Contamination Assessment and Reduction Project (CARP)

A Model for the Evaluation and Management of Contaminants of Concern in Water, Sediment, and Biota in the NY/NJ Harbor Estuary

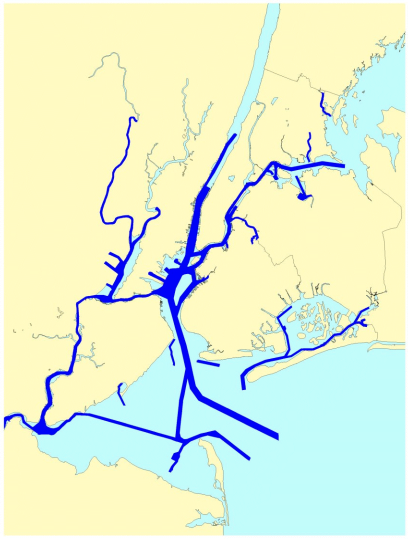

Contaminant Fate & Transport & Bioaccumulation Sub-models

July 2007

HydroQual

PREFACE

The modeling work reported here is one of several efforts undertaken in connection with the Contamination Assessment and Reduction Project (CARP). CARP is a landmark project bringing together federal, state and non-government partners in a determined effort to better understand and reduce contamination within the New York/New Jersey Harbor Estuary. This contamination has led to environmental harm and economic hardships. In particular, dredging and disposal activities connected to port activities were severely curtailed in the early 1990ôs as dredging managers and regulators struggled with finding management options for handling contaminated dredged material. While dredging has since proceeded, the costs have escalated to 10 to 30 times previous levels, largely because of sediment contamination. Other negative impacts continue to plague the system, including fish advisories and substandard water quality, which are impeding the recovery and utilization of many of the estuaryôs natural resources.

Through workgroup deliberations in connection with the Dredged Material Forum and the NY/NJ Harbor Estuary Program (HEP), a general plan was developed to address the problem of continued contamination of sediments requiring dredging. The operative management questions included: Which sources of contaminants need to be reduced or eliminated to render future dredged material clean? Which actions can yield the greatest benefits? And, which actions are necessary to achieve the 2040 targets recommended in the Dredged Material Management Plan for the Harbor? CARP was initiated to address these questions. The primary funding mechanism for CARP was the 1996 *Joint Dredging Plan for the Port of New York and New Jersey*, an agreement between the States of New York and New Jersey that was funded by the Port Authority of New York and New Jersey (Port Authority). Additional funds were obtained from the New Jersey Department of Transportation (NJDOT), the Empire State Development Corporation, The U.S. Army Corps of Engineers, the Hudson River Estuary Management Program, HEP, and the Hudson River Foundation.

The specific objectives of the CARP are to:

1. Identify and quantify sources of contaminants of concern to the NY/NJ Harbor Estuary from a dredged material standpoint;
2. Establish baseline levels of contaminants of concern in water, sediments, and biota;
3. Determine the relative significance of contaminant inputs in controlling the concentrations of those contaminants in water, sediment and biota:
4. Forecast future conditions in light of various contaminant reduction scenarios;
5. Take action to reduce levels of contaminants of concern in water, sediments, and fish tissue.

CARP is a unique partnership of governmental and non-governmental entities whose activities have been guided by a management committee composed of representatives from the U.S. Environmental Protection Agency, U.S. Army Corps of Engineers, New Jersey Department of Environmental Protection (NJDEP), New York State Department of Environmental Conservation (NYSDEC), NJDOT, Empire State Development

Corporation, Port Authority, Environmental Defense and the Hudson River Foundation. NYSDEC and NJDEP completed objectives 1 and 2 above through a comprehensive data collection (sampling and testing) program, which represents about 90% of the $32 million total funding for CARP. It was the consensus of the CARP Management Committee that mathematical modeling tools were needed to help understand the results of the data collection program and the fate and transport of contaminants through the Harbor. These models provide a means for integrating data in a mass balance framework such that relationships between loadings and contaminant concentrations in water, sediment and biota can be evaluated and quantified. Moreover, these models can provide the predictive capacity that managers and scientists need to assess the consequences of existing contaminant loads and potential remedial actions. The modeling work performed by HydroQual, Inc., therefore addresses Objectives 3 and 4 above, and represents about 10% of the total funding for CARP.

The major focus of CARP has been on an objective evaluation of the fate and transport of contaminants throughout the entire NY/NJ Harbor Estuary system. The CARP Management Committee hopes that its work will lead to action to reduce both ongoing and historic contamination. The CARP Management Committee includes representatives of federal and state government agencies and is therefore mindful of the various regulatory programs that are in place to address contaminant issues. Consequently, since the inception of CARP, agencies on the Committee have made comments and recommendations to make CARP as relevant as possible to these programs. However, the CARP data collection and modeling efforts were not designed specifically to comply with the requirements of any particular regulatory program. CARP products, particularly the modeling results, will no doubt provide important new information for these programs to consider, but further data collection and model refinement may be necessary to suit the scale and requirements of any particular program. And it is only those charged with regulatory responsibilities that can judge whether CARP products comply with their requirements.

Given the vast complexities of the entire estuary and the processes that affect contaminant fate and transport, modeling of this system has been a great technical challenge. From the initiation of CARP, it was understood that the modeling would be limited in some aspects because of scientific uncertainties in fully understanding all of the relevant processes. To ensure that the model components would be *state-of-the-science* upon completion, a Model Evaluation Group (MEG) was established at the outset of the project. Experts in organic and inorganic geochemistry, hydrodynamics, sediment transport and contaminant modeling were solicited to be members of the MEG. The MEGôs first responsibility was to be part of the team to select a modeling contractor. It then has met repeatedly over the past five years, reviewing and commenting on the acceptability of modeling concepts and formulations to reproduce estuarine processes, including the review of model validation and hindcast results. The comments and suggestions of the MEG have been addressed by HydroQual, Inc., and a summary of the responses are included in this report. In addition, the MEG has provided comments and guidance on the future use and application of the modeling products.

While some model components have been verified, refined and successfully used in other venues, other components were newly designed for this project. The CARP modeling has elements that could be considered *applied science and engineering*, while others would be better characterized as *research and development*. The MEG has generally found that the CARP modeling effort has advanced the understanding of contaminant behavior in the estuary and does a very credible job of characterizing the relationships between contaminant loadings and concentrations in the environment.

One of the more challenging issues that the CARP Management Committee addressed was the development of realistic contaminant reduction scenarios to use as an illustration of the modelôs capability. As the modeling activities progressed, it became increasingly clear that legacy contamination of sediments was a dominant feature in controlling levels of contaminants in the system. Since two large-scale sediment remediation projects (namely the Hudson River Superfund and Lower Passaic River Superfund projects) were being developed, it made sense to include these projects in our initial CARP scenario analyses. While neither project is fully defined as yet, the model scenario gives a glimpse of the potential for these sites (remediated or not) to influence sediment and water quality in the Harbor over the long term.

The completed modeling components should not only be viewed as management tools, but as research tools from which fuller understandings of the fate and transport of contaminants can be gleaned. In addition, it is the hope of the CARP Management Committee that this modeling work serve as a foundation from which more advanced models can be developed and applied to new and emerging management issues.

Dennis J. Suszkowski, Ph.D.
Hudson River Foundation
Co-chair, CARP Management Committee

W. Scott Douglas
NJ Dept. of Transportation
Co-chair, CARP Management Committee

LEGAL NOTICE

CONTENTS

CONTENTS (Continued)

Section Page

CONTENTS (Continued)

CONTENTS (Continued)

CONTENTS (Continued)

Section Page

CONTENTS (Continued)

CONTENTS (Continued)

FIGURES

FIGURES (Continued)

FIGURES (Continued)

FIGURES (Continued)

FIGURES (Continued)

FIGURES (Continued)

FIGURES (Continued)

TABLES

EXECUTIVE SUMMARY

For the Contamination Assessment and Reduction Program (CARP), numerical models have been developed to assist managers in determining which sources of contaminants would have to be eliminated or reduced in order for future sediments in the NY/NJ Harbor to be considered "clean" in terms of meeting dredged material benchmarks. The CARP models account for the fate, transport, and bioaccumulation of sixty-three hydrophobic organic and metal contaminants of concern. Specifically, these contaminants include ten PCB homologs, seventeen dioxin/furan congeners with 2,3,7,8 substitutions, twenty-two PAHs, six DDT related chemicals, five chlordane related chemicals and the metals cadmium, mercury, and methylmercury. The contaminant fate, transport, and bioaccumulation models are forced by several others CARP models (i.e., hydrodynamic transport, sediment transport, organic carbon production) which are fully described in other CARP modeling technical reports (HydroQual, 2007a; HydroQual, 2007b).

In order to develop the CARP contaminant fate, transport, and bioaccumulation models, several data analysis and data synthesis tasks were completed. The modeling work relied primarily on the use of a multimillion-dollar data set collected for CARP by the States of New York and New Jersey between 1998 and 2002. Additional data used for model calibration include data collected by EPA's REMAP and data from the peer-reviewed literature.

CARP data related to contaminant inputs were synthesized for purposes of specifying detailed contaminant loading inputs for numerous individual contaminant sources representing a variety of source types (i.e., tributary head-of-tide, STP, CSO, stormwater, atmospheric deposition, landfill leachate, in-place sediments, open boundaries, etc.). It was also necessary to use the CARP data to calculate site-specific phase partition coefficients and volatilization rates for each contaminant. The calculated phase partition coefficients included temperature and salinity dependencies. For PCBs, the calculated volatilization rates included temperature dependencies.

The CARP contaminant fate, transport, and bioaccumulation model calibration process involved numerous model and data comparisons, sensitivity analyses, and a hindcast verification. A Model Evaluation Group (MEG) convened by the Hudson River Foundation (HRF) oversaw the development of the contaminant fate, transport, and bioaccumulation models as well as their calibration and application. Model calibration, sensitivity, verification, and application are summarized below.

Model Calibration

The CARP contaminant model calibration processes included:

- contaminant specific assessments of the overall level of agreement between model results and measured data
- checking for biases in the level of agreement between model results and data collected by one state or another
- confirming that outliers were randomly distributed rather than systematic
- assessing level of agreement between model and data for specific phases
- explaining and analyzing seasonal, episodic, and long-term variations in model results and data

For PCB homologs, the model and data agree reasonably well for the majority of the homologs (i.e., tri-CB, tetra-CB, penta-CB, hexa-CB, hepta-CB, octa-CB, nona-CB, and deca-CB). For example, for hexa-CB, 97% of the water column particulate measurements on an organic carbon normalized basis are within a factor of ten of the CARP model calculations. More significantly, 74% of the water column particulate measurements on an organic carbon normalized basis are within a factor of 3 of the CARP model calculations. The model tends to overpredict mono-CB measurements and, to a lesser extent, the di-CB measurements. It is noted that loading measurements for the mono-CB and di-CB homologs were often lumped together. Additional statistical comparisons of model results and data for the PCB homologs are included in Section 4.0 and Appendix 4B.

For 17 dioxin/furan congeners with 2,3,7,8 substitutions, 90% of the water column particulate measurements on an organic carbon normalized basis and 100% of the sediment particulate measurements on an organic carbon normalized basis are within a factor of ten of the CARP model calculations. More significantly, 65% of the water column particulate measurements on an organic carbon normalized basis and 80% of sediment particulate measurements on an organic carbon normalized basis are within a factor of 3 of the CARP model calculations.

In general, the level of agreement between model results and measured data for cadmium is similar to that for PCB homologs and dioxin/furan congeners. The agreement between model calculations and the limited available methylmercury data is not as good as for other contaminants. Mercury comparisons are favorable for particulate concentrations in the water column and sediment, less so for water column dissolved. Additional statistical comparisons of model results and data for PCB

homologs, dioxin/furan congeners, mercury, and cadmium are included in Section 4.0 and Appendices 4B-4D.

For PAHs and organochlorine pesticides related to DDT and chlordane, additional model skill assessments were performed. The twenty-two PAH compounds for which the CARP HOC model has been applied include: benzo[a]pyrene, dibenzo[a,h]anthracene, benzo[a]anthracene, benzo[b/j/k]fluoranthene, indeno[1,2,3,cd]pyrene, chrysene, benzo[g,h,i]perylene, acenaphthene, acenaphthylene, fluoranthene, fluorene, pyrene, anthracene, naphthalene, phenanthrene, 1-methylnaphthalene, 2-methylnaphthalene, perylene, 1-methylphenanthrene, 2,3,5-trimethylnaphthalene, 2,6-dimethylnaphthalene, and benzo[e]pyrene. To the extent that the dissolved water column PAH measurements are credible (i.e., there were technical issues with the manner in which these data were collected and only a limited number of paired measurements of dissolved and particulate phases), the CARP model somewhat overpredicts both the dissolved and particulate measurements. The model overprediction can be characterized as being within the range of the data and is likely due to any or all of: analytical problems with loading data (described in Section 3.3.1.2.1), underestimation of the volatilization rate, or other transformation/degradation processes unique to PAHs and not considered in the CARP HOC model kinetics. Although the model does well for most PAHs in the sediment bed, there is a clear problem in the model's ability to calculate measurements of 1-methyl and 2-methyl naphthalenes (log Kow 3.84 and 3.86, respectively) in the sediment bed. Further improvement on this calibration would require the collection of additional site specific data. Specifically, data on water column dissolved phase PAH concentrations are needed as well as any site specific fate information on naphthalene and its methylated forms that distinguishes these chemicals from other PAHs. The analytical methods may not yet be available to make the needed measurements.

The six contaminants related to DDT for which the CARP model has been applied include: 2,4'-DDT, 4,4'-DDT, 2,4'DDE, 4,4'DDE, 2,4'DDD, and 4,4'DDD. The CARP model performs better for the DDE and DDD isomers than for the DDT isomers. In general there is more range in the water column data for DDT related contaminants than is captured by the CARP model. When there is disagreement between model and data for the DDT related contaminants, the model usually underestimates the highest measurements. In most cases, there is 90% or better agreement within a factor of ten between water column measurements and calculations and even better agreement for sediment bed measurements and calculations. These results are suggestive of the fact that the model includes the major sources of the DDT related contaminants and that the model is accurately representing the overall transport and phase partitioning behavior of these contaminants. The model does not capture the degradation processes. This is consistent with some of the underprediction of

DDE and DDD but inconsistent with underprediction of DDT. The overall conclusion is that there does not appear to be any systematic biases (e.g., model always higher than data) in the organochlorine pesticide calibrations.

The five contaminants related to chlordane for which the CARP model has been applied include:

α-chlordane (also known as cis-), γ-chlordane (also known as trans-), oxychlordane, cis-nonachlor, and trans-nonachlor. Model results and measured data for the chlordane related contaminants are overall in reasonable agreement. This indicates that the CARP model captures the major sources of the chlordane related contaminants and is properly accounting for their overall transport and phase partitioning. The comparisons also indicate that transformation processes not accounted for in the CARP model kinetics likely play a relatively minor role in determining levels of contamination in the Harbor water column and bed over the time horizon of the current conditions calibration.

Overall, the CARP contaminant fate and transport models were successfully calibrated for a large number of different contaminants. Across the large number of HOC's there was no adjustment in model coefficients beyond prescribed adjustments in partition coefficients and volatilization rate coefficients. The CARP contaminant fate and transport model was also calibrated to cadmium and mercury with reasonable success. These results are further indication that the underlying CARP hydrodynamic, sediment transport, and organic carbon production models are all well calibrated. The calibrations of the underlying models are described in separate reports (HydroQual, 2007a; HydroQual, 2007b).

Model Sensitivity

Sensitivity analyses and diagnostic work performed as part of CARP model calibration include: clean bed/time to steady state simulations (i.e., sediment initial conditions sensitivity), organic carbon partitioning sensitivities, and volatilization sensitivities. Sensitivity results demonstrate that the CARP HOC model was relatively insensitive to the volatilization formulation and temperature and salinity dependencies on partitioning. On the other hand, sensitivity results show that site-specific rather than octanol-water based partitioning to organic carbon, the value selected for A_{DOC} for specifying HOC binding to DOC, and the selection of sediment initial conditions were all critical in determining model responses. In particular, results of the clean bed/time to steady state simulations were important from a management perspective. Clean bed results quantitatively suggest that observed contaminant

concentrations in sediments can not be explained by current day loadings. This implies that current levels of contamination in Harbor sediments are likely due, in large part, to historical sources, the remnants of which still persist in sediments. Further, clean bed results indicate that given a full remediation of contamination in the sediment bed, some level of recontamination will occur from the continuance of current loadings. The recontamination, however, will produce contaminant concentrations that are much lower than current contaminant levels.

Model Verification

Hindcast verifications were performed as a further test of the critical time constants (i.e., those model inputs that are controlling the time response of contaminants in Harbor sediments). Hindcast verifications were performed for cesium (^{137}Cs), 2,3,7,8-TCDD, and selected PCB homologs (di-BC, tetra-CB, hexa-CB, octa-CB). The hindcast process involved estimating historical loadings and historical sediment initial conditions. In the case of cesium, the historical loadings were well known. For this reason, the cesium hindcast is the most important test of the critical time constants in the model controlling contaminant responses. In the case of 2,3,7,8-TCDD, historical loadings are believed to have been dominated by a single source and the time history of the single source discharge was inferred from proximal dated sediment cores. Other sources of 2,3,7,8-TCDD were left at present day loading levels for the hindcast. For PCBs, the historical loadings were developed both by scaling current day loadings using site-specific scale factors and by taking advantage of measurements made on the Upper Hudson River upstream of Troy Dam. Initial conditions for the hindcast simulations representative of 1965 concentrations were established based on dated sediment cores for each of the contaminants. Overall the agreement between hindcast model results and data were very good for cesium and 2,3,7,8-TCDD. Hindcast results were not as good for PCBs. This is most likely due to uncertainties in PCB hindcast loadings.

Model Application

The CARP contaminant fate and transport model was applied to evaluate several unit loading component responses which span all current-day loading source categories. These components are: atmospheric deposition, ocean boundary, STPs, CSOs, runoff, head of tide, and in-place sediment bed (i.e., sediment initial conditions). These components were evaluated for 2,3,7,8-TCDD, 2,3,4,7,8-PCDF, di-CB, tetra-CB, hexa-CB, octa-CB, Hg, MeHg and Cd. In addition, subset components which more specifically target known loading sources were also run. These include: Passaic River in-place sediments, Newark Bay in-place sediments, and the Hudson River at Troy Dam. These components were

evaluated for 2,3,7,8-TCDD, 2,3,4,7,8-PCDF, di-CB, tetra-CB, hexa-CB, and octa-CB. The CARP component analysis was used to estimate the future response of contaminants in the water column and sediment bed to continuing loadings and the 1998 in-place contamination in the Harbor. Long term responses of the system to current loadings were gauged by carrying out the loading component simulations for 32 years.

For many of the contaminants, loading component results show that legacy sources of contamination as represented by sediment initial conditions will have a greater effect on ambient levels of contamination than current day sources for many years into the future. This trend is more apparent for HOCs than for metals. Of the current day sources, stormwater runoff and head of tide loadings tend to provide the greatest contributions to ambient contamination. The water column is more responsive to current day loadings than the sediment bed. For the conditions modeled, 1998 Passaic River sediments have little future impact on sediments in other regions of the model with the exception of perhaps Newark Bay and the Kills. Similarly, for the conditions modeled, the future influence of 1998 Newark Bay sediment initial conditions is for the most part limited to Newark Bay and the Kills and is less than the influence of 1998 Passaic River sediment initial conditions. These results do not say anything about the origins of the 1998 in-place contamination. Component results indicate that the 1998-2002 Upper Hudson River loading, if unchanged, is the dominant future source of sediment contamination for di-CB throughout the Harbor, but is not a dominant source for the tetra-, hexa-, and octa- CB homologs. The Upper Hudson is not an appreciable source of contamination to Harbor sediments for either 2,3,7,8-TCDD or 2,3,4,7,8-PCDF.

Results of the CARP contaminant fate and transport model for contaminant concentrations in water and sediments were expanded to predict contaminant concentrations in organisms. For purposes of predicting concentrations of contaminants in organisms under present and potential future loading conditions, site-specific BAFs and BSAFs were calculated based on biological data collected by CARP investigators. In addition, steady-state and time variable CARP bioaccumulation models were developed for purposes of better understanding and explaining observed trends in measured BAFs and BSAFs.

CARP loading component results have been stored in a spreadsheet-based user interface. The interface allows stakeholders to specify their own loading conditions by scaling (i.e., either up or down) each of the individual loading components simultaneously for an infinite number of "what if?" calculations. The spreadsheet includes tabular and graphical displays of expected contaminant

concentrations for the water column, sediment bed, and several pelagic and benthic species under the user-specified loading conditions.

The CARP models have also been applied to project contaminant levels in the year 2040 under three loading conditions: future with current loadings, future with 17-mile remediation of the Passaic River and the enactment of the Upper Hudson River Superfund Record of Decision (ROD), and future with lower 7-mile remediation of the Passaic River and the enactment of the Upper Hudson River Superfund ROD. The projection runs were performed for the same selected contaminants as the component runs. Results of the projection runs have many potential applications. For the immediate purposes of CARP, results of the projection runs were used to predict HARS suitability in the future.

For HARS suitability determinations, worm BSAFs based on dredged material testing rather than field-derived BSAFs were used. For existing conditions, 2,3,7,8 concentrations in sediments of the Kills and several other Harbor areas are generally suitable for HARS disposal while sediments of Newark Bay, the Passaic River, and the Hackensack River are not. In terms of PCBs, most of the sediments of the Harbor, including Newark Bay and the Kills, are not HARS suitable under existing conditions. HARS suitability will be achieved by 2040 for 2,3,7,8-TCDD in Newark Bay and the Kills under all three conditions evaluated: the future with current loadings and the future with the Upper Hudson River ROD implemented with either of two Passaic River remediation scenarios. HARS suitability will almost be achieved for PCBs by 2040 in Newark Bay and the Kills only with the Upper Hudson River ROD implemented and either of two Passaic River remediation scenarios. For PCBs, a future with current loadings condition would not achieve HARS suitability for Newark Bay and the Kills and several other areas of the Harbor.

CONCLUSIONS

This report section represents conclusions reached as a direct result of the development and initial applications of the CARP contaminant fate, transport, and bioaccumulation numerical models. The conclusions have been broadly sorted into categories including overall understanding, Port and Harbor management implications, and specific needs for further research or data collection.

Overall Understanding

- The CARP models simulate very complex estuarine processes for a large suite of contaminants. The management questions for which the CARP models were designed to answer require that estuarine processes are well characterized over broad spatial scales. The CARP model development effort therefore included a compilation and synthesis of data from many sources to achieve a well-integrated whole system model. The modeling, coupled with data collected to characterize contaminant loads and to calibrate the model, provides a valuable tool from which reasonable forecasts can be made of the direction and rate of change in contaminant concentrations in the water, sediments, and biota of the Harbor in light of changes to contaminant inputs.

- Detailed analyses of specific sections of the Harbor will require further model refinement and data collection. In this regard, the data collected to support the development of the CARP models, although unprecedented, were somewhat marginal and would not be fully sufficient for sub-regional evaluations.

- The CARP models represent an advancement over the contaminant fate modeling state-of-the-science in that hydrodynamic transport, sediment transport, organic carbon production/dissolved oxygen dynamics, and contaminant partitioning and bioaccumulation have all been integrated into a single framework.

- The comprehensive linked and integrated approach followed in the development of the CARP models will allow for important management questions to be addressed (e.g., How will nutrient load reductions and corresponding changes in carbon and sulfur cycles in the Harbor affect PCB or mercury exposure concentrations and bioaccumulation behavior?).

- An important aspect of the CARP models is correctly representing the rates of exchange of contaminants between the water column and sediment bed . For the most part, the CARP

models do this well in the core area of the Harbor for which dredged material management questions are relevant. The cesium hindcast results, in particular, are a good demonstration of the ability of the CARP models to capture sediment response times.

- Residence time of contaminants, especially particle reactive contaminants, in the NY/NJ Harbor system and the time to steady state are related to the exchange between the sediment bed and the overlying water column. For most of the CARP model domain, settling, resuspension, and the particle mixing rate across the water-sediment interface controls this exchange. In addition to mixing rates, the effect of sediment transport and "estuarine trapping" also impact the time to steady state. In many parts of the Harbor, particulate phase contaminants are continually resuspended by tidal action, transported (oftentimes by near bottom waters moving in a net landward direction), and redeposited. The "estuarine trapping" process works to retain particle-reactive contaminants in the estuary for long time periods and impedes the loss of contaminants to the ocean.

- As a result of the long-term estuarine trapping of particles and the persistence of many of the contaminants, contamination observed in NY/NJ Harbor surficial sediments is due to both current day and historical legacy pollution sources.

- Neither the data collected nor the modeling work performed for CARP indicate that chemical transformations, such as photolysis, dechlorination, or other degradation mechanisms, are occurring appreciably in the NY/NJ Harbor for either PCB homologs or dioxin/furan congeners over the time horizon modeled. This is also true for organochlorine pesticides.

- Field-derived and model-derived BioAccumulation Factors (BAFs) for hydrophobic organic contaminants followed expected trends. Specifically , BAFs were generally higher for more hydrophobic PCBs (i.e., higher K_{ow} homologs); BAFs increased with trophic levels due to biomagnification of PCBs in the food chain; and BAFs were lower for migrating fish populations. In addition, metabolism of PAHs in zooplankton and fish was shown to be important. Field-derived BAFs for dioxin/furans were however lower than expected, suggesting that metabolism of dioxin/furan congeners is possibly occurring in fish.

- Field-derived and model-derived Biota Sediment Accumulation Factors (BSAFs) for hydrophobic organic contaminants were found to vary significantly as a function of K_{ow}. For example, for low K_{ow} PCB homologs, BSAFs are less than one and are believed to be controlled

by respiratory exchange. For mid-range Kow PCB homologs, BSAFs are often greater than one due to the relative importance of dietary exposure. Finally, for high K_{ow} PCB homologs, BSAFs are reduced to values less than one. This reduction is attributed to diffusion limitations through membranes for high K_{ow} PCB homologs. Based on limited data, BSAFs were also found to be lower in the more contaminated areas of the Harbor. The effect of contaminant levels on benthic organism response and/or geographic differences in the quality of food supply may be possible explanations for this observed behavior.

Port and Harbor Management Implications

- The results of the "clean bed" analysis suggest that historical sources were much larger than current sources for most contaminants. Further, the "clean bed" results indicate that if NY/NJ Harbor were to undergo remediation, current day sources would likely produce some surficial recontamination, but not to the extent of current observed levels of contamination.

- Component analysis findings confirm results of the "clean bed" analysis in that sediment initial conditions, specified based on observed sediment contaminant levels, are a major component of contamination. The component results indicate that over several decades, contamination in surficial sediments will decline as current sources of contamination are smaller than legacy sources. Of the current sources of contamination, runoff and head-of-tide appear to be dominant for many of the contaminants.

- A HARS suitable Newark Bay, in terms of PCB and dioxin/furan levels of contamination in worms, may be attained in the future if the Superfund ROD for the Upper Hudson River is implemented and a cleanup of the in-place sediments in the Passaic River is undertaken. For the HARS suitability calculations, BSAFs from the Harbor dredged material laboratory testing program, rather than field-derived BSAFs, were used.

- To the extent that sediment cleanup targets will be established based on bioaccumulation by benthic organisms in the field, observed differences in measured BSAFs for discrete locations within the Inner (i.e., Arthur Kill, Newark Bay, and Upper Bay) and Outer (Long Island Sound, Jamaica Bay, Raritan Bay and Sandy Hook) Harbor have serious implications. The observations (based on seven worm-sediment pairs of contaminant measurements) suggest that as sediments are cleaned up, BSAFs may increase. If this is in fact true, stricter cleanup goals may be required.

- Additional conclusions are likely to emerge as existing CARP model outputs are further studied and as additional model simulations are performed. CARP model results can help focus future TMDL, Superfund, and Restoration data collection and modeling efforts.

Specific Needs for Further Research or Data Collection

- For many of the contaminants, concentrations measured by CARP investigators were higher in storm water than in CSOs. Similarly, model results (i.e., "clean bed" and components) indicate that of the ongoing sources of contamination, runoff and head-of-tide are most important for many contaminants. Additional monitoring of storm water and runoff is recommended.

- One of the challenges faced in modeling PCBs for CARP is related to the mono-CB and di-CB homologs. In many cases, measurements of loading concentrations for these homologs were lumped together for analytical reasons. There also may have been analytical difficulties with the ambient measurement of these homologs, particularly in the water column. Other studies have adopted a "tri-CB +" convention to avoid analytical difficulties with mono-CB and di-CB. In the NY/NJ Harbor, however, the mono-CB and di-CB are important for a number of reasons including: (1) there was inadvertent production of PCB11 (a di-CB congener) that was discovered because of CARP's measurement of elevated di-CB in several areas of the Harbor and (2) the Upper Hudson River source is dominated by lower chlorinated homologs and di-CB could potentially serve as a good marker or tracer of an Upper Hudson influence. Further investigation into analytical methods for resolving congeners within the mono-CB and di-CB homologs without co-elution would be beneficial.

- A limited number of contaminant samples for the Passaic River head-of-tide source were collected by CARP investigators at Little Falls, New Jersey. From a modeling perspective, it would have been more useful to collect these samples at the Dundee Dam since there are many potential sources of contamination between Little Falls and the Dundee Dam. Additionally, we have some concern specifically for 2,3,7,8-TCDD related to the limited number of samples collected. For the case of 2,3,7,8-TCDD, one of the Little Falls samples had elevated concentrations. Our ability to specify the upstream boundary condition for the Passaic River was somewhat compromised by the design of the sampling program. Additional sampling at the Dundee Dam should be conducted for both dissolved and particulate contaminant phases

with coincident measurements of suspended sediment, particulate organic carbon, and dissolved organic carbon.

- Dissolved phase concentrations of dioxin and furan congeners, which are in the pico- to nano-gram per liter and lower range, are extremely difficult to measure. For CARP modeling, only a limited number of dissolved phase measurements were available for dioxin/furan congeners and the validity of those measurements was questionable. Fortunately, the dioxin/furan congeners have relatively high log K_{OW} values and are predominantly present in the particulate phase. CARP model calibrations for dioxin/furan congeners, therefore, focused on particulate phase concentrations which contain a large portion of the total mass. Additional dissolved phase measurements would be helpful in assessing the bioavailability of dioxin/furan congeners.

- Reliable measurement of dissolved phase PAHs was problematic for CARP investigators. From a modeling perspective, lack of paired dissolved and particulate phase measurements made it difficult to calculate site-specific, three-phase organic carbon partitioning coefficients. Given that log K_{OW} values for PAH compounds are relatively low, this presented a greater problem for model calibration than lacking dissolved phase measurements for dioxin/furan congeners which have relatively higher log K_{OW} values . Although the final CARP model calibration results for PAHs are reasonable, further improvement on this calibration would require collection of additional site-specific PAH data to test field-derived partition coefficients.

- Although site-specific, three-phase organic carbon partitioning coefficients were successfully developed and applied in the CARP model, log K_{OW} values were used in the calculation of the freely dissolved phase (that portion of dissolved phase which is not complexed with DOC). There is some uncertainty in the log K_{OW} values obtained for CARP modeling primarily using the EPA Structure-activity Estimation Program (SPARC). Log K_{OW} values derived from SPARC and other sources should be checked and updated as may be appropriate in the future, particularly if the CARP model is being applied in a context such as risk assessment where bioavailability is a critical issue. In particular, the log K_{OW} values for the organochlorine pesticides are a concern.

- A potential weakness of the CARP model is the Hudson River between Albany and Poughkeepsie. Although hydrodynamics for this stretch of the River had been included in the calibration of the predecessor hydrodynamic model used in SWEM, the organic carbon production model had never been implemented above Poughkeepsie prior to CARP. CARP

did not provide an opportunity (i.e., data, budget, schedule, etc.) for a rigorous calibration of the organic carbon production model in this stretch of the River. Further, the CARP model computational grid has only one lateral element in this portion of the domain which could impact both the hydrodynamic and sediment transport model calculations. Due to the PCB source from the Upper Hudson River, potential deficiencies in organic carbon production or hydrodynamic and sediment transport on the Hudson River above Poughkeepsie would affect PCB calculations more so than calculations for other contaminants. A project targeted at collecting hydrodynamic, nutrient, carbon, solids, and productivity data on the Hudson River between Albany and Poughkeepsie and performing additional model skill assessment is desirable. Additional contaminant measurements to supplement CARP water column and sediment data would also be beneficial.

- Although the mechanistic mercury methylation model developed and applied for CARP represents a true technological advancement, the state-of-the-science for understanding the behavior of mercury in the environment has continued to evolve in parallel with the development of the CARP model. Thus, as the CARP model is just now becoming publically available, so too are the results of other investigations on mercury dynamics in the Harbor. Several publications in the peer reviewed literature became available after the completion of the CARP metals model and other publications are anticipated to become available in the near future. For example, we anticipate that a manuscript currently in preparation by Richard Bopp and others on mercury deposition in sediments of the NY/NJ Harbor will become available in the peer reviewed literature in the near future. We therefore recommend that an effort be undertaken to perform a post-audit assessment of the CARP mercury model relative to all the new information. It is possible that refinements and enhancements to the CARP mercury model, based on the latest research, would benefit the utility of the model in assessing mercury contamination.

- The specification of the atmospheric deposition of mercury in the CARP model was based on site-specific measurements collected by Yuan Gao and reported in 2001. Since then, additional atmospheric deposition data for mercury in the NY/NJ Harbor region have been collected by other researchers or are anticipated. In 2004, Reinfelder et al. prepared a report for the NJDEP on monitoring completed by the New Jersey Atmospheric Deposition Network (NJADN). Richard Bopp's group at Rensselaer Polytechnic Institute (Kroenke, 2003, Bopp et al., 2006, Gagne, 2006) has recently undertaken efforts to quantify regional atmospheric fluxes of mercury. Information on loadings of mercury from sources other than atmospheric deposition

has also recently become available (Balcom et al., 2004). These data should be evaluated and possibly incorporated into the model as part of TMDL or other future CARP model applications.

- Measurements of methylmercury by CARP investigators were fewer in number and less reliable than the CARP measurements for other contaminants. In this regard, additional measurements of methylmercury in the NY/NJ Harbor would be useful for additional model verification. We would recommend that, once available, the methylmercury data collected by Hammerschmidt et al. (submitted) be considered in a post-audit assessment of the CARP mercury model prior to further CARP mercury model applications for management decisions. Soon to be available estimates for rates of methylmercury production and other new mercury speciation considerations (Balcom et al., submitted, Hammerschmidt et al., submitted, Miller et al., 2007, Sunderland et al., 2006, Lambertsson and Nilsson, 2006, Kerin et al., 2006, Heyes et al., 2006) will also be useful.

- CARP bioaccumulation data and modeling results suggest that varying levels of contamination throughout different geographic regions of the NY/NJ Harbor (i.e., at seven discrete locations in the Inner and Outer Harbor) may be affecting bioaccumulation behavior (i.e., growth and other bioenergetic behaiviors) of benthic organisms. Further, the modeling and data suggest that dioxin/furan metabolism may be occurring in fish. Additional biological data need to be collected to support these findings.

- BSAFs calculated using coincident measurements of contaminants in collocated sediments and worms collected by CARP investigators are different than BSAFs measured during dredged material laboratory testing. Further data collection is advisable for purposes of developing robust protocols for extrapolating between field and laboratory exposures and applying HARS-based and human-health based endpoints for benthic invertebrates.

SECTION 1.0

INTRODUCTION

This report presents the technical details of the development of the Contamination Assessment and Reduction Project (CARP) contaminant fate and transport and bioaccumulation sub-models. The report focuses on the development and calibration of the CARP contaminant fate and transport and bioaccumulation sub-models for the four water years beginning in October 1998 and ending in September 2002 for both hydrophobic organic and metal contaminants. This report also includes a description of hindcast verifications of the model and application of the model for management (i.e., diagnostic and projection) purposes. This report is the third in a series describing CARP sub-models. Additional reports relating to CARP models include:

HydroQual, 2007a. A model for the evaluation and management of contaminants of concern in water, sediment, and biota in the NY/NJ harbor estuary. Hydrodynamic Sub-model. Report prepared for the Hudson River Foundation on behalf of the Contamination Assessment and Reduction Project (CARP). 552 pp.

HydroQual, 2007b. A model for the evaluation and management of contaminants of concern in water, sediment, and biota in the NY/NJ harbor estuary. Sediment Transport/Organic Carbon Production Sub-model. Report prepared for the Hudson River Foundation on behalf of the Contamination Assessment and Reduction Project (CARP). 1379 pp.

The CARP contaminant fate and transport and bioaccumulation sub-model originates from a mathematical model of the long-term behavior of PCBs in the Hudson River Estuary (Thomann et al., 1989) and an integrated model of organic chemical fate and bioaccumulation in the Hudson River Estuary (Farley et al., 1999), collectively called the Thomann-Farley model. Since the Thomann-Farley model is the predecessor model to the CARP contaminant fate and transport and bioaccumulation sub-models, some of the features of the Thomann-Farley model which will not be detailed in other sections of this report are described below.

The Thomann-Farley model is a large space scale, seasonal time scale model for contaminant fate and bioaccumulation of PCBs, PAHs, and dioxin in the Hudson River Estuary. It was developed to assess the impact of various loads of contaminants in the ecosystem, particularly with regard to fisheries and port activities associated with dredging and disposal of contaminated sediments. The

Thomann-Farley model includes: (1) a fully time-variable chemical transport and fate model for calculating PCBs, PAHs, and dioxin in the water column and sediment bed; (2) a time-variable, age-dependent food chain model for calculating PCB concentrations in phytoplankton, zooplankton, small fish, perch, and striped bass; and (3) Biota-Sediment-Accumulation Factors (BSAFs) for calculating PCB, PAHs, and dioxin concentrations in dredged material test organisms (*Macoma nasuta* and *Nereis virens*). Within the overall Thomann-Farley mass balance modeling approach, the primary focus was on the development and application of sub-models of contaminant fate and bioaccumulation. Hydrodynamic, organic carbon, and sediment transport were not modeled directly in the Thomann-Farley model but rather were specified based on field observations, the modeling work of others (i.e., SWEM calculations), or simple mass balances. Some of the technical advantages of the CARP model over the Thomann-Farley model include: better spatial resolution of contaminant hot spot and dredging areas, vertical resolution of the water column to capture estuarine two-layer flow dynamics (represented in ten vertical depth layers), open boundaries away from the zone of influence of NY/NJ Harbor contaminant loads, inclusion of the HARS within the model domain, a mechanistic consideration of hydrodynamic transport, suspended sediment and organic carbon through fully-linked sub-models, incorporation of kinetics for a broader range of hydrophobic organic contaminants, incorporation of kinetics for metal contaminants including mercury methylation/demethylation processes, and inclusion of additional species in bioaccumulation calculations (i.e., polychaete worms, clams, striped bass, white perch, American eel and blue crab). Additionally the Thomann-Farley model did not have the benefit of the comprehensive ambient and loading source data collected by CARP.

The water quality model source code underlying the Thomann-Farley model is WASTOX (Connolly and Thomann, 1985; Connolly, 1991). The water quality model source code underlying both the CARP contaminant fate and transport and sediment transport/organic carbon production sub-models is Row Column Aesop (RCA). Both RCA and WASTOX originate from the Water Analysis Simulation Program (WASP) developed by Hydroscience (HydroQual's predecessor firm) in the 1970's (DiToro et al., 1981, DiToro and Paquin, 1984). RCA code has been used to develop numerous models outside of the NY/NJ Harbor region. The code has been constantly refined and upgraded to include both more realistic representations of chemical and biological processes occurring in open waters and underlying sediments, and more robust numerical solution techniques. The code has evolved to include the capacity to interface directly with the outputs of hydrodynamic and sediment transport models. Since the early 1990's, HydroQual has maintained a users manual for the RCA code. An updated version of the users manual recently completed by HydroQual is available to the CARP MEG and management committee upon request and includes a detailed description of the basic equations of the

model, characteristics of the model, characteristics of the computer code, and descriptions of input and output files associated with the code.

The principal attributes of the RCA source code include:

- RCA is a general purpose code used to evaluate a myriad of water quality problem settings. The user is able to customize an RCA sub-routine to address water body specific water quality issues.
- RCA formulates mass balance equations for each model segment for each water quality constituent or state-variable of interest. These mass balance equations include all horizontal, lateral and vertical components of advective flow and dispersive mixing between model segments; physical, chemical and biological transformations between the water quality variables within a model segment; and point, nonpoint, fall-line, and atmospheric inputs of the various water quality variables of interest.
- The partial differential equations, which form the water quality model, together with their boundary conditions, are solved using several mass conserving finite difference techniques.

The purpose of this report is to provide the CARP MEG with a comprehensive description of the CARP contaminant fate and transport and bioaccumulation sub-models for hydrophobic organic and metal contaminants. The report is broken down into twelve technical sections including: contaminant modeling approach, contaminant model setup, contaminant model calibration for current conditions, contaminant model sensitivities, contaminant model hindcast verification, application of models for additional contaminants, bioaccumulation model approach, bioaccumulation model setup, bioaccumulation results, bioaccumulation model sensitivities, contaminant loading source component simulations, and 2040 projections.

SECTION 2.0

CONTAMINANT FATE AND TRANSPORT MODELING APPROACH

This report section will describe the contaminant fate and transport modeling approach along with the corresponding model equations. Two approaches were followed: one for hydrophobic organic contaminants (HOCs) and one for metals. These are described separately in Sections 2.1 and 2.2, respectively. The HOCs include ten PCB homologs and 17 dioxin and furan congeners. The HOC modeling approach and kinetics were further tested in an application to 22 individual PAH compounds and 11 organochlorine pesticides as described in Section 7.0. The metals include mercury, methylmercury, and cadmium.

2.1 HYDROPHOBIC ORGANIC CONTAMINANTS KINETICS

This report section will describe the kinetic processes included in the CARP contaminant fate and transport model for hydrophobic organic contaminants in the water column and sediment bed.

2.1.1 Water Column Processes

The CARP contaminant fate and transport model includes the ability to represent numerous hydrophobic organic contaminant processes in the water column including: partitioning of contaminants to dissolved and particulate organic carbon, settling and resuspension of particle associated contaminants, diffusive and mixing exchanges across the water column and sediment bed interface, and volatilization of contaminants across the water column and atmosphere interface. The CARP contaminant fate and transport model code has the capability to also consider, photolysis, dechlorination, and other degradation processes; however, absent strong evidence indicating that these processes are occurring in the Harbor for the hydrophobic organic contaminants of concern, these model features were not implemented.

2.1.1.1 Three Phase Partitioning to Organic Carbon

For purposes of hydrophobic organic contaminants, three contaminant phases are modeled: freely dissolved (C_D), DOC-complexed dissolved (C_{DOC}), and POC-complexed (C_{POC}):

$$C_T = C_D + C_{DOC} + C_{POC} \tag{2-1}$$

In order to model the three phases, partition coefficients, K_{POC} and K_{DOC}, are used to express the relationship between POC-complexed contaminant (C_{POC}) and freely dissolved contaminant (C_D), and between DOC-complexed contaminant (C_{DOC}) and freely dissolved (C_D) contaminant. Following the approach of Burkhard (2001), K_{DOC} is equal to the contaminant specific octanol-water partition coefficient (K_{ow}) times a scale factor (A_{DOC}) to account for the more hydrophilic nature and lower binding affinity of contaminants to DOC. Substituting the relationships for K_{POC} and K_{DOC} into equation 2-1 yields the following expression:

$$C_T = C_D + C_D \times DOC \times A_{DOC} \times K_{OW} + C_D \times POC \times K_{POC} \quad (2\text{-}2)$$

Our initial approach for the derivation of K_{POC} values from site specific data is described below. The derivation involves a consideration of the definition of fraction dissolved chemical, f_D:

$$f_D = \frac{C_D}{C_D + C_{DOC} + C_{POC}} \quad (2\text{-}3)$$

Based on equations 2-1 and 2-2, equation 2-3 may be re-written as:

$$f_D = \frac{C_D}{C_D + C_D \times DOC \times A_{DOC} \times K_{OW} + C_D \times POC \times K_{POC}} \quad (2\text{-}4)$$

Dividing the numerator and denominator of the right side of equation 2-4 by the freely dissolved concentration, C_D, yields:

$$f_D = \frac{1}{1 + DOC \times A_{DOC} \times K_{OW} + POC \times K_{POC}} \quad (2\text{-}5)$$

Re-arranging terms in equation 2-5 yields:

$$\frac{1}{f_D} = 1 + DOC \times A_{DOC} \times K_{OW} + POC \times K_{POC} \quad (2\text{-}6)$$

and:

$$\frac{1}{f_D} - 1 - DOC \times A_{DOC} K_{OW} = POC \times K_{POC} \quad (2\text{-}7)$$

Finally, a log-linear equation is developed:

$$\log\left(\frac{1}{f_D} - 1 - DOC \times A_{DOC} K_{OW}\right) = \log(POC) + \log(K_{POC}) \quad (2\text{-}8)$$

Equation 2-8 may be used for the derivation of site specific values of K_{POC} for each contaminant if a value of A_{DOC} is known or assigned. For initial evaluations, an interim A_{DOC} value of 0.1 was used as part of model calibration (see Section 4.3.2). Site-specific K_{POC} values were derived by using water column measurements of contaminants, DOC, and POC to plot the left side on equation 2-8 on the y-axis and the first term on the right side of equation 2-8 on the x-axis. For such a plot for a given contaminant, if the slope is forced to 1, the y-intercept is the log of the partition coefficient for POC-complexed and freely dissolved contaminant, K_{POC}. Section 4.3.3 presents the data plots developed in deriving site-specific values of K_{POC} for each contaminant used in initial CARP model calibration.

Due to the large amount of variability in the site-specific contaminant measurements of the fraction dissolved and the uncertainty in the derived y-intercept described above, particularly for contaminants predominantly in the dissolved phase, a second approach was developed for calculating K_{POC}. In this case, site-specific K_{POC} values for all hydrophobic organic contaminants (HOCs) were calculated by solving equation 2-2 for K_{POC} for each set of observations, by taking the log of the calculated K_{POC} values, and by averaging the calculated log K_{POC} values across observations for each contaminant.

As part of the CARP current conditions calibrations, this latter approach was extended to consider the effects of temperature and salinity on K_{POC}. This was done for PCB homologs using enthalpies for water-octanol phase changes for K_{POC} temperature corrections. The enthalpies were not readily available for other contaminant groups. For this exercise, the van't Hoff equation (equation 2-9) was used for the relationship between temperature and octanol water partitioning:

$$\log K_{ow}(T) = \log K_{ow}(25°) + \frac{\Delta H_{ow}}{2.303R}\left(\frac{1}{298.15} - \frac{1}{273.15+T}\right) \quad (2\text{-}9)$$

where:

$$T = temperature\ (^{\circ}C)$$
$$\Delta H_{ow} = Enthalapy\ change\ of\ phase\ transfer\ (kJ / mole)$$
$$R = Gas\ constant\ \left(= 8.314 \times 10^{-3}\ kJ / mole\text{–}^{\circ}K\right)$$

The Setschenow equation (2-10) was used for the relationship between salinity and octanol water partitioning:

$$\log K_{ow}(salt) = \log K_{ow}(freshwater) + K^{salt} \cdot [salt] \qquad (2\text{-}10)$$

where:

$$K^{salt} = Setschenow\ constant\ (\approx 0.35\ for\ PCBs)$$
$$[salt] = molar\ salt\ concentration\left(\approx 0.6 \cdot \frac{salinity}{35\ ‰}\right)$$

In applying the van't Hoff equation (equation 2-9), values of the enthalpy change for each PCB homolog were obtained from relationships given in Li et al., 2003 and log K_{OW} values were taken from Hawker and Connell, 1988. Due to the geographic variability in measured congener distributions, homolog averages were determined from a direct average (i.e., rather than a weighted average) of congener-specific values. Both the van't Hoff (equation 2-9) and Setschenow (equation 2-10) equations were applied simultaneously. The value of the Setschenow constant for PCBs, 0.35, was taken from Sobek et al., 2004. Further discussion of partitioning is found in the calibration (see section 4.0) and sensitivities (see section 5.0) sections of this report.

2.1.1.2 Chemical Transformations

The CARP contaminant fate and transport model code has the capability to also consider photolysis, dechlorination, and other degradation processes; however, absent strong evidence indicating that these processes are occurring in the Harbor for the hydrophobic organic contaminants of concern, these model features were not implemented.

2.1.1.3 Matrix Transfers

Transfer of contaminants across the air-water and sediment-water interfaces are included in the CARP model calculations. Transfers across the air-water interface are described below in section 2.1.1.3.1.

Sections 2.1.1.3.2 through 2.1.1.3.4 below describe the approach for transfer of contaminants across the sediment-water interface.

2.1.1.3.1 Volatilization

Contaminant transfer across the air-water interface is considered in two ways in the CARP model: as an independent external loading (i.e., wet and dry deposition plus forward diffusion gas exchange) and a dynamic back diffusion gas exchange which is dependent upon water column concentrations of freely dissolved chemical. For purposes of initial CARP model calibration, the back diffusion gas exchange rate was specified as a single value of 1 m/day, consistent with results of several gas exchange rate measurements using sulfur hexafluoride, SF_6, and helium-3, ^3He, tracers in both the tidal freshwater Hudson and the NY/NJ Harbor Estuary. This approach was later revised to calculate the back diffusion gas exchange rate. A discussion of the available measurements and our calculation procedure follows.

A 2.8 to 9.2 cm/hr CO_2 gas exchange rate for the tidal freshwater Hudson River has been reported (Clark et al., 1996). As calculated in Farley et al., 1999, the Clark et al., 1996 CO_2 gas exchange measurements correspond to a PCB volatilization rate of 0.34 to 1.1 m/day, consistent with the CARP model gas exchange rate of 1 m/day. For converting CO_2 gas exchange rates to PCB volatilization rates, a molecular weight correction of $(44/300)^{0.355}$ was used. The exponent of 0.355 is derived from raising the exponent in the Schwarzenbach et al., 1993 relationship between diffusivity (D_W) and molecular weight (MW), 0.71, to the ½ power (i.e., taking the square root). Effectively, raising an exponent to a power corresponds to the multiplication of the two exponents, 0.71 x ½ = 0.355. The square root dependency originates from Surface Renewal Theory (Dankwerts, 1951) that is used in the O'Connor-Dobbins formulation for calculating mass transfer coefficients through the water side of the interface. The molecular weight relationship from Schwarzenbach et al., 1993 and the O'Connor-Dobbins formula are presented below.

O'Connor-Dobbins Equation (O'Connor and Dobbins, 1958):

$$k'_{\ell} = \sqrt{\frac{U \times D_w}{h}} \qquad (2\text{-}11)$$

where D_W is the molecular diffusivity of a substance in water, U is the average water velocity (often taken as the average tidal velocity in estuaries), and h is the mean water depth.

Molecular Diffusivity (D_w)and Molecular Weight (MW) Relationship (Schwarzenbach et al., 1993):

$$D_w \propto \frac{1}{MW^{0.71}} \qquad (2\text{-}12)$$

Similarly, the initial CARP model gas exchange rate of 1 m/day used for HOCs is supported by more recent work of Ho et al. 2002 who performed SF_6 experiments in the tidal Hudson River near Newburgh, NY in July/August 2001. An average gas transfer velocity for SF_6 of 1.56 $\pm$ 0.12 m d^{-1w} was reported (Ho et al., 2002). Following the molecular weight adjustment described above, this corresponds to a gas exchange rate of approximately 1.1 to 1.3 m d^{-1} for HOC's with molecular weights around 300 and is in reasonable agreement with the CARP gas exchange rate of 1.0 m d^{-1}. It is acknowledge that marked improvements have taken place in SF_6 resolution since the work of Clark et al., 1996 (Ho et al., 2002).

Additionally, SF_6 experiments were conducted in the East River near Randall's Island, north of Hellgate and opposite Sunken Meadow (about 13.5 km or 8.4 miles away from the Battery) (Caplow et al., 2004). Gas exchange rates ranging from 4.5 to 10.7 cm/hr for CO_2 were reported. After molecular weight adjustment, these values correspond to 0.55 m/day to 1.3 m/day, and agree well with the CARP model volatilization rate of 1 m/day, for HOCs with a molecular weight near 300. During July 2002, SF_6 experiments were conducted in Newark Bay (Caplow et al., 2003) near the confluence with the Hackensack and Passaic Rivers. Gas exchange rates of 7.0 $\pm$ 0.4 cm/hr were estimated for CO_2. These values correspond to HOC gas exchange rates of 0.8 to 0.9 m/day.

The sensitivity of the CARP HOC fate and transport model to temperature effects on the back diffusion gas exchange rate for PCB homologs was explored and resulted in a modification to the volatilization rate specified in the current conditions calibrations for PCB homologs and dioxin/furan congeners. Our consideration of temperature effects is described in Section 5.3. The gas exchange rate previously set at 1 m/day was calculated in the CARP model as a function of the concentration gradient of the contaminant between air and water, the dimensionless Henry's constant, and a depth normalized overall transfer rate. Since wet and dry deposition and forward gas exchange are already considered as external loadings, the contaminant concentration in air, C_A, was set to 0 for these calculations. The overall volatilization rate coefficient, or k'_v was calculated using velocity, diffusivity, and depth dependence (see Equation 2-11 for the water transfer rate), the dimensionless Henry's constant and a specified gas transfer exchange rate coefficient of 100 m/day. A final expression of the form in 2-13 was used for the contaminant mass rate of volatilization:

$$\frac{k'_v}{h} \cdot \left(\frac{C_A}{K'_H} - C_D \right) \tag{2-13}$$

where K'_H is the dimensionless Henry's Law constant, C_D is the dissolved contaminant concentration, and h is the water depth.

The overall volatilization rate coefficient, k'_v was calculated as described above by:

$$k'_v = \frac{1}{\underbrace{\frac{1}{k'_\ell}}_{\text{Water transfer}} + \underbrace{\frac{1}{K'_H \cdot 100}}_{\text{Air transfer}}} \tag{2-14}$$

It is noted that wind effects on volatilization were not specifically considered for the CARP model. Our rationale is that tidal velocities in the Harbor are strong enough that water velocity, and not wind velocity, would control the water side of the volatilization interface. Further, it is unlikely that wind velocities over the Harbor are available at sufficient temporal and spatial resolution over the model domain to drive the volatilization calculation with any more rigor than using the tidal velocity calculation.

Independent external loadings associated with wet and dry deposition plus forward gas exchange are described below in Section 3.3.1.2.5.

2.1.1.3.2 Pore Water/Diffusive Exchange

The exchange of dissolved contaminants across the water column and sediment bed interface is described below in section 2.1.2.2.2 as a sediment bed process.

2.1.1.3.3 Settling

Formulations of coagulation induced settling that were used to describe the removal of particles from the water column and to the sediment bed are presented in detail in HydroQual, 2007b. POC-complexed contaminants are subject to this water column removal mechanism in the CARP contaminant fate and transport sub-model. The necessary interfacing between the CARP contaminant fate and transport and sediment transport/organic carbon production sub-models is discussed in sections 3.2 and 4.3.1 of this report.

2.1.1.3.4 Resuspension

Analogous to settling, kinetic formulations for resuspension processes which bring particles from the sediment bed to the water column are presented in detail in HydroQual, 2007b. POC-complexed contaminants are subject to this water column source term in the CARP contaminant fate and transport sub-model. The necessary interfacing between the CARP contaminant fate and transport and sediment transport/organic carbon production sub-models is discussed in sections 3.2 and 4.3.1 of this report.

2.1.2 Sediment Bed Processes

Similar to the water column, modeled sediment kinetics for HOCs include partitioning, chemical transformations, and matrix (i.e., water and sediment) transfers. Important sediment processes that are modeled include diffusive exchange of dissolved contaminants between sediment pore water and the water column, sediment layering, and mixing processes of particle-bound contaminants. The sediment mixing processes ultimately determine the response time that contaminant concentrations in surface sediments and the overlying water column experience as a consequence of future changes in external loadings and other management actions. Modeling the sediment mixing processes correctly is a critical component of the CARP model. Each of the CARP model sediment kinetic processes for HOC's are described more fully below.

2.1.2.1 Three Phase Partitioning to Organic Carbon in the Sediment Bed

In the CARP contaminant fate and transport model, partitioning of hydrophobic organic contaminants is handled in the same manner in the sediment bed as in the water column. The description of water column partitioning provided in Section 2.1.1.1 applies for partitioning in the sediment bed. A noteworthy difference is that POC concentrations in the sediment are significantly greater than POC concentrations in the water column. Accordingly, although the ratio of particulate contaminant per mass of POC to dissolved contaminant, as defined by the partition coefficient, is identical in both the water column and sediment bed, there is significantly more POC and contaminant per volume of sediment bed than per volume of water column. Measurements of contaminants in sediment bed pore water were not available to confirm the partitioning relationships in the sediment bed. Absent information to the contrary, we would not expect the partitioning between POC-complexed contaminant (C_{POC}) and freely dissolved contaminant (C_D) to change between the water column and sediment. However, based on HydroQual's experience on another system, the Housatonic River, DOC in sediment bed pore water could bind more (i.e., ten times more) of the freely dissolved

contaminant (C_D) as DOC-complexed contaminant (C_{DOC}) than water column DOC on a mass of DOC basis. Pore water data were not available for NY/NJ Harbor to confirm whether or not this feature, i.e., a higher value of A_{DOC} in the sediment than in the water column, should be included in the CARP model.

2.1.2.2 Sediment Bed Mixing Processes

In the CARP contaminant fate and transport sub-model, sediment mixing processes include both particle mixing and diffusive exchange. These are described below in sections 2.1.2.2.1 and 2.1.2.2.2. Part of our effort in developing the HOC sediment kinetics for the CARP model was to avoid artificial, i.e., caused by "numerical dispersion", mixing of contaminants between sediment layers. Numerical dispersion was found to occur by Blasland, Bouck, and Lee, Inc. (1997) in a model of the Fox River in areas experiencing alternating periods of erosion and deposition. Problems of numerical mixing were attenuated in the CARP model by following the archival stack approach of Limno-Tech (1998).

An added benefit of applying an archival stack in the CARP contaminant sub-model was to reduce the computational burden and model simulation times. An archival stack is an established modeling technique whereby contaminant concentrations in deeper sediment layers are effectively removed from the model calculations, but are archived in a storage matrix. During a major storm event or dredging operation, contaminant concentrations in the deeper sediment layers can be re-introduced into the model calculations. For CARP calibration runs, the archival stack was handled as a reservoir of uniform contaminant concentration. The archive stack could be configured to include multiple layers of varying concentrations for future applications. Further discussion of the structure of the sediment bed in the various CARP sub-models is provided in section 3.2.2.

2.1.2.2.1 Particle Mixing

Transfer of particle-bound contaminants across the sediment-water interface and between sediment layers is in part due to bioturbation (Aller, 1988). Bioturbation varies seasonally (Balzer, 1996), is proportional to the biomass of the macrobenthos inhabiting the sediment (Matisoff, 1982), and is influenced by temperature (Gerino et al., 1998). Benthic biomass was not modeled directly in the CARP contaminant fate and transport sub-model, but rather it was assumed that the benthic biomass present is proportional to the concentration of labile organic carbon in the sediment which was calculated by the organic carbon production model and passed to the contaminant fate and transport model. The direct relationship between sediment labile organic carbon and benthic biomass, and the basis of our assumption, is that the flux of labile organic carbon deposited to the sediment, D_p, is the food source

for the macrobenthos and the source of labile organic carbon in the sediment. For purposes of the CARP bioaccumulation sub-model, benthic biomass will be handled differently as described in report sections 8.0 to 11.0. The CARP bioaccumulation sub-model shall consider direct measurements of contaminant body burdens in worms and clams.

2.1.2.2.2 Diffusive Exchange

Mixing of pore water with overlying water and between sediment layers may include the effects of "hydrodynamic pumping" of water through sediment bed forms (Elliott, 1990) and/or "bioirrigation" due to the activity of sediment organisms (Boudreau, 1996; Schluter et al., 2000). For estimating rates of diffusive exchange of dissolved contaminants in the CARP contaminant fate and transport sub-model, including benthic enhancement, we took advantage of the pore water diffusion coefficients, D_d, used in the calibrated/validated System Wide Eutrophication Model (SWEM) which is the basis of the CARP organic carbon production model. D_d as taken from SWEM is approximately two to three times higher than molecular diffusion. D_d in SWEM was calibrated against pore water ammonia concentrations, which are highly dependent upon pore water diffusion. Of particular importance for CARP is the influence of the pore water diffusion coefficients on the contaminants with low octanol-water partition coefficients such as the low molecular weight PAH compounds (see section 7.0).

As applied in CARP, the D_d term is not varied or corrected for molecular weights across contaminants. The rationale for this approach is that the biological effects are the more predominant component driving pore water mixing.

Fluxes of dissolved contaminants, both HOCs and to a lesser extent metals, from the pore water to the overlying water column occur almost entirely as DOC complexes. A noted weakness of the CARP model kinetic formulation of diffusive exchange is that the CARP organic carbon production model does not explicitly calculate pore water DOC concentrations. The CARP model accounts for this by using an assigned concentration of pore water DOC, which is not included in the overall carbon balance.

2.2 METAL CONTAMINANTS KINETICS

2.2.1 Water Column Processes

Relevant process occurring in the water column for metals include aquatic speciation, and specifically for mercury, methylation and demethylation. Other transfer processes are analogous to those experienced by HOCs.

2.2.1.1 Aquatic Speciation

For metals, a full speciation calculation including dissolved and particulate forms was used instead of a simpler partitioning approach. Incorporating detailed chemical speciation allowed the CARP model to consider how variations in salinity and organic matter would effect the distribution of metals in the water column. The availability of a detailed breakdown of metal distribution by chemical form was also beneficial for considering how metal bioavailability changed in response to changing water chemistry. These latter considerations were especially useful for the mercury methylation calculations as described in Section 2.2.1.2.1 and bioaccumulation calculations as described in Section 8.3. Free ions, Cd^{+2} and Hg^{+2}, from speciation calculations were used as the bioavailable form of the metals for bioaccumulation model calculations.

Stability constants and reaction stoichiometry for inorganic complexes for Cd, Hg, and meHg were compiled from the National Institutes of Standards and Technology database (NIST Version 7, Smith et al., 2003) and supplemented with other sources (e.g., Benoit, Gilmour et al. 1999). Inorganic speciation included complexation with hydroxides, chlorides, carbonates, sulfates, and sulfides (Table 2-1). Concentrations of major ions used in these complexation reactions were estimated from salinity values calculated by the SWEM-based CARP hydrodynamic model.

Table 2-1. Inorganic reactions used in metal speciation calculations for mercury, methylmercury, and cadmium. Most of these reactions were derived from information in the NIST Critical Stability Constants Database (Martell et al., 2004) except for mercury sulfide complexes, which were based on Benoit et al. (1999).

Hydroxides									
Mercury									LogK
Hg+2	+	OH-			=	HgOH-			10.2
Hg+2	+	2OH-			=	Hg(OH)2			21.83
Hg+2	+	3OH-			=	Hg(OH)3-			20.9
Methylmercury									LogK
MeHg+	+	OH-			=	MeHgOH			9.47
MeHg+	+	2OH-			=	MeHg(OH)2-			11.67
Cadmium									LogK
Cd+2	+	OH-			=	CdOH+			3.92
Cd+2	+	2OH-			=	Cd(OH)2			7.65
Cd+2	+	3OH-			=	Cd(OH)3-			10.30
Cd+2	+	4OH-			=	Cd(OH)4-2			8.70
Chlorides									LogK
Mercury									LogK
Hg+2	+	Cl-			=	HgCl-			7.3
Hg+2	+	2Cl-			=	HgCl2			14
Hg+2	+	3Cl-			=	HgCl3-			15
Hg+2	+	4Cl-			=	HgCl4-2			15.6
Hg+2	+	OH-	+	Cl-	=	HgOHCl			18.1
Methylmercury									LogK
MeHg+	+	Cl-			=	MeHgCl			5.23
Cadmium									LogK
Cd+2	+	Cl-			=	CdCl+			1.98
Cd+2	+	2Cl-			=	CdCl+			2.60
Cd+2	+	3Cl-			=	CdCl+			2.40
Carbonates and Sulfates									
Mercury									LogK
Hg+2	+	SO4			=	HgSO4			2.4
Methylmercury									LogK
MeHg+	+	CO3-2			=	MeHgCO3-			6.1
MeHg+	+	SO4-2			=	MeHgSO4-			0.94
Cadmium									LogK
Cd+2	+	CO3-2			=	CdCO3			3.50
Cd+2	+	CO3-2	+	H+	=	CdHCO3+			11.80
Cd+2	+	SO4-2			=	CdSO4			2.40

Sulfides									
Mercury									LogK
Hg+2	+	2S-2	+	H+	=	Hg(HS)S-			63
Hg+2	+	2S-2	+	2H+	=	Hg(HS)2			68.5
Hg+2	+	S-2			=	HgS			42
Hg+2	+	2S-2			=	HgS2-2			54.5
Methylmercury									LogK
MeHg+	+	S-2			=	MeHgS-			22.5
2MeHg+	+	S-2			=	MeHg2S			38.8
3MeHg+	+	S-2			=	MeHg3S-			45.8
Cadmium									LogK
Cd+2	+	S-2	+	H+	=	CdHS+			23.1
Cd+2	+	2S-2	+	2H+	=	Cd(HS)2			45.59989
Cd+2	+	3S-2	+	3H+	=	Cd(HS)3-			63
Cd+2	+	4S-2	+	4H+	=	Cd(HS)4-2			80.9

Complexation of metals by organic matter is described by multiple binding-sites on both DOC and POC. Consideration of multiple binding sites allowed development of a concentration-dependent apparent binding strength that increased at lower metal concentrations. As these mixtures of binding sites in natural organic matter are titrated with metal, the strong binding sites are preferentially filled first. Weaker sites will eventually interact with the metal as the concentration is titrated to higher concentration, but only after strong sites are completely saturated with metal. As a result, weaker sites appear to have higher site densities (i.e., are active at higher metal loadings). This formulation is consistent with general models of trace-metal binding with organic matter (e.g., Tipping 1998). For the organic matter formulations used here it was generally sufficient to include only two or three types of sites, with site densities that bracketed the range of metal concentrations in the simulation (Table 2-2).

Table 2-2. Dissolved and particulate organic complexation reactions used in metal speciation calculations for mercury, cadmium, and methylmercury.

Dissolved Organic Carbon							
Mercury					LogK	Moles/mgC	Sources
Hg^{+2}	+	L_1	=	HgL_1	28.7	1.00E-08	Haitzer et al. 2003
Hg^{+2}	+	L_2	=	HgL_2	38	1.20E-09	Calibration to CARP data
Methylmercury					LogK	Moles/mgC	Sources
$MeHg^+$	+	L_3	=	$MeHgL_3$	20	1.00E-11	Calibration to CARP data
$MeHg^+$	+	L_4	=	$MeHgL_4$	13.4	5.72E-11	O'Driscoll and Evans 2000
$MeHg^+$	+	L_5	=	$MeHgL_5$	11	1.28E-09	O'Driscoll and Evans 2000
Cadmium					LogK	Moles/mgC	Sources
Cd^{+2}	+	L_6	=	CdL_6	9.00	8.00E-09	Based on apparent binding
Cd^{+2}	+	L_7	=	CdL_7	10.40	5.00E-10	
Cd^{+2}	+	L_8	=	CdL_8	4.00	1.00E-11	
Particulate Organic Carbon							
Mercury					LogK	Moles/mgC	Sources
Hg^{+2}	+	P_1	=	HgP_1	29.7	1.00E-08	Haizter et al 2003 * 10
Hg^{+2}	+	P_2	=	HgP_2	40	1.20E-09	Calibration to CARP data
Methylmercury					LogK	Moles/mgC	Sources
$MeHg^+$	+	P_3	=	$MeHgP_3$	21	1.00E-11	Calibration to CARP data
$MeHg^+$	+	P_4	=	$MeHgP_4$	11.87	1.28E-09	Simplified Amirbahman et al 2002
Cadmium					LogK	Moles/mgC	Sources
Cd^{+2}	+	P_5	=	CdP_5	11.50	8.00E-09	Calibration to CARP data
Cd^{+2}	+	P_6	=	CdP_6	10.70	5.00E-10	Based on apparent binding
Cd^{+2}	+	P_7	=	CdP_7	4.00	1.00E-11	

2.2.1.2 Chemical Transformations

2.2.1.2.1 Mercury Methylation/Demethylation

Although mercury methylation in these simulations only occurs in the sediments, demethylation does occur in the water column. Photolysis of methylmercury (resulting in the formation of inorganic mercury) is calculated using CARP organic carbon production model calculated light intensities in the water column multiplied by dissolved water column methylmercury concentrations and a rate constant taken (K = 3.09E-4) from the literature (Sellers et al., 1996) with the following form:

Photolysis (mg L^{-1} day^{-1}) = Light (uE m^{-2} s^{-1}) * K (uE^{-1} m^2 s^1 day^{-1}) *
Dissolved Methylmercury (mg L^{-1}) (2-11)

2.2.1.3 Matrix Transfers

Matrix transfers (i.e., volatilization, pore water/diffusive exchange, settling, and resuspension) which cadmium and mercury experience are analogous to those experienced by HOC's. Refer to section 2.1.1.3 above.

2.2.1.3.1 Volatilization

The evasion, or volatilization, of elemental mercury was modeled using "2-film" theory, in the same manner as the volatilization of PCB homologs and dioxin furan congeners as described in Section 2.1.1.3.1.

2.2.2 Sediment Bed Processes

2.2.2.1 Phase Partitioning/Speciation

The chemical speciation reactions in the sediment are largely based on the same chemical reactions used to calculate speciation in the water column (see section 2.2.1.1). All of the inorganic and organic reactions in the water column are duplicated in the sediment. In addition, metals in the sediment are also allowed to react with iron monosulfide mineral phases that are widespread in sediments (commonly measured as acid volatile sulfide or AVS). Binding of both mercury and cadmium with AVS is very strong, and therefore dominates the speciation of either metal in sediments when AVS is available. Because mercury interactions with AVS are stronger than all other metals, it is assumed to bind to AVS regardless of what other metals are present. For cadmium, however, many other metals bind to AVS more strongly, including for example copper and mercury. It is more likely, therefore, that a portion of AVS in sediments bound with other metals is unavailable for binding cadmium. Since we are not simulating other metals such as copper in this modeling analysis we cannot build these competitive interactions in directly. Instead we assume that only a fraction (10%) of the total AVS in sediments is available for binding cadmium, based on the observed distribution of metals from sediments collected in the CARP domain. The AVS phase is calculated as a particulate sulfide phase in the CARP sediment transport/organic carbon production model, ST-SWEM.

Table 2-3 AVS model parameters					
Mercury					LogK
Hg+2	+	AVS-2	=	HgAVS	40
Cadmium (only 10% of AVS is assumed to be available)					LogK
Cd+2	+	AVS-2	=	CdAVS	15

2.2.2.2 Chemical Transformations

2.2.2.2.1 Mercury Methylation

Net mercury methylation in sediments is a balance between the formation of methylmercury and demethylation processes. Mercury methylation is directly tied to sulfate reduction rates in sediments (King et al., 2000; King et al., 2001; King et al., 1999) and is also influenced by pore water sulfide concentrations (Benoit et al., 1999).

The SWEM-based CARP organic carbon production model computes both the rate of sulfate reduction as a critical step in the generation of sediment oxygen demand and the pore water sulfide concentrations. Sulfide reacts with pore water inorganic mercury to form many different chemical species of which only neutral (uncharged) compounds (e,g., HgS^0, $Hg(HS)_2^0$) are available for methylation (Benoit et al., 1999). The CARP methylation model was calibrated to measured methylation rates in the Hudson River (Heyes et al., 2004) and Long Island Sound (Hammerschmidt and Fitzgerald, 2004) making use of model calculated sulfate reduction rates and mercury speciation (i.e., concentrations of HgS^0, $Hg(HS)_2^0$).

The methylation rate takes on the following form:

Mercury Methylation Rate = k * Sulfate Reduction Rate * Concentration of Available Mercury as HgS^0 and $Hg(HS)_2^0$

The Mercury Methylation Rate (MMR) initially has units of moles * L^{-1} * day^{-1} at the source code level. The constant 'k' has a value of 44,140 and units of m^2 * $mg^{-1}O_2$. The Sulfate Reduction Rate (SRR) calculated in the SWEM-based CARP organic carbon production model, has units of mg O_2 m^{-2} day^{-1} and the concentration of Available Mercury (AvlHg) has units of moles * L^{-1}. For the MMR, volume-normalized units can be converted to areal units by taking into account the assumed active layer depth of 0.10 meters (i.e., 10 cm) as follows:

MMR (moles L^{-1} day^{-1}) * 1000 L m^{-3} = MMR (moles m^{-3} day^{-1}) * 0.1 meters
active layer depth = MMR (moles m^{-2} day^{-1}) (2-19)

2.2.2.2.2 Mercury Demethylation

As noted in section 2.2.1.2.1 demethylation by photolysis of methylmercury occurs in the water column. Demethylation can also occur in sediments. There are several possible pathways for methylmercury degradation that are discussed in the literature (Marvin-DiPasquale et al., 2000; Oremland et al., 1995; Pak and Bartha, 1998) but due to a lack of detailed process information all demethylation processes are grouped together in one model formulation. It is clear that demethylation is largely a microbial process in sediment and is strongly tied to redox (Compeau and Bartha, 1984) and sulfate reduction rates (Oremland et al., 1991) with greater rates of demethylation generally occurring under anoxic conditions. Consequently, the CARP demethylation function has two rate constants for use in either oxic or anoxic portions of the sediment. The sediment demethylation model has the following formulation:

Demethylation Rate = k * Total Sediment Methylmercury * Carbon Decay Rate

The Demethylation Rate constant has units of moles * L^{-1} * day^{-1}. The second-order rate constant 'k' has values of 0.202 in oxic layers of the sediment and 8.08 in anoxic layers. These values were determined by calibration to project data by comparing model-calculated sediment methylmercury concentrations produced with calibrated MMR to measured methylmercury concentrations in the sediment. The units of 'k' are m^2 * $mg^{-1}O_2$. Total Sediment Methylmercury has units of moles L^{-1} for the 10 cm active layer and finally Carbon Decay Rate (CDR) has units of mg O_2 m^{-2} day^{-1}. In anoxic sediment layers Carbon Decay Rate is equal to SRR and oxic layer CDR is equal to the anoxic layer CDR. The demethylation rate is linked to the SRR throughout the model but continues to be active in oxic sediment layers when SRR is equal to zero and the corresponding MMR is also zero.

2.2.2.3 Mixing Processes

Physical and biological processes (i.e., volatilization, pore water/diffusive exchange, settling, and resuspension) which cadmium and mercury experience are analogous to those experienced by HOC's. Refer to section 2.1.2.2 above.

SECTION 3.0

CONTAMINANT FATE AND TRANSPORT MODEL SETUP

This report section will describe the information necessary to use the contaminant kinetics described above in Section 2.0 in the CARP contaminant fate and transport sub-model. The requisite information for the contaminant fate and transport sub-model includes both outputs from other CARP sub-models (i.e., hydrodynamic transport, suspended sediment transport, and organic carbon production) and forcing data inputted directly to the contaminant fate and transport model.

3.1 INTERFACING WITH CARP HYDRODYNAMIC MODEL OUTPUTS

In general, the CARP hydrodynamic sub-model calculates the water circulation and transport patterns that are passed to the other CARP sub-models on an hourly averaged basis. Transport information across each interface in the CARP model computational grid is passed to each sub-model through the use of an information file, a gcm_tran file, that is outputted by the hydrodynamic sub-model. Report sections 3.1.1 and 3.1.2 describe the content of a gcm_tran file and discuss the importance for modeling contaminant fate and transport of specific pieces of information contained in the gcm_tran file. The CARP hydrodynamic sub-model is more fully described in HydroQual, 2007a.

3.1.1 General Hydrodynamic Information Passed to CARP Sub-Models

The CARP hydrodynamic sub-model produces an output file which includes as time histories in three dimensions the calculated (i.e., one hour average) water depths, volume transport rates, dispersions, salt concentrations, and temperatures. The volume transport rates and dispersions are reported in the longitudinal, lateral, and vertical directions. Calculated water depths are tracked as changes in elevation over time.

3.1.2 Specific Hydrodynamic Information Shared with CARP Sub-Models

The organic carbon production and contaminant fate and transport CARP sub-models rely upon temperature and salinity calculated by the hydrodynamic sub-model for calculating temporally and spatially varying values of partition coefficients, various rate constants and kinetic coefficients which have temperature and/or salinity dependencies. For example, for metals fate and transport, water column salinities calculated by ECOM in near bottom waters are used for the calculation of major ion

sediment bed pore water chemistry. The CARP sub-models also rely upon the volume transport rates calculated by ECOM. Specifically for the calculation of suspended sediment, organic carbon, and other particulate matter transport, including particulate contaminants, bottom shear stress provided by the hydrodynamic sub-model is of critical importance (i.e., bottom shear stress determines whether or not resuspension of particulate matter can occur). Bottom shear stresses in ECOM are typically calculated without considering the effects on bottom roughness of wind wave interactions with velocity currents. As part of the CARP specific application of ECOM, the effect of wave-current interaction on the bottom roughness coefficient is considered. Specifically, as described in HydroQual, 2007b, for sediment transport calculations, bottom roughness coefficients calculated by ECOM in Haverstraw Bay were adjusted to account for wind wave effects.

3.2 INTERFACING WITH CARP SEDIMENT TRANSPORT/ORGANIC CARBON PRODUCTION MODEL OUTPUTS

In general, the CARP sediment transport/organic carbon production sub-model calculates concentrations of suspended sediment, particulate organic carbon, and dissolved organic carbon over time and in longitudinal/lateral space in ten vertical layers of the water column and in the sediment bed in active layer aerobic and anaerobic zones and in an anerobic archive (a.k.a., archival stack). The carbon is type identified based on its reactivity.

In addition to organic carbon concentrations and vertical transport rates, the CARP sediment transport/organic carbon production sub-model outputs numerous other concentrations and fluxes in the water column and sediments relevant to eutrophication including: algal biomass as either carbon or chlorophyll a; particulate and dissolved organic and dissolved inorganic phosphorus; particulate and dissolved organic and dissolved inorganic nitrogen; available and biogenic silicon; algal exudate carbon; hydrogen sulfide; dissolved oxygen; and porewater and bulk sediment concentrations and fluxes of nitrogen, phosphorus, silica, oxygen, and sulfides.

Correct calculation of suspended sediment and organic carbon concentrations and vertical transport rates of carbon, in particular, is needed for calculating concentrations of contaminants bound to particles. Information calculated by the sediment transport/organic carbon production sub-model and specifically passed to the contaminant fate and transport sub-model is described below in greater detail.

3.2.1 General Sediment Transport/Organic Carbon Production Information Passed to CARP Fate and Transport Sub-models

The CARP sediment transport/organic carbon production sub-model produces a large output file (i.e., approximately 7.4 gigabytes per year) specifically for the CARP contaminant fate and transport sub-models. The output file includes as time histories in three dimensions the calculated (i.e., one hour average) water column phytoplankton settling rate and phytoplankton biomass; labile, refractory, and inert particulate organic carbon concentrations; refractory and labile dissolved organic concentrations; average light intensity; settling rate for particulate organic carbon; and hydrogen sulfide concentrations. For the sediment, the output file includes as time histories in two dimensions the calculated (i.e., one hour average) diffusive and particle mixing rates; resuspension and burial rates for the active sediment bed; erosion rates from the sediment bed archival stack to the active sediment bed; rates of change of the depth of the active sediment bed; concentrations of labile, refractory and inert (also referred to as G1, G2, and G3 carbon) in the active sediment bed; depths and rates of change in depth of the archival stack sediment bed; and concentrations of labile, refractory and inert carbon in the archival stack sediment bed. This output file is read by the CARP contaminant fate and transport sub-models for both hydrophobic organic chemicals (HOCs) and metals.

3.2.2 Sediment Bed Correspondence Between CARP sub-models

The CARP hydrodynamic sub-model does not consider a sediment bed explicitly, but considers the interaction of the water column and the bed through the assignment of bottom roughness coefficients. The CARP sediment transport/organic carbon production sub-model includes a sediment bed that is represented by a 9.9 to 10.1 cm active layer and a deeper archive layer. For purposes of the CARP sediment transport/organic carbon production model, the 9.9 to 10.1 cm active sediment bed layer may be further sub-divided at two different operational levels: redox chemistry and erodibility. From the redox chemistry perspective, the aerobic and anaerobic regions of the 9.9 to 10.1 cm active layer are allowed to vary as depth of oxygen penetration changes, but the depths of the aerobic and anaerobic regions must always sum in the 9.9 to 10.1 cm range. From the erodibility perspective, the uppermost 0 to 0.2 cm of the 9.9 to 10.1 cm active layer are easier to resuspend than deeper portions of the active layer and the archive layer. These features of the CARP sediment transport/organic carbon production sub-model bed structure have been described previously (HydroQual, 2007b). For purposes of the CARP contaminant fate and transport sub-model, the 9.9. to 10.1 cm active sediment bed layer from the sediment transport/organic carbon production sub-model is broken out into ten 1 cm chemical layers. The archive layer used in the CARP sediment transport/organic carbon production

sub-model is retained in the CARP contaminant fate and transport sub-model to track contaminant levels in more deeply buried sediment.

3.2.3 Additional Sediment Transport/Organic Carbon Production Information Passed to the Metals Fate and Transport Sub-Model

In addition to the information passed from the sediment transport/organic carbon production sub-model to the contaminant fate and transport sub-models for HOCs and metals via the output file described above, supplemental sediment bed outputs, including sediment bed concentrations of dissolved and particulate hydrogen sulfide and sulfate reduction rates (as carbon decay rates), are passed as two-dimensional time histories specifically to the metals fate and transport sub-model.

3.3 DEVELOPMENT OF CONTAMINANT LOADINGS AND OTHER MODEL INPUTS

This report section will describe forcing data input directly to the contaminant fate and transport model.

3.3.1 Contaminant Loadings

HydroQual developed protocols for assigning contaminant loadings estimates for purposes of driving the CARP contaminant fate and transport model calculations. The protocols developed have been applied to all CARP contaminant groups: PCB homologs, dioxin/furan congeners, the metals mercury and cadmium, PAH compounds, and organochlorine pesticides related to chlordane and DDT. The development of the loading estimates is summarized below.

It is noted that contaminant loadings estimates were developed for methyl mercury based on a very few methyl mercury measurements which were mostly dissolved measurements. To a certain extent, this represents a very minor "double-counting" of loading as the methyl mercury measurements are reflected in the total particulate and total dissolved mercury loading estimates. However, the mercury methylation kinetics are so fast that any external inputs into the system of methyl mercury are likely masked by the in-situ net methylation/demethylation processes and external inputs of methyl mercury are insignificant in magnitude as compared to inputs of total mercury.

3.3.1.1 Flow Component of Contaminant Loadings

Loadings (i.e., mass per time) of contaminants and other substances may be expressed as the product of a flow component (i.e., volume per time) and a concentration component (i.e., mass per volume). For contaminant loadings, the flow component was determined and described previously as part of the development of the hydrodynamic model (HydroQual, 2007a). As described in HydroQual 2004, the flow component is based on both direct measurements and landside modeling of flows coming from tributary headwater, STP, CSO, and landside runoff sources. Conditions for which flow component loadings have been developed include the six water years 1988-89, 1994-95, and 1998-2002. These water years cover the period of the CARP monitoring program (i.e., 1998-2002) and include a variety of conditions. For example, Hurricane Floyd occurred in the fall of 1999 and the there was virtually no rainfall in August of 1995.

3.3.1.2 Concentration Component of Contaminant Loadings

Estimates of the concentration component of contaminant loadings on a mass per volume basis have been developed for use in the CARP contaminant fate and transport model for a variety of different contaminant sources including: tributary headwater, STP, CSO, overland runoff, atmospheric deposition, and landfill leachate. Protocols for specifying loadings for each contaminant source type are described below.

3.3.1.2.1 Tributary Headwater Contaminant Loading Concentrations

Contaminant concentrations were measured at the heads of tide for five New York and five New Jersey tributaries as part of the CARP sampling program. The measured tributaries in New York include: the Bronx, Hudson, Mohawk, Sawmill, and the Wallkill Rivers. The measured tributaries in New Jersey include: the Hackensack, Passaic, Raritan, Rahway, and Elizabeth Rivers. Quality assurance of the tributary data is briefly addressed below and is followed by a more complete description of our analysis of the contaminant data and our evaluation of daily contaminant loads.

Quality Assurance

The contaminant data were subject to quality assurance checks by NYSDEC and NJDEP prior to our use and subsequently by a formal CARP QA/QC review. Additional checking of the data (e.g.,

identifying possible outliers and other inconsistencies in data sets) was performed throughout our evaluations.

For PCB homologue evaluations, the effect of non-detectable congener measurements on loading estimates was also considered by cross-plotting PCB homologue concentrations with non-detectable congener concentrations set equal to their detection limit versus PCB homologue concentrations with non-detectable concentrations set equal to zero (Figure 3-1). The only significant differences in the assignment for non-detectable congeners were for samples with low concentrations. Since these samples are not expected to have a significant effect on our loading estimates, non-detectable congener concentrations were not considered a major concern and values of the non-detectable congeners were set equal to 0 in our analysis of tributary loadings.

It is noted, for the case of PAHs, that the CARP QA/QC review process resulted in a recommendation for virtually all PAH measurements of "use with caution". In many instances, only a particle phase measurement is available. Calculation of tributary loadings for PAHs using CARP concentration measurements at tributary heads of tide was therefore difficult. Measurements of PAHs in water samples are often problematic because of tradeoffs involved with sampling methods. Large volume sampling devices such as TOPS which were appropriate for sampling PCBs and dioxin/furans are not appropriate for PAHs because XAD resin columns used in the TOPS device give high background levels of some PAH compounds, causing an overestimate of the dissolved fraction. This was avoided to some extent in the New York CARP data set by taking the dissolved measurements from the effluents of the TOPS glass fiber cartridge filters rather than from the XAD resins (Litten, 2003). On the other hand, using whole water samples (as was done for the New Jersey CARP data set) is not a perfect solution either in that small sample size can give rise to small analyte masses such that even low levels of contamination could significantly impact the overall measured PAH levels. Naphthalene (and associated methylated compounds), fluorene, acenaphthene, phenathrene, ideno(1,2,3-cd)pyrene, and benz(g,h,i) perylene are most impacted (Joel Pecchioli, NJDEP, personal communication).

Contaminant Concentration Distributions

Total contaminant concentrations for each of the measured tributaries were plotted as log probability distributions. As an example, measurements for tetra-CB for the Wallkill River are shown in Figure 3-2, panel 1 (where the data are ordered from "1" for the lowest flow to "13" for the highest flow). As shown, the median concentration for tetra-CB in the Wallkill is 0.2 ng/L with a large variation

of one and a half orders of magnitude (i.e., approximately a factor of thirty) from the lowest to the highest concentration.

In an attempt to explain this variability in measured concentrations, the data were also plotted in several other formats including dissolved concentrations (panel 2), DOC-normalized dissolved concentrations (panel 3), particulate concentrations (panel 4), suspended sediment-normalized particulate concentrations (panel 6), and POC-normalized particulate concentrations (panel 5). Plots of the dissolved concentrations (panel 2) and the POC-normalized particulate concentrations (panel 5) show that a large portion of the variability in the data can be explained by separating the dissolved and particulate concentrations and normalizing the particulate concentrations by the measured POC values. This finding is consistent with two expectations: (1) that POC serves as the dominant sorbent phase, particularly for hydrophobic organic contaminants like PCBs and dioxins, and (2) that the binding of contaminant by DOC is likely to be important only for highly hydrophobic contaminants (e.g., with log Kow's > 6.5 or 7). Figures 3-3a an 3-3b depict the reductions in variability, as represented by standard deviation when dissolved and particulate concentrations are separated and particulate concentrations are POC normalized. This approach which works well in reducing variability for PCBs, dioxins, furans, and to a lesser extent, metals, was followed for all contaminant groups including PAH compounds and organochlorine pesticides related to DDT and chlordane.

A summary of final median dissolved and POC-normalized particulate concentrations for the 10 PCB homologs, 17 dioxin/furan congeners, cadmium and mercury, PAH compounds and organochlorine pesticides is given in the tables found in Appendix 1A for all the measured tributaries. Since only four samples were collected for most of the measured tributaries, median concentrations were calculated by taking the average of the log transformed concentrations and converting the results back to arithmetic values.

It is noted that there are minor discrepancies between some of the figures and tables presented in this section of the report and the final median contaminant concentrations presented in the tables of Appendix 1A. These discrepancies relate to the fact that all of the contaminant loading concentration data were not available to HydroQual at the time the loadings generation protocols were developed. Final loadings used in model calibration, which incorporate all of the contaminant concentration data are tabulated in Appendix 1A.

Interim (i.e., non-final but substantially representative) median concentration values are also shown graphically on Figures 3-4 and 3-5. For purposes of this display, PCB homologs were summed

as were dioxin and furan congeners. Interim median particulate concentrations are shown on Figure 3-4 and interim median dissolved on Figure 3-5. A notable feature on Figures 3-4 and 3-5 are the relatively high Hudson River PCB concentrations consistent with the known source on the Upper Hudson. Another feature is deceptively high Bronx River particulate contaminant concentrations due to low POC measurements. There is a somewhat consistent pattern across contaminants in terms of "clean" and "contaminated" tributaries. This consistency is more apparent for particulate concentrations. In terms of dissolved, there are some apparently high concentrations of dissolved dioxin and furan congener sums, particularly for the Hudson River, which do not agree with other dissolved contaminant measurements or with particulate measurements. These elevated dissolved dioxin and furan congener sums are not attributable to elevated concentrations of dissolved organic carbon. Although seemingly high, the elevated dissolved dioxin and furan congener sum concentration are a small fraction of the total loading when compared to particulate concentrations and should not compromise our ability to specify reliable loadings.

Tributary Contaminant Loads

Based on our analysis of measured contaminant concentrations, tributary loads of contaminant were developed on a daily basis using median dissolved and POC-normalized concentrations. For New York and New Jersey tributaries that were not sampled, default median carbon normalized particulate contaminant and dissolved contaminant concentrations were assigned based on the most often "cleanest" monitored tributaries in the respective states (i.e., the Wallkill River in New York and the Hackensack River in New Jersey). The New York values were also applied to the Connecticut tributaries. Although some of the Connecticut tributaries are expected to be more contaminated than the "cleanest" New York monitored tributary, this inherent underestimation of loads from the Connecticut tributaries is not likely to significantly impact contaminant concentrations in the core Harbor areas, but may result in an underprediction of contaminant concentrations in Long Island Sound. The default values for all contaminant groups are given in several tables presented in Appendix 1A. These values represent a likely lower limit on the contaminant concentration contributed by an unmeasured tributary. The footnote in each table lists the unmeasured tributaries. As noted on the tables in Appendix 1A, default values were also applied to measured tributaries in cases where data were missing (e.g., dissolved dioxin and furan congeners in New Jersey tributaries).

Two protocols were established for developing daily contaminant loads from median dissolved and POC-normalized particulate concentrations. These methods are based on the availability of POC data for the tributary and are described below.

1. For tributaries with sufficient POC data, USGS gaging flow data and POC loading estimates were used to evaluate daily contaminant loads as follows:

$$Load = Flow \times Dissolved\ Conc. + POC\ Load \times POC\ Normalized\ Part.\ Conc.$$

In this approach, POC loading estimates were determined using the Normalized POC Loading Function (NPL). NPL is analogous to the Normalized Sediment Load Function (NSL), as described by HydroQual previously as part of its report on the development of suspended sediment loads. Site-specific applications of NPL were developed based on the available USGS historical records of POC and flow for the following tributary rivers: Hudson, Mohawk, Passaic, Raritan, Elizabeth, Rahway, Saddle, Wallkill, Rondout, Connecticut, Toms, and Great Egg. For the Mohawk, Connecticut, Passaic, Raritan, and Rahway Rivers, available data supported development of relationships for both non-flood (i.e., flow rate less than or equal to twice the mean flow rate) and flood condition for each river. For the Hudson, Wallkill, Elizabeth, Saddle, Toms, and Great Egg rivers, available data supported a single relationship applied under both non-flood and flood conditions. Calculated and observed relationships between normalized POC loadings and normalized flow for each of these eleven rivers are shown in Appendix 2.

2. For the remainder of the tributaries where sufficient POC data were not available, a slight revision was made to the above method for calculating loads. For these tributaries, POC loading estimates were determined from NSL-generated sediment loads multiplied by an estimate for the fraction organic carbon (foc) on suspended sediment. The foc values used in this evaluation were determined from generic relationships between POC and suspended sediment that were developed using USGS data compiled for 13 rivers within the CARP model domain (see Figure 3-6). Much of the data came from the Mohawk River, particularly for suspended sediment values greater than 200 mg/L. The relationships between particulate organic carbon and suspended sediment shown on Figure 3-6 are exponential (i.e., log linear) with foc, the ratio between particulate organic carbon and suspended sediment, decreasing as suspended sediment increases. foc values range between 20% and 3% when suspended sediment concentrations are less than 40 mg/L and between 3% and 1% when suspended sediment concentrations are greater than 40 mg/L. The final equation for evaluating contaminant loads from these tributaries is expressed in terms of USGS gaging flow data, NSL-estimated sediment loads, and fraction organic carbon estimates as follows:

$$Load = Flow \times Dissolved\ Conc. + f_{oc} \times SS\ Load \times POC\ Normalized\ Part.\ Conc.$$

Results for daily flows, POC loads, and contaminant loads for tetra-CB from the Wallkill River are shown in Figure 3-7 for the 1999-2000 water year. As expected, contaminant loads are highly dependent on flow, and more specifically on the POC load, with most of the contaminant load associated with particle-bound contaminant during high flow periods. For less hydrophobic contaminants (e.g., di-CB, tri-CB), contaminant loads which are associated with dissolved contaminant loads throughout the year may also be significant.

Finally, a comparison of daily loadings developed based on median dissolved and median carbon normalized particulate contaminant concentrations, calculated by the protocols described above, and loadings developed based on directly measured concentrations for tetra-CB in ten tributaries is given in Figure 3-8. As shown, the calculated values provide a good estimate of the measured values, particularly during high loading periods. The methods outlined in this section are therefore considered to provide reasonable approaches for evaluating contaminant loads from tributaries with limited contaminant measurements.

Other Considerations for Tributary Load Estimates

The load generation protocol outlined above was not followed for PCB homolog loadings from the Upper Hudson River over the Federal Dam at Troy. For the Upper Hudson, PCB concentrations at Thompson Island Dam (RM 189) have been measured continuously by the General Electric (GE) Corporation since April 1991. This data set represents a more complete description for the downstream migration of PCBs from the General Electric plant site at Hudson Falls and the contaminated sediments in Thompson Island Pool. A comparison of the concentrations of tri-CB over Thompson Island Dam for 1999 - 2000 (from the GE data set) and for the seven CARP measurements taken further downstream near Waterford (RM 160) is shown in Figure 3-9. As shown, there is good agreement in load estimates from the GE data at Thompson Island Dam and the CARP data near Waterford for the spring 1999 samples. During the late spring and summer (2000 and 2001 samples), the GE data show a large increase in loads, particularly for the lower chlorinated homologs. This trend has been attributed to enhanced release of PCBs from sediments in Thompson Island Pool by bioturbation during the late spring/summer productivity period. A similar increase is not observed in the CARP measurement from August 2000 and 2001. Therefore, it is not entirely clear whether PCB loads from the continuous GE record at Thompson Island Dam or from the limited CARP sampling near Waterford provide a more

representative estimate of PCB loads entering the Lower Hudson River. The GE data were used for model simulations based on the greater number of measurements available.

3.3.1.2.2 STP Contaminant Loading Concentrations

Measured STPs

Effluents of the major STPs within the CARP model domain were sampled for contaminant concentrations as part of CARP. Sampling frequencies at the individual plants range between two and eight times with most being sampled three to four times. For each STP sampled, final median contaminant concentrations were identified and are tabulated in various tables found in Appendix 1B. These concentrations were paired with time varying flow records (i.e., from monthly Discharge Monitoring Reports (DMRs) or more detailed NYCDEP records) at each STP to produce loadings for use in the model. A decision was made not to vary STP effluent contaminant concentrations for purposes of model input due to the temporally sparse (i.e, 3 to 4 or fewer points in most cases) data collected for each STP. Representative interim (i.e., before all CARP measurements were fully available) median contaminant concentrations are shown in a summary format on Figure 3-10. A more complete description of HydroQual's analysis of the STP effluent contaminant data and loadings generation procedure for unmeasured plants follows.

Unmeasured STPs

For purposes of assigning effluent contaminant concentrations to unmeasured plants, the STP effluent data for each state were screened to eliminate facilities with elevated effluent concentrations potentially attributable to industrial dischargers in their headworks. From each state, median concentrations were determined for each contaminant based on measured effluents for all plants which were not eliminated in the screening process . These median values which are assigned to unmeasured plants are tabulated in various tables found in Appendix 1B. The footnote in each table identifies the unmeasured STPs. The screening procedure is illustrated on Figures 3-11 and 3-12 for cadmium. Figure 3-11 shows a probability distribution of cadmium in STP effluents. Figure 3-12 shows the same data, however the high values (i.e., indicative of potential drainage area specific industrial influences) have been eliminated. In this case, data from STP 6, Newtown Creek, have been eliminated. A median value calculated based on the distribution shown in Figure 3-12 rather than Figure 3-11 was used for assigning effluent concentrations.

3.3.1.2.3 CSO Contaminant Loading Concentrations

CSO contaminant concentration data collected under CARP by both states were considered for specifying contaminant model loadings. For dioxin/furan congeners, PAH compounds, organochlorine pesticides, and metals, data from both states were pooled to calculate natural logarithmic mean concentrations. For the case of PCB homologs, there were notable differences between New York and New Jersey measurements with the New York measurements being biased high. It is noted that normalizing CSO PCB homolog concentrations by organic carbon did not help to explain or account for the observed concentration differences between New York and New Jersey measurements. Therefore, datasets for New York and New Jersey were handled separately in assigning appropriate CSO concentrations. CSO concentration loadings for PCB homologs in the CARP model were assigned in the following manner:

- New Jersey PCB homolog measurements were used to calculate a natural logarithmic mean concentration for each homolog which was assigned to all CSO's in New Jersey.

- Within New York, PCB homologs measured within the 26th Ward and Red Hook sewer districts were particularly high. New York PCB homolog measurements, omitting those collected in the 26th Ward and Red Hook sewer districts, were used to calculate a natural logarithmic mean concentration for each homolog which was assigned to all CSO's in New York and Connecticut.

- PCB homolog measurements collected within the 26th Ward and Red Hook sewer districts were assigned to New York CSO's within those sewer districts.

The representative contaminant concentrations for CSOs as described above were combined with flows varying on an hourly basis to develop hourly loading estimates for more than 700 CSO outfall locations that were aggregated to the level of CARP model grid cell resolution (304 locations in the model with stormwater). The hourly flows, also used to drive the hydrodynamic model and described in the CARP report on hydrodynamic modeling, were generated for each water year using detailed landside loading models developed previously by HydroQual. CSO contaminant concentrations are tabulated in Appendix 1C.

3.3.1.2.4 Runoff Contaminant Loading Concentrations

Representative stormwater runoff concentrations assigned to contaminants in the model are based mostly on concentration estimates collected by New Jersey CARP investigators but also include two samples collected by New York CARP investigators in industrial and commercial portions of the Jamaica Bay drainage area. New Jersey CARP investigators collected stormwater contaminant measurements at five locations. In addition New York CARP investigators conducted a supplemental data collection program targeted at obtaining measurements of dioxin and furan congeners in more rural drainage areas than were sampled previously by either New Jersey or New York CARP investigators (Litten, 2005).

For PCB homologs, PAH compounds, organochlorine pesticides, and metals, natural logarithmic concentration means were calculated and assigned to all stormwater outfall locations. For dioxin/furan congeners, natural logarithmic concentration means were calculated separately for urban and rural areas. These representative concentration estimates were paired with hourly flows generated from detailed landside models for each water year. For load estimates, more than 1000 stormwater outfalls to the estuary were aggregated to the level of CARP model grid cell resolution (304 locations in the model with CSOs). Stormwater contaminant concentrations are tabulated in Appendix 1D.

Overall, the limited stormwater contaminant concentration samples available suggest a high degree of variability across the seven (note: for dioxin and furan congeners additional rural locations were sampled) sampling locations for each contaminant; however, there is not sufficient information available to incorporate this variability into the specified loadings. Organic carbon normalization of the data did not help to reduce variability. Some of the data were flagged by NJDEP as not useable; however, the flagged data were not outliers and fell within the range of the useable data.

3.3.1.2.5 Atmospheric Deposition Loadings

Atmospheric deposition loadings were calculated based on data provided by the New Jersey Atmospheric Deposition Network (NJADN). The NJADN data were collected by researchers from Rutgers and Princeton Universities with support from the Hudson River Foundation, New Jersey Sea Grant, and New Jersey Department of Environmental Protection. Up to 4 NJADN stations were identified for application to model input:

- Liberty State Park - Applied to Harbor core (i.e., Hudson River below Haverstraw Bay, Upper Bay, Newark Bay, Arthur Kill and Kill van Kull, East River, Harlem River, Jamaica Bay).

- Sandy Hook - Applied to open water areas (i.e, Lower Bay and New York Bight, Raritan Bay, Long Island Sound).

- New Brunswick - Applied to urban tributary areas (i.e., Hackensack, Passaic, and Raritan Rivers). Applied to northern less urbanized areas (i.e., Hudson River above Haverstraw Bay) when the NJADN station at Chester was not available.

- Chester - When available, applied to northern less urbanized areas (i.e., Hudson River above Haverstraw Bay).

For the case of PCB homologs, atmospheric deposition fluxes at each of the four stations including gas, particle, and precipitation were available from NJADN. These values were applied directly to the model on an annual basis. For the case of mercury and cadmium, annual estimates for particle and precipitation fluxes were available from NJADN on a Harbor wide basis. These fluxes, 0.080 mg m^{-2} yr^{-1} for cadmium and 0.0067 mg m^{-2} yr^{-1} for mercury, were applied to the entire model domain. For dioxin/furan congeners, NJADN did not calculate fluxes, but provided gas and particle concentration measurements for the Liberty State Park, Sandy Hook, and New Brunswick stations. HydroQual followed NJADN protocols (Totten et al., in press) to develop the concentration measurements into fluxes. New Brunswick data were applied to both urban and northern less urbanized tributary areas since Chester data were not available for dioxin/furan congeners.

For particle deposition fluxes, dioxin/furan congeners flux calculations for the particle phase were performed using particle concentration estimates available from NJADN and assuming a particle deposition velocity of 0.5 cm/sec, consistent with NJADN's development of PCB fluxes. For gaseous fluxes, dioxin/furan congeners flux calculations were performed using gas phase concentration estimates from NJADN and an estimate for the air-water exchange rate coefficient. In this analysis, the air-water exchange rate coefficient was determined as a function of wind speed (1 m/sec), temperature (15 ^{o}C), and Henry's Law constants for each congener following the approach of Totten et al., in press.

To account for the temperature dependence of the air-water exchange rate coefficient, Henry's law constants were adjusted for ambient temperature using congener specific log-linear regression relationships as developed by the EMEP Meteorological Synthesizing Centre-East (MSCE) that account

for temperature dependency. The regression equations are tabulated in Table 3-1. Using these regression equations, Henry's law constants for each congener were computed for 15°C, approximately the annual average temperature. As a check, Henry's law constants were also calculated using EPA's structure based program, SPARC (Hilal, et al.,1994), at 25°C and compared to those estimated from the MSCE regression equations at 25°C. The relevant constants generated from SPARC are tabulated in Table 3-2. The comparison, presented in Figure 3-13, shows good agreement with SPARC generated values as well as a range of Henry's constants found in the literature.

Table 3-1

EMEP Temperature Dependency Equations for PCDD/F Henry's Law Constants

Congener	Temperature Dependence of Henry Law Constant Log(K_H, Pa m^3/mol)
2,3,7,8-TCDD	-4388/T + 15.02
1,2,3,7,8-PeCDD	-4522/T + 15.32
1,2,3,4,7,8-HxCDD	-4978/T + 16.08
1,2,3,6,7,8-HxCDD	-4936/T + 15.92
1,2,3,7,8,9-HxCDD	-5090/T + 16.60
1,2,3,4,6,7,8-HpCDD	-5621/T + 17.95
1,2,3,4,6,7,8,9-OCDD	-4004/T +13.27
2,3,7,8-TCDF	-3908/T + 13.24
1,2,3,7,8-PeCDF	-4392/T + 14.11
2,3,4,7,8-PeCDF	-4468/T + 14.69
1,2,3,4,7,8-HxCDF	-4832/T + 16.35
1,2,3,6,7,8-HxCDF	-4816/T + 15.91
1,2,3,7,8,9-HxCDF	-4816/T + 16.00
2,3,4,6,7,8-HxCDF	-4801/T + 15.93
1,2,3,4,6,7,8-HpCDF	-5211/T + 16.42
1,2,3,4,7,8,9-HpCDF	-5241/T + 16.62
1,2,3,4,6,7,8,9-OCDF	-4537/T + 14.59

Table 3-2
Henry's Law Constants for Dioxin/Furan Congeners Calculated Using SPARC

CONGENER	HENRY'S LAW CONSTANT (25°C, 760 Torr) (atm-m^3/mol)	(Pa-m^3/mol)
2,3,7,8 - TCDD	1.01 E-05	1.026
1,2,3,7,8 - PeCDD	8.20 E-06	0.831
1,2,3,7,8,9 - HxCDD	6.00 E-06	0.608
1,2,3,4,7,8 - HxCDD	6.20 E-06	0.628
1,2,3,6,7,8 - HxCDD	6.64 E-06	0.673
1,2,3,4,6,7,8 - HpCDD	4.81 E-06	0.488
OCDD	3.94 E-06	0.399
2,3,7,8 - TCDF	1.86 E-05	1.881
1,2,3,7,8 - PeCDF	1.38 E-05	1.400
2,3,4,7,8 - PeCDF	1.37 E-05	1.385
1,2,3,4,7,8 - HxCDF	9.90 E-06	1.003
1,2,3,6,7,8 - HxCDF	9.67 E-06	0.979
1,2,3,7,8,9 - HxCDF	9.77 E-06	0.990
2,3,4,6,7,8 - HxCDF	1.01 E-05	1.019
1,2,3,4,6,7,8 - HpCDF	7.27 E-06	0.737
1,2,3,4,7,8,9 - HpCDF	7.35 E-06	0.745
OCDF	5.25 E-06	0.532

NJADN did not measure dioxin/furan congeners in precipitation. Dioxin/furan congener concentrations were therefore estimated using two approaches as outlined below:

- Dioxin/furan congener concentrations in stormwater were used for our initial estimates of concentrations in precipitation. To test the validity of this approach, an independent check was performed by HydroQual which compared PCB loading concentration estimates for both precipitation and stormwater runoff. Figure 3-14 demonstrates that PCBs in precipitation collected by NJADN tend to be an order of magnitude lower than PCBs measured in stormwater collected by New Jersey CARP investigators.

- Dioxin/furan congener concentrations in precipitation were estimated from measured particulate and gaseous concentrations using the approach outlined in Eitzer and Hites (1989). In this approach, the congener concentrations in precipitation are determined from:

$$C_{rain} = W_g C_g + W_p C_p$$

where W_g = washout ratio due to gas scavenging (unitless); W_p = washout ratio due to particle scavenging (unitless); C_g = gas phase contaminant concentration (fg/m^3); C_p = volumetric particulate concentration of contaminant (fg/m^3). Table 3-3 summarizes the gas and particle washout ratio computed by Eitzer and Hites for their study area.

Table 3-3
Washout Ratios Computed by Eitzer and Hites

	Washout ratio	
PCDD/F	**W_g**	**W_p**
Tetra-CDD	170,000	18,000
Penta-CDD	6,300	9,300
Hexa-CDD	5,600	10,000
Hepta-CDD	270,000	62,000
Octa-CDD	2,700,000	90,000
Tetra-CDF	16,000	19,000
Penta-CDF	9,300	12,000
Hexa-CDF	8,600	9,800
Hepta-CDF	58,000	32,000
Octa-CDF	210,000	21,000

Figure 3-15 is a comparison of the estimated precipitation concentrations at NJADN stations with CARP New Jersey stormwater concentrations. Like PCBs, the precipitation concentrations tend to be an order of magnitude lower than the stormwater concentrations. On this basis, it was determined that stormwater is not a suitable surrogate for precipitation and that estimates from NJADN particulate and gaseous concentrations using the approach of Eitzer and Hites (1989) are likely to be more representative.

The resultant dioxin/furan fluxes for particle, gas, and precipitation for a one meter rainfall condition (i.e., 1998-99) are shown in Table 3-4. Fluxes vary slightly for other years based on rainfall.

Table 3-4

Dioxin/Furan Atmospheric Deposition Fluxes (ng/square meter/day)

New Brunswick	wet	dry	gas	total
2,3,7,8-TCDD	0.09	0.07	0.08	0.25
1,2,3,7,8-PeCDD	0.04	0.27	0.19	0.50
1,2,3,7,8,9-HxCDD	0.02	0.30	0.00	0.32
1,2,3,4,7,8-HxCDD	0.05	0.66	0.09	0.80
1,2,3,6,7,8-HxCDD	0.04	0.48	0.09	0.62
1,2,3,4,6,7,8-HpCDD	2.67	5.52	0.35	8.53
OCDD	42.14	23.99	1.82	67.95
2,3,7,8, TCDF	0.74	0.87	4.30	5.91
1,2,3,7,8 PeCDF	0.19	0.94	1.43	2.57
2,3,4,7,8 PeCDF	0.19	1.20	0.84	2.23
1,2,3,4,7,8 HxCDF	0.11	1.50	0.26	1.87
1,2,3,6,7,8 HxCDF	0.09	1.20	0.19	1.47
1,2,3,7,8,9 HxCDF	0.02	0.26	0.04	0.32
2,3,4,6,7,8 HxCDF	0.09	1.32	0.13	1.54
1,2,3,4,6,7,8 HpCDF	1.11	5.34	0.26	6.71
1,2,3,4,7,8,9 HpCDF	0.20	0.99	0.02	1.22
OCDF	0.56	3.97	0.19	4.72

Sandy Hook	wet	dry	gas	total
2,3,7,8-TCDD	0.092	0.00	0.09	0.18
1,2,3,7,8-PeCDD	0.028	0.13	0.35	0.50
1,2,3,7,8,9-HxCDD	0.056	0.37	0.80	1.22
1,2,3,4,7,8-HxCDD	0.078	0.55	1.03	1.66
1,2,3,6,7,8-HxCDD	0.071	0.66	0.59	1.32
1,2,3,4,6,7,8-HpCDD	4.650	10.23	0.48	15.36
OCDD	60.379	51.18	2.16	113.72
2,3,7,8, TCDF	0.244	0.32	1.31	1.87
1,2,3,7,8 PeCDF	0.071	0.29	0.64	1.00
2,3,4,7,8 PeCDF	0.064	0.36	0.39	0.81
1,2,3,4,7,8 HxCDF	0.051	0.52	0.32	0.89
1,2,3,6,7,8 HxCDF	0.038	0.40	0.23	0.66
1,2,3,7,8,9 HxCDF	0.019	0.26	0.04	0.32
2,3,4,6,7,8 HxCDF	0.041	0.52	0.14	0.71
1,2,3,4,6,7,8 HpCDF	0.425	1.75	0.25	2.43
1,2,3,4,7,8,9 HpCDF	0.066	0.32	0.01	0.40
OCDF	0.510	3.23	0.20	3.94

Table 3-4
Dioxin/Furan Atmospheric Deposition Fluxes (ng/square meter/day)

Liberty Science Center	wet	dry	gas	total
2,3,7,8-TCDD	0.10	0.07	0.08	0.25
1,2,3,7,8-PeCDD	0.03	0.21	0.13	0.37
1,2,3,7,8,9-HxCDD	0.03	0.34	0.01	0.37
1,2,3,4,7,8-HxCDD	0.06	0.71	0.06	0.83
1,2,3,6,7,8-HxCDD	0.05	0.61	0.01	0.67
1,2,3,4,6,7,8-HpCDD	3.80	9.13	0.22	13.15
OCDD	50.35	35.27	2.00	87.62
2,3,7,8, TCDF	0.15	0.21	0.75	1.11
1,2,3,7,8 PeCDF	0.07	0.36	0.56	0.99
2,3,4,7,8 PeCDF	0.06	0.37	0.27	0.70
1,2,3,4,7,8 HxCDF	0.06	0.78	0.20	1.04
1,2,3,6,7,8 HxCDF	0.04	0.56	0.16	0.77
1,2,3,7,8,9 HxCDF	0.01	0.08	0.00	0.09
2,3,4,6,7,8 HxCDF	0.05	0.69	0.07	0.81
1,2,3,4,6,7,8 HpCDF	0.74	3.62	0.15	4.51
1,2,3,4,7,8,9 HpCDF	0.09	0.44	0.03	0.57
OCDF	0.54	3.96	0.18	4.67

Atmospheric deposition loadings were also developed for the organochlorine pesticide and PAH contaminant groups. The organochlorine pesticides include cis- and trans- chlordane; cis- and trans-nonachlor; oxy- chlordane; and 4,4' and 2,4' DDT, DDE, and DDD. For the case of organochlorine pesticides, atmospheric deposition fluxes at each of the three stations (i.e., Liberty State Park, Sandy Hook, and New Brunswick) including gas, particle, and precipitation were available from NJADN (Gioia, unpublished data). These values were applied directly to the model on an annual basis.

Similarly, for PAHs, atmospheric deposition fluxes at each of four stations (i.e., Liberty State Park, Sandy Hook, New Brunswick, and Chester) including gas, particle, and precipitation were available from NJADN. These fluxes were applied directly to the model on an annual basis. Atmospheric deposition fluxes were available specifically for 1-methylphenanthrene, anthracene, benz[a]anthracene, benzo[a]pyrene, benzo[b,j,k]fluoranthenes, benzo[e]pyrene, benzo[g,h,i]perylene, chrysene, dibenz[a,h]anthracene, fluoranthene, fluorene, ideno[1,2,3,cd]pyrene, perylene, phenanthrene, and pyrene.

3.3.1.2.6 Landfill Contaminant Loadings Concentrations

Landfill leachate loadings were developed based on volumetric information provided by NYSDEC (Litten, 2003) as well as CARP contaminant concentration measurements. For six landfills in New York (i.e., Pelham, Pennsylvania Ave, Fountain Ave, Edgemere, Fresh Kills, and Brookfield) which comprise 2000 acres, an estimated leachate flow volume of 2.6 MGD for a 1.1 meter rainfall year was available. This flow volume estimate was apportioned across landfills based on acreage and was also scaled either up or down based on annual rainfall for the six water years being modeled. The largest landfill, Fresh Kills, which comprises 1200 of the 2000 acres considered would contribute 1.56 MGD of the 2.6MGD in a 1.1 meter rainfall year. Fresh Kills has a leachate treatment system which captures and treats much of the leachate from Fresh Kills. Expected volumes for the Fresh Kills treatment system were up to 1 MGD, but actual operation has been on order of 0.5 MGD. Leachate from the Pelham landfill was not included as a loading in the model since Pelham landfill leachate is diverted to the Hunts Point STP and is therefore already included in the model as Hunts Point effluent. Leachate contaminant concentration measurements collected as part of New York's CARP effort include measurements characteristic of both landfill treatment plant effluent and untreated leachate coming off of mounds. Contaminant concentrations in the leachate coming off of mounds represent upper limits on the contaminant concentrations actually reaching the estuary. An arithmetic average of the natural (ln) logs of the contaminant concentrations coming off of the various mounds was calculated for each contaminant and assigned to leachate volumes not undergoing treatment. For treated leachate volumes, contaminant concentrations were assigned based on arithmetic averages of the natural (ln) logs of the landfill treatment plant effluent data. It is noted that New York's CARP effort for landfills included contaminant concentration measurements for leachate collected from Hackensack Meadowlands Development Commission landfills. These data were not used because location information and volumetric estimates for leachate coming from the Hackensack Meadowlands Development Commission landfills were not available. These data may be incorporated into the model at a later date as location and volumetric information become available. It is noted that a portion of the leachate coming from the Hackensack Meadowlands Development Commission landfills is treated at the Passaic Valley STP (Litten, 2003) and is already included in the CARP model.

3.3.1.2.7 Open Ocean Boundary Loading Concentrations

The ocean boundaries of the CARP model were selected to be sufficiently far enough away from the Harbor core area so as not to be strongly influenced by internal contaminant loadings. Accordingly concentrations at the open ocean boundary for contaminants are likely to be small relative to other

contaminant sources. The CARP monitoring program included limited (i.e., 3 stations) contaminant sampling in the New York Bight, but this sampling did not go as far out into the ocean as the CARP model boundaries. Without data from CARP, open ocean boundary contaminant concentrations assigned in the CARP model were either inferred from preliminary calibration results or based on literature values. In the case of the PCB homologs and dioxin/furan congeners, concentrations at the open ocean boundary were considered negligible and were specified as 0.

3.3.2 Contaminant Loading Initial Dilution Simulations

Once interim (i.e., initial dilution simulations were performed when a majority, but not all, of the CARP loading concentration had become available to HydroQual) contaminant loadings and open boundary conditions were established for current conditions, initial dilution simulations were performed with the CARP model. Initial dilution simulations consist of running the present day loadings of contaminants to the system as conservative (i.e., subject to hydrodynamic transport only, no phase partitioning or other kinetic processes) tracers. Care was taken to run the initial dilution simulations sufficiently long enough (i.e., based on CARP model experience one year of "spin-up" prior to a year for consideration was sufficient in Harbor core areas. Outlying areas such as the Sound and the Bight might require more time) to reach an equilibrium condition. There were several purposes for performing initial dilution simulations with the CARP current conditions contaminant loadings.

When compared to ambient water column data, initial dilution simulation results serve as a cursory initial check on the agreement or consistency between the assigned loadings (which are based on the loading measurements) and the measured ambient concentrations in the water column. In the case of comparing CARP initial dilution simulation results to measured ambient concentrations in the water column, model and data comparisons suggest that CARP loading estimates are reasonable (i.e., we did not see several orders of magnitude differences between calculated and observed values. Comparing CARP initial dilution simulation contaminant concentration results to ambient water column contaminant concentration data also provided a preliminary assessment of areas of the CARP model domain where historical contamination in sediments is potentially acting as an active source of contaminants to the water column or where a present day loading has not been accounted for. The CARP initial dilution simulations results served as an excellent basis for building the CARP model calibration up in a stepwise fashion. There was the opportunity to gain insights and understandings into controlling processes in advance of developing and applying the full CARP contaminant fate and transport model.

Results of the CARP initial dilution simulations are presented in Appendix 3 in a summary format. Model and data were binned by region and compared as the ratio of calculated to observed values. Perfect agreement between model and data would result in a ratio of 1, suggesting that observed water column contaminant concentrations are more likely influenced by current rather than historical loadings and that important processes such as volatilization, partitioning, settling, or resuspension were offsetting one another. There is a noted caution for over interpreting initial dilution simulation results in that the degree to which such calculations are mechanistic is extremely limited. A ratio of 1 between initial dilution simulation results and observed data could result purely by coincidence.

3.3.3 Initial Conditions for Contaminant Concentrations

Since the period selected for the current conditions calibrations corresponds to the period of CARP data collection, the water years October 1998 through September 2002, initial conditions representative of October 1998 were needed for both the water column and the sediment. Sections 3.3.3.1 and 3.3.3.2 below describe the derivation of initial conditions.

3.3.3.1 Initial Conditions for Contaminant Concentrations in the Sediment

The assignment of sediment initial conditions is an important aspect of the current conditions calibration. Sediment initial conditions are significant because of the relatively larger magnitude of the sediment in comparison to the water column in terms of particulate organic matter to which contaminants may bind. Sediment initial conditions tend to persist longer in the calculation than the initial conditions assigned in the water column and also build up or develop over longer time horizons.

For purposes of the CARP current conditions calibrations, sediment initial concentrations for PCB homologs were assigned on the basis of interpolating sediment data collected by NYSDEC for CARP. For the dioxin/furan congeners and mercury and cadmium, sediment initial conditions were assigned on the basis of interpolating a hybrid of REMAP data collected in 1998 and sediment data collected by NYSDEC for CARP. All sediment initial concentration estimates were assigned on a mass contaminant per mass sediment organic carbon basis.

Exploration of how the assigned sediment initial conditions compare to concentrations that would have resulted in the sediments if the only sources of contaminants to the sediments over time were current day loadings was also performed and is explained in section 5.1.

3.3.3.2 Initial Conditions for Contaminant Concentrations in the Water Column

Initial contaminant concentrations in the water column were assigned on the basis of using model calculated concentrations from the initial dilution simulations described above in section 3.3.2. The assigned initial conditions in the water column do not strongly influence or control model calculations since a model spin-up period, described in section 4.2, was used in the current conditions calibrations. Essentially, the model is run for four years of spin-up before results are considered. The spin-up procedure dampens the importance of the assigned initial conditions.

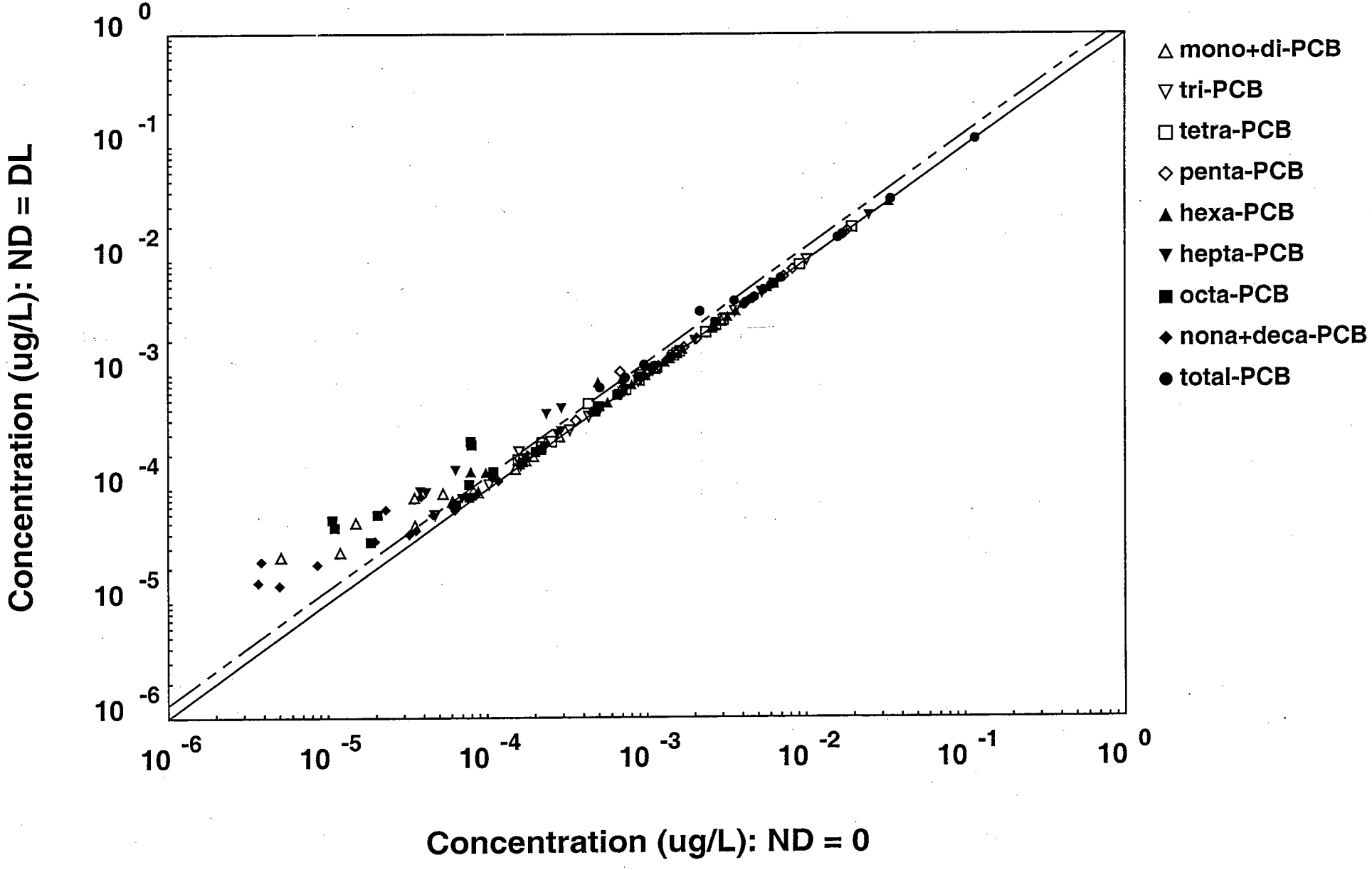

Figure 3-1. Comparison of PCB congener non-detectable measurements set at detection limit and at zero.

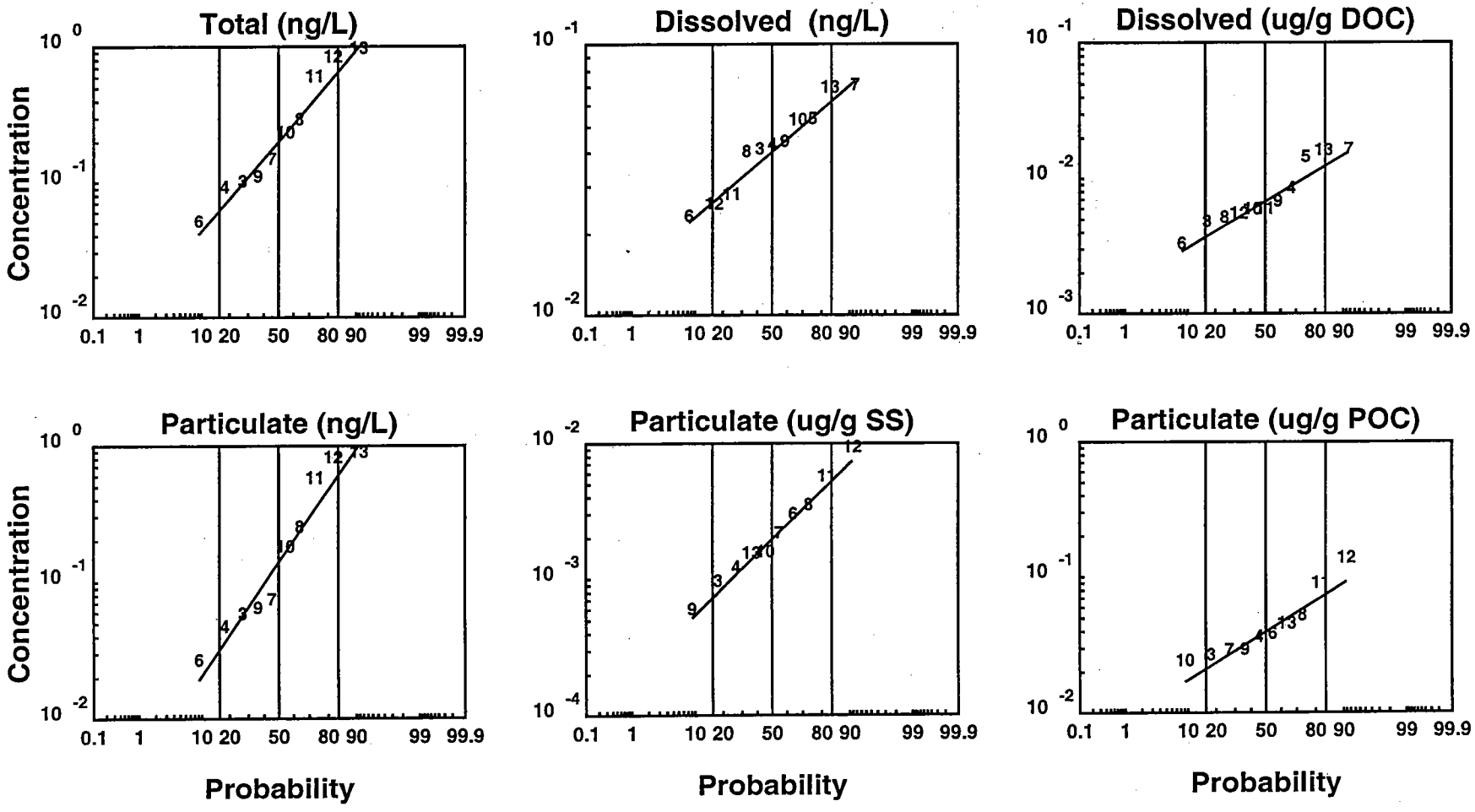

Figure 3-2. Example of approach for explaining variability in tributary contaminant conentration measurements.

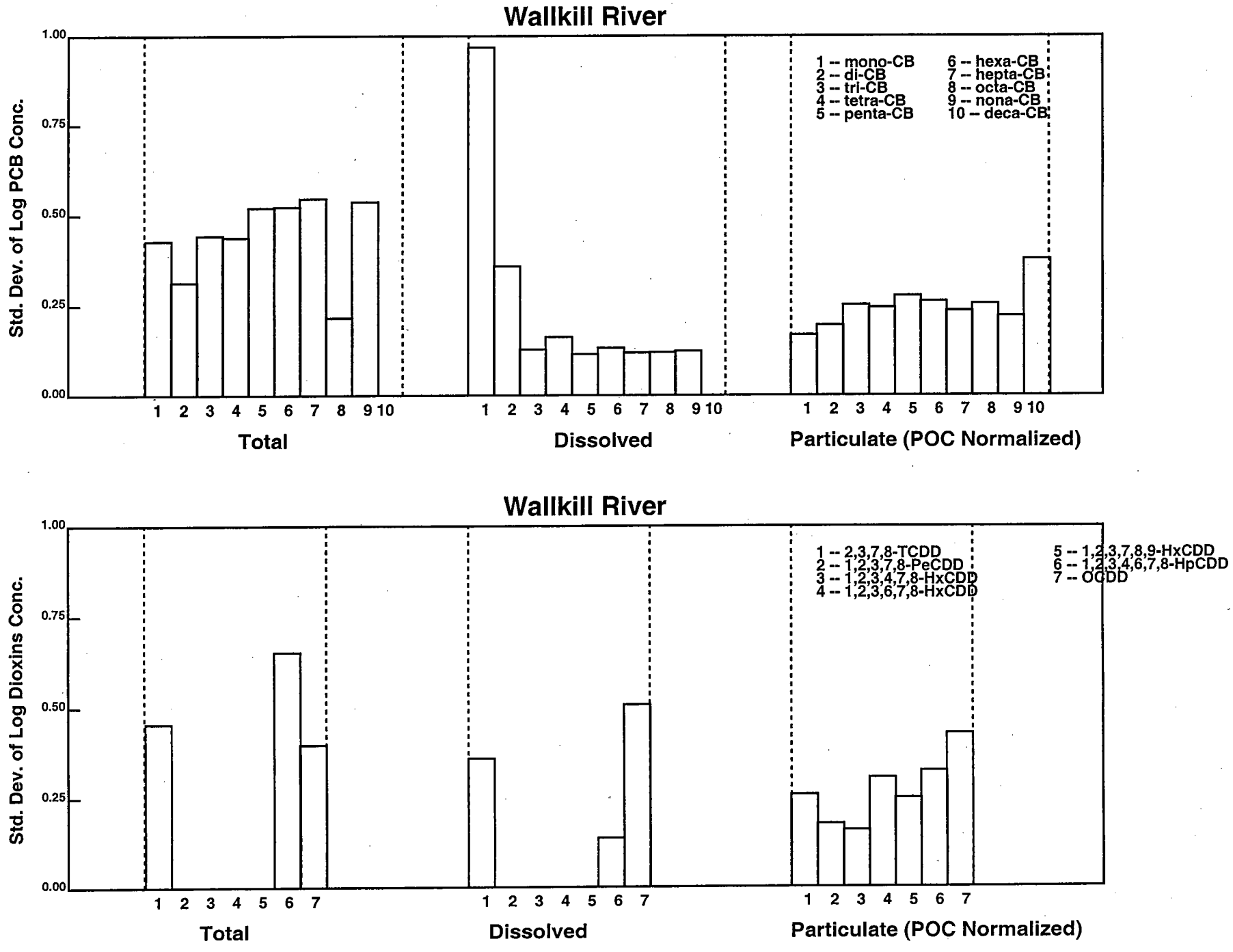

Figure 3-3a. Comparisons of standard deviations across same tributary measurements for various fractions for PCB homologs and dioxin cogeners.

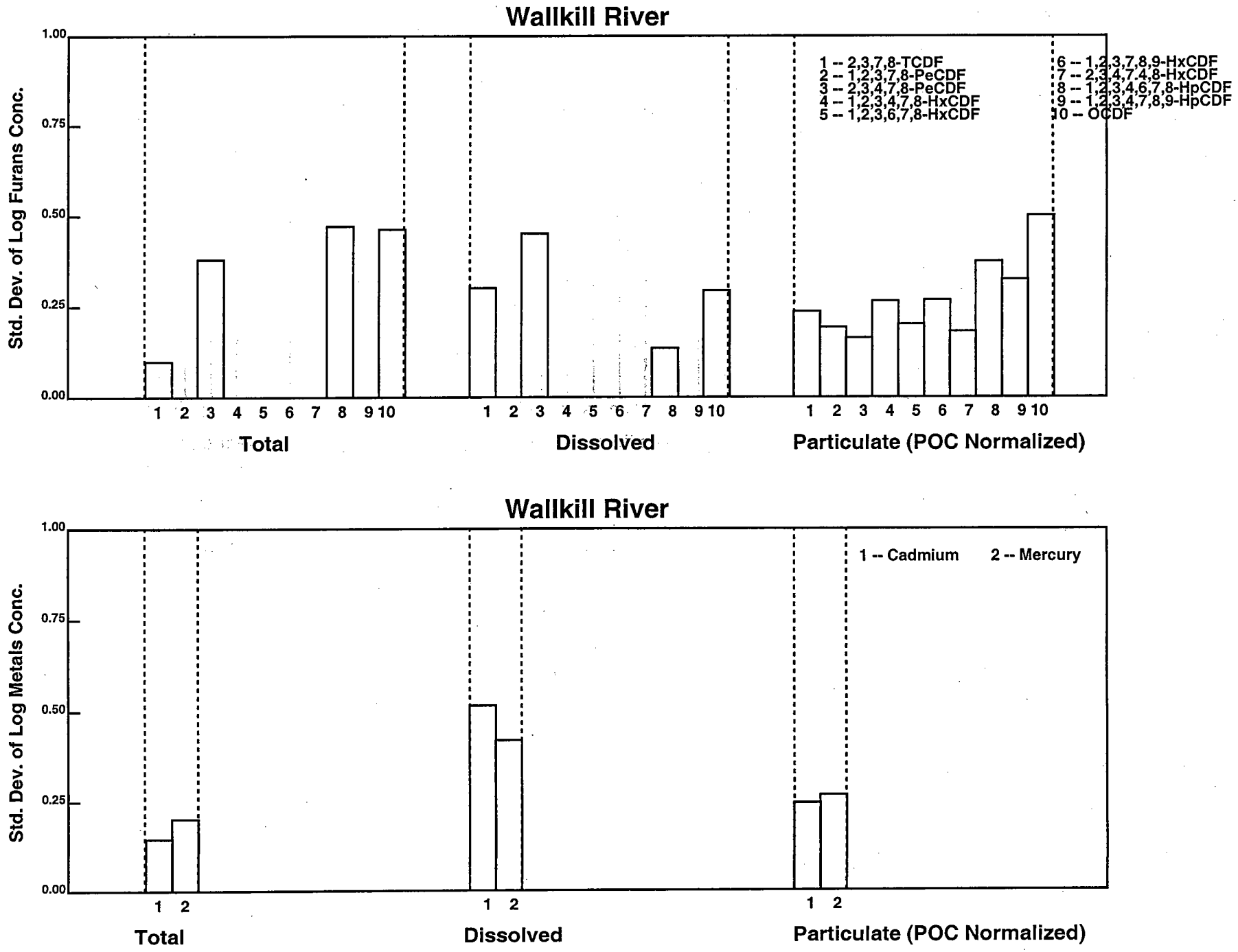

Figure 3-3b. Comparison of standard deviations across same tributary measurements for various fractions for furan congeners and metals.

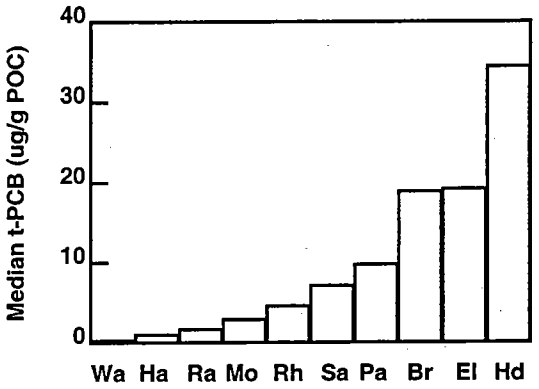

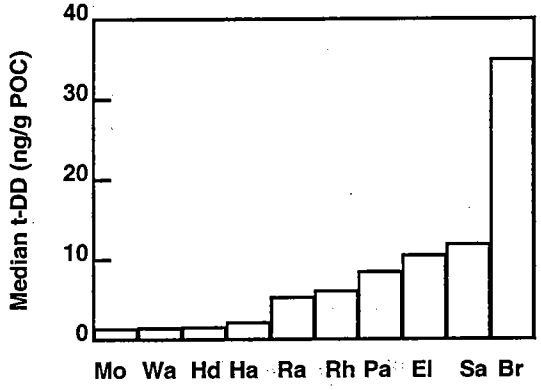

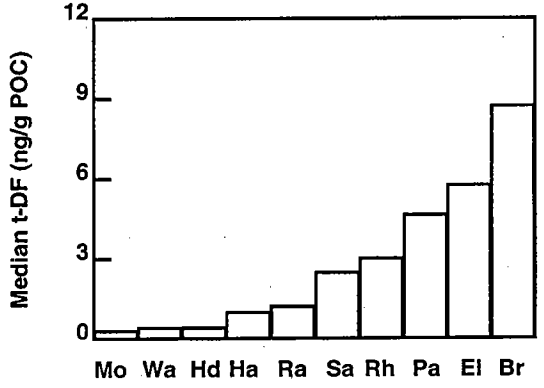

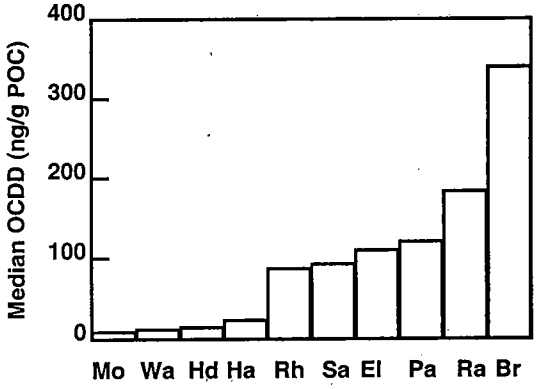

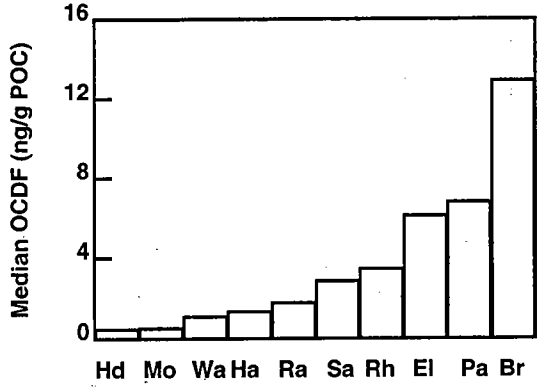

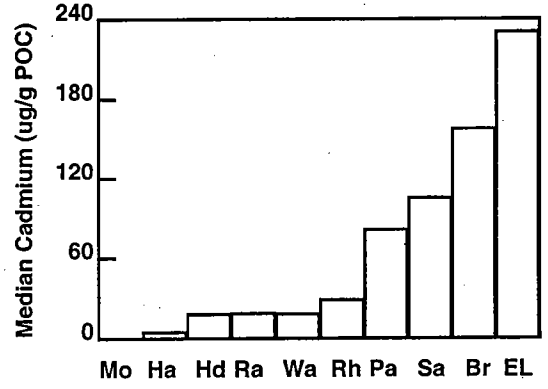

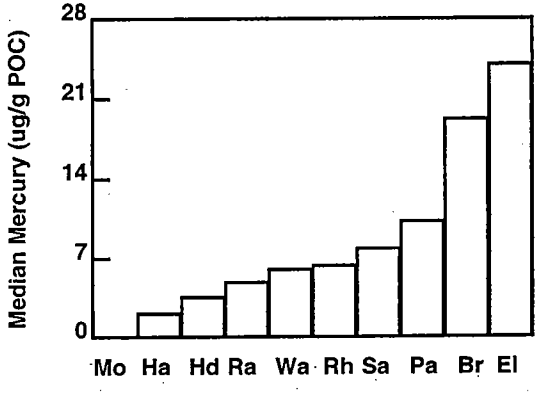

Br -- Bronx River
Hd -- Hudson River At Waterford
Mo -- Mohawk River
Sa -- Saw Mill River
Wa -- Wallkill River
El -- Elizabeth River
Ha -- Hackensack River
Pa -- Passaic River
Ra -- Raritan River
Rh -- Rahway River

Figure 3-4. Median particulate contaminant concentrations for measured tributaries.

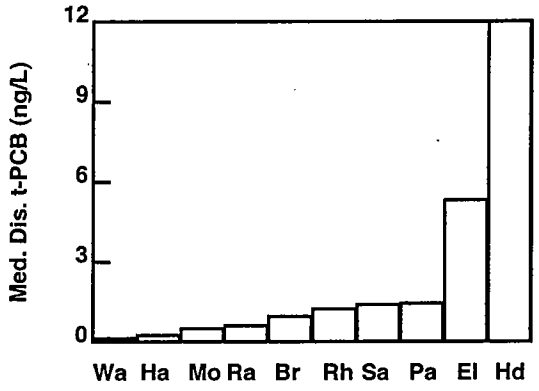

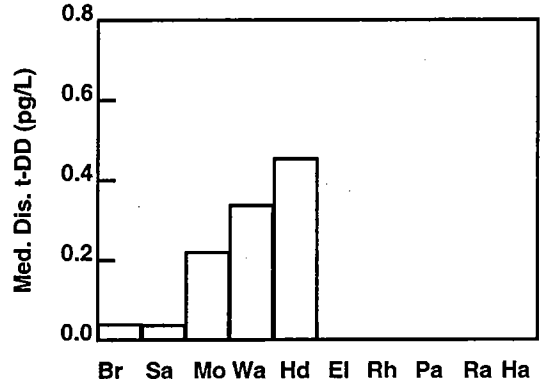

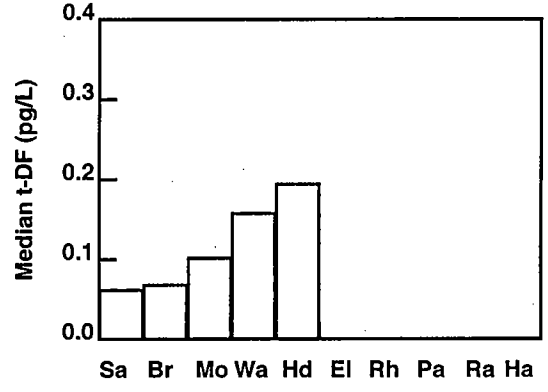

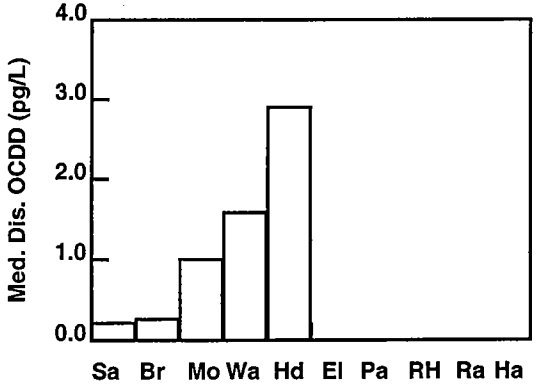

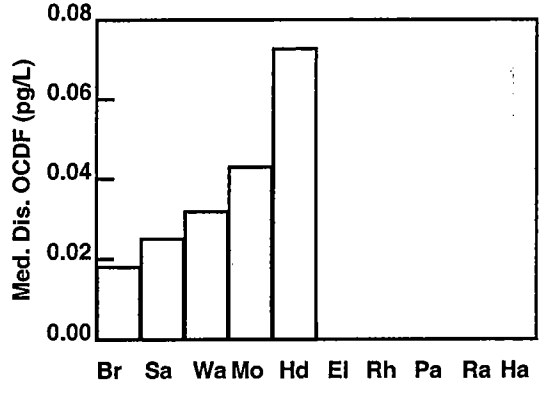

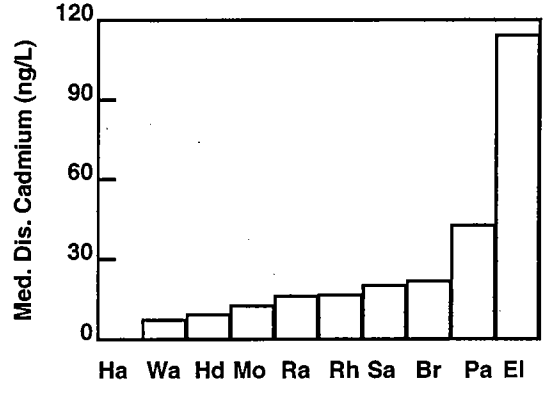

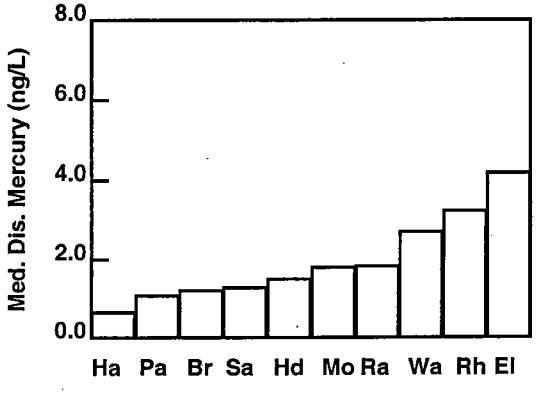

Br -- Bronx River
Hd -- Hudson River At Waterford
Mo -- Mohawk River
Sa -- Saw Mill River
Wa -- Wallkill River
El -- Elizabeth River
Ha -- Hackensack River
Pa -- Passaic River
Ra -- Raritan River
Rh -- Rahway River

Figure 3-5. Median dissolved contaminant concentrations for measured tributaries.

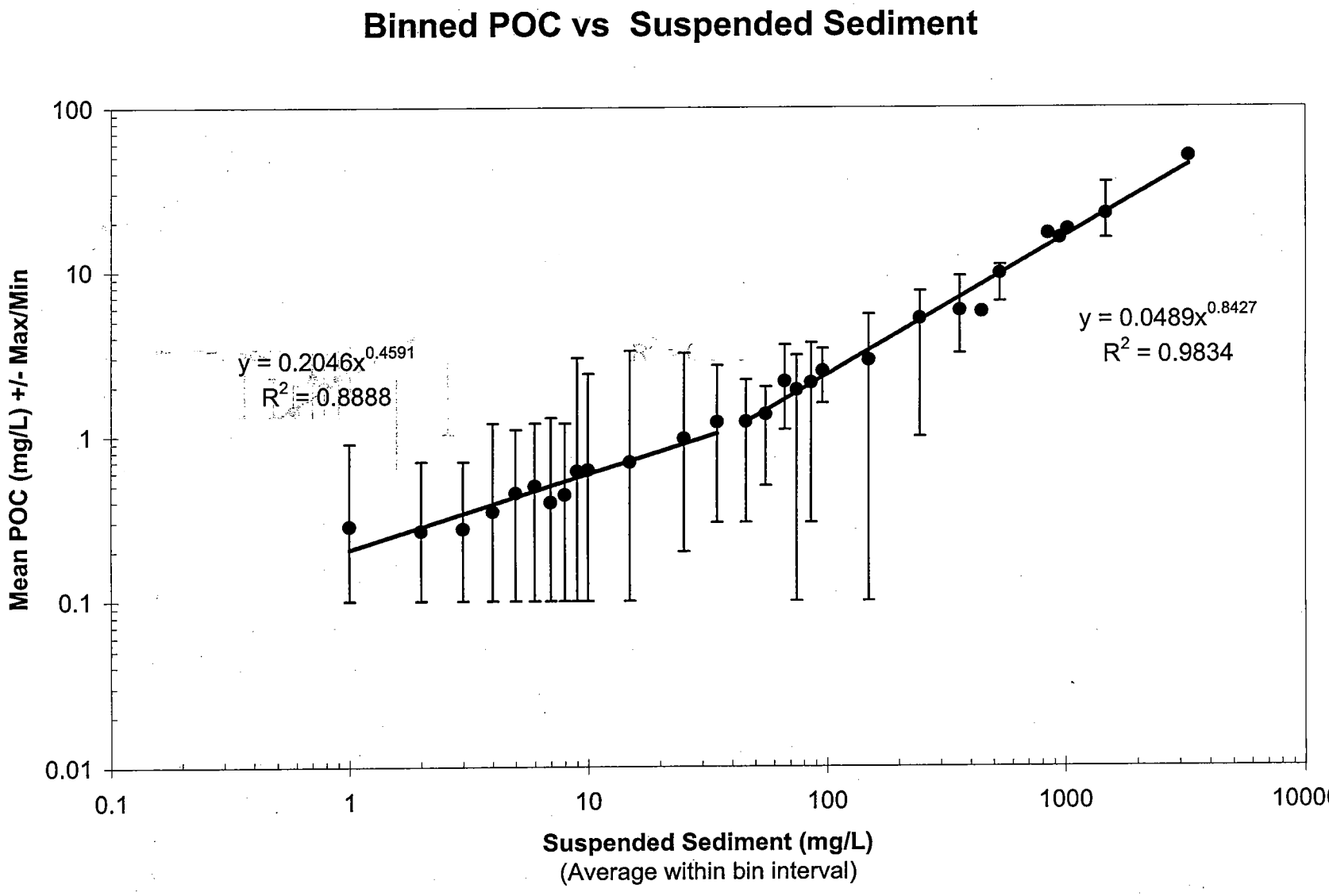

Figure 3-6. Tributary relationship between POC and SS.

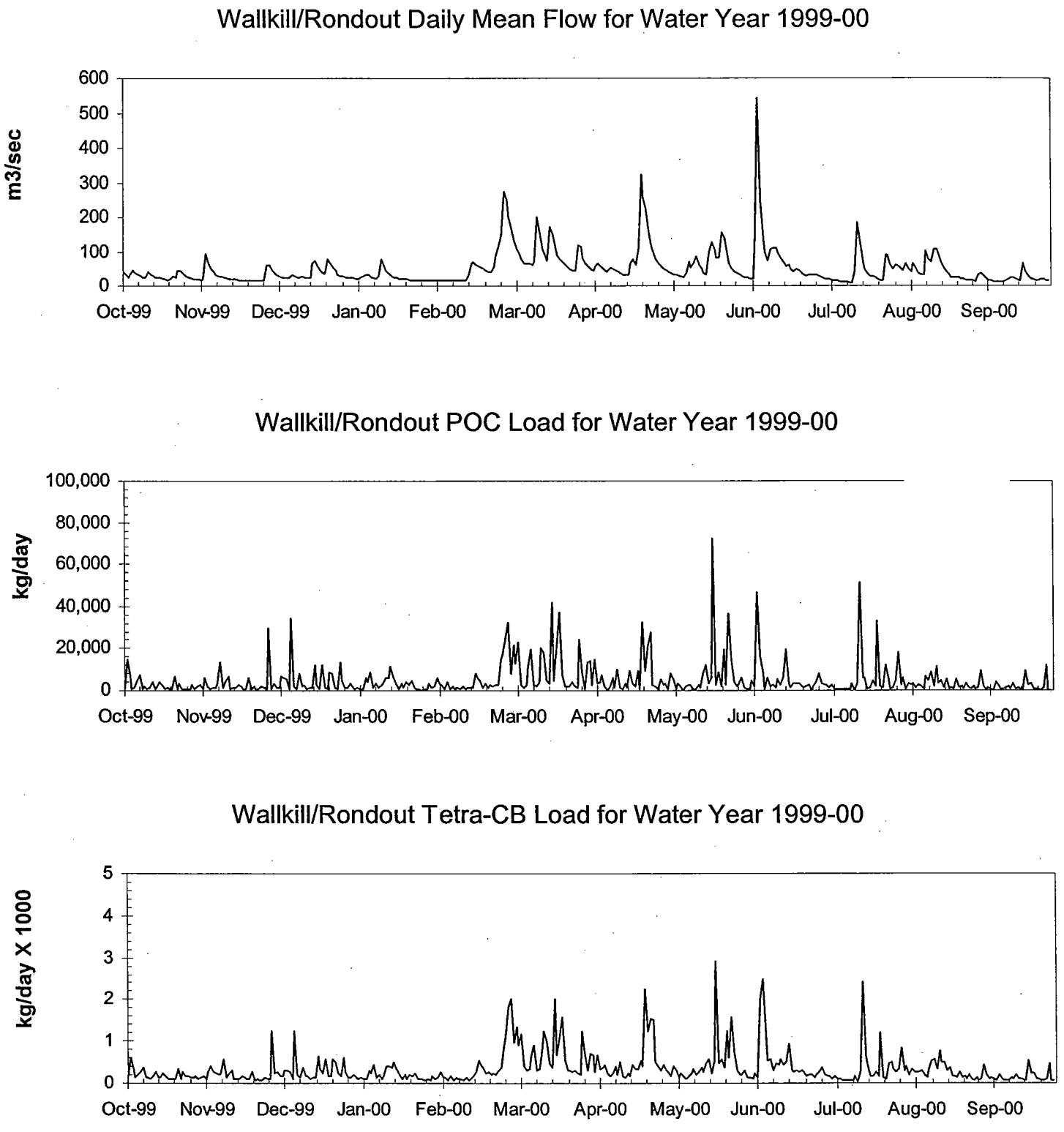

Figure 3-7. Flow, POC loads, and tetra-CB loads calculated for the Wallkill River for the 1999-2000 water year.

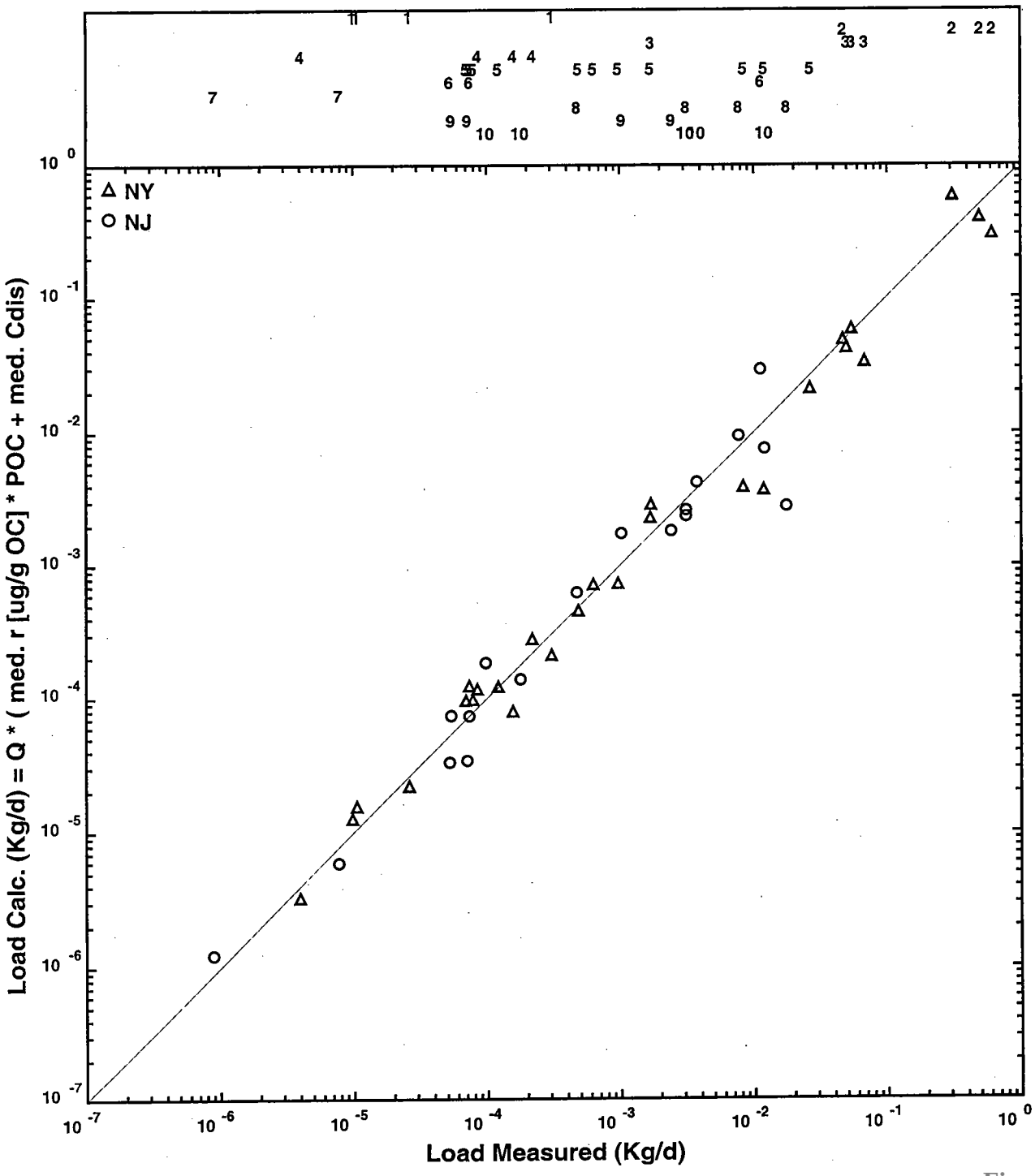

1 Bronx River

2 Hudson River

3 Mohawk River

4 Saw Mill River

5 Wallkill River

6 Elizabeth River

7 Hackensack River

8 Passaic River

9 Rahway River

10 Raritan River

Figure 3-8. Calculated vs. observed loads for tetra-CB in ten tributaries.

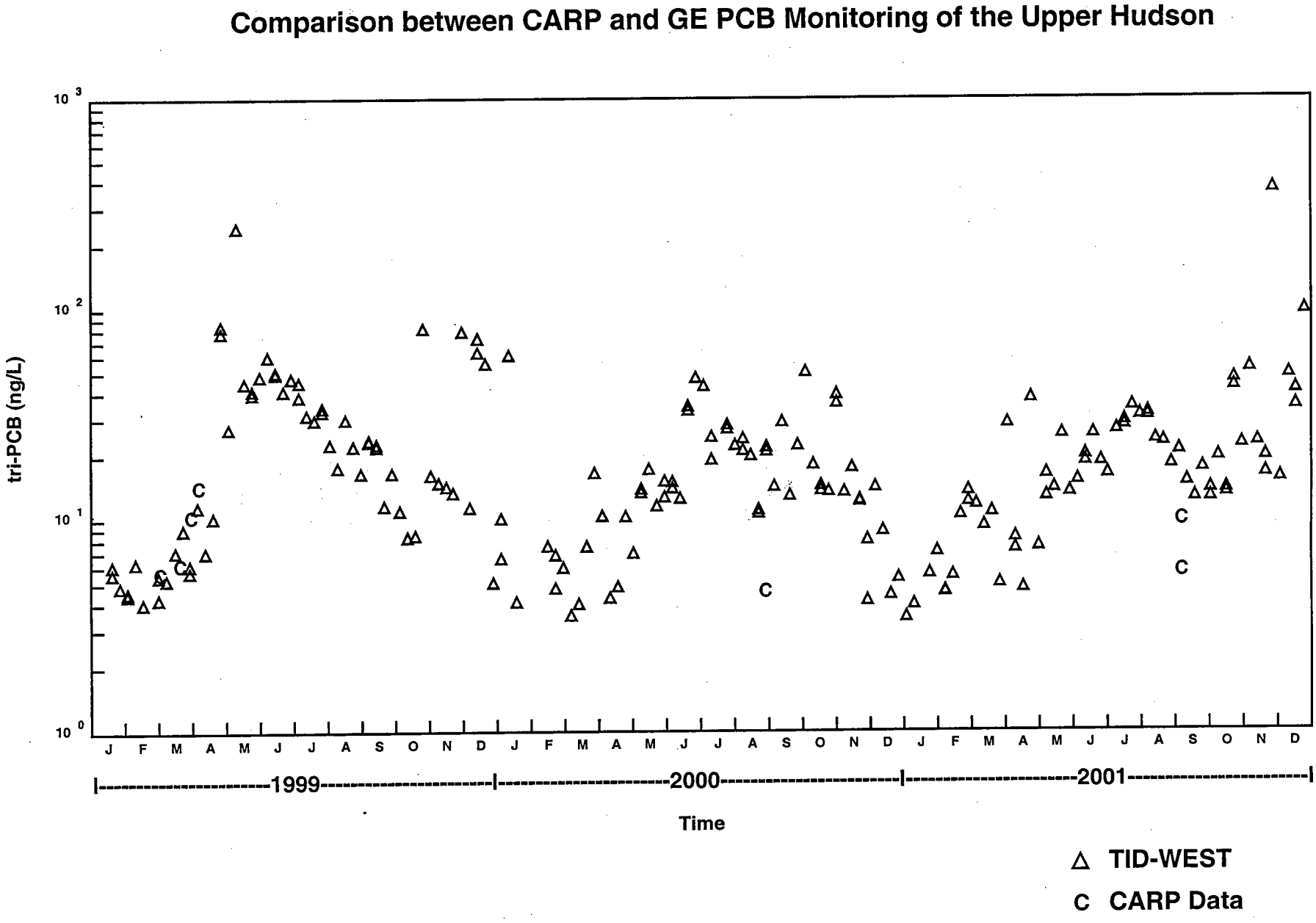

Figure 3-9. A comparison of tri-CB concentrations over Thompson Island Dam for 1999-2000 (GE data set) and for seven CARP measurements taken near Waterford (RM160).

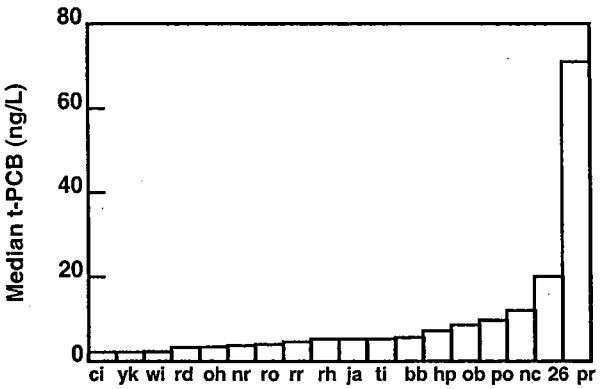

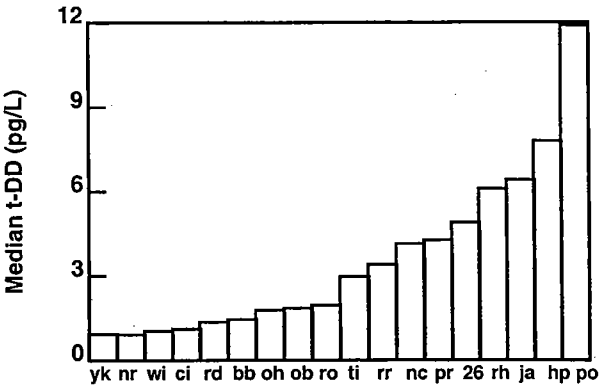

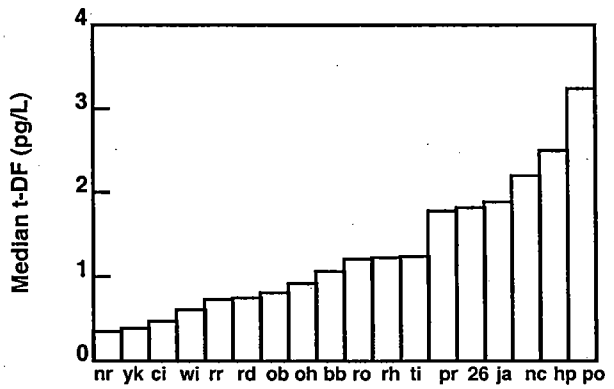

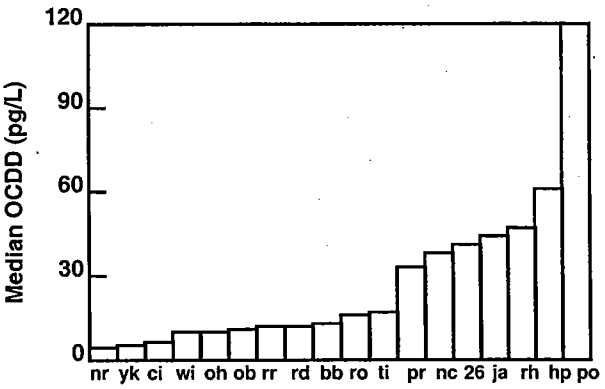

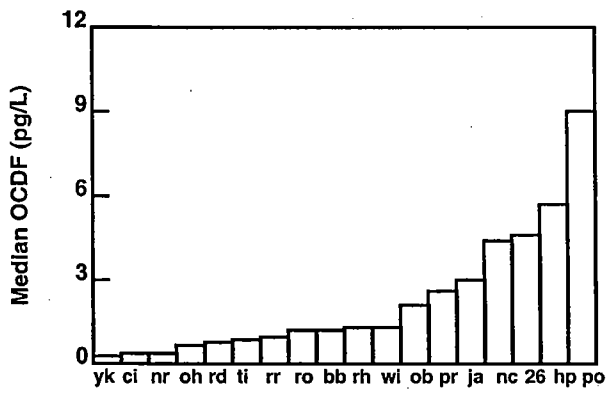

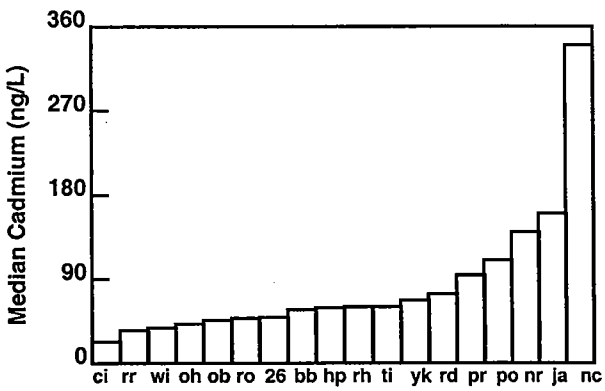

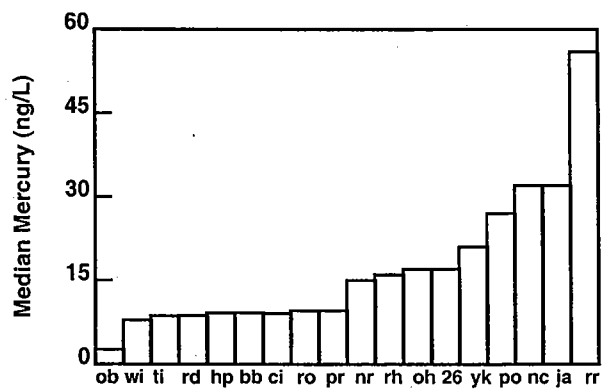

ci -- Coney Island
yk -- Yonkers
wi -- Wards Island
rd -- Red Hook
oh -- Owls Head
nr -- North River
ro -- Rockaway
bb -- Bowery Bay
ob -- Oakwood Beach
nc -- Newtown Creek
pr -- Port Richmond
26 -- 26th Ward
ja -- Jamaica
hp -- Hunts Point
po -- Poughkeepsie
rh -- Rensselaer
ti -- Tallman Island
rr -- Rockland

Figure 3-10a. Measured median STP effluent concentrations in New York.

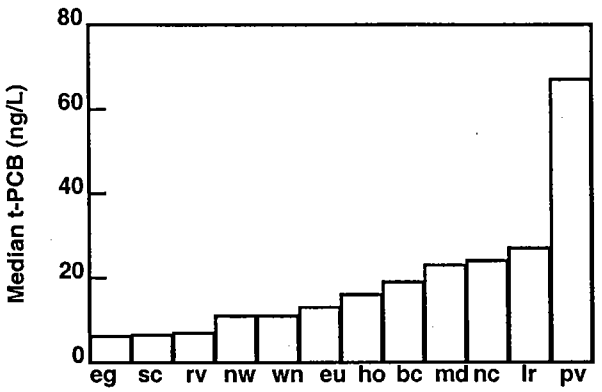

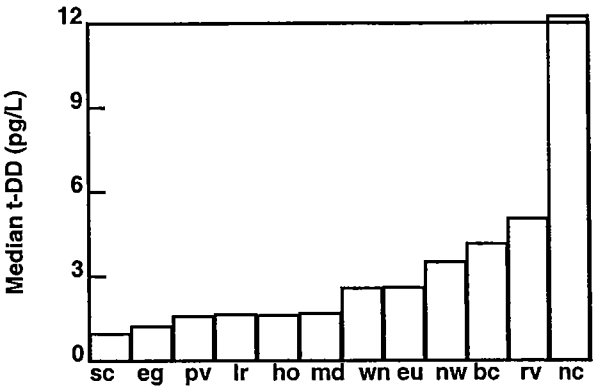

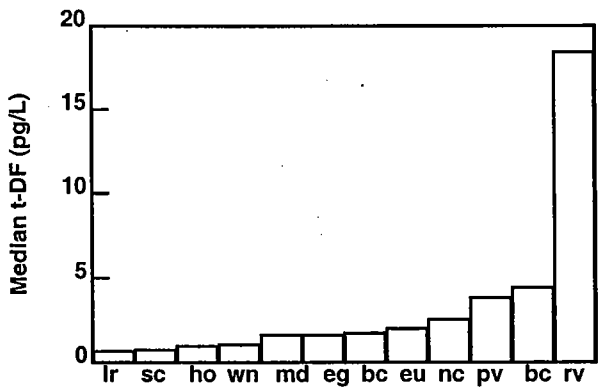

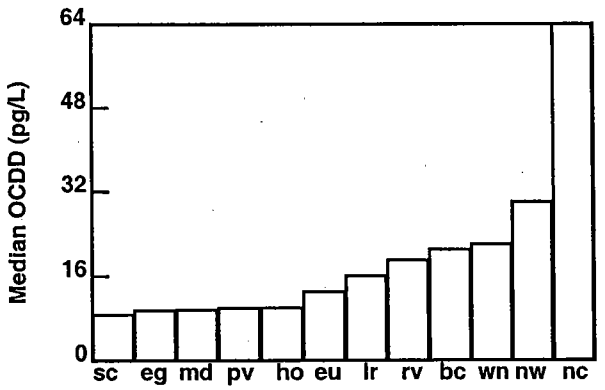

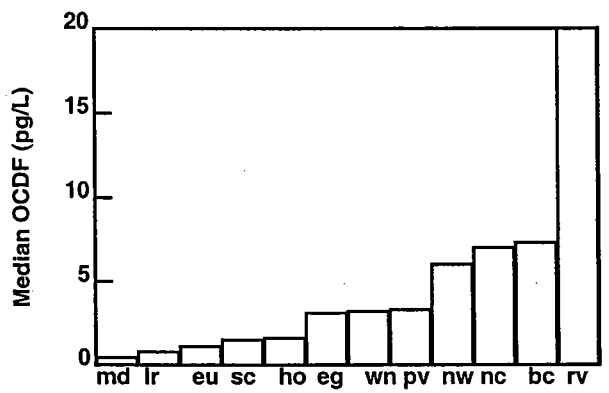

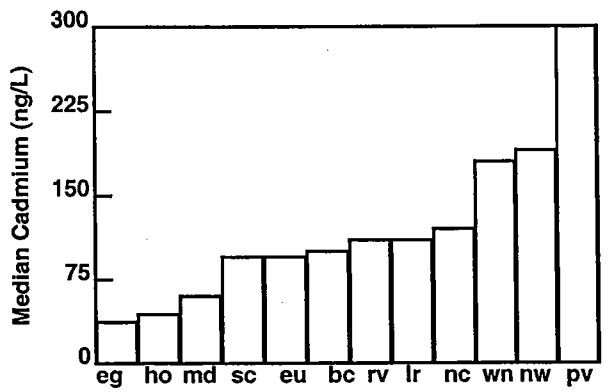

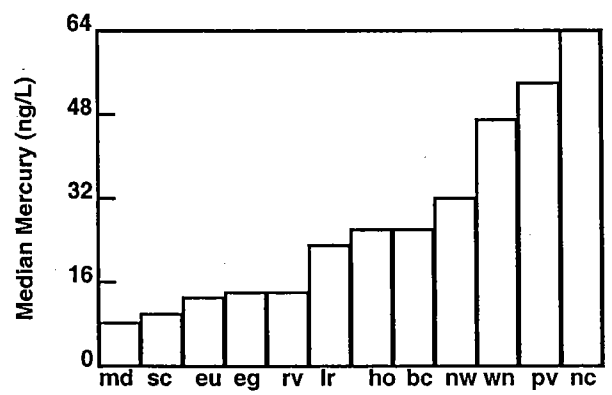

eg -- Edgewater
eu -- Essex and Union Co.
ho -- Hoboken
sc -- Secaucus
wn -- West New York
nw -- NB-Woodcliff
pv -- Passaic Valley
nc -- NB-Central
bc -- Bergeb Co.
md -- Middlesex
lr -- Linden Roselle
Rv -- Rahway Valley

Figure 3-10b. Measured median STP effluent concentrations in New Jersey.

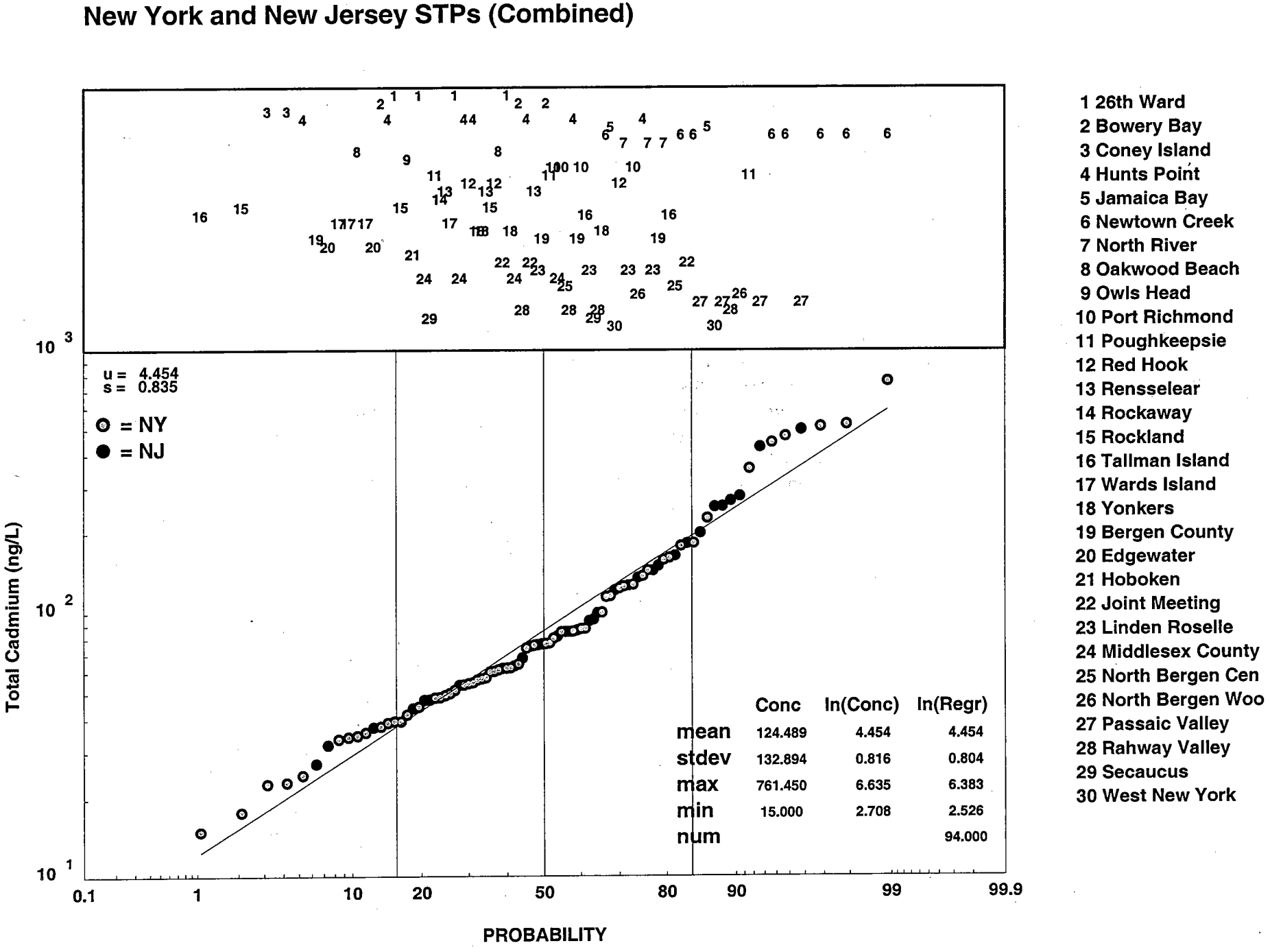

Figure 3-11. Probability distribution of STP effluent cadmium concentrations.

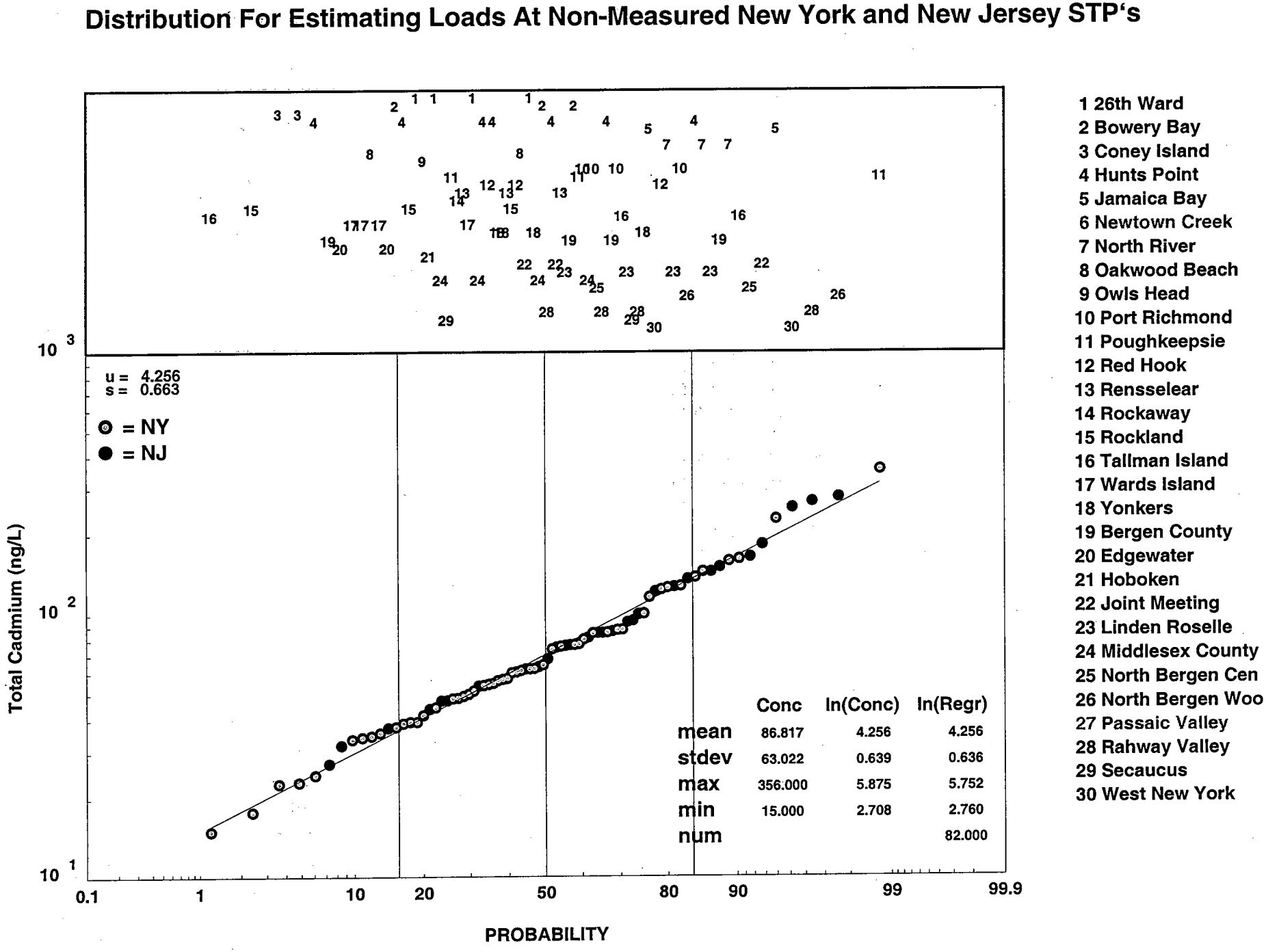

Figure 3-12. Probability distribution of STP effluent cadmium concentrations used for assigning concentrations to unmeasured effluents.

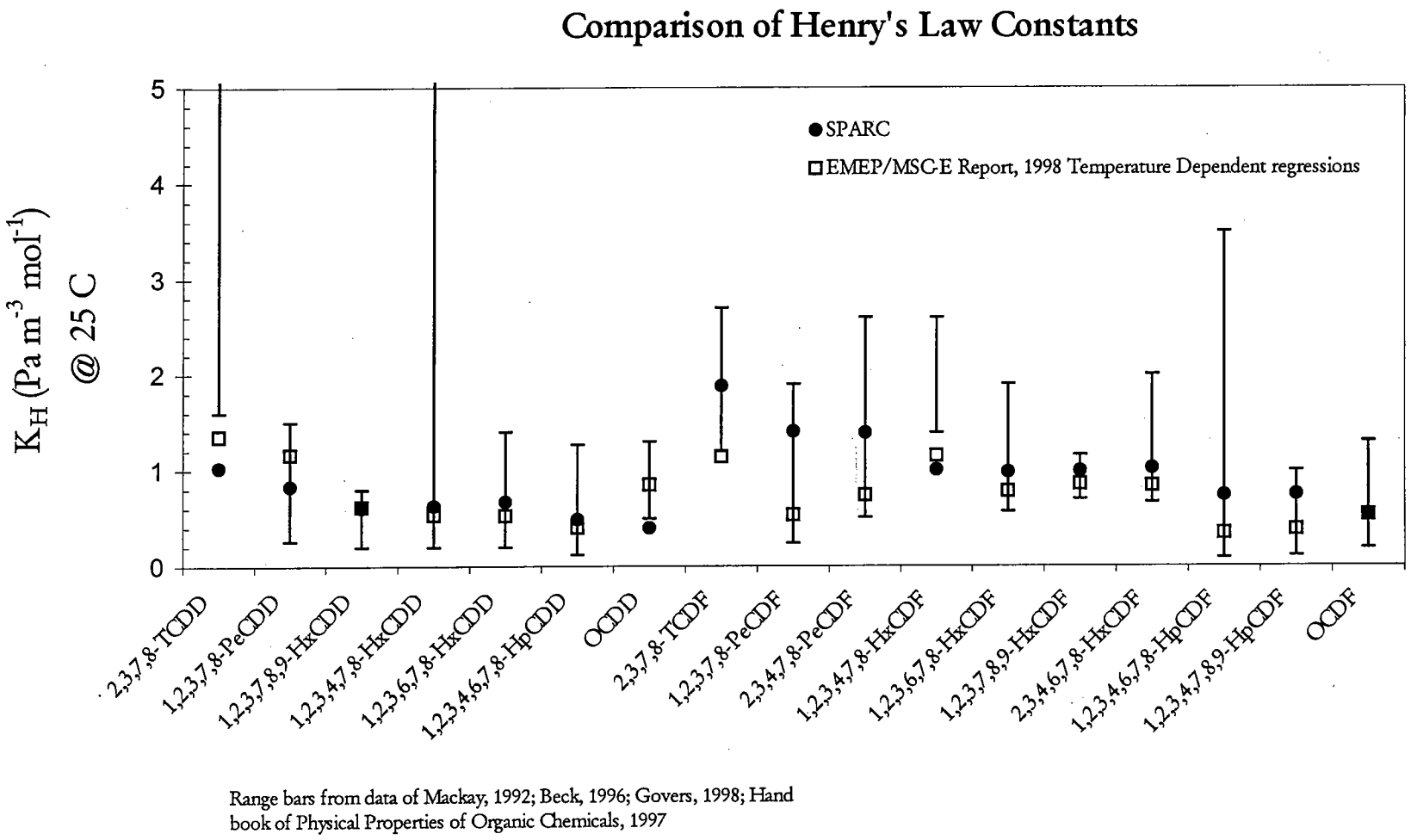

Range bars from data of Mackay, 1992; Beck, 1996; Govers, 1998; Hand book of Physical Properties of Organic Chemicals, 1997

Figure 3-13. Comparison between SPARC generated and literature reported Henry's Constants.

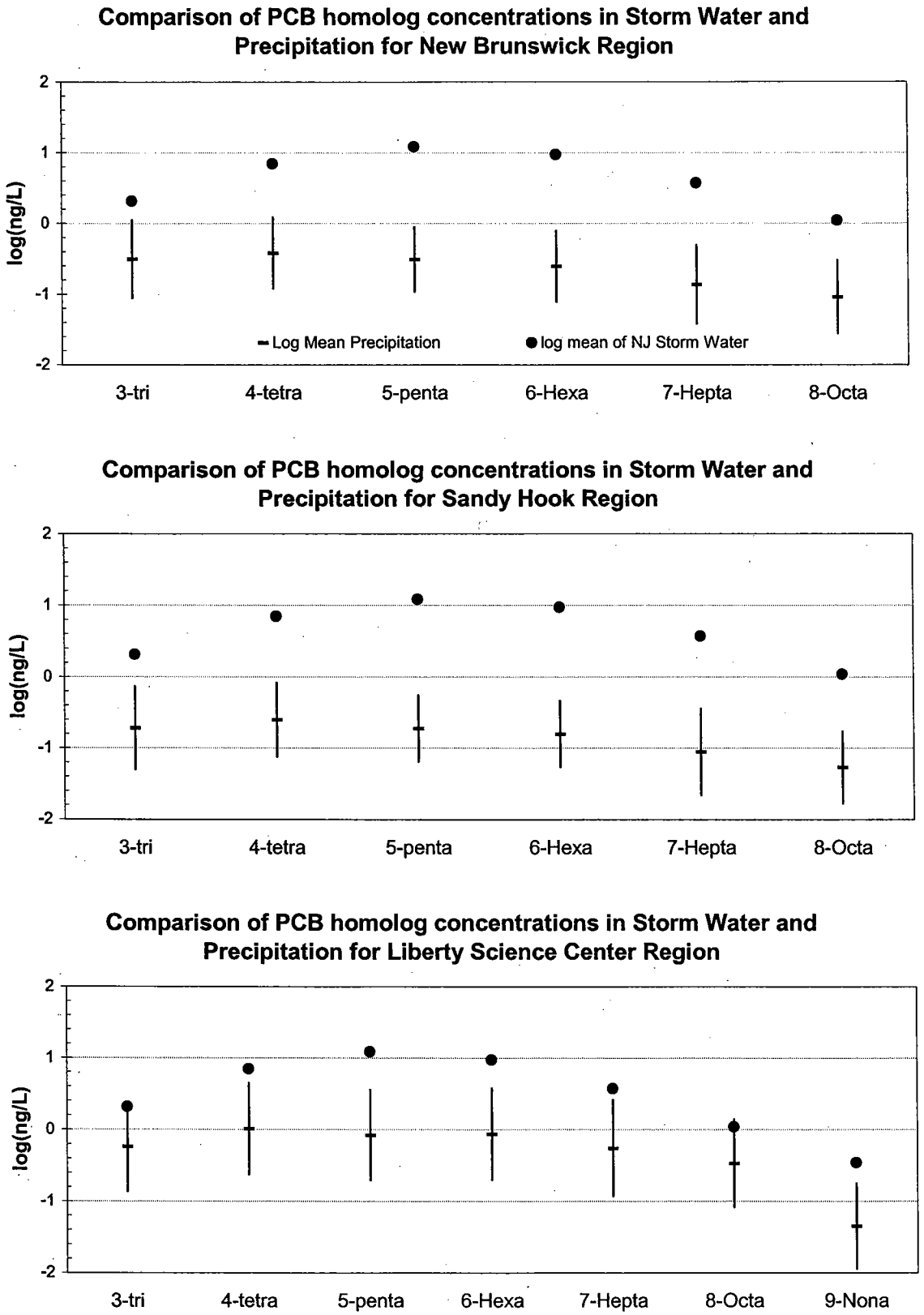

Figure 3-14. Comparison between PCB concentrations measured in precipitation and stormwater runoff.

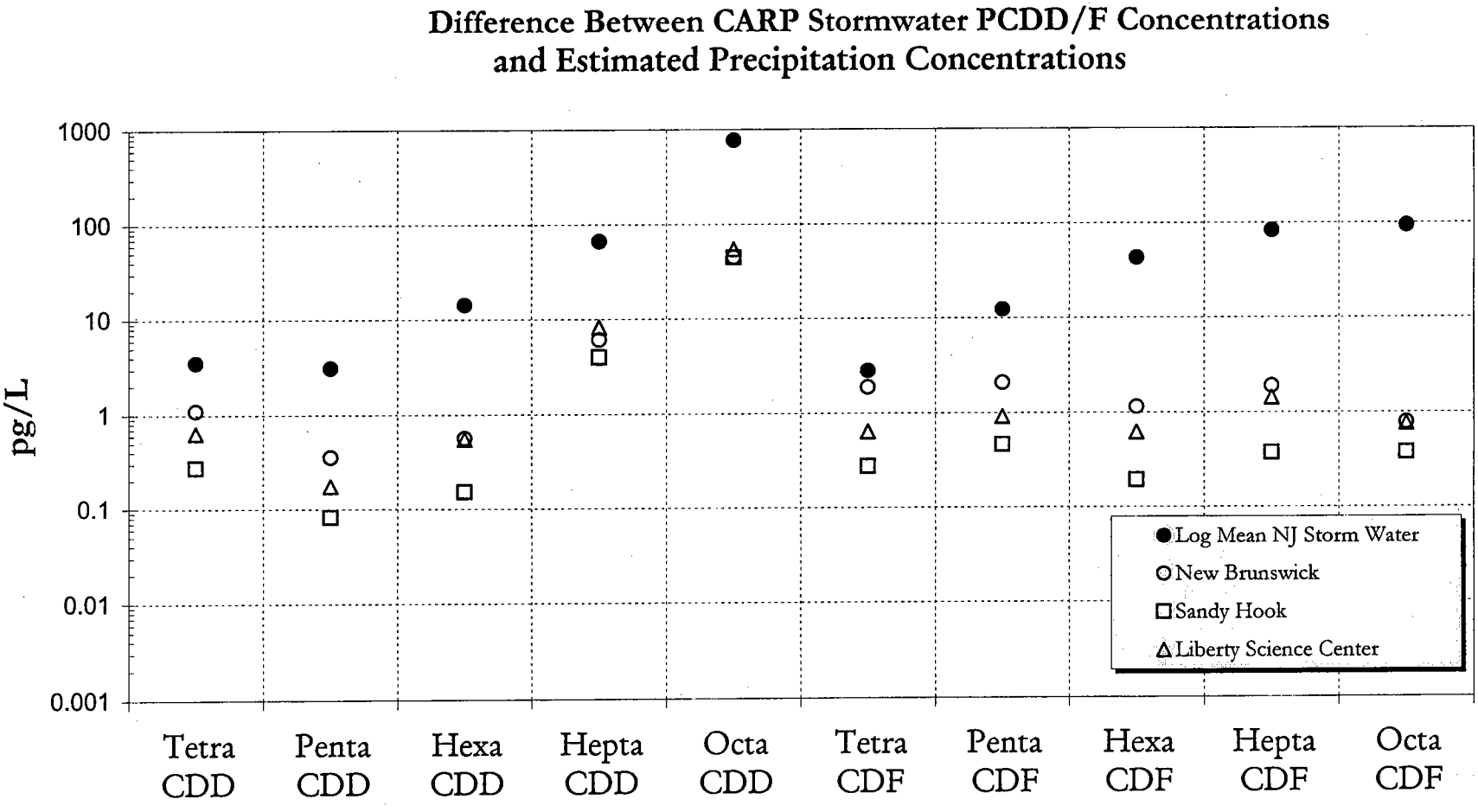

Figure 3-15. Comparison of measured stormwater concentrations and estimated precipitaiton concentrations for selected dioxin and furan congeners.

SECTION 4.0

CONTAMINANT FATE AND TRANSPORT MODEL CURRENT CONDITIONS CALIBRATION

The CARP Contaminant Fate and Transport sub-model has been calibrated for current (i.e., 1998-2002) conditions for two major groups of HOCs (i.e., 10 PCB homologs and 17 dioxin/furan congeners) and the metals cadmium and mercury. The mercury calibration also includes a methylmercury calibration. The overall calibration procedure also includes a hindcast verification which is described in Section 6.0 and application to two additional groups of HOCs (i.e., 22 PAHs and 11 organochlorine pesticides related to DDT and chlordane) as described in Section 7.0. Details of the current conditions calibrations for the PCB homologs, dioxin/furan congeners and the metals are described in this report section.

4.1 DATA AVAILABLE FOR CURRENT CONDITIONS CALIBRATIONS

Calibration of the CARP contaminant fate and transport model for current conditions made use of data in both water column and sediments collected specifically for CARP during 1998 through 2002 by NYSDEC and NJDEP. The NYSDEC data collection program supporting the CARP contaminant fate and transport current conditions calibrations included both water column (Litten, 2003), biological, and sediment measurements. The NJDEP (implemented by Stevens Institute of Technology) data collection program supporting the CARP contaminant fate and transport current conditions calibrations included only water column measurements. The CARP data are described and available for download from the internet at http://www.carpweb.org. Additional data sources considered for the current conditions calibration include measurements of contaminants in sediments from EPA's 1998 Regional Environmental Monitoring Assessment Program (REMAP) (Adams and Benyi, 2003). Model calculations and data comparisons for the current conditions calibrations are displayed in Section 4.3.

4.2 CALIBRATION STRATEGY

The approach taken for calibrating the contaminant fate and transport model for current conditions included performing the model calculations for two four-year cycles with the first cycle being treated as model spin-up and the second cycle as the calibration cycle. A spin-up cycle in the calibration procedure was used to decrease the importance of assigned initial conditions in the water column, and

to allow for some re-distribution of the assigned initial conditions in sediments (e.g., from localized erosion zones to sediment depositional areas).

A hierarchical approach was taken for evaluating the model calibration relative to the handling of a few key model inputs. These include: the application of solid phase transport terms from the sediment transport/organic carbon production sub-model, contaminant specific partition coefficients for POC, contaminant specific partition coefficients for DOC, and volatilization rates.

4.3 CALIBRATION PARAMETERS

4.3.1 Application of Solid Phase Transport Terms

The vertical transport terms for each grid element for the solid phase (i.e., settling, resuspension, and burial) calculated by the CARP sediment transport/organic carbon production model are passed forward directly to the contaminant fate and transport model on an hourly basis as described in Section 3.2. During the calibration process for the contaminant fate and transport model, we investigated two methods for applying the hourly solid phase vertical transport terms across the water column/sediment bed interface: 1) as separate settling and resuspension fluxes, and 2) as a combined net flux. The contaminant fate and transport model performed better (i.e., greater numerical stability) when the hourly fluxes calculated by the sediment transport/organic carbon production model were first condensed to a net flux between the water column and sediment before being applied in the contaminant fate and transport model. This suggests that on an hourly basis resuspension and deposition are not occurring simultaneously.

4.3.2 HOC Partition Coefficients for DOC-Complexed and Freely Dissolved Contaminant, A_{DOC}

The numerical formulations used in the CARP model for expressing the partitioning of freely dissolved contaminant to DOC are presented above in report section 2.1.1.1. Values for A_{DOC} were assigned based on the work of others (Farley et al., 1999 and Burkhard, 2000 and tested as part of the site specific data analysis to develop the partitioning relationship between POC complexed contaminant and freely dissolved contaminant as presented below in section 4.3.3.

A challenge in modeling the partitioning behavior of the contaminants of concern relates to measurement limitations. For example, XAD columns used as part of CARP monitoring capture the

freely dissolved portion of the dissolved contaminant plus some unspecified fraction of the DOC complexed portion of the dissolved contaminant. Researchers at the State University of New York (SUNY) at Syracuse are attempting to quantify how much of the DOC-complexed dissolved contaminant is actually captured by XAD as a function of several factors such as flow rate, column age, etc. We took this uncertainty into account in assigning values of A_{DOC} during the CARP model calibration. That is to say, we expected in some cases that model calculations of total dissolved contaminant would exceed the measured dissolved concentration since the measurements missed some of the DOC complexed portion of the dissolved contaminant. Similarly, we expected that the calculation of freely dissolved contaminant would be less than or, in some cases, equal to the measured dissolved concentrations. A final calibration value for A_{DOC} of 0.08 was developed and is consistent with previous findings of Burkhard (2000).

4.3.3 HOC Partition Coefficients for Poc-Complexed and Freely Dissolved Contaminant, K_{POC}

The numerical formulations used in the CARP model for expressing the partitioning of freely dissolved contaminant to POC are presented above in report section 2.1.1.1. Site specific data plots used for calculation of preliminary partition coefficients without temperature and salinity adjustment are presented in Appendix 4A. Final calibration values for K_{POC} for PCB homologs which consider temperature and salinity effects are tabulated below in Table 4-1.

Table 4-1. Final K_{POC}[1] Values for CARP PCB Current Conditions Calibration

Homolog	log K_{OW}	log K_{POC}
mono	4.63	6.39
di	5.00	6.04
tri	5.60	6.20
tetra	6.00	6.27
penta	6.45	6.62
hexa	6.85	7.15
hepta	7.22	7.75
octa	7.63	8.21
nona	7.99	8.72
deca	8.18	9.01

Notes:

[1] Assumes an A_{DOC} = 0.08 and temperature and salinity dependencies on K_{POC}

It is noted that the calculated salinity and temperature dependent log K_{POC} values are not linearly related to log K_{ow} values for the lower chlorinated PCB homologs (i.e., as indicated in Table 4-1 and

Figure 4.1) as would be expected. This in part can be explained by the partitioning behavior of congeners with varying degrees of ortho chlorine substitutions. When our calculations of K_{POC} were restricted to congeners with 2-, 3-, and 4- ortho chlorines (omitting 0- and 1-ortho chlorine substitutions), calculated K_{POC} values were linearly related to log K_{ow} values even for the lower chlorinated PCB homologs (see Figure 4–2). The enhanced binding of planar PCB congeners (i.e., congeners with 0- and 1- ortho substituted chlorines) are apparent from our data evaluations (see Figure 4-3). This behavior is believed to be associated with the binding of planar PCB congeners to black carbon or soot particles that are present in the water column and sediment (Lohmann et al., 2005).

Final calibration values for K_{POC} for dioxin/furan congeners are tabulated below in Table 4-2. These were calculated following the method described in Section 2.1.1.1.

Table 4-2 . Final K_{POC}[1] Values for CARP Dioxin/Furan Current Conditions Calibration

Congener	log K_{POC}
2,3,7,8-TCDD	6.81
1,2,3,7,8-PeCDD	7.18
1,2,3,4,7,8-HxCDD	8.20
1,2,3,6,7,8-HxCDD	8.53
1,2,3,7,8,9-HxCDD	8.59
1,2,3,4,6,7,8-HpCDD	9.89
OCDD	10.88
2,3,7,8-TCDF	6.87
1,2,3,7,8-PeCDF	7.28
2,3,4,7,8-PeCDF	7.38
1,2,3,4,7,8-HxCDF	7.97
1,2,3,6,7,8-HxCDF	8.16
1,2,3,7,8,9-HxCDF	6.97
2,3,4,6,7,8-HxCDF	8.04
1,2,3,4,6,7,8-HpCDF	9.37
1,2,3,4,7,8,9-HpCDF	8.74
OCDF	10.32

Notes:

[1]Assumes and A_{DOC} = 0.08 and salinity dependencies on K_{POC} and no temperature dependencies.

The site specific log K_{POC} values calculated from the CARP data for the dioxin and furan congeners are significant in terms of furthering the overall understanding of the behavior of dioxin and furan congeners in natural ecosystems. As described in USEPA 1993, historically, there has been great uncertainty across a limited number of available estimates of octanol water partitioning for dioxin and furan congeners. Further, the value of octanol as a surrogate for naturally occurring organic phase interactions with chemicals such as 2,3,7,8-TCDD may also have limitations (Miller et al. 1985).

For 2,3,7,8-TCDD, reported log K_{OW} direct measurements range from 4.4 to 6.95 (Marple et al., 1986; Sijm et al., 1989). Reported log K_{OW} values estimated by other techniques are generally higher than 7 (Burkhard and Kuehl, 1986; Leo and Weininger, 1989). Shlu et al. 1988 developed correlation equations as a function of chlorine number and molar volume which enable the K_{ow} to be estimated with an accuracy within a factor of 2 for dioxin congeners. Shlu et al. 1988, compare their calculations of K_{ow} to those reported by a variety of other researchers. HydroQual's selections for log K_{ow} are based on the EPA structure-activity estimation program (SPARC) (Hilal et al., 1994). SPARC estimates agree well with the range of values reported in Shlu et al. For 2,3,7,8-TCDD, a range for log K_{ow} of 5.5 to 7.02 is reported and a range of 6.6 to 7.0 is recommended by Shlu et al. HydroQual used a log K_{ow} of 6.65 based on SPARC for the CARP model. For 1,2,3,4,7,8-HxCDD, 7.79 to 10.22 is reported and 7.3 to 8.3 is recommended by Shlu et al. HydroQual selected 7.76 based on SPARC. For 1,2,3,4,6,7,8-HpCDD, 8.2 to 11.05 is reported and 7.5 to 8.5 is recommended by Shlu et al. HydroQual selected 8.56 based on SPARC.

Additionally, a wide range of log K_{POC} values are also reported for 2,3,7,8-TCDD: 7.4 to 7.6 (Jackson et al., 1985); 6.66 (Walters et al., 1989); greater than 7.3 (Lodge and Cook, 1989). Broman et al. 1991 report a log K_{POC} of 6.8 for 2,3,7,8-TCDD and values of 6.8 to 7.9 for congeners with greater chlorination. On this basis, we believe the site specific log K_{POC} values calculated from CARP measurements and presented in Table 4-2 are reasonable, and are the most appropriate for use in the CARP model.

4.3.4 HOC Volatilization Rates

The numerical formulations used in the CARP model for expressing the exchange of hydrophobic organic contaminants across the air water interface, from water to air, are described in detail in report sections 2.1.1.3 and 5.3. Exchange of contaminants between air and water due to

external loadings associated with wet and dry deposition and forward gas diffusion are described in section 3.3.1.2.5.

The calibration approach included the initial specification of a single volatilization rate of 1 m/d, consistent with the results of site specific CO_2 and SF_6 experiments. These experiments are described in section 2.1.1.3. The volatilization rate was further modified for PCB homologs and dioxin/furan congeners through calculation of the volatilization rate as a function of contaminant concentration, Henry's constant, velocity, and molecular diffusivity, as described in section 2.1.1.3. Further sensitivity analysis on the calibration was performed to consider temperature effects as will be described in section 5.3.

4.4 CONTAMINANT FATE AND TRANSPORT MODEL CURRENT CONDITIONS CALIBRATION RESULTS

For purposes of the current conditions calibration of the CARP contaminant fate and transport model, model calibration results are presented as comparisons to CARP water column and sediment contaminant data in a variety of formats including x-y, probability, and time series plotting formats. Each plotting format is described briefly below:

X-Y Plots - CARP data and model results coincident in time and space are paired. In each ordered pair, the abscissa, or x-coordinate, represents the measured data and the ordinate, or y-coordinate, represents the model results (e.g., see Figure 4-4 for hexa-CB calibration results). The ordered pairs are plotted using different plotting symbols to identify New York collected (blue circles) and New Jersey collected (orange downfacing triangles) data. Diagonal lines are drawn on the plots showing 1:1 correspondence and +/- a factor of ten correspondence. If the model and data were in perfect agreement, all of the points shown would lie along the line of 1:1 correspondence. Reported in the lower right hand corner of each x-y plot is an accounting that details the number of ordered pairs plotted, N, as well as the number of ordered pairs with elements corresponding to each other within factors of ten, five, three, and two. Outliers are not plotted with either plotting symbol, but are referenced by a numeric location identifier created by HydroQual. X-Y plots have been generated for each contaminant modeled and for several contaminant phases including water column total, water column dissolved, water column particulate on both an organic carbon and a dry weight basis, and sediment bed particulate on both an organic carbon and dry weight basis. These plots are useful for identifying the overall level of agreement between model results and measured data, whether or not there are any biases in the level

of agreement between the model and data collected by one state or the other, and, by researching the numeric location identifiers of outliers, whether or not there is a systematic miss. For example, are all the outliers from one region of the model or are the outliers randomly distributed? Further, these plots give an indication of the level of agreement between modeled and measured contaminant phases. For example, do the measured data underpredict the dissolved phase consistently? Under prediction of the dissolved contaminant phase by the measured data was an expected result based on observations that XAD columns may miss a fraction of DOC-complexed dissolved contaminant.

Probability Plots - Probability plots were constructed to compare the underlying distributions of measured and calculated contaminant concentrations (e.g., see Figure 4-5). Measurements (red circles) and model results (blue triangles) coincident in time and space were each independently ordered, ranked, and plotted on probability axes. Perfect agreement between measured and modeled contaminant concentrations would result in identical probability distributions. Similar to the X-Y plots described above, probability plots have been generated for all contaminants modeled and for several contaminant phases. Probability plots are useful for assessing whether or not the model and data represent the same overall range (i.e., slopes of the distributions and maxima and minima values) and whether or not the model and data have the same central tendency (i.e., 50^{th} percentile values and 50^{th} percentile values plus/minus one standard deviation).

Time Series Plots - Time series plots were constructed to display the time record of model results and data at a given location (e.g., see Figure 4-6 for four locations in the Passaic River). Time series results are presented for water column total contaminant on a mass per volume basis, water column particulate contaminant on an organic carbon normalized basis, water column dissolved on a mass per volume basis, and sediment contaminant on an organic carbon normalized basis. These plots display the temporal variation in model results and observatons over the CARP data collection period from October 1998 through September 2002. Different plotting symbols are used to display New York collected (i.e., blue triangles) and New Jersey collected (i.e., blue circles) CARP data. Also shown on the plots are the assigned model initial conditions for contaminants in the sediment bed. Multiple station locations are arranged on a page so that the time series plots are useful to some extent in assessing spatial variability. Since the time series results are shown for the four years modeled, they display seasonal or episodic variations in the model results and data rather than long term trends. Features such as spring freshets and the timing of seasonal algal blooms are evident on these plots. These plots were useful for diagnosing the causability of some of the features in the distributions of contaminant concentrations. For example, in producive areas such as the Hackensack River or Long

Island Sound, seasonal algal blooms effectively serve to dilute particulate contaminant concentrations and result in a corresponding decrease in dissolved concentrations. Further, in some instances these plots showed artifacts of the way the models were set up such as differences in the synchronization of tributary carbon and contaminant loadings.

Each of these plottings formats are considered below on a contaminant specific basis in a discussion of the CARP calibration results.

4.4.1 PCB Homologs

The CARP model caibration results for PCB homologs are presented in Appendix 4B for each of the three plotting types described above. An overall summary of the CARP model and data comparisons is provided for PCB homologs on Figure 4-7. The overall conclusions of the model and data comparisons for PCB homolog concentrations is that the model and data agree reasonably well for the majority of the homologs (i.e., tri-CB, tetra-CB, penta-CB, hexa-CB, hepta-CB, octa-CB, nona-CB, and deca-CB). It is noted that due to a weakness in the organic carbon production model above Poughkeepsie, for the tidal, freshwater Hudson, we relied more on model and data comparisons on a dry weight rather than an organic carbon basis. The model tends to overpredict the mono-CB measurements and, to a lesser extent, the di-CB measurements.

Some of the explanations as to why this overprediction of mono- and di-CB occurs include:

- There may be some general analytical difficulties with obtaining reliable measurements of the monochlorinated compounds.
- CARP monitoring of loading sources lumped mono and di homologs together in some cases. When this occurred, HydroQual's consideration of these measurements assumed that 50% was mono- and 50% was di-.
- Volatilization or some other loss mechanism specific to the lower chlorinated PCBs may have been underestimated or missed in the CARP model.

4.4.2 Dioxin/Furan Congeners

The CARP model calibration results for dioxin/furan congeners are presented in Appendix 4C and include plots in the three formats described above. A summary of the CARP model and data comparisons is provided for 17 individual 2,3,7,8 substituted dioxin and furan congeners on Figure 4-2. Overall, the model and data comparisons for the dioxin and furan congeners are quite good. Generally, 90% of the water column particulate measurements on an organic carbon normalized basis and 100% of the sediment particulate measurements on an organic carbon normalized basis are within a factor of ten of the calculations. More significantly, 65% of the water column particulate measurements on an organic carbon normalized basis and 80% of sediment particulate measurements on an organic carbon normalized basis are within a factor of 3 of the calculations. The model and data agreement is less apparent for dissolved water column concentrations. Generally, the calculated dissolved concentration is higher than the measured dissolved concentration. This in part relates to the fact that dioxin and furan congeners were usually measured by CARP investigators only in the particulate form and the dissolved measurements are a sparse data set. Limited dissolved measurements were made by CARP investigators; however, the margin between the detection limit and the amount recovered was usually very small. It is not clear to what extent the dissolved measurements are accurate and the calculated concentrations might actually be more credible. Therefore, comparisons of measured and calculated dissolved concentrations were considered to be of somewhat questionable merit for model calibration. In 1993, EPA found that typical analytical procedures are inadequate to reliably measure dioxin in water at the low concentrations expected to elicit ecological effects. This analytical limitation is especially true for dissolved dioxin. According to EPA 1993, a high priority should be given to applying new techniques and instrumentation to lower the detection limit for dioxin in water samples.

4.4.3 Cadmium

Relatively little calibration was needed to assign parameter values for processes that affect cadmium. The chemical distribution among inorganic forms was determined from thermodynamic parameters available from NIST without additional calibration (Table 2-1). For cadmium binding to organic matter, well-calibrated models already exist for determining cadmium binding to both fulvic and humic acids. Parameters for this modeling analysis were generated from simulated cadmium binding to humics and fulvics, where the behavior of humic acids was assumed to represent cadmium binding to particulate organic matter, and the simulated behavior of fulvic acids was assumed to represent the binding behavior of dissolved organic matter. The Windermere Humic Aqueous Model, WHAM VI,

(Tipping 1998) was used to simulate cadmium titrations to humics and fulvics in water with composition similar to water in the NY and NJ Harbor, and apparent binding strengths and binding capacities were generated from these simulated titrations. The simulated behavior was simplified from the 56 individual binding interactions simulated in WHAM VI, to a three-site binding model for both dissolved and particulate carbon. The three-site model was designed to include both strong cadmium binding (at sites with limited capacity) and weak interactions at sites with greater capacity. This mixture of sites provides a concentration-dependent binding model such that the apparent binding strength of cadmium with organic matter will increase at lower cadmium concentrations. After developing parameters for three-site descriptions appropriate for both dissolved and particulate organic matter, the model (including all organic and inorganic reactions in Tables 2-1 and 2-2) was used to calculate the distribution of dissolved and particulate cadmium and was compared with measured dissolved and particulate cadmium in the CARP field data. Based on these comparisons, a single site (referred to as P5) in the three-site particulate carbon model was adjusted to improve the fit. These apparent binding strengths and capacities are listed in Table 2-2.

The cadmium calibration results are presented in Appendix 4D for each of the three plotting types described above. An abbreviated summary of the model and data comparisons is presented here as Figure 4-9. In general, the level of agreement between model results and measured data for cadmium is similar to that for HOCs. Overall, the agreement is very good. For sediments, the overall range of calculated cadmium concentrations is not as wide as the range of measurements. This is evident on the probability distribution presented in Appendix 4D.

4.4.4 Mercury and Methylmercury

Chemical distribution of mercury and methylmercury include both inorganic and organic forms. For inorganic forms, suitable binding constants were available in the literature (Table 2-1). A number of sources were also found for describing organic matter binding. With a procedure and rationale similar to that described for cadmium, these sources were assembled into a multiple site model appropriate for mercury and methylmercury (Table 2-2).

Mercury methylation rates were simulated as a function of the calculated rate of sulfate reduction obtained from the SWEM-based CARP organic carbon production model, given the assumption that only non-ionic forms of mercury are available for methylation. The combination of sulfate-reduction and bioavailability is based on a conceptual model of mercury methylation proposed by Gilmour and

Henry (1991) that predicts variable methylation potential across a salinity gradient (Figure 4-10). This conceptual model is supported by studies that have documented relationships between measured methylation rate and measured sulfate reduction (such as King et al. 1999, 2001). Measured methylation rates in the CARP model domain, paired with calculated sulfate reduction rates taken from the CARP organic carbon production model, show a similar relationship (Figure 4-11).

The other element of this conceptual model is that non-ionic forms of mercury (e.g., HgS^o, $Hg(HS)_2^o$) are more bioavailable to sediment microorganisms. Using the detailed chemical speciaton model developed for CARP, the bioavailability of sediment mercury can be simulated over a range of sulfide concentrations and pH values (Figure 4-12). At low sulfide concentrations mercury is largely bound with sediment organic matter is not bioavailable. As sulfide concentrations increase, mercury is increasingly drawn away from the organic matter resulting in the formation of non-ionic mercury sulfide species (HgS^o, $Hg(HS)_2^o$) that are bioavailable for methylation by sulfate reducing bacteria. As sulfide concentrations continue to increase, the distribution of mercury sulfide complexes is shifted from non-ionic mercury sulfides to charged polysulfide species (e.g., HgS_2^{2-}, $Hg(HS)_3^-$) resulting in reduced bioavailability and inhibited methylation at high sulfide concentrations.

These combined relationships were used to calibrate rate constants for methylation rate as functionally described in Figure 4-11. The resulting model describes spatial and seasonal patterns of mercury methylation that agree remarkably well with measured methylation rates in the CARP model domain. Comparison of predicted rates with measured rates in the Hudson River (Heyes et al., 2004) and Long Island Sound (Hammerschmidt and Fitzgerald, 2004) are shown in Figure 4-13.

Net methylation rates are dependent on both the methylation rate and the demethylation rates. Initial demethylation kinetic constants and rate coefficients were based on the Aquatic Cycling of Mercury in the Everglades (ACME) data collected by Marvin-DiPasquale and Oremland (1998) in the sediments and soils of the Florida Everglades. The relatively high concentrations used in the ACME data have likely resulted in demethylation rates lower than may be appropriate under field condition. Calibration and comparison with CARP data have supported the use of higher demethylation rates. The sediment methylation concentrations that result from calibrated methylation and demethylation is shown in Figure 4-14.

The mercury and methylmercury model and data comparisons are presented in Appendix 4D. It is noted that methylmercury measurements were limited to the water column only in CARP. The

agreement between model calculations and the limited available methylmercury data is not as good as for other contaminants. Mercury comparisons are favorable for particulate concentrations in the water column and sediment, less so for water column dissolved. Some of the reasons for discrepancies include:

- The laboratory analysis method for methylmercury involved a distillation which does not have a full recovery. All of the net methylmercury measurements were corrected using an historic mean methylmercury distillation recovery of 90.6%. This historic mean efficiency factor may not be exactly correct for each measurement to which it was applied. In this sense, the methylmercury measurements have some uncertainty.
- The methylmercury data are the weakest of the CARP metal measurements. These measurements were most often non-detect, showed the worst reproducibility, and most frequently had blank contamination.

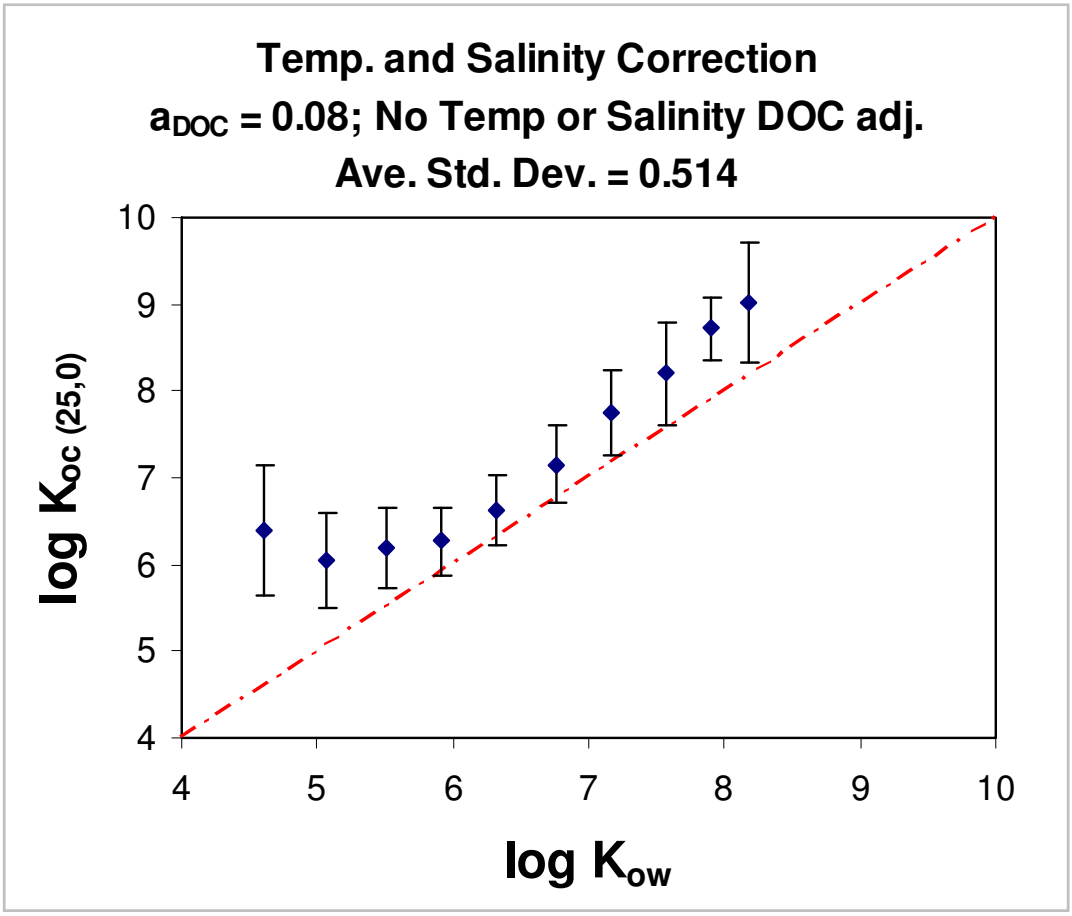

Figure 4-1. Final calculation of log K_{POC} for PCB homologs with temperature and salinity corrections

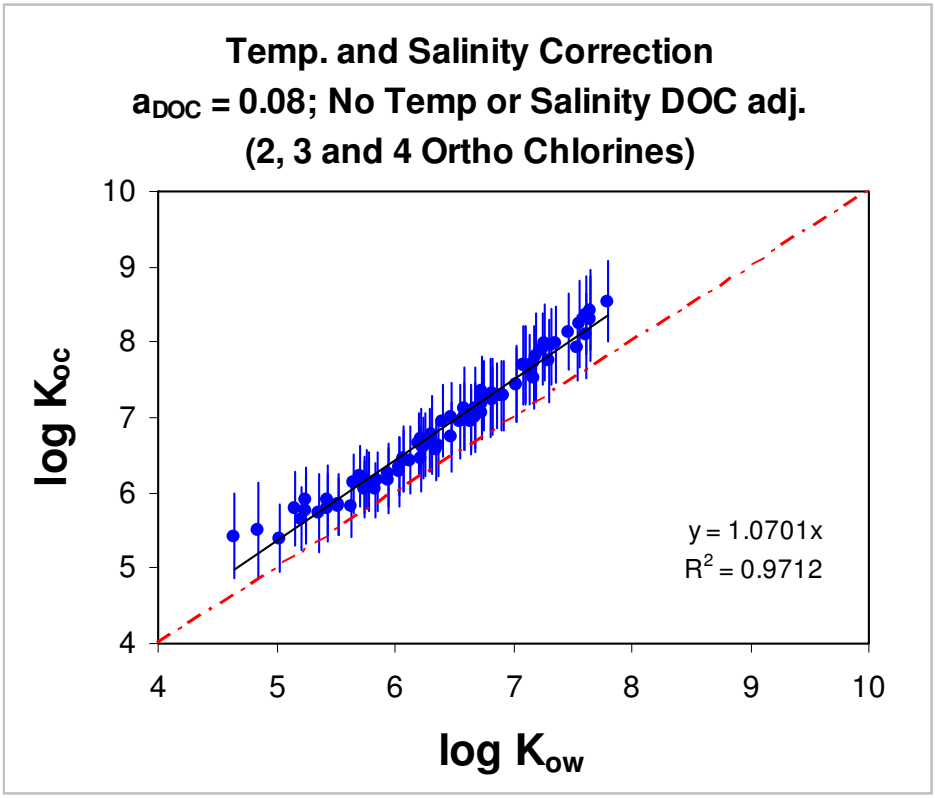

Figure 4-2. Consideration of log K_{POC} for individual PCB congeners with temperature and salinity corrections. Congeners with 0- and 1- ortho chlorine substitutions have been omitted.

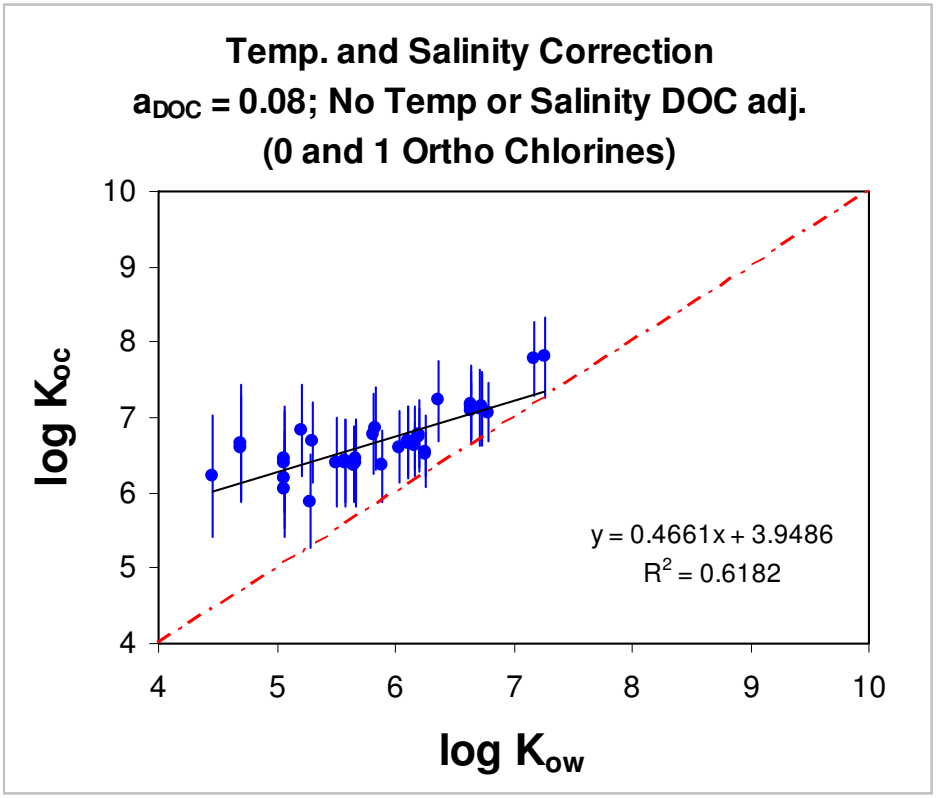

Figure 4-3. Consideration of log K_{POC} for individual PCB congeners with temperature and salinity corrections. Results for congeners with 0- and 1-ortho chlorine substitutions.

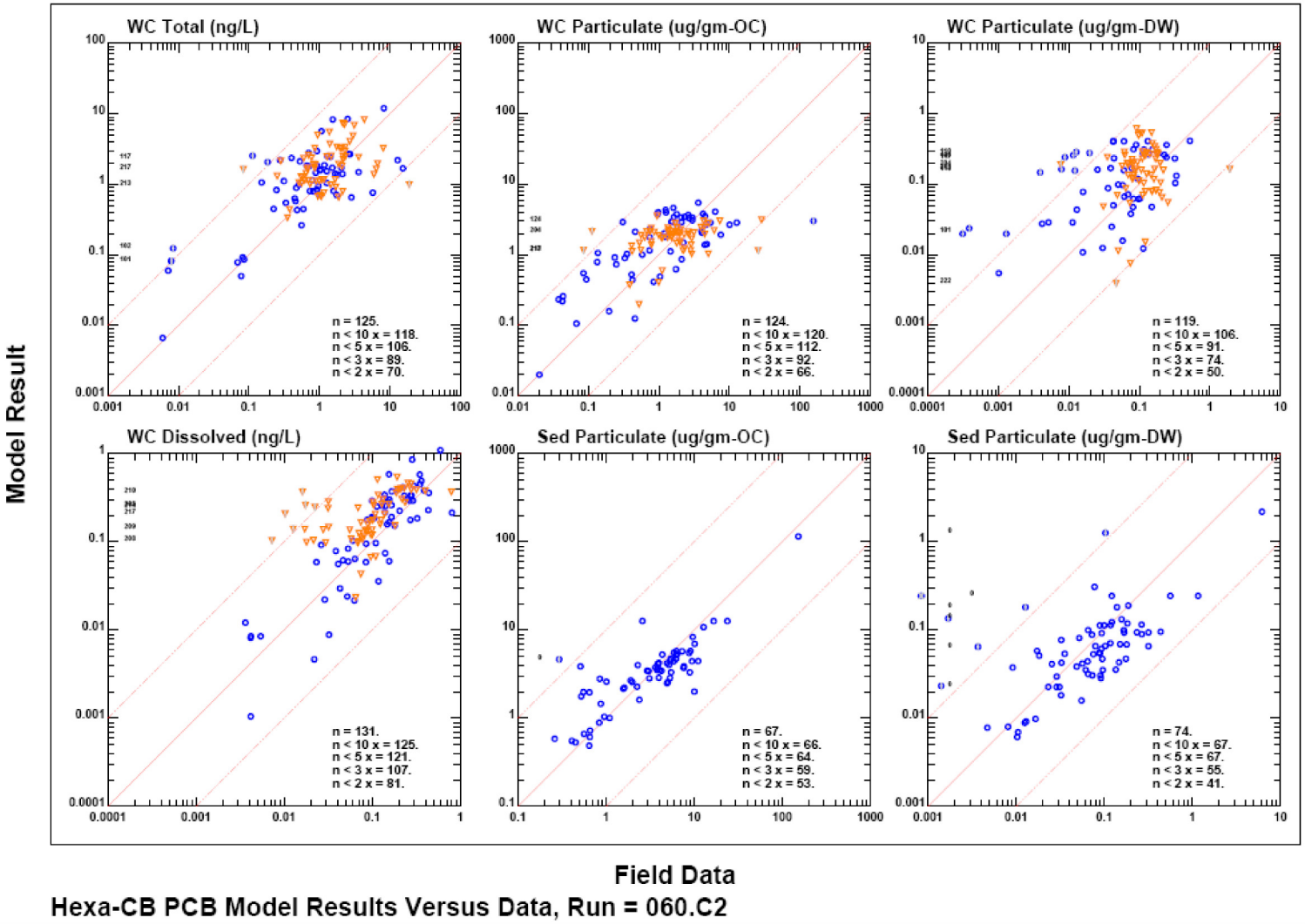

Figure 4-4. Example x-y plots for hexa-CB model and data comparisons

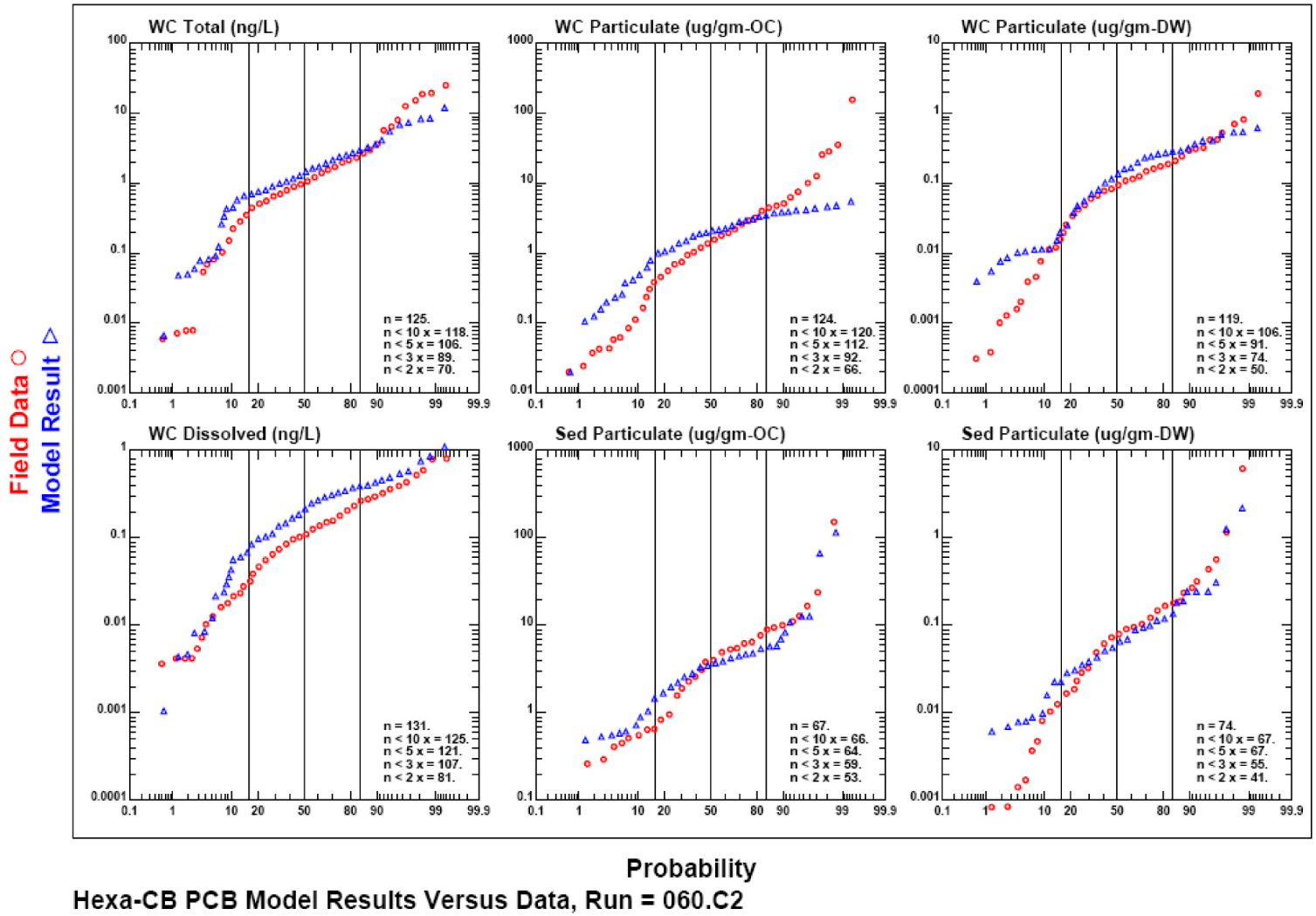

Figure 4-5. Example probability plots for hexa-CB model and data comparisons.

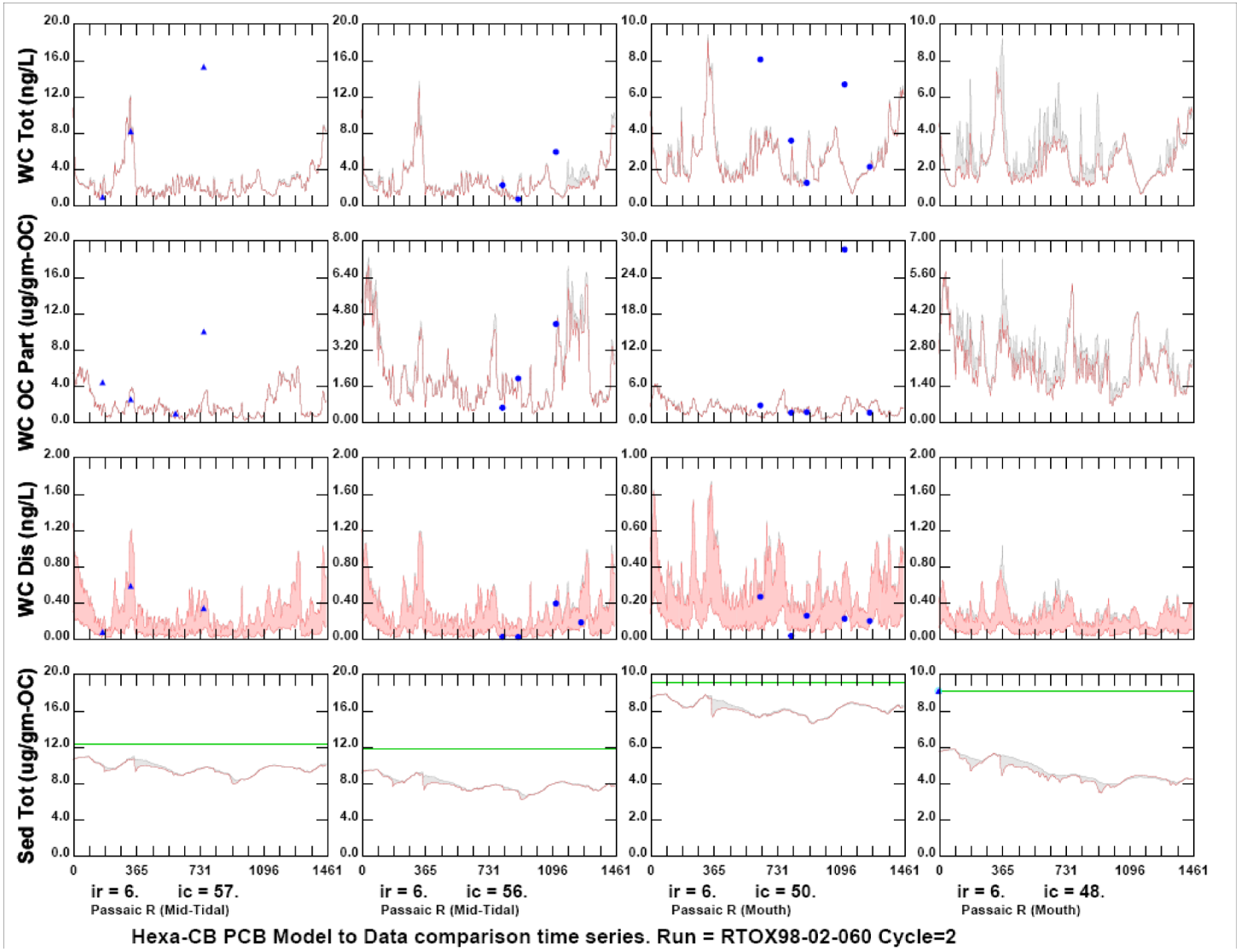

Figure 4-6. Example time series model and data comparisons for hexa-CB.

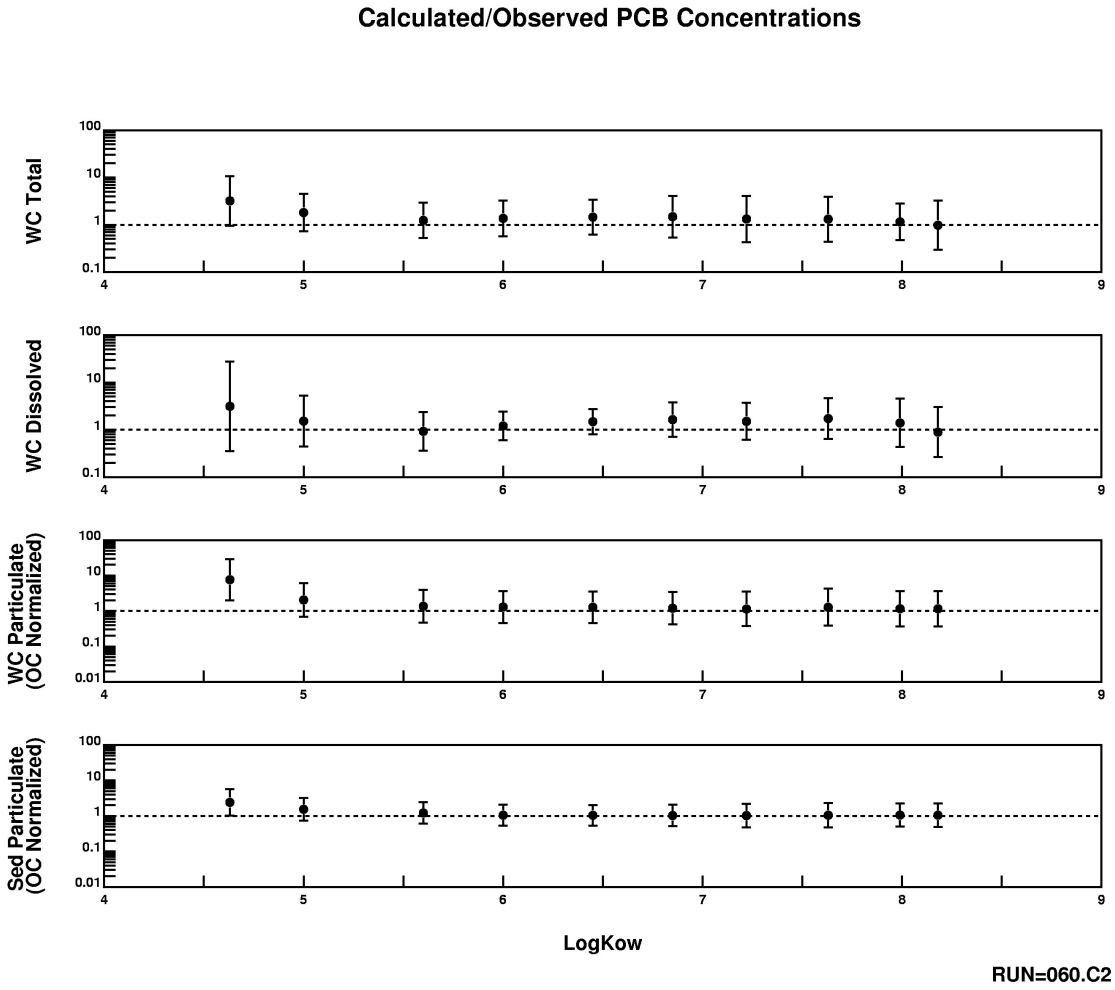

Figure 4-7. PCB Current Conditions Model and Data Comparison Summary

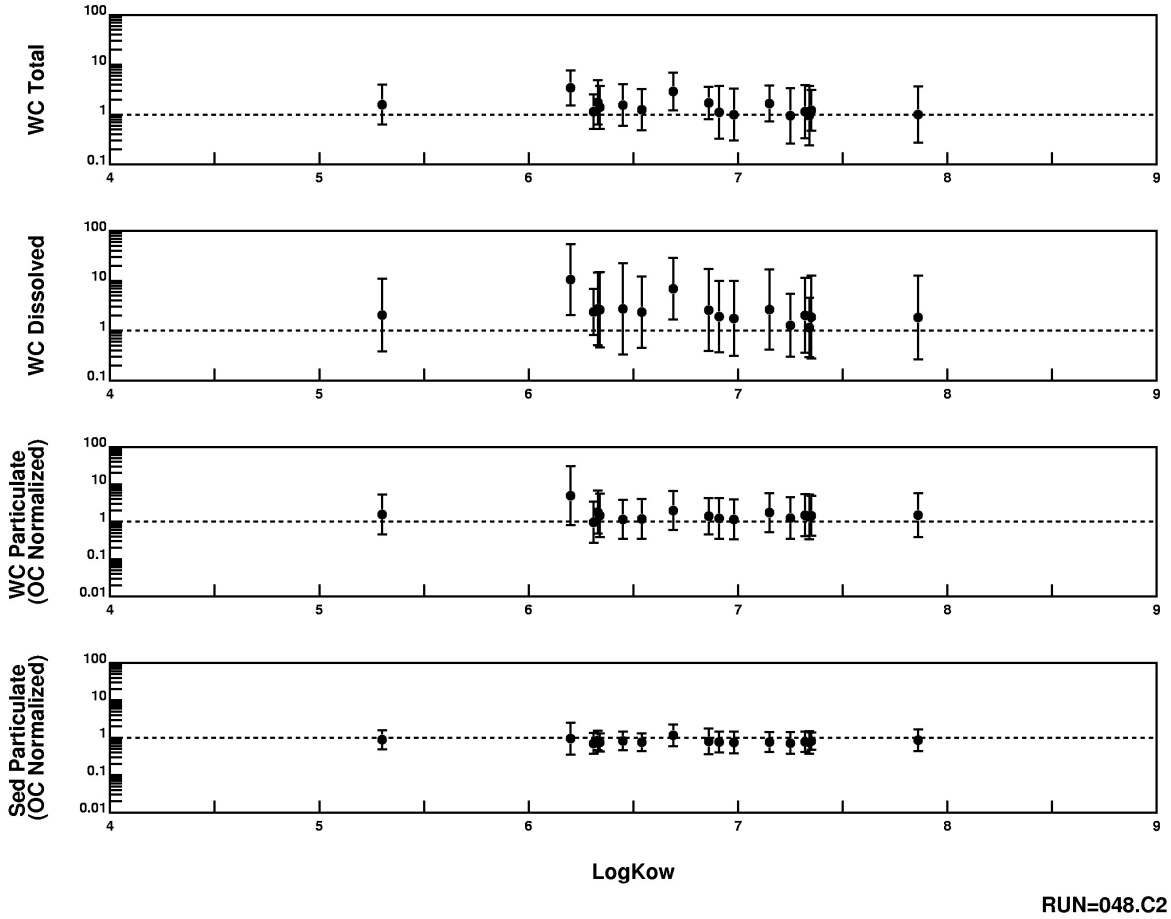

Figure 4-8. Dioxin/furan Congeners Current Conditions Model and Data Comparison Summary

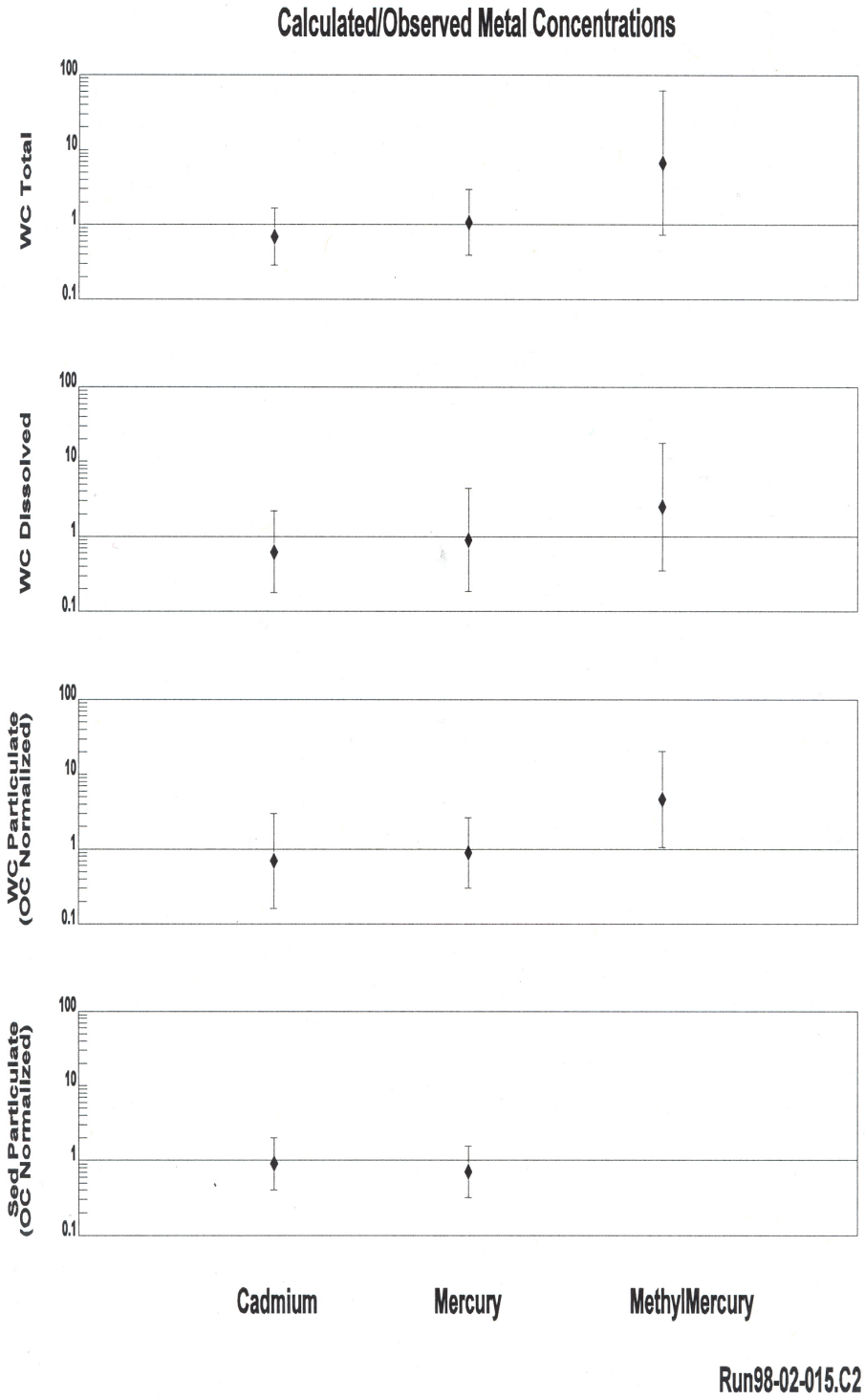

Figure 4-9. Cadmium and Mercury Current Conditions Model and Data Comparison Summary

Conceptual model of Mercury Methylation

(Gilmour and Henry 1991 as redrawn by Langer et al 2001)

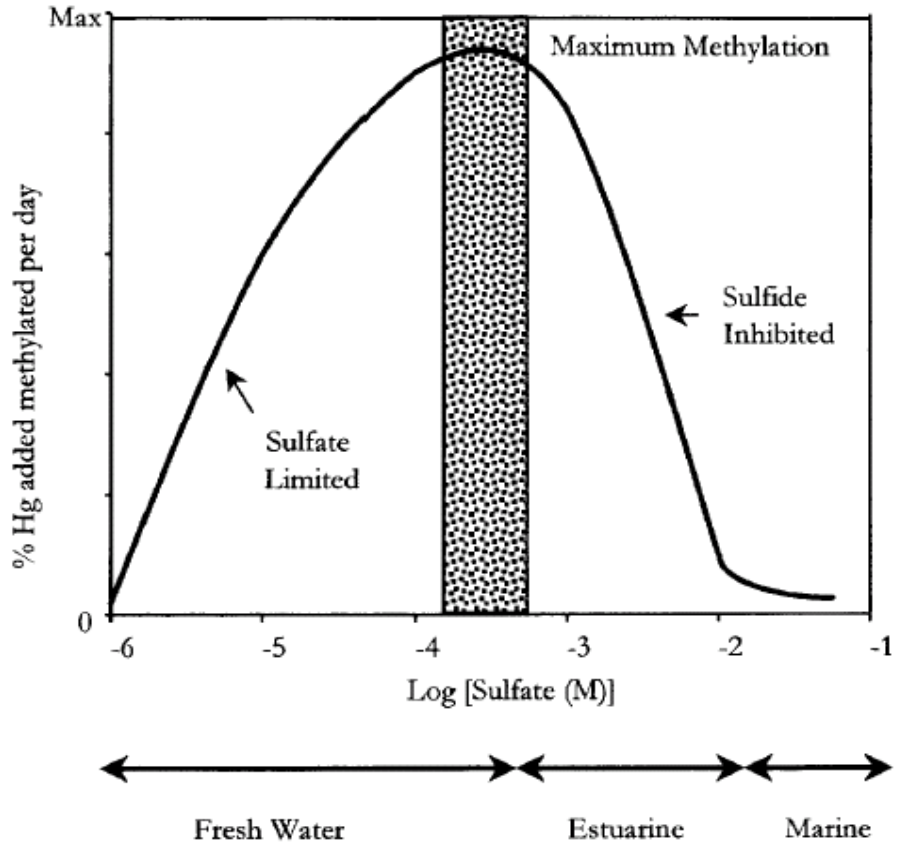

Figure 4-10. Conceptual Model of Mercury Methylation

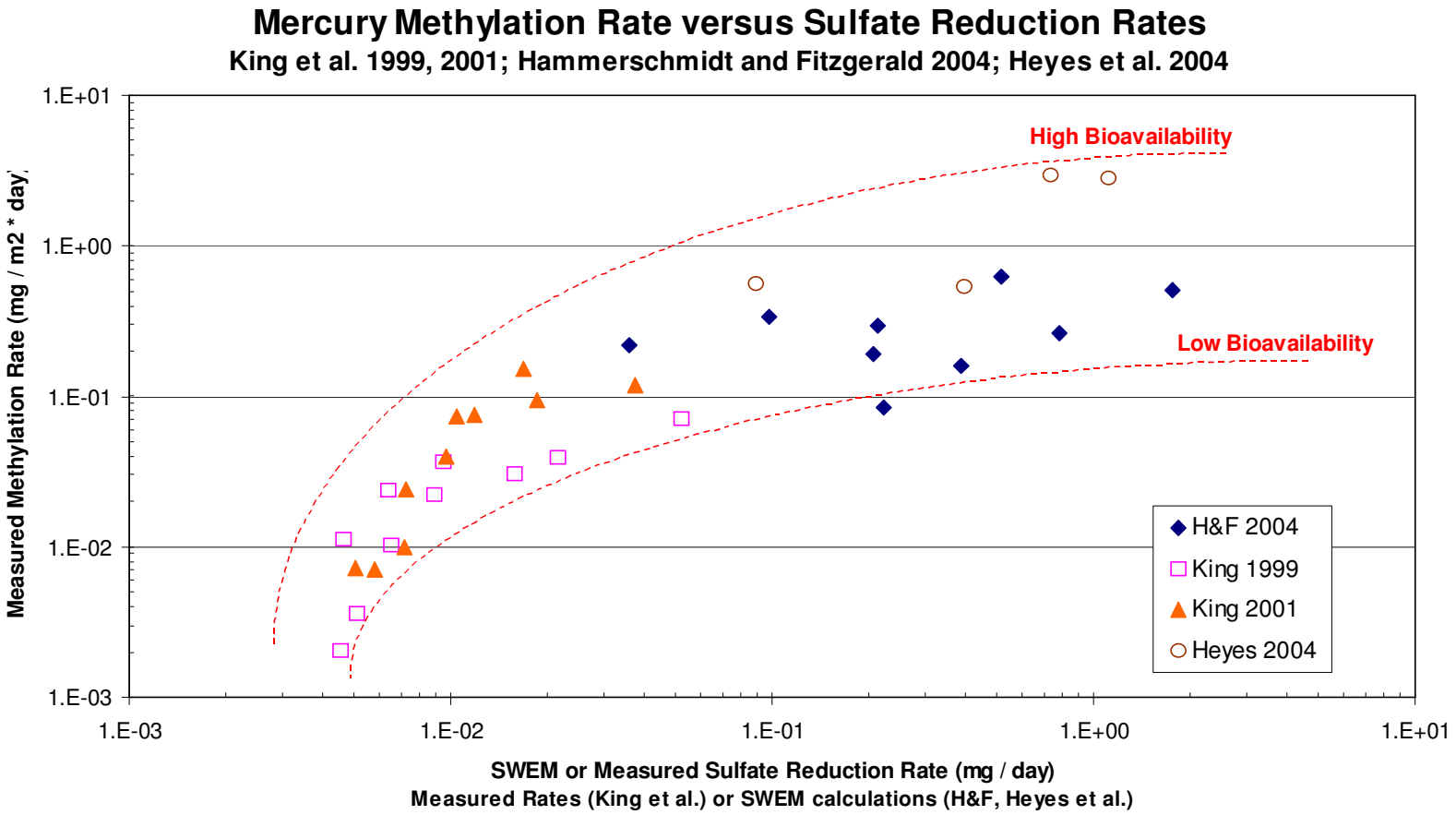

Figure 4-11. Mercury Methylation Rates vs. Sulfate Reduction Rates

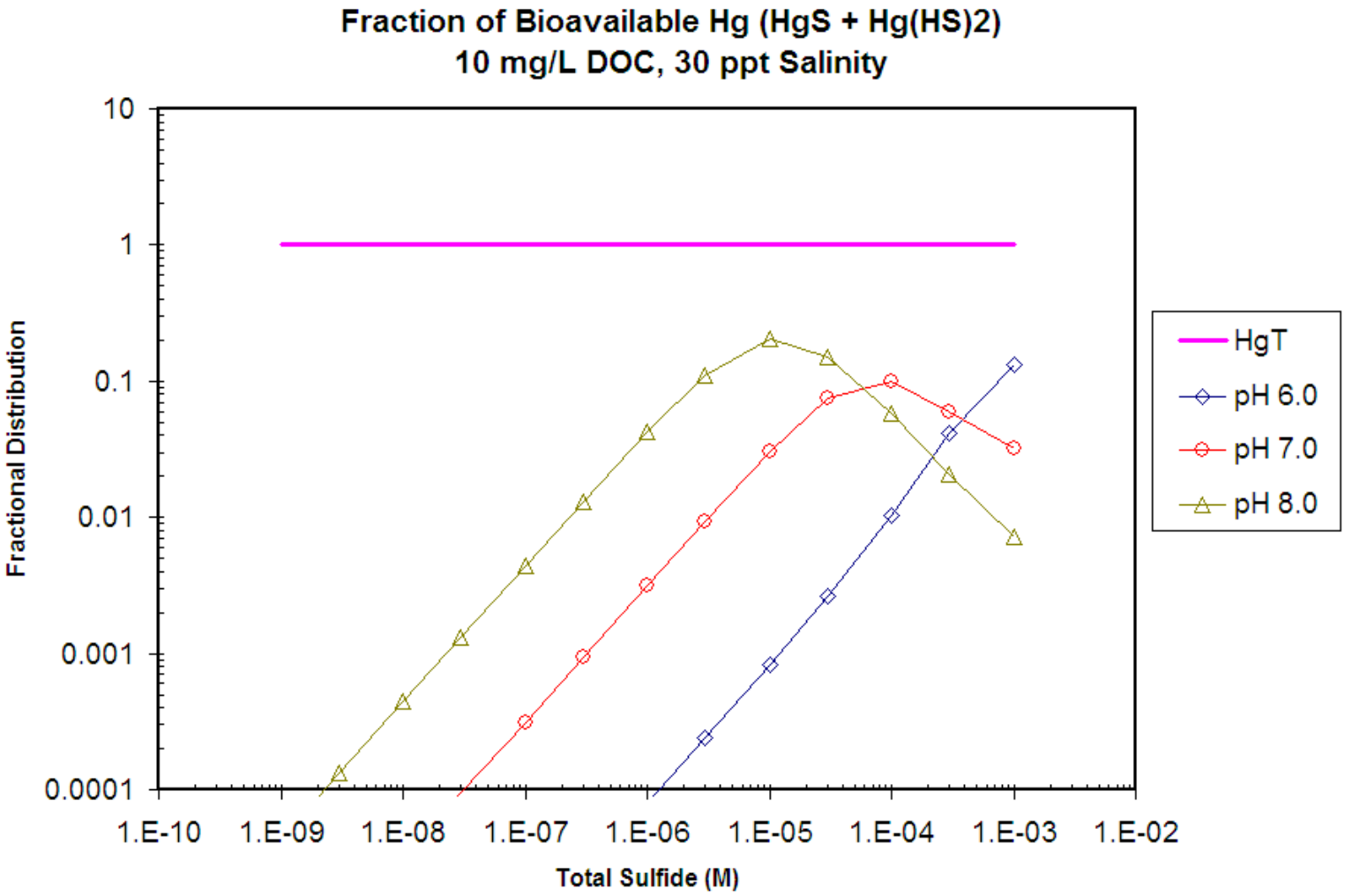

Figure 4-12. Fraction of Bioavailable Hg (HgS + Hg(HS)2)

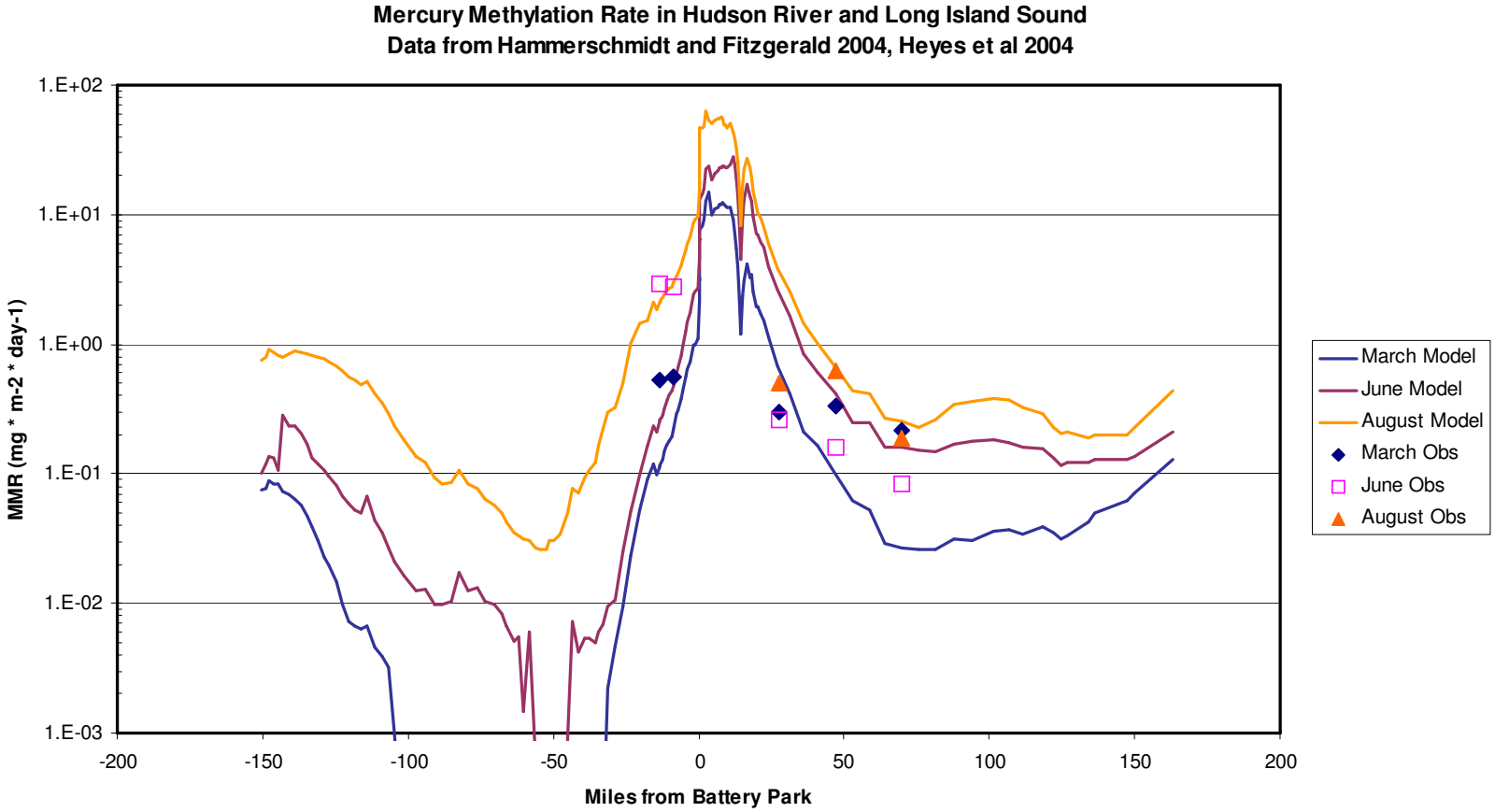

Figure 4-13. Mercury Methylation Rate in Hudson River and Long Island Sound

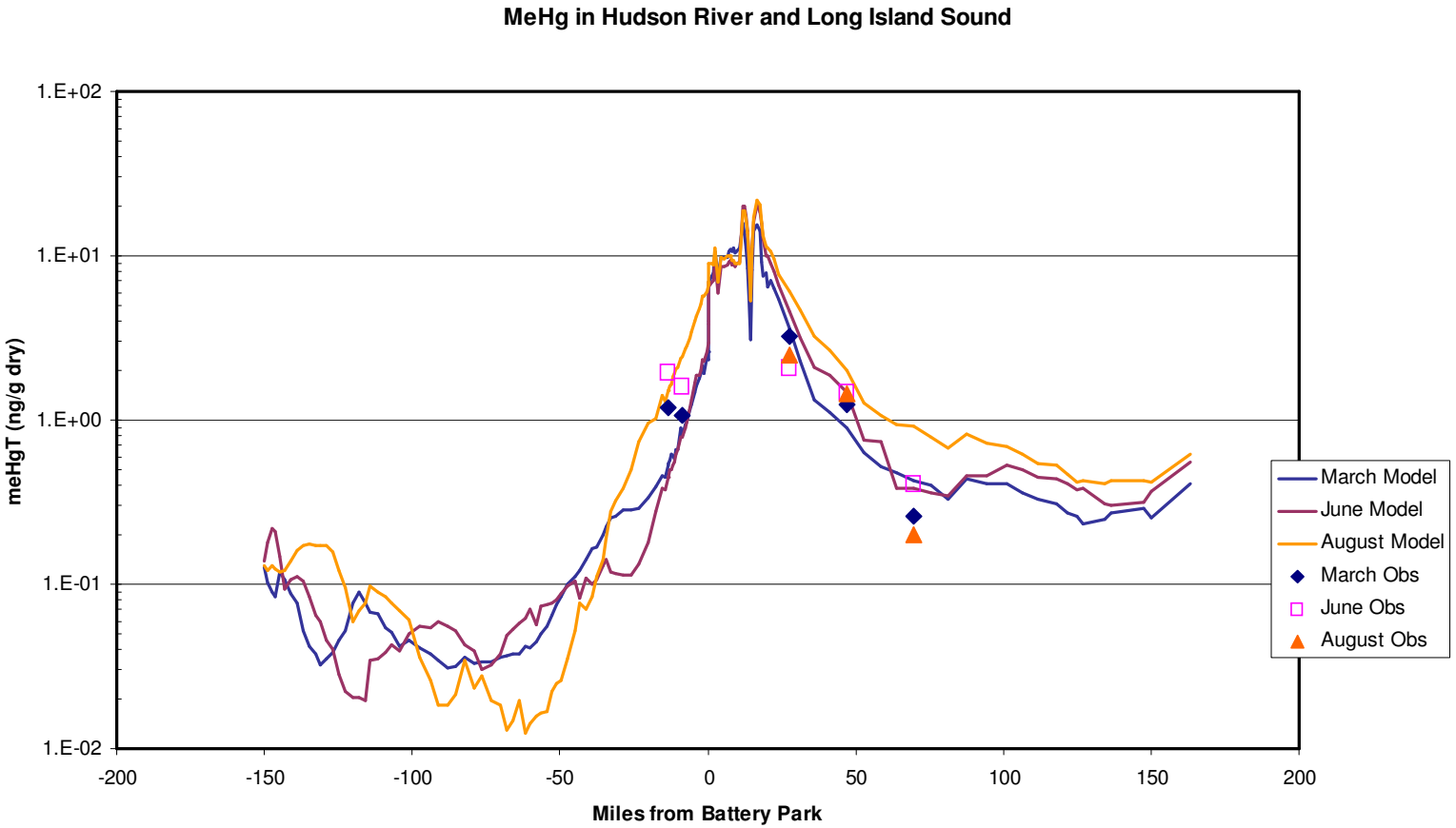

Figure 4-14. MeHg in Hudson River and Long Island Sound

SECTION 5.0

CONTAMINANT FATE AND TRANSPORT MODEL SENSITIVITY ANALYSES

Sensitivity analysis is a process consisting of varying individual selected model input parameters (while holding the other parameters constant) to determine the individual effect on model response. The resulting variations in calculated state variables are a measure of the sensitivity of model predictions to the parameter whose value was varied. Sensitivity analysis is different than uncertainty analysis, which consists of propagating the relative error in individual selected parameters to determine the resulting error in model predictions. A probabilistic model (e.g. Monte Carlo Analysis) is one method for performing an uncertainty analysis (EPA provides guidance on uncertainty analysis at http://www.epa.gov/superfund/programs/risk). Uncertainty analysis is discussed in an EPA Office of Solid Waste and Emergency Response guidance document on sediment remediation for hazardous waste sites (U.S. EPA, 2005). The guidance document describes that, in general, while quantitative uncertainty analyses are possible and practical to perform with watershed loading models and food chain/web models, they are not so (at the current time practical) for fate and transport models.

Uncertainty analyses were beyond the scope of HydroQual's contract agreement for the development of the CARP model and, as described above, are not part of the standard of practice for contaminant fate and transport models. On this basis, uncertainty analyses with the CARP contaminant fate and transport model were not performed. Numerous sensitivity analyses however were performed with the CARP model. These sensitivity analyses are described below.

5.1 CLEAN BED/TIME TO STEADY STATE SIMULATIONS

At an interim point in the CARP HOC model calibration process (i.e., before the calibration strategy for phase partitioning and volatilization had been finalized), a sensitivity analysis was performed on the assignment of initial contaminant concentrations in the sediment bed. For purposes of these sensitivity calculations, the initial sediment bed concentrations of ten PCB homologs and seventeen dioxin/furan congeners were set to 0 rather than the concentrations interpolated from observed data. "Clean bed" model simulations were carried out for 96 years. The "clean bed" model simulations are included as part of the CARP model sensitivities analysis to the extent that they examine the response of the model to a change in one of its input parameters, in this case, the sediment bed initial conditions. The "clean bed" analysis also provided useful, albeit preliminary, information with management implications in terms of the time behavior of the system and separating observed sediment bed contaminant concentrations into those associated with either current-day or legacy source inputs.

The "clean bed" analysis shows that the time to steady state, or the time required for the contaminant in the sediment bed to increase to a steady concentration in response to a continuous loading source, is less than 96 years for most areas in the core of the NY/NJ Harbor as represented by the CARP model computational grid. It is noted that there are some CARP grid cells for which a leveling off of sediment contaminant concentrations did not occur, even after 96 years. For the most part, these locations were at the oceanward edges of the CARP model domain. In general, a runtime of approximately 32 years is probably sufficient to approach steady state. This is important information for the loading component analysis described in Section 12.0.

Residence time of contaminants in the system and the time to steady state are related to exchange between the water column and sediment bed. For most of the CARP model domain, the particle mixing rate (see Sections 3.2 and 2.1.2.2) controls this exchange. One exception to this is the majority of the East River where shear stresses are extremely high and suspended solids concentrations are relatively low. In major portions of the East River, almost no particle accumulation or particle exchange occurs and the dissolved mixing rate controls exchange between the water column and sediment bed. When/where diffusive mixing controls, particularly for high K_{ow} compounds, time to steady state can be upwards of one hundred years. If any of the mixing processes were overestimated, the CARP model would not be able to maintain elevated contaminant concentrations in the sediment bed.

It is noted that in addition to mixing rates, the effects of sediment transport and "estuarine trapping" also impact the time to steady state. Over the course of a 96 year simulation, particulate phase contaminants are continually resuspended, transported (oftentimes by bottom waters moving in a net landward direction), and redeposited, and this process works to further impede the loss of contaminants to the ocean.

From the perspective of a sensitivity calculation, the results from the "clean bed" analysis show that:

- For most of the CARP domain, the time for the top 10 cm of the sediment bed to reach steady state is approximately 30 years.
- Some areas at the outer fringes of the CARP model domain required 100 years or longer to reach steady state.
- The "clean bed" analysis results indicate that the "memory" of Harbor sediments to past contaminant loads is likely on the order of 30 years (since it takes that long for sediments to reach a steady-state with current continuous loadings) and that the assignment of initial contaminant conditions in the sediment bed is critical in computing long-term responses.

In addition to interesting sensitivity results, the "clean bed" analysis results also had management implications. The "clean bed" analysis shows how much of the contaminant concentrations observed in surficial bed sediments today can be accounted for by current contaminant loading sources. These results are summarized on the diagrams contained in Appendix 10. Each diagram contained in Appendix 10 presents results of the "clean bed" analysis for a different PCB homolog or dioxin/furan congener. Calculated contaminant concentrations in the sediment bed are presented in a color concentration map format on each diagram in three ways: based on interpolated data, based on the results of a CARP model "clean bed" simulation, and based on the subtraction of interpolated data and "clean bed" simulation results. The interpolated data represent the contamination due to both current and legacy sources of contamination. The "clean bed" simulation results represent contamination due only to the current loading sources included in the CARP model. The subtraction of the "clean bed" results from the interpolated data indicates the contribution to sediment contaminant concentrations from loading sources not included in the CARP model, interpreted to be legacy sources. Example diagrams from Appendix 10 are presented here as Figure 5-1 for 2,3,7,8-TCDD.

The diagrams contained in Appendix 10 and Figure 5-1 demonstrate that for the majority of the contaminants, the observed contaminant concentrations in the sediment bed can not be explained by the current day loadings and are therefore likely due to historical sources. This is particularly evident for some of the higher chlorinated PCB homologs, 2,3,7,8-TCDD, and 1,2,3,4,7,8-HxCDF. Specific features represented on the diagrams in Appendix 10 include:

- There appears to be a PCB loading source to the lower East River in the vicinity of Newtown Creek which is not included in the CARP current loadings. The lower East River is known for being a "hard bottom" environment with the exception of a few discrete depositional areas. Many of the field programs that HydroQual has been involved with have, in general, been unable to collect cores or biological samples from the lower East River bed without specialized equipment suited to hard bottom environments. Consistent with the "hard bottom" conditions in the East River, it is possible that historical contamination would not be buried by deposition of more recently deposited cleaner material and would persist in surficial sediments. On this basis, it is likely that there was a historical PCB loading in the lower East River; however, we cannot fully rule out the possibility that an ongoing industrial source was not sampled by CARP and is not represented or captured in CARP STP, CSO, or SW sampling.

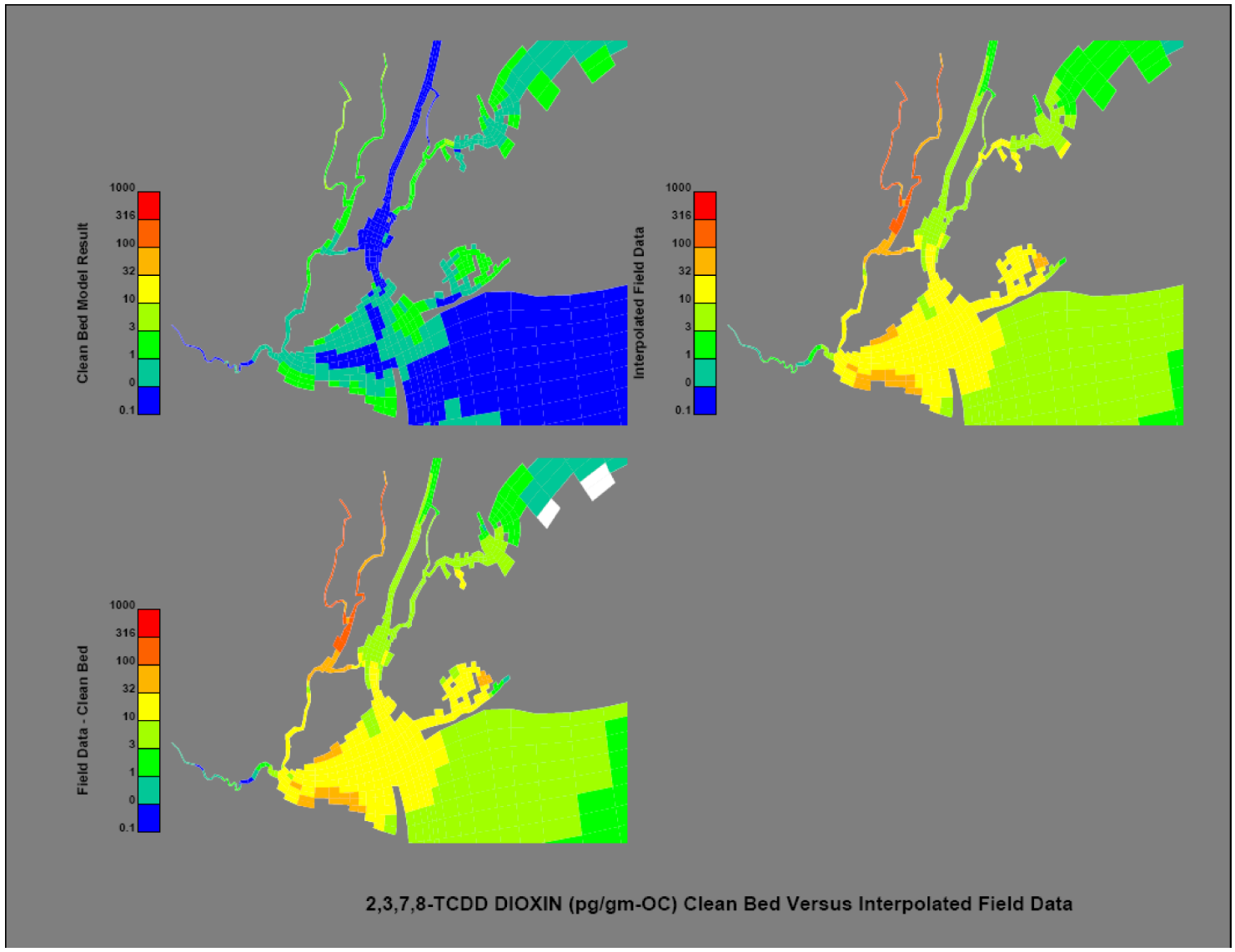

Figure 5-1. "Clean Bed" analysis diagrams for 2,3,7,8-TCDD

- Overall the mono- and di- chlorinated homologs do not appear to be as dominated by historical loading sources as some of the higher chlorinated PCB homologs. This is consistent with the fact that mono- and di- chlorinated homologs have lower partitioning to organic carbon and therefore have greater opportunity to exit the estuary over time (i.e., via dissolved phase volatilization and ocean exchange).

- The influence of historical PCB contamination in the North River (i.e., the Hudson River opposite Manhattan) appears to be a combination of 1.) historical loadings dominated by lower chlorinated homologs transported somewhat rapidly from upstream and 2.) the longer residence time of more particle associated higher chlorinated homologs in the bed coming from local Harbor and upstream sources.

- In the case of 2,3,7,8-TCDD, historical sources in the Passaic River and Jamaica Bay are apparent. On the basis of CARP "clean bed" model results, it is not clear whether or not elevated concentration levels around the edges of Raritan Bay, not accounted for by current CARP model loadings, are due to historical loading sources along the Raritan Bay shorelines or the previous transport of contaminated particles from the Passaic River.

- For 1,2,3,4,7,8-HxCDD, 1,2,3,6,7,8-HxCDD, and 1,2,3,7,8,9-HxCDD there is some suggestion of historical sources in Jamaica, Raritan, and Little Neck Bays as well as elevated current day sources to the East River, Jamaica Bay, and Hackensack River. For 1,2,3,7,8-PeCDD, the suggestion of a historical source to Little Neck Bay is also apparent. For 1,2,3,7,8-PeCDF, historical sources to the East River, Raritan Bay, and Jamaica Bay are also apparent.

- For several of the dioxin and furan congeners other than 2,3,7,8-TCDD, there is a suggestion of an Upper Newark Bay/lower Hackensack River historical source.

- An historical source of 2,3,7,8-TCDF to the western Upper Bay, north of the confluence with Kill van Kull, is suggested.

The reader is reminded that the diagrams presented in Appendix 10 and Figure 5-1 were prepared using an interim version of the CARP model. Before any final conclusions are drawn or actions taken, findings should be confirmed, under an independent effort, by running the final CARP model and/or applying a more localized rather than a system-wide model in areas such as the Hackensack and Passaic Rivers and Jamaica Bay. Further, the representativeness of the interpolated observed data should also be checked and factored into any decision making or conclusion drawing.

Where historical contaminant sources are implicated, effort, beyond the scope of this project, should be undertaken to check former land uses and practices.

5.2 ORGANIC CARBON PARTITIONING SENSITIVITY ANALYSIS

5.2.1 Site Specific vs. K_{ow} Based Partitioning to Organic Carbon

The sensitivity of the CARP contaminant model was tested for PCB homologs under a number of different formulations for partitioning of contaminants between dissolved and particulate phases. These sensitivities included consideration of both two phase (i.e., POC complexed and total dissolved) and three phase (i.e., POC complexed, DOC complexed, and freely dissolved) partitioning. The partition coefficient to POC was specified in sensitivity calculations based on both octanol-water partitioning and site-specific partitioning relationships. Additional sensitivity work performed on the three-phase partitioning using site-specific partitioning relationships are described below.

5.2.2 Potential Temperature and Salinity Effects on Site Specific Partitioning to Organic Carbon

The derivation of the site-specific partition coefficients used in the CARP contaminant model for partitioning to POC and DOC are described above in Sections and 2.1.1.1, 2.1.2.1, 4.3.1, and 4.3.2. The plots showing preliminary field derived partition coefficients and the site-specific data are presented in Section 4.3.2 and illustrate that there is a large amount of variability in the site-specific contaminant measurements of fraction dissolved contaminant. These plots also illustrate that observed partitioning behavior in the NY/NJ Harbor system on average deviates significantly from that which in theory is suggested by octanol-water partitioning. An exercise was undertaken to discern whether or not any of the observed variability in ratio of POC-complexed contaminant to freely dissolved contaminant across locations and survey periods for PCB homologs could be attributed to either or both of temperature and salinity differences and/or chlorine substitution patterns. The exercise resulted in bringing the partitioning closer to octanol-water partitioning, but did not eliminate or account for the observed variability. Specific model simulations performed using three phase partitioning include various combinations of K_{POC} specified as a function of temperature and salinity and several values of A_{DOC} (i.e., 0.02, 0.1, and 0.08). We concluded from these analyses that the model was sensitive to the selection of an A_{DOC} value and that by using 0.08, overall, the model best represented the observed data. We also concluded that temperature and salinity dependency considerations in the calculation of site-specific partition coefficients did little to change the overall model calibration.

5.3 VOLATILIZATION SENSITIVITY ANALYSIS

The sensitivity of the CARP HOC fate and transport model to temperature effects on the Henry's constant controlling the back diffusion gas exchange rate was tested at the request of the CARP MEG for PCB homologs. The specific formulations used are described below.

For each PCB homolog, the value of both the Henry's Constant (K_H) and the enthalpy for air water exchange (ΔH_{AW}) were needed. These are tabulated below in table 5-1. Enthalpies for air water exchange used in the model were obtained from Bamford et al., 2002. It is noted that these enthalpies are in disagreement with those reported in Li et al., 2003. After consultation with the CARP MEG, the enthalpies reported by Bamford et al were used in the CARP model.

Table 5-1. Constants Used in Volatilization Rate Calculations

Homologue	K_H (Pa-m^3/mol)	[1]ΔH_{AW} (KJ/mol)	[2]ΔH_{AW} (KJ/mol)
Mono-CB	20.44	50.69	48.37
Di-CB	23.75	48.65	50.79
Tri-CB	28.08	42.55	53.28
Tetra-CB	36.04	27.73	55.78
Penta-CB	45.19	33.47	58.33
Hexa-CB	57.50	67.25	60.97
Hepta-CB	58.07	110.93	63.48
Octa-CB	40.76	160.30	66.08
Nona-CB	63.78	154.00	68.57
Deca-CB	97.48	145.00	71.09

[1] Bamford et al., 2002 (used in model calculations)
[2] Li et al., 2003 (not used)

The final equation used for calculating the dependence of the Henry's Law Constant on temperature is shown below as equation 5-1.

$$K_H'(T(°K)) = K_H'(298°K) \times EXP\left(\frac{\Delta H_{AW}}{R} \times \left(\frac{1}{298°K} - \frac{1}{T(°K)}\right)\right) \qquad (5\text{-}1)$$

where:

ΔH_{AW} is the enthalpy of phase change, R is the universal gas constant expressed as 8.314×10^{-3} (KJ mol^{-1} $^{o}K^{-1}$), and $K_{H'}$ is the dimensionless Henry's Law Constant. The dimensionless Henry's Law Constant, $K_{H'}$, is defined as the Henry's Law Constant, K_H (Pa m^3 mol^{-1}), divided by the universal gas constant, R (8.314 Pa m^3 mol^{-1} $^{o}K^{-1}$), and the absolute temperature (^{o}K).

The temperature effects on the Henry's constant controlling the back diffusion gas exchange rate were incorporated into the final calibrations for PCB homologs. It was not possible to include these effects for other HOCs (i.e., dioxin/furan congeners, PAHs, and pesticides) because we did not have reliable values for the enthalapies of phase change. Based on model results for PCB homologs, the modification to a more sophisticated formulation for volatilization had only minor impact on the model response.

SECTION 6.0

CONTAMINANT FATE AND TRANSPORT MODEL HINDCAST VERIFICATION

As a further test of the critical time constants (i.e., those model inputs controlling rates of contaminant exchange between the sediment and the water column) developed during the current conditions calibration of the CARP contaminant fate and transport model, hindcast verification calculations were performed. Hindcast simulations starting in 1965 and calculating forward through the conclusion of the CARP monitoring program in 2002 were performed. Direct calculations of hydrodynamics, sediment transport, and organic carbon production for all thirty-seven of these years were not possible . Instead, hydrodynamics, sediment transport, and organic carbon were simulated for thirty-seven years in series based on selecting surrogate conditions. Individual years included in the thirty-seven year series were selected, based on similarities to the observed flow of the Hudson River, from six water years for which CARP model inputs are available: 1988-89, 1994-95, and 1998-2002. Sediment transport and organic carbon were calculated continuously based on the pattern of selected hydrodynamics. The mapping of the actual water years to modeled water years are shown below in Table 6-1.

Table 6-1. Mapping of actual water years to surrogate years for which CARP hydrodynamic, sediment transport, and organic carbon production model inputs are available.

Water Year	Year Used	Water Year	Year Used	Water Year	Year Used	Water Year	Year Used
1965-66	1994-95	1975-76	1999-00	1985-86	2000-01	1995-96	1999-00
1966-67	1994-95	1976-77	1999-00	1986-87	1988-89	1996-97	1999-00
1967-68	2000-01	1977-78	2001-02	1987-88	2001-02	1997-98	2000-01
1968-69	2001-02	1978-79	1999-00	1988-89	itself	1998-99	itself
1969-70	2000-01	1979-80	1994-95	1989-90	1999-00	1999-00	itself
1970-71	1988-89	1980-81	1994-95	1990-91	1999-00	2000-01	itself
1971-72	1999-00	1981-82	2000-01	1991-92	2001-02	2001-02	itself
1972-73	1999-00	1982-83	2000-01	1992-93	1999-00		
1973-74	1999-00	1983-84	1999-00	1993-94	2000-01		
1974-75	1999-00	1984-85	1994-95	1994-95	itself		

The chemicals for which CARP hindcast calibration verifications were performed include: cesium, 2,3,7,8-TCDD, and 4 PCB homologs (di-, tetra-, hexa-, and octa-). A description of the hindcasts for each these contaminants is provided below.

6.1 HINDCAST VERIFICATION FOR CESIUM

There are known historical sources of ^{137}Cs to NY/NJ Harbor as well as extensive data in sediments. For this reason, ^{137}Cs is an excellent substance for which to perform a CARP model hindcast verification. A successful calibration of the CARP model for cesium increases the credibility of the CARP model for contaminants of concern.

6.1.1 Development of Cesium Hindcast Loadings

Historical cesium loadings included in the CARP model hindcast calculation include three sources: The Indian Point Power Plant, direct atmospheric deposition over the open water surface from fallout due to weapons testing, and atmospheric deposition in both the upstream watershed and over land from fallout due to weapons testing resulting in tributary head of tide and stormwater runoff loadings. A CARP model load generation mechanism is described for each of these sources. An additional consideration is setting a sediment initial condition for cesium given that weapons testing started in the early 1950's and peaked in the early 1960's before the startup of the CARP hindcast calculations.

6.1.1.1 Indian Point Power Plant Cesium Loadings

Indian Point Power Plant liquid effluent releases of ^{137}Cs to the Hudson River have been monitored and reported to the Nuclear Regulatory Commission and appear in Table 1-5 of Chillrud, 1996. The release of liquid effluent ^{137}Cs from the Indian Point Power Plant as reported in Chillrud, 1996 have been included as a loading source in the CARP ^{137}Cs hindcast verification. Between 1966 and 1992, 49.2 Ci of ^{137}Cs were released from the Indian Point Power Plant. The maximum annual release, 22.5 Ci, occurred in 1971.

The ^{137}Cs load to the Hudson River from the Indian Point Power Plant was inputted into the CARP contaminant hindcast model uniformly over ten water column depth layers. Figures 6-1 and 6-2 display the Indian Point Power Plant ^{137}Cs load as a time series. Figure 6-1 displays the tabulation from Chillrud 1996 by calendar year. Figure 6-2 displays the CARP model inputs by water year.

6.1.1.2 Cesium Atmospheric Deposition

The atmospheric input of ^{137}Cs considered in the CARP hindcast verification calculation was generated by Thomann et al., 1989 using the data on ^{90}Sr areal loading rates given in Bopp and Simpson, 1984. A ^{137}Cs to ^{90}Sr ratio of 1.59 was used. The areal loading rates were inputted directly into the CARP model which is structured to accept rates of atmospheric deposition on an areal basis. The loading rates were adopted from Figure 5-1 in Thomann et al., 1989 and are in agreement with those tabulated in Table 1-2 of Chillrud, 1996 (shown here as Figure 6-3). Peak deposition occurred in 1963, prior to the start of the CARP hindcast simulations. Actual cesium atmospheric deposition inputs used in the CARP model are shown on Figure 6-4 as solid blue bars. For reference, loads prior to the CARP hindcast period are shown by hatched bars.

6.1.1.3 Tributary Head of Tide and Stormwater Runoff Cesium Inputs

Atmospheric deposition of ^{137}Cs over land from weapons testing would have appeared in tributary headwaters and storm water runoff. Inputs of cesium from the heads of tide of all rivers discharging to the CARP model domain and stormwater runoff were calculated as follows:

a. From the sediment core of Bopp et al.,1991 taken on the Passaic River above the Dundee Dam, sediment concentrations (r_2) for each year were estimated. Several core measurements were available from Bopp et al., 1991 for 1965 through 1985. Subsequent measurements were described directly by Richard Bopp during several CARP MEG meetings and conference calls in 2005.

b. Using a fresh water partition coefficient of 10^5 L/kg from Thomann et al., 1989, daily varying SS concentrations for each tributary calculated using the NSL procedure, and the assumption that the particle bound sediment Cs concentrations (r_2) equals the water column particle bound Cs concentration (r_1), time variable particulate and dissolved cesium concentrations for each river were calculated. The particulate cesium concentration calculation is straight forward (i.e., $r_1 = r_2 \times SS$ water column). The particulate cesium concentration and the partition coefficient were used to calculate dissolved concentrations. The total cesium concentration at each head of tide then is ($r_2 \times SS + r_2 \times SS \times$ fraction dissolved/fraction particulate).

c. Step b was also applied using storm water runoff SS concentrations.

d. Loadings were calculated using concentrations from steps b and c and time variable flow rates used in the CARP hydrodynamic model. Figure 6-5 depicts the core data used to calculate the loads.

A noted minor shortcoming of this approach for the specific case of the Hudson River head of tide loading is that there may be an influence of additional discharges from the Knolls Atomic Power Laboratory (KAPL) located upstream of Lock 7 on the Mohwak River which were not accounted for. The major release of ^{137}Cs from Knolls, 20.1 Ci, however, occurred between July 1962 and December 1963, prior to the start of the CARP hindcast simulation. Between 1966 and 1971, less than 0.09 Ci were released from Knolls (Chillrud, 1996).

Figures 6-6 and 6-7 display all of the ^{137}Cs loadings by source type and by source location.

6.1.1.4 ^{137}Cs Sediment Initial Condition

Initial conditions in the bed sediment were set based on available dated sediment core data for 1965 (TAMS, 2005; Chaky, 2003; Bopp et al., 1982; Chillrud, 1996; Olsen et al., 1984). The initial conditions in the sediment reflect the majority of the loading associated with fallout from weapons testing prior to 1965.

6.1.2 Development of Cesium Kinetics

Since ^{137}Cs was not a CARP contaminant of concern, ^{137}Cs model kinetics had to be developed specifically for hindcast purposes. The CARP cesium kinetics include phase partitioning to suspended sediment and decay. Decay of ^{137}Cs was modeled with a half-life of 30.2 years or a first order decay rate of 0.2295 per year. The partitioning of cesium to suspended sediment is somewhat complicated, potentially having salinity (through ionic strength and seawater cation competition), suspended sediment, and age dependencies. Numerous partitioning relationships for cesium partitioning with salinity dependencies were considered.

Thomann et al., 1989, developed a partitioning relationship which incorporated both salinity and suspended sediment concentration effects, but was based on a sediment bed solids concentration of 250,000 mg/L rather than 500,000 mg/L as porosity data indicated. Testing of the Thomann et al.,

1989 partitioning relationship in the CARP model resulted in severe underprediction of particulate cesium in the sediments of estuarine portions of NY/NJ Harbor. Other relationships and data sets, for which ^{137}Cs partitioning to particles over a range of salinity were examined, were therefore considered for the CARP hindcast. These include: Ciffroy et al., 2003; Linsalata, 1984; Linsalata et al., 1985; Turner and Millward, 1994; Olsen 1979 modified from Hairr, 1974; and Mulholland and Olsen, 1992. Based on this information, the following ^{137}Cs partitioning relationship was developed for CARP:

$$\log K = -0.0116 \times SALT + 4.0741 \quad (6\text{-}1)$$

6.1.3 Cesium Hindcast Results

Model and data comparisons for ^{137}Cs are presented in Appendices 5a - 5c. The figures in Appendix 5a present a comparison between model calculations in the sediment bed and dated core measurements along eight spatial transects spanning key Harbor areas. As indicated on the figures, the dated sediment cores are from Lamont Doherty investigators (Chaky, 2003) and the high resolution cores collected as part of the Hudson River PCB Reassessment RI/FS (TAMS, 2005). On each page, the results for a different water year, starting in 1965-66 and going through 2001-02, are shown for the top ten cm of the sediment bed. Results are presented on both logarithmic and arithmetic scales. Example results are shown here for the 1971-72 and 1988-89 water years as Figures 6-8 and 6-9. Model results are very consistent with core data overall. In particular, the model does a good job of capturing the spatial trends in abundant core data collected in the Hudson River, Upper Bay, and Lower Bay. Over the progression of the hindcast, however, the model tends to over predict levels in some of the sediment cores, most notably the Hudson River PCB Reassessment Database high resolution core, HR-010, and the Lamont-Doherty cores, RB17, NB13, NB20, and NB13B (TAMS, 2005; Chaky, 2003). Further checking of the model against measured sediment concentrations of ^{137}Cs was performed at selected locations in the form of sediment chronologies. Sediment chronologies are presented in Appendix 5c. An example chronology is shown here as Figure 6-10 for core HR-006. It is noted that by virtue of data collection programs, the chronologies are generally available for depositional areas of the Harbor. In particular, we had trouble matching the "HAST" core data. We believe that this miss is related to the location of the core, near Hasting-on-Hudson, New York, an embayment area not well resolved by the CARP model grid. Reproducing sediment concentrations of ^{137}Cs was the main focus of the hindcast verification since the sediment concentration measurements were the most credible.

In addition, the hindcast verification calculations were compared to the limited available water column measurements of ^{137}Cs in the Hudson River. Hudson River water column measurements included both dissolved (Jinks and Wrenn, 1976; Hairr, 1974) and particulate (Hairr 1974; Olsen, 1979)

forms. Appendix 5-b displays the model and data comparisons for particulate ^{137}Cs in the water column for the waters years between 1970 and 1977. Model and data for the water years between 1970 and 1976 are in excellent agreement. In the 1976-1977 water year, there is a lone data point in the Hudson River in the vicinity of mile point 75 which the model under-predicts. Figures in Appendix 5-b display the model and data comparison for dissolved ^{137}Cs in the water column for the waters years between 1965 and 1974. The model calculations of dissolved ^{137}Cs in the water column are reasonable relative to the measured data; however, there are clear discrepancies, particularly in the 1970-71 water year. These discrepancies might relate to the fact that loadings were available and specified on an annual basis rather than with the inter-annual temporal variability that is likely to have characterized releases of dissolved ^{137}Cs from the Indian Point facility.

We interpret the cesium hindcast results to be a positive verification of the CARP model rates of exchange between the sediment bed and the water column over a relatively long time period.

6.2 HINDCAST VERIFICATION FOR 2,3,7,8-TCDD

One of the challenges of a hindcast verification is the problem of estimating historical contaminant loadings in the absence of direct measurements. In the case of 2,3,7,8-TCDD, its production was the unintended consequence of other activities. As an unintended consequence, the production of 2,3,7,8-TCDD within the watershed of the CARP model domain was not systematically documented and studied until relatively recently. There are no direct data on the release of 2,3,7,8-TCDD. This limitation aside, 2,3,7,8-TCDD is suitable for a hindcast analysis since its release to the NY/NJ Harbor estuary was largely from the Lister Avenue site along the Passaic River and dated sediment cores of 2,3,7,8-TCDD profiles are available for verification purposes (Chaky, 2003; Bopp, 1991). Nonetheless, Ayers et al., 1985 concluded that there were not enough data available to estimate emissions of dioxins in the Hudson-Raritan basin or to make any reasonable hindcast. In this sense, the CARP hindcast for 2,3,7,8-TCDD represents an unprecedented effort in terms of estimating past and present sources of 2,3,7,8-TCDD to the NY/NJ Harbor Estuary.

6.2.1 Approach for Calculating 2,3,7,8-TCDD Loadings

HydroQual has included 2,3,7,8-TCDD loadings from a variety of sources in the CARP hindcast model calculation. The approach for developing the loadings is described for three major functional groups:

- estimates of historical inputs at current source locations (i.e., atmospheric deposition, STPs, CSOs, runoff, tributary headwaters, ocean boundaries, etc.)
- estimates of contributions from in-place sediments in 1965 (i.e., sediment initial conditions)
- estimates of contributions from Lister Avenue after 1965

6.2.1.1 Historical 2,3,7,8-TCDD Inputs at Current Source Locations

HydroQual used the current loadings (i.e., atmospheric deposition, STPs, CSOs, runoff, tributary headwaters, ocean boundaries) of 2,3,7,8-TCDD developed for the CARP model to drive hindcast calculations.

6.2.1.2 2,3,7,8-TCDD Inputs from 1965 In-Place Sediments

To set sediment initial conditions for the 2,3,7,8-TCDD hindcast calculation which begins in 1965, HydroQual spatially interpolated over the CARP model domain dated sediment core data available from Chaky, 2003 and Bopp et al., 1991. These data include: lower Passaic River, 7600 ppt; Newark Bay, 1100 - 1400 ppt; Upper Bay, 120 - 150 ppt; Arthur Kill, 180 ppt; Raritan Bay, 16 ppt; Jamaica Bay, 43 ppt; Hudson River mile 59.55, 3.5 ppt; and Hudson River near Hasting-on-Hudson 16 ppt. Also, sediment data from 1998 on from CARP and other programs were scaled to 1965 levels to better approximate the 1965 concentration spatial patterns in the interpolation. The derivation of the scale factor, using cores 2072, 1845, and 436 is shown on Figure 6-11.

6.2.1.3 2,3,7,8-TCDD Inputs from Lister Avenue

Although major chemical production operations at the Lister Avenue site ceased in 1969, it is likely that the facility continued to release some amount of 2,3,7,8-TCDD. To characterize the Lister Avenue input, HydroQual needed to make two estimates: the magnitude of the release from Lister Avenue between 1965 and 2002 and the time trend of the release from 1965 through 2002. Based on dated sediment core data presented in Bopp et al., 1991 (i.e., 1960, 1100 ppt 2,3,7,8-TCDD; 1972, 680 ppt 2,3,7,8-TCDD; 1984, 1200 ppt 2,3,7,8-TCDD; and 1986, 180 ppt 2,3,7,8-TCDD) for sediment core F1 in Newark Bay, the time trend for the Lister Avenue release of 2,3,7,8-TCDD has been estimated as following two exponential decay trends: from 1965 up until the large storm in 1984 and from after the 1984 storm onward through 2002. Estimating the magnitude of the Lister Avenue release is more difficult to do. Bopp et al., 1991 estimate that the total deposition of 2,3,7,8-TCDD to Newark Bay from 1948 to 1985 was from 4 to 8 kg. Assuming that the release from Lister Avenue from 1948 to

1985 was probably greater than the deposition to Newark Bay (i.e., some of the contaminant was likely trapped in the sediments of the Passaic River or transported further downstream in the estuary than Newark Bay), HydroQual's original proposal was to use 6 kg as the release from Lister Avenue into the CARP model for 1965 to 2002 when releases were likely to be lower than the 1948 to 1985 period. However, based on advice from Richard Bopp, it was suggested that the release from Lister Avenue from 1965 to 2002 was likely closer to 1 to 2 kg. A 2 kg release from Lister Avenue did not appear to be sufficient in some preliminary hindcast simulations. A 4 kg release was therefore used for the final hindcast. Both the estimated magnitude and time trend of the release from Lister Avenue is shown on Figure 6-12.

Figures 6-13 and 6-14 summarize the CARP hindcast loadings for 2,3,7,8-TCDD by source type and by source location.

6.2.2 Development of 2,3,7,.8-TCDD Kinetics for Hindcast

Unlike cesium, 2,3,7,8-TCDD is a CARP contaminant of concern. It was not necessary to develop 2,3,7,8-TCDD kinetics specifically for hindcast purposes. CARP current conditions calibration kinetics were used in the 2,3,7,8-TCDD hindcast.

6.2.3 2,3,7,8-TCDD Hindcast Results

The major tool for verifying the 2,3,7,8-TCDD hindcast simulation results are the sediment bed spatial transect plots presented in Appendix 6A. The results in Appendix 6A are presented on both an organic carbon normalized and a dry weight basis for years with data during the thirty-seven year hindcasting period. The plots are shown with both logarithmic and arithmetic scales. Example spatial transects for water years 1978-79 and 1999-2000 are shown in Figure 6-15 and 6-16. The agreement between model and data is very good given the uncertainty in the historical loadings of 2,3,7,8-TCDD and the spatial heterogeniety of contaminant concentrations in sediments. The spatial heterogeniety is illustrated to some extent by the variability in the measured data presented along the transects by the various plotting symbols. Comparing concentrations obtained from core data to concentrations averaged over the larger area represented by grid cells of the CARP model is a difficult test of the model's ability to capture depositional areas. The data were obtained from a variety of researchers and programs as indicated on the diagrams. The model results are shown as annual maxima, means, and minima with shading and lines at each point along each transect. We gratefully acknowledge the cooperation of the reserachers and agencies in furnishing the data.

In interpreting the model and data comparisons presented in Appendix 6A, we gave the greatest emphasis to reproducing the data provided by Bopp and Chaky (presented as orange/red downward triangles). Also, given the fact that the hindcast procedure used surrogate rather than actual hydrodynamic and meteorologic conditions, we paid greater attention to model and data comparisons on a dry weight rather than an organic carbon normalized basis. Further, we did not have organic carbon measurements available for many of the data sets. For further verification, comparison of the CARP model concentration calculations to core top data collected over the hindcasting period are presented as time series results in Appendix 6B. Time series results are least favorable in the vicinity of Newtown Creek and at one station in each of the Kills and Passaic River.

6.3 HINDCAST VERIFICATION FOR SELECT PCB HOMOLOGS

6.3.1 Approach for PCB Loadings

A method for scaling present day contaminant loadings developed for the CARP model to historical periods based on changes in United States atmospheric emissions was originally intended for the CARP hindcast and was previously applied by HydroQual to the Delaware River PCB TMDL model. The United States emissions trends, which would form the basis of the scale factors that would be applied to present day loading concentrations to develop hindcast loading concentrations, were developed based on information contained in Breivik et al., 2002a, 2002b. This approach however proved to be problematic for two reasons: the loadings developed were significantly higher than previous estimates (Thomann et al.,1989; Ayers et al., 1985) and the loadings resulted in extreme model over-prediction of measured concentrations in sediments.

HydroQual implemented the following approach for scaling present day contaminant loading concentrations using site-specific, rather than national, scale factors developed by Thomann et al., 1989 based on the work of Ayers et al. 1985 for total PCBs. Scale factors presented in Table A-10 from Thomann et al. 1989 for 1966 through 1987 were used. A trend was developed for 1987 through 1998 based on linearly interpolating the 1987 loading estimate from Thomann et al., 1989, and loading estimates developed for CARP. The basis of the Thomann et al. 1989 scaling method was 37.5 lb/day of PCB loadings for all sources other than the Upper Hudson for 1980. Figure 6-17 displays the two information resources used, Thomann et al 1989 loading estimates and CARP present day loading estimates, along with the CARP hindcast loading estimates based on the scale factors. Homolog distributions measured by CARP investigators for various individual loading types were maintained in

the hindcast. Sediment initial conditions were set based on both Hudson River core data and scaled CARP data as shown on Figure 6-18 and in Table 6-2.

Table 6-2. Scale factors used for assigning sediment bed initial conditions for selected PCB homologs for CARP model hindcast simulations

Homologue	1965 Core Data : CARP Data
di-	.20
tetra-	.30
Hexa-	.17
Octa-	.20

One exception to HydroQual's scaling approach is the Upper Hudson above the Troy Dam for which loadings data are available from 1991 on, from measurement made on the Upper Hudson by USEPA/General Electric. For periods before the 1991 measurements from USEPA/General Electric are available, i.e., 1965 to 1990, annual loading estimates based on Thomann et al., 1989, for di-, tetra, and hexa- homologs are used. The upper Hudson hindcast loading estimates are displayed on Figure 6-19.

The Hudson River loading estimates developed by Thomann et al., 1989 from 1965 through 1975 are based on sediment PCB concentrations in cores of reaches 1 through 5 above the Troy Dam (Hetling et al., 1978) corrected for conditions just upstream of the Dam (i.e., a factor of 0.38 to account for losses in reaches 1 through 5). The assumptions made in the calculations of Thomann et al., 1989 are that there is an annual equilibrium of solid phase concentrations of PCBs between the overlying water and surface sediments, that there are no significant decay mechanisms between reach 1 and the Dam, and that the materials in the cores of Hetling et al., 1978 were deposited at the net rate of 2 inches/year. An independent check on the trend in Upper Hudson total PCB loading estimates between 1966 and 1975, per Richard Bopp, is a core at Hudson River mile point 163.6. This core, 163.6v, suggests that the PCB loadings used in the hindcast should be much higher; however, this is contrary to the hindcast results presented in Section 6.3.3.

The Hudson River loading estimates developed by Thomann et al., 1989 for 1976 through 1987 are based on water column PCB measurements from the USGS which are indicative of an exponential decline likely due to decreasing discharges to the river, upstream decay of PCBs in sediments, and/or net burial of PCBs in sediments. The analysis of Thomann et al., 1989 suggests a Hudson River PCB

load decay rate of 0.2765 per year for 1980 through 1987 which is used by Thomann et al. for making future projections of loadings.

In summary then, the Upper Hudson loads for the majority of the CARP hindcast years are based on direct water column measurements (i.e., USEPA/General Electric data from 1991-2002 and USGS data from 1976 to 1987). For the years 1988 to 1990, the trend in USGS water column measurements was extrapolated. Only the years 1966 to 1975 were indirectly estimated from sediment cores. Some potential room for improvement in the methodology described above for the years 1966 to 1975 has been identified but was not possible to implement. An analysis of Troy area cores, planned by Bopp and Chaky, has yet to be completed. Once fully analyzed, these cores could serve the purpose of identifying the time series of upriver inputs.

Some of the controlling factors on the release of PCBs from the Upper Hudson include the break of the Fort Edward Dam in 1974 and the 100 year flood in 1976.

A summary of PCB loadings by homolog included in hindcast calculations is shown on Figures 6-20 to 6-27 by both source type and source location.

6.3.2 Development of PCB Homolog Kinetics for Hindcast

Similar to 2,3,7,8-TCDD, PCB homologs are CARP contaminants of concern. It was not necessary to develop PCB homolog kinetics specifically for hindcast purposes. CARP current conditions calibration kinetics were used in the PCB homolog hindcast.

6.3.3 PCB Homolog Hindcast Results

Time series model and data comparisons at thirteen sediment core locations are shown in Appendix 7A for the PCB homologs included in the CARP hindcast verification: di-, tetra-, hexa-, and octa-. On each page, model and data comparisons are shown for the four homologs on both a dry weight and an organic carbon normalized basis. The comparisons are presented on logarithmic scales and are repeated on arithmetic scales. In addition, transect model and data comparison plots are also presented in Appendix 7B. The measured spatial heterogeneity of contaminant concentrations in sediments is illustrated to some extent by the variability in the data presented along the transects by the various plotting symbols. The model results are shown as annual maxima, means, and minima with shading and lines at each grid cell along each transect. Example transect model and data comparison

plots are shown for tetra-CB for the water years 1979-80 and 1999-2000 in Figures 6-28 and 6-29, respectively.

Overall the agreement between model and data is reasonable, but not as strong as the model and data agreement for the other CARP hindcast contaminants, 2,3,7,8-TCDD and ^{137}Cs. Level of agreement between model and data for each PCB homolog varies by location. There does not appear to be a clear bias for any one of the four homologs. Some of the reasons for the less favorable agreement in this hindcast as compared to the other CARP hindcasts include:

- Homolog compositions for the loading estimates made on a total PCB basis were inferred based on current CARP data. Homolog composition for specific loadings may have deviated historically from those currently observed. Homolog composition considerations were not an issue for the 2,3,7,8-TCDD and ^{137}Cs hindcasts.

- For the lower chlorinated homologs in particular, the PCB contamination is driven by a tributary headwater input. The major tributary headwater source for this hindcast, unlike the other hindcasts, has several implications. The importance of incorporating actual rather than surrogate event level details in the PCB loadings is magnified. Using surrogate rather than actual hydrodynamics is more important in this hindcast than for the other CARP hindcasts.

- The organic carbon production model applied for CARP was rigorously calibrated and validated for areas south of Poughkeepsie. For purposes of CARP, the estuarine organic carbon production model was extended north of Poughkeepsie. Areas north of Poughkeepsie did not have the benefit of the multi-million dollar data collection program and calibration/validation effort performed south of Poughkeepsie prior to CARP. Also, carbon and nutrient dynamics specific to the freshwater portions of the Hudson River (e.g., zebra mussels) were not considered per se. For this reason, we placed greater emphasis on contaminant model and data comparisons on a dry weight basis rather than an organic carbon normalized basis in the Upper Hudson.

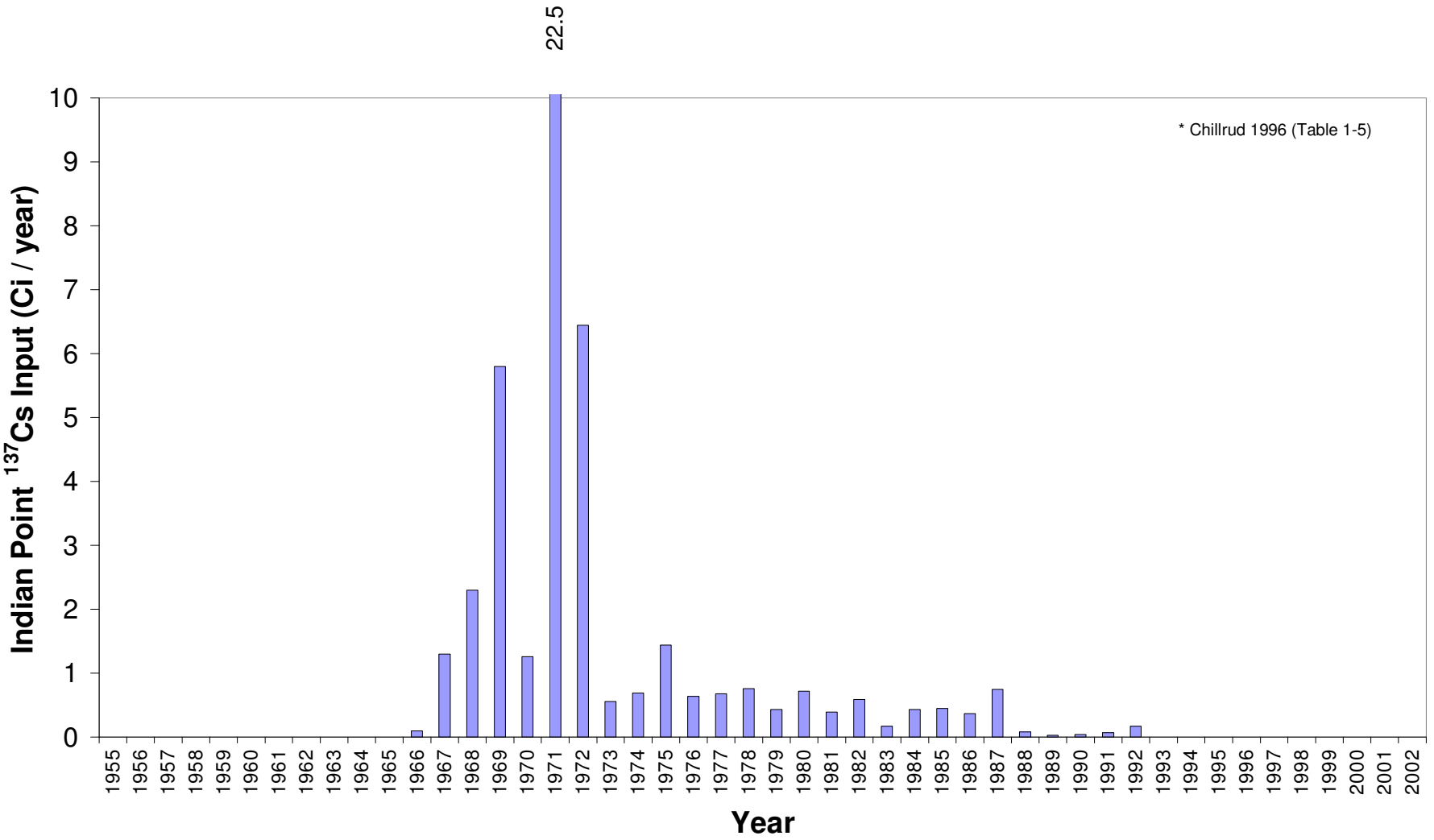

Figure 6-1. Annual releases of ^{137}Cs from Indian Point as reported by Chillrud 1996.

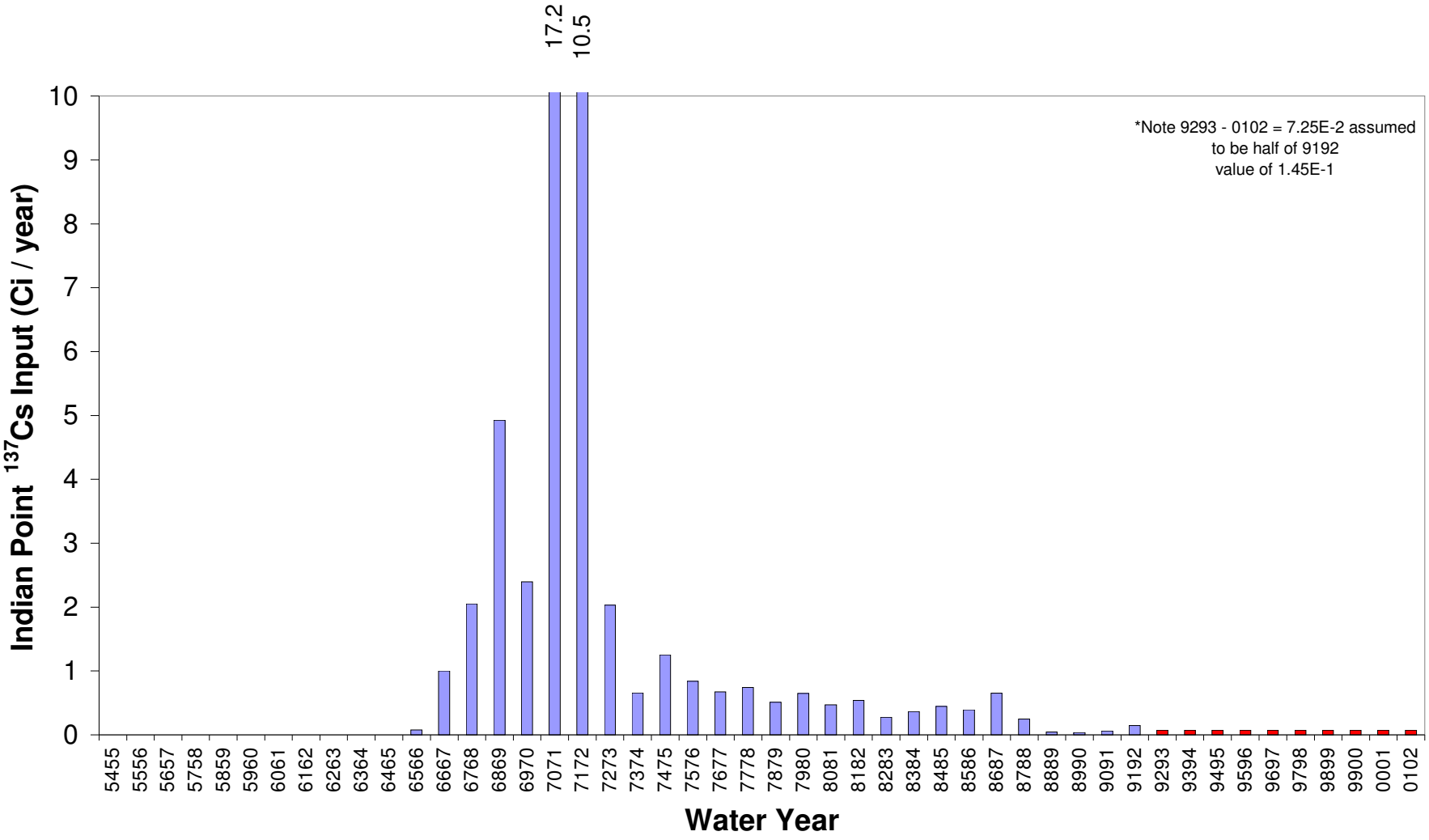

Figure 6-2. Indian Point release of ^{137}Cs per water year applied in CARP model hindcast simulations.

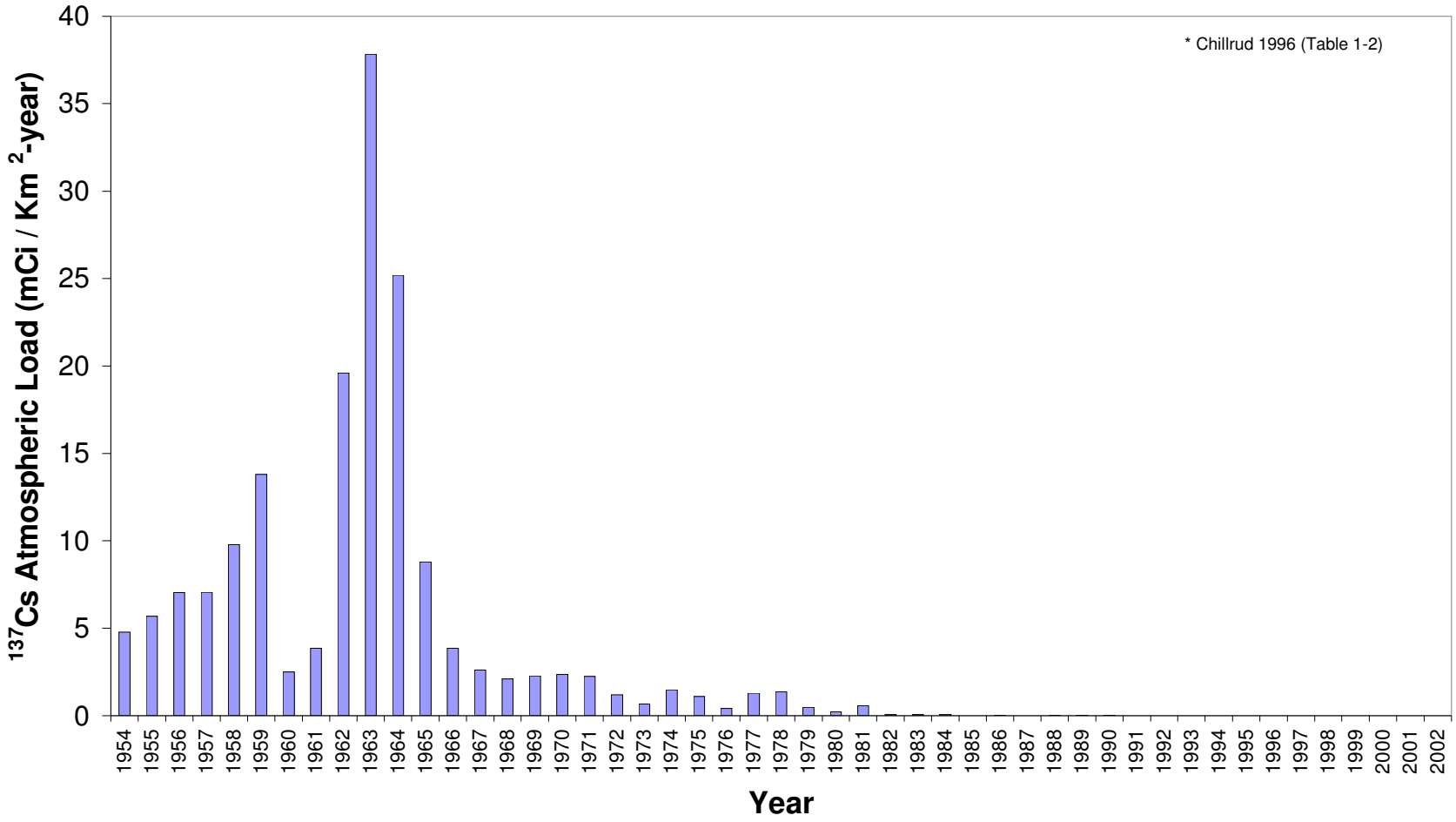

Figure 6-3. Annual release of ^{137}Cs from atmospheric deposition as reported by Chillrud 1996.

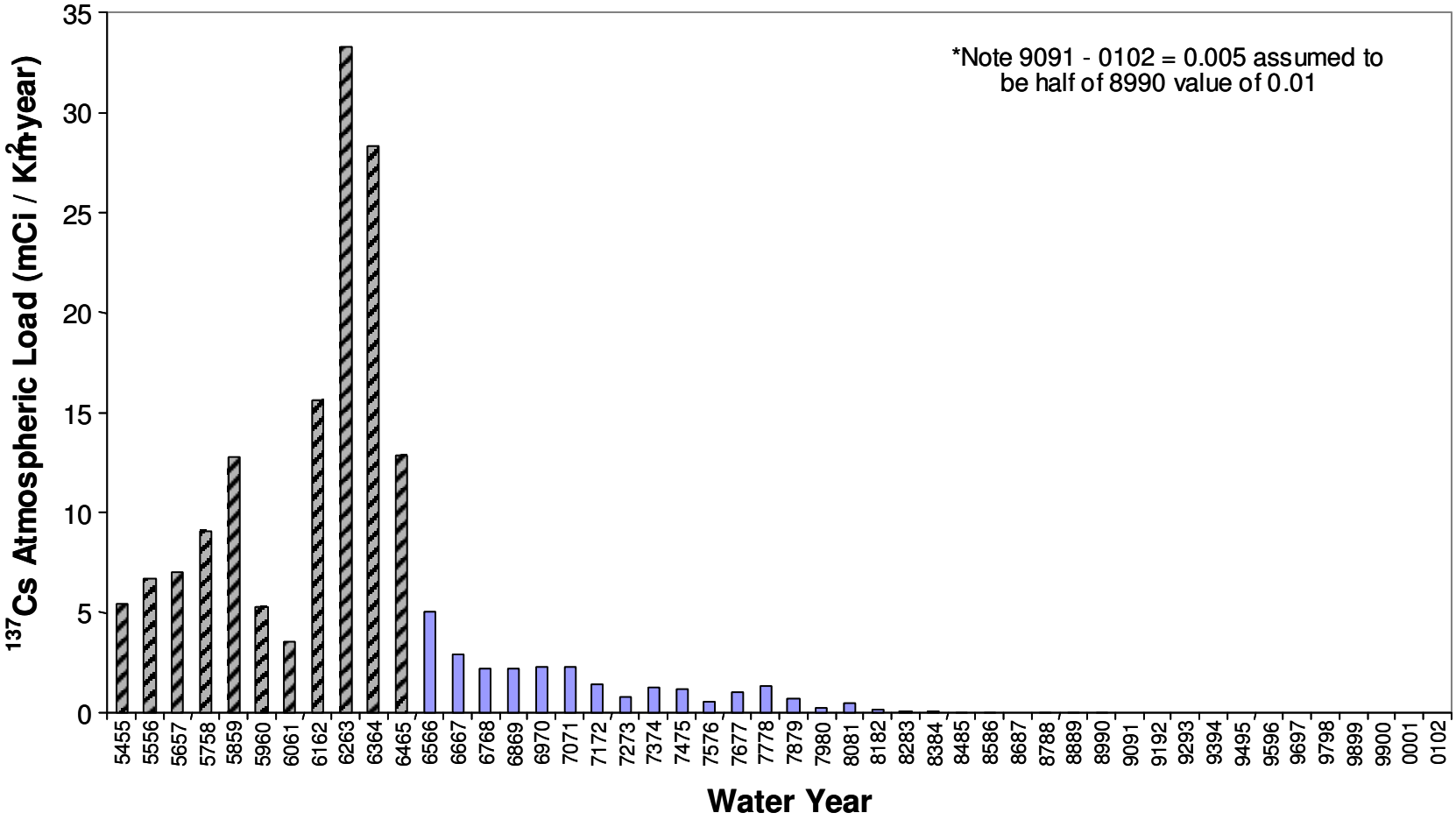

Figure 6-4. Atmospheric deposition of ^{137}Cs per water year applied in CARP model hindcast simulations.

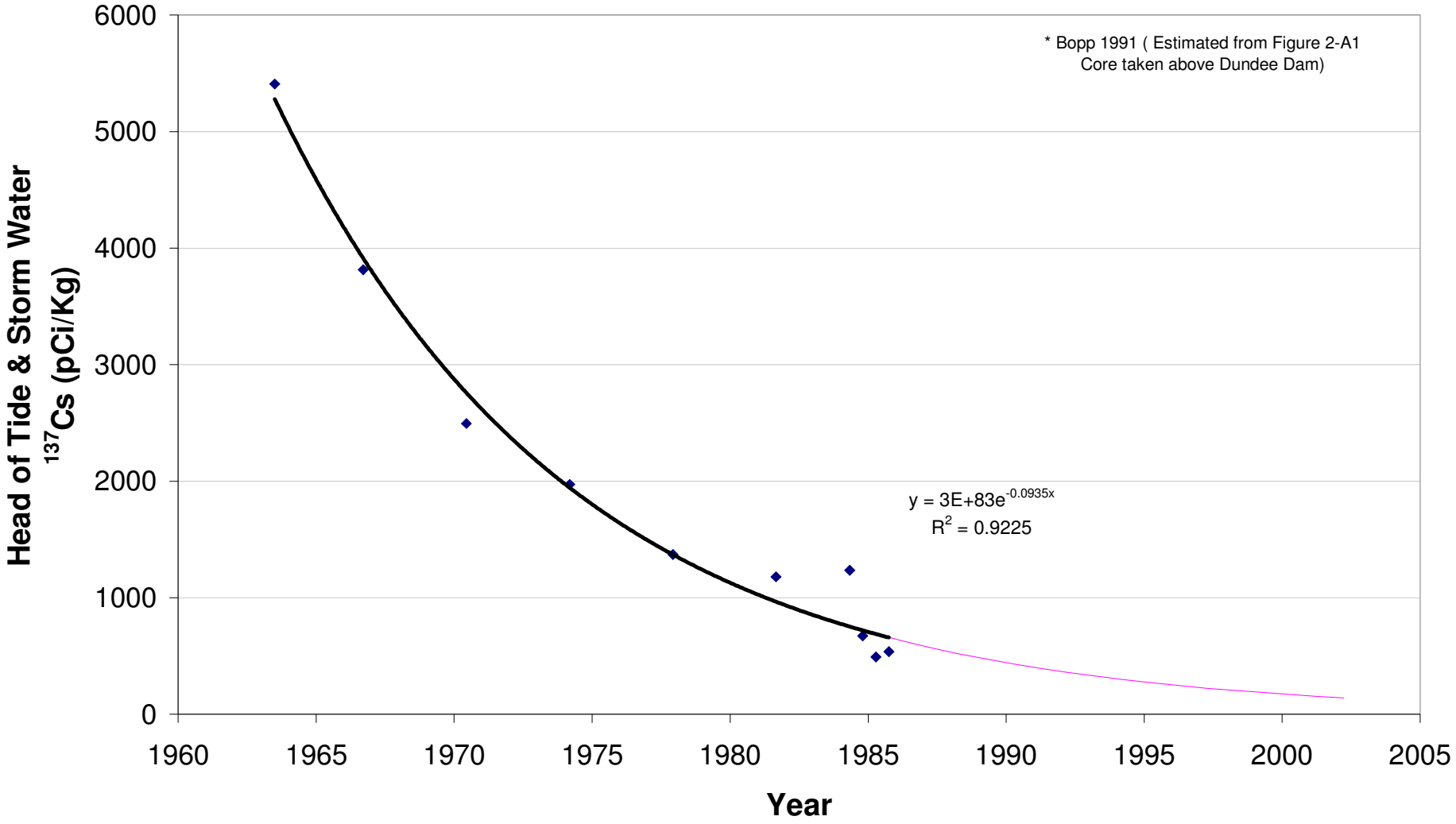

Figure 6-5. Time trend, inferred from dated sediment core data, of head of tide and storm water ^{137}Cs inputs used in CARP model hindcast simulations.

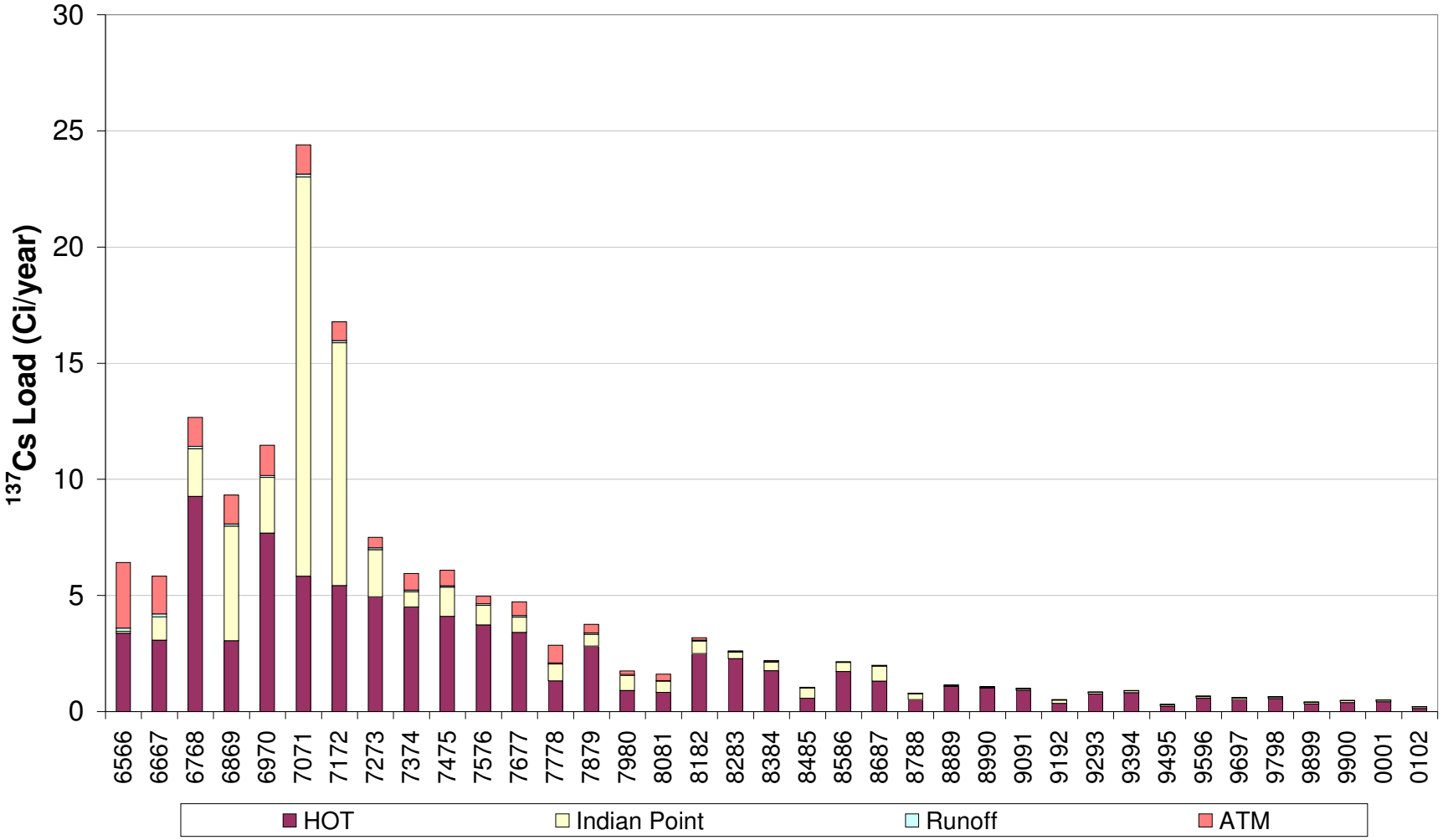

Figure 6-6. All CARP model hindcast simulation loads for ^{137}Cs by source type.

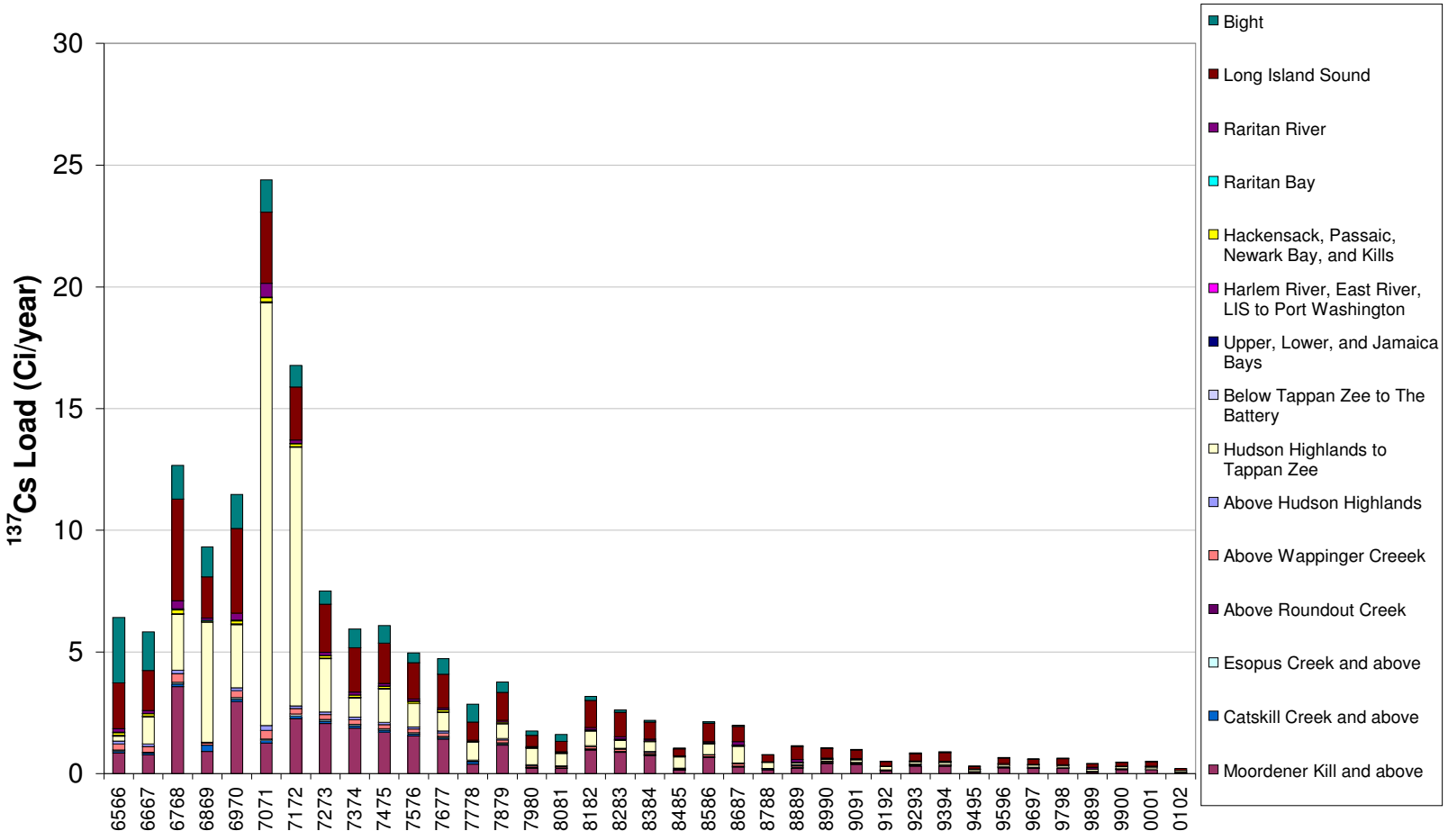

Figure 6-7. All CARP model hindcast simulation loads for ^{137}Cs by source location.

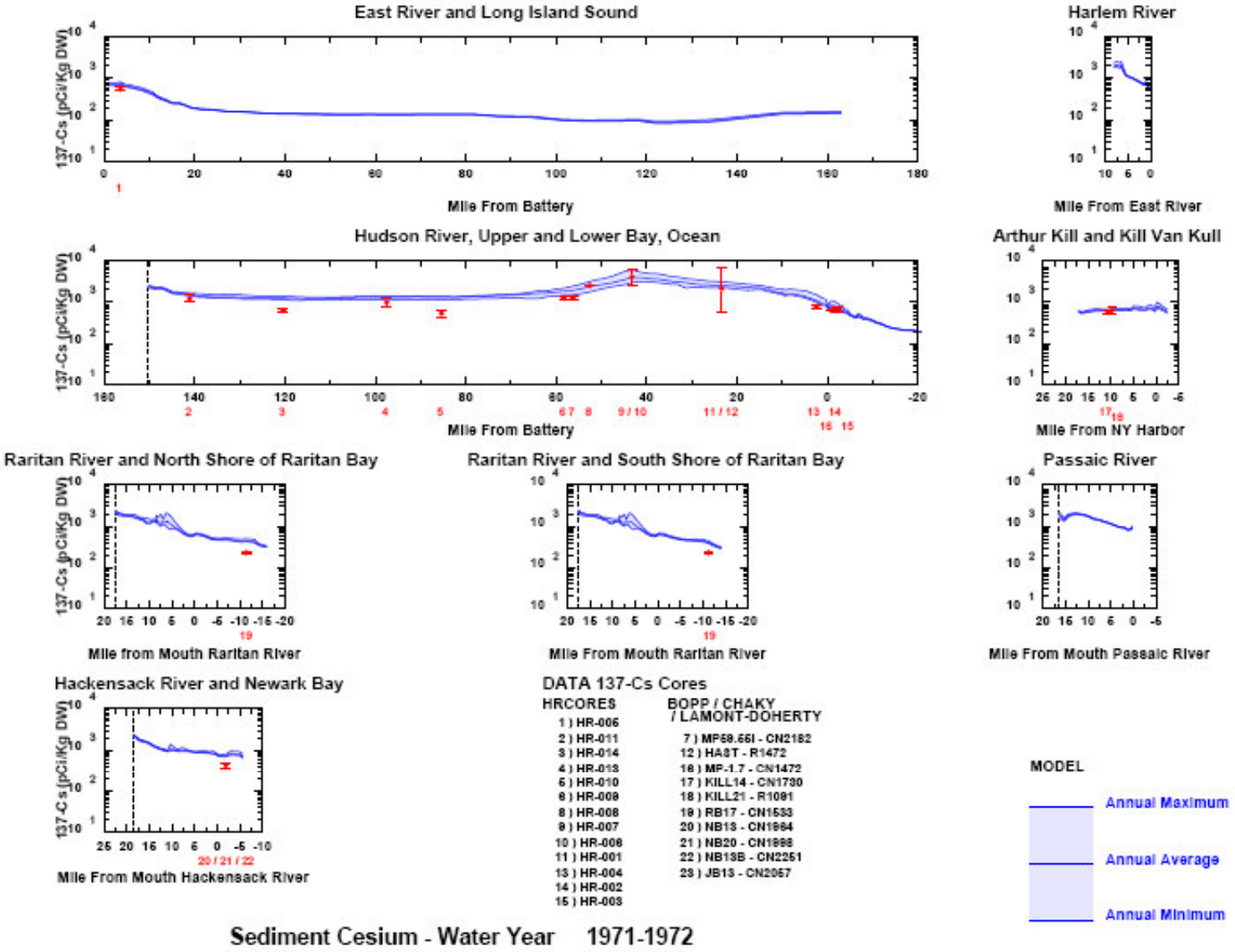

Figure 6-8. Example sediment spatial transect model and data comparisons for CARP ^{137}Cs hindcast – 1971-72.

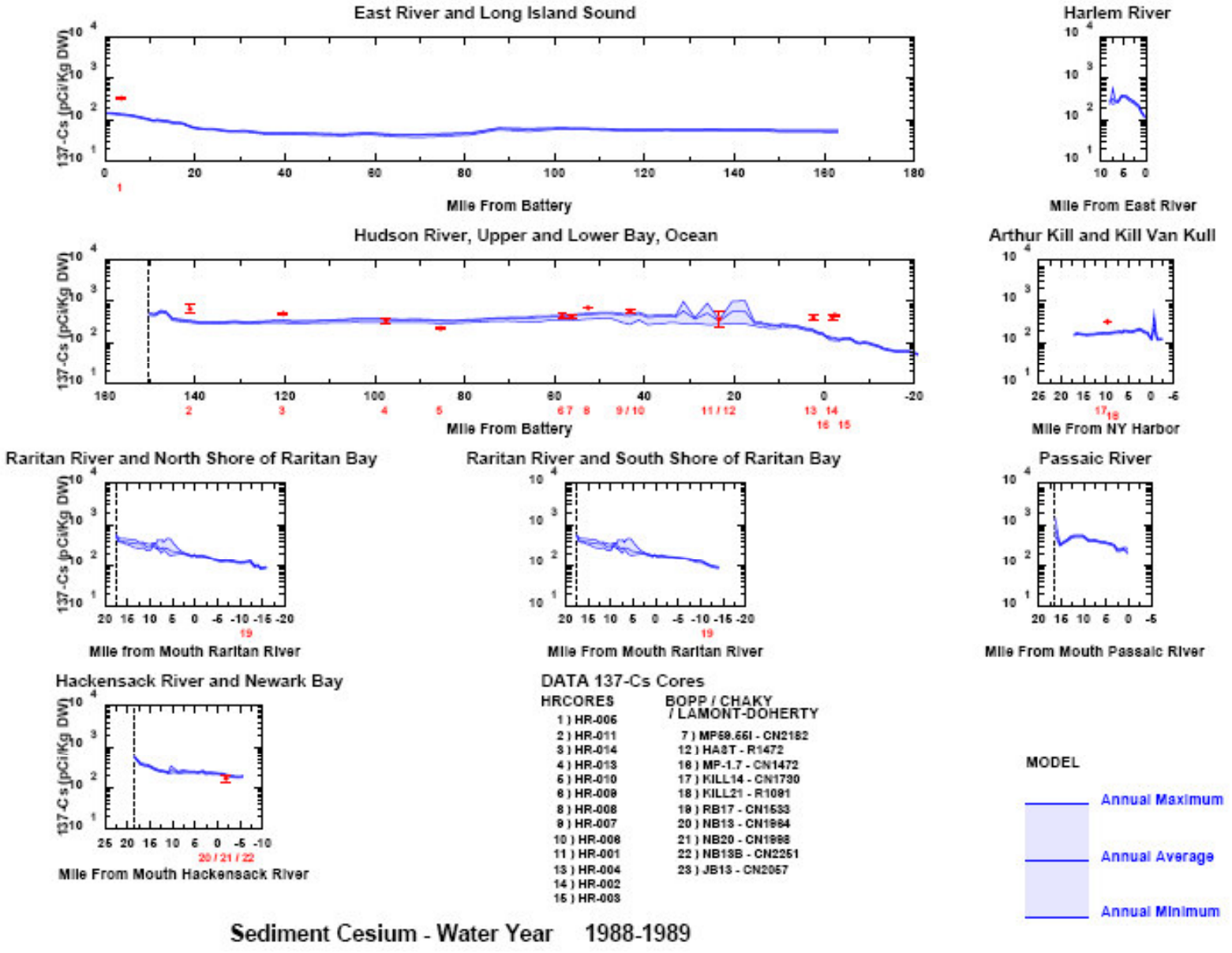

Figure 6-9. Example sediment spatial transect model and data comparisons for CARP ^{137}Cs hindcast – 1988-89.

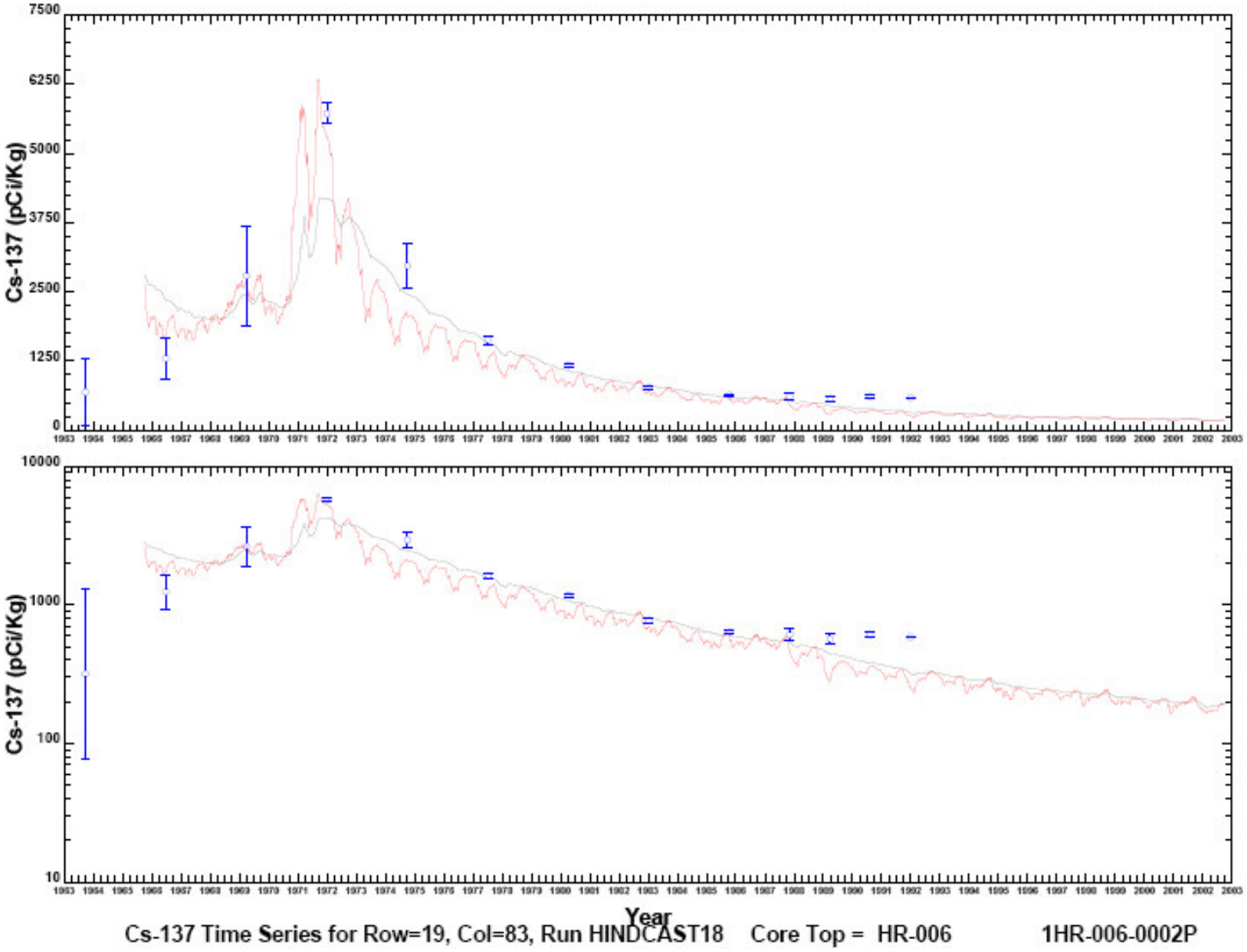

Figure 6-10. Example sediment chronology model and data comparisons for core HR-006.

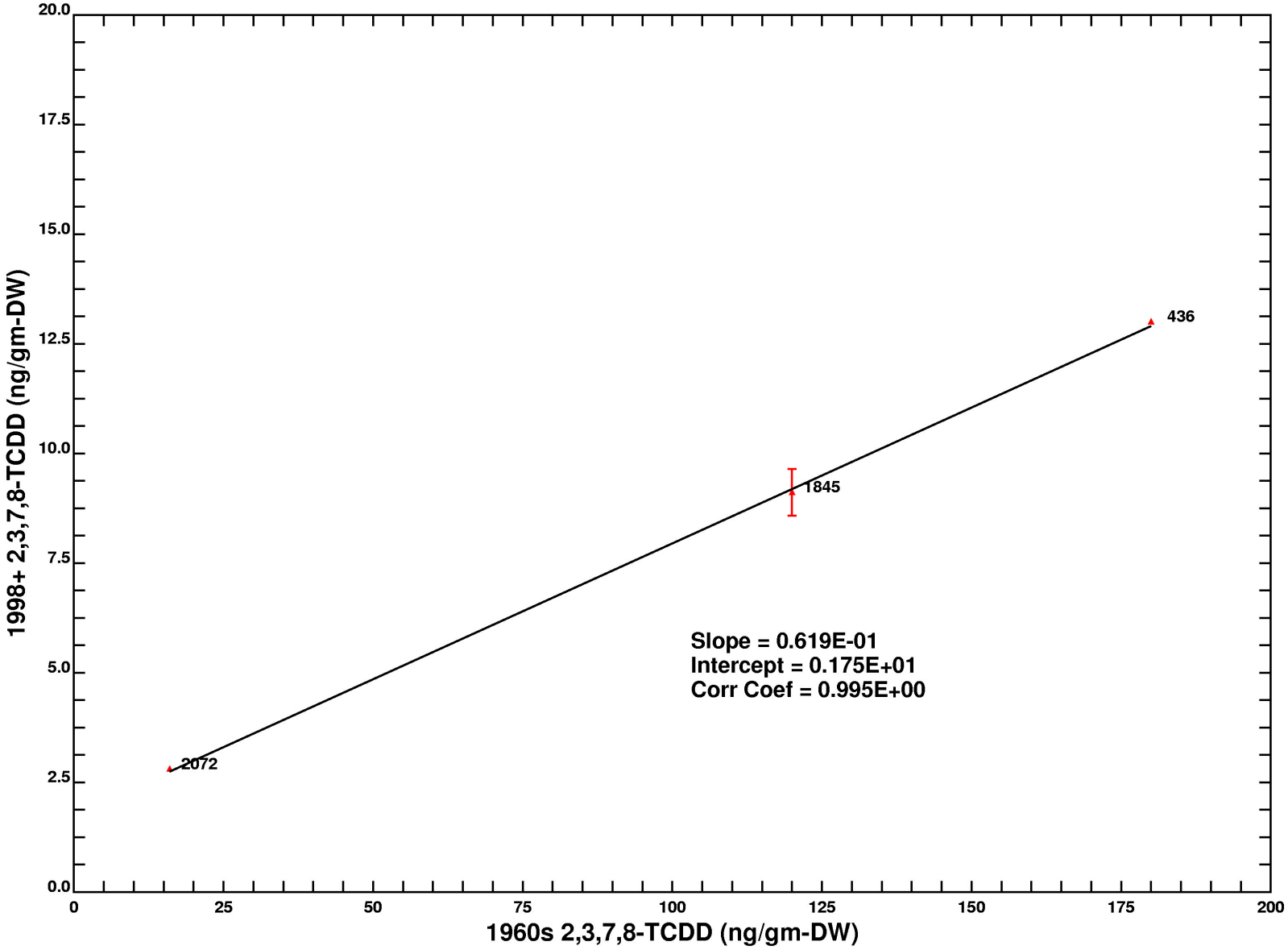

Figure 6-11. Time trend, inferred from dated sediment core data, used for assigning CARP model 2,3,7,8-TCDD hindcast simulation sediment bed initial conditions.

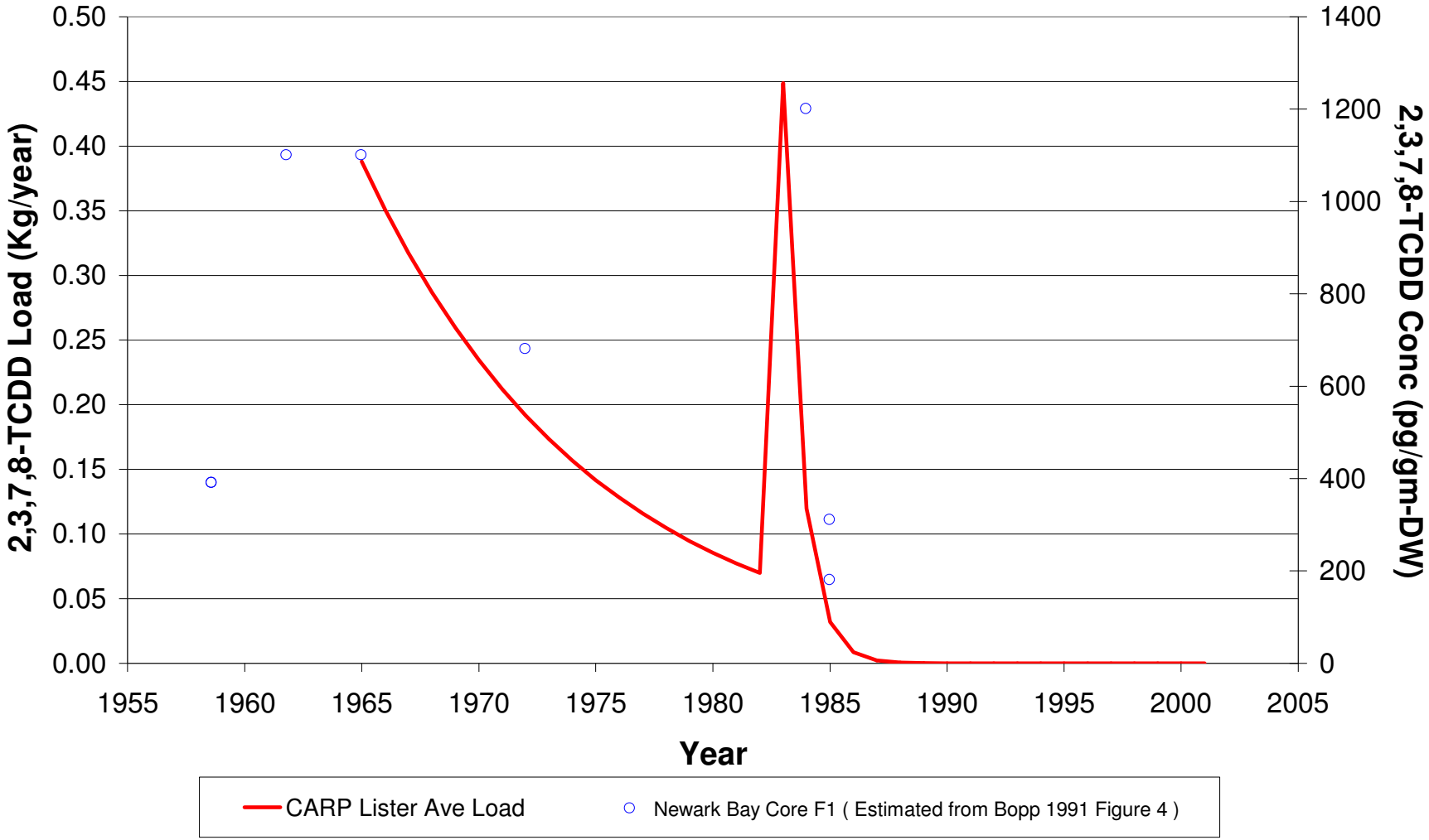

Figure 6-12. Lister Avenue input of 2,3,7,8-TCDD assigned, based on dated sediment core measurements, in CARP model hindcast simulation.

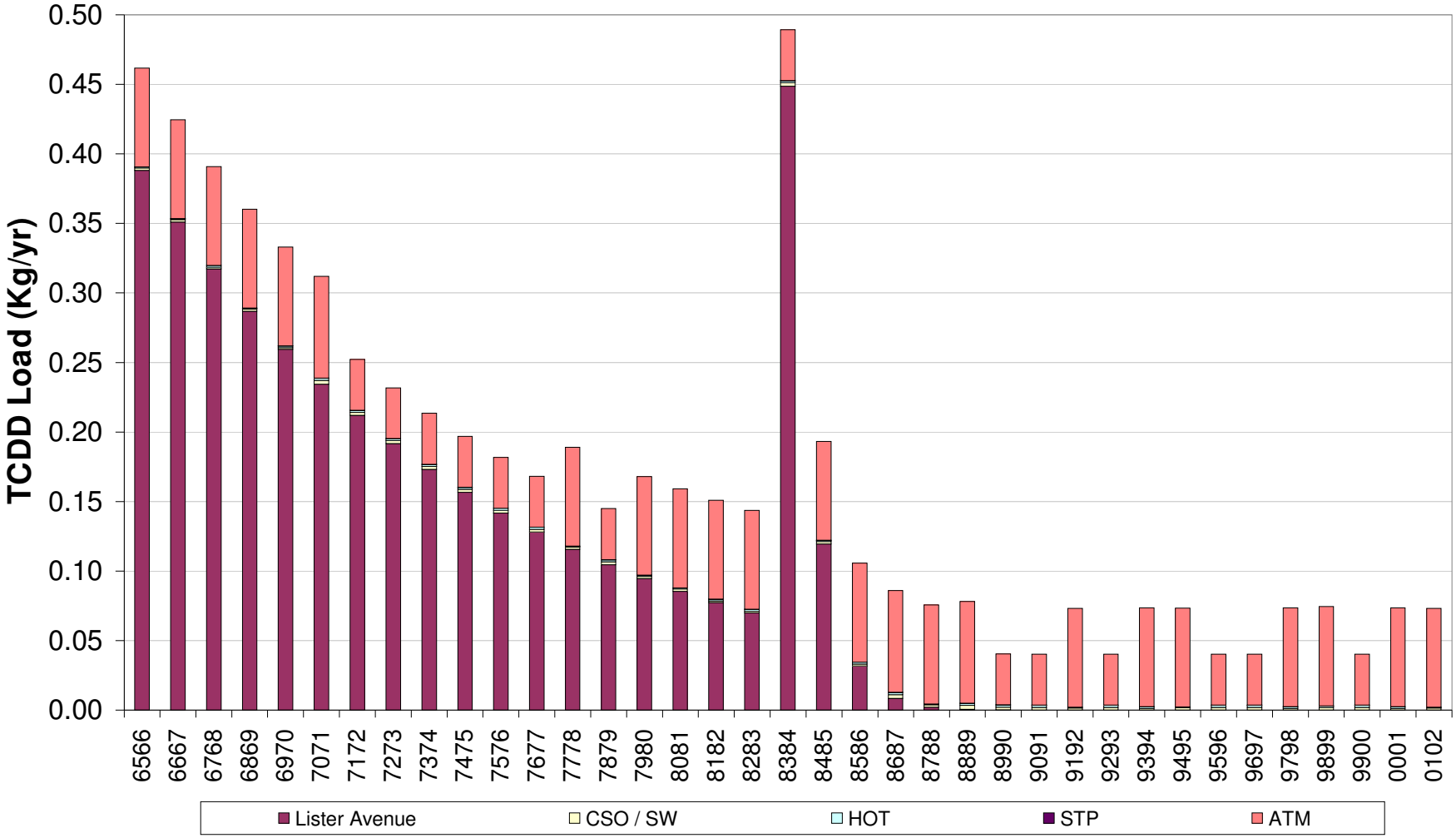

Figure 6-13. All CARP model hindcast simulation loads for 2,3,7,8-TCDD by source type.

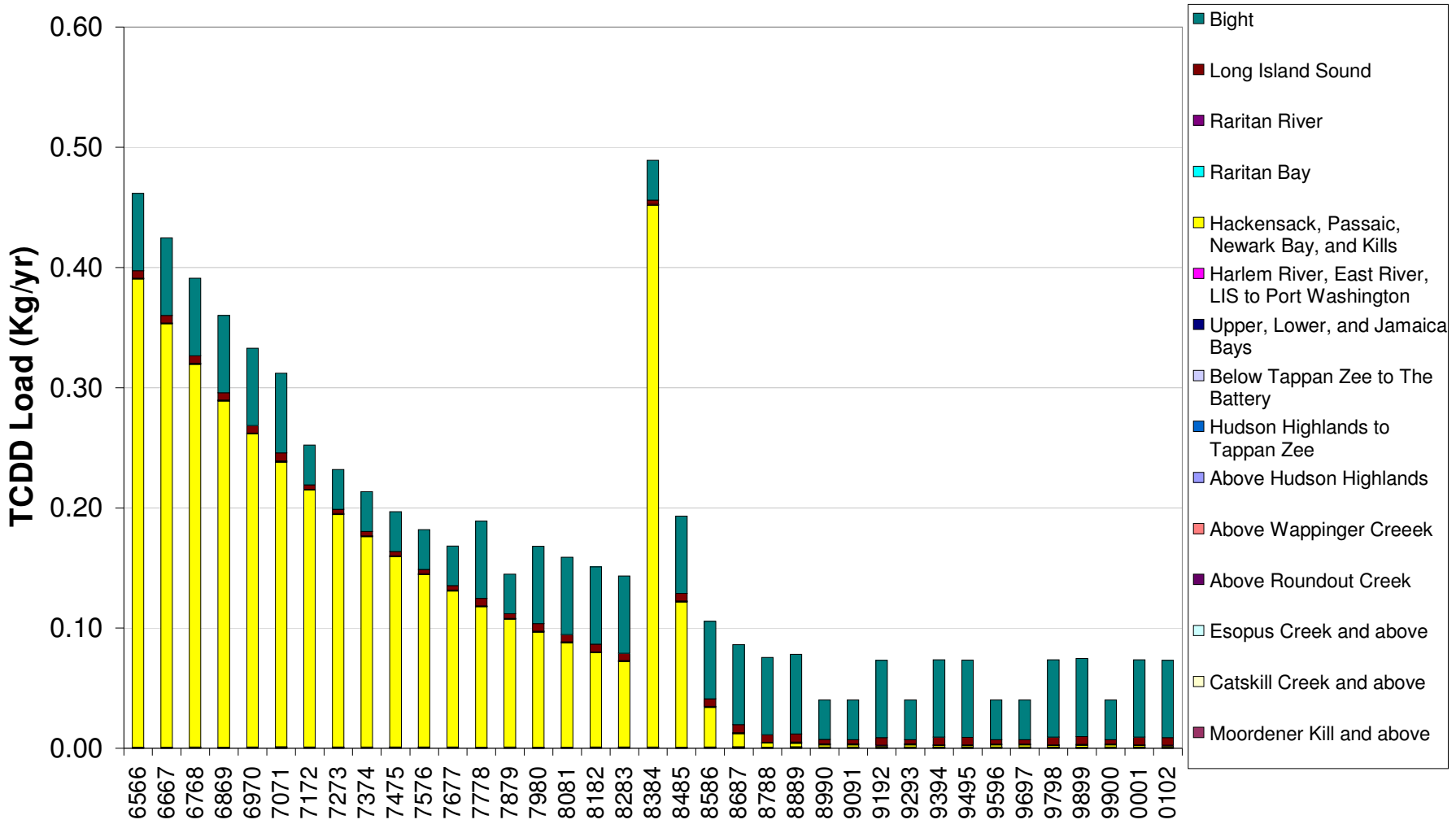

Figure 6-14. All CARP model hindcast simulation loads for 2,3,7,8-TCDD by source location.

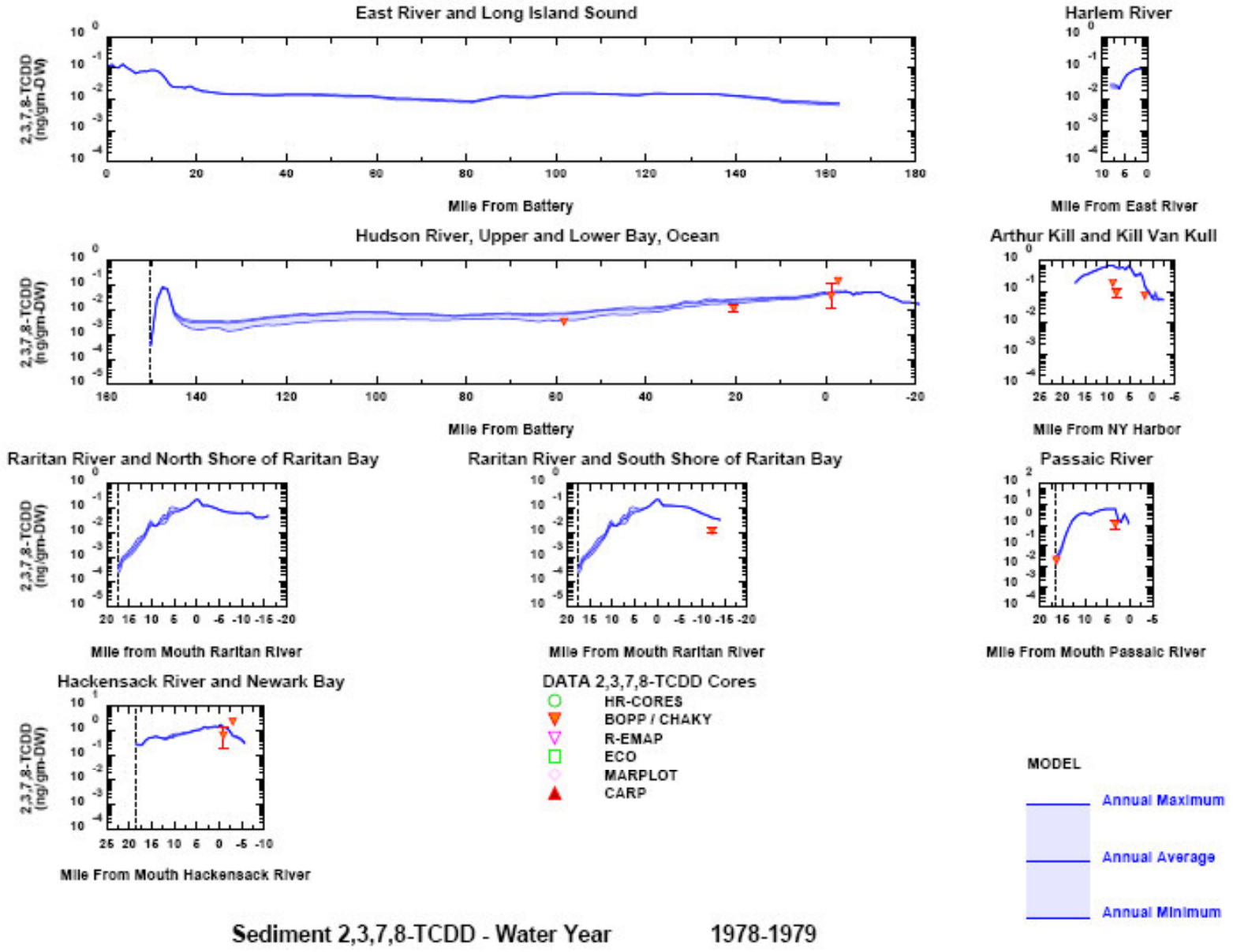

Figure 6-15. Example spatial transect model and data comparisons for CARP 2,3,7,8-TCDD hindcast – 1978-79.

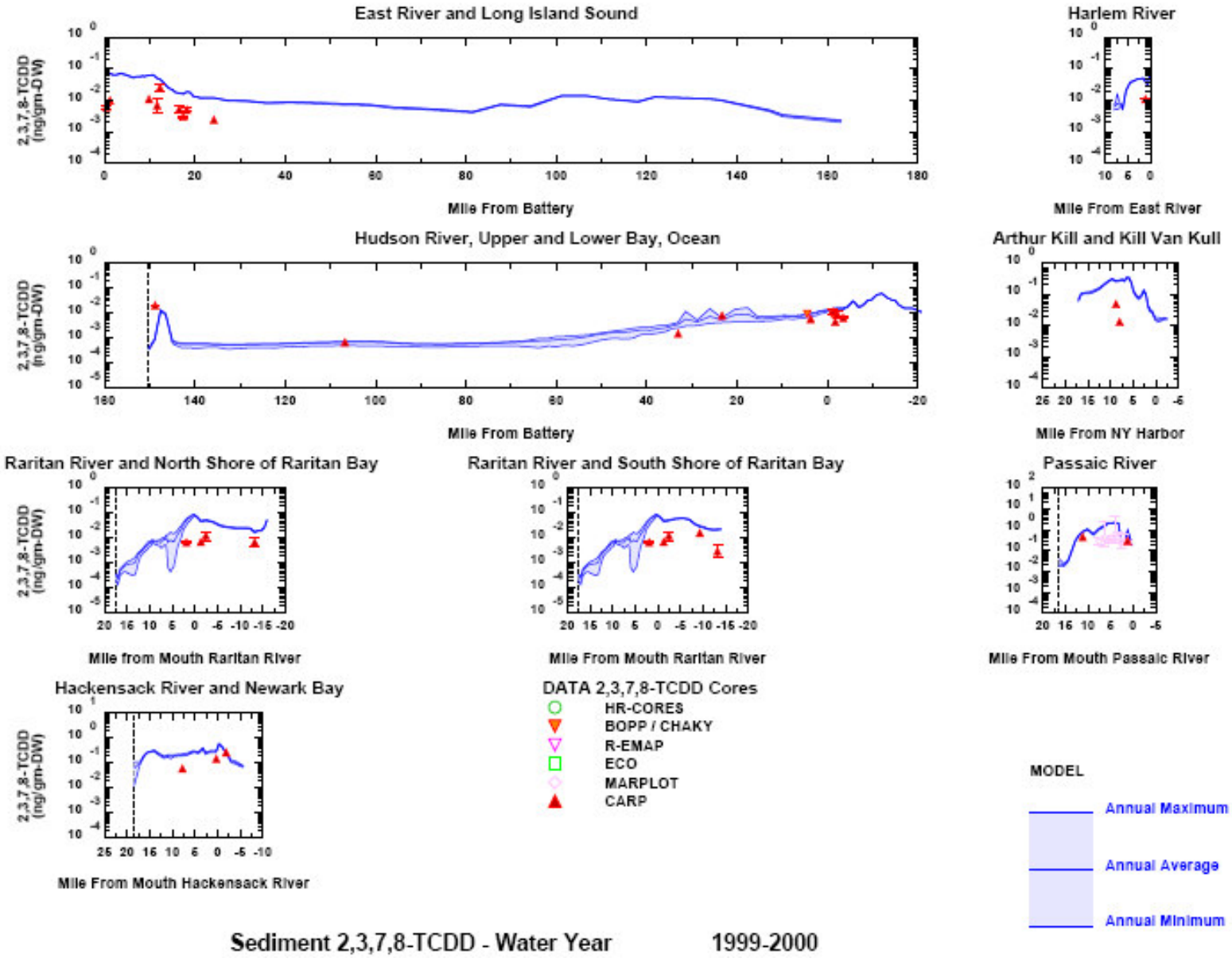

Figure 6-16. Example spatial transect model and data comparisons for CARP 2,3,7,8-TCDD hindcast – 1999-2000.

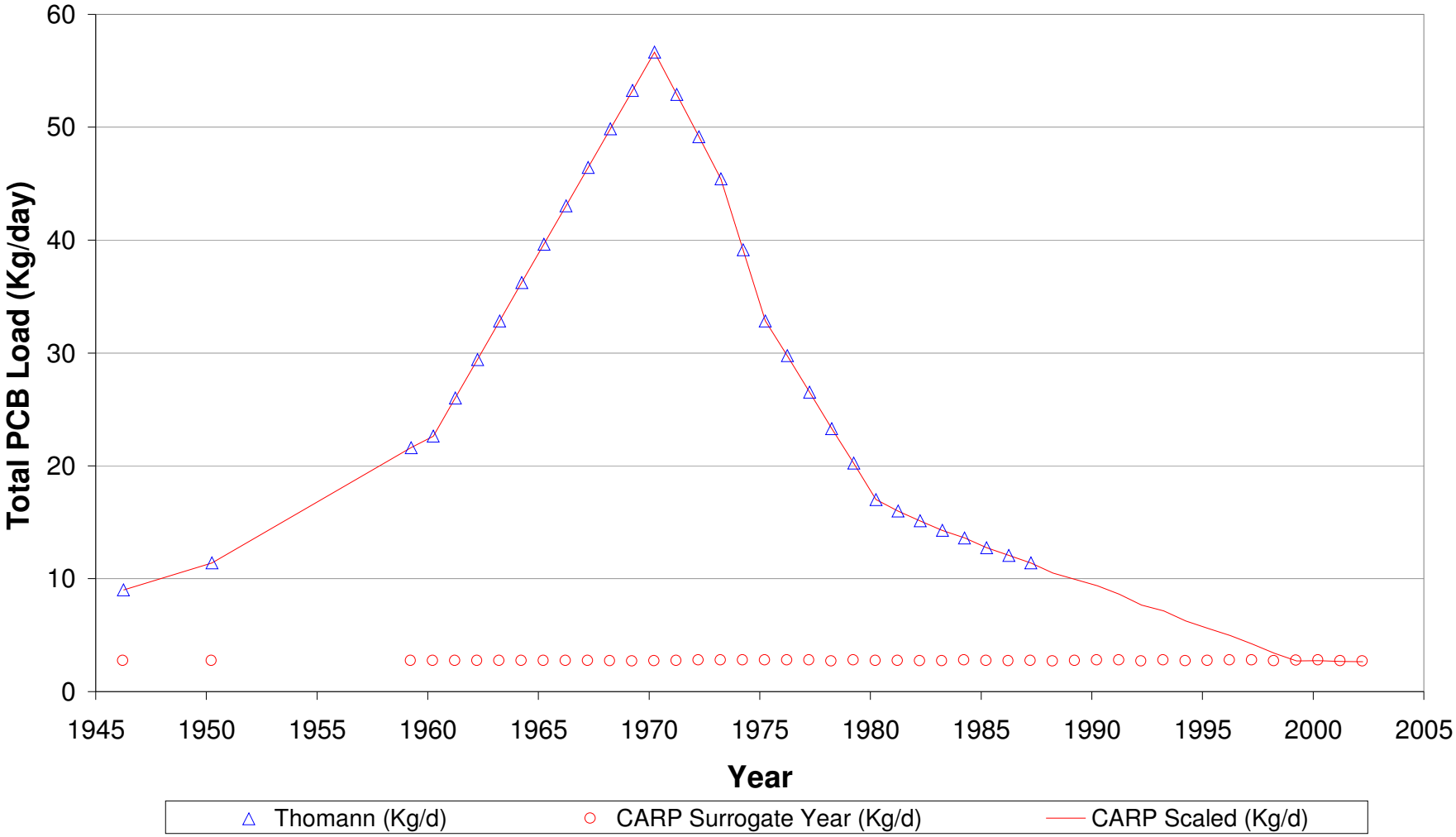

Figure 6-17. Time trend of PCB inputs (red line), excluding the Upper Hudson, assigned in CARP model hindcast simulations for selected homologs based on CARP current data (red circles) and loading estimates of Thomann (blue triangles).

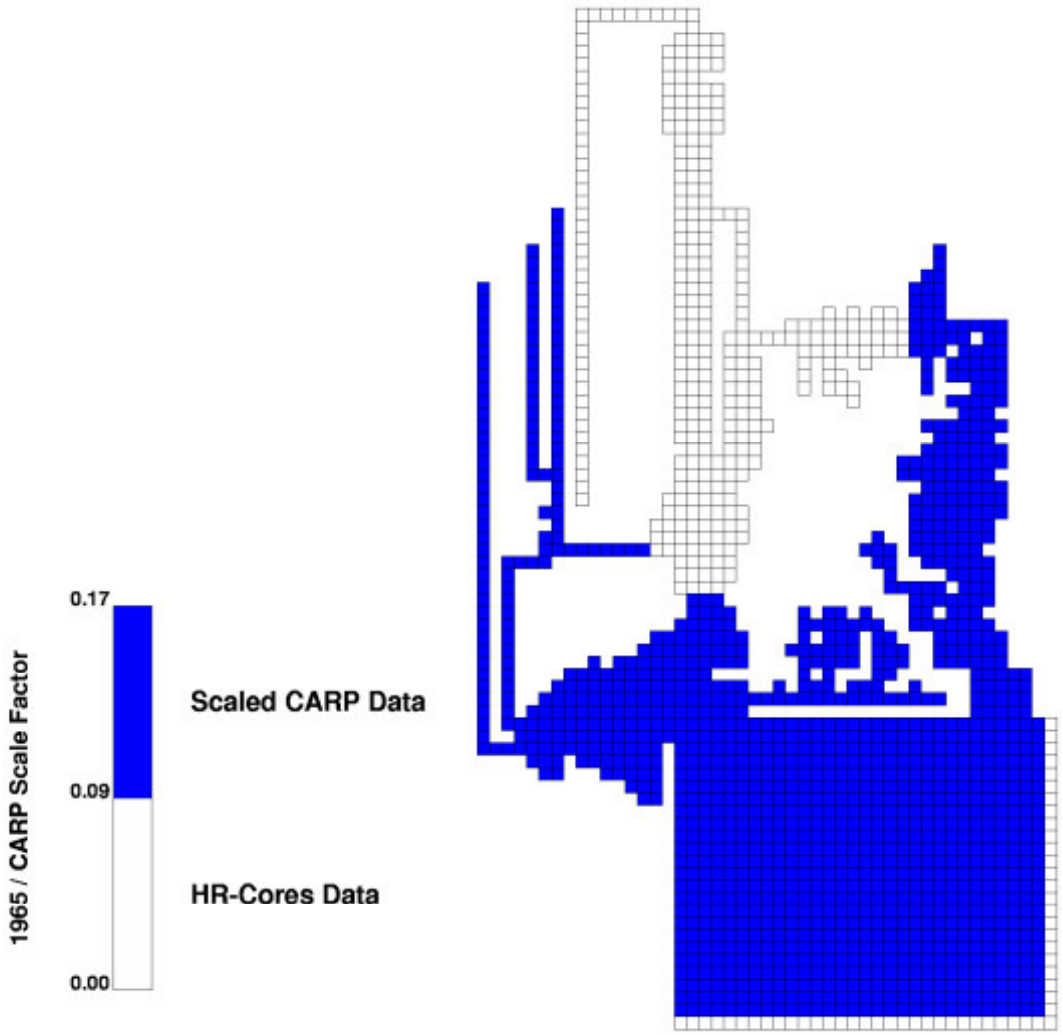

Figure 6-18. Computational grid view of data sources applied for deriving PCB homolog sediment bed initial conditions for CARP model hindcast simulations.

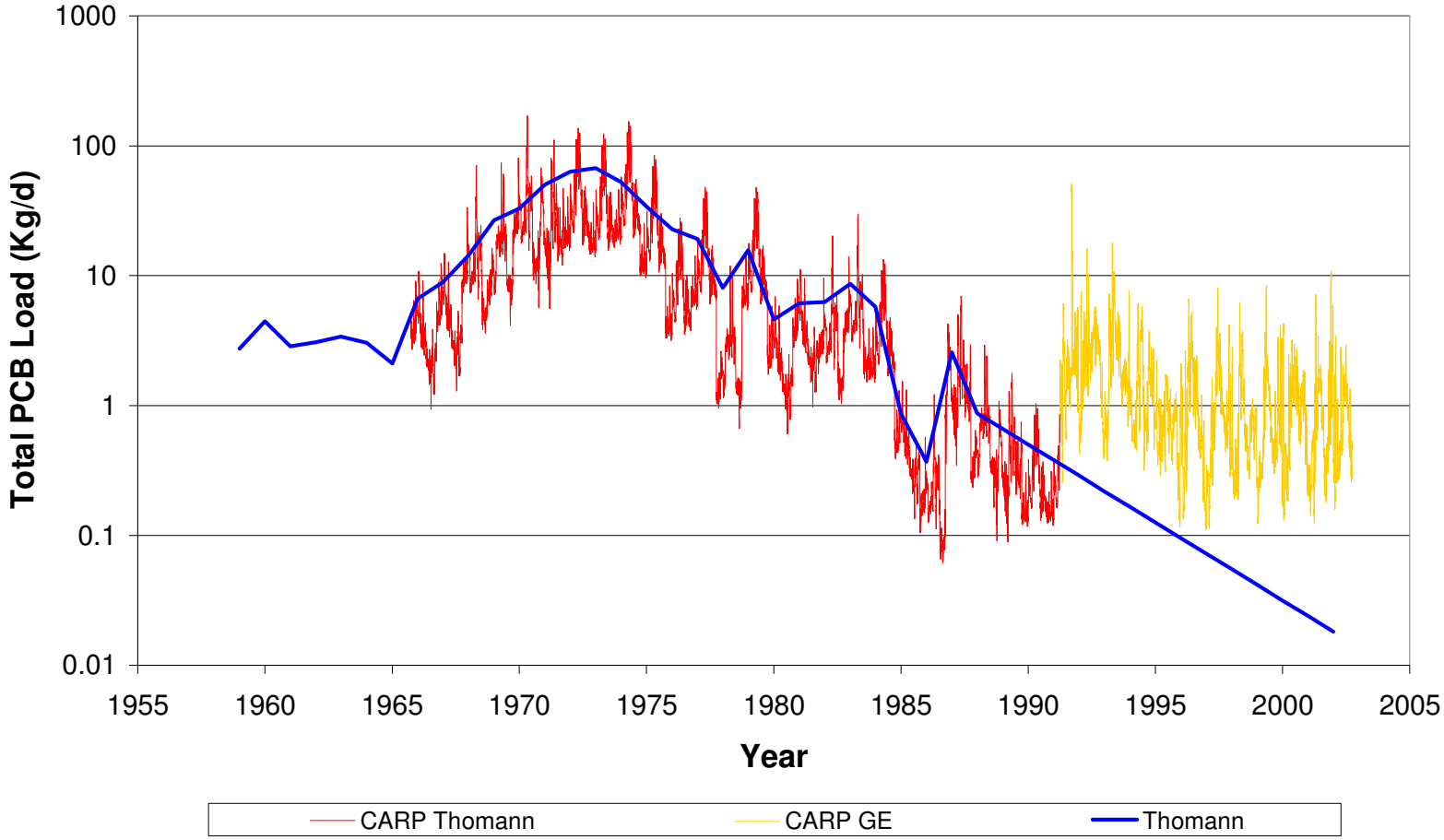

Figure 6-19. Time trend of PCB inputs from the Upper Hudson assigned in CARP model hindcast simulations for selected homologs based on data collected by General Electric (yellow line) and estimates of Thomann (red line).

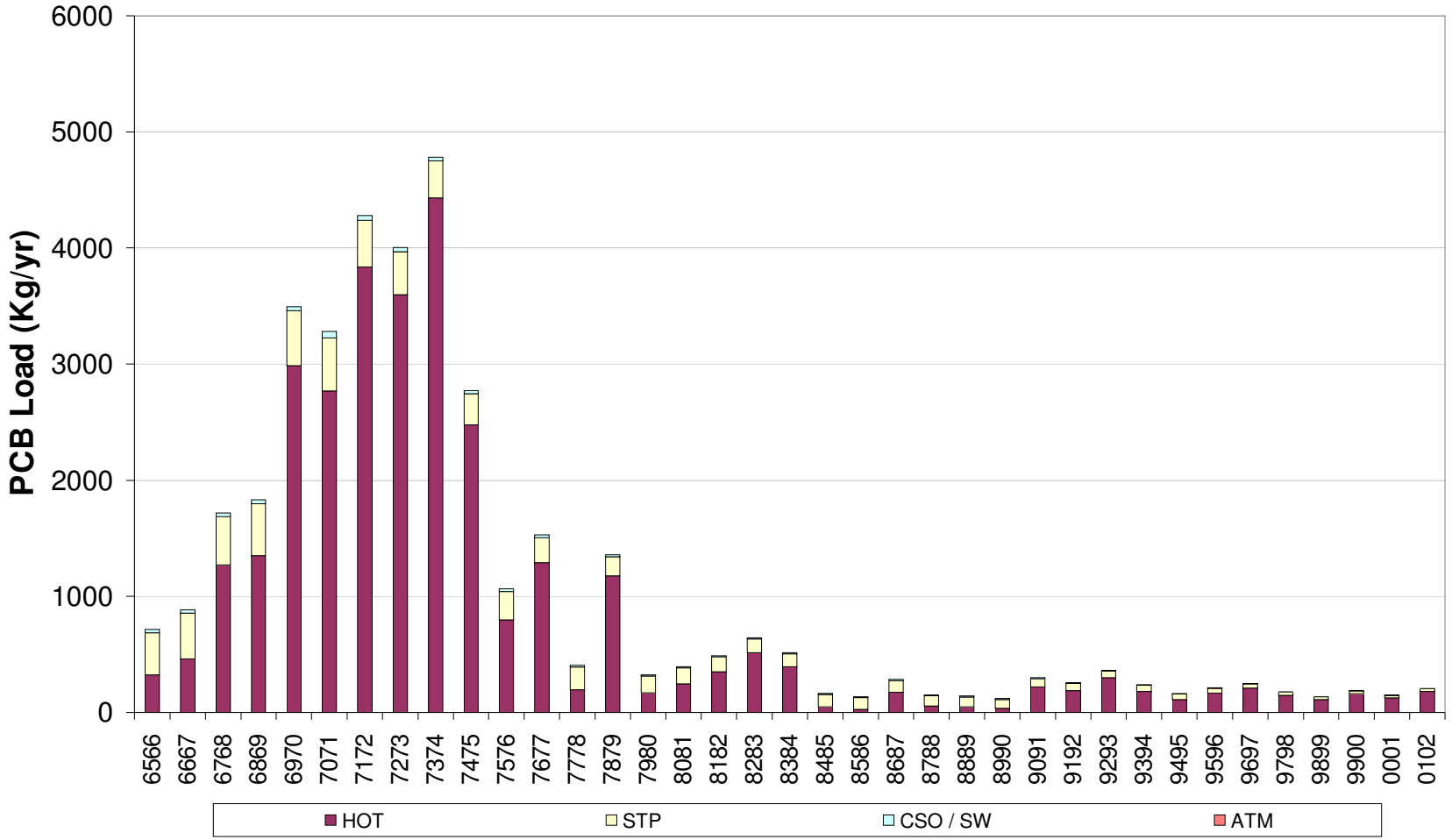

Figure 6-20. All CARP model hindcast simulation loads for di-CB by source type.

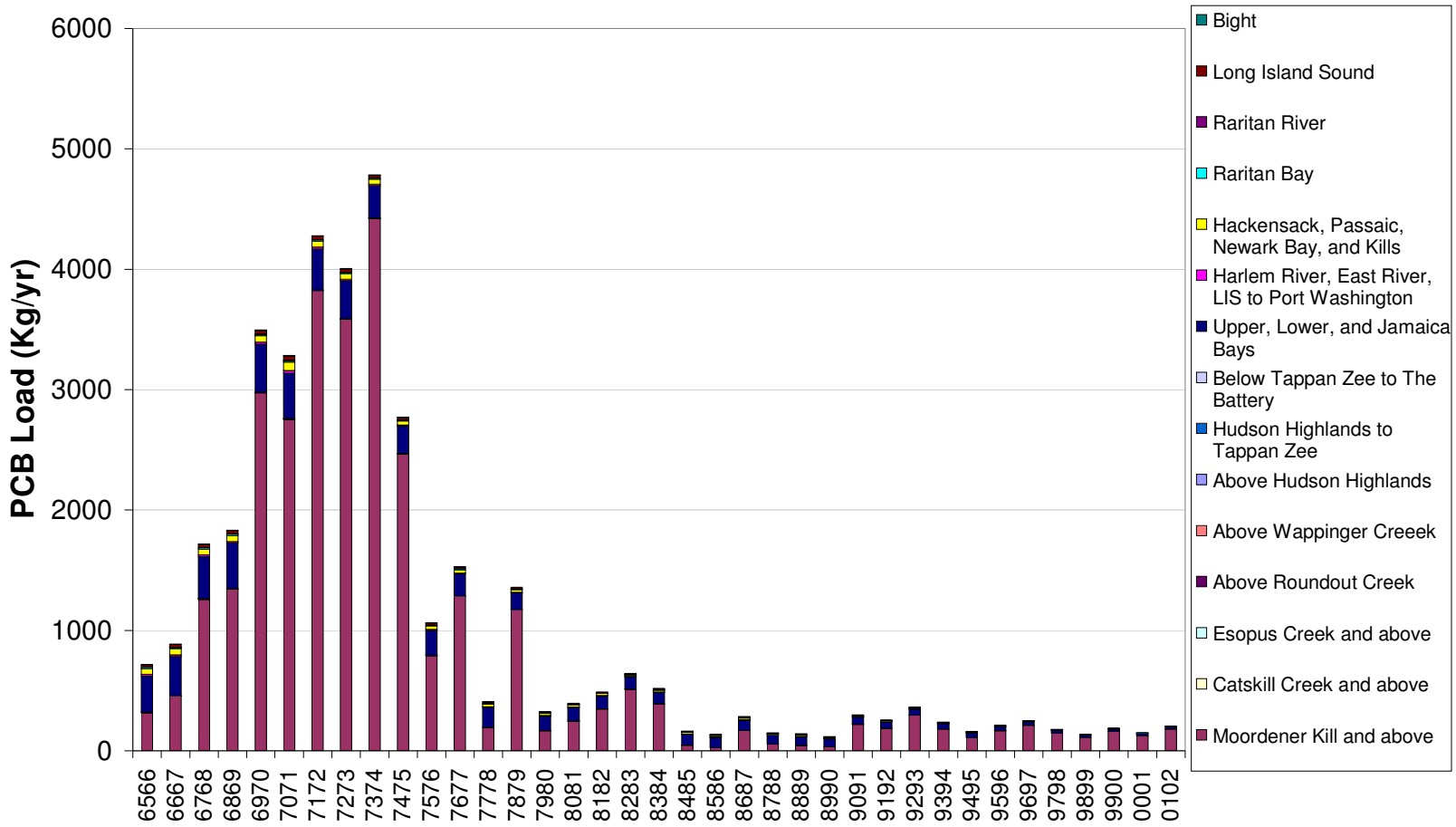

Figure 6-21. All CARP model hindcast simulation loads for di-CB by source location.

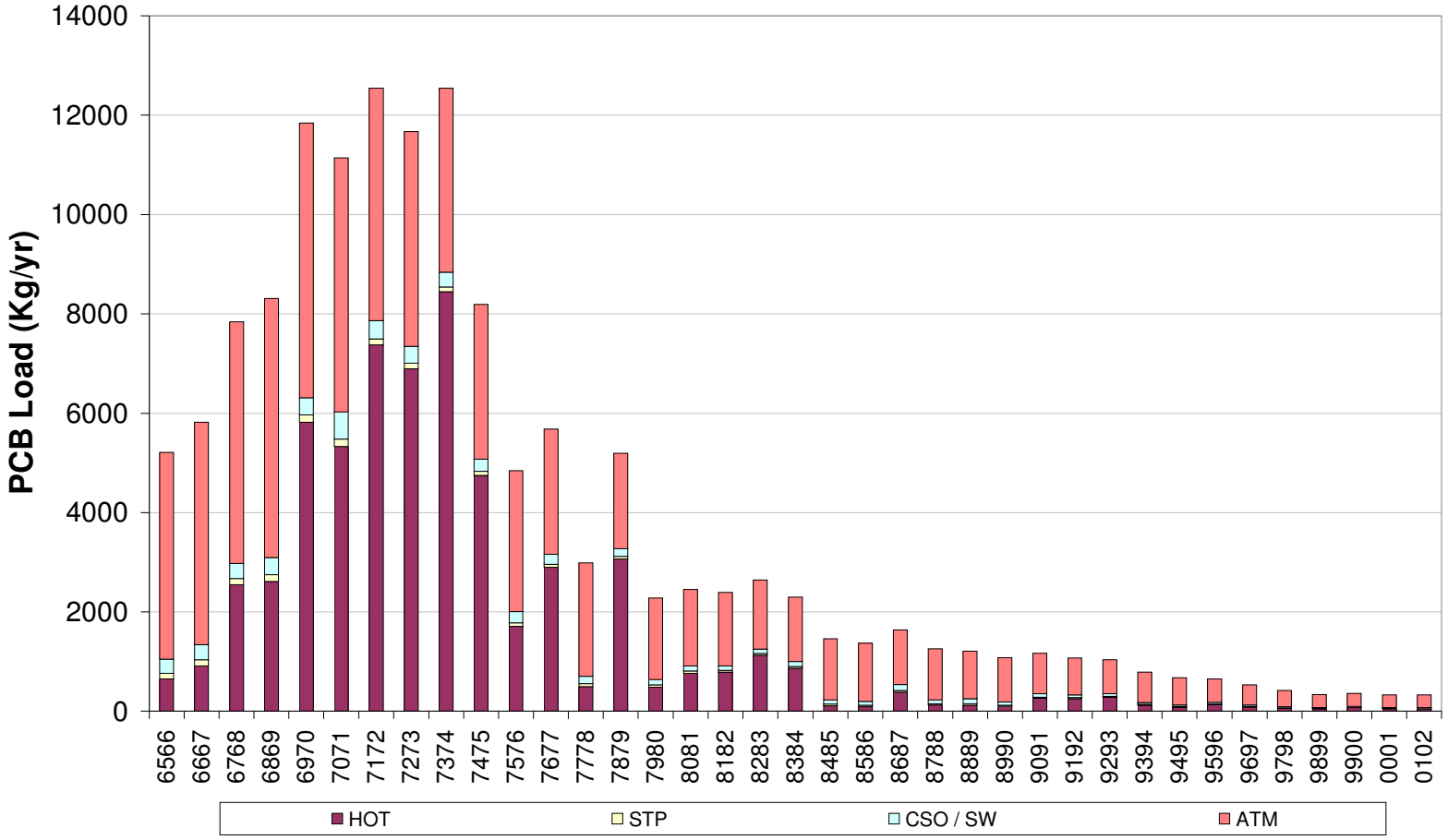

Figure 6-22. All CARP model hindcast simulation loads for tetra-CB by source type.

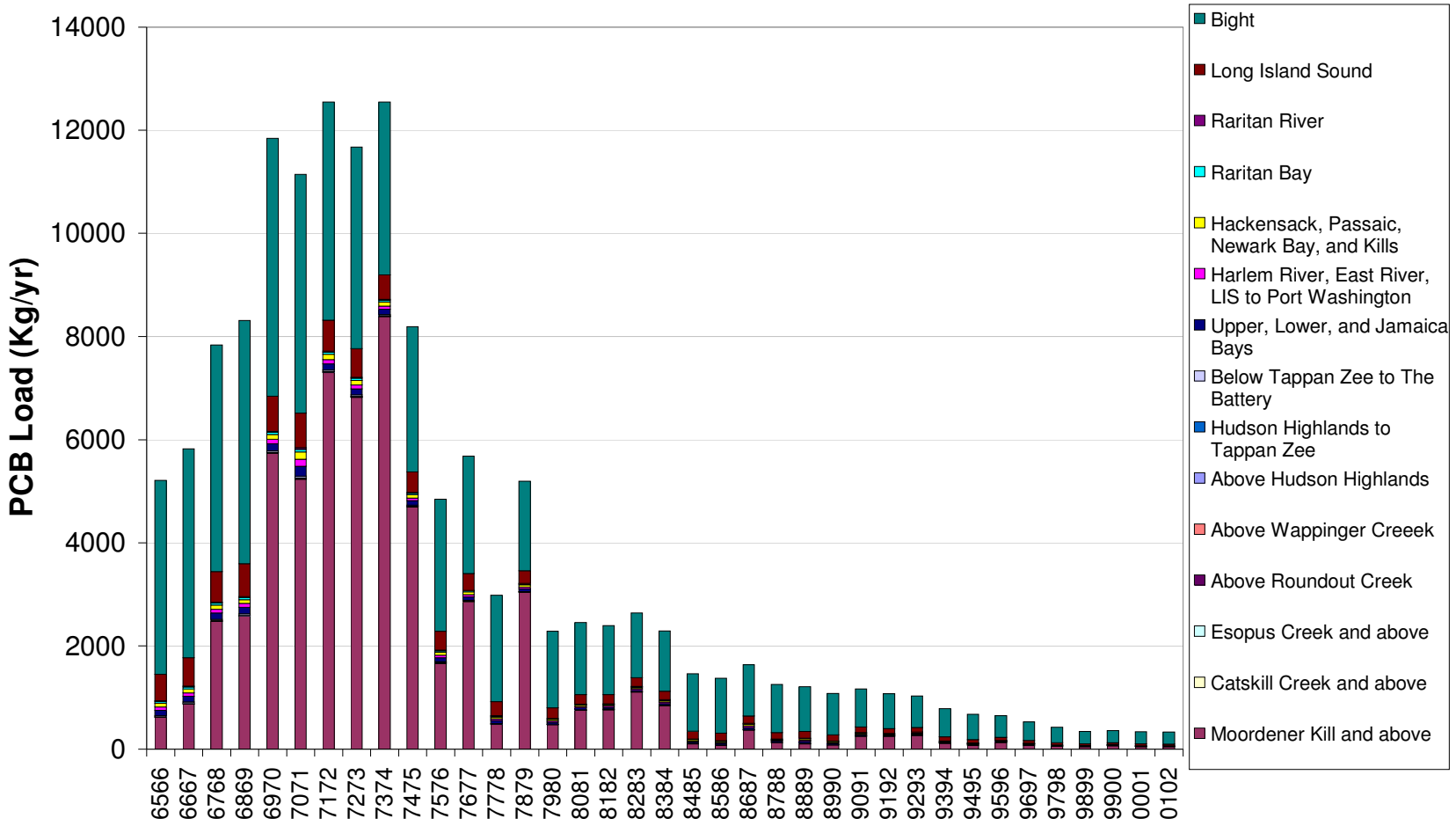

Figure 6-23. All CARP model hindcast simulation loads for tetra-CB by source location.

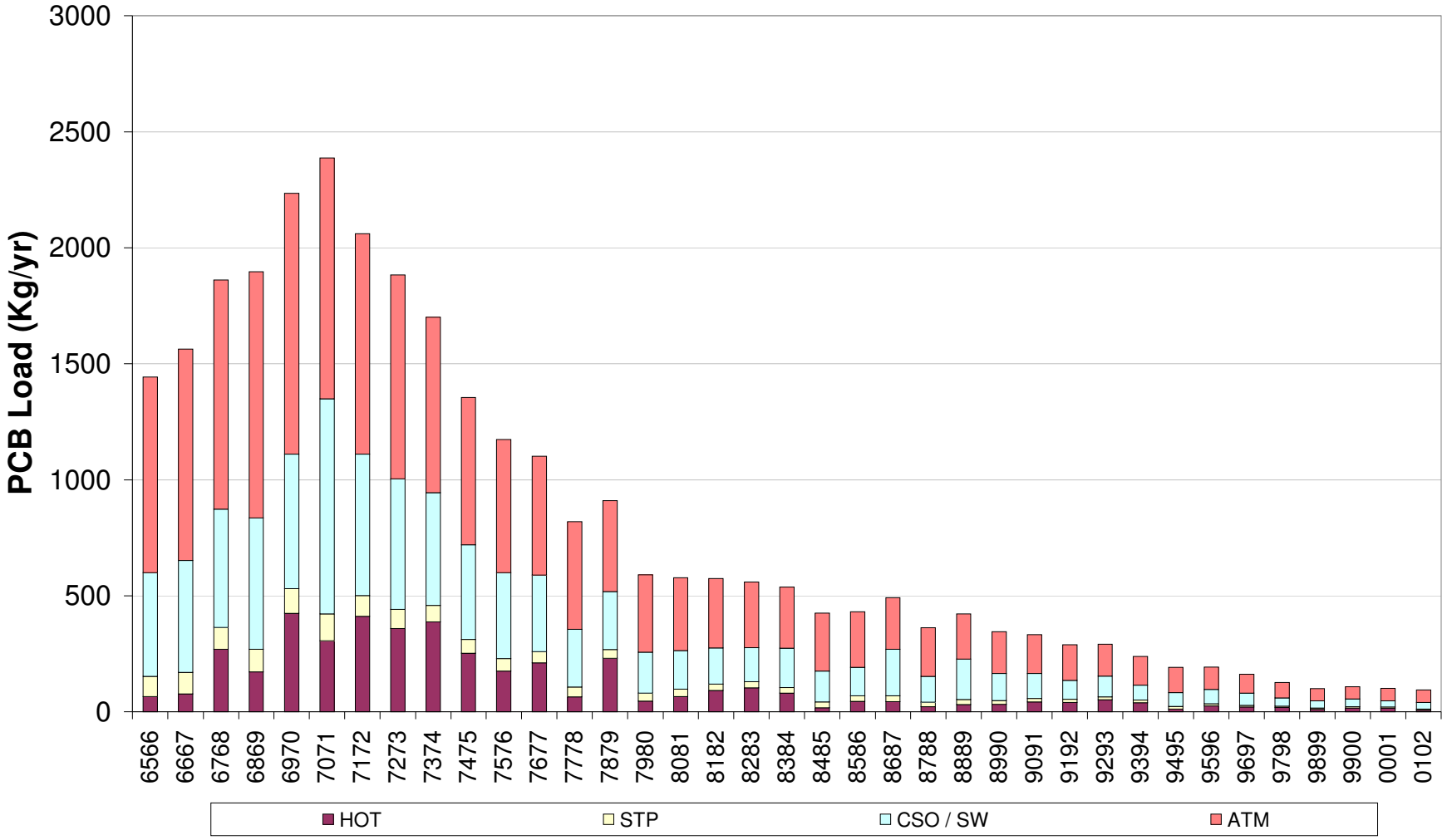

Figure 6-24. All CARP model hindcast simulation loads for hexa-CB by source type.

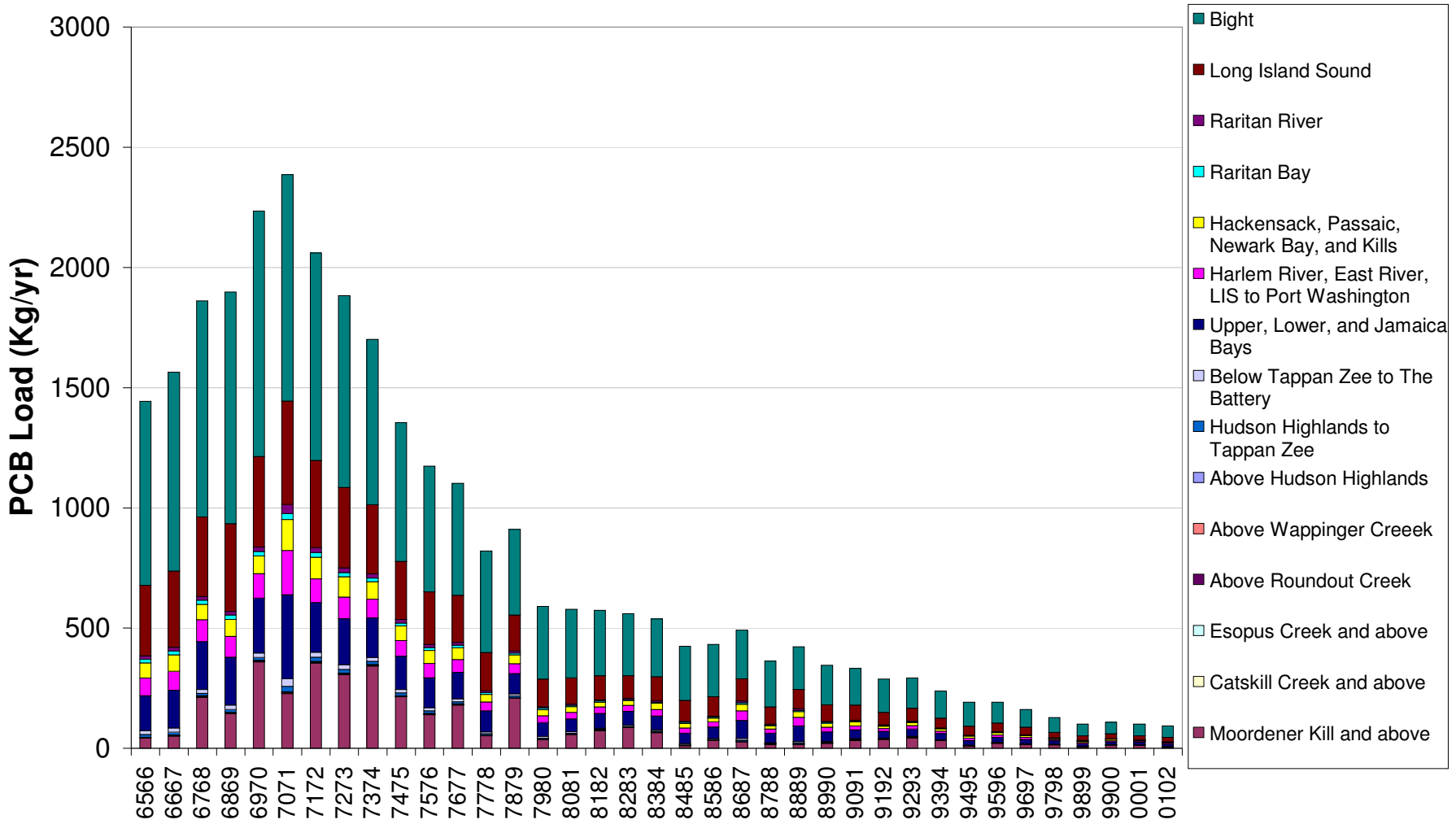

Figure 6-25. All CARP model hindcast simulation loads for hexa-CB by source location.

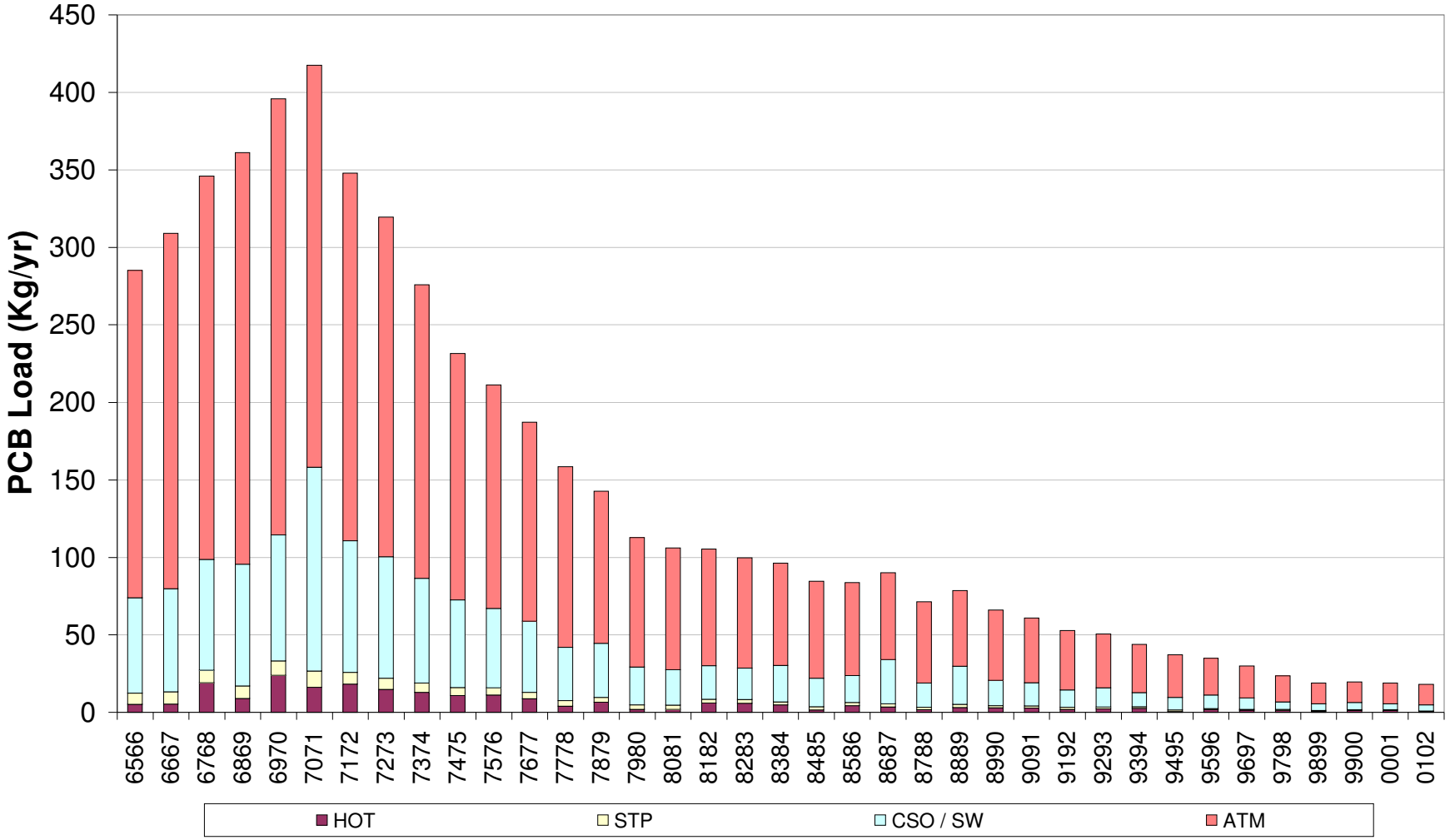

Figure 6-26. All CARP model hindcast simulation loads for octa-CB by source location.

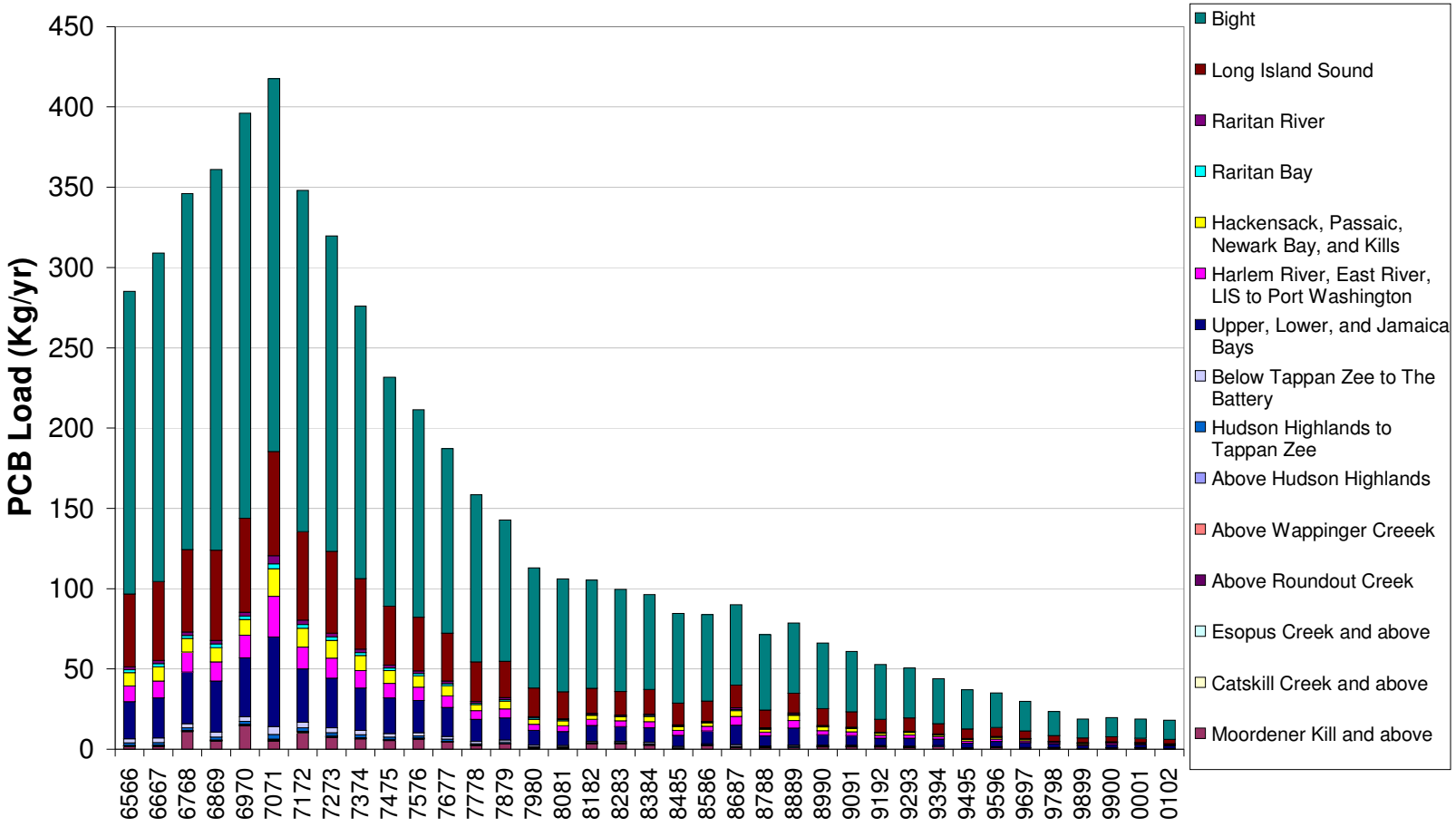

Figure 6-27. All CARP model hindcast simulation loads for octa-CB by source location.

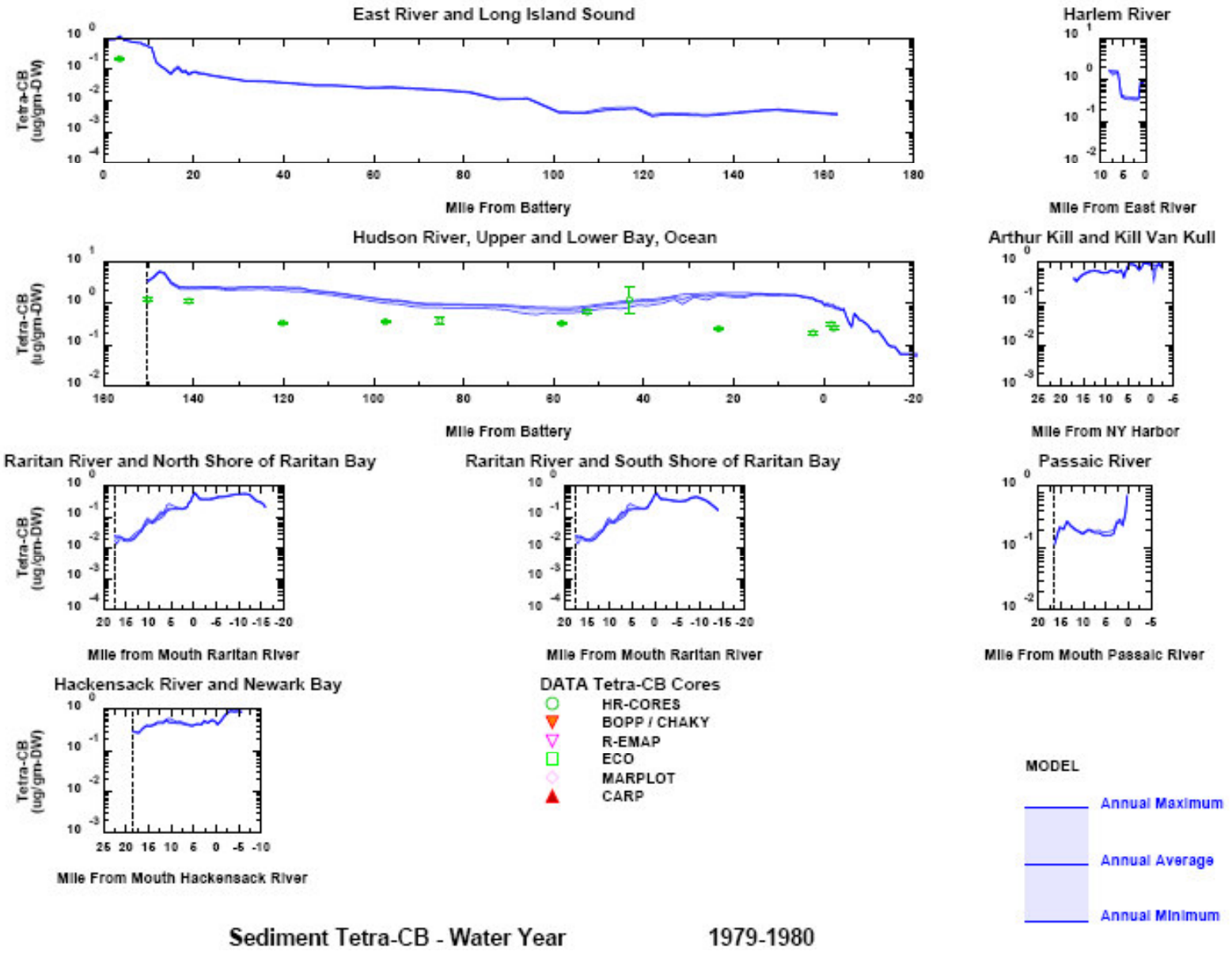

Figure 6-28. Example tetra-CB hindcast model and data comparisons along spatial transects – 1979-80.

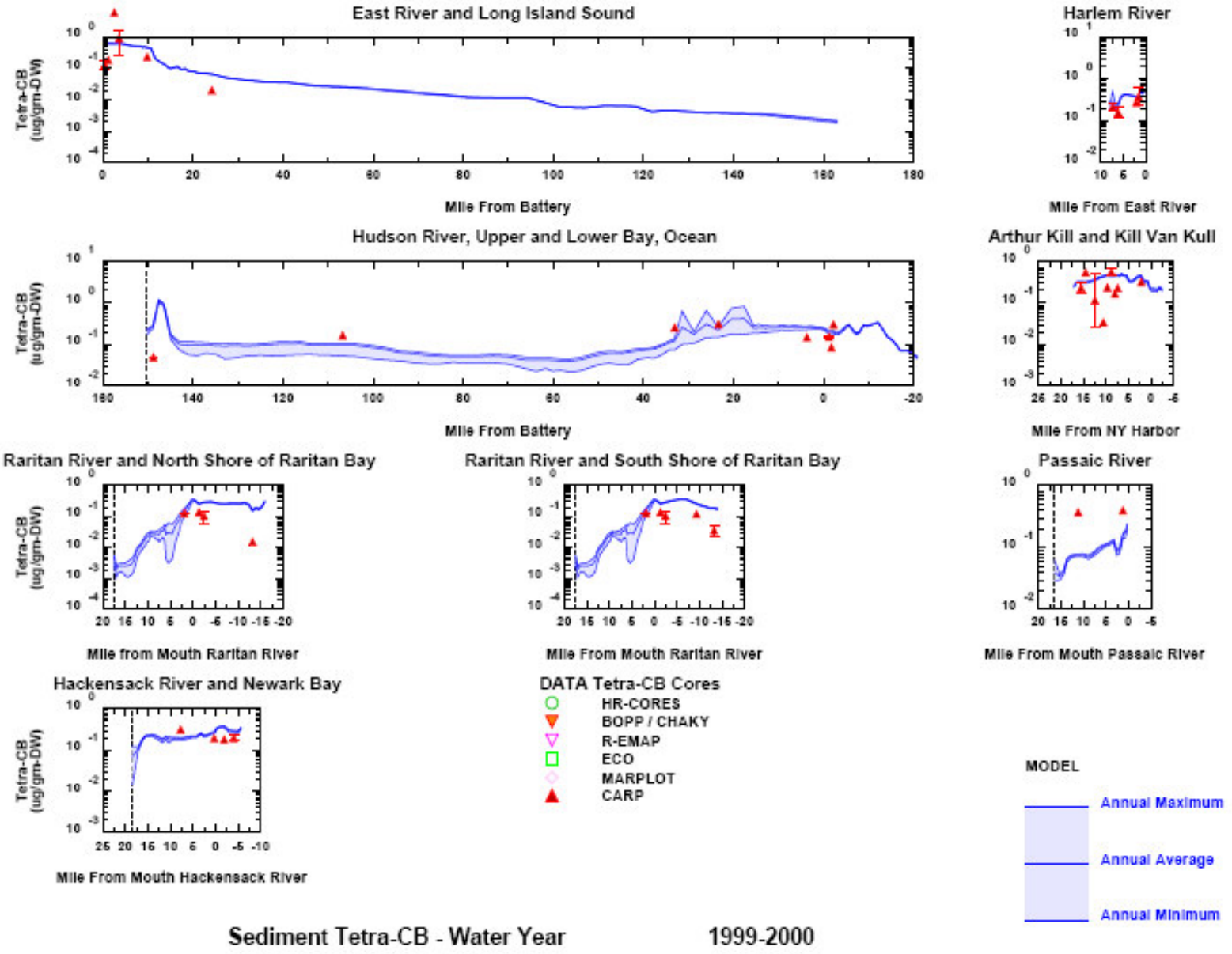

Figure 6-29. Example tetra-CB hindcast model and data comparisons along spatial transects – 1999-2000.

SECTION 7.0

APPLICATION OF CONTAMINANT FATE AND TRANSPORT MODEL TO ADDITIONAL CONTAMINANTS

As described in Sections 2 and 4, the CARP model was developed and calibrated to current conditions (i.e., 1998 -2002) based on measurements of contaminant concentrations in the water column and sediment collected by CARP investigators. Contaminants for which the model was calibrated include: 10 PCB homologs, 17 dioxin and furan congeners, and the metals mercury (including methyl mercury) and cadmium. Both the analytical integrity of the CARP data and the state of the science for understanding behavior in the estuary were considered strong for PCB homologs and dioxin/furan congeners. As a follow up, the calibrated hydrophobic organic contaminant (HOC) model was then further tested for 22 PAH compounds, DDT and its metabolites and chlordane related contaminants. This report section will describe the application of the HOC model kinetics to selected PAHs and organochlorine pesticides.

As part of the application of the CARP HOC model kinetics to selected PAHs and organochlorine pesticides, source terms were developed specifically for each contaminant modeled based on measured loadings and sediment bed initial conditions as described in Section 3.3. Physical constants and coefficients (e.g., critical shear stress) were the same for all contaminants. Chemical specific constants and parameters were varied by contaminant (e.g., Henry's constants, octanol water partition coefficients). In all cases, contaminant specific loading source terms were not adjusted during calibration.

7.1 PAHs

The twenty-two PAH compounds for which the CARP HOC model has been applied include: benzo[a]pyrene, dibenzo[a,h]anthracene, benzo[a]anthracene, benzo[b/j/k]fluoranthene, indeno[1,2,3,cd]pyrene, chrysene, benzo[g,h,i]perylene, acenaphthene, acenaphthylene, fluoranthene, fluorene, pyrene, anthracene, naphthalene, phenanthrene, 1-methylnaphthalene, 2-methylnaphthalene, perylene, 1-methylphenanthrene, 2,3,5-trimethylnaphthalene, 2,6-dimethylnaphthalene, and benzo[e]pyrene. It is noted that Table 1 in the CARP Modeling RFP indicates 17 individual PAH compounds and 4 groups of PAH compounds. Based on the data available from CARP and the specification of the CARP Modeling RFP, the 22 modeled individual PAH compounds include: the 17

individual compounds from Table 1 of the CARP Modeling RFP, two C1 naphthalene compounds, one C2 naphthalene, one C3 naphthalene, and one C1 phenanthrene/anthracene.

Application of the CARP HOC model to the PAH compounds made it necessary to obtain octanol water partition coefficients, K_{OW} , and to calculate site specific organic carbon based partition coefficients, K_{POC}. The calculation of site specific three-phase K_{POC} values for all HOCs included in the CARP model is decribed in Sections 2 and 4 . It is recognized that the calculation method applied for site specific log K_{POC} values works best for contaminants for which both dissolved and particulate phases were routinely and reliably measured. For PAH's, use of XAD columns in the TOPS device to measure the dissolved phase was problematic. Often, particularly as part of the New Jersey CARP data collection, smaller volume whole water grab samples were collected and analyzed or only the filter portion of the TOPS device was used. To avoid the problem of background contaminantion from the methylated naphthalenes and phenanthrenes on XAD columns, the New York CARP investigators used either whole water samples, like New Jersey, or attempted other "non-XAD" methods to separate PAH samples by phase. These attempts were disappointing and the PAH data are considered problematic (Litten, 2003). As a result, our calculations of site-specific log K_{POC} values for PAH compounds, following the protocol utilized for the other HOCs, were based on a very limited number of paired phase-specific measurements. Table 7-1 below tabulates both SPARC-derived log K_{OW} values and final log K_{POC} values for PAH compounds.

Table 7-1. Final K_{POC}[1] Values for CARP Model PAH Application

Compound	log K_{OW}	log K_{POC}
benzo[a]pyrene	6.11	6.18
dibenzo[a,h]anthracene	6.71	6.07
benzo[a]anthracene	5.89	6.15
benzo[b/j/k]fluoranthene	6.27	6.18
indeno[1,2,3,cd]pyrene	6.72	6.47
chrysene	5.71	6.14
benzo[g,h,i]perylene	6.51	6.37
acenaphthene	4.01	5.19
acenaphthylene	3.22	5.61
fluoranthene	5.08	5.95
fluorene	4.21	5.54
pyrene	4.92	5.86
anthracene	4.53	5.83

Table 7-1. Final K_{POC}[1] Values for CARP Model PAH Application

Compound	log K_{OW}	log K_{POC}
naphthalene	3.36	5.00
phenanthrene	4.57	5.98
1-methylnaphthalene	3.84	4.38
2-methylnaphthalene	3.86	3.80
perylene	6.44	6.30
1-methylphenanthrene	5.04	5.72
2,3,5-trimethylnaphthalene	4.86	5.32
2,6-dimethylnaphthalene	4.37	5.59
benzo[e]pyrene	6.44	6.25

Notes:

[1] Assumes an A_{DOC} = 0.08 and represents average observed temperature and salinity conditions.

PAH compounds, like the other HOCs considered by CARP, were subject to volatilization as a function of contaminant concentration, Henry's constant, velocity, and molecular diffusivity, as descibed in section 2.1.1.3.

Model and data comparisons for PAH compounds are shown on the diagrams presented in Appendix 8. The format of these diagrams has been described peviously in Section 4.4. Example diagrams are shown here for benzo[a]pyrene in X-Y, probability, and time series model and data comparison formats in Figures 4-1, 4-2, and 4-3, respectively. Model and data comparison summary diagrams are presented in Figure 4-4 for all PAH compounds modeled. Our interpretation of these diagrams is:

- To the extent that the dissolved water column PAH measurements are credible (i.e., there were technical issues with the manner in which these data were collected and only a limited number of paired measurements of dissolved and particulate phases were available), the model does a reasonable job in describing PAH observations. As shown in the summary diagrams (Figure 4-4), the model somewhat overpredicts both the dissolved and particulate measurements. The model overprediction can be characterized as being within the range of the data and is likely due to any or all of: analytical problems with loading data (described in section 3.3.1.2.1), underestimation of the volatilization rate, or other transformation/degradation processes unique to PAHs that the CARP HOC model kinetics do not account for.

- Although the model does well for most PAHs in the sediment bed, there is a clear problem in the model's ability to calculate measurements of 1-methyl and 2-methyl naphthalenes (log K_{OW} 3.84 and 3.86, respectively) in the sediment bed.
- Further improvement on this calibration would require the collection of additional site specific data. Specifically, data on water column dissolved phase PAH concentrations are needed as well as any site specific fate information on naphthalene and its methylated forms that distinguishes these chemicals from other PAHs. The analytical methods may not yet be available to make the needed measurements.

7.2 ORGANOCHLORINE PESTICIDES

This report section will describe the application of the CARP model to selected organochlorine pesticides including contaminants related to DDT and chlordane.

7.2.1 DDT Related Compounds

The six contaminants related to DDT for which the CARP model has been applied include: 2,4'-DDT, 4,4'-DDT, 2,4'DDE, 4,4'DDE, 2,4'DDD, and 4,4'DDD. The numerical substitution designations may also be referenced as ortho- (o) and para- (p). It is noted that 2,4'-DDT and 4,4'DDT are the major isomers found in technical DDT and that 2,4'DDE, 4,4'DDE, 2,4'DDD, and 4,4'DDD are DDT breakdown products. 2,2'-DDT, an additional isomer found in technical DDT, was not measured by CARP. For purposes of the CARP current conditions model application, the DDT isomers and breakdown products were each modeled as independent contaminants. The justification for this approach is that the processes by which the DDT isomers are converted to DDE and DDD isomers, photolysis and biodegradation, occur very slowly, particularly in the sediment bed where the largest reservoir of these previously used chemicals exists. Essentially, similar to other HOCs modeled under CARP, the DDT related contaminants experience 3-phase partitioning and volatilization.

Application of the CARP HOC model to the DDT related contaminants required octanol water partition coefficients, K_{OW}, and site specific organic carbon based partition coefficients, K_{POC}. The calculation of site specific three-phase K_{POC} values for all HOCs included in the CARP model is decribed in Sections 2 and 4 . For each DDT related contaminant, following the protocol utilized for the other HOCs, we calculated average observed three-phase K_{POC} values based on obervations and applied those as model inputs. Table 7-2 below tabulates both SPARC-derived log K_{OW} values and final log K_{POC} values for DDT related contaminants.

Table 7-2. Final K_{POC}[1] Values for CARP Model DDT Application

Compound	log K_{OW}	log K_{POC}
2,4'-DDD	6.07	6.41
2,4'-DDE	6.73	7.07
2,4'-DDT	6.61	6.85
4,4'-DDD	6.17	6.42
4,4'-DDE	6.79	7.26
4,4'-DDT	6.72	7.38

Notes: [1] Assumes an A_{DOC} = 0.08 and represents average observed temperature and salinity conditions.

Model and data comparisons for the DDT related compounds are shown on the diagrams presented in Appendix 9. The format of these diagrams (i.e., X-Y, probability, and time series) has been described peviously in Section 4.4. Figures 7-5, 7-6, and 7-7 show examples of these model and data comparison diagrams for 4,4'-DDD. Figure 7-8 shows the model and data comparisons for the DDT related contaminants, along with the chlordane related contaminants, in a one page summary format. Our interpretation of these diagrams is that the CARP model performs better for the DDE and DDD isomers than for the DDT isomers. In general there is more range in the water column data than is captured by the model. When there is disagreement between model and data, the model is usually calculating low for the highest measurements. In most cases, there is 90% or better agreement within a factor of ten between water column measurements and calculations and even better agreement for sediment bed measurements and calculations. Within a factor of three, there is 60% or better agreement in most cases between measurements and calculations for the DDE and DDD isomers. For the DDT isomers, there is 30% or better agreement within a factor of three between water column measurements and calculations. For the DDT isomers in the sediment, the agreement within a factor of three between measured and calculated is 40% or better. These results are suggestive of the fact that the model includes the major sources of the DDT related contaminants and that the model is accurately representing the overall transport and phase partitioning behavior of these contaminants. The model does not include degradation processes. This is consistent with some of the underprediction of DDE and DDD but is not consistent with underprediction of DDT. The overall conclusion is that there doesn't appear to be any systematic biases (e.g., model always higher than data) in the organochlorine pesticide calibrations.

7.2.2 Chlordane Related Compounds

The five contaminants related to chlordane for which the CARP model has been applied include:α-chlordane (also known as cis-), γ-chlordane (also known as trans-), oxychlordane, cis-nonachlor, and trans-nonachlor. α-Chlordane and γ-chlordane are the dominant chlordane isomers in technical chlordane and in bed sediments. Oxychlordane is a highly toxic chlordane by-product. Trans-nonachlor, and to a lesser extent cis-nonachlor, are major ingredients found in chlordane and were also modeled with the chlordane isomers and by-product. The nonachlors were selected for modeling because, along with oxychlordane, they are the dominant forms of chlordane usually found in fish. Heptachlor, which was first isolated from technical chlordane, was produced and used on its own. Heptachlor epoxide is a heptachlor metabolite. Since heptachlor was manufactured and applied independent of chlordane, heptachlor and heptachlor epoxide were not included in the CARP model application for chlordane. Other CARP researchers have also defined total chlordane to include: include:α-chlordane, γ-chlordane, oxychlordane, cis-nonachlor, and trans-nonachlor (Litten, 2003).

Exact details of the transformations between the chlordane related contaminants in the environment are poorly understood. Accordingly, the application of the CARP model to the chlordane related contaminants considered each contaminant independently and did not attempt to account for the transformations. Modeling the transformations would require data and information beyond the scope of CARP.

Application of the CARP HOC model to the chlordane related contaminants required octanol water partition coefficients, K_{OW}, and site specific organic carbon based partition coefficients, K_{POC}. The calculation of site specific three-phase K_{POC} values for all HOCs included in the CARP model is decribed in Sections 2 and 4 . For each chlordane related contaminant, following the protocol utilized for the other HOCs, we calculated average observed three-phase K_{POC} values based on obervations and applied those as model inputs. Table 7-3 below tabulates both SPARC-derived log K_{OW} values and final log K_{POC} values for chlordane related contaminants.

Table 7-3. Final K_{POC}[1] Values for CARP Model Chlordane Application

Compound	log K_{OW}	log K_{POC}
α-chlordane	6.01	6.27
γ-chlordane	6.01	6.30
Oxychlordane	4.82	5.60
Cis-nonachlor	6.50	6.70
Trans-nonachlor	6.50	6.67

Notes: [1] Assumes an A_{DOC} = 0.08 and considered to be representative of average temperature and salinity conditions.

Model and data comparisons for chlordane related compounds, along with the comparisons for DDT related compounds, are shown on the diagrams presented in Appendix 9. The format of these diagrams has been described peviously in Section 4.4 where example plots are shown. As described in Section 7.2.1, a one page summary format plot is available for the calibration results for the chlordane related contaminants, along with the DDT related contaminants (see Figure 7-8). The comparisons in Figure 7-8 demonstrate that the model and data comparisons for the chlordane related contaminants are overall in reasonable agreement (see bars plotted at logKow 4.82, 6.01, and 6.50). The α-, γ, and oxy- chlordanes have relatively strong comparisons given the simplified modeling approach. There is greater than 90% concurrence within a factor of ten between water column measurements and calculations as shown on the X-Y plots in Appendix 9. Within a factor of three, there is 40% or greater agreement between measurements and calculations. Agreement in the sediment bed is even greater. For the nonachlors, the water column comparisons are somewhat weaker. Overall, there tends to be more of a range represented by the New York collected than the New Jersey collected CARP data, probably related to the greater spatial coverage of the New York collected CARP data. When the model and data are in disagreement, particularly for the α and γchlordanes and trans-nonachlor, the model tends to overpredict the lowest measurements as shown on the probability diagrams in Appendix 9. The comparisons for oxychlordane and cis-nonachlor are more uniform. We believe these comparisons demonstrate that the CARP model is capturing the major sources of the chlordane related contaminants and is properly accounting for their overall transport and phase partitioning. These comparisons also indicate that the transformation processes not accounted for in the CARP model kinetics play a relatively minor role in determining levels of contamination in the Harbor water column and bed over the time horizon of the current conditions calibration.

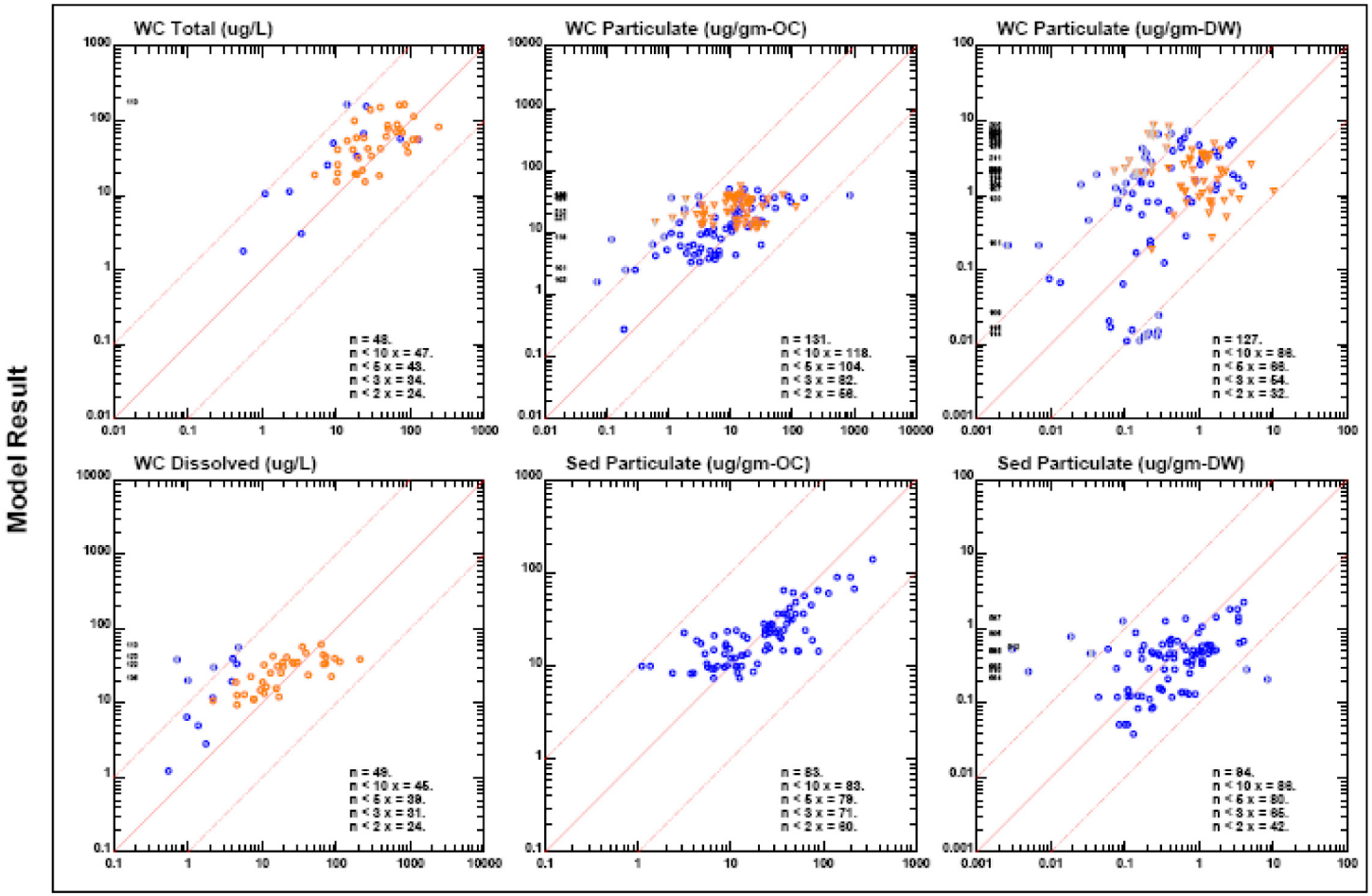

Figure 7-1. Example X-Y model and data comparison plots for benzo[a]pyrene

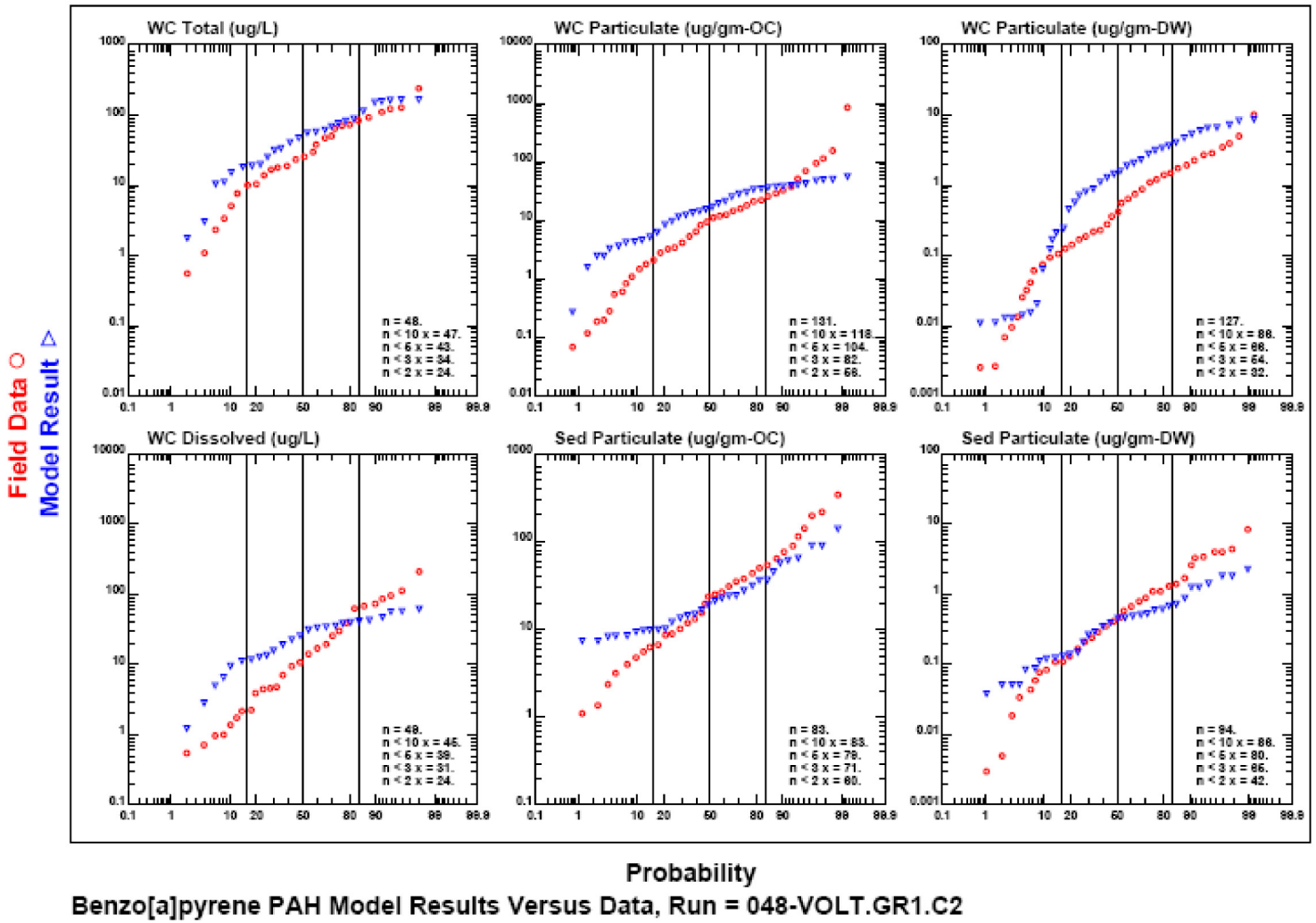

Figure 7-2. Example probability model and data comparison plot for benzo[a]pyrene

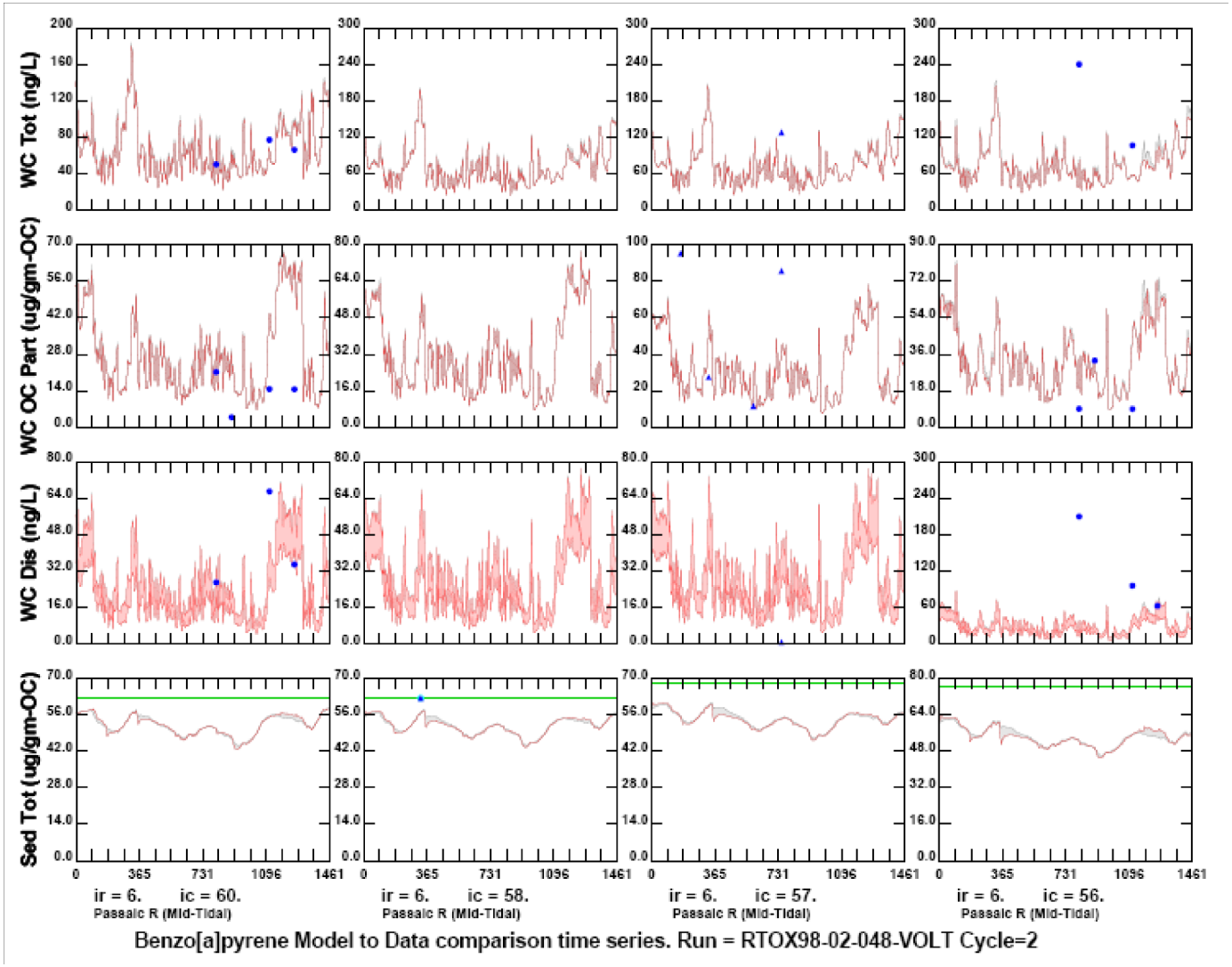

Figure 7-3. Example time series model and data comparison plots for benzo[a]pyrene at four locations in the Passaic River

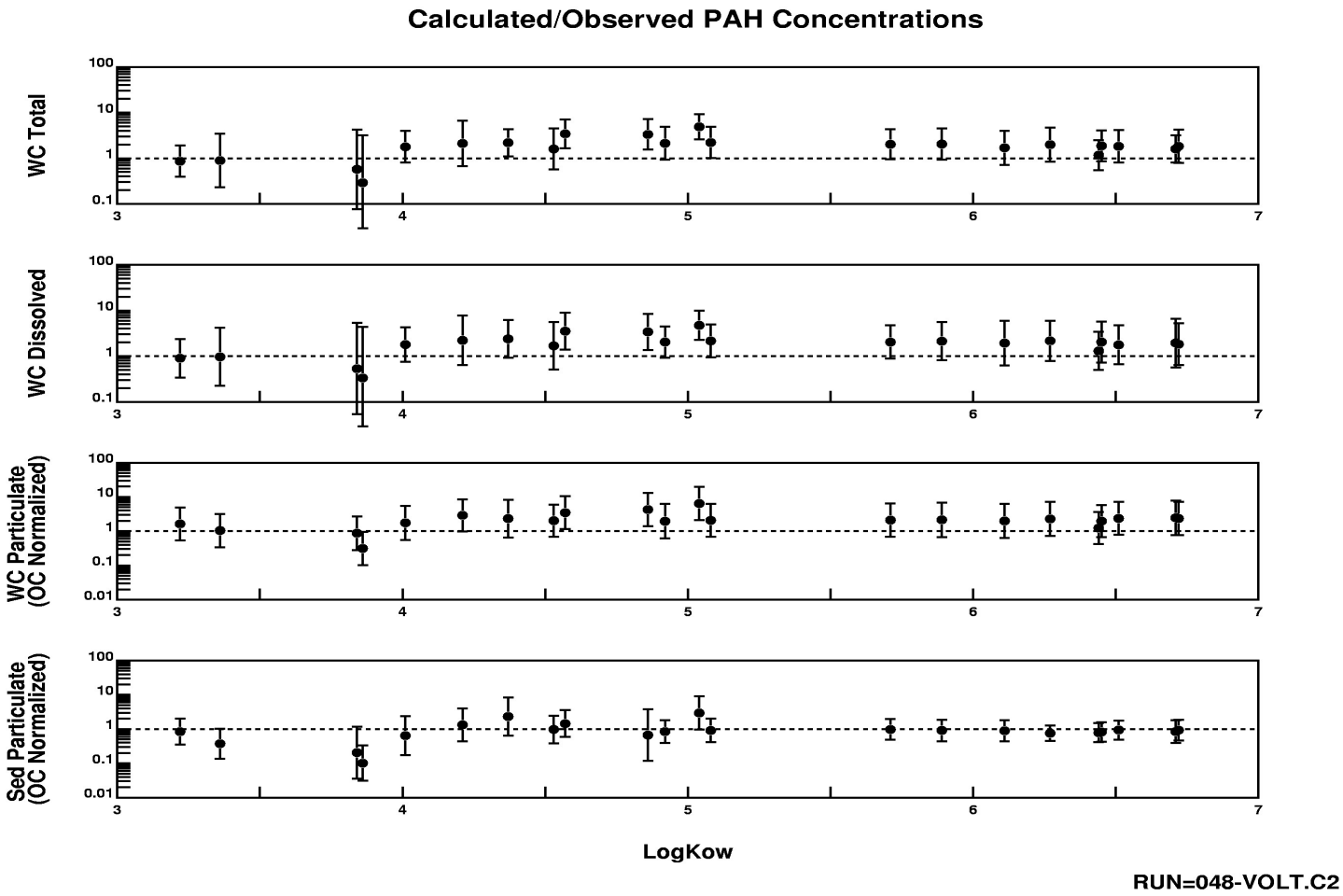

Figure 7-4. Calibration summary for 22 PAH compounds.

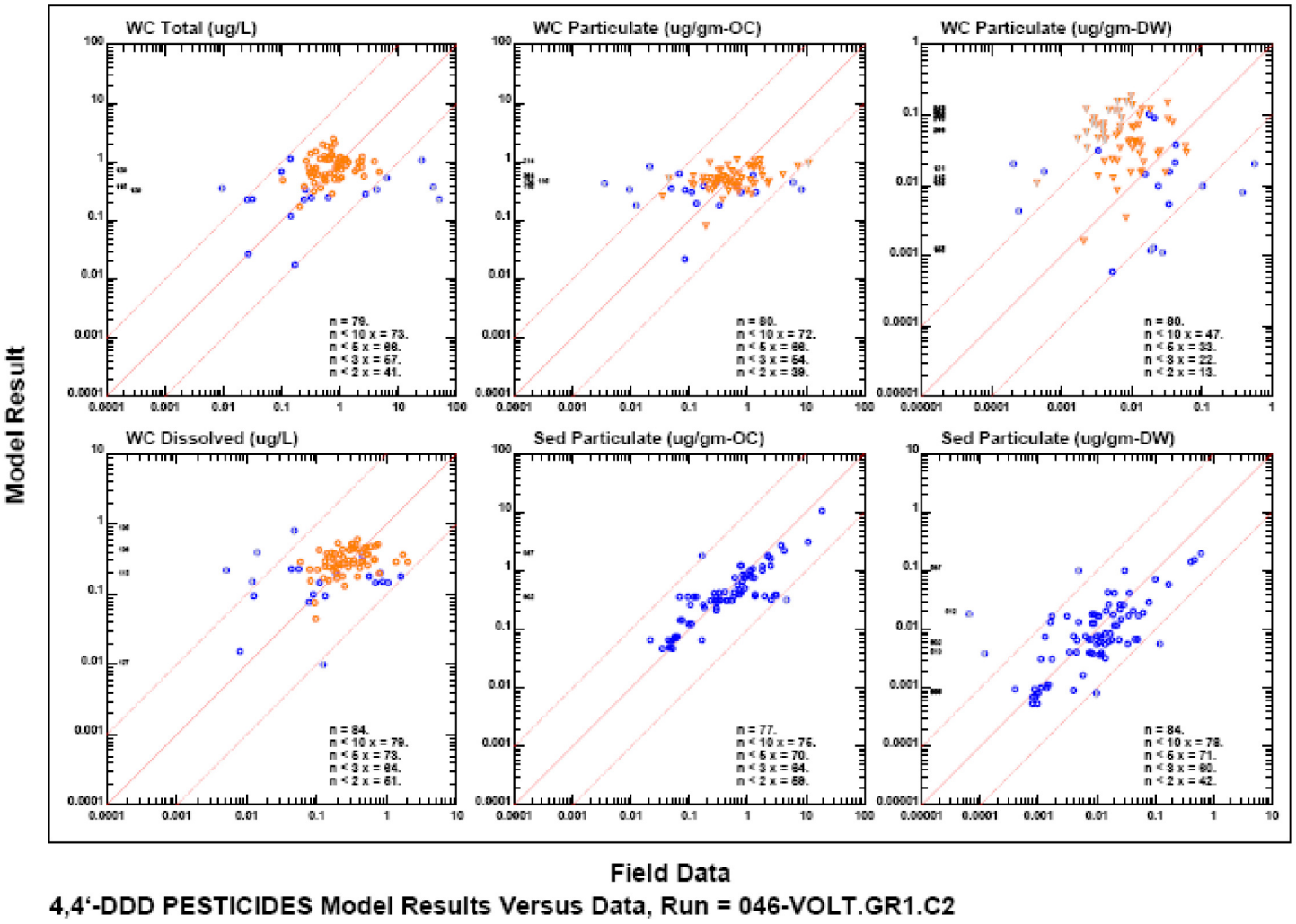

Figure 7-5. Example X-Y model and data comparisons for 4,4'-DDD

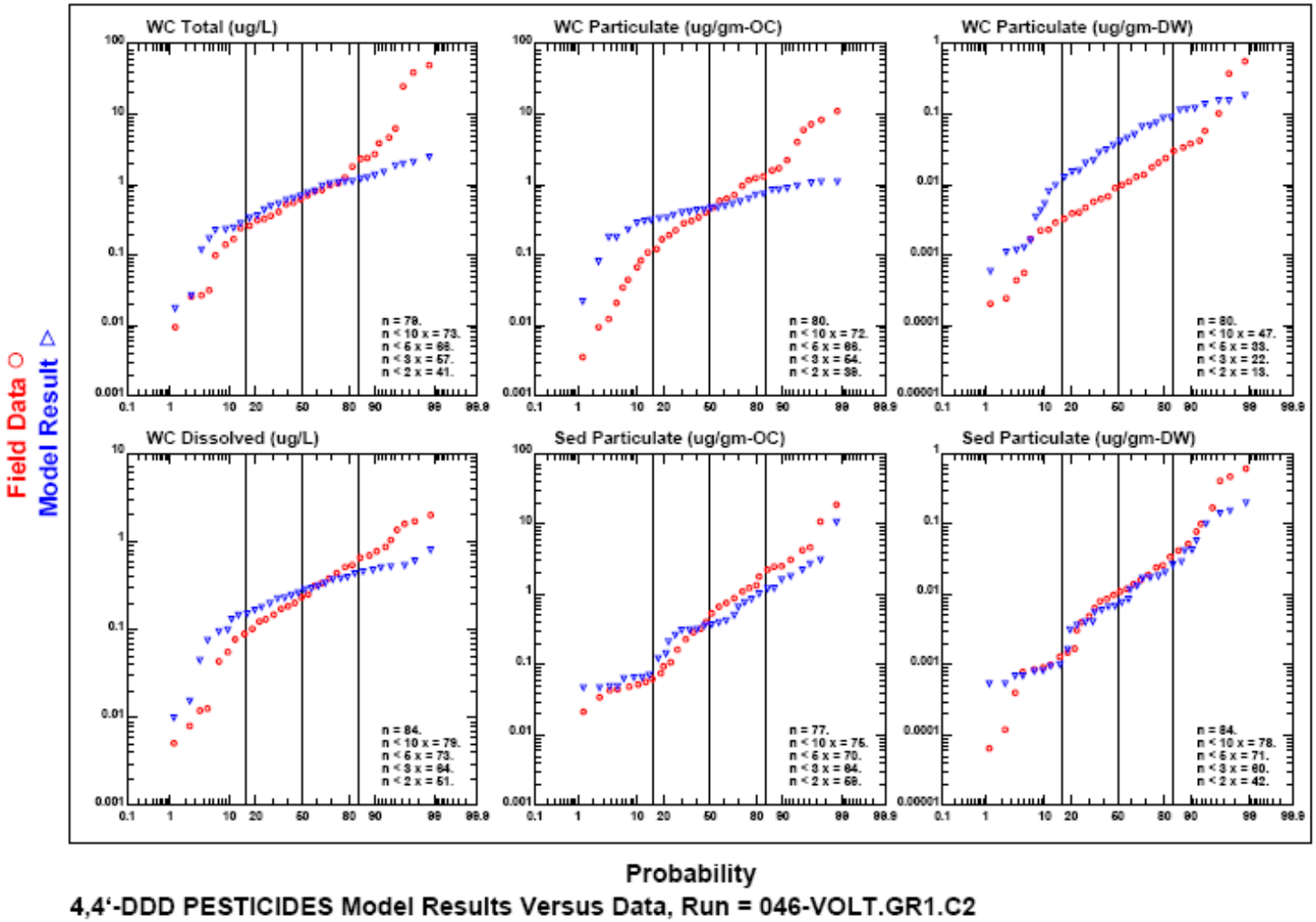

Figure 7-6. Example probability model and data comparisons for 4,4'-DDD

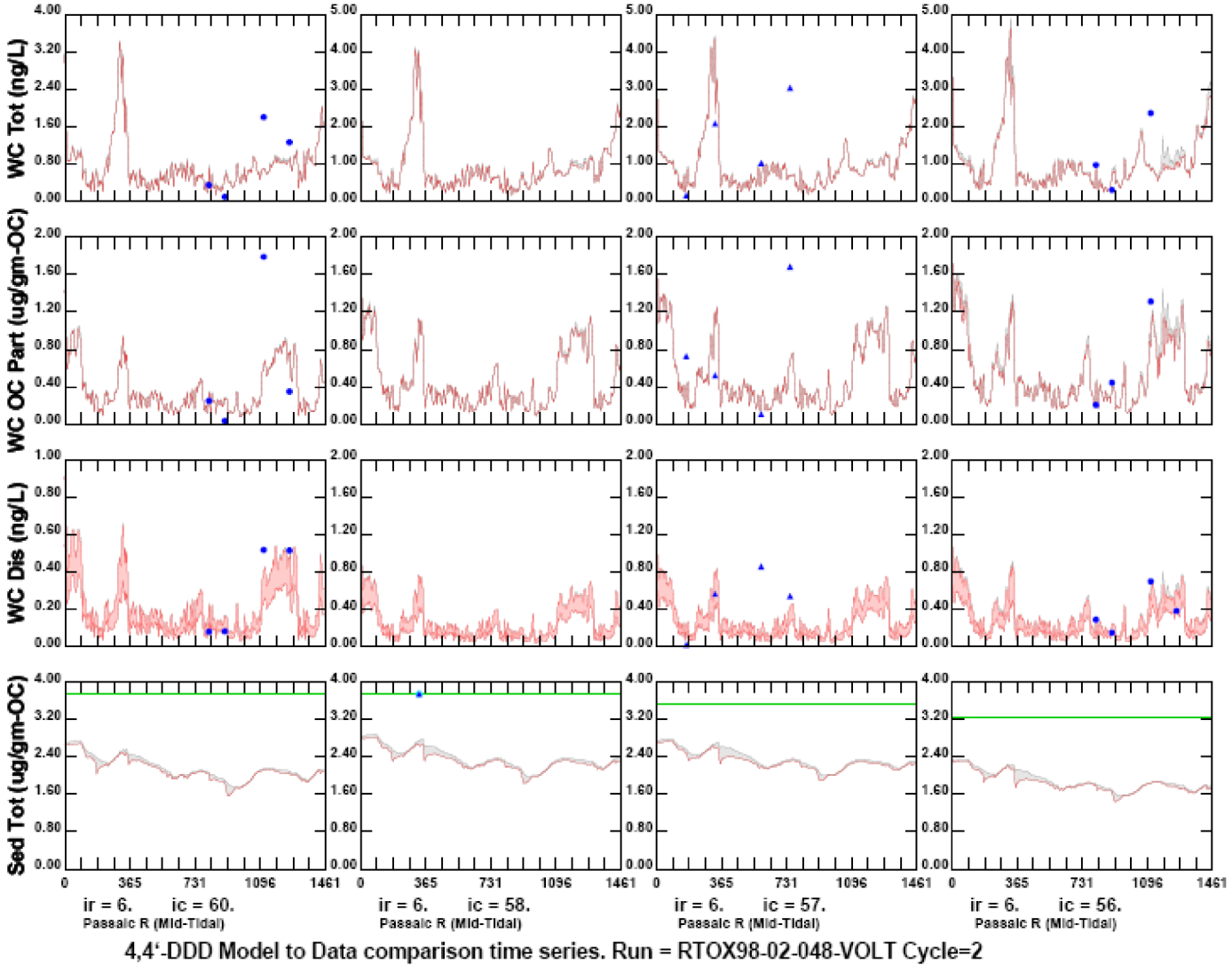

Figure 7-7. Example time series model and data comparisons for 4,4'-DDD at four locations in the Passaic River

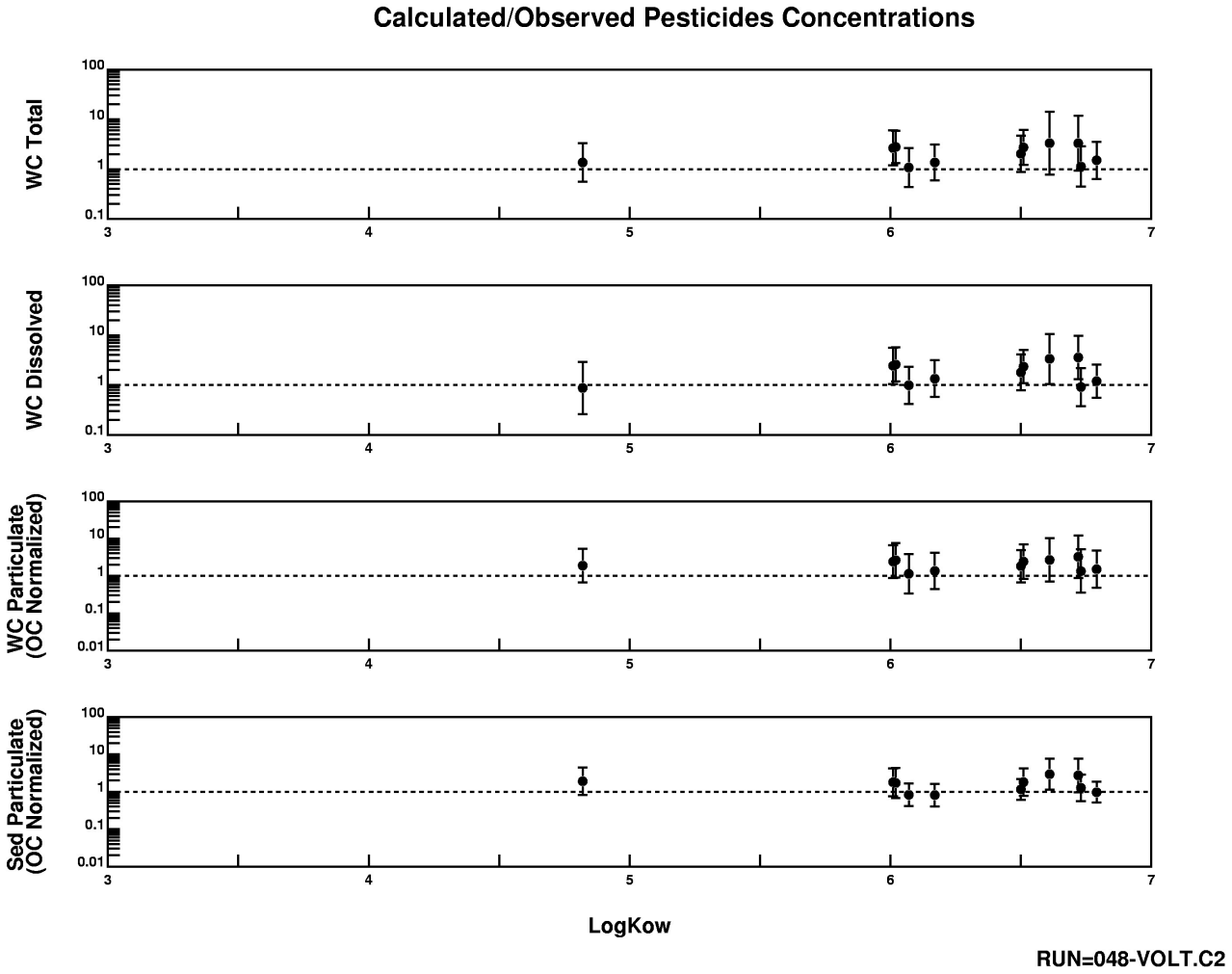

Figure 7-8. Calibration summary for DDT related and chlordane related organochlorine pesticides.

SECTION 8.0

FOOD CHAIN / BIOACCUMULATION MODELING APPROACH

A bioaccumulation model is necessary for CARP specifically to: (1) evaluate the link between current contaminant concentrations in the water column and sediment to levels in the biota; and (2) to evaluate the response of the biota to changes in the contaminant concentrations in the water column and in sediments. For purposes of CARP, several descriptions of bioaccumulation of HOCs and metals have been developed ranging from field-derived bioaccumulation and biota-sediment accumulation factors (BAFs and BSAFs) to time-variable, age-dependent bioaccumulation models. This report section will describe (1) the evaluation of field-derived BAFs for water column species and field-derived BAFs and BSAFs for benthic species, (2) the general formulation of the bioaccumulation model, (3) the time-variable bioaccumulation model for the white perch and striped bass food chain, and (4) the steady-state bioaccumulation model calculation for Harbor worms. This is followed by a description of the setup for BAF, BSAF and bioaccumulation model evaluations (Section 9), the BAF and BSAF results (Section 10), and more detailed bioaccumulation model results and sensitivity calculations (Section 11). It is noted that the BAF and BSAF results presented in Section 10 are used for subsequent management projections as presented in Sections 12 and 13.

The overall approach followed on CARP for bioaccumulation is based on the calculation of and application of BAFs and BSAFs developed from the CARP biological data collected by NYSDEC. Steady-state model calculations for Harbor worms and time-variable model calculations for the white perch and striped bass food chain were performed for reasons of sensitivity and to develop possible causal explanations for trends observed in the measured BAFs and BSAFs. In this sense, the bioaccumulation model was used to evaluate, or add value to, field-derived BAFs and BSAFs. Whether or not the BAFs and BSAFs were directly calculated by the model or measured in the field, their predictive capability would remain tied to predicting changes in exposure concentrations. BAFs and BSAFs do not forecast changes in trophic sturcture.

8.1 EVALUATION OF BIOACCUMULATION FACTORS (BAFs)

BioAccumulation Factors (BAFs) have been used as a static descriptor for the accumulation of HOCs and metals in water column species. In this context, a BAF is the ratio of the contaminant concentration in the organism (expressed either on a wet weight or lipid normalized basis) to the concentration of freely dissolved chemical in water (e.g., in μg / L) based on exposure to contaminated water and food.

$$BAF = \frac{v}{C_{dis}^{freely}} \quad or \quad BAF_{lipid} = \frac{v_{lipid}}{C_{dis}^{freely}} \tag{8-1}$$

Initial evaluation of the CARP biota data for water column species was performed using field-derived BAFs for PCB homologs, dioxin / furan congeners, pesticides, PAHs, mercury and cadmium. For this purpose, measured body burdens for PCB homologs, dioxin / furan congeners, pesticides and PAHs were lipid normalized, and body burdens for mercury and cadmium were expressed on a wet weight basis. Since corresponding water concentrations were not collected during fish sampling, freely-dissolved contaminant concentrations for HOCs were obtained for each sample location and time period as five day averages from the CARP contaminant fate model. For metals, the free metal ion concentration for cadmium and mercury (i.e., Cd^{2+} and Hg^{2+}) and the freely dissolved methyl mercury concentrations were obtained for each sample location and average five day time period from the CARP contaminant fate model. Water column species considered in this evaluation included zooplankton, white perch, striped bass, mummichog, American eel, and winter flounder.

8.2 EVALUATION OF BIOTA-SEDIMENT ACCUMULATION FACTORS (BSAFs)

Biota-Sediment Accumulation Factors (BSAFs) have been used as a static descriptor for the accumulation of HOCs and metals in benthic species. In this context, a BSAF is the ratio of the contaminant concentration in the organism (expressed either on a wet weight or lipid normalized basis) to the contaminant concentration in sediment (expressed either on a dry weight or organic carbon normalized basis).

$$BSAF = \frac{v}{r} \quad or \quad BSAF_{lipid,oc} = \frac{v_{lipid}}{r_{oc}} \tag{8-2}$$

Initial evaluation of the CARP biota data for benthic species was performed using field-derived BSAFs for PCB homologs, dioxin / furan congeners, pesticides, PAHs, mercury and cadmium. For this purpose, measured body burdens for PCB homologs, dioxin / furan congeners, pesticides and PAHs were lipid normalized, and body burdens for mercury and cadmium were expressed on a wet weight basis. Since corresponding sediment samples were not collected during the initial CARP benthic sampling, sediment contaminant concentrations were obtained for each sample location and time period as five day averages from the CARP contaminant fate model on an organic carbon normalized basis. Benthic species considered in this evaluation included clams and blue crabs.

For a special worm sampling program that was conducted subsequent to CARP sampling, co-located worm and sediment samples were collected at seven locations throughout the Harbor. For this

dataset, measurements of contaminant concentrations in worms and sediment were used directly in calculating field-derived BSAFs.

As described in Section 10, field-derived BSAFs for harbor worms are also compared to laboratory-derived BSAFs for the dredged material test organism *Nereis virens* (a polychaete worm). The laboratory-derived BSAFs are based on 28-day laboratory exposure data from dredged material testing studies. The data were furnished to HydroQual electronically by Mark Reiss of USEPA Region 2. The data are described, in part, in a series of technical reports prepared by a USACE-New York District contractor (Battelle 1996a-e). As a further examination of bioaccumulation behavior, we performed similar evaluations of BSAFs for 10-day laboratory exposure data for *Armandia brevis* (a polychaete worm) (Meador et al., 1997).

8.3 GENERAL BIOACCUMULATION MODEL FORMULATION

The accumulation of toxic chemicals into aquatic organisms is typically viewed as a dynamic process that depends on direct uptake from the water, food ingestion, depuration (from back diffusion, urine excretion and egestion of fecal matter) and metabolic transformation of the contaminant within the organism. For phytoplankton and possibly lower trophic species, direct uptake from the water is described by diffusion of the contaminant through cell membranes. For fish and other higher trophic organisms, diffusion (e.g. through gill membranes or dermal layers) and food ingestion may both play important roles. The basic modeling approach, which has largely been developed for HOCs, is described below.

In general, model equations for the uptake and release of contaminants are often written in terms of μg contaminant per g organisms (ν) where organism weight is expressed in terms of wet weight or lipid content (Thomann et al., 1992a). The general form of bioaccumulation equations is given below:

$$\frac{d\nu_i}{dt} = k_{u_i} C_{dis} - k_{b_i} \nu_i + \sum_j \alpha_{i,j} I_{i,j} \nu_j \left[\frac{f_{dry\ wt_j}}{f_{dry\ wt_i}} \right] - \left(k_e + k_m + k_g \right) \nu_i \qquad (8\text{-}3)$$

where ν_i is the concentration of the chemical in organism i (μg contaminant/g organism i), t is time, k_{ui} is the diffusive uptake rate of dissolved contaminant from the water and into the organism (L/g organism i/day), C_{dis} is the freely-dissolved contaminant concentration (μg contaminant/L) and typically does not include complexed forms of the contaminant, k_{bi} is the back diffusive transfer rate of contaminant from the organism and into the water (1/day), α_{ij} is the efficiency of organism i to assimilate contaminant from feeding on organism j (unitless), $I_{i,j}$ is the ingestion rate of organism i on

organism j (g prey/g predator/day), $f_{dry\ wt}$ is the fraction dry weight of the predator and the prey, k_e is the excretion/egestion rate coefficient for contaminant removal from organism i (1/day), k_m is the metabolic transformation rate coefficient for contaminant in organism i (1/day), and k_g is the growth rate coefficient (1/day) and is included to account for the reduction in ν_i due to the increase in the size of the organism (i.e., growth dilution). For phytoplankton, which serve as the base of the food web, only diffusion of dissolved contaminant across the cell membrane is considered as an uptake mechanism. The equation for phytoplankton is therefore analogous to Equation 8.3 but does not include a term for contaminant uptake through ingestion of contaminated prey.

Equation 8.3 or similar equations have been applied to multiple trophic levels in the development of food chain models (Thomann and Connolly, 1984; Thomann et al., 1991; Connolly, 1991; Thomann et al., 1992a,b; Gobas, 1993; Park, 1998; Barber et al., 1991). Overall, the models are similar in their construct and reflect a cross-fertilization of ideas among investigators (e.g., see the comparison of the Thomann and Gobas models presented in Burkhard, 1998). As an example, a generic food chain model proposed by Thomann et al. (1992a,b) is presented in Figure 8-1. Five interactive biological compartments are considered, together with the particulate and freely-dissolved contaminant concentrations in the water column and in sediments. In these types of models, the contaminant concentration in phytoplankton is often considered to be in equilibrium with dissolved contaminant concentrations. The accumulation of contaminant in higher trophic organisms is dependent on both diffusive transfer (e.g. through gills) and feeding as described in eq 8-3. Here, zooplankton obtain their food from the ingestion of phytoplankton, benthic invertebrates obtain contaminant through the ingestion of contaminated sediment particles (and possibly from phytoplankton and detrital matter at the sediment-water interface, not shown), forage fish feed on zooplankton and benthic invertebrates, and piscivorous fish feed primarily on forage fish.

For specific model applications, feeding patterns, ingestion rates (I_{ij}), growth rates (k_g), and egestion rates (k_e) are determined from bioenergetic models of energy flows through food chains and/or from stomach content, fish growth, and fecal matter production data. Because age may play an important role in describing feeding patterns and in determining the accumulation of contaminant, a further breakdown in age classes may be required. Other model parameters for diffusive uptake and backward diffusive transfer (k_{ui} and k_{bi}), assimilation efficiencies (α_{ij}), and egestion and the metabolic rate coefficients (k_e and k_m) are usually taken from previous laboratory studies or are determined from model calibration of field data.

8.4 BIOACCUMULATION MODEL FOR WHITE PERCH AND STRIPED BASS FOOD CHAIN

A time-variable, age-dependent striped bass food chain model was previously developed by Thomann et al. (1989; 1991), and later applied by Farley et al. (1999; 2006) in a subsequent study of PCB contamination in the Lower Hudson and NY-NJ Harbor. The model includes a five component, water-column food chain that consists of phytoplankton, zooplankton, small fish, seven age classes of perch, and seventeen age classes of striped bass (see Figure 8-2). As shown, phytoplankton serve as the base of the food chain. Phytoplankton are preyed upon by a zooplankton compartment, the characteristics of which is considered to be represented by *Gammarus*. The small fish compartment, which feeds on zooplankton, is meant to reflect a mixed diet of fish of about 10 g in weight and includes age 0-1 tomcod and herring. White perch is considered as a representative size-dependent prey of the striped bass and is assumed to feed exclusively on zooplankton. Based on feeding studies where stomach contents of striped bass were examined (Gardinier and Hoff 1982; O'Connor 1984; Setzler et al. 1980), the 0-2 year old striped bass are assumed to feed on zooplankton; 2-5 year old striped bass are assumed to feed on a mixture of small fish and 0-2 year old perch; and 6-17 year old striped bass are assumed to feed on 2-5 year old perch.

This model forms the basis of the CARP bioaccumulation model and is used in bioaccumulation modeling and sensitivity studies for 10 PCB homologs, 17 dioxin / furan congeners, cadmium and mercury in the white perch-striped bass food chain (see Section 11). In applying the model to the Lower Hudson, freely dissolved concentrations of PCBs, dioxins and furans, free cadmium, free mercury and methyl mercury concentrations in water are taken directly from the CARP contaminant fate model. For PCBs, dioxins and furans, contaminant accumulation in phytoplankton is then described by equilibrium partitioning based on the lipid content of the phytoplankton and chemical-specific, octanol-water partition coefficients. Octanol-water partition coefficients for PCBs were adjusted for temperature and salinity using the van't Hoff equation and Setschenow's equation, respectively (see previous description in Section 2). Since reliable estimates for enthalpies of phase change are not available for dioxins and furans, only salinity adjustments were made. For cadmium, mercury and methylmercury, POC-bound metal concentrations were taken directly from the CARP contaminant fate model and were assumed to be representative of metal concentrations in phytoplankton.

Respiration rates for zooplankton, small fish, white perch, and striped bass were estimated using formulations given in Thomann and Connolly (1984) and Connolly and Tonelli (1985). These values are used along with dry weight fractions, food assimilation efficiency (a), the gill transfer efficiency (β), and chemical assimilation efficiency from food (α) to calculate the remaining bioenergetic parameters. These include the gill uptake rates ($k_u = \beta \cdot R_{oxygen}/C_{oxygen}$) and food ingestion rates ($I = (R+k_g)/a$). For

model applications for PCB homologs and dioxin / furan congeners, chemical-specific K_{ow}'s were used along with gill uptake rates (k_u) and lipid content to determine back-diffusion rates ($k_b = k_u/(f_{lipid} K_{ow})$). For model applications for cadmium and mercury, back-diffusion rates were assumed to be negligible. In the bioaccumulation model calculations, migration patterns for striped bass are also required in evaluating time-dependent exposure concentrations in the water and in the striped bass prey.

The assignment of model parameters and striped bass migration patterns are discussed in more detail in Section 9. These values were used in conjunction with chemical exposure concentrations from the CARP contaminant fate model calculations to determine chemical concentrations in zooplankton, small fish, white perch and striped bass. Testing of the model was performed by comparing model results to observed contaminant concentrations in zooplankton, white perch and striped bass. Final calibration values for all chemicals are discussed as part of the bioaccumulation model results and sensitivity calculations in Section 11.

8.5 BIOACCUMULATION MODEL FOR HARBOR WORMS

A steady-state, bioaccumulation model was formulated to examine the accumulation of PCB homologs in Harbor worms as part of our bioaccumulation modeling and sensitivity studies in Section 11. The model was based largely on the work on Thomann et al. (1992) and considers the chemical accumulation in worms to be a function of ingestion, egestion and ventilation as depicted in Figure 8-3. The resulting equation for bioaccumulation in worms is similar to Equation 8-3 and is given as:

$$\frac{d\nu_{lipid}}{dt} = k_u C_{dis} - k_b \nu_{lipid} + \alpha I_{oc} r_{oc} \left[\frac{K_{lipid}}{K_{oc}^{app}} \right] - \left(k_e + k_m + k_g \right) \nu_{lipid} \quad (8\text{-}4)$$

where ν_{lipid} is the concentration of the chemical in the worm (μg contaminant/g lipid), t is time, k_{ui} is the diffusive uptake rate of dissolved contaminant from the porewater and into the organism (L/g organism i/day), C_{dis} is the freely-dissolved contaminant concentration (μg contaminant/L), k_b is the back diffusive transfer rate of contaminant from the worm and into the porewater (1/day), α_{ij} is the efficiency of the worm to assimilate contaminant from feeding on sediment (unitless), I_{oc} is the ingestion rate of the worm on sediment organic carbon (g org C/g lipid/day), r_{oc} is the chemical concentration in sediment (μg contaminant/g org C), K_{oc} is the partition coefficient of the contaminant to "digestable" organic carbon and is assumed to be equal to the octanol-water partition coefficient (L/kg org C), K_{oc}^{app} is the apparent or field-derived partition coefficient for contaminant onto organic carbon and includes the effects of "non-digestable" organic carbon (e.g., soot or black carbon) (L/kg org C), k_e is the excretion/egestion rate coefficient for contaminant removal from the worm (1/day), k_m is the metabolic transformation rate coefficient for contaminant in the worm (1/day), and k_g is the growth rate

coefficient (1/day) and is included to account for the reduction in ν_{lipid} due to the increase in the size of the organism (i.e., growth dilution).

The steady-state solution for worm BSAFs on a lipid-organic carbon basis is given as:

$$BSAF_{lipid,oc} = \frac{\nu_{lipid}}{r_{oc}} = \frac{\frac{k_u}{K_{oc}^{app}} + \alpha \cdot I_{oc} \cdot \left[\frac{K_{lipid}}{K_{oc}^{app}}\right]}{k_b + k_e + k_m + k_g} \quad (8\text{-}5)$$

For model calculations, the respiration and growth rates are determined from relationships given in Thomann et al. (1992): kg = $0.01 \cdot w^{-0.2}$ and R = $0.036 \cdot w^{-0.2}$ where the organism weight (w) is given in g(wet wt). This information is used along with values for the respiratory transfer efficiency (β), the food assimilation efficiency (a), and the dietary chemical assimilation efficiency (α) to calculate the remaining bioenergetic parameters including the respiratory uptake rate:

$$k_u = \frac{\beta \cdot R_{oxygen}}{C_{oxygen}} \quad (8\text{-}6)$$

and the organic carbon ingestion rate:

$$I_{oc} = \frac{R + k_g}{a} \cdot f_{dry\,wt}^{worm} \cdot \frac{0.4}{f_{lipid}^{worm}} \quad (8\text{-}7)$$

where 0.4 represents the grams of organic carbon per grams of dry weight in the sediment organic matter.

Finally, chemical-specific K_{ow}'s for PCB homologs are used along with respiratory uptake rates (k_u) and lipid content to determine back-diffusion rates:

$$k_b = \frac{k_u}{f_{lipid}^{worm} \cdot K_{ow}} \quad (8\text{-}8)$$

The assignment of model parameters is described in more detail in Section 9. Comparison of model results to field data, along with model sensitivity studies are discussed in Section 11. Final BAFs and BSAFs used for projection purposes are described in Section 10.

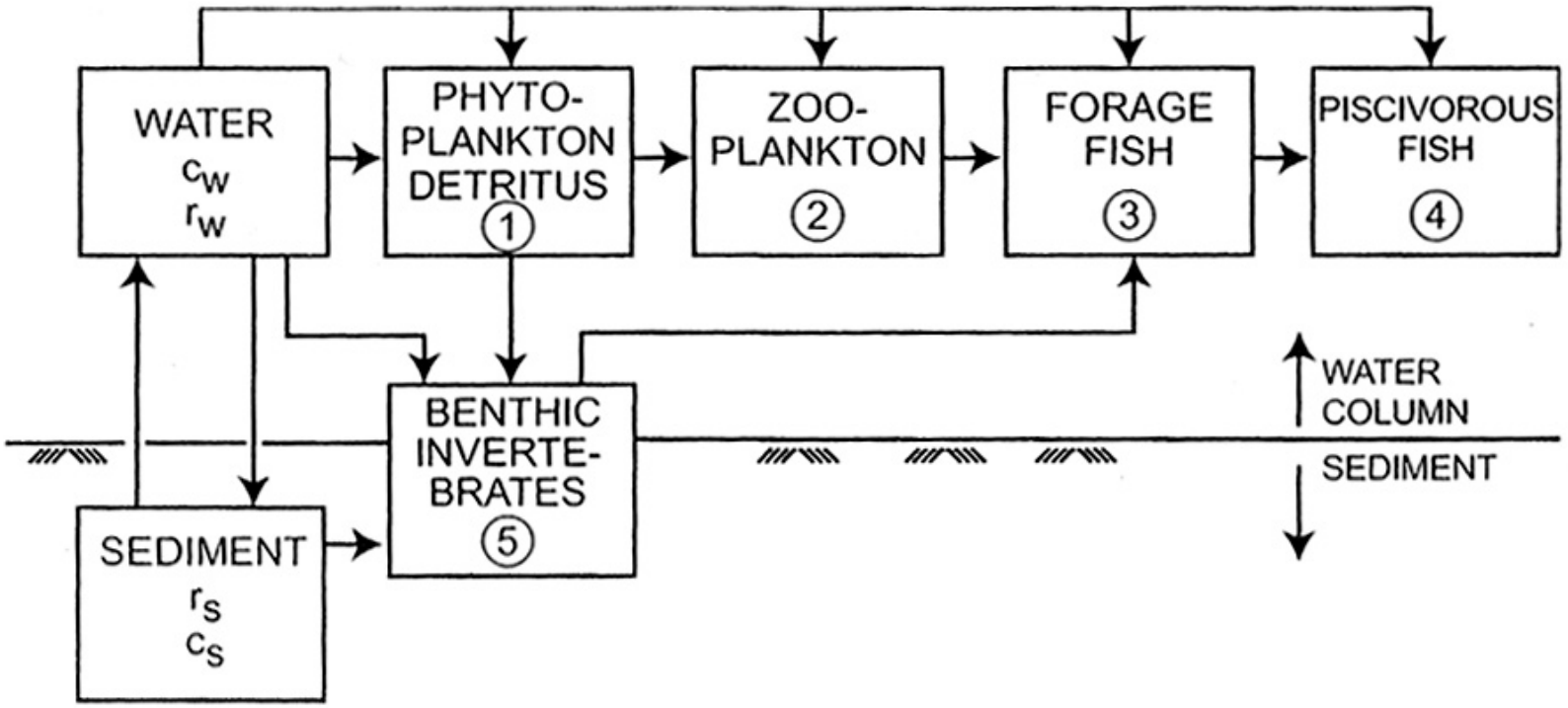

Figure 8-1. Generic Food Web Model (Thomann et al., 1992)

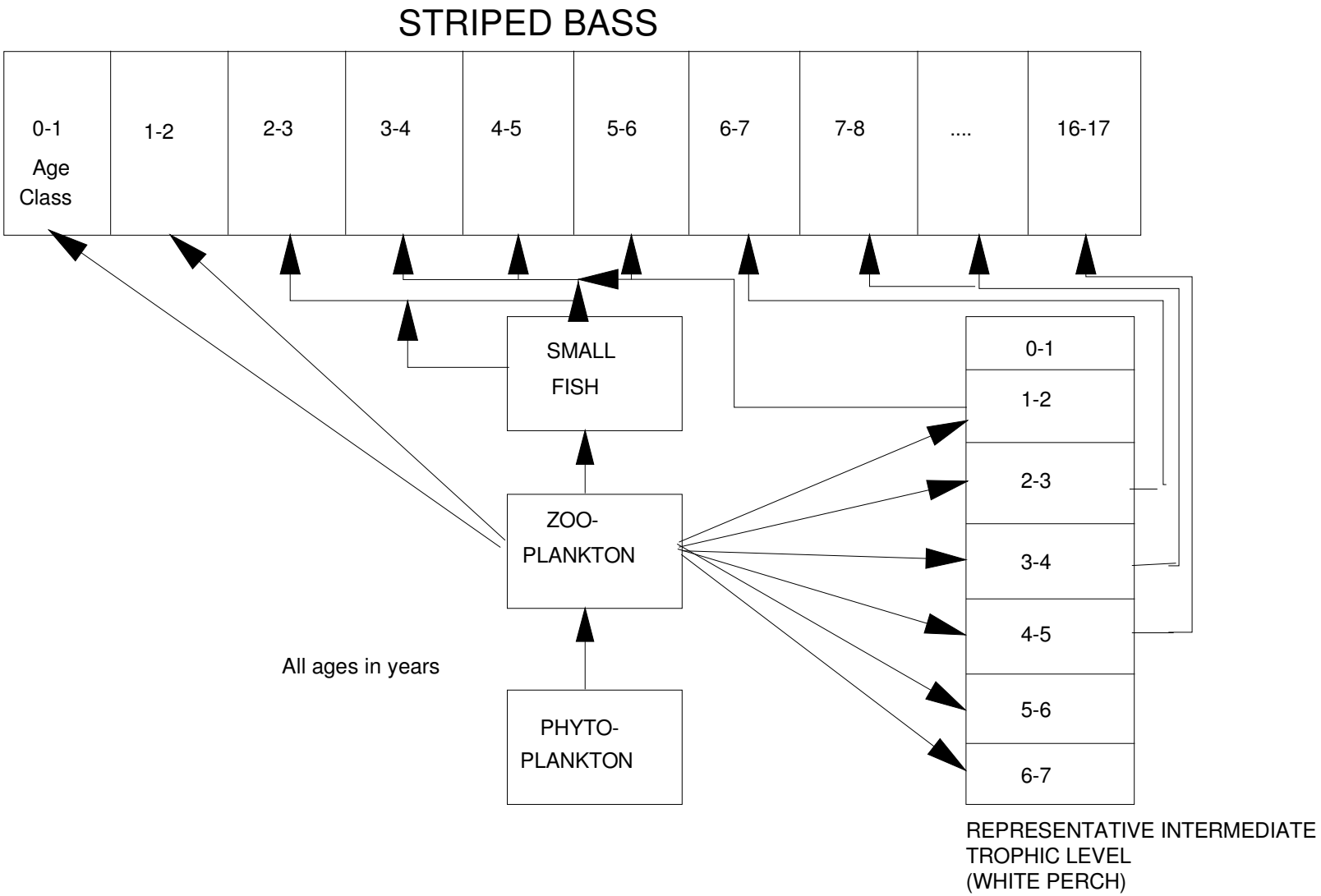

Figure 8-2. Age-dependent striped bass food chain.

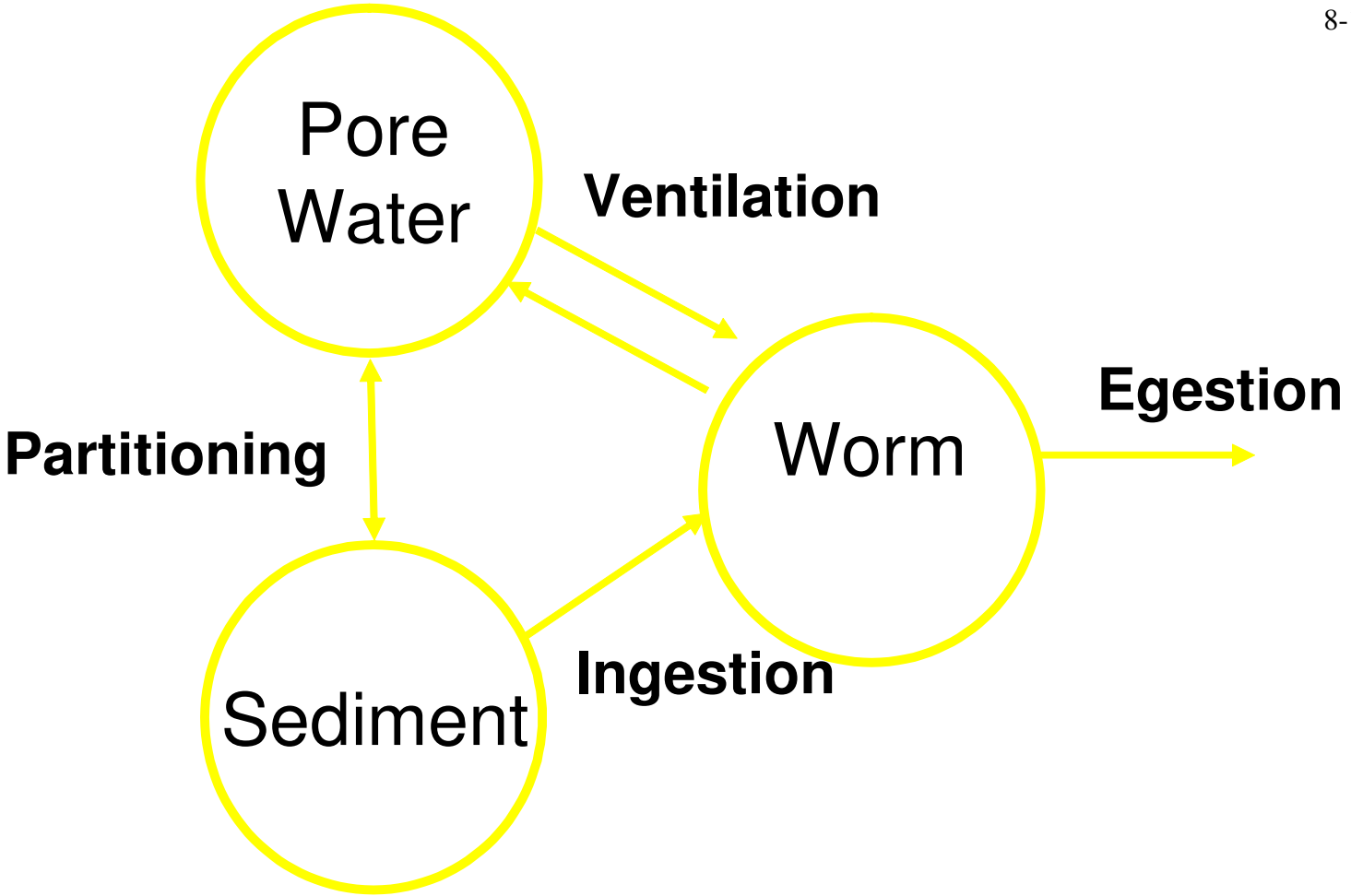

Figure 8-3. Bioaccumulation pathways for Harbor worms.

SECTION 9.0

SETUP FOR BIOACCUMULATION CALCULATIONS

As part of CARP bioaccumulation evaluations, field-derived BAFs and/or BSAFs were evaluated for zooplankton, white perch, striped bass, mummichog, American eel winter flounder, blue crab, clams, and worms. In addition, bioaccumulation model calculations were performed for the white perch-striped bass food chain and for bioaccumulation in Harbor worms. Governing equations for BAFs, BSAFs and bioacccumulation model calculations were discussed in detail previously in Section 8.0. The computer code for the CARP bioaccumulation model, RCAFC, based on the generic Foodchain model (Connolly and Thomann, 1985; Connolly, 1991), has been developed as part of HydroQual's multi-purpose Fortran-based source code, Row Column Aesop (RCA). RCAFC provides a flexible platform for modeling bioaccumulation in complex food webs and allows a full coupling of the benthic and pelagic food webs along with capabilities to model migrating fish species such as striped bass and American eel. Further RCAFC is fully consistent with the CARP contaminant fate model developed using RCATOX. This report section will describe the input information necessary to perform field-derived BAF and BSAF evaluations and to implement the CARP bioaccumulation model for the white perch-striped bass food chain and for the Harbor worms.

9.1 INFORMATION FOR BAF AND BSAF EVALUATIONS

Since water and sediment measurements were not coincident with most of the biota sampling, BAF and BSAF evaluations were performed using exposure concentrations from the CARP contaminant fate model. For BAF evaluations, freely-dissolved PCB, dioxin/furan, PAH and pesticide concentrations, free ion metal concentrations (Cd^{2+} and Hg^{2+}) and freely-dissolved methyl mercury concentrations were extracted from the CARP fate model for the bottom layer of the water column. For BSAF evaluations, organic carbon normalized concentrations for PCB, dioxin/furans, PAHs, pesticides, cadmium, inorganic mercury and methylmercury were extracted from the CARP fate model for the top 10-cm of sediment. For both the water column and sediment, concentrations were taken at coincident locations and times based on 5-day time-averaged results. This information was used along with the measured concentrations of contaminants in biota and lipid contents to evaluate field-derived BAF and BSAF values for 10 PCB homologs, 17 dioxin/furan congeners, 22 PAHs, and 11 chlorinated pesticides (including DDT, chlordane and their derivatives).

9.2 INFORMATION FOR BIOACCUMULATION MODEL CALCULATIONS

Time-variable, age-dependent bioaccumulation model calculations for the white perch-striped bass food chain were performed using water column exposure concentrations from the CARP contaminant fate model, along with detailed information on bioenergetic parameters for each organism in the food chain and a prescribed migration pattern for striped bass. Steady-state, bioaccumulation model calculations for Harbor worms were also performed using measured sediment exposure concentrations and bioenergetic parameters for the worms. A description of how these exposure concentrations, bioenergetic parameters and migration patterns were defined is given in the following subsections.

9.2.1 Exposure Concentrations

For the white perch - striped bass food chain model, exposure concentrations were extracted from the CARP contaminant fate model as 5-day averages for the bottom layer of the water column. For PCBs, dioxin/furans, PAHs and pesticides, water column exposure concentrations were based on freely-dissolved concentration. In addition, HOC concentrations in phytoplankton serve as an important route of dietary intake to zooplankton, and were calculated using the freely-dissolved HOC concentrations, octanol-water partition coefficients, and an averaged phytoplankton lipid content of 5 percent for phytoplankton. For PCB homologs, octanol-water partition coefficients were adjusted for temperature and salinity using the van't Hoff and Setschenow's equations, respectively. For dioxin/furan congeners, PAHs, and pesticides, only salinity adjustment were made because sufficient and/or reliable information was not available on the enthalpies of phase change for these chemicals.

For metals, water column exposure concentrations were based on free cadmium and mercury ion concentrations (Cd^{2+} and Hg^{2+}) and freely-dissolved methyl mercury concentrations. Metal concentrations in phytoplankton were assumed to be equal to POC-bound concentrations and were taken directly as 5-day averages from the CARP contaminant fate model.

For BSAF calculations for Harbor worms, exposure concentrations for PCBs and dioxin/furans were taken directly from measurements of collocated sediments that were analyzed as part of the CARP special worm study. For dredged material bioaccumulation testing data (Battelle, 1996a-e), exposure concentrations for PCBs were taken directly from measured sediment concentrations. For both cases, sediment concentrations were given as organic carbon normalized concentrations for BSAF calculations.

9.2.2 Aggregating Model Grid Cells into Food Web Regions

The spatial resolution of the CARP model was largely driven by a balance between the requirements of the hydrodymanic and sediment transport models and the spatial expanse of the Harbor-Bight-Sound system. For the white perch-striped bass food chain bioaccumulation model, it was not considered necessary to perform bioaccumulation model calculations at the resolution of the CARP grid for the following reasons: (1) the home range (or areal feeding range) of resident fish is expected to extend over many grid cells; (2) in a well-mixed, estuarine system, sharp gradients in chemical exposure concentrations are not likely to occur except for short-term events; and (3) the kinetics for the higher trophic levels are not likely to be fast enough to rapidly respond to short-term events. Contaminant fate model results for individual CARP computational grid segments were therefore aggregated into food web regions before being applied in the bioaccumulation model. For CARP model calculations, the five food web regions used in the Thomann-Farley model (see Figure 9-1) were subdivided into a total of 39 CARP food web subregions (see Figure 9-2). Maps of the food web regions are presented in Figures 9-1 and 9-2 on the model grid (upper left panel) in computational row-column space and as three projections in real-world space.

For model calculations, resident fish were considered to remain in a given CARP food web region throughout their lives. For striped bass, migration patterns of striped bass were assigned based on Waldman (1988; 1990) and are described in Thomann et al. (1989; 1991). These are summarized as follows: Striped bass are born on May 15th of each year and the yearlings are assumed to remain in the mid estuary (as defined by Km 30 to 126; RM 18.5 to 78.5). The 2-5 year old striped bass are considered to migrate from the mid estuary into New York Harbor in June and spend the summer months (July through September) in Long Island Sound and the New York Bight. Lastly, 6-17 year old striped bass are assumed to spend most of their year in the open ocean, but migrate into Long Island Sound and the New York Bight around March 15th and into the mid estuary around April 15th to spawn. They remain in the mid estuary until the middle of July. Application of the striped bass migration patterns to the 39 CARP food web regions is given in Figure 9-3. Since striped bass migrate over large distances within the model domain, field observations for the 39 CARP food web regions were grouped into the five Thomann-Farley food web regions for final striped bass model-data comparisons.

9.2.3 Bioenergetic Information for the White Perch-striped Bass Food Chain

In addition to exposure concentrations extracted from the CARP contaminant fate model, information on growth rates, weights, respiration rates, lipid content, feeding diets, etc. are required for bioaccumulation model calculations. In applying the bioaccumulation model to the white perch-striped bass food chain, these parameters were specified as follows:

Growth rates were determined from results of Poje et al. (1988) for zooplankton; from a generalized growth-weight relationship for small fish (Thomann et al. 1989); from the age-weight data of Bath and O'Connor (1982) for perch; and from the age-weight data of Setzler et al (1980) and Young (1988) for striped bass. Details of age-dependent weights and growth rates are given in Thomann et al (1989) and are summarized in Table 9-1.

Respiration rates for zooplankton, small fish, perch, and striped bass were estimated using formulations given in Thomann and Connolly (1984) and Connolly and Tonelli (1985). Details of respiration rates, along with lipid content, dry weight fractions, and food assimilation efficiency, are given in Thomann et al (1989) and are summarized in Table 9-2. These values are used with the gill transfer efficiency (β) to calculate gill uptake rates ($k_u = \beta \cdot R_{oxygen}/C_{oxygen}$) and food ingestion rates ($I = (R+k_g)/a$). For these calculations, C_{oxygen} is taken directly from the CARP sediment transport-organic carbon model as 10-day averages, and the feeding structure of the white perch-striped bass food chain, which was previously outlined in Section 8, is prescribed as follows: Phytoplankton serve as the base of the food chain, and are preyed upon by a zooplankton compartment, the characteristics of which is considered to be represented by *Gammarus*. The small fish compartment, which feeds on zooplankton, is meant to reflect a mixed diet of fish of about 10 g in weight and includes 0-1+ tomcod and herring. Perch is considered as a representative size-dependent prey of the striped bass and is assumed to feed exclusively on zooplankton. Based on feeding studies where stomach contents of striped bass were examined (Gardinier and Hoff 1982; O'Connor 1984; Setzler et al. 1980), the 0-2 year old striped bass are assumed to feed on zooplankton; 2-5 year old striped bass are assumed to feed on a mixture of small fish and 0-2 year old perch; and 6-17 year old striped bass are assumed to feed on 2-5 year old perch.

For model applications for PCB homologs and dioxin/furan congeners, chemical-specific K_{ow}'s were used along with gill uptake rates (k_u) and lipid content to determine back-diffusion rates ($k_b = k_u/(f_{lipid} K_{ow})$). For these calculations, the gill transfer efficiency (β) was set equal to 0.6. The chemical assimilation efficiency (α) was set equal to the food assimilation efficiency of 0.3 for zooplankton. For small fish, white perch and striped bass, the chemical assimilation efficiency (α) was initially specified as a constant, (1/2.3) based on information in Kelly et al. (2004) for mid-range K_{ow} compounds. In addition, the egestion rate coefficient (k_e) was set equal to 0.005 / day and the metabolic rate coefficient (k_m) was set equal to zero for initial calibration studies.

Bioaccumulation model parameters for cadmium, mercury and methylmercury are similar to those cited above with the following exceptions. The back-diffusion rate coefficient (k_b) was assumed to be negligible and the chemical assimilation efficiency (α) was assumed to be equal to 0 for cadmium and mercury and to 0.3 and 0.8 for methylmercury in zooplankton and fish, respectively. As before, the gill transfer efficiency (β) was again set equal to 0.6, and the egestion rate coefficient was set equal to

0.005 / day for initial calibration studies. Final calibration values for all chemicals are discussed as part of the bioaccumulation model results and sensitivity calculations in Section 11.

Table 9-1
Weights and Growth Rates for Zooplankton, Small Fish, White Perch, and Striped Bass

Organism	Year Class	Weight [a] (g wet wt)	Growth Rate (1/day)
Zooplankton	-	1.04 (mg dry wt)[b]	0.10
Small Fish	-	10.	0.00631
White Perch	0-1	0.176	0.0125
	1-2	16.9	0.0033
	2-3	56.3	0.00127
	3-4	89.6	0.00056
	4-5	110.0	0.00040
	5-6	127.5	0.00028
	6-7	141.5	0.00031
Striped Bass	0-1	2.0	0.006302
	1-2	20.08	0.005464
	2-3	148.4	0.003825
	3-4	601.8	0.002185
	4-5	1,339.4	0.001366
	5-6	2,208.4	0.001366
	6-7	3,641.	0.000905
	7-8	5,072.	0.000518
	8-9	6,131.	0.000456
	9-10	7,247.	0.000408
	10-11	8,417.	0.000369
	11-12	9,637.	0.000337
	12-13	10,904.	0.000310
	13-14	12,217.	0.000287
	14-15	13,572.	0.000267
	15-16	14,969.	0.000250
	16-17	16,406.	0.000235
	17-18	17,881.	0.000221

[a] Weights given for the beginning of the year class.
[b] Zooplankton weight is given in mg dry weight; all other weights given in g wet weight.

Table 9-2
Bioenergetic Parameters for Zooplankton, Small Fish, White Perch, and Striped Bass

	Zooplankton	Small Fish	White Perch	Striped Bass
Food Assimilation Efficiency (a)	0.3	0.8	0.8	0.8
Fraction lipid (f_{lipid})	0.022	0.047	0.047	0.037
Fraction dry weight ($f_{dry\ wt}$)	0.2	0.25	0.25	0.25
Egestion Rate Coef. (k_e)(1/day)	0.005	0.005	0.005	0.005
Respiration Rate (R) (g wet wt resp/g wet wt-day)	$R = 0.01249\, e^{\rho T}$	$R = 0.0047\, e^{\rho T}$	$R = \beta\, w^{\gamma} e^{\rho T} e^{\nu u}$ $u = \omega\, w^{\delta} e^{\phi T}$	$R = \beta\, w^{\gamma} e^{\rho T} e^{\nu u}$ $u = \omega\, w^{\delta} e^{\phi T}$
Respiration Parameters: β	-	-	0.043	0.043
γ	-	-	-0.3	-0.3
ρ	0.06293	0.06293	0.03	0.03
ν	-	-	0.0176	0.0176
ω	-	-	1.19	1.19
δ	-	-	0.32	0.32
ϕ	-	-	0.0405	0.0405
Respiration Rate (R_{O2}) [a] (g O_2/g wet wt-day)	$R_{O_2} = a_{oxygen-carbon}\, a_{carbon-dry\ wt}\, f_{dry\ wt}\, R$			

[a] For respiration rates in oxygen equivalents, $a_{oxygen-carbon}$ and $a_{carbon-dry\ wt}$ are taken as 2.67 and 0.4, respectively.

9.2.4 Bioenergetic Information for Harbor Worms

A steady-state bioaccumulation model was used to calculate BSAFs for Harbor worms at two representatives sites: Newark Bay (inner Harbor) and Sandy Hook (outer Harbor). Model parameters for sediment organic carbon fracton and the lipid fraction of worms were obtained directly from field measurements. The average weight of the worms was taken as 2 mg and the food assimilation efficiency was set at 0.2 based on information in Thomann et al. (1992). (Note that model sensitivity showed that calculated BSAFs were not affected by the assigned weight of the worms.) Values for f_{oc}, f_{lipid}, weight and food assimilation efficiency were used along with relationships given in Section 8 to calculate the growth rate, respiration rate and organic carbon ingestion rate of the worms. A summary of the bioenergetic model parameters is given in Table 9-3.

Table 9-3. Summary of Initial Bioenergetic Parameters for Harbor Worms

	Newark Bay	Sandy Hook
f_{oc}	0.025	0.035
fl_{ipid}	0.009	0.014
Food Assimilation Efficiency	0.2	0.2
Growth Rate (1/day)	0.035	0.035
Respiration Rate (g wet / g wet / day)	0.125	0.125
Ingestion Rate (g OC / g lipid / day)	5.1	3.3

In addition, the respiratory transfer efficiency (β) was set equal to 0.6. The chemical assimilation efficiency (α) was initially set equal to the food assimilation efficiency of 0.2. The egestion rate coefficient (k_e) was set equal to 0.005 / day and the metabolic rate coefficient (k_m) was set equal to zero for initial calibration studies. Final calibration values for all chemicals are discussed as part of the bioaccumulation model results and sensitivity calculations in Section 11.

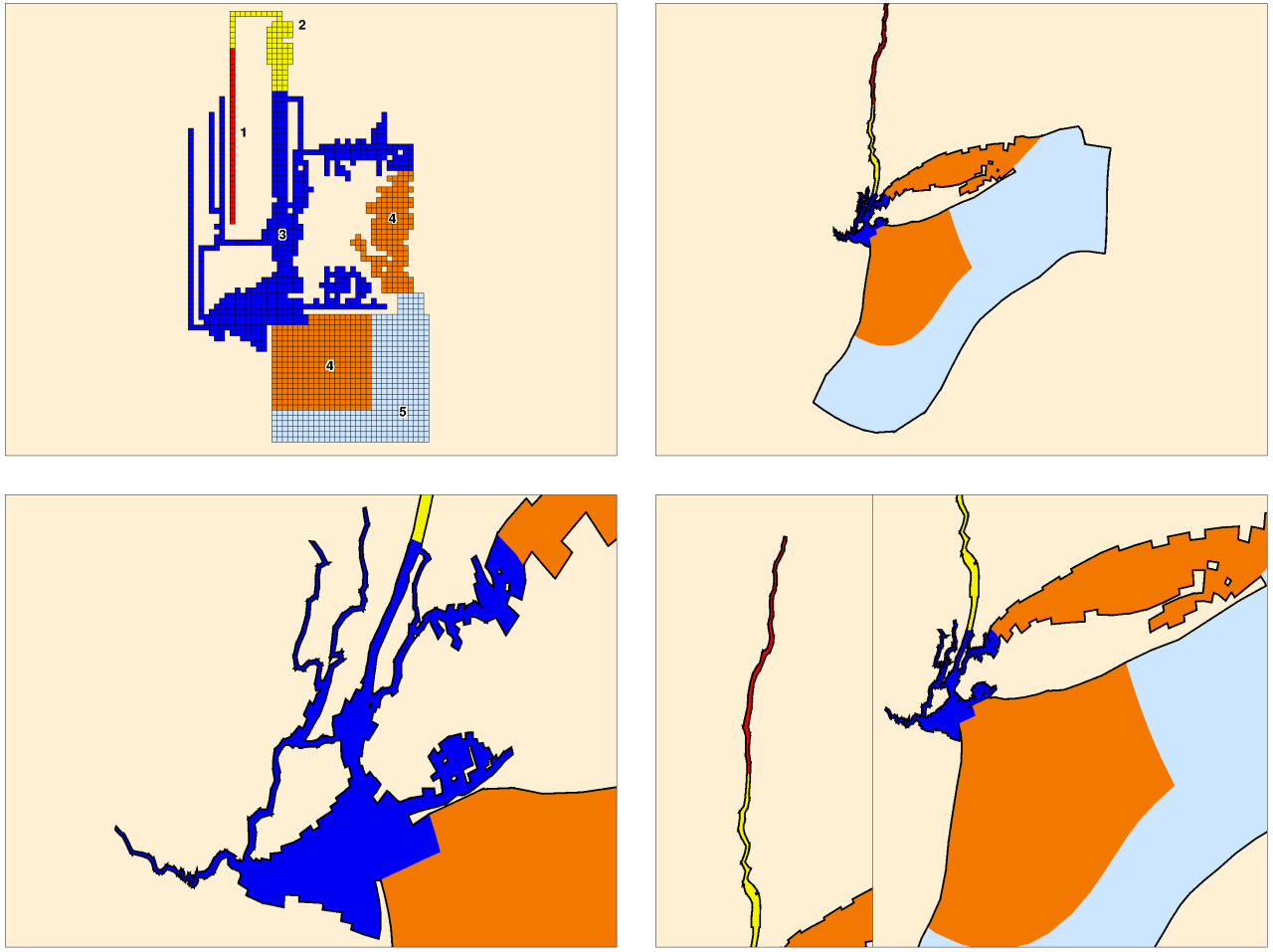

Figure 9-1. Thomann-Farley model food web regions overlain on the CARP model grid. Shown in both computational row-column and real-world projected space

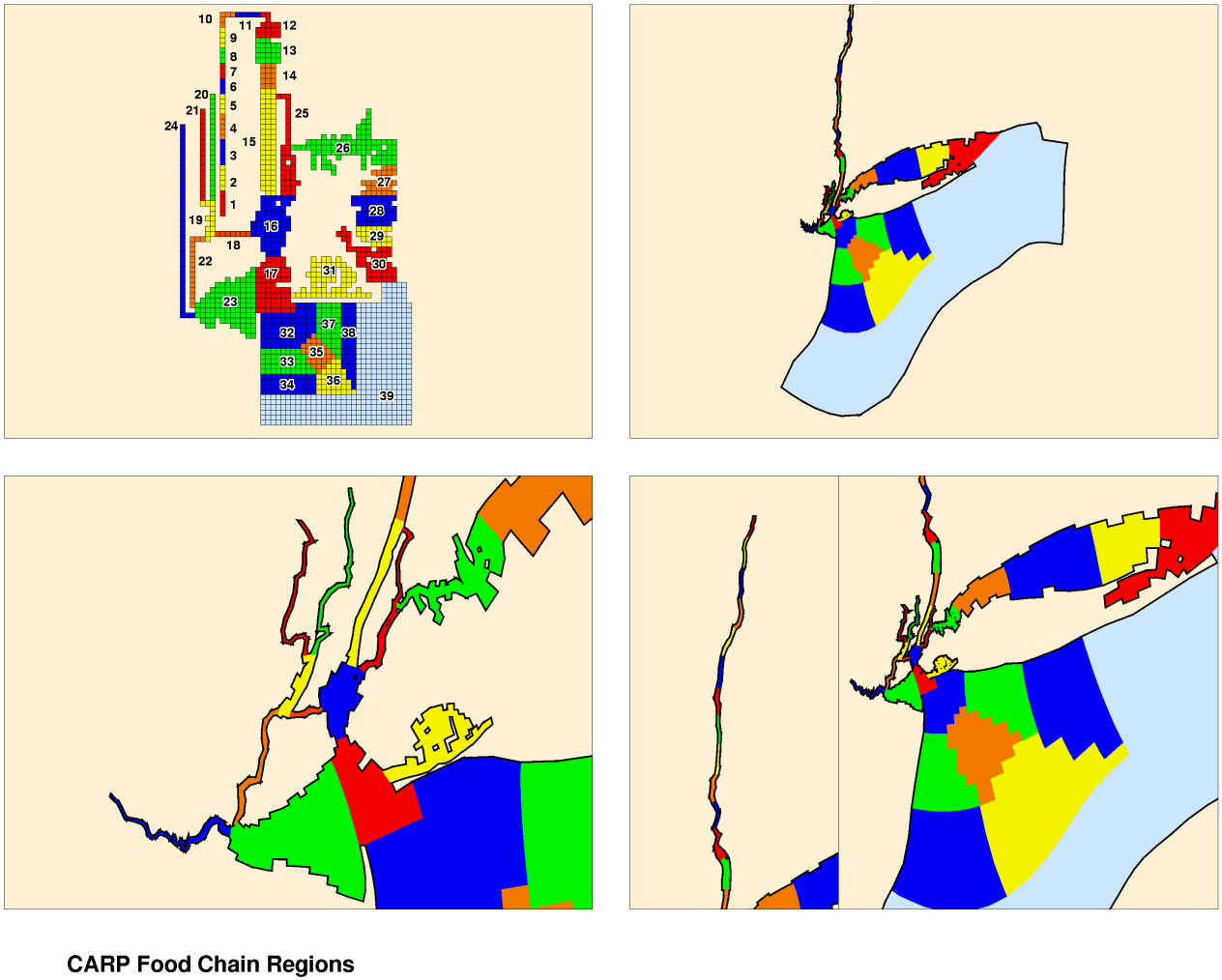

Figure 9-2. CARP model food web regions overlain on the model grid. Shown in both computational row-column and real-world projected space.

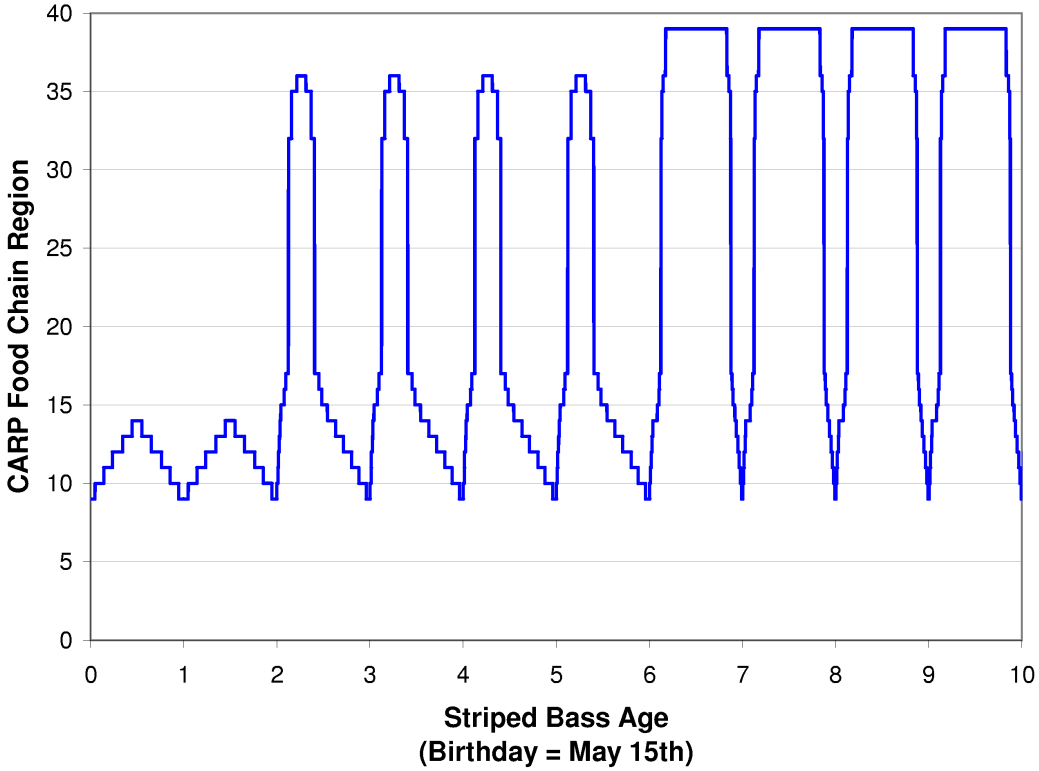

Figure 9-3. Application of the striped bass migration pattern to the 39 CARP model food web regions.

SECTION 10.0

BAF AND BSAF EVALUATIONS

As part of the CARP sampling plan, measurements were performed on chemical concentrations in the fish and lower trophic levels species. Since CARP water and sediment measurements were not coincident with most of the biota sampling, water and sediment exposure concentrations from the CARP contaminant fate model were used in conjunction with the biota measurements to determine Harbor-specific BAFs and BSAFs. This section of the report describes the results of the BAF and BSAF evaluations. More detailed bioaccumulation modeling and sensitivity studies, which were performed to examine the dominant factors affecting the bioaccumulation behavior of Harbor biota, are presented in Section 11.

10.1. DATA AVAILABLE FOR BAF AND BSAF EVALUATIONS

BAF and BSAF evaluations were performed using measured chemical concentrations in various organisms collected specifically as part of CARP biota sampling. The samples were collected from 1998 through 2002 by NYSDEC. The CARP biota data are available for download from the internet at http://www.carpweb.org. As part of its CARP effort, NYSDEC is preparing reports summarizing the CARP biological data. Additional data sources considered for the BAF and BSAF evaluations include coincident measures of contaminants in worms and sediments of the Harbor collected by an independent contractor at the request of NJDOT OMR, dredged material testing data for worm PCB provided by USEPA Region 2, and the published, site-specific data of Meador et al. 1997.

10.2 BAF RESULTS FOR HOCs IN WATER COLUMN SPECIES

Field-derived BAFs were calculated from measured biota concentrations and corresponding water exposure concentrations that were extracted for the bottom layer of the water column from the CARP contaminant fate model. For PCB homologs, dioxin/furan congeners, PAHs and pesticides, BAFs were calculated on a lipid basis as:

$$BAF_{lipid} = \frac{\nu_{lipid}}{C_{dis}^{freely}} \qquad (10\text{-}1)$$

where ν_{lipid} is the chemical concentration in the organism (μg chemical/g lipid) and the exposure concentration is given as the freely-dissolved chemical concentration.

A summary of lipid-normalized BAFs for PCB homologs in zooplankton, white perch, striped bass, mummichog, American eel and winter flounder are presented in Figure 10-1 as a function of K_{ow}. Solid lines on the individual panels of the figure represent the 1:1 line and are used to indicate trends in BAFs with K_{ow} and also the magnitude of the BAFs relative to K_{ow} values. As shown for zooplankton, the field-derived BAFs for PCB homologs increase linearly as a function of K_{ow} and on average are approximately six times greater than K_{ow} (i.e., BAF $\approx 6 \times K_{ow}$). BAFs for fish show somewhat similar behavior. BAFs for the more chlorinated homologs in fish however are sometimes higher than the corresponding BAFs in zooplankton suggesting that PCB homologs are biomagnified as they are passed through the food chain. For less chlorinated PCB homologs, BAFs in fish are typically lower than the corresponding BAFs in zooplankton, suggesting that dietary exposure is less important for the lower K_{ow} homologs or that metabolism of certain lower chlorinated congeners may be occurring. For example, a greater percentage of the lower chlorinated congeners may be more susceptible to enzymatic attack due to adjacent non-chlorinated sites on the biphenyl structure.

Lipid-normalized BAFs for dioxin/furan congeners in zooplankton (Figure 10-2) are similar to the BAFs for PCBs in zooplankton. Although there is more scatter in the results, BAFs for dioxin/furan congeners in zooplankton are again approximately six times greater than the K_{ow} values. BAFs for dioxin/furan congeners in fish however show very different behavior. In almost all cases, BAFs are anywhere from one to three orders of magnitude lower than the corresponding BAFs in zooplankton (see Figure 10-2). This unexpected result suggests that either there is an inefficient trophic transfer of dioxin/furan congeners through the food chain, or that fish possess the capacity to metabolize dioxins and furans. Further examination of dioxin/furan metabolism in fish is presented in Section 11.

The lipid-normalized BAFs for chlorinated pesticides in zooplankton and fish are shown in Figure 10-3. Although there is more scatter in the results, the BAFs for pesticides are similar to those previously shown for PCBs (Figure 10-1) with two exceptions. First, the lipid-normalized BAFs for pesticides are on average only a factor of three greater than the K_{ow} values (i.e., BAF $\approx 3 \times K_{ow}$). Second, the extremely high BAF value for oxy-chlordane is likely the result of a poor estimate for the chemical K_{ow} value.

Lipid-normalized BAFs for PAHs in zooplankton and fish are presented in Figure 10-4. As shown, the BAFs for zooplankton and fish are relatively flat as a function of K_{ow}, and for log K_{ow} > 4, are below the 1:1 K_{ow} equivalents line. This is an expected results because metabolism of PAHs by

fish and some lower trophic level organisms has been shown to occur in other studies. For PAHs which fall on or above the 1:1 K_{ow} equivalents line (i.e., PAHs with log K_{ow} values approximately equal to or less than 4), it is quite likely that, for these compounds, the time required for the organisms to equilibrate with the surrounding water is relatively fast compared to metabolic rates.

10.3 BAF RESULTS FOR CADMIUM AND MERCURY IN WATER COLUMN SPECIES

Field-derived BAFs for cadmium and mercury were also calculated from measured biota concentrations and corresponding water exposure concentrations that were extracted for the bottom layer of the water column from the CARP contaminant fate model. For cadmium and mercury, BAF evaluations were performed on a wet weight basis as:

$$BAF = \frac{\nu}{C_{exposure}} \tag{10-2}$$

where ν_{lipid} is the chemical concentration in the organism (μg chemical/g wet weight) and the water exposure concentrations were taken as the free metal ion concentration (Cd^{2+}) for cadmium and as the summation of the free metal ion concentration (Hg^{2+}) and the free methyl mercury concentration for mercury. (In all cases, the free methyl mercury concentration was the dominant contributor to the mercury exposure concentration.)

A summary of BAFs for cadmium in zooplankton, white perch, striped bass, mummichog, American eel and winter flounder are presented in Figure 10-5. As shown, the field-derived BAFs for zooplankton are an order of magnitude greater than the BAFs for white perch, mummichog and American eel, and two orders of magnitude greater than BAFs for striped bass and winter flounder. These results which show lower BAFs for higher trophic organisms suggest that cadmium uptake through dietary exposure is not an important pathway. This is consistent with reports of strong binding of cadmium in organisms (e.g., by metallothioneins) which in effect may limit dietary exposure. Differences in BAFs that are apparent for the various species are likely to be associated with differences in the bioenergetics and migration of the organisms (e.g., as manifested in respiratory uptake, egestion rates, growth rates, and migration patterns).

BAFs for mercury in zooplankton, white perch, striped bass, mummichog, American eel and winter flounder are presented in Figure 10-6. For zooplankton, two BAF values are given and are based on measured total mercury and methylmercury concentrations in zooplankton samples. The results indicate that a small portion of the total mercury in zooplankton (i.e., < 10%) is expected to be as methylmercury. This is in contrast to fish where a large portion of the mercury in fish samples is

expected to be methylmercury (Back et al., 2003; Kainz et al., 2002; Mason et al., 2000, 1996; Post et al., 1996; Wang and Fisher 1998 a and b; Wang and Fisher 1999; Watras et al., 1998). Assuming that total mercury in fish is predominately methylmercury, we expect (1) that, like cadmium, dietary exposure is not expected to be an important pathway of non-methylated forms for fish, and (2) that dietary exposure of methylmercury is very important and that concentrations of methylmercury are biomagnified as they are passed through the food chain. BAFs for methylmercury in the various fish species however will likely depend not just on trophic level, but also on ingestion rates, egestion rates, growth rates and exposure history, particularly for migratory fish.

10.4 BAF AND BSAF RESULTS FOR HOCs IN SEDIMENT SPECIES

Since bottom-dwelling organisms may receive a portion of their exposure from the filtration of overlying water and a portion from ingestion of contaminated sediment, field-derived BAFs and BSAFs were calculated for the sediment species. The BAF and BSAF calculations were performed using measured biota concentrations and corresponding bottom-water and sediment exposure concentrations from the CARP contaminant fate model. For PCB homologs, dioxin/furan congeners, PAHs and pesticides, BAFs were again calculated on a lipid basis as:

$$BAF_{lipid} = \frac{\nu_{lipid}}{C_{dis}^{freely}} \tag{10-3}$$

where ν_{lipid} is the chemical concentration in the organism (μg chemical/g lipid) and the exposure concentration is given as the freely-dissolved chemical concentration in the bottom layer of the water column. BSAFs were calculated on a lipid-organic carbon basis as:

$$BSAF_{lipid,oc} = \frac{\nu_{lipid}}{r_{oc}} \tag{10-4}$$

where ν_{lipid} again is the chemical concentration in the organism (μg chemical/g lipid) and the exposure concentration is taken as the organic carbon normalized concentration of chemical in the top 10 cm of sediment.

A summary of lipid normalized BAFs is presented in the top panels of Figure 10-7 for PCB homologs in edible tissue, muscle and hepatopancreas of blue crab. Solid lines on the panels of the figure represent the 1:1 line and are again used to indicate trends in BAFs with K_{ow}. As shown, the field-derived BAFs for PCB homologs increase linearly as a function of K_{ow} and on average are approximately five to ten times greater than K_{ow} for the higher K_{ow} homologs. This suggests that dietary uptake is an important pathway for the higher K_{ow} homologs. At lower K_{ow} values, BAFs in blue crab

are typically closer to the 1:1 K_{ow} equivalents line, suggesting that dietary uptake is less important for the lower chlorinated homologs. As with fish, metabolism of certain lower chlorinated congeners may be occurring in crabs, but this is more difficult to surmise from the crab results.

Lipid/organic carbon-normalized BSAFs, which serve as more useful indicators of bioaccumulation potential for dredged material evaluations, are presented in the bottom panels of Figure 10-7. Solid lines on the bottom panels of the BSAF plots represent a BSAF value of one and can be interpreted as an equal affinity of the chemical for lipid and for sediment organic carbon. As shown, BSAF values increase with increasing K_{ow} values for the lower chlorinated homologs, reach maximum values of approximately one for the middle K_{ow} range, and decrease for the highest K_{ow} homologs. As discussed in more detail in Section 11, the lower BSAF values for the lower K_{ow} homologs is likely the result of stronger binding of planar PCBs to a strong binding phase(s) in sediment (e.g., soot or black carbon). For the higher K_{ow} range, the decrease in BSAFs is likely associated with reductions in the efficiency of chemical transfer for the more chlorinated homologs. Finally, differences in calculated BAF and BSAF values for edible tissue, muscle and hepatopancreas of blue crab are small for PCBs, and as will be shown in subsequent figures, for dioxin/furan congeners, PAHs and pesticides.

Lipid-normalized BAFs and lipid/organic carbon-normalized BSAFs for dioxin/furan congeners in blue crabs are presented in Figure 10-8. Although there is more scatter in the results, the calculated BAF values fall on or below the 1:1 K_{ow} equivalents line and the BSAF values are approximately 10 times lower than BSAFs for PCBs (see Figure 10-7). As previously discussed for fish, these results suggest that either there is an inefficient trophic transfer of dioxin/furan congeners through the food chain, or that crabs may also possess the capacity to metabolize dioxins and furans.

The lipid-normalized BAFs and lipid/organic carbon-normalized BSAFs for chlorinated pesticides in blue crabs are shown in Figure 10-9. Although there is more scatter in the results, calculated BAFs and BSAFs are comparable to results previously shown for the mid-range PCB homologs (Figure 10-7). Results for oxy-chlordane (log K_{ow} = 4.81) again appear as outliers. This is likely due to a poor estimate for the K_{ow} value for oxy-chlordane, as previously noted in Section 10.2.

Lipid-normalized BAFs and lipid/organic carbon-normalized BSAFs for PAHs in blue crabs are presented in Figure 10-10. As shown, the BAFs for crabs are relatively flat as a function of K_{ow}, and for log K_{ow} > 4, are below the 1:1 K_{ow} equivalents line. The corresponding BSAFs for PAHs are approximately 10^{-2}. These results provide further evidence for the metabolism of PAHs by aquatic organisms.

Lipid-normalized BAFs and lipid/organic carbon-normalized BSAFs for PCBs, dioxin/furans,

pesticides and PAHs in clams are presented in Figures 10-11 through 10-14, respectively. Results are presented for three clam species: Wedge Rangia (taken primarily from Haverstraw Bay), soft shell clams from the Harbor, and surf clams from the New York Bight. By and large, calculated BAFs and BSAFs for clams are comparable with results previously presented for blue crab. Finally, differences in calculated BAF and BSAF values for the three clam species, depurated and non-depurated, are small for PCBs, dioxin/furans, PAHs and pesticides.

10.5 SPECIAL STUDY: BSAF RESULTS FOR HOCs IN HARBOR WORMS

Since insufficient information was collected on polychaetes in the CARP sampling program, a special study of contaminant accumulation in Harbor worms was conducted by an independent contractor at the request of NJDOT OMR. The study consisted of coincident measurements of worms and sediment for seven locations in the Harbor and its adjoining waters. In analyzing the data, BSAFs were calculated on a lipid-organic carbon basis as:

$$BSAF_{lipid,oc} = \frac{v_{lipid}}{r_{oc}} \tag{10-5}$$

where v_{lipid} again is the chemical concentration in the organism (μg chemical/g lipid) and the exposure concentration is taken as the organic carbon normalized concentration of chemical in the sediment sample. For comparison, lipid-organic carbon normalized BSAFs were also calculated using CARP contaminant fate model results for organic carbon normalized concentration of chemical in the top 10 cm of sediment.

A summary of lipid/organic carbon-normalized BSAF calculations from measured and model-derived sediment concentrations is presented in Figure 10-15 for PCB homologs in worms. As shown, the calculated BSAFs for PCBs are similar to results previously presented for blue crabs (Figure 10-7) and clams (Figure 10-11), with values at each location much less than one for low K_{ow} homologs, approximately equal to one in the middle K_{ow} range, and decreasing below one for the highest K_{ow} homologs. BSAFs shown on the diagram were calculated using both the measured sediment concentrations and model calculated sediment concentrations as indicated by the different plotting symbols. For the Inner Harbor locations (the Upper Bay, Newark Bay, and the Arthur Kill), BSAFs calculated from measured sediment concentrations correspond closely to BSAF calculated from sediment concentrations extracted from the CARP contaminant fate model (based on the agreement of the results presented with different symbols). For the Outer Harbor locations (Raritan Bay, Long Island Sound, and Jamaica Bay), BSAFs from model-derived sediment concentrations are comparable to BSAF values for the Inner Harbor sites. BSAFs from measured sediment concentrations for the Outer Harbor locations however show a distinct increase from both the BSAFs from model-derived

sediment concentrations and the Inner Harbor BSAFs. These findings are important in two respects. First, the correspondence between BSAFs from model-derived and measured sediment concentrations for the Inner Harbor locations provides greater confidence in using our previously calculated BSAFs for blue crab and clams that were based on model-derived sediment concentrations. Second, geographic differences in BSAFs may be related to the quality of the food supply, the degree of contamination, or the type of worm present at the various locations. A more complete description of this finding will be presented in Section 11.

A similar presentation of lipid/organic carbon-normalized BSAF calculations from measured and model-derived sediment concentrations is given in Figure 10-16 for dioxin/furan congeners in worms. As shown, the calculated BSAFs for dioxin/furan congeners are similar to results previously presented for blue crabs (Figure 10-8) and clams (Figure 10-12), with BSAFs approximately 10 times lower than BSAFs for PCBs (Figure 10-15). This result again suggests that either there is an inefficient transfer of dioxin/furan congeners from sediment, or that worms also possess the capacity to metabolize dioxin and furan congeners. Again, there is a close correspondence between BSAFs calculated from measured and model-derived sediment concentrations for the Inner Harbor locations (the Upper Bay, Newark Bay, and the Arthur Kill). Differences in BSAFs calculated from measured and model-derived sediment concentrations are present for the Outer Harbor locations (Raritan Bay, Long Island Sound, and Jamaica Bay), but are much less obvious than differences observed for PCBs (see Figure 10-15). The smaller differences for dioxin/furan congeners may be associated with the possible loss of chemical in the organism by metabolism.

A summary of lipid/organic carbon-noramlized BSAFs from measured and model-derived sediment concentrations is given in Figure 10-17 for chlorinated pesticides in worms. As with previous BSAF results for pesticides in blue crab (Figure 10-9) and clams (Figure 10-13), there is more scatter in the results and BSAFs are comparable to results for middle range PCB homologs (Figure 10-15).

Lipid/organic carbon-normalized BSAFs from measured and model-derived sediment concentrations are presented in Figure 10-18 for PAHs in worms. The calculated BSAFs are again similar to results previously presented for blue crab (Figure 10-10) and clams (Figure 10-14), with BSAFs approximately 10 times lower than BSAFs for PCBs (Figure 10-15). These results provide further evidence for PAH metabolism by worms. Comparisons of BSAFs from measured and model-derived sediment concentrations for PAHs at the Inner and Outer Harbor locations are similar to those discussed above for dioxin/furan congeners.

It is noted that differences in BSAFs calculated using measured sediment concentrations and model calculated sediment concentrations for the Outer Harbor sites do not necessarily imply that there is a model deficiency or discrepancy with measured data. Part of the differences might relate to the fact that a sediment grab sample represents only a small fraction of the very heterogeneous sediment area that is represented as an average in a model grid cell. In general, model grid cells in the Outer Harbor tend to have larger lateral areas than model grid cells in the Inner Harbor.

10.6 BSAF RESULTS FOR DREDGED MATERIAL TESTING

Field-derived BSAFs for PCB homologs were also calculated for *Nereis virens*, a polychaete used in dredged material bioaccumulation tests for NY-NJ Harbor. Data for these analyses were obtained from 28-day bioaccumulation tests for sediments that were collected from various locations in the Harbor (for example, those described in Battelle, 1996a-e) and were provided to HydroQual in electronic form from Mark Reiss, USEPA Region 2. Data for deeper sediments with low organic content that were collected as part of the channel deepening project around Port Jersey were excluded from the analyses.

A summary of lipid / organic carbon normalized BSAFs calculations for the PCB homologs is presented in Figure 10-19. As shown, the BSAFs for Nereis in 28-day exposures are approximately equal to 0.15 (log BSAFs ≈-0.8) and are lower than the BSAFs for PCBs in Harbor worms previously reported in Figure 10-15. Lower BSAFs for *Nereis*, the dredged material test organism, as compared to Harbor worms may, in part, be due to the fact that contaminant concentrations in the test organisms may not have reached a steady-state equilibrium within the 28-day test period. Harbor worms collected *in-situ* are more likely to be at equilibrium with ambient contaminant concentrations associated with a longer exposure period. Standard deviations in BSAF values are also given on Figure 10-19 and are indicative of large variation in BSAF values for various locations in the Harbor. Possible explanations for observed geographic differences in BSAFs are address in more detail in Section 11.

10.7 BAF AND BSAF RESULTS FOR CADMIUM AND MERCURY IN SEDIMENT SPECIES

Field-derived BAFs and BSAFs were calculated for the sediment species using measured biota concentrations and corresponding bottom-water and sediment exposure concentrations from the CARP contaminant fate model. For cadmium and mercury, BAFs and BSAFs were calculated on a wet weight basis following Equation 10-2 and Equation 10-6 below.

$$BSAF = \frac{v}{r} \quad (10\text{-}6)$$

A summary of BAFs is presented in the top panels of Figure 10-20 for cadmium in worms, clams and blue crab. As shown, the field-derived BAFs for cadmium range from $10^{5.2}$ for clams, to approximately 10^{6} for worms and edible tissue in blue crabs, to approximately 10^{7} for the hepatopancreas in blue crab. This latter result is expected because higher concentrations of inorganic metals have been reported to accumulate in the hepatopancreas. BSAFs, which serve as more useful indicators of bioaccumulation potential for dredged material evaluations, are presented in the bottom panels of Figure 10-20. As shown, BSAF values range from 0.05 to 0.2 (-1.3 to -0.7 on a log scale) for the worms. Most of the clams, and the edible tissue in blue crabs fall within a similar range. As expected, the BSAF for cadmium in the hepatopancreas of the blue crab is much higher and approximately equal to 1.3 (0.11 on a log scale).

A summary of BAFs for non-methylated mercury and methylmercury is presented in Figure 10-21 for worms, clams and blue crabs. Average BAFs for methylmercury in clams and blue crab fall within a limited range from $10^{5.1}$ to $10^{5.3}$ in L/ng-WW units. Average BSAFs for methylmercury in certain clams (wedge rangia) and crabs are elevated as compared to other clams (surf and soft shell) and worms (based on model calculated sediment concentrations). Reason for this behavior is not clear at the present time.

Figures 10-20 and 10-21 present the BSAF calculations for worms in two ways: (1) using measured biota concentrations and corresponding sediment exposure concentrations derived from the CARP contaminant fate model and (2) using measured biota concentrations and measured collocated sediment concentrations. There is excellent agreement between the worm BSAFs based on the model-derived and the field-measured sediment concentrations for each of cadmium and mercury, highlighting the strength of the CARP contaminant fate model. In the case of methylmercury, the agreement between the two worm BSAF calculation methods is poor, but it is noted that only one biota/sediment pairing was available for methylmercury. Mercury and cadmium BSAFs presented for the worms were based on seven biota/sediment pairings.

10.8 TABULATION OF HARBOR-SPECIFIC BAFs AND BSAFs

As part of CARP component and scenario runs (see Section 12), calculations of chemical concentrations in biota are performed using water and sediment exposure concentrations along with Harbor-specific BAFs and BSAFs. For this purpose, geometric mean BAFs previously presented in Figures 10-1 through 10-6 are used for selected water column species. A listing of these values is given

in Appendix 11. For PCB homologs, dioxin/furan congeners, PAHs and pesticides, chemical concentrations in biota are calculated as follows:

$$\nu = BAF_{lipid} \cdot C_{dis}^{freely} \cdot f_{lipid} \quad (10\text{-}7)$$

where ν is the chemical concentration in the organism (μg chemical/g wet wt), BAF_{lipid} is the lipid normalized BAF (L/kg lipid), C_{dis}^{freely} is the freely dissolved chemical concentration, and f_{lipid} in the lipid fraction in the organism. For cadmium, non-methylated mercury and methylmercury, chemical concentrations in biota are calculated as:

$$\nu = BAF \cdot C_{exposure} \quad (10\text{-}8)$$

where BAF is given in L/kg wet wt, and $C_{exposure}$ is taken as the free metal ion concentration (Cd^{2+}) for cadmium and as the summation of the free metal ion concentration (Hg^{2+}) and the free methyl mercury concentration for mercury.

For sediment species (blue crab, clams, worms), bioaccumulation calculations will be performed using geometric mean BSAFs previously presented in Figures 10-7 through 10-21. A listing of these values are given in Table 10-2. For PCB homologs, dioxin/furan congeners, PAHs and pesticides, chemical concentrations in biota are calculated as follows:

$$\nu = BSAF_{lipid,oc} \cdot r_{oc} \cdot f_{lipid} \quad (10\text{-}9)$$

where $BSAF_{lipid,oc}$ is the lipid normalized BSAF (kg org C/kg lipid), and r_{oc} is the organic carbon normalized concentration of chemical in top 10 cm of the sediment. For cadmium, non-methylated mercury and methylmercury, chemical concentrations in biota are calculated as:

$$\nu = BAF \cdot r \quad (10\text{-}10)$$

where BAF is given in L/kg wet wt, and r is taken as the dry weight concentration of cadmium, non-methylated mercury (i.e., total mercury - methylmercury), and methylmercury in the top 10 cm of sediment.

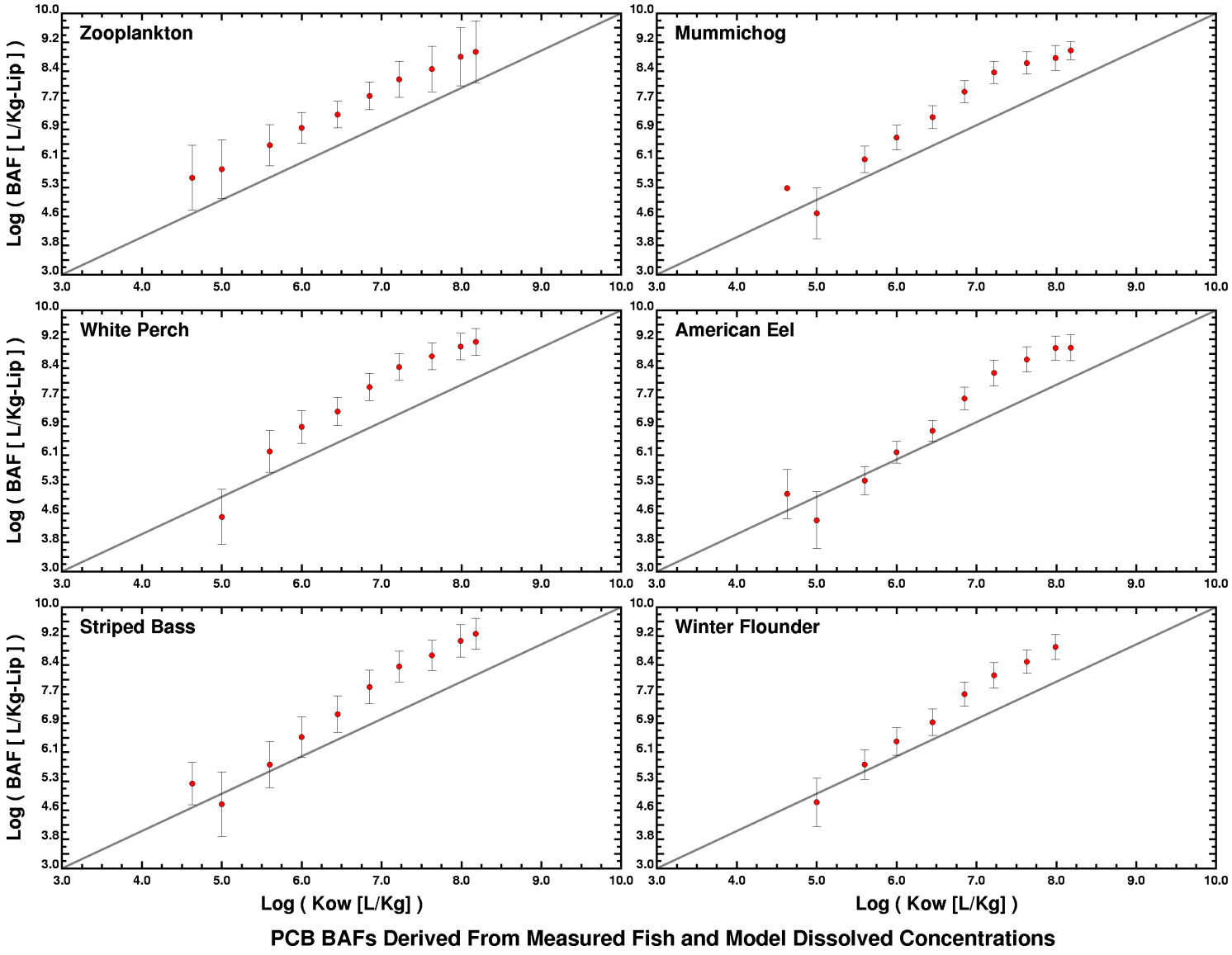

Figure 10-1. Summary of lipid-normalized BAFs for PCB homologs.

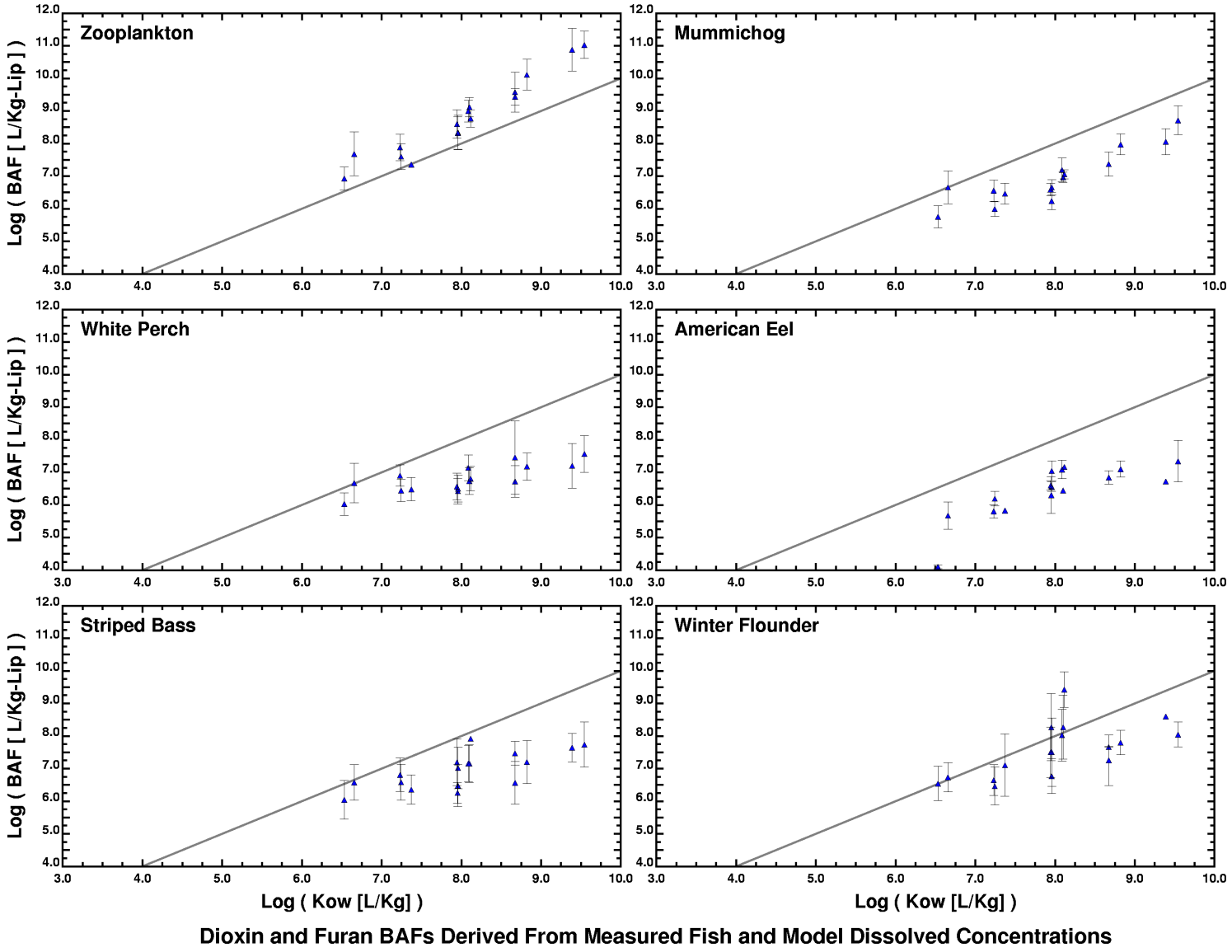

Figure 10-2. Summary of lipid-normalized BAFs for dioxin and furan congeners.

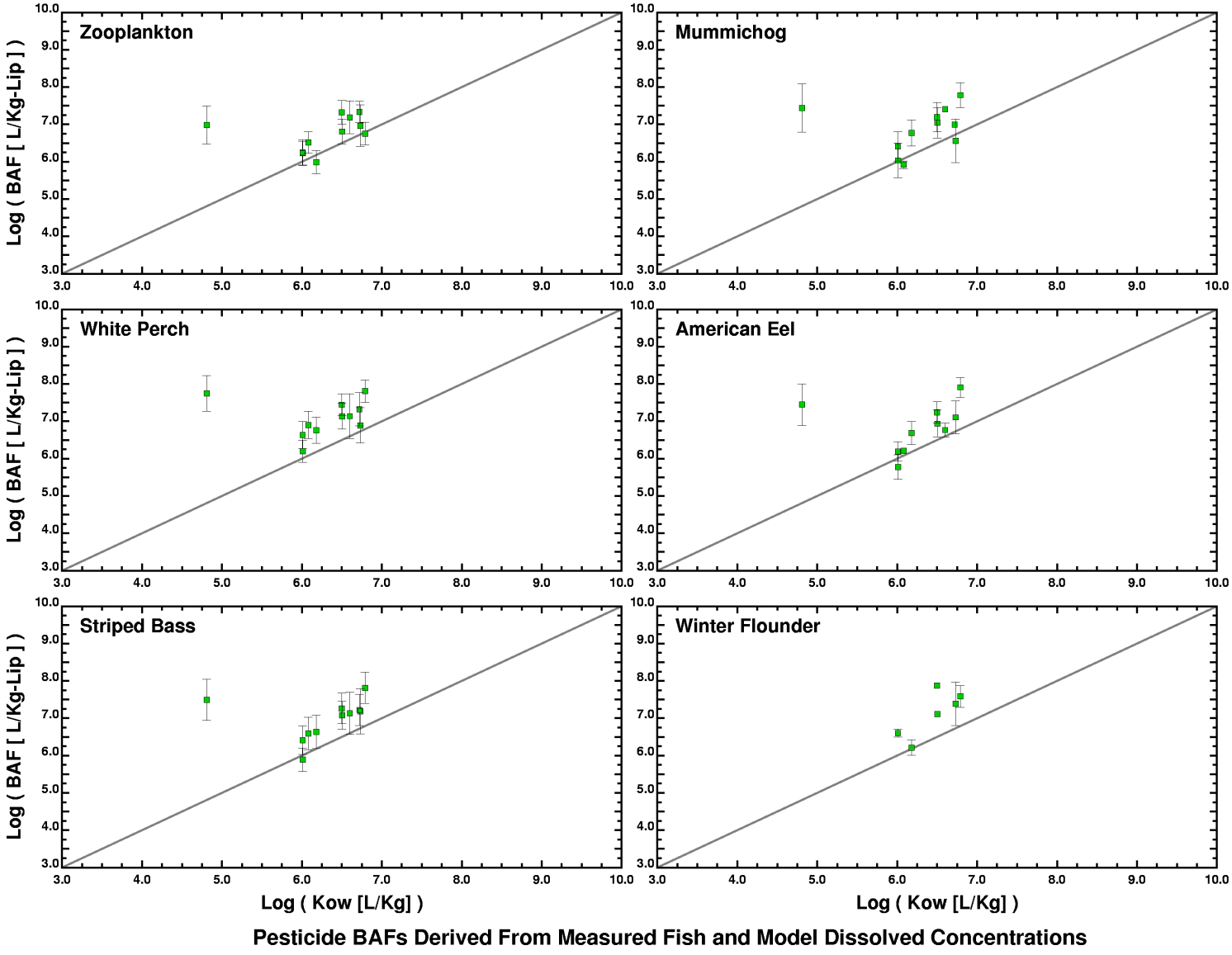

Figure 10-3. Summary of lipid-normalized BAFs for organochlorine pesticides.

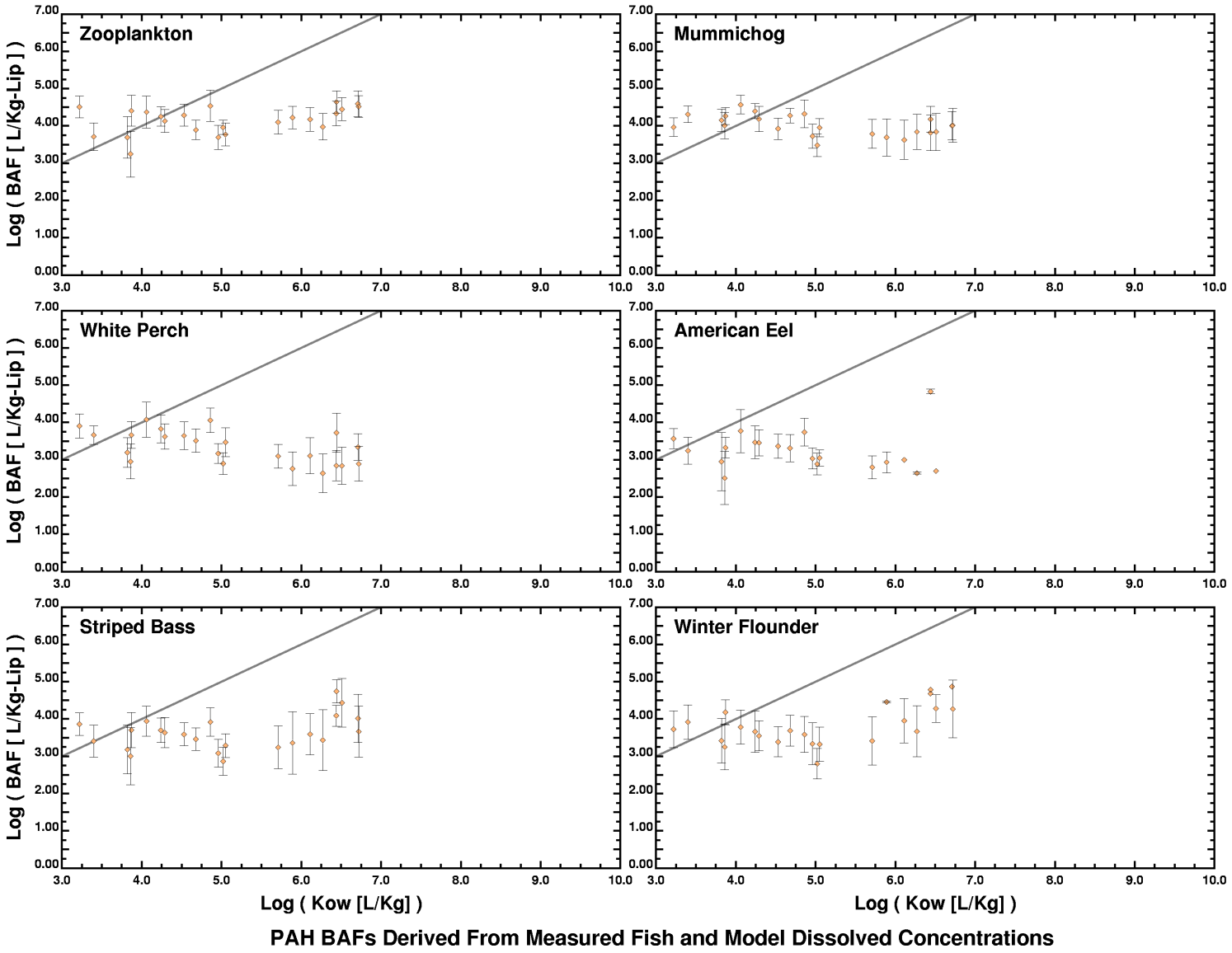

Figure 10-4. Summary of lipid-normalized BAFs for PAHs.

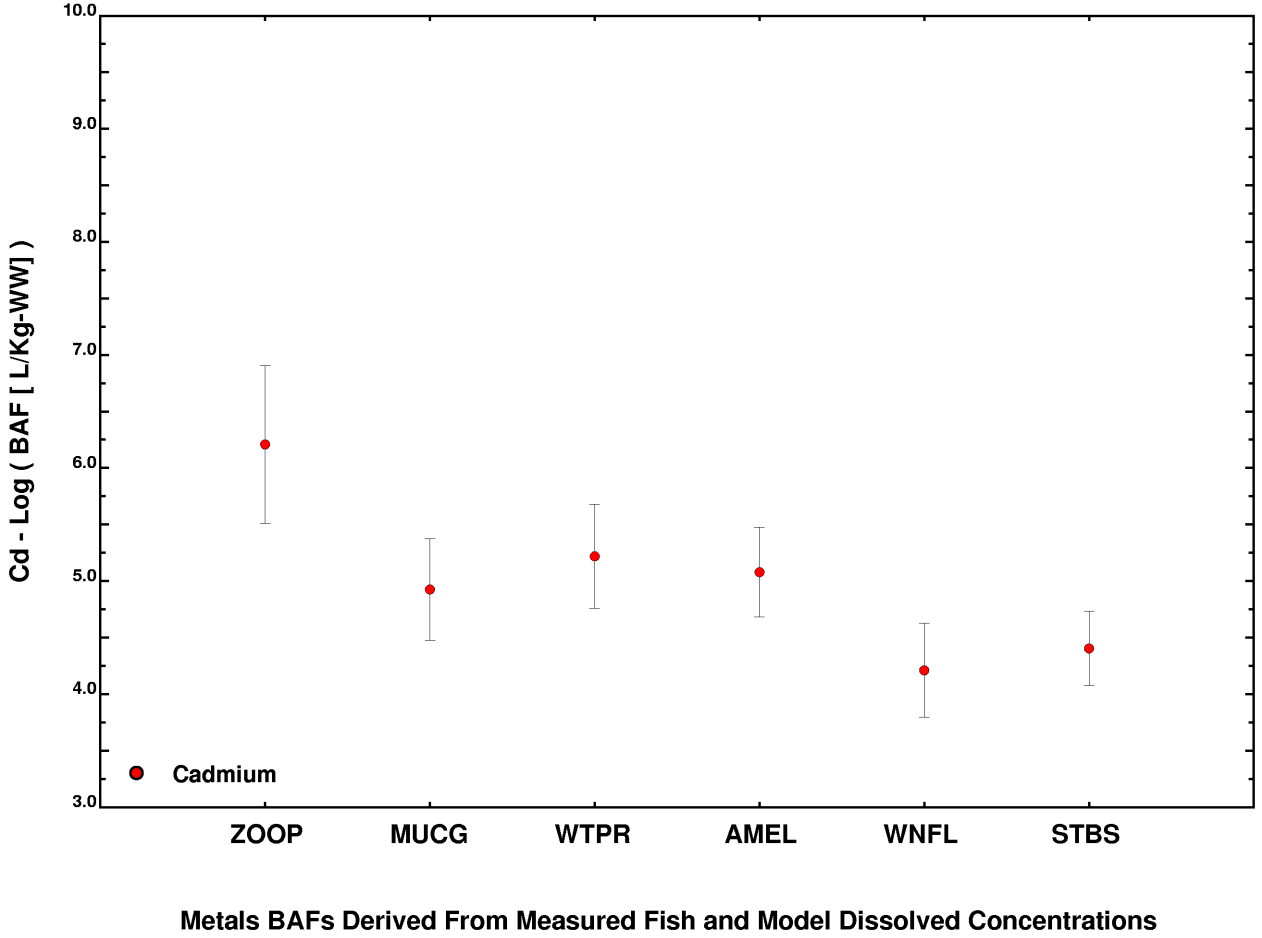

Figure 10-5. Summary of BAFs for cadmium.

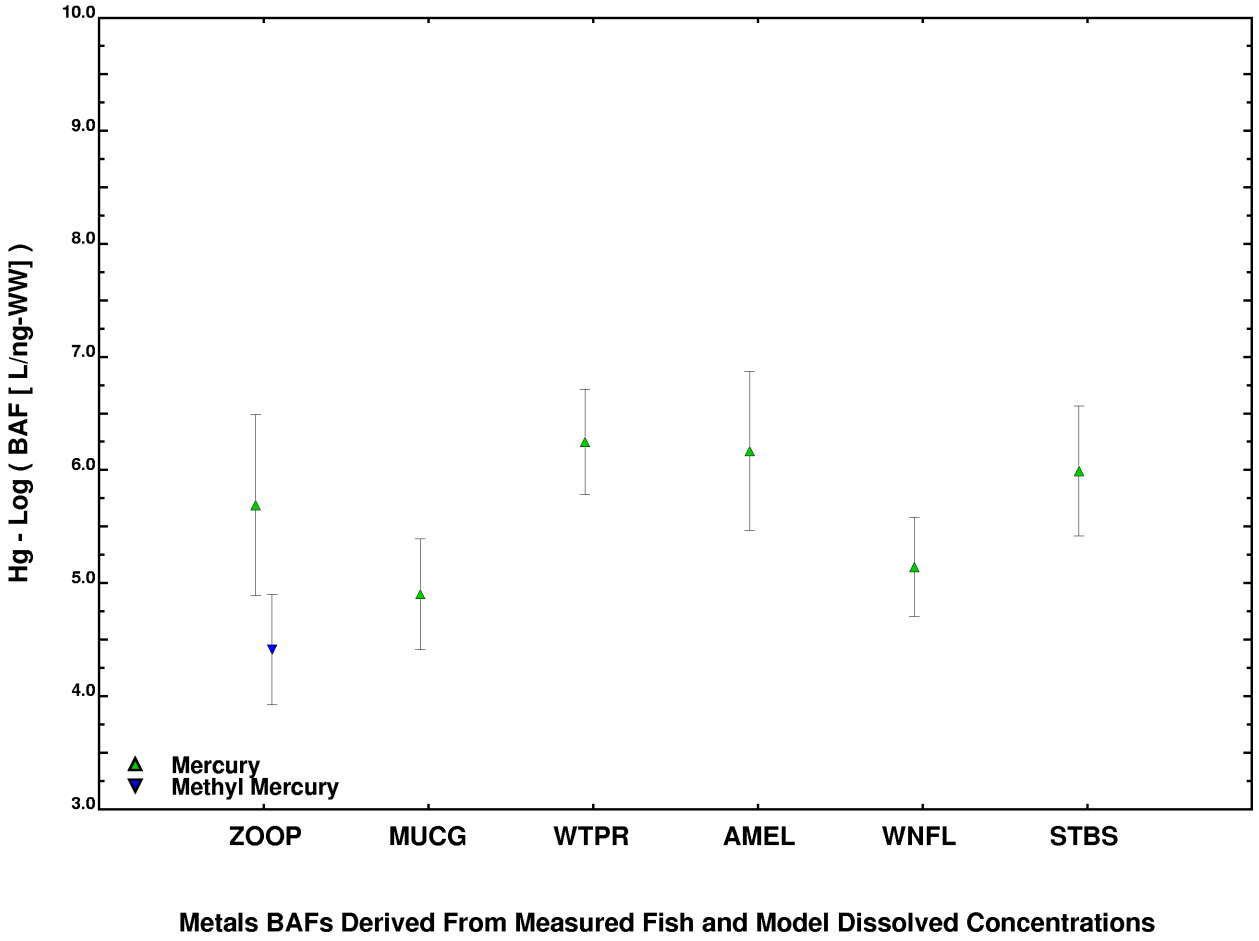

Figure 10-6. Summary of BAFs for total mercury and methyl mercury.

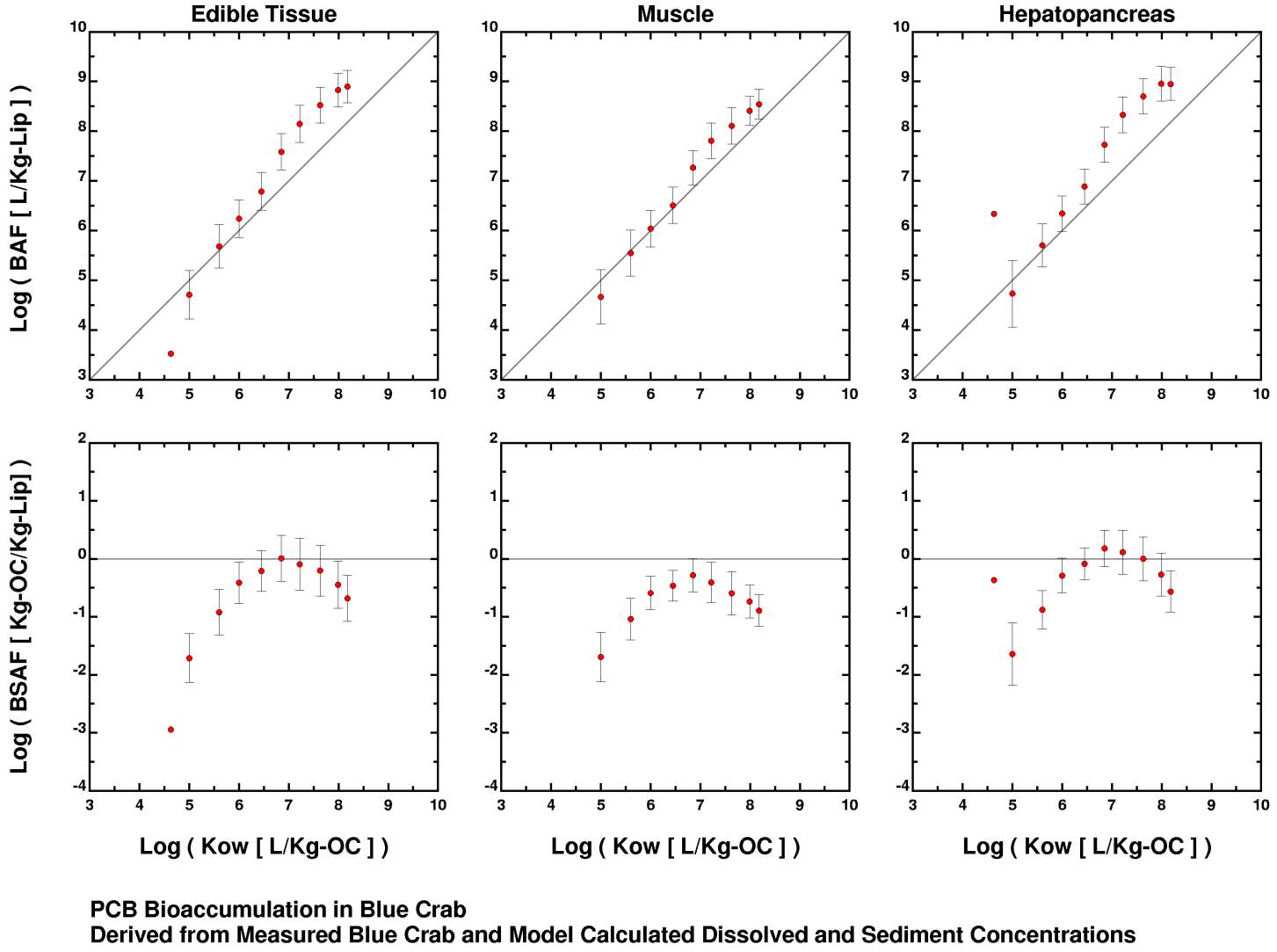

Figure 10-7. Lipid-normalized BAFs and lipid/organic carbon - normalized BSAFs for PCB homologs in blue crab.

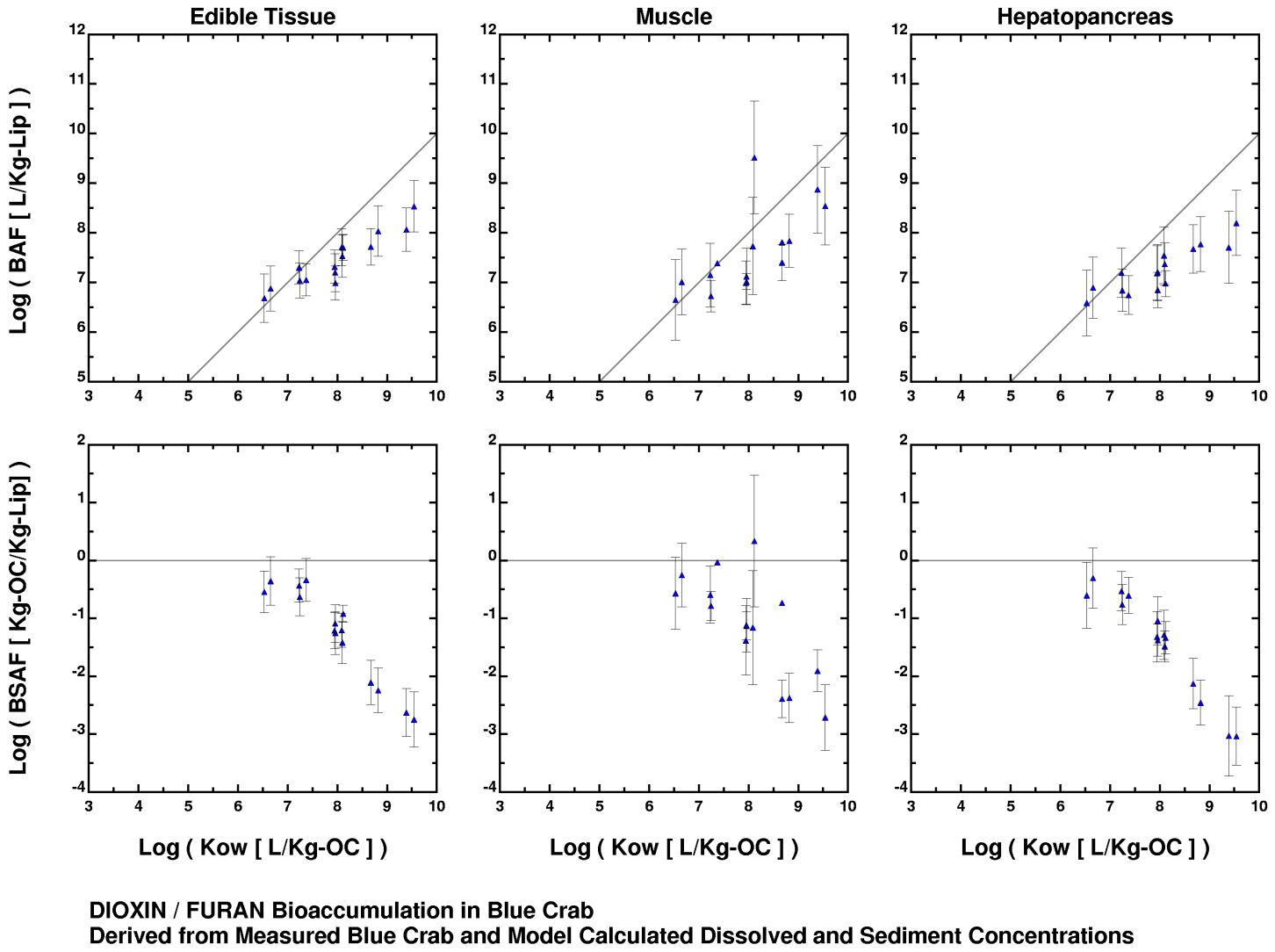

Figure 10-8. Lipid-normalized BAFs and lipid/organic carbon-normalized BSAFs for dioxin and furan congeners in blue crab.

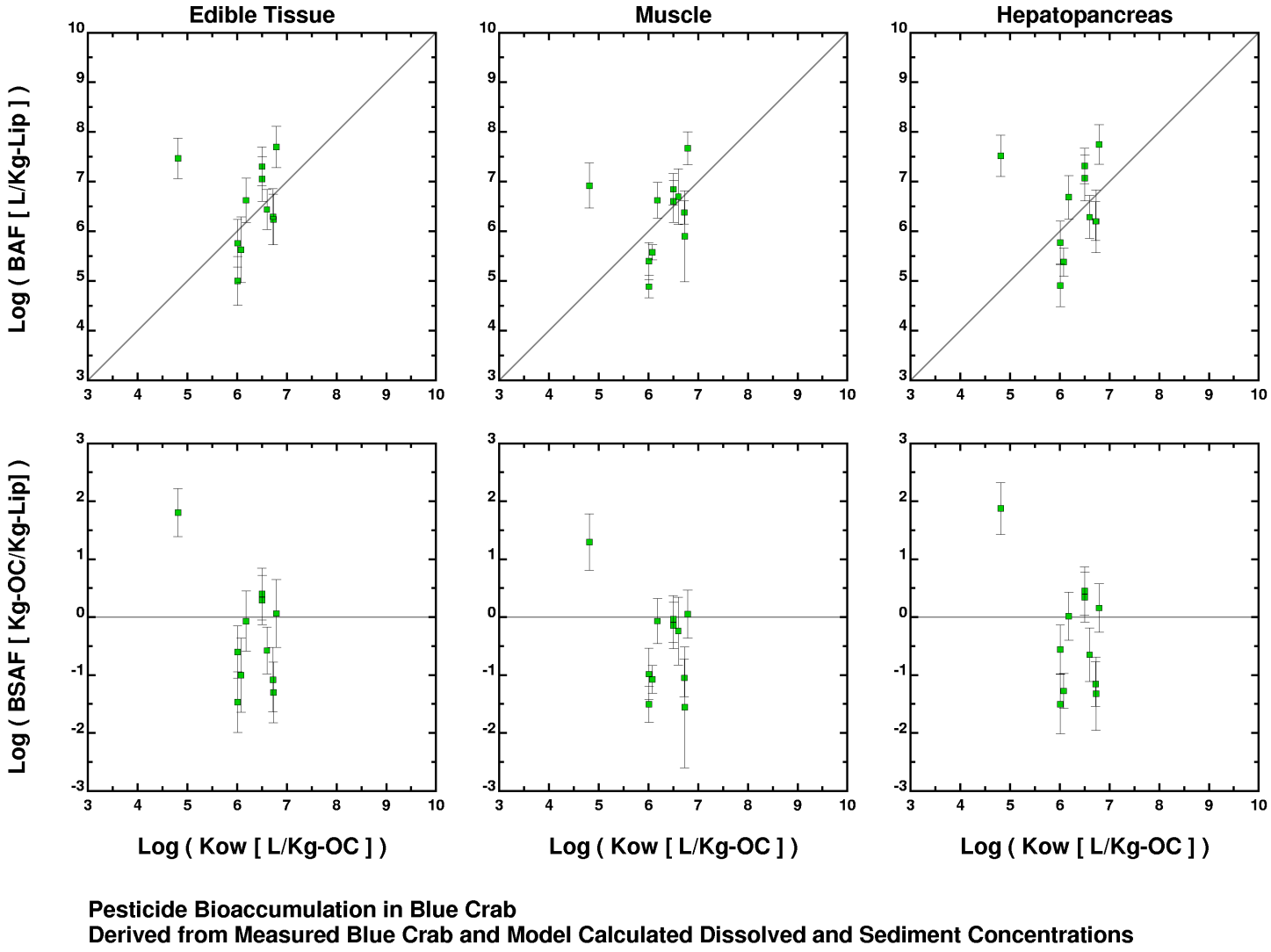

Figure 10-9. Lipid-normalized BAFs and lipid/organic carbon-normalized BSAFs for chlorinated pesticides in blue crabs.

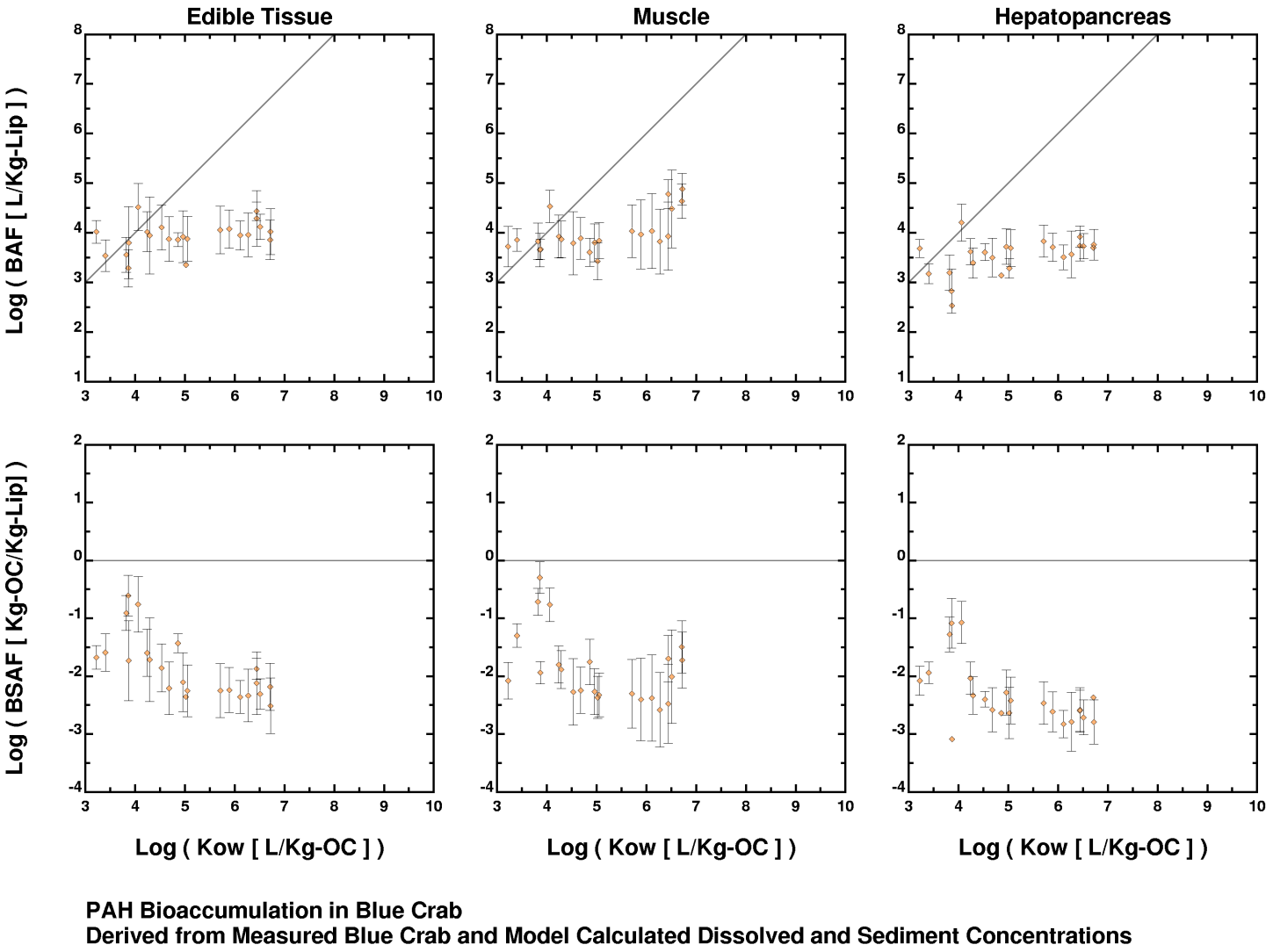

Figure 10-10. Lipid-normalized BAFs and lipid/organic carbon-normalized BSAFs for PAHs in blue crabs.

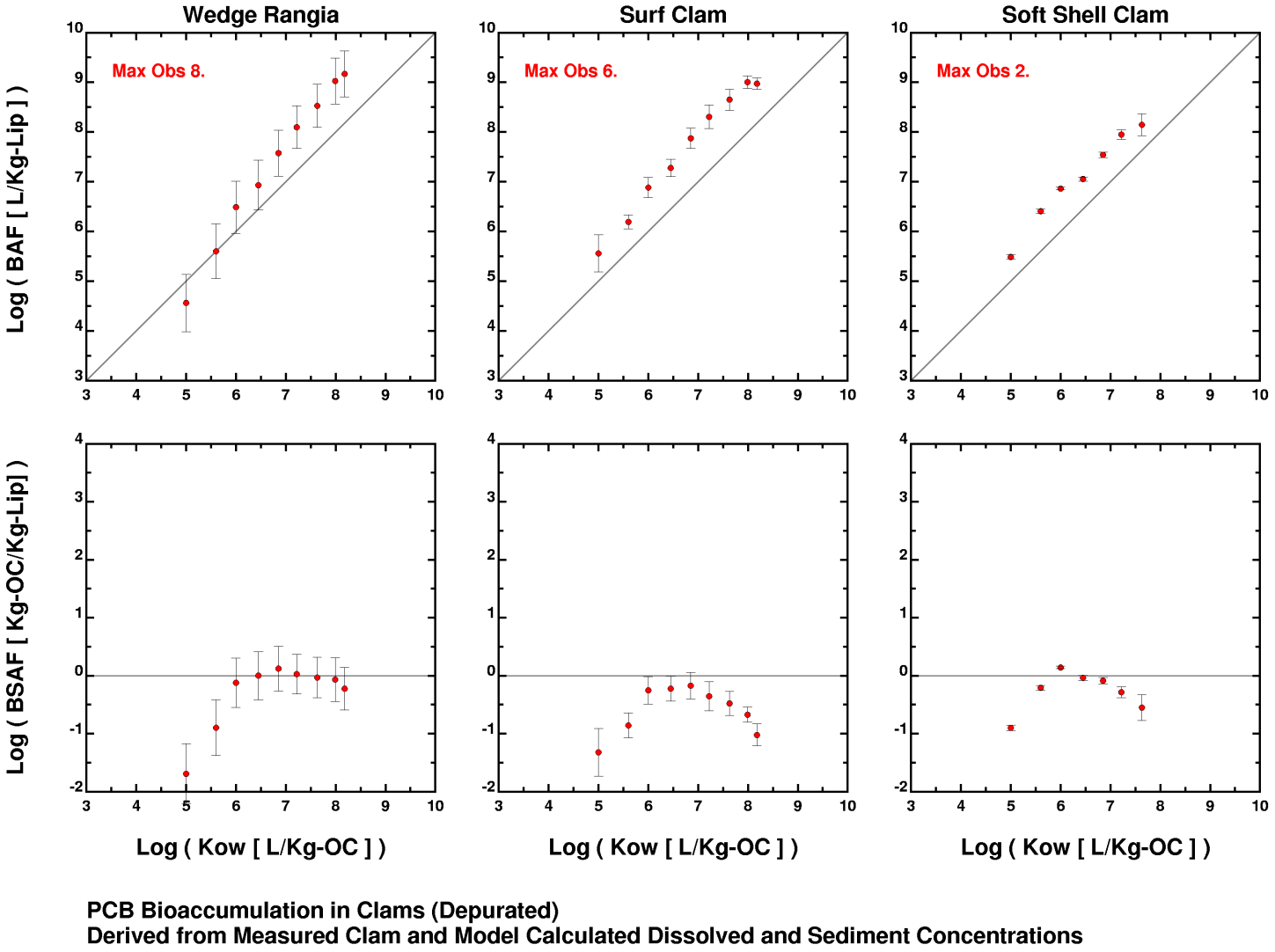

Figure 10-11a. Lipid-normalized BAFs and lipid/organic carbon-normalized BSAFs for PCB homologs in depurated clams.

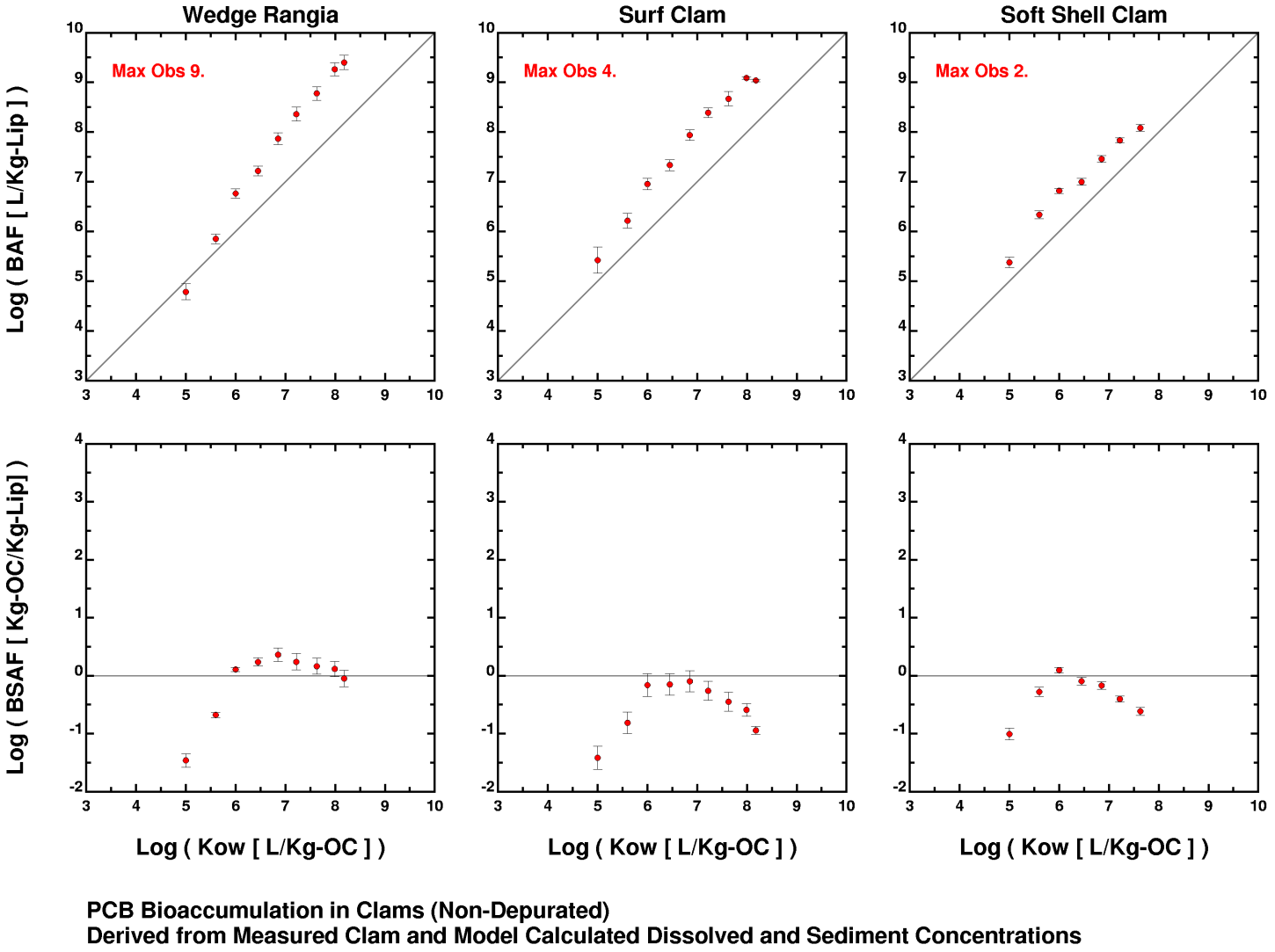

Figure 10-11b. Lipid-normalized BAFs and lipid/organic carbon-normalized BSAFs for PCB homologs in non-depurated clams.

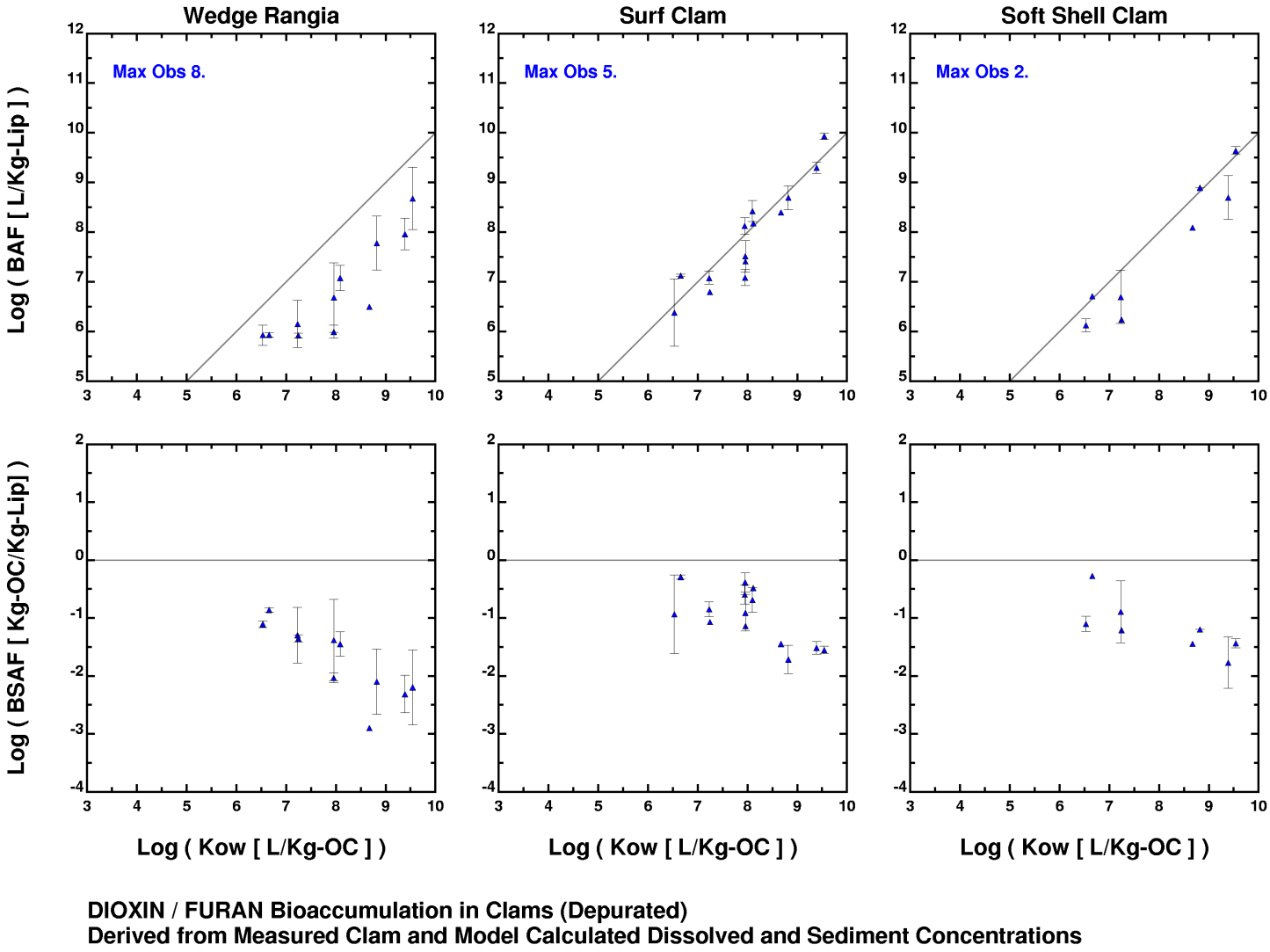

Figure 10-12a. Lipid-normalized BAFs and lipid/organic carbon-normalized BSAFs for dioxin and furan congeners in depurated clams.

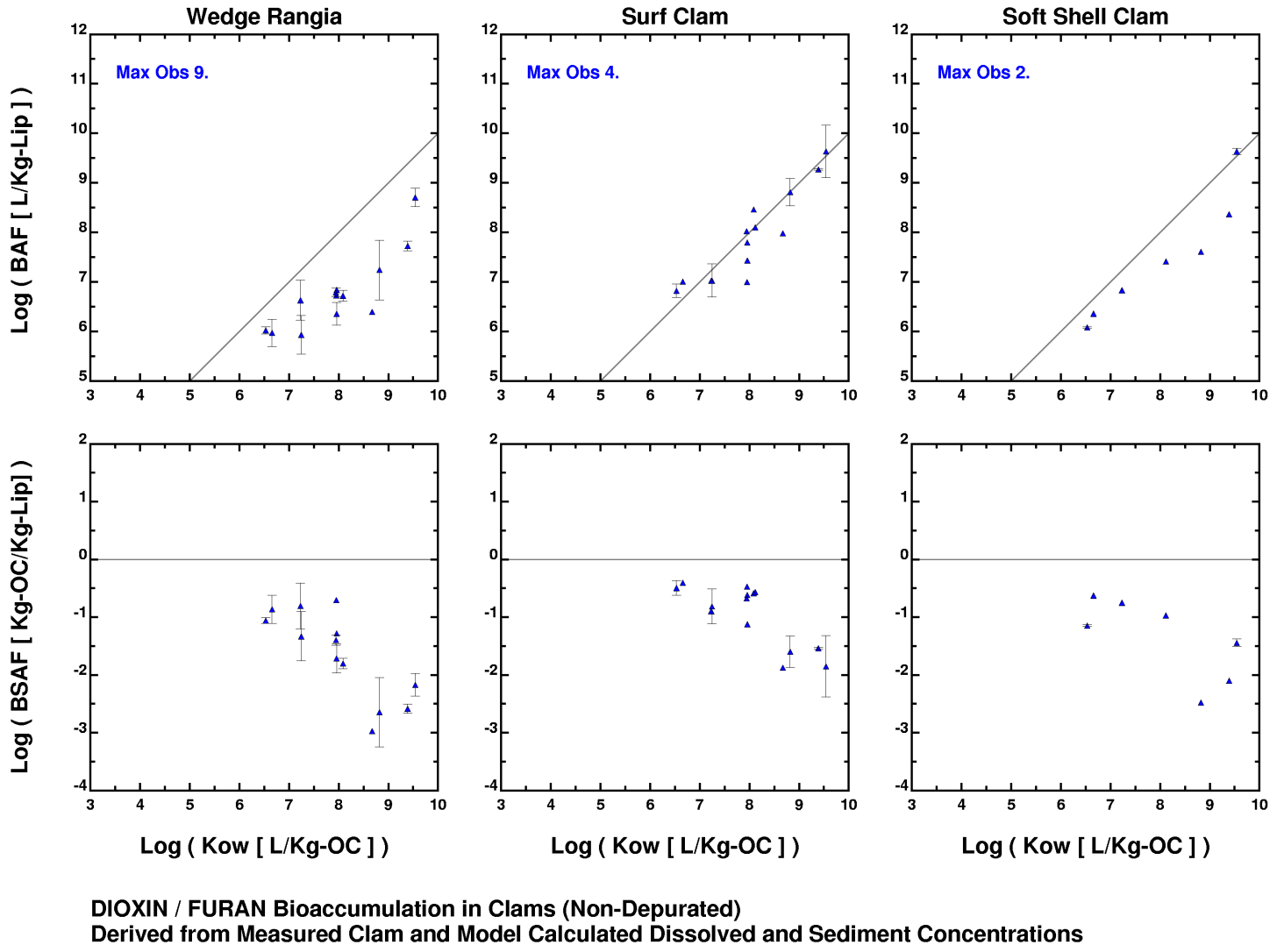

Figure 10-12b. Lipid-normalized BAFs and lipid/organic carbon-normalized BSAFs for dioxin and furan congeners in non-depurated clams.

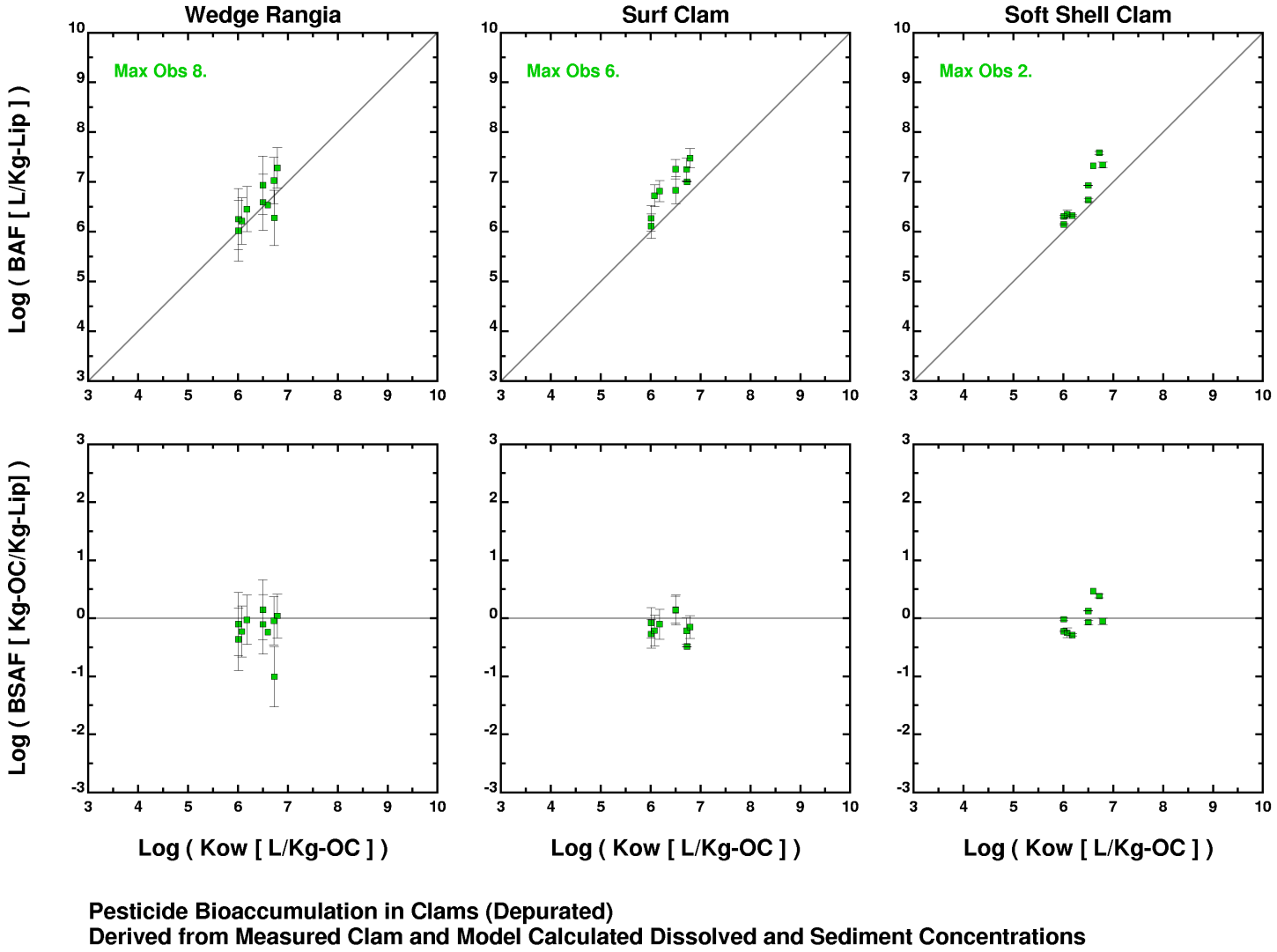

Figure 10-13a. Lipid-normalized BAFs and lipid/organic carbon-normalized BSAFs for organochlorine pesticides in depurated clams.

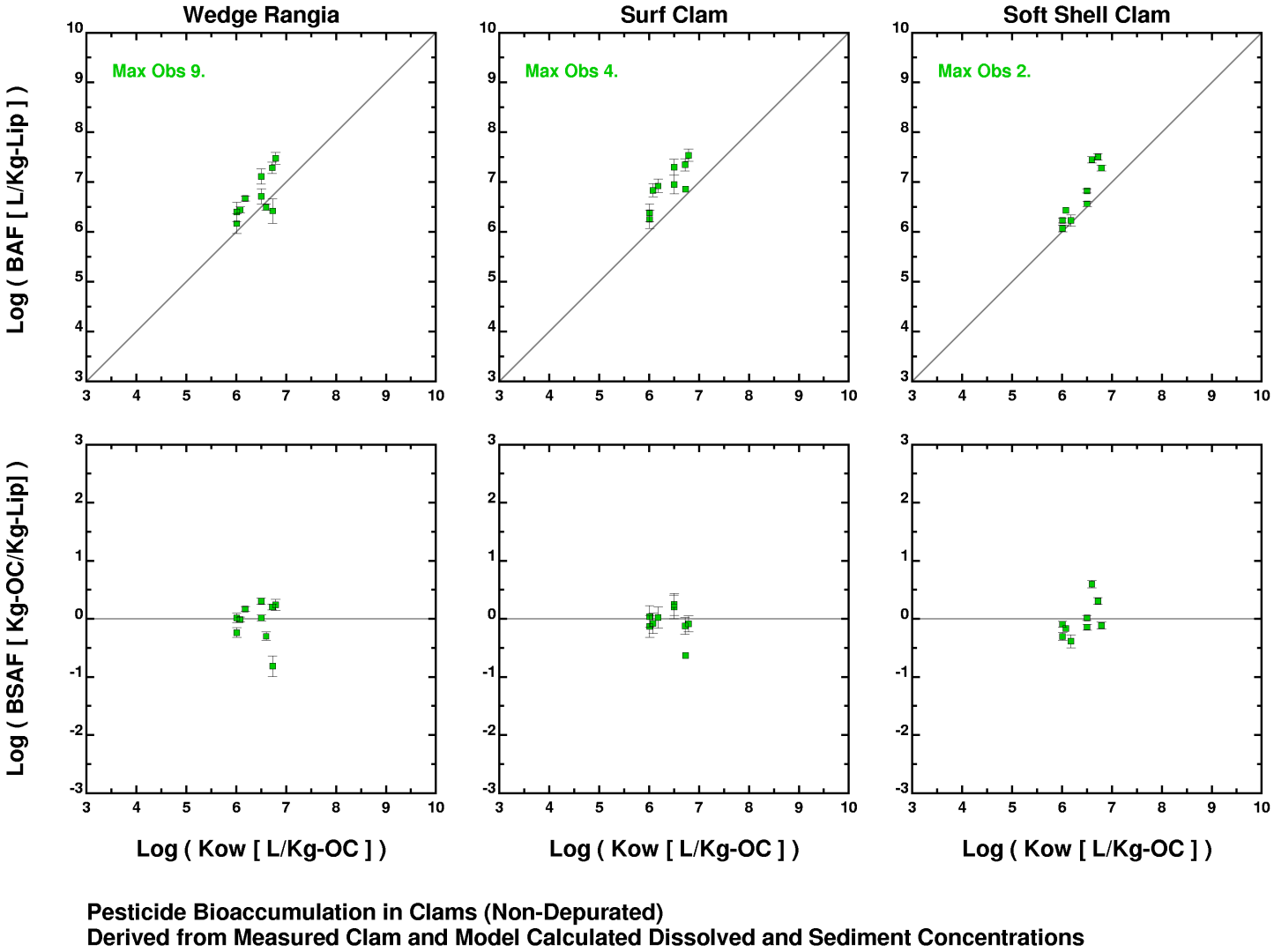

Figure 10-13b. Lipid-normalized BAFs and lipid/organic carbon-normalized BSAFs for organochlorine pesticides in non-depurated clams.

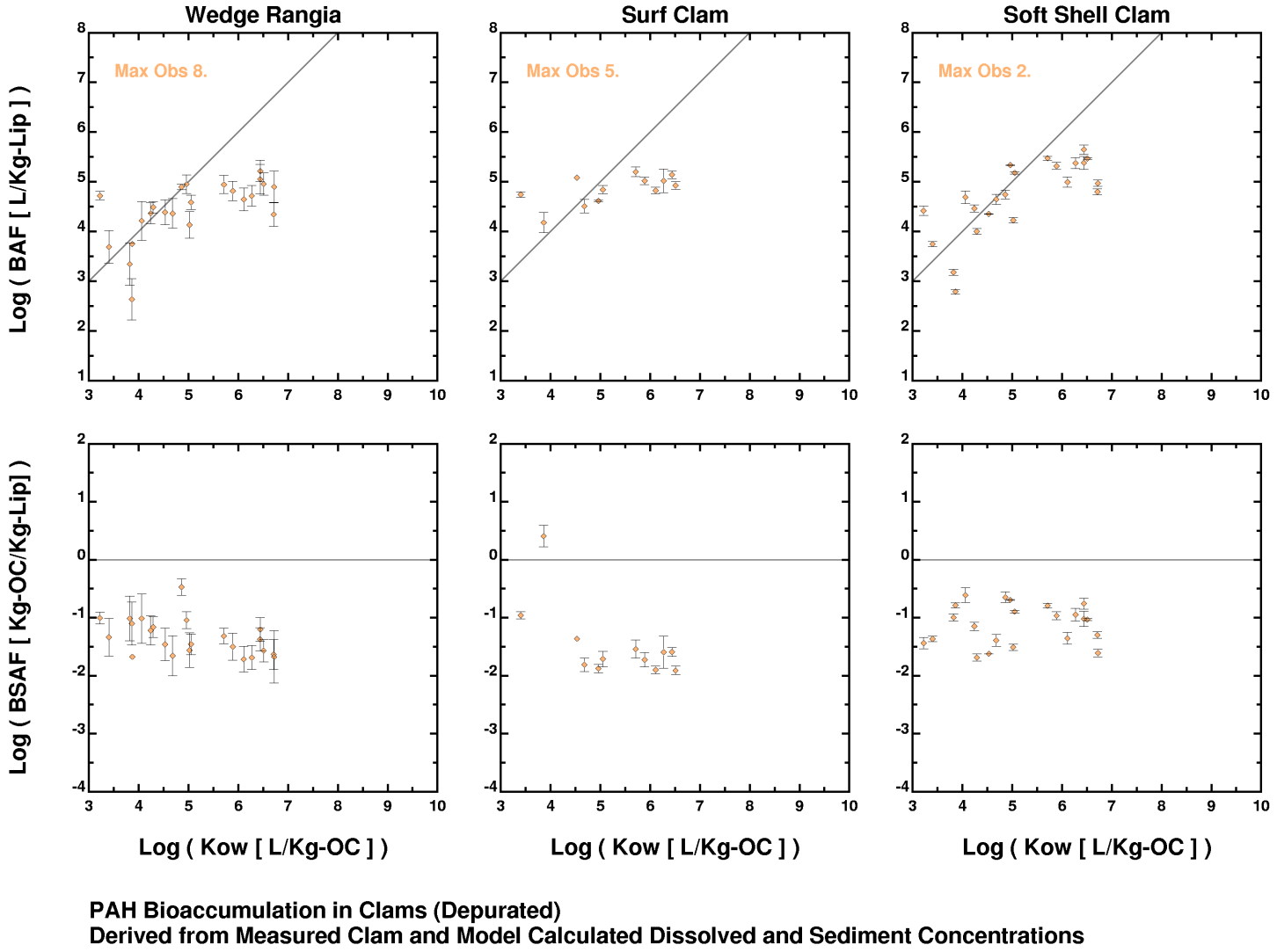

Figure 10-14a. Lipid-normalized BAFs and lipid/organic carbon-normalized BSAFs for PAHs in depurated clams.

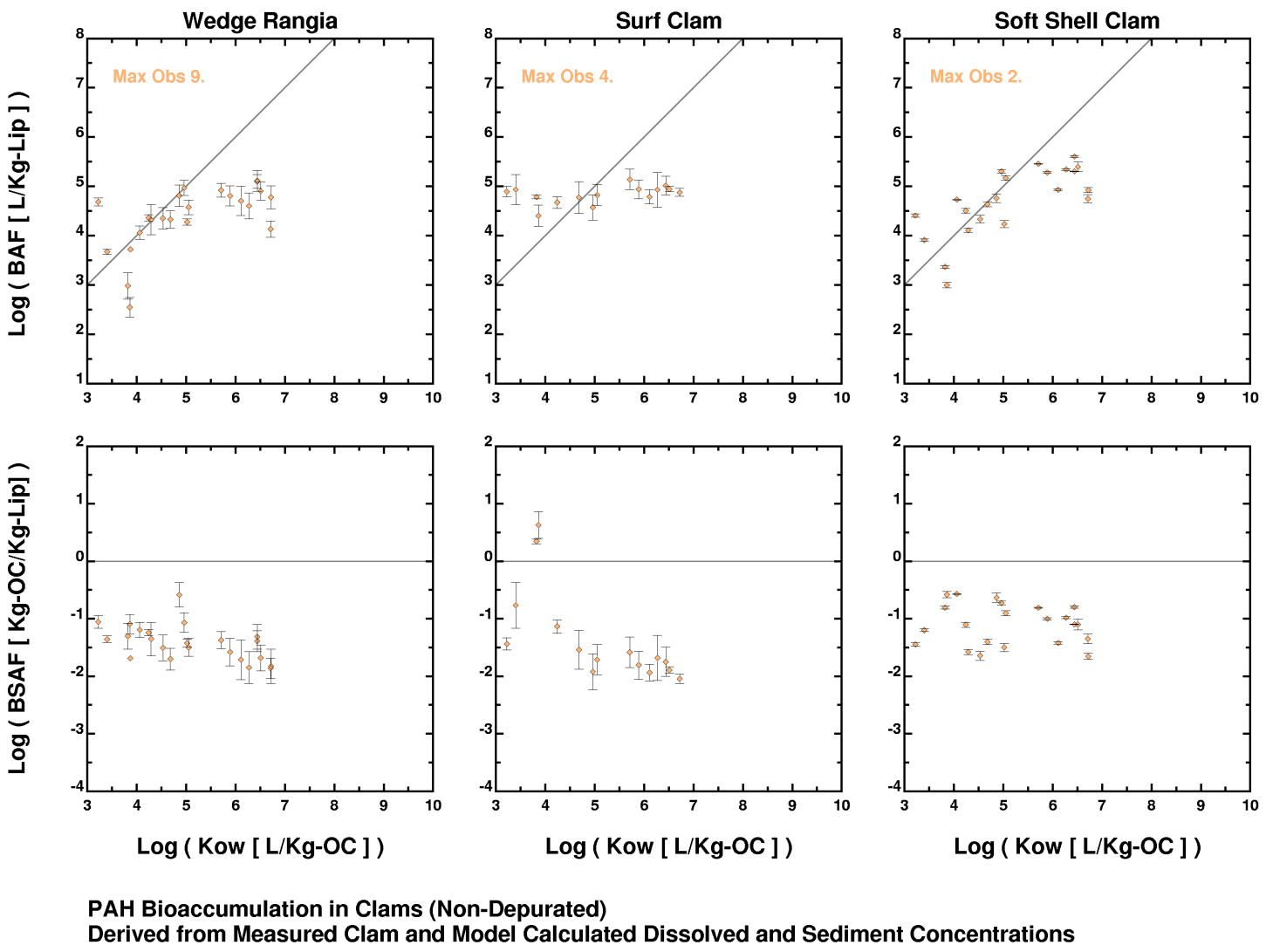

Figure 10-14b. Lipid-normalized BAFs and lipid/organic carbon-normalized BSAFs for PAHs in non-depurated clams.

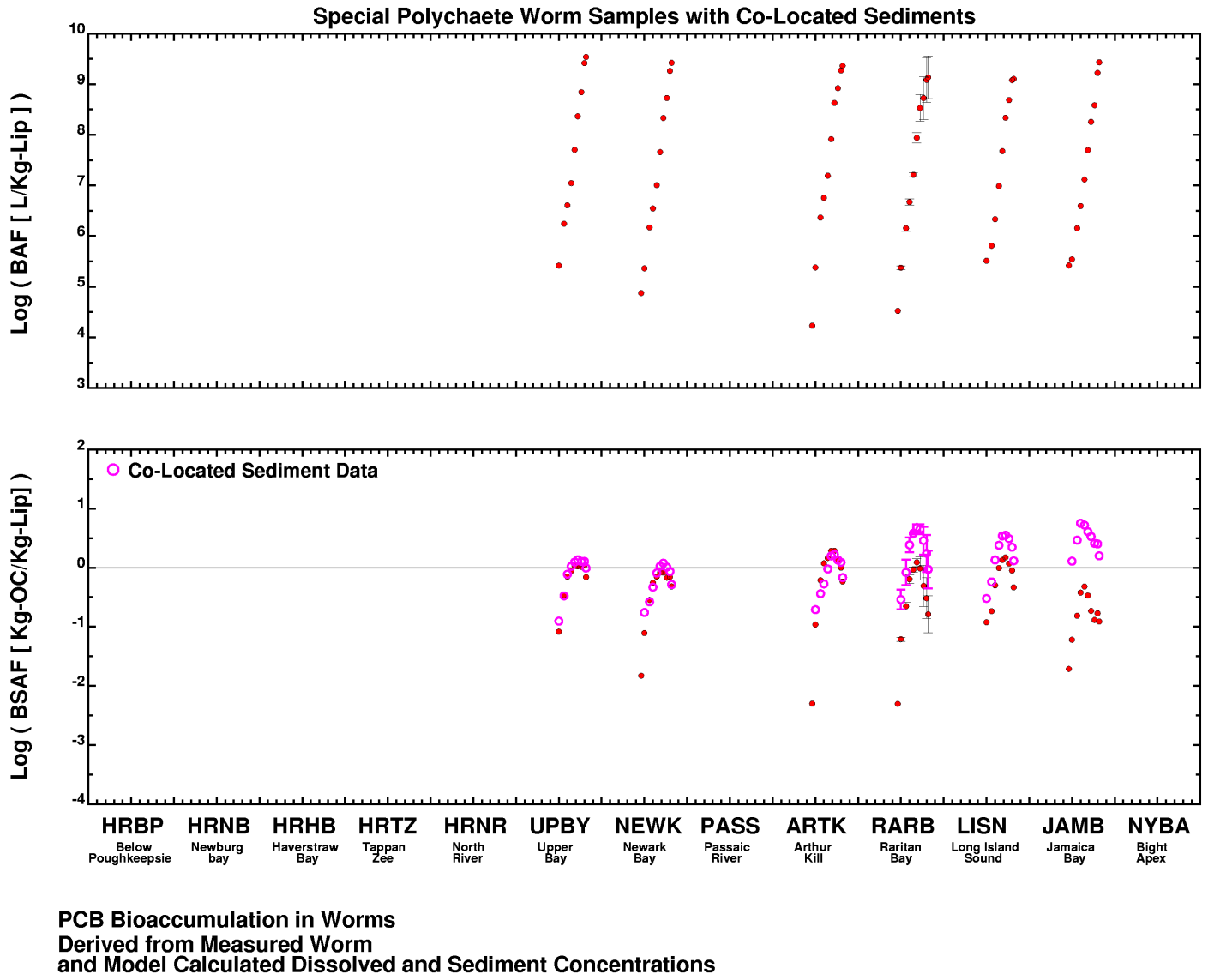

Figure 10-15. Lipid/organic carbon-normalized BSAFs for PCB homologs in worms.

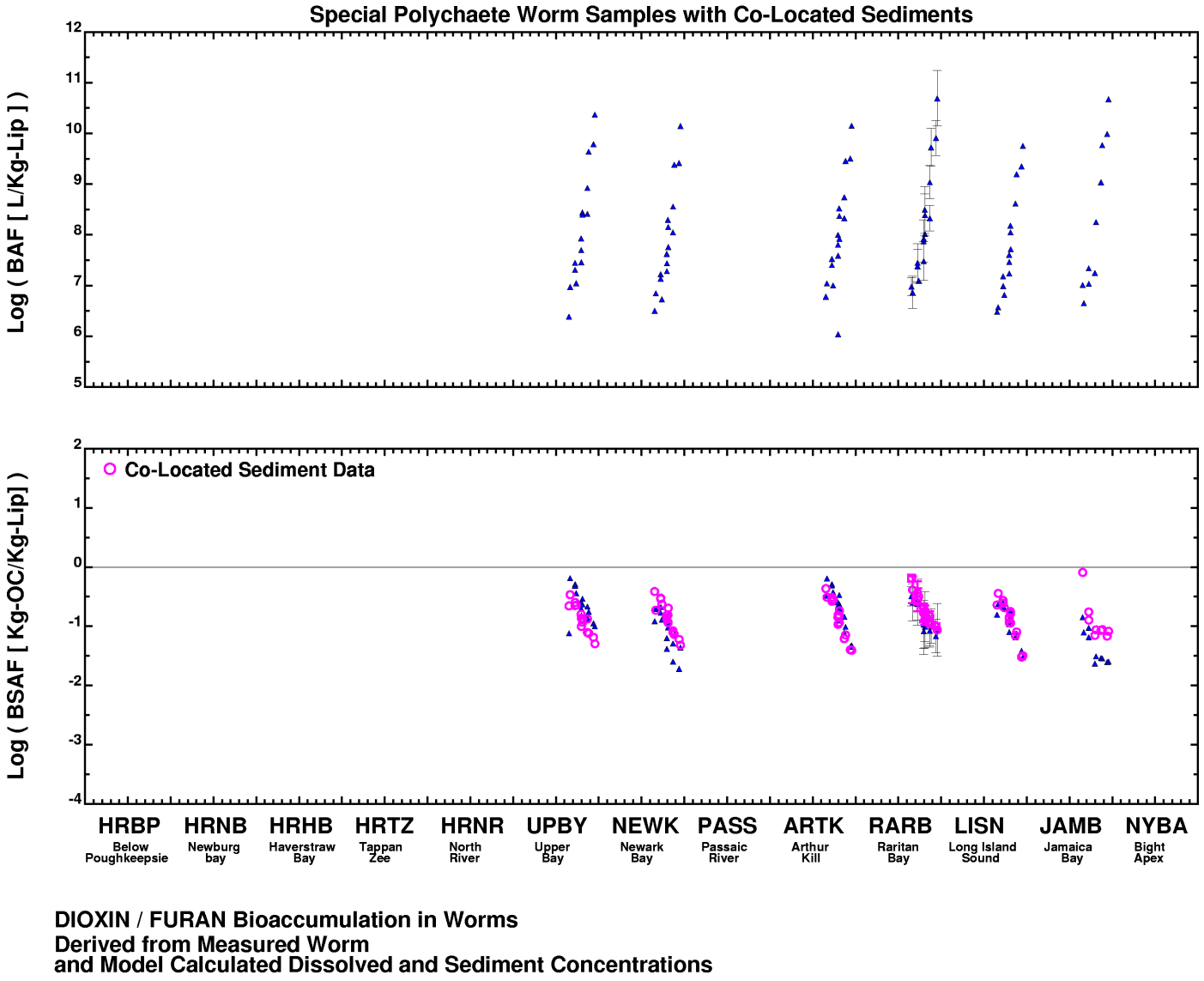

Figure 10-16. Lipid/organic carbon-normalized BSAFs for dioxin and furan congeners in worms.

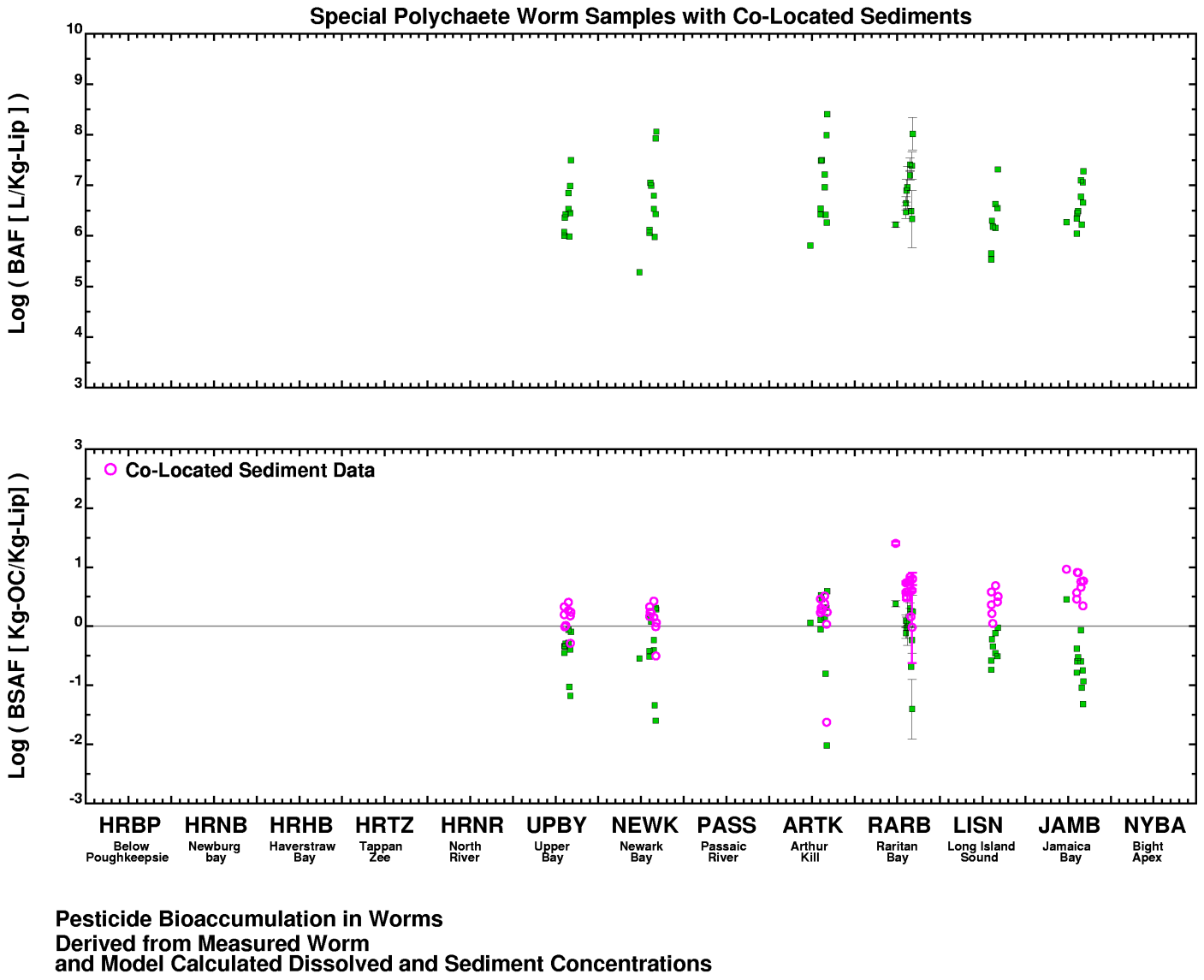

Figure 10-17. Lipid/organic carbon-normalized BSAFs for organochlorine pesticides in worms.

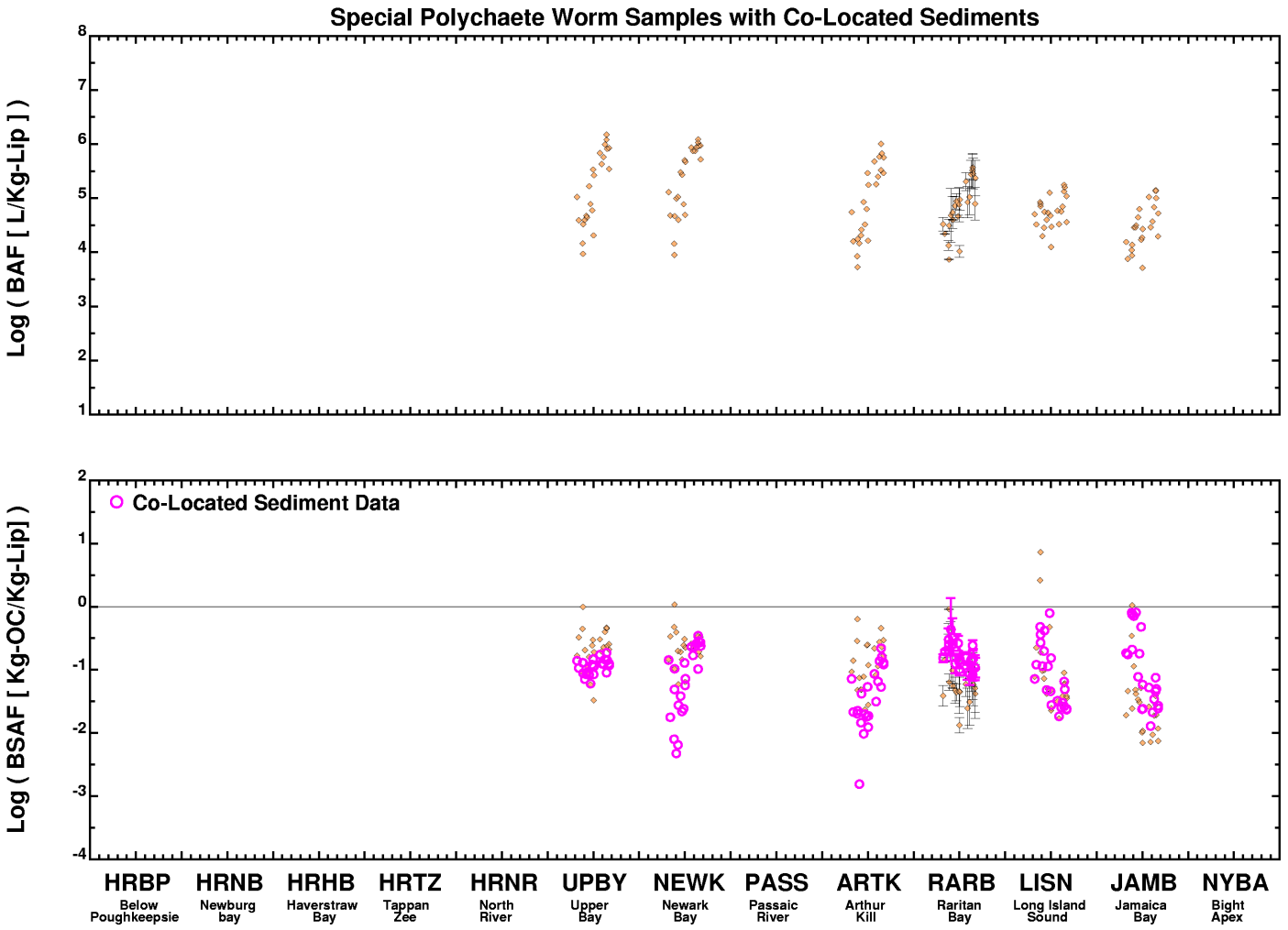

PAH Bioaccumulation in Worms Derived from Measured Worm and Model Calculated Dissolved and Sediment Concentrations

Figure 10-18. Lipid/organic carbon-normalized BSAFs for PAHs in worms.

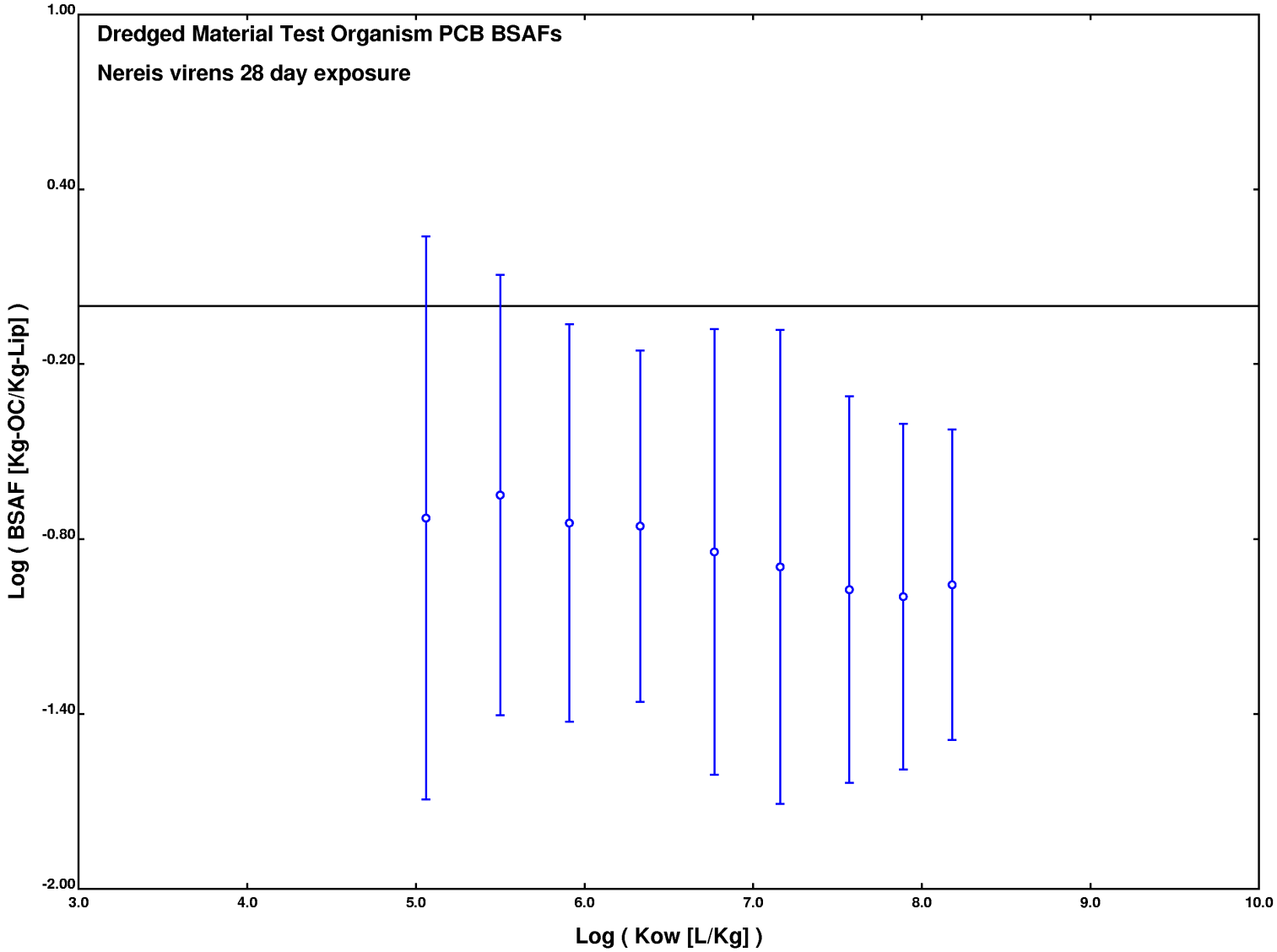

Figure 10-19. Summary of *Nereis* PCB BSAFs calculated from NY/NJ Harbor dredged material testing data.

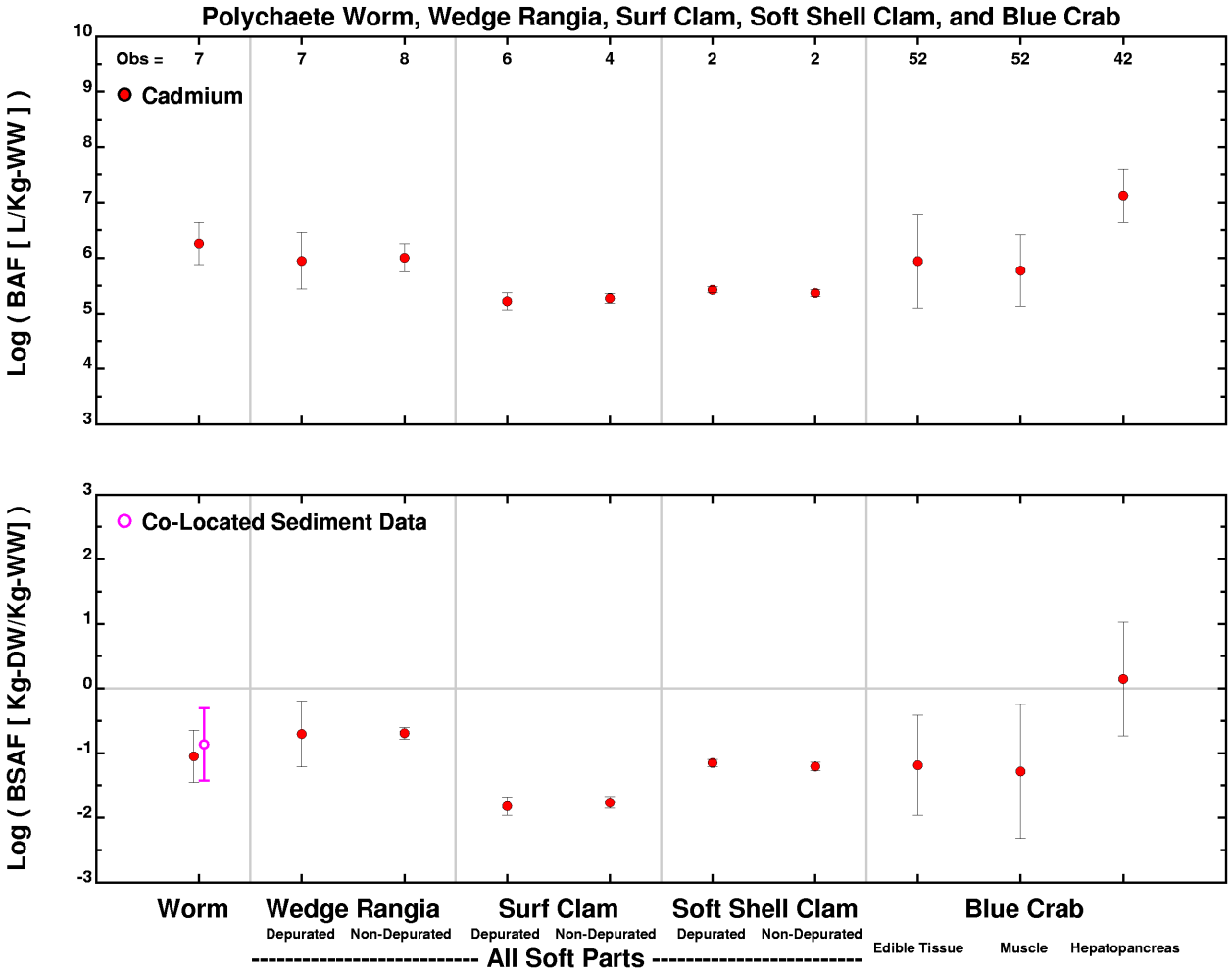

Cadmium Bioaccumulation in Benthic Species
Derived from Measured Body Burden and Model Calculated Dissolved and Sediment Concentrations

Figure 10-20. BAFs and BSAFs for cadmium in benthic species.

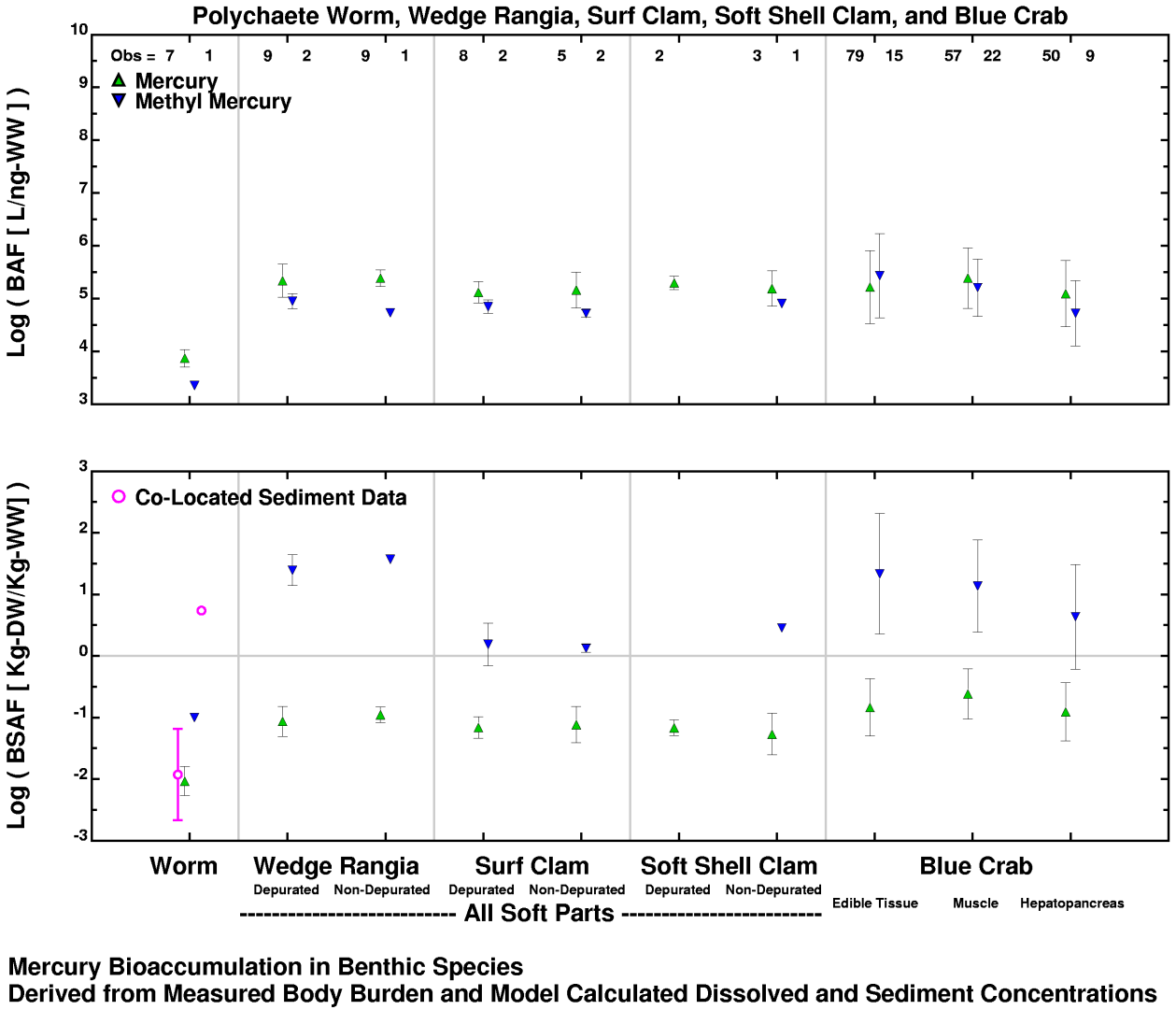

Mercury Bioaccumulation in Benthic Species
Derived from Measured Body Burden and Model Calculated Dissolved and Sediment Concentrations

Figure 10-21. BAFs and BSAFs for nonmethyl mercury and methyl mercury in benthic species

SECTION 11.0

FOOD CHAIN/BIOACCUMULATION MODEL SENSITIVITIES

In addition to field-derived BAF and BSAF evaluations in Section 10, detailed model calculations were performed to examine the dominant factors affecting bioaccumulation in Harbor biota. Evaluations included fully time-variable, age-dependent bioaccumulation model calculations for 10 PCB homologs, 17 dioxin/furan congeners, cadmium and mercury in the white perch-striped bass food chain, and steady-state bioaccumulation model calculations for 10 PCB homologs in Harbor worms. Formulations for the time-variable, white perch-striped bass bioaccumulation model and the steady-state worm bioaccumulation model were previously presented in Section 8. Determination of model input parameters, including water and sediment exposure concentrations, organism weight, growth rate, lipid content, respiration relationships, migration patterns, etc. were described in Section 9. This section of the report describes the results of the bioaccumulation model evaluations and sensitivity studies. The model evaluations and sensitivity studies were performed for informational and explanatory purposes only. Ultimately, field-derived BAFs and BSAFs were used for management purposes.

11.1 BIOACCUMULATION OF PCBs IN FISH

The fully time-variable, age-dependent bioaccumulation model was used to examine PCB bioaccumulation in the white perch-striped bass food chain. Model calculations were performed using model parameters described in Section 9. For the base case, the gill transfer efficiency was specified as a constant value of 0.6 for all species based on information given in McKim et al. (1985) for mid-range K_{ow} compounds. The chemical assimilation efficiency was set equal to the food assimilation efficiency of 0.3 for zooplankton. For small fish, white perch and striped bass, the chemical assimilation efficiency was specified as 0.435 based on information in Kelly et al. (2004) for mid-range K_{ow} compounds.

Detailed comparisons of lipid-normalized PCB model results and field observations for the base case are presented for zooplankton and the individual age classes of white perch and striped bass in Appendix 12a. For comparisons, model results and field observations for zooplankton were matched based on sample collection time and location (which is represented by one of the 39 CARP food web regions). For white perch, comparisons were made based on matched time, location (which is represented by one of the 39 CARP food web regions), and weight (which is used as a surrogate for age). Finally, model results and field observations for the migratory striped bass were compared based on sample collection time, location (as represented by one of the the five larger Thomann-Farley food web regions) and weight. A summary of these comparisons are given in Figure 11-1 as ratios of model

calculated and field observed concentrations for the 10 PCB homologs. (In this presentation, a ratio of one indicates perfect agreement between model calculated and field observed concentrations.)

As shown, the bioaccumulation model provides a good description of PCB homolog concentrations in zooplankton (Figure 11-1 top). With the exception of di-CB, very good agreement between model calculated and field observed concentrations were also obtained for white perch (Figure 11-1 middle). As shown in the detailed comparisons in Appendix 12a, the model does very well in describing PCB accumulation in white perch across all seven age classes of white perch. The model results for all PCB homologs however consistently fall slightly below the field observations for PCB accumulations for the three year olds. This slight underprediction is most likely be due to a slight difference in the assigned growth or respiration rates (see Section 9) and the actual growth or respiration rates for the three year old white perch.

For striped bass, base case model calculations were performed for the following migration pattern: striped bass are assumed to remain in the mid-Hudson for their first two years; the 2-5 year old striped bass are considered to migrate from the mid-Hudson into the Harbor in June and spend the summer months in Long Island Sound and the New York Bight before returning to the mid-Hudson in the fall; the 6-17 year old striped bass are assumed to spend most of their year in the open ocean, but migrate into Long Island Sound and the New York Bight around March 15th and into the mid-Hudson around April 15th to spawn (see Section 9 for details). A summary of model-field observation comparisons for striped bass is given in Figure 11-1 bottom. As shown, base case model results overpredict concentrations in striped bass for the lower chlorinated homologs, but provide a very good description of chemical accumulation for the higher homologs (hexa through deca-CB). The overprediction of PCB accumulations in the lower chlorinated homologs may be associated with the assignment of striped bass migration, particularly into and out of areas with higher concentrations of lower chlorinated homologs (e.g., the mid Hudson).

As a sensitivity calculation, the white perch-striped bass bioaccumulation model was also run with a redefined striped bass migration pattern. For this case, striped bass are again assumed to remain in the mid-Hudson for their first two years; migration from the mid-Hudson to the Harbor in June and to Long Island Sound and the New York Bight for the summer is assigned only to the 2 and 3 year old striped bass; and the 4 year olds and 5 year olds (along with the older striped bass) are assumed to spend most of their year in the open ocean, and migrate into the estuary in the spring. Detailed comparisons of PCB model results and field observations for this sensitivity case are given in Appendix 12b. Since only the striped bass migration pattern was changed, zooplankton and white perch results are the same as the base case. Overall, striped bass model results for the redefined migration pattern are slightly lower and tend to underpredict field observations for the higher chlorinated homologs (Figure 11-2

bottom). This sensitivity calculation however does demonstrate the effect of migration on PCB accumulation in striped bass. Based on these results, several migration patterns should probably be considered in the future to help describe not just the average but also the expected distribution of PCBs in the migratory striped bass.

Lastly, a sensitivity calculation for the white perch-striped bass bioaccumulation model was performed with a refined description of the chemical assimilation efficiency (α) and egestion rate coefficient (k_e) for small fish, white perch and striped bass. For this case, the base case was used in describing striped bass migration and the chemical assimilation efficiency for all fish was specified as a function of K_{ow} following the relationship given in Kelly et al. (2004).

$$\alpha = \frac{1}{5.3 \cdot 10^{-8} \cdot K_{ow} + 2.3} \tag{11-1}$$

This relationship provides a decrease in the chemical assimilation efficiency for the higher K_{ow} compounds and is consistent with previous observations that have been reported in the literature (e.g., Gobas et al., 1988). A similar relationship was used to describe reductions in the egestion rate coefficient for higher K_{ow} homologs and is given as:

$$k_e = \frac{1}{4.6 \cdot 10^{-6} \cdot K_{ow} + 200} \tag{11-2}$$

Detailed comparisons of PCB model results and field observations for this sensitivity case are again presented for zooplankton and the individual age classes of white perch and striped bass in Appendix 12c. A summary of these comparisons are given in Figure 11-3 for the 10 PCB homologs. Since only the chemical assimilation efficiency for fish was changed, zooplankton results (Figure 11-3 top) are the same as the base case. Comparisons of model results and field observations for white perch (Figure 11-3 middle) and striped bass (Figure 11-3 bottom) are also the same for the lower chlorinated homologs. For the higher chlorinated homologs, model predictions for chemical accumulations in white perch are slightly lower than the base case. For striped bass, reductions in model predictions for the higher chlorinated homologs are more apparent. Although a decrease in chemical accumulations of higher chlorinated homologs is expected due to the reduction in chemical assimilation efficiency (as described by Eq. 11-1), the results were smaller than expected. This is because corresponding reductions in the egestion rate coefficient (Eq. 11-2) slowed the overall loss of chemical from the fish.

11.2 BIOACCUMULATION OF DIOXIN/FURANS IN FISH

The fully time-variable, age-dependent bioaccumulation model was also used to examine the bioaccumulation of dioxin/furan congeners in the white perch-striped bass food chain. Model

calculations were performed using model parameters described in Section 9. For the base case, the gill transfer efficiency was again specified as a constant value of 0.6 for all species. The chemical assimilation efficiency was set equal to the food assimilation efficiency of 0.3 for zooplankton. For small fish, white perch and striped bass, the chemical assimilation efficiency was specified as 0.435 based on information in Kelly et al. (2004) for mid-range K_{ow} compounds.

Detailed comparisons of lipid-normalized model results and field observations for the base case are presented for zooplankton and the individual age classes of white perch and striped bass in Appendix 12d. A summary of these comparisons is given in Figure 11-4 as ratios of model calculated and field observed concentrations for the 17 dioxin/furan congeners. As shown, the bioaccumulation model provides a good description of dioxin and furan concentrations in zooplankton (Figure 11-4 top). Model results for congeners with the highest K_{ow} values however tend to fall slightly below the observed concentrations. Model results for white perch and striped bass however typically overpredict observed dioxin and furan concentrations by factors of ten to a thousand (Figure 11-4 middle,bottom).

One possible explanation for this large discrepancy in the calculated and observed concentrations in fish is metabolism. In this case, metabolism of dioxin and furan congeners may occur through enzymatic attack across the carbon-oxygen bonds on the dioxin and furan structures. Previous work by van der Linde et al. (2001) suggest that first-order rate coefficient for dioxin/furan metabolism in fish is in the range of 0.01 to 0.1/day. For this sensitivity study, a metabolic rate coefficient of 0.1/day was assigned for small fish, white perch and striped bass. Detailed comparisons of the lipid-normalized model results and field observations for this sensitivity calculation are presented in Appendix 12e, and a summary of the comparisons is given in Figure 11-5. As shown, the model results for white perch provide a better description of field observations, particularly for dioxin and furan congeners with log K_{ow}'s of approximately 7. Model results however show an increasing overprediction of field observations for the higher K_{ow} congeners.

A subsequent sensitivity run was performed by considering both dioxin/furan metabolic rate coefficient of 0.1/day and the refined description of the chemical assimilation efficiency (α) and the egestion rate coefficient (k_e) for small fish, white perch and striped bass previously presented in Eq 11-1 and Eq 11-2, respectively. A summary of the comparisons is given in Figure 11-6 and more detailed comparisons are given in Appendix 12f. As shown, model results provide a good description of observed concentrations in white perch over the whole range of dioxin and furan congeners. As opposed to previous results for PCBs, the inclusion of a decreasing chemical assimilation efficiency and egestion rate coefficient for the higher K_{ow} compounds had a large effect on the accumulation of dioxins and furans in white perch. This is because decreasing chemical assimilation efficiencies for the higher

K_{ow} congeners had a large effect in reducing the rate of dietary uptake, but the decrease in the egestion rate coefficient did not significantly affect the overall loss rate which is largely due to metabolism.

Lastly, the metabolic rate coefficient for striped bass was reduced to a value of 0.01/day to provide a better match of model results and field observations. A possible justification for this reduction in the metabolic rate coefficient for striped bass may be related to slow rates of respiration (on a gram respired per gram wet weight of organism per day) for the larger fish. Detailed comparisons for this sensitivity run is presented in Appendix 12g and a summary of the comparisons is given in Figure 11-7. These results provide a good description of observed concentrations and provide further evidence that metabolism of dioxin and furan congeners may be occurring in fish.

11.3 BIOACCUMULATION OF CADMIUM AND MERCURY IN FISH

The fully time-variable, age-dependent bioaccumulation model was also used to examine the bioaccumulation of cadmium and mercury in the white perch-striped bass food chain. Model calculations were performed using model parameters described in Section 9 along with specified values for the gill transfer efficiency (β) and the dietary chemical assimilation efficiency (α). For the base case, the gill transfer efficiency was again specified as a constant value of 0.6. The chemical assimilation efficiency for cadmium and non-methylated mercury was set equal to zero based on the assumption that inorganic metal is strongly bound to ligands (e.g., metallothionen) in the food. For methylmercury, the chemical assimilation efficiency was set equal to the food assimilation efficiency of 0.3 for zooplankton and 0.8 for small fish, white perch and striped bass. Finally, since cadmium, non-methylated mercury and methylmercury are all considered to be strongly bound within the organism, back-diffusion across the gill was set equal to zero.

Detailed comparisons of wet-weight metal concentrations for model results and field observations are presented for zooplankton and the individual age classes of white perch and striped bass in Appendix 12h. A summary of these comparisons is given in Figure 11-8 as ratios of model calculated and field observed concentrations for cadmium, total mercury and methylmercury. As shown, the bioaccumulation model severely underpredicts observed concentrations of cadmium in zooplankton, but provides a good description for observed cadmium concentrations in white perch and in striped bass standard fillets. (The bioaccumulation model is set up to describe Cd concentrations in whole fish and not the higher concentrations that accumulate in fish livers.) These results strongly suggest that the primary exposure pathway for cadmium is through the gill and not through dietary exposure. The underprediction of cadmium in zooplankton, which may in part be explained by binding of cadmium to zooplankton shells, is therefore not expected to have a significant effect on accumulations in fish.

For mercury, the bioaccumulation model provides a good description of observed concentrations of total mercury for zooplankton, white perch and striped bass. Based on model results, approximately half of the total mercury in zooplankton and more than 90 percent of the total mercury in fish is expected to be methylmercury. This is consistent with previous reports in the literature. For zooplankton analyzed as part of the CARP dataset, methylmercury typically accounted for only 10-20 percent of the total mercury concentrations, and may require re-evaluation. Based on these results, the CARP mercury model is shown to provide a good description of how mercury is methylated in harbor sediments and how methylmercury is transferred to fish through dietary exposure.

11.4 BIOACCUMULATION OF PCBs IN HARBOR WORMS

Field-derived BSAFs for PCBs were previously presented for worms at various sites in the Harbor (see Section 10). A summary of the field-derived BSAFs are given in Figure 11-9 and show: (1) variation in BSAFs as a function of K_{ow}, and (2) significant differences in BSAFs for inner and outer Harbor sites. To evaluate possible reasons for this behavior, a steady-state bioaccumulation model was used to calculate BSAFs for Harbor worms at two representative sites: Newark Bay (inner Harbor) and Sandy Hook (outer Harbor) performed using Eq. 8-5 and bioenergetic parameters from the literature (Table 9-1).

For model calculations, partitioning of PCB homologs to sediment organic carbon was approximated as:

$$K_{oc}^{app} \approx K_{ow} + f_{BC} \cdot 10^{7.5} \qquad (11\text{-}3)$$

to simulate the overall effects of PCB binding to natural organic matter and black carbon in sediments. In this relationship, f_{BC} was taken as 0.06 which is equivalent to 6% of the sediment organic carbon being comprised of black carbon or soot. The respiratory exchange rate coefficient (β) was set equal to 0.6. Finally, the dietary assimilation efficiency (α) was specified as a function of K_{ow} following a relationship similar to Kelly et al. (2004) and given as:

$$\alpha = \frac{2.3 \cdot \alpha_o}{5.3 \cdot 10^{-8} \cdot K_{ow} + 2.3} \qquad (11\text{-}4)$$

where α_o represents the maximum dietary chemical efficiency (which in effect corresponds to the dietary chemical assimilation efficiency for low to mid-range K_{ow} compounds). The value of α_o was used as a calibration parameters in fitting field-derived BSAFs.

An initial model calibration was performed for worms collected at the Newark Bay site using an α_o value of 0.025 (Figure 11-10a). As shown, the model provides a very good description of the observed variation in BSAFs for PCB homologs. For comparison, model calculations were also performed using a constant α value of 0.025 over the entire K_{ow} range and assuming that no soot is present in sediment (i.e., $K_{oc} \approx K_{ow}$) (see dashed line in Figure 11-10 top left). Differences in these results and the calibrated model show that: (1) black carbon primarily influences the BSAF for the lower K_{ow} homologs, and (2) the drop in the dietary assimilation efficiency (α) has a dominant effect at higher K_{ow} values. Finally, calculations with no dietary uptake (dotted line in Figure 11-10 top left) were compared to the calibrated model. Differences in the two responses clearly demonstrate the importance of dietary uptake in controlling BSAFs for PCB homologs with log K_{ow}'s > 5.8.

Based on calibrated results for the Newark Bay worms (Figure 11-10 top left), three sensitivity analyses were performed to examine possible causes for the large discrepancies in BSAFs for the inner Harbor and outer Harbor sites. For the first analysis, differences in the dietary chemical assimilation efficiency (α) from the Newark Bay (inner Harbor) and Sandy Hook (outer Harbor) sites were considered. For this evaluation, the α_o value was increased from 0.025 to 0.13 to describe observed BSAFs at Sandy Hook (Figure 11-10 bottom left). This result would suggest that sediment at Sandy Hook and the other outer harbor sites provide a higher quality food supply to the worms (e.g., either by being more enriched in readily digestable lipids or less contaminated by black carbon) than sediment at the inner Harbor sites.

As a second sensitivity analysis, differences in respiration and growth rates at the two sites were considered. Based on this evaluation, a factor of 6.5 increase in the respiration rate (Figure 11-10 top right), or a factor of 6.5 decrease in the growth rate (not shown), or some combination of the two could account for differences in observed BSAFs at the Newark Bay and Sandy Hook sites. A possible increase in respiration rates at Sandy Hook could be indicative of a less stressed environment (e.g., with a higher quality food supply or reduced chronic toxicological effects). As an alternative explanation, slower growth rates at the outer Harbor sites may be indicative of a more stable and well-established worm population.

Finally, the presence of predatory worms at the outer Harbor sites was considered as another possible explanation of BSAF differences between inner and outer Harbor sites. For this scenario, model calculations were performed by considering that worms at Sandy Hook were feeding on other worms at the site. This places the predatory worms at a higher trophic level, where biomagnification of PCBs would be more pronounced. As shown in Figure 11-10 bottom right, model results for predatory worms at Sandy Hook also provide a reasonable description of differences in BSAFs for the inner and outer Harbor.

Based on these sensitivity studies, it is not possible to ascribe the differences in BSAFs at the inner and outer Harbor sites to differences in the quality of the food supply, in the bioenergetics of the worms, in the presence of predatory worms at the outer Harbor sites, or some combination of the three. An additional datasets was therefore examined to try to better understand the factors affecting observed geographic differences in BSAFs.

11.5 ADDITIONAL BSAF EVALUATIONS

A previous study of PCB bioaccumulation was conducted by Meador et al. (1997). In this study, sediment was collected from various locations in NY-NJ Harbor and used in ten-day, laboratory bioaccumulation tests using two infaunal invertebrates: *Rhepoxynius abronius* (a non-deposit feeding amphipod which was assumed not to feed during the test) and *Armandia brevis* (a non-selective, deposit-feeding polychaete that ingested sediment). *Armandia* results from this work are consistent with the CARP worm data, showing the same effect of K_{ow} on BSAFs (see Figure 11-11 top). Comparison of the *Armandia* results and results for *Rhepoxynius*, the non-feeding amphipod, were also used to demonstrate the importance of dietary exposure in determining BSAF values for the higher chlorinated PCB homologs.

For our studies, a further analysis of the *Armandia* dataset was performed to examine the possibility of geographic differences in observed BSAFs. As shown in Figure 11-11 top, there is a trend of decreasing BSAFs from the outer Harbor sites (Chapel Hill and The Narrows) and the inner Harbor sites (Shooters Island and Newark Bay). These results provide confirmation of the geographic differences in BSAFs that were observed in the CARP worm study. In addition, because the studies of Meador et al. (1997) were conducted under controlled laboratory conditions with a specific polychaete, these results show that possible geographic differences in worm populations or the presence of predatory worms can not be used as the sole explanation for differences in BSAFs at the inner and outer Harbor sites.

The analysis of Meador's dataset therefore leads us to conclude that differences in BSAFs for the inner and outer Harbor sites is in large part due to either differences in the quality of the food supply or changes in bioenergetics of the organisms resulting from chronic toxicological effects. Studies by Rice et al. (1995) provide evidence to support differences in bioenergetic behavior. In their work, the same sediment from NY-NJ Harbor was used in evaluating growth and mortality effects for *Armandia* in 20-day laboratory exposures. Results of their growth studies are presented in Figure 11-11 bottom and show a decrease in growth rate from the outer Harbor (Chapel Hill, Narrows) and inner Harbor (Shooters Island, Newark Bay). Although we would expect a decrease in growth rate to actually cause an increase and not a decrease in BSAFs for the inner Harbor sites, we view the decrease in growth as

an indicator of other changes (e.g., a decreased respiration rate and/or a poor quality food supply) that would be associated with a decrease in BSAFs.

At this time, we can not say with certainty what factor or factors are responsible for the observed differences in BSAFs for the inner and outer sites. Our concern is that if chronic toxicity is in fact playing an important role, then chronic toxicological effects may decrease and BSAFs for the inner Harbor sites may increase as contaminant levels in sediment are reduced over time. Further monitoring and complementary laboratory studies should therefore be considered to examine possible effects of sediment contaminant levels on bioaccumulation in worms and other benthic organisms.

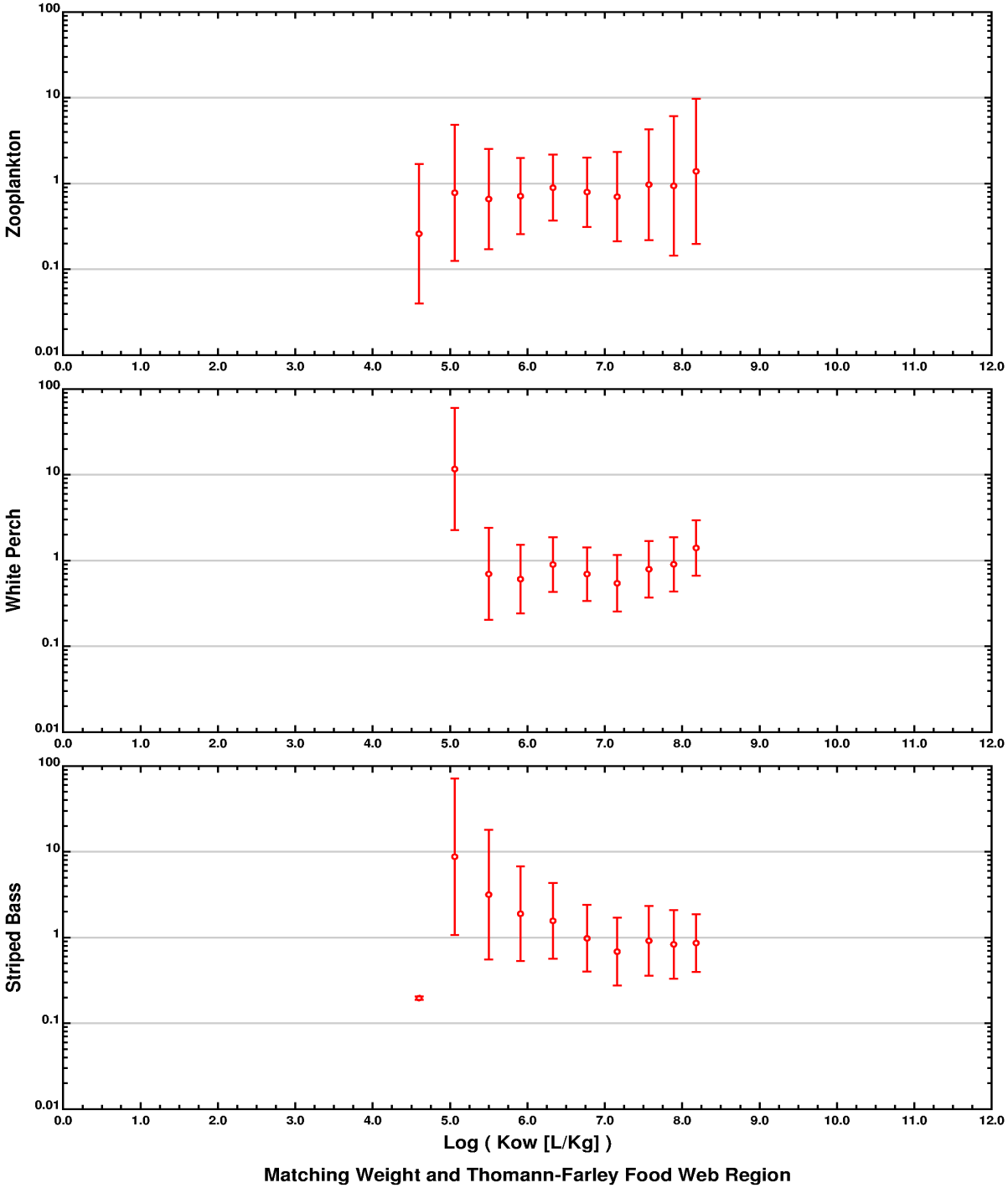

Figure 11-1. Summary comparison between field observed and model calculated PCB concentrations in organisms - base case

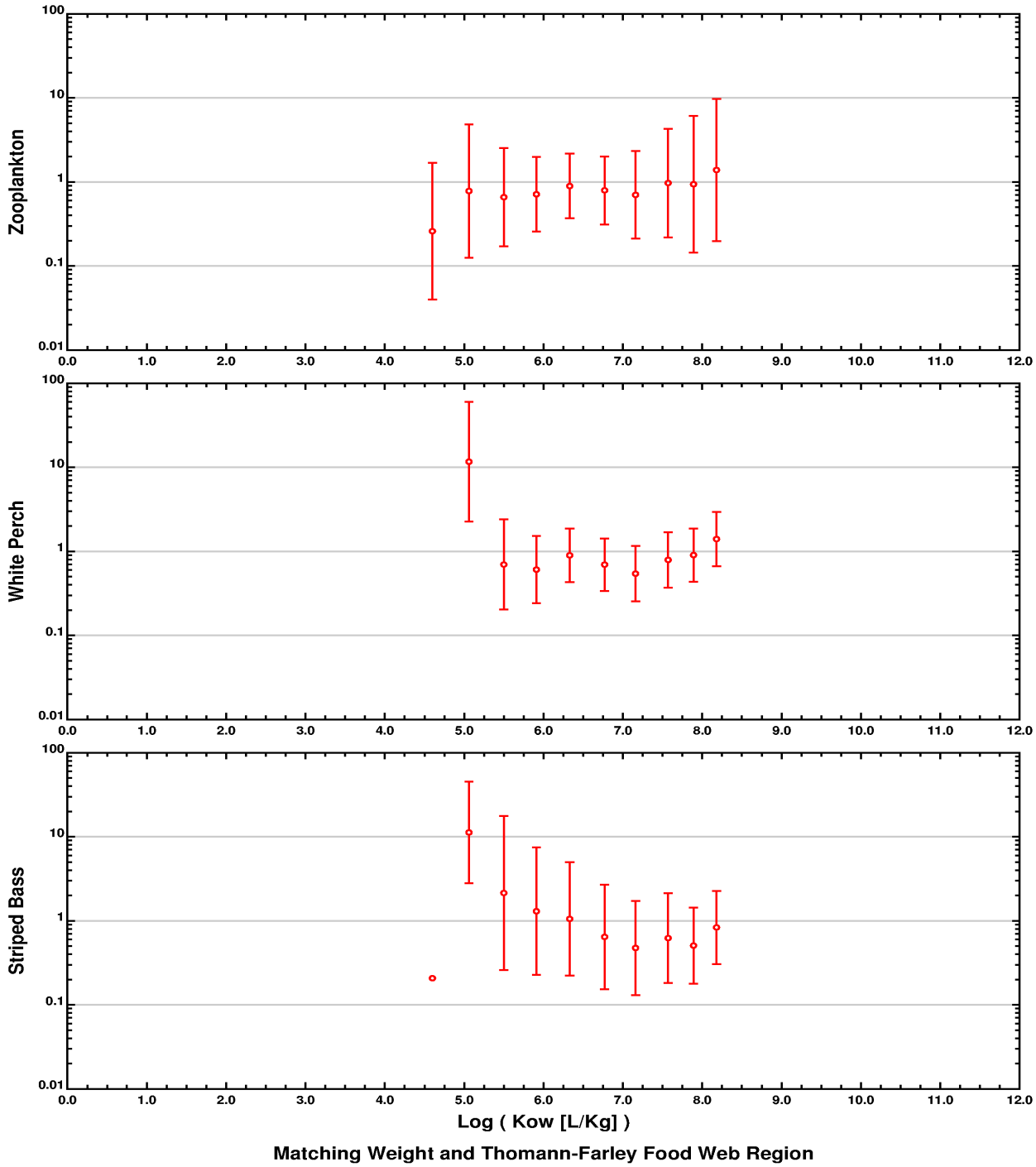

Figure 11-2. Summary comparison between field observed and model calculated PCB concentrations in organisms - sensitivity calculation for the alternate striped bass migration pattern

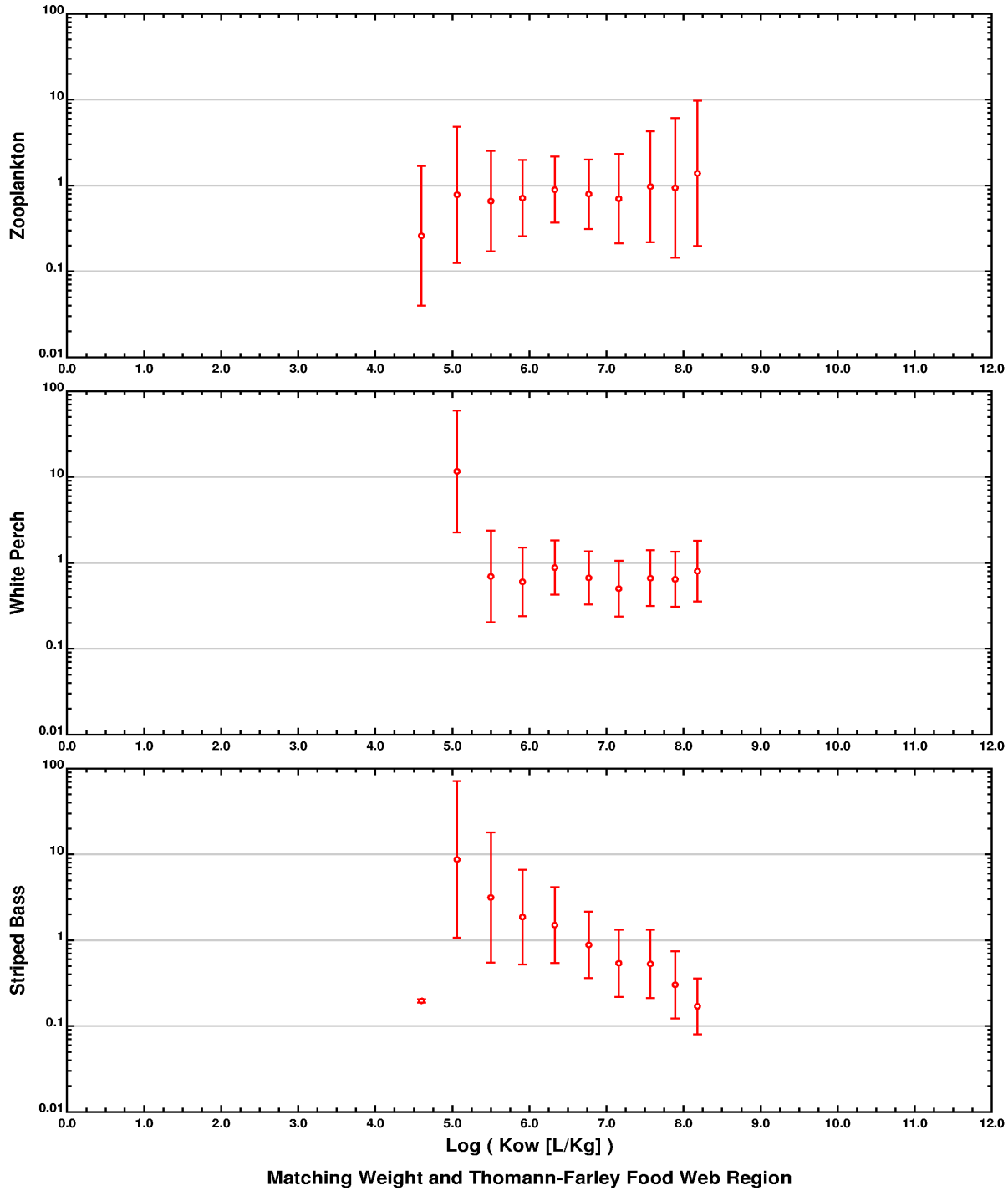

Figure 11-3. Summary comparison between field observed and model calculated PCB concentrations in organisms - sensitivity calculation for variations in chemical assimilation efficiency and egestion rate as a function of K_{ow}

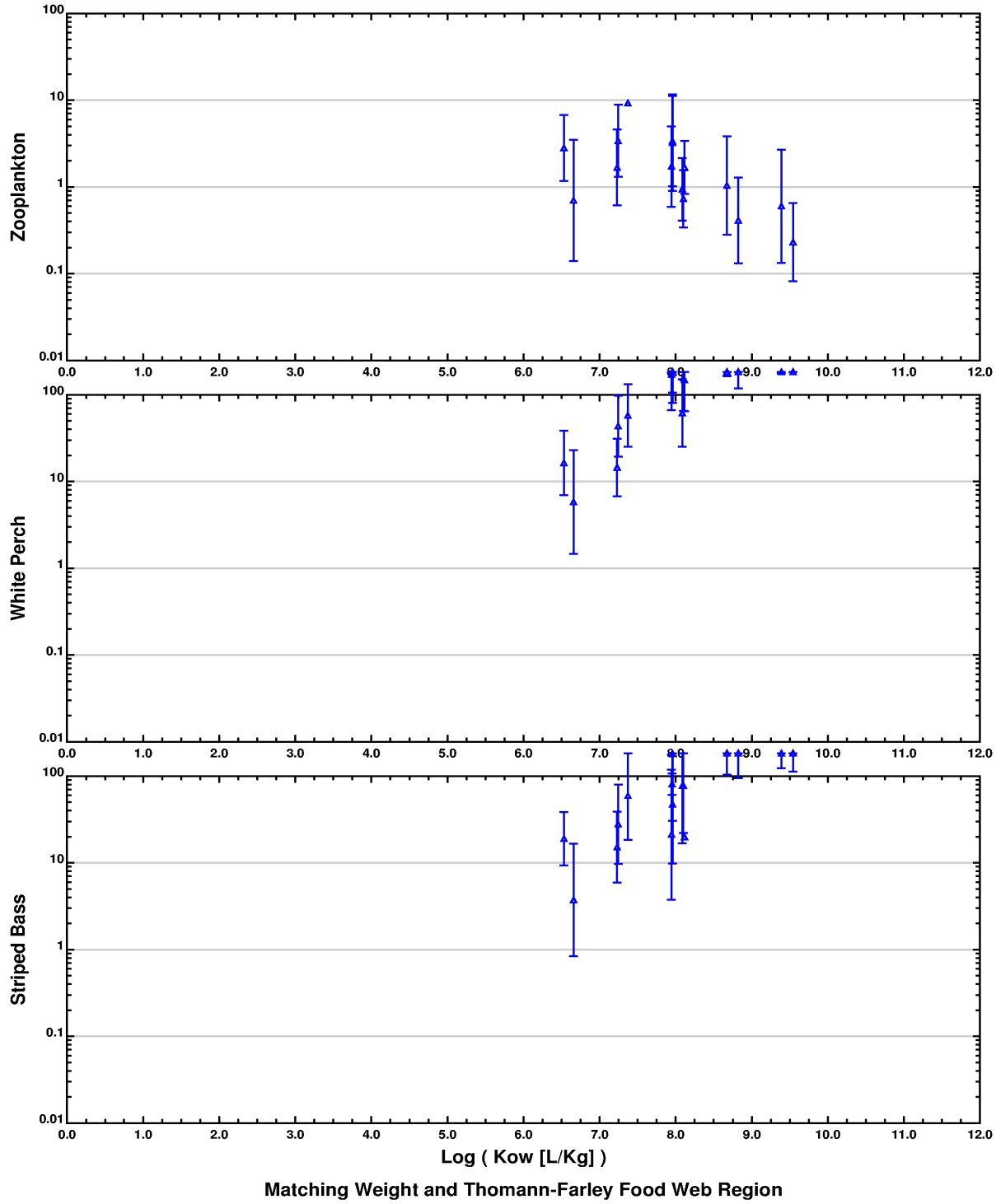

Figure 11-4. Summary Comparison between field observed and model calculated dioxin/furan concentrations in organisms - base case

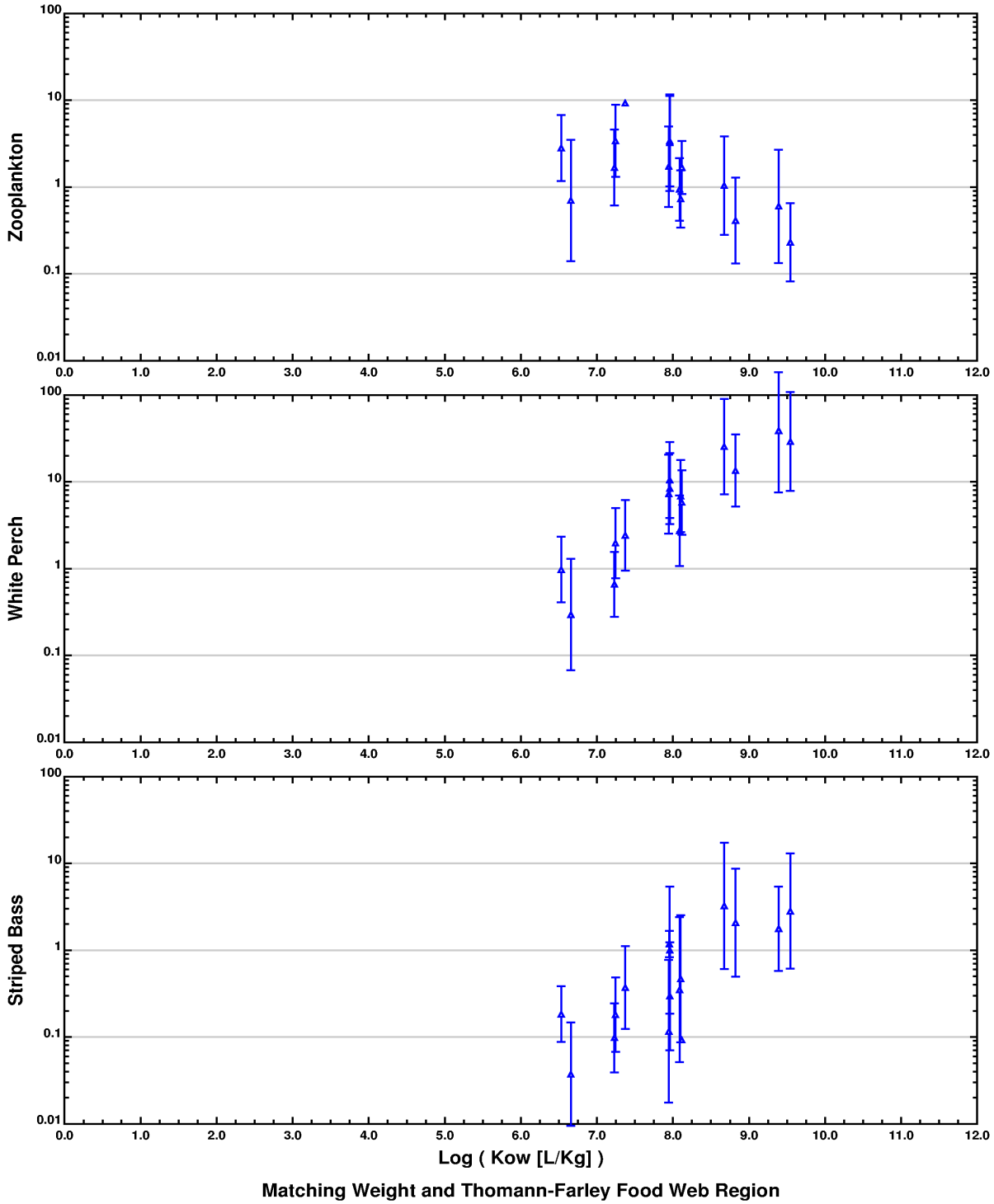

Figure 11-5. Summary comparison between field observed and model calculated dioxin/furan concentrations in organisms - sensitivity calculation for metabolism in fish

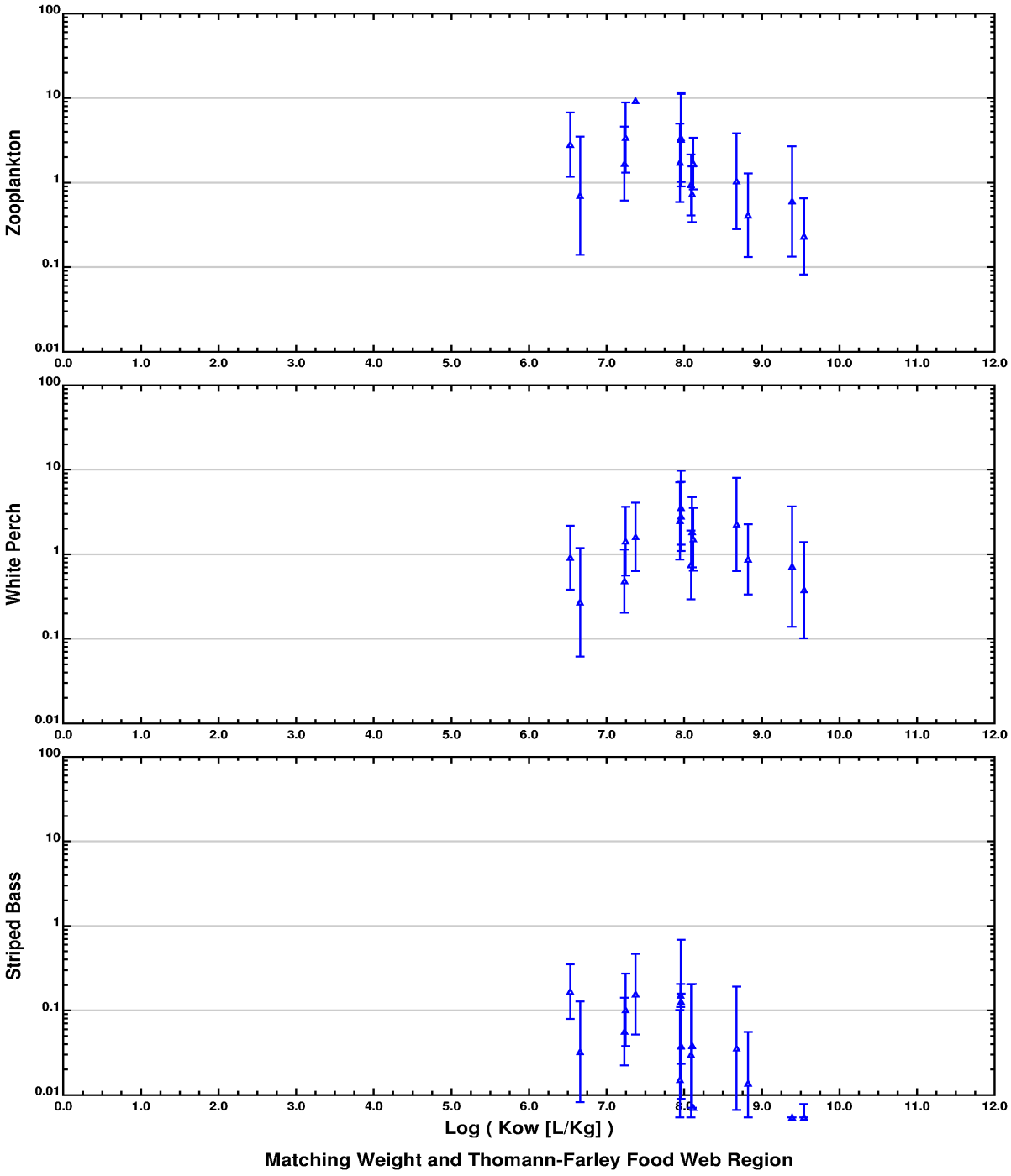

Figure 11-6. Summary comparison between field observed and model calculated dioxin/furan concentrations in organisms - sensitivity calculation for metabolism plus variations in chemical assimilation efficiency and egestion rate as a function of K_{ow}

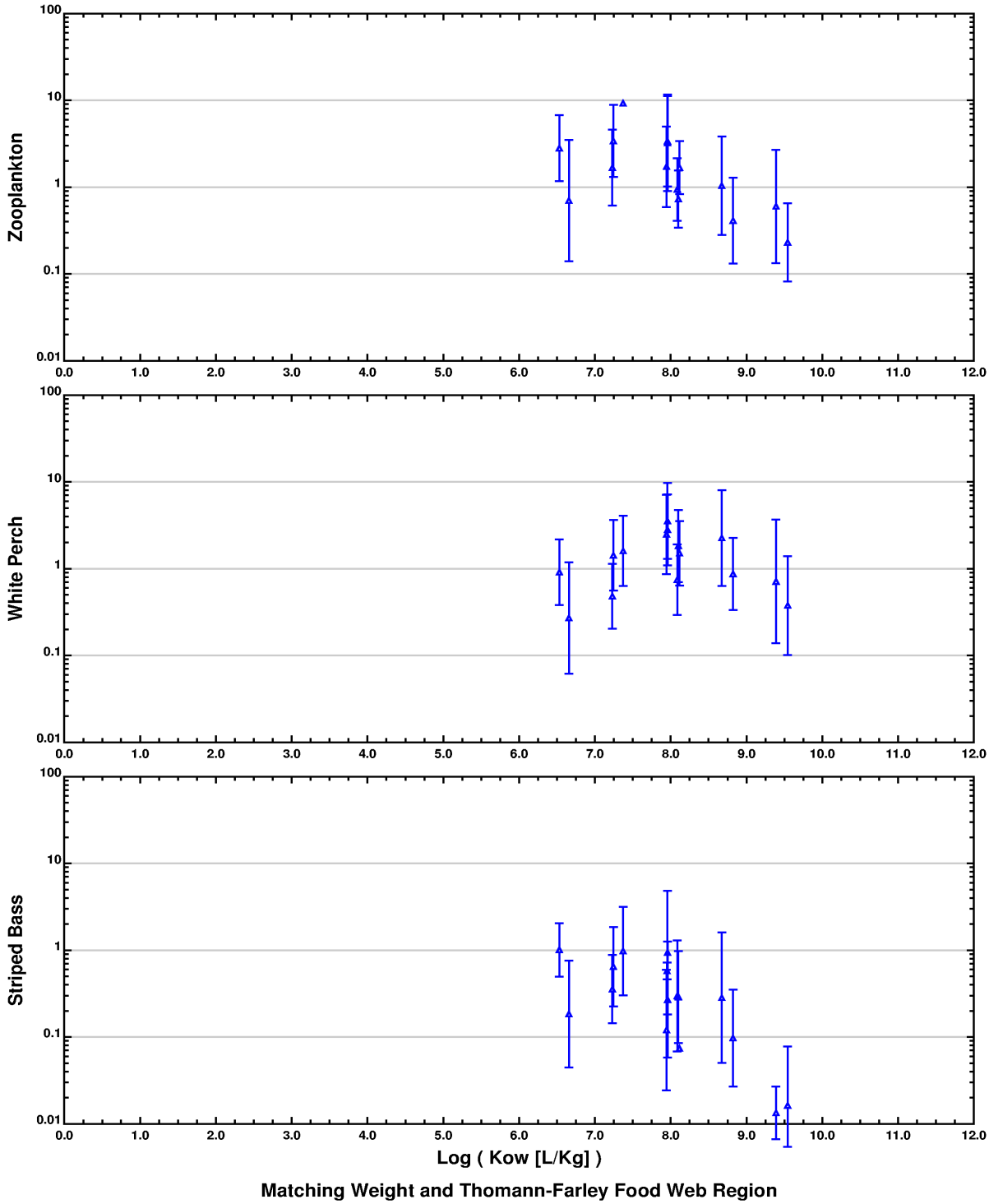

Figure 11-7. Summary comparison between field observed and model calculated dioxin/furan concentrations in organisms - sensitivity calculations for reduced metabolism rate for striped bass

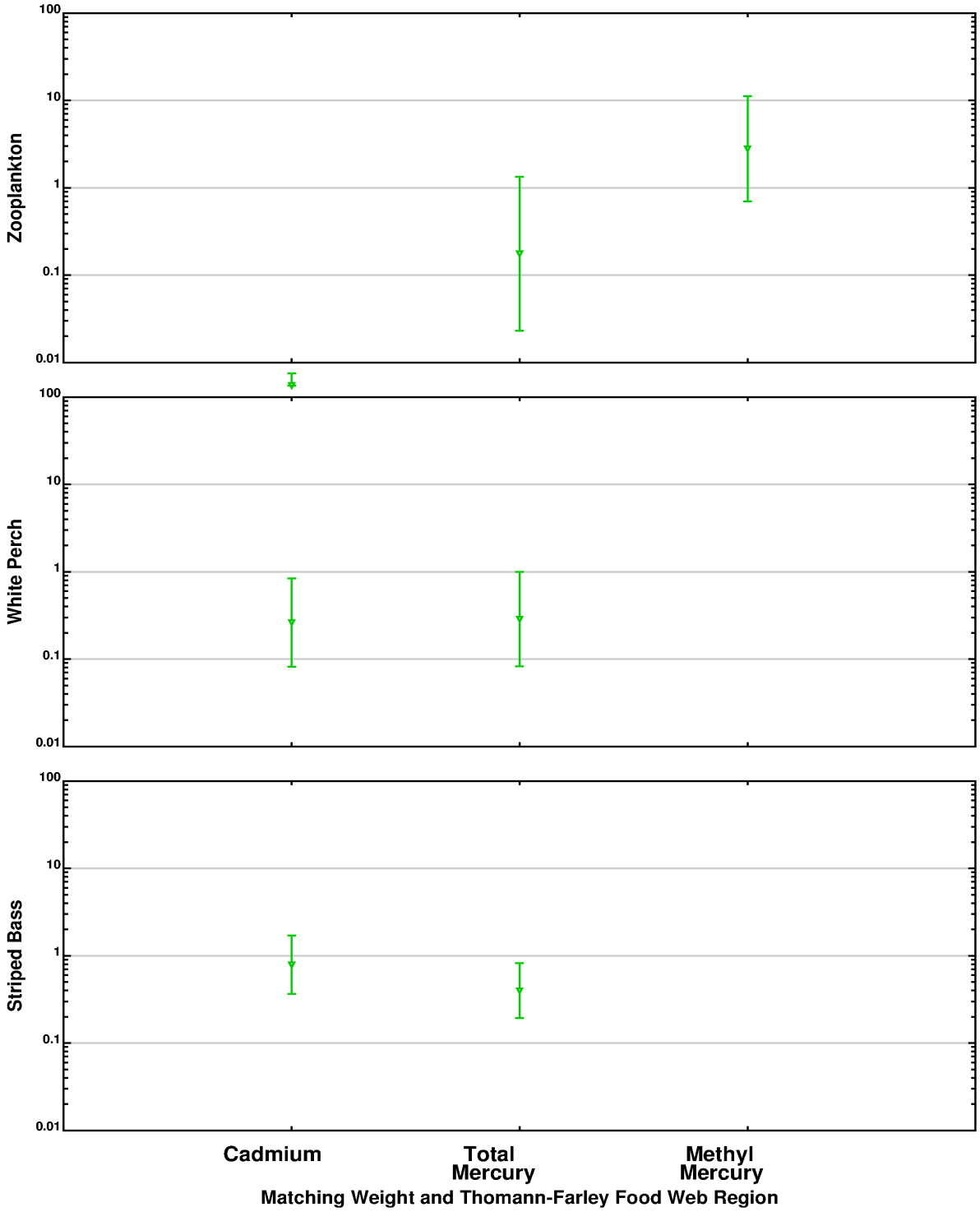

Figure 11-8. Summary comparison between field observed and model calculated metal concentrations in organisms

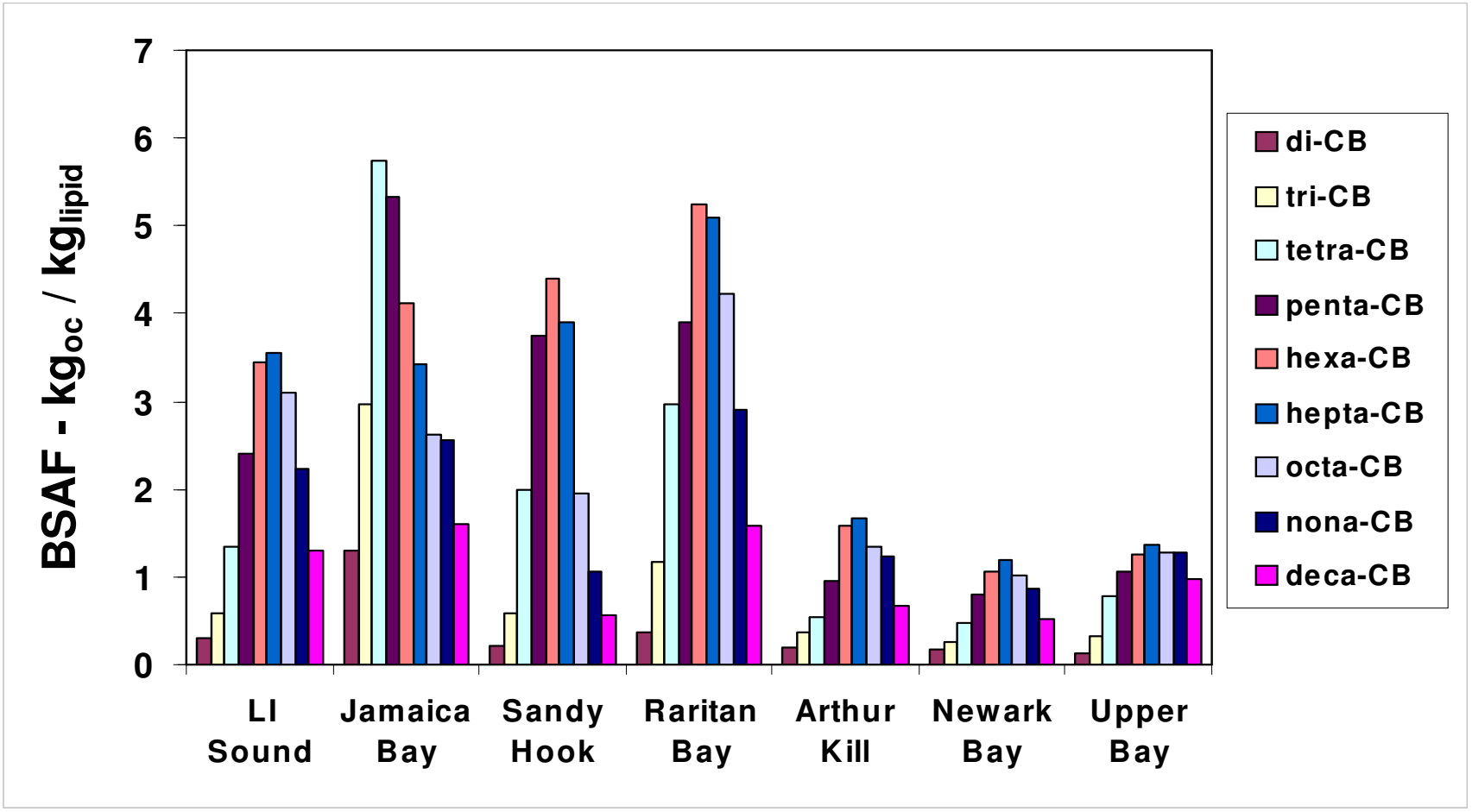

Figure11-9. Summary of field-derived BSAFs for PCBs in Harbor worms.

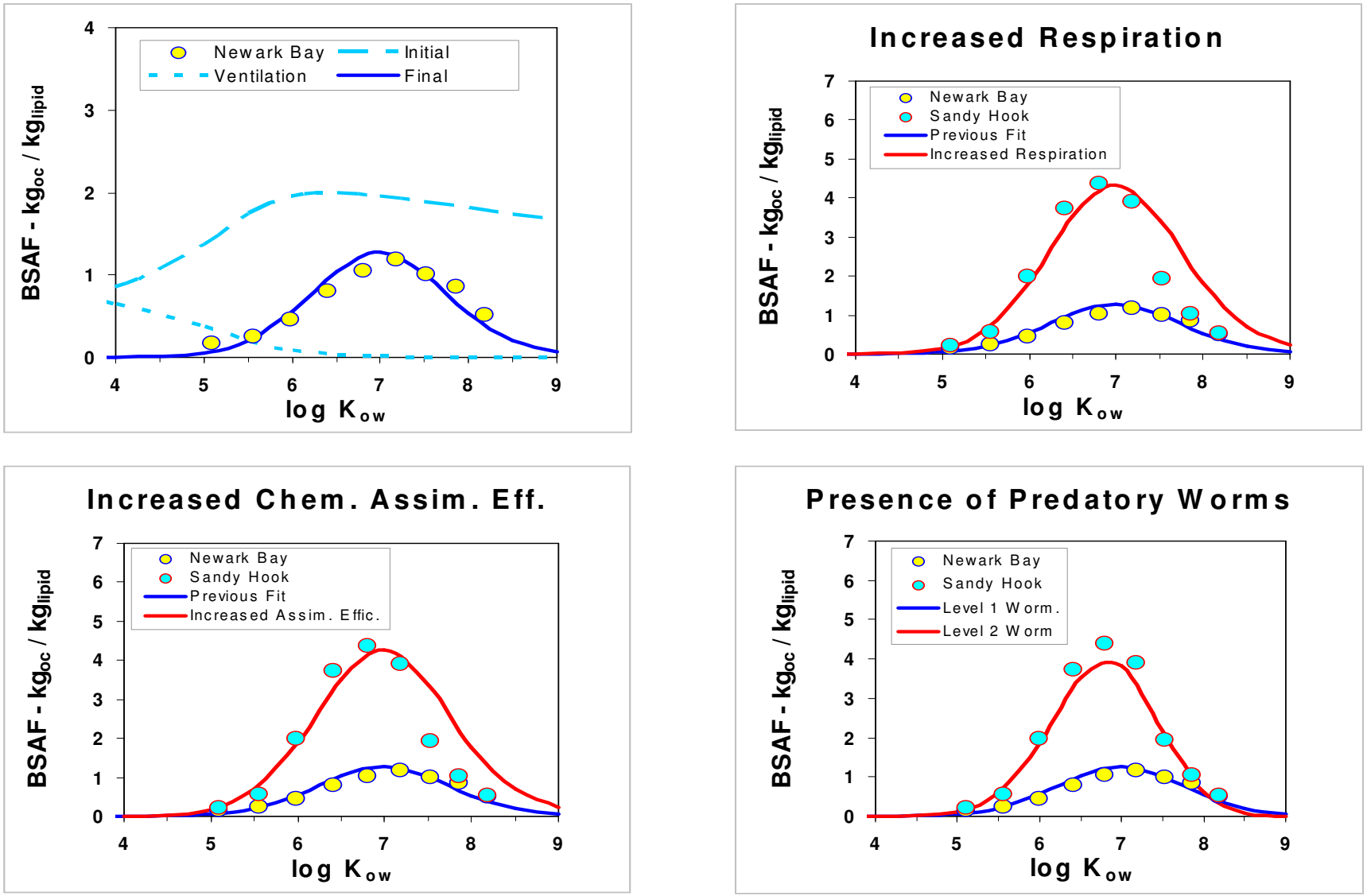

Figure11-10. Model baseline and sensitivity evaluations for PCB worm BSAFs.

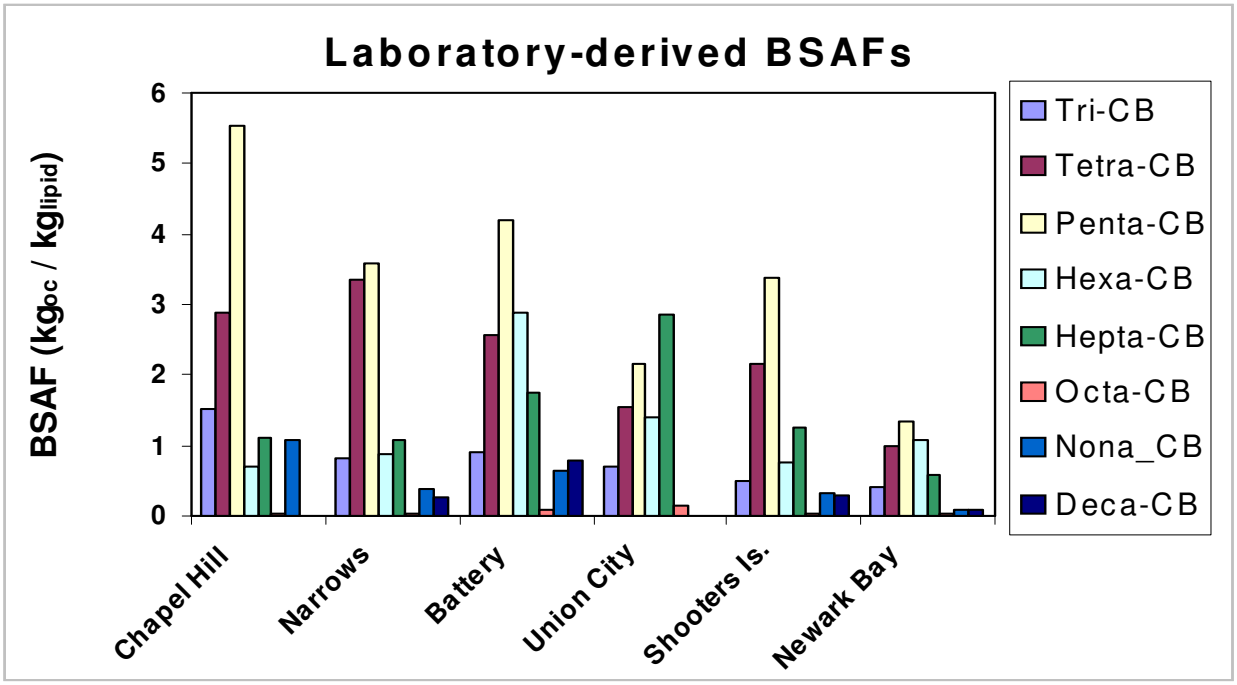

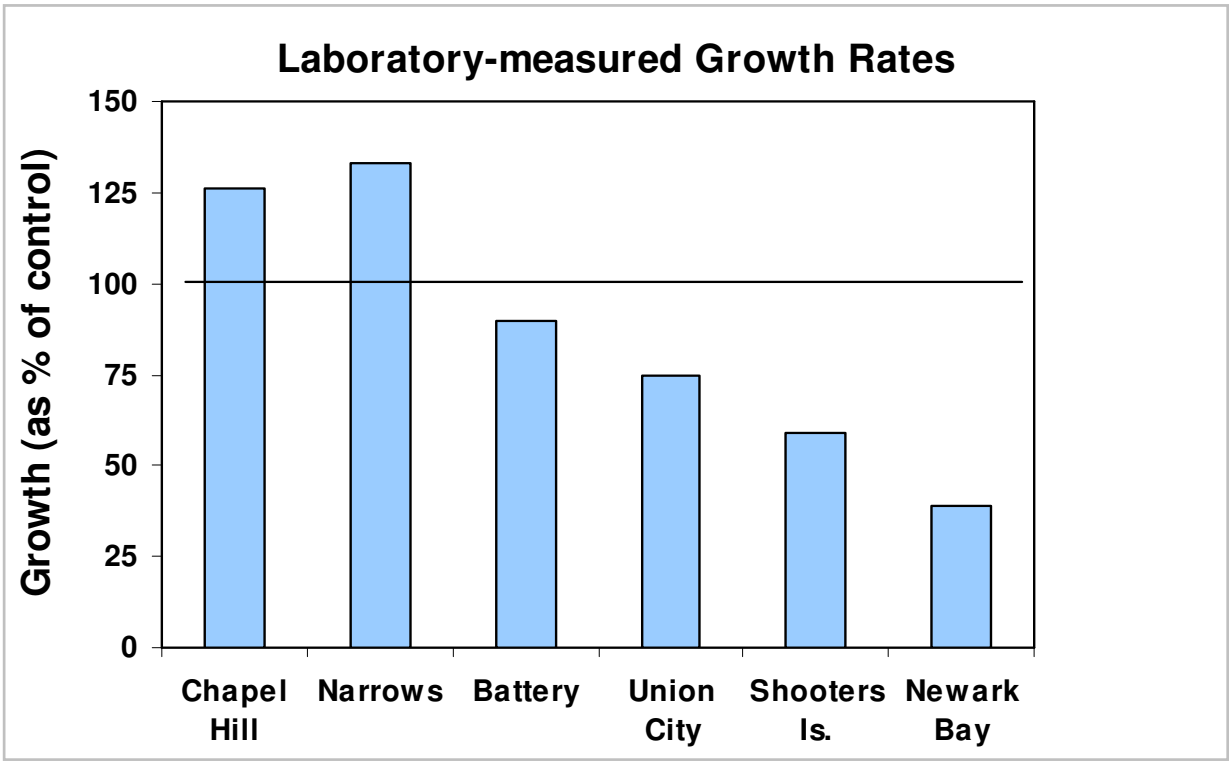

Figure 11-11. Laboratory derived BSAFs (top) and growth rates for Armandia. Based on bioaccumulation studies (Meador et al., 1997) and effects testing (Rice et al., 1995).

SECTION 12.0

LOADING COMPONENT SIMULATIONS

The calibrated CARP contaminant model has been applied to diagnose the causality of ambient contaminant concentrations in water, sediment, and biota. For this purpose, simulations with the CARP model have been performed to define the influence of known external, or baseline, contaminant loading source types on ambient contaminant concentrations. In addition, model simulations have also been performed with the calibrated CARP model to determine the influence of additional selected sources of contamination on ambient contaminant levels throughout the Harbor. The CARP loading source component simulations are described below. Results for the components are presented in Sections 12.1 and 12.2 in terms of the sediment bed and water column responses. The corresponding responses of pelagic and benthic biota to the various loading components were also calculated in the analysis by using water column and sediment bed component responses and field-derived BAFs and BSAFs. The responses of biota to the various loading components are included as part of the loading component response matrix presented in Section 12.3.

12.1 BASELINE COMPONENTS

The CARP model has been applied to evaluate several base loading components which span all current source categories for selected contaminants of concern. These base loading components are: atmospheric deposition, ocean boundary, STPs, CSOs, runoff, head of tide inputs, and in-place sediments (i.e., sediment initial conditions).

Preliminary baseline contaminant loading component simulations were performed by HydroQual in two ways to test the linearity of the model responses. The first loading component approach, the "zeroing out" approach, investigated by HydroQual consisted of shutting off the contaminant loadings related to a specific component (e.g., STP), running the model for multiple years and calculating the component response over time. The component responses were calculated by subtracting the calculated ambient contaminant concentrations when a loading component had been removed from those calculated when all loadings were active. This process was repeated for each of the loading components.

The second loading component approach, the "turn-on" approach, consisted of running the calibrated model with only the contaminant loads from a specific loading component active. Each "turn on" loading component was run for mutiple years and the component response over time was calculated. Ambient concentrations calculated in "turn-on" components for individual loading

components were summed. Results of the "turn-on" contaminant loading components are further described below.

Both loading component approaches produced the same results for HOCs and nearly identical results for metals. These findings confirm that the contaminant processes in the HOC fate model are based on linear equations and that contaminant processes in the metals fate model are all relatively linear for the modeling conditions. The CARP loading component analysis is different than loading component analyses performed previously for nutrients in the region using LIS3.0 and SWEM where the "zeroing out" approach had to be used for nutrients because of nonlinear changes in biological responses associated with nutrient limitations. If the "turn-on" approach were used for nutrients, each nutrient loading component simulation would likely result in an unrealistic ambient nutrient-stressed condition. The "zeroing out" approach maintained simulated nutrient levels that were more realistic. The point is specifically made here for those readers familiar with loading component response analyses performed previously in the region for EPA and other entities for TMDL related evaluations.

The CARP loading component evaluation is also different than the SWEM and LIS3.0 analyses because of the slow response times for HOC and metal contamination in Harbor sediments. For the CARP loading component analysis, ambient contaminant concentrations change over a longer time period. It is therefore not possible to present the CARP loading component results as single "equilibrium" concentration responses as was possible for nutrients/dissolved oxygen. Rather, the CARP loading component analysis is used to evaluate the contribution of continuing current loads and initial conditions (as represented by 1998 in-place contamination in sediment) on future contaminant levels on a time series basis. It is important to note that the CARP component analysis is not an appropriate tool to identify the origins or sources of 1998 in-place contamination. Rather, the CARP component analysis is used to estimate the future response of contaminants to continuing loads and the 1998 in-place contamination in the Harbor. For this purpose, we gaged long term responses of the system to current loadings by carrying out the loading component simulations for 32 years.

Results of the baseline loading components, simulated using the "turn-on" approach, are described below in Sections 12.1.1 to 12.1.5. For each of the eight contaminants (i.e., 4 PCB homologs, 2,3,7,8-TCDD, 2,3,4,7,8-PCDF, mercury, and cadmium) considered in the loading component analysis, component results are presented at twelve selected locations as time series responses. The time series for each contaminant are presented in a two page format which highlights locations in both the western and eastern portions of the NY/NJ Harbor estuary (see Appendix 13A and 13C). As an example of time series component results, the 2,3,7,8-TCDD loading component analysis at milepoint 6.4 in the Passaic River is shown in a summary format for both the water column and sediment bed on Figure 12-1. Results shown in Figure 12-1 demonstrate that the initial conditions, as represented by 1998 in-place

contaminant levels in sediments, are attenuated over the course of a model simulation. Further, the current-day, continuing loadings cause a build-up to steady-state ambient concentrations.

In the component analysis, the first four years of simulation are considered a spin-up period to allow for correction of any inaccuracies in the specification of sediment initial conditions (through redistibution of sediments) which were based on the interpolation of relatively sparse data Years five through eight correspond to the 1998-2002 CARP data collection and model calibration period. Years between 9 and 32, are considered to be a preliminary projection of future conditions without management actions. It is noted that over the thirty-two year component simulation period for which the CARP contaminant fate and transport model was run, the same four years of hydrodynamic and sediment transport conditions (i.e., October 1998 through September 2002) were cycled eight times. A somewhat different approach will be taken for projection of future conditions in the 2040 projection scenarios described in Section 13.

Final component responses were calculated on the basis of the last four years of the component simulation runs, years 29 to 32, which represent conditions including a long-term exposure for each loading source component and a reworking of the specified initial conditions. Final component response results are also shown graphically along spatial transects which cover major sections of the Harbor (Appendix 13B and 13D). All of the graphical displays of the component responses, both temporal and spatial, are provided for both the water column and sediment bed. These results are contained in Appendix 13 and are described below more fully on a contaminant specific basis.

It is noted that while we attempt to describe some of the major features of the loading component results below, the component results can inform a wide variety of management objectives within the region. It is not possible to anticipate all of the potential management applications for the component results here. The application of the component results is further addressed in Section 12.3.

12.1.1 Component Results for Four Selected PCB Homologs

Water column and sediment component results were generated for four selected PCB homologs. An example of the sediment component results for six selected locations in the Harbor core is shown in Figure 12-2 for the tetra-CB homolog. A complete presentation of the component results for the four selected PCB homologs are given in Appendix 13. Review of the figures in Appendix 13 demonstrates:

- In both the water column and sediments in western and eastern portions of the NY/NJ Harbor estuary, head of tide loadings are a dominant source for di-CB. Head of tide loadings are less

important for tetra-CB, hexa-CB, and octa-CB. In the case of the upper Hudson River PCB source, this observation is consistent with the upstream source signature which is more heavily weighted toward lower chlorinated homologs.

- For hexa-CB and octa-CB, runoff and STPs appear to be important sources.
- The role of legacy sources represented by sediment initial conditions becomes more apparent for the higher chlorinated homologs. This is consistent with the fact that higher chlorinated compounds are more strongly associated with particles and therefore have greater residence time in the system due to estuarine trapping, decreased volatilization and smaller effects of other diffusive exchange processes.

It is noted that the four selected homologs for which component analyses were performed, when summed, represent about 50% of the total PCB concentration. Diagrams displaying the PCB components results are shown in Appendix 13 for each of the four homologs considered and as the summation of the four homologs.

12.1.2 Component Results for 2,3,7,8-TCDD

The results for the 2,3,7,8-TCDD component simulations are found in Appendix 13 and are presented in both temporal and spatial graphical formats. A subset of these results are shown here as Figure 12-3. As shown, legacy sources of contamination represented by sediment initial conditions have a greater effect than current day sources (i.e., the legacy source components dominate the scales of the graphical displays). The contributions of the current day sources to ambient 2,3,7,8-TCDD concentrations are due mainly to stormwater runoff and, at certain locations, head-of-tide loadings.

12.1.3 Component Results for a Selected Furan Congener

Similar to 2,3,7,8-TCDD, the results for the 2,3,4,7,8-TCDF component simulations are found in Appendix 13 and are presented in both temporal and spatial graphical formats. Legacy sources of contamination reflected in sediment initial conditions are larger than current day sources and dominate the y-axis scales. The contributions of the current day sources to ambient 2,3,4,7,8-TCDF concentrations are due mainly to stormwater runoff and, at certain locations, head-of-tide loadings.

12.1.4 Component Results for Mercury

Component results for mercury and methyl mercury in both the water column and the sediment bed are presented in Appendix 13. The diagrams in Appendix 13 illustrate that like many of the other contaminants, mercury and methylmercury concentrations in sediments and the water column are

mostly attributable to legacy contamination represented by the assigned sediment initial conditions. Of the current loadings, stormwater runoff and tributary head of tide have the largest impacts on sediment concentrations. CSO's also play a role at certain locations. It is likely that the relatively large contributions from stormwater runoff and head of tide are associated with atmospheric deposition occuring in the watershed and over land upstream of tributary headwaters. In contrast, direct atmospheric deposition over the open water surface does not have as significant of an impact on ambient contaminant concentrations. Another notable trend is that the impact of current loadings is more pronounced in the sediments underlying western Habor waters and tapers off significantly in sediments underlying eastern Harbor waters. Note that the white space on the methylmercury plots represents the difference between the sum of individual component response concentrations and concentrations produced when all component loadings are run simultaneously. These small differences are due to nonlinearities in the methylmercury model. Trends in methylmercury component response concentrations are similar to those observed for total mercury. For both mercury and methylmercury, as is true for other contaminants, the watercolumn tends to be more responsive to current day loadings than the sediment bed.

12.1.5 Component Results for Cadmium

Component results for cadmium in both the water column and the sediment are fully presented in Appendix 13. Summary results are shown here for cadmium component responses in the sediment bed in Figure 12-4. This figure was selected in particular because the cadmium responses in sediments are somewhat different than for the other contaminants, most notably at the location presented in the Passaic River. Inspection of the cadmium results in Appendix 13 and in Figure 12-4 indicates that although the water column response to current day loadings is relatively uniform over the time horizon of the simulation, the impact of current sources of cadmium in the sediments of the Passaic River and other locations appear to increase with time. There are several possible explanations for this behavior including greater deposition of a local source of cadmium than reflected in the assigned initial conditions (which were based on sparse data) and/or migration of cadmium from other parts of the Harbor greater than indicated by assigned initial conditions. In general for cadmium, the major sources of sediment bed contamination are stormwater runoff and tributary headwaters. The effects of current sources are increasing over time, and the current sources are more important relative to legacy sources /initial conditions in the bed of the Newark Bay complex than in eastern portions of the Harbor sediment bed.

12.2 DISCRETIONARY COMPONENTS

Three additional loading component simulations were performed for four selected PCB homologs, 2,3,7,8-TCDD, and a selected furan congener. The loading components were selected to

isolate known problems and include the Upper Hudson and in-place sediments from the Passaic River and Newark Bay. The results of these discretionary components are incorporated in the displays of the baseline loading component results presented in Figures 12-1 through 12-4 and Appendix 13. Some additional discussion is provided below for each discretionary component.

12.2.1 Passaic River Sediment Component Results

For purposes of this calculation, the initial sediment contaminant concentrations in the Passaic River below Dundee Dam to the confluence with Newark Bay were run as the only source term in the model. Thus, the results of this simulation show how in-place contamination present in the sediments underlying the Passaic River in 1998 (whatever their origin source) continue to influence concentrations in the water column and sediments of the Passaic River and other parts of the system. The results of this simulation indicate that while the Passaic River 1998 sediment initial conditions for several PCB homologs, 2,3,7,8-TCDD, and 2,3,4,7,8-TCDF dominate the concentrations observed in the sediments of the Passaic River, the Passaic River 1998 sediment initial conditions have very little impact on sediment concentrations in other regions of the model with the exception of perhaps Newark Bay and the Kills. Examples of the expected future effects of Passaic River 1998 sediment concentrations of 2,3,7,8-TCDD throughout the system are shown in Figure 12-5 for the water column and Figure 12-6 for the sediment bed. Additional transect displays of the results are presented in Appendix 13.

12.2.2 Newark Bay Sediment Component Results

In this component simulation, the initial sediment contaminant concentrations in Newark Bay were run as the only source term in the model. The component results show that the contaminantion present in the sediments of Newark Bay account for very little of the contamination observed throughout the system for PCBs For 2,3,7,8-TCDD the influence of the Newark Bay sediment initial conditions is for the most part limited to Newark Bay and the Kills and is less than the influence of Passaic River sediment initial conditions. For 2,3,4,7,8-PCDF, the role of the Newark Bay sediment initial conditions is even more limited to the proximity of Newark Bay than for 2,3,7,8-TCDD.

12.2.3 Upper Hudson Component Results

In this component simulation, the contaminant concentrations entering the model over the Troy Dam on the Hudson River near Albany, New York were run as the only source term in the model. For the di-CB homolog, the Upper Hudson River is the dominant source of sediment contamination throughout the Harbor, but is not a dominant source for the tetra-, hexa-, and octa-CB homologs. Further, it is likely that the Upper Hudson was a contributor to 1998 sediment initial conditions for di-

CB not associated with either the Passaic River or Newark Bay sediment initial conditions. For 2,3,7,8-TCDD and 2,3,4,7,8-PCDF, the Upper Hudson source does not appreciably account for ambient concentrations. An example of the expected future effects of the current Upper Hudson River source is shown along spatial transects in the water column and sediment bed for the summation of the di-CB, tetra-CB, hexa-CB and octa-CB homologs in Figures 12-7 and 12-8.

12.3 COMPONENT MATRIX

The CARP loading component simulations provide a wealth of information that could be applied toward a variety of management decisions (e.g., sediment remediation, TMDLs, future planning, etc.). For this reason, CARP loading component response results have been stored in a spreadsheet-based matrix to afford CARP member agencies the opportunity to perform "what if" calculations without necessarily running the full CARP model. Based on the matrix, CARP member agencies will have the opportunity to explore the impacts of loading reductions by source type and/or broad scale sediment remediations by scaling the already completed CARP loading component simulations within a spreadsheet user interface. For example, a question that could be answered with the matrix is: what contaminant concentrations could be expected in Harbor worms based on a 25% reduction in current stormwater runoff and a 50% reduction of Passaic River and Newark Bay in-place sediment concentrations?

In preparing the CARP matrix, it was necessary to aggregate the CARP loading component responses in time and space. The CARP domain which includes approximately 1600 wet grid elements in each of ten depths had previously been divided into thirty-nine food chain regions as discussed in Section 9 and shown in Figure 9-2. The matrix includes this same spatial averaging. Contaminant responses included in the matrix have been averaged over depth.

As was described in Section 12.1, there is a time dynamic to the loading component responses. For purposes of the matrix, the last four years of the component responses, years 29 through 32, were selected for the matrix. The advantage of selecting this time period is the ability to have a diagnostic of the behavior of the system after a long-term exposure to the current loadings and a reworking of specified sediment initial conditions. It is appropriate to consider the long-term effects of the current loadings in formulating plans for managing the loadings. Further, considering this time horizon allows management plans to take into account the expected natural attenuation of contaminant levels. A shortcoming of selecting years 29 through 32 rather than the 1998-2002 CARP calibration period, years 5 through 8, is missing the opportunity of answering the question with the matrix of why we measure or calculate a given level of contamination right now. This question of why we measure or calculate a given level of contamination right now, however, has already been answered, although not in the matrix,

by virtue of the time series analysis of the component responses presented in Sections 12.1 and 12.2.

The matrix was designed to be self contained and self explanatory. A users manual is not required. Some of the informational and instructional features of the matrix include a help screen which provides a table of contents and plan view of the layout of the matrix and pie diagrams which depict the current external loadings entering the full model domain and the domain excluding Long Island Sound and the New York Bight.

The loading component ambient responses stored in the matrix include water column, sediments, and biota reported in a variety of different units conventions. The biota include: worms, clams, blue crabs, zooplankton, mummichogs, white perch, American eel, winter flounder, and striped bass. Component responses in biota were calculated based on the field-derived, site-specific BAFs and BSAFs developed using CARP data. The BAFs and BSAFs used for the matrix are described in Section 10. It is recommended that users of the matrix are familiar with Sections 10, 11.4, and 11.5 which explain the uncertainties associated with observed geographic variations in Harbor BSAFs and differences with dredged material testing data.

Distribution of the loading component response matrix shall be coordinated through the Hudson River Foundation.

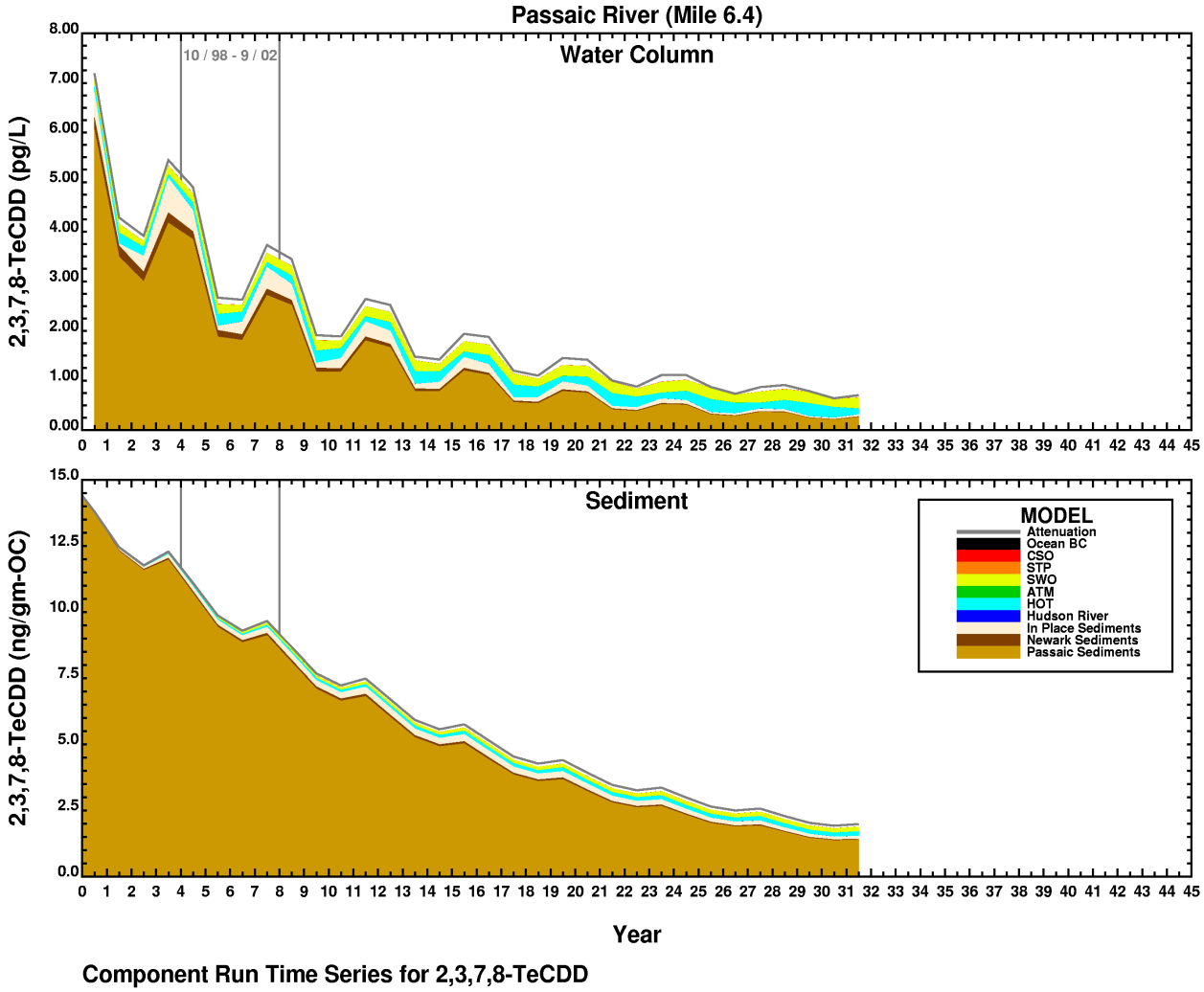

Figure 12-1. Example loading component responses for 32 simulation years

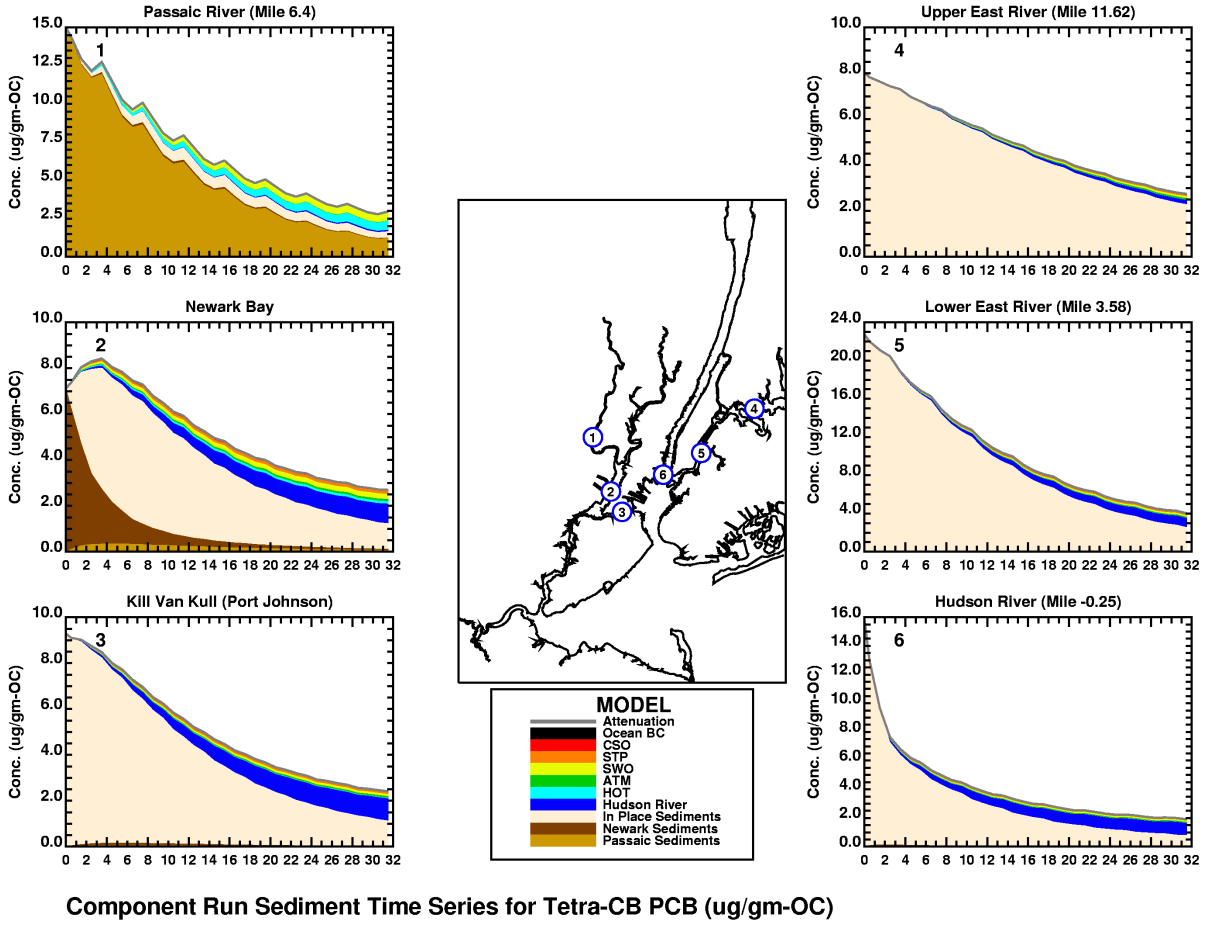

Figure 12-2. Time series component results for sediments at six selected locations - Tetra-CB example.

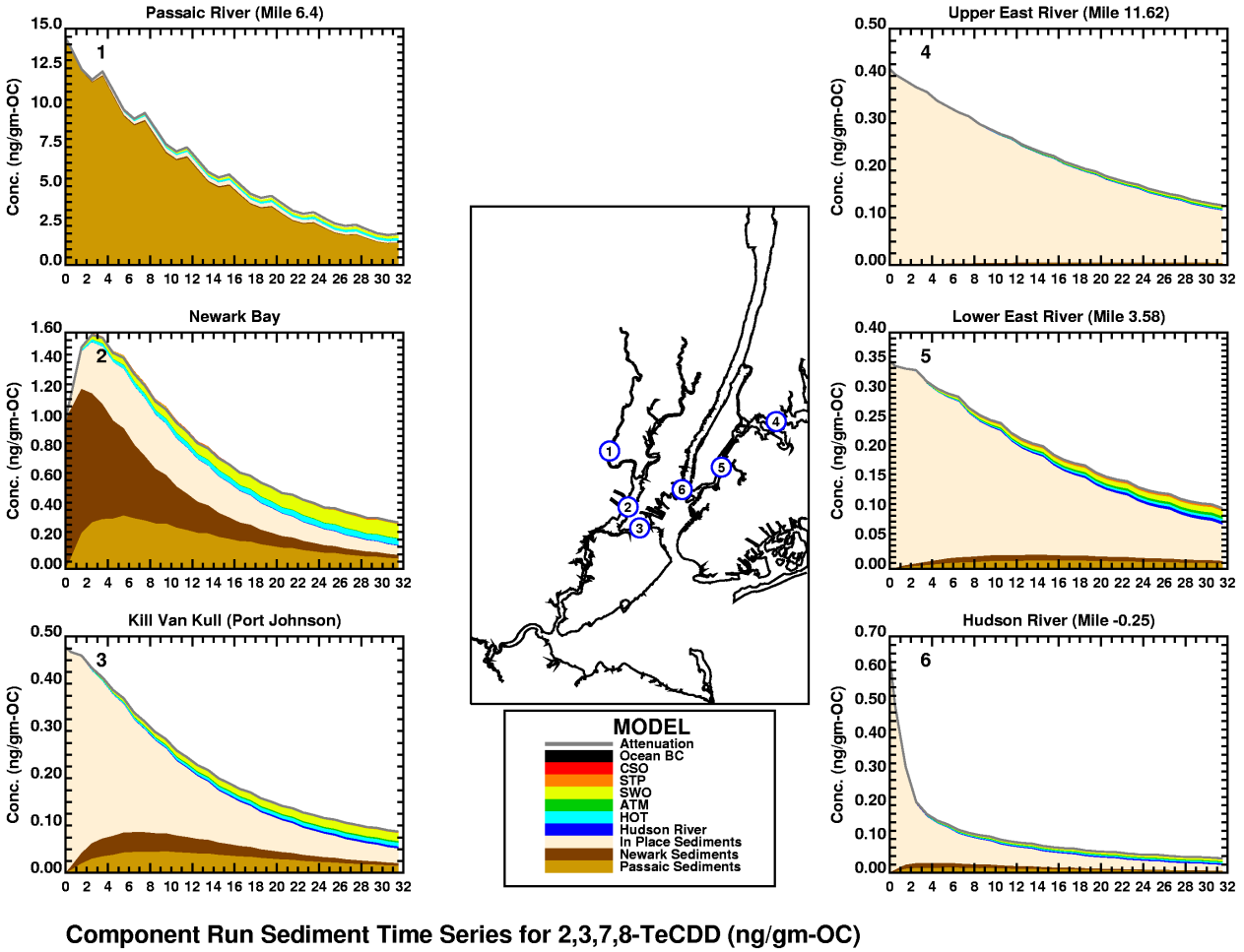

Figure 12-3. Time series component results for sediments at six selected locations - 2,3,7,8-TCDD example.

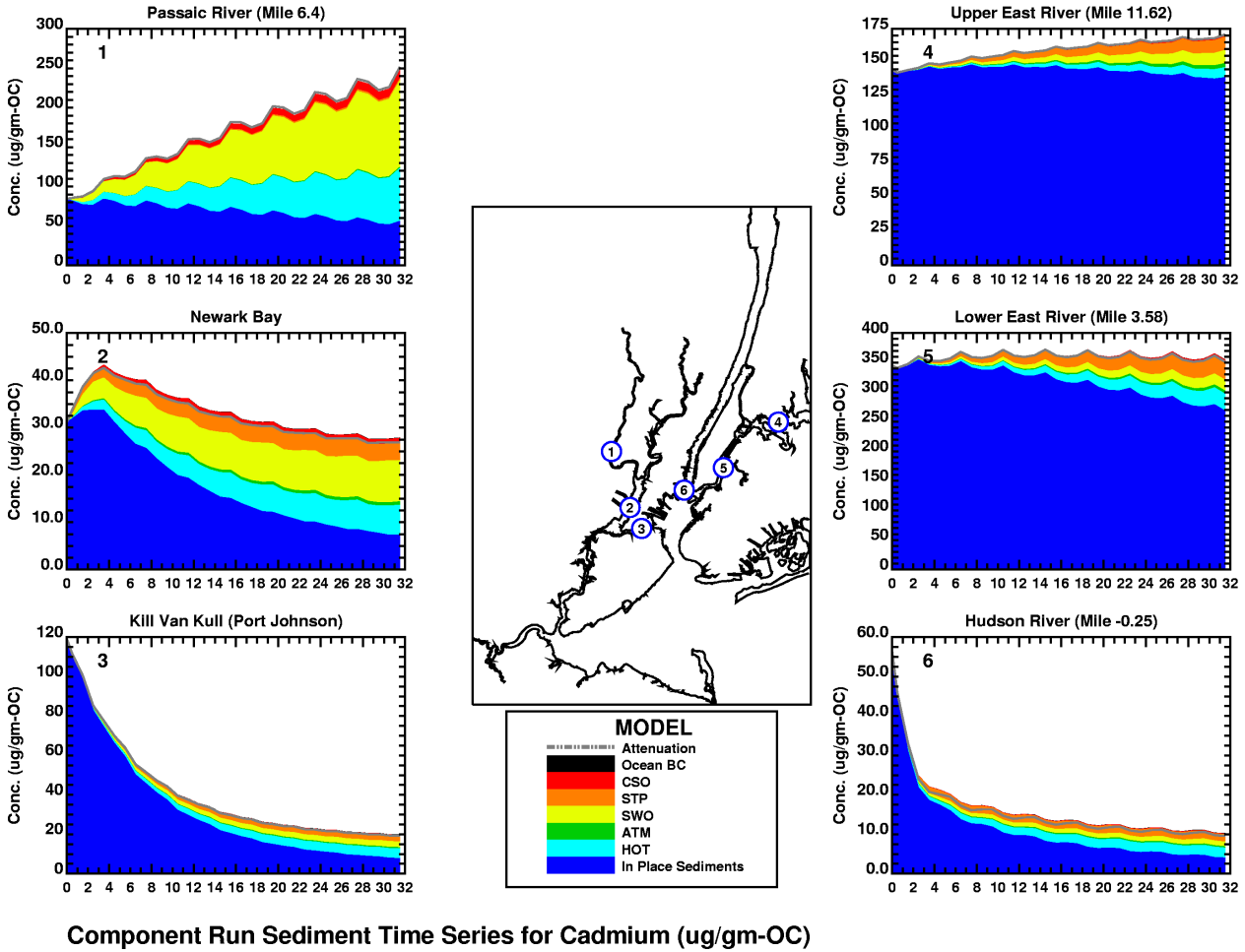

Figure 12-4. Time series component results for sediments at six selected locations - Cadmium Example.

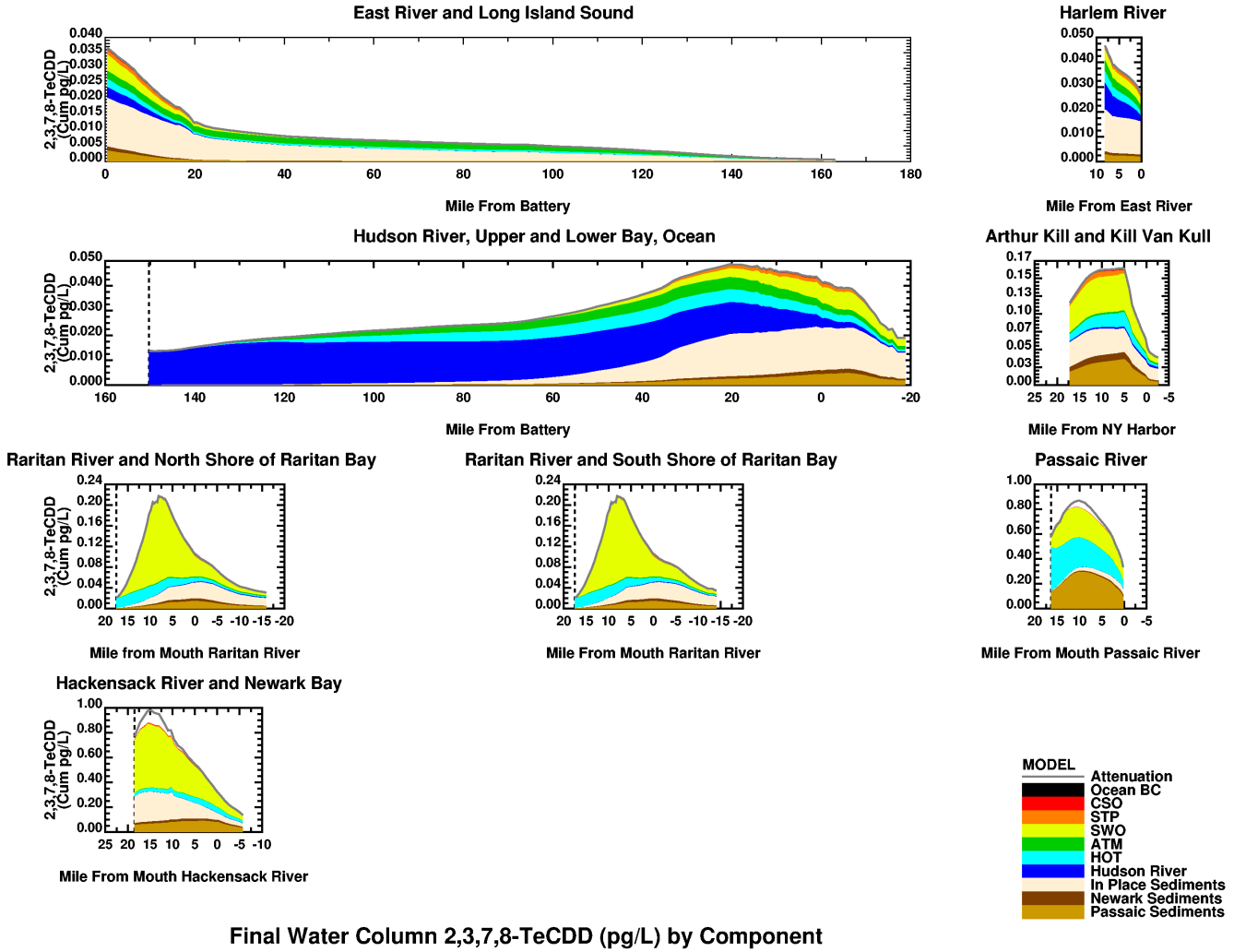

Figure 12-5. Example water column loading component responses along spatial transects for simulation years 29-32 for 2,3,7,8-TCDD.

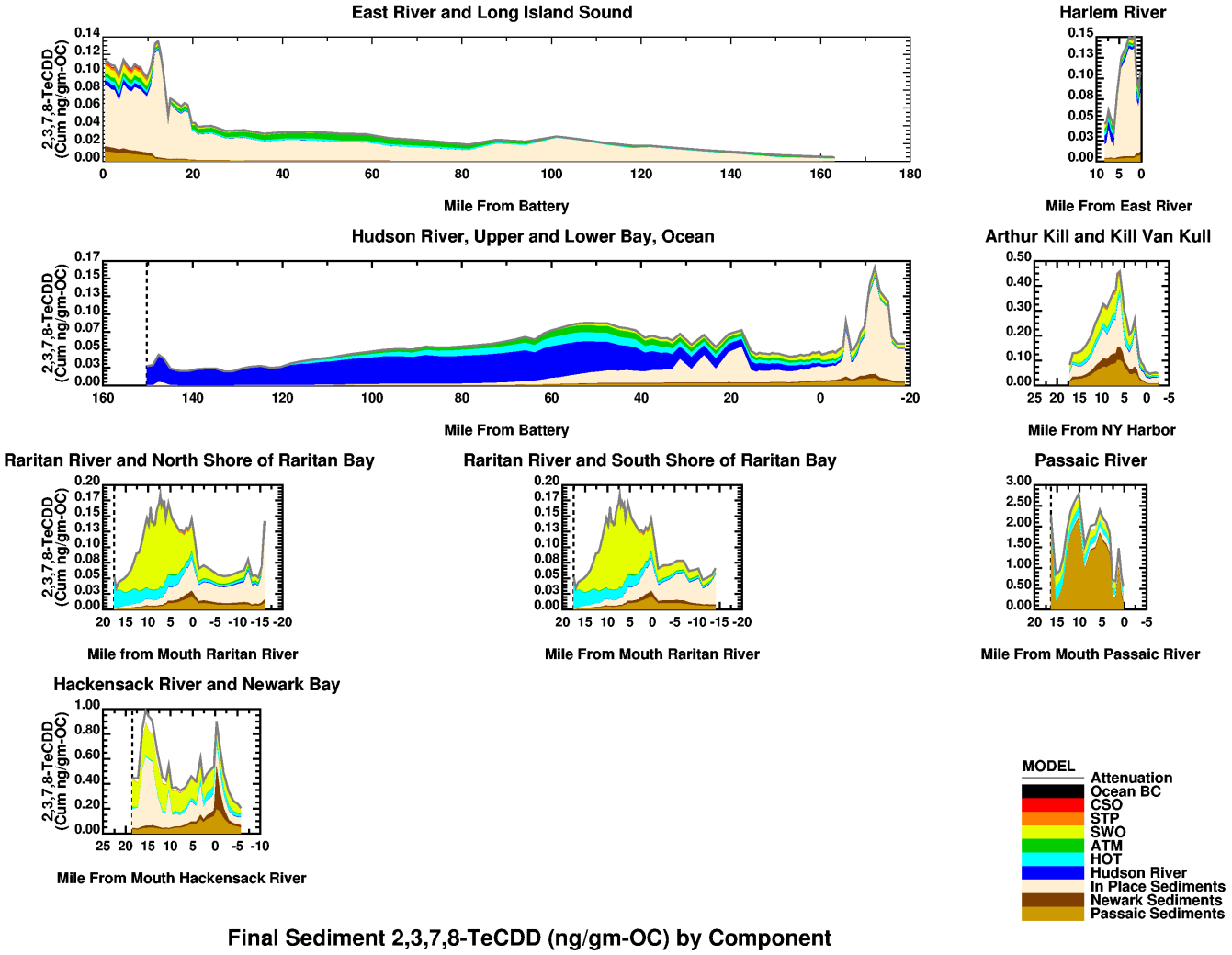

Figure 12-6. Example sediment bed loading component responses along spatial transects for simulation years 29-32 for 2,3,7,8-TCDD.

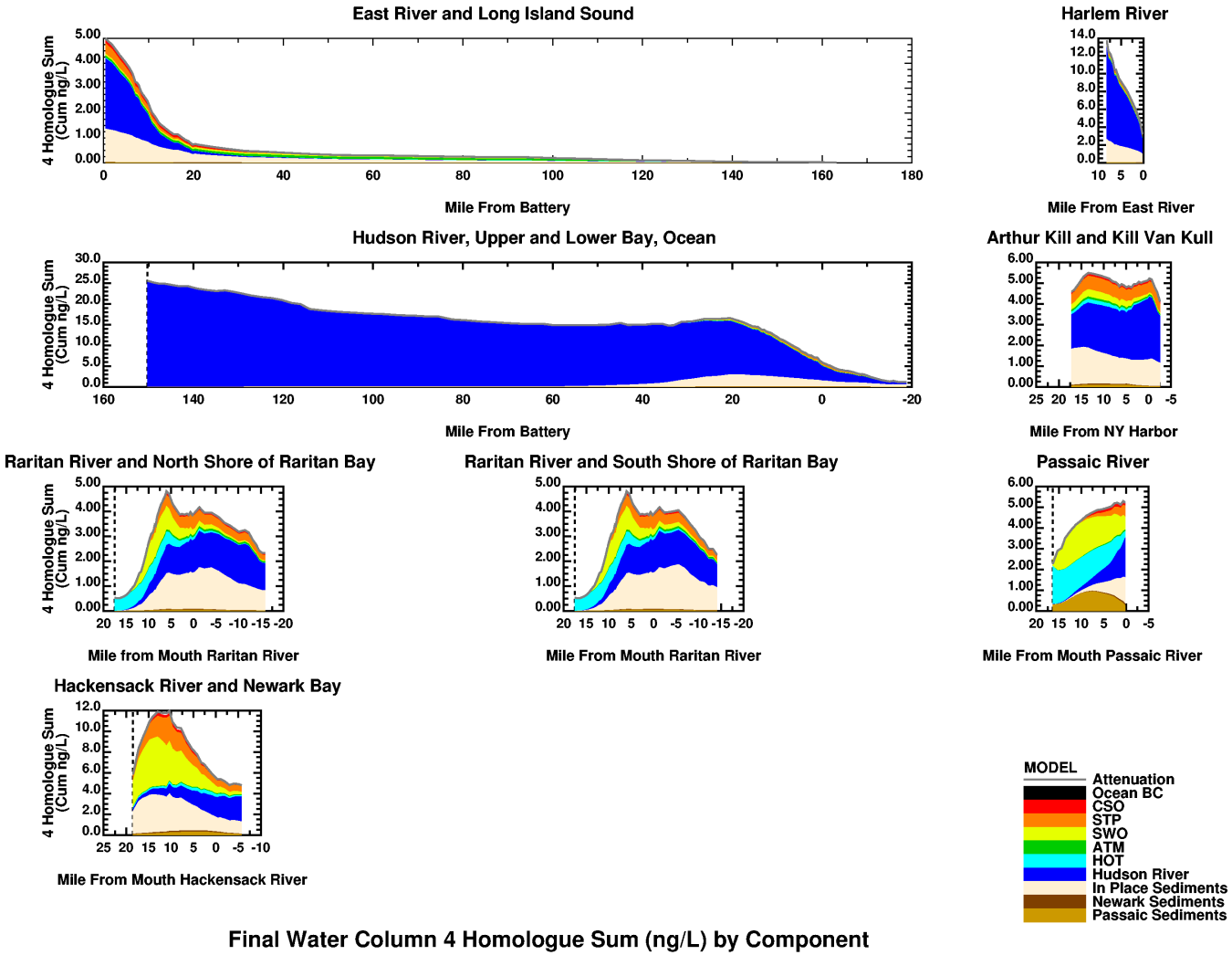

Figure 12-7. Example water column loading component responses along spatial transects for simulation years 29-32 for the summation of di-CB, tetra-CB, hexa-CB, and octa-CB homologs.

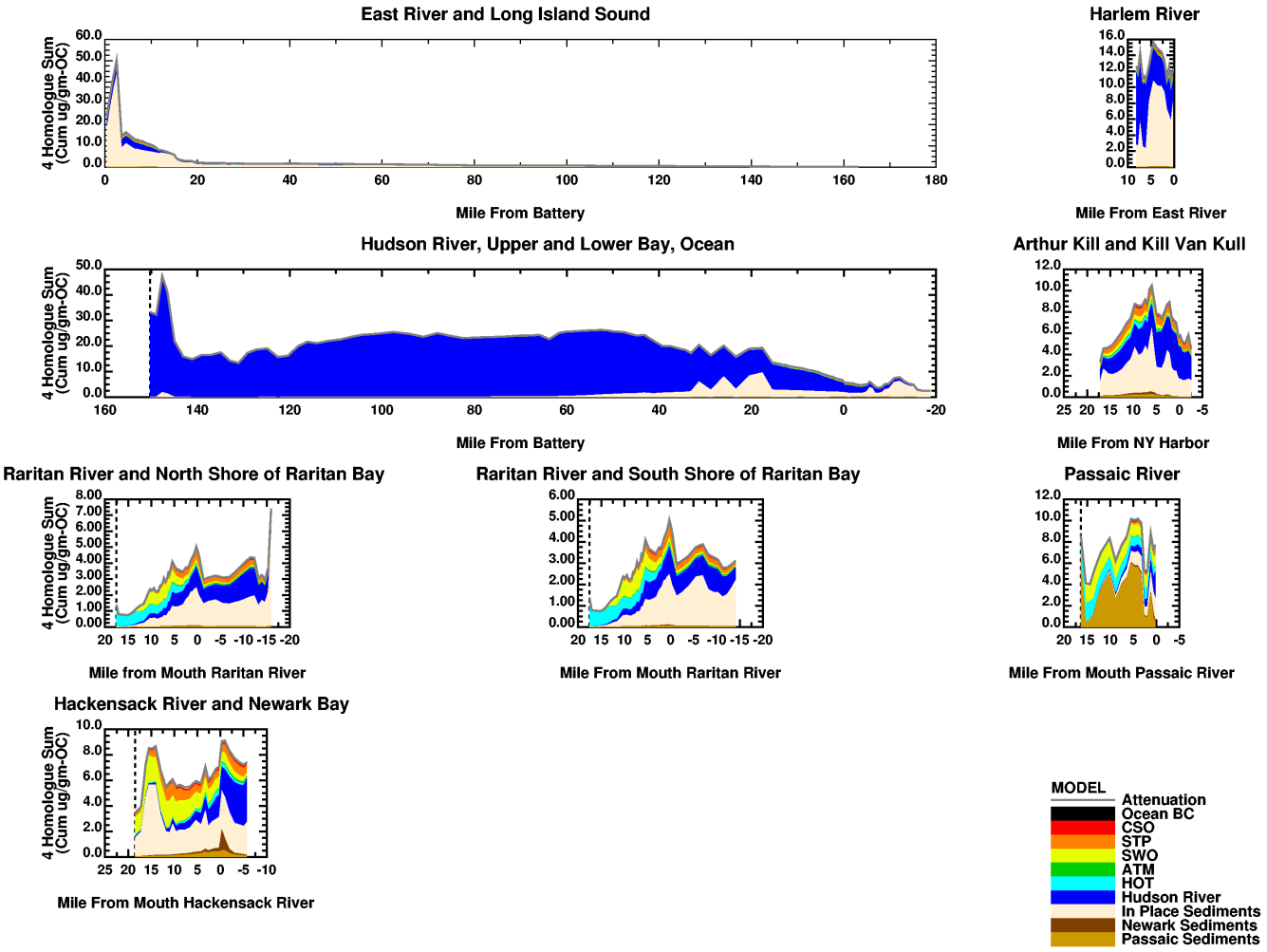

Figure 12-8. Example sediment bed loading component responses along spatial transects for simulation years 29-32 for the summation of di-CB, tetra-CB, hexa-CB, and octa-CB homologs.

SECTION 13.0

SCENARIO EVALUATIONS/FUTURE PROJECTIONS

Projection runs were performed using the calibrated CARP contaminant fate and transport and bioaccumulation models in order to estimate future concentrations in the water column, sediment, and biota under current loading conditions as well as alternative conditions. The projection runs were performed for the same selected contaminants as the component runs. These contaminants are the four PCB homologues: dichlorobiphenyl (di-CB), tetrachlorobiphenyl (tetra-CB), hexachlorobiphenyl (hexa-CB), and octachlorobiphenyl (octa-CB), the dioxin congener 2,3,7,8-TCDD, the furan congener 2,3,4,7,8-PeCDF, and the metals cadmium, mercury, and methyl-mercury. Three different projections were simulated for these contaminants: (1) the future with the current loads, (2) the future with the Upper Hudson PCB loads that are expected based on the Superfund Record of Decision (ROD) and full remediation (i.e., zero contaminant concentrations in the sediment bed) of the lower seven miles of the Passaic River, and (3) the future with the Upper Hudson PCB loads that are expected based on the ROD and full remediation (i.e., zero contaminant concentrations in the sediment bed) in the lower seventeen miles of the Passaic River.

The fate and transport model results include time series for each model grid element of expected future contaminant concentrations in the water column and sediment bed. Fate and transport model results for the projection simulations were used along with the field-derived BAFs/ BSAFs described in Sections 8 through 11 to estimate the expected temporal and spatial changes in contaminant concentrations in fish and benthos over time. Appendix 14 provides a display of the expected future time series responses of the contaminant concentrations in the water column and sediment bed calculated by the fate and transport model for the projection simulations for twelve selected locations throughout the system. These water column and sediment bed time response results are also summarized in a tabular format for 40 regions of the model. The regions are identified on Figure 13-1.

Regarding the time series diagrams for the sediment bed presented in Appendix 14, the user is cautioned that model results are displayed for discrete locations and do not necessarily reflect the expected temporal behavior for an entire region. One example of this is the location in the southern portion of Newark Bay for which time series results are presented. At this location, the temporal response of PCB concentrations in sediments is very sensitive to the inactment of the Upper Hudson River Superfund ROD. This is consistent with conventional sediment mass balances of Newark Bay that indicate a movement of particles from the Harbor to Newark Bay (i.e., suspended sediments coming down from the Hackensack and Passaic Rivers do not account for the mass of solids accumulating in Newark Bay). Di-CB in particular comprises a large fraction of the response in

southern Newark Bay to the Upper Hudson ROD. Had a model grid cell been selected further north in Newark Bay, the influence of the Upper Hudson River on PCB concentrations would not be a dominant feature. This finding is consistent with dated sediment core work performed by Richard Bopp in the northern portion of Newark Bay. Dr. Bopp's measurements for PCBs on a "tri +" (i.e., omitting mono-CB and di-CB) PCB basis show no indication of a Hudson River signal in northern Newark Bay.

Particular focus here in this report section is given to estimated future hydrophobic organic contaminant concentrations in polychaete worms. Worm concentrations were predicted using both field-derived BSAFs and BSAFs based on dredge material testing (DMT) data. Predicted worm contaminant concentrations were compared to Historic Area Remediation Site (HARS) criteria to examine suitability of sediments for future HARS disposal under the various projection scenario conditions.

Attainment of HARS suitable contaminant levels was largely dependent on the BSAF values chosen and varied by location. In general the use of field-derived BSAFs to calculate worm concentrations resulted in more areas of the Harbor failing to obtain HARS criteria than the use of the DMT BSAFs. Based on discussions with the CARP Management Committee and the MEG, DMT BSAFs, rather than field-derived BSAFs, are considered more appropriate for HARS suitability determinations. In the Passaic River, Hackensack River, Newark Bay, the Arthur Kill, and Jamaica Bay, 2,3,7,8-TeCDD generally controlled HARS suitability. For the rest of the Harbor, total-PCB concentrations were the controlling factor in determining HARS suitability.

13.1 FUTURE WITH CURRENT LOADINGS

The future with current loadings projection was run using the model results at the end of the CARP calibration period as initial conditions and the same thirty-seven year sequence of hydrodynamic and sediment transport conditions used in the hindcast analysis (see Section 6.0 for a description). External contaminant loads over the entire projection period were based on the same contaminant concentrations used to specify the current conditions loadings, but included the water volumes and suspended sediment and carbon content associated with the sequence of hydrodynamic conditions. Calculated sediment concentrations and worm BSAF values under these assumed conditions were used to determine future suitability for HARS disposal if current loadings were allowed to continue.

Related to the input conditions for this simulation, there were discussions among the CARP Management Committee as to whether or not any future natural attenuation should be assumed for the Upper Hudson River PCB loading. For this simulation, we did not assume any future attenuation of the Upper Hudson River PCB load for several reasons: (1) the objective of the simulation was to

illustrate the future under current loadings (i.e., to determine the effects on in-place contaminants on future contaminant concentrations), (2) measured PCB conconcentrations and calculated loadings for the Upper Hudson River were relatively steady between 1992 and 2002 as described in Section 6.3.1 and shown by the yellow line on Figure 6-19 in Section 6, and (3) subsequent projection runs rigorously addressed the expected improvement in the PCB loadings from the Upper Hudson River. It is recognized that as discussed in Section 6.3.1, there was evidence of a decline in Upper Hudson PCB concentrations between 1976 and 1987 that may be related to any or all of the Fort Edward Dam break in 1974, the 100 year flood in 1976, decreasing PCB discharge to the River, upstream decay of PCBs in sediments , and/or net burial of PCBs in sediments.

Results of the "future with current loadings" simulation show that over the 37 year period of the projection run, the sediment concentrations were generally reduced by about half with greater or lesser reductions depending on location and contaminant. Figure 13-1 shows the ratio of the concentration in the sediment bed calculated after 37 years to the initial concentration. The greatest reductions were calculated in the 2,3,7,8-TCDD concentrations and the least in di-CB. The areas with the lowest contaminant concentrations tended to remain the same or occasionally increased due to the migration of chemical from more contaminated areas. The areas with the greatest contamination tended to see the greatest reductions in concentration with the exception of areas where the elevated contaminant concentration was due to current loads.

Two possible BSAF values were considered for each of 2,3,7,8-TCDD and the PCB homologues. The first set of BSAFs were derived from the collocated sediment and worm field samples collected by CARP and discussed in Sections 8 through 11. The second set of BSAFs were derived from DMT data provided by USEPA Region 2 (Mark Reiss) for PCBs and from Schrock et al.1997 for 2,3,7,8-TCDD. For both 2,3,7,8-TCDD and the PCB homologues, the field-derived BASFs tended to be greater than the laboratory-based DMT BSAFs. It is not uncommon for there to be differences in field-derived and laboratory-derived BSAFs. Potential reasons for this disparity relate to dredged material test organisms not necessarily being in full steady-state equilibrium with the exposure after 28 days or that the DMT values were obtained using *Neries virens* and the field-derived BSAFs are based on undocumented various species of polychaete worms that may have varied within or between sampling sites. Table 13-1 shows the BSAFs used to predict worm concentrations. Total PCB concentrations were estimated as two times the sum of the individual concentrations of the four modeled homologues. Estimated worm 2,3,7,8-TCDD, 2,3,4,7,8-PCDF, and PCB concentrations are shown in Figure 13-2 and Figure 13-3 for the field-derived and DMT BSAFs, respectively.

There are two dioxin/furan requirements for HARS disposal. The *Neries virens* 28-day bioaccumulation tests can not result in total tissue TCDD concentrations greater than 1 ppt and the

Toxicity Equivalency Quotient (TEQ) values cannot exceed 4.5 ppt. The TEQ for 2,3,7,8-TCDD alone is 1 ppt. Based on the field-derived BSAFs, for almost all sediments in the Harbor, the ratio of 2,3,7,8-TCDD concentration to TEQ is greater than 1:4.5 suggesting that the 2,3,7,8-TCDD concentration controls HARS suitability determination on a TEQ basis. Since the full suite of dioxin/furan chemicals and coplanar PCB homologs required to calculate a TEQ was not run in the projection, and since 2,3,7,8-TCDD concentrations generally control HARS suitability for Harbor sediments, the 2,3,7,8-TCDD concentrations predicted in worms were compared to the 1 ppt standard to determine HARS suitability.

Table 13-1
Worm BSAFs (gm-DW/gm-WW)

	2,3,7,8-TCDD	2,3,4,7,8-PCDF	Di-CB	Tetra-CB	Hexa-CB	Octa-CB
Field-Derived	0.170	0.198	0.200	0.972	1.808	1.407
Dredged Material Testing	0.052[1]	NA	0.243[2]	0.300[2]	0.496[2]	0.216[2]

Notes:

1. Schrock et al., 1997. BSAF = 0.363 gm-sed-DW/gm-worm-DW divided by approximately 7 gm-worm-WW/gm-worm-DW
2. Dredged material testing data provided by USEPA Region 2

Worm 2,3,7,8-TCDD concentrations were calculated with both the field-derived and DMT BSAFs and predicted surface sediment concentrations. These values were then compared to the 1 ppt HARS disposal criteria. Under current loading conditions for thirty-seven years using the field-derived BSAF, most of the sediments in the model domain would be suitable for disposal at the HARS (Figure 13-2 and Figure 13-4); however, almost the entire Passaic River, about half of the Hackensack River , and portions of Jamaica Bay would still exceed HARS criteria. The worst model segments exceed the 1 ppt standard by a factor of two to three. On Figure 13-4 and in similar diagrams, portions of the Harbor shown in green are HARS suitable under projection conditions. Those areas shown in shades of red are not expected to be HARS suitable. For the red and green shading on the diagrams, the darkest colors are used for the largest deviations from HARS suitable. Areas shaded in darkest red are expected to have concentrations more than eight times greater than the HARS criterion. In contrast, using the DMT BSAFs, the entire domain of the model would achieve HARS suitability before 37 years (Figure 13-3 and Figure 13-5). Thus, depending upon which BSAF is used, different conclusions are reached about future HARS suitability. It is not clear that the DMT BSAFs should be applied to exposure concentrations in the field nor is it clear that field-derived BSAFs are appropriate for HARS suitability determinations. Discussions with the CARP Management Committee and MEG favor application of DMT BSAFs to ambient model results for HARS suitability determinations.

Total PCB concentrations in worms were estimated using both sets of homolog specific BSAFs and were compared to the HARS human health non-cancer criterion of 113 ppb. Consistent with the

practice of the dredged material testing program in the region, DMT BSAFs were doubled for purposes of comparing to the HARS human health non-cancer PCB criterion. This practice attempts to reconcile differences in the 28-day test and exposure durations associated with the human health criterion. Based on the field-derived BSAFs, the majority of the mainstem Hudson River, and the eastern and western Harbor would not achieve the HARS criterion. The worst segments are expected to exceed the criterion by more than a factor of ten (Figure 13-2 and Figure 13-6). Using DMT-based BSAFs, results in somewhat broader expected attainment of the HARS criterion (Figure 13-3 and Figure 13-7). Segments in the upper 30 to 40 miles of the Hudson River however are still expected to exceed 113 ppb, as well as some segments in the Lower Bay, Jamaica Bay, the Hackensack River, Raritan Bay, and the Lower and Upper East River, with the worst segments expected to exceed the criterion by more than a factor of eight.

13.2 WITH ACTION ALTERNATIVES

Two projection runs considered likely action alternatives. These alternatives listed from greatest level of remediation action to least are full sediment remediation of the lower seventeen miles of the Passaic River and full sediment remediation of the lower seven miles of the Passaic River. Both of the Passaic River sediment remediation evaluations include reductions in the Upper Hudson PCB load. Under the recommendation of USEPA Region 2, the expected future Upper Hudson River PCB loads over the Troy Dam were taken from the Upper Hudson River Superfund Record of Decision (ROD). Specifically, the future loadings assumed for the Upper Hudson River over Troy Dam are identified in the ROD as "ID R20RS, REM3/10/Select-w/0.13% resuspension - 6 yr dredge". These anticipated loadings provided by EPA include both dredging assumptions and a "step-down" assumption for the Hudson River loading above the dredging area on the Upper Hudson River. These loadings were applied as indicated in the ROD (Table 363150-7) from 2002 onward. No attempt was made to accelerate or delay these loadings based on actual implementation and performance since 2002. For 1998 through 2002, loadings calculated based on actual measurements and used for CARP model calibration were used for projections.

13.2.1 17-Mile Passaic River Sediment Remediation

As the most extensive remediation scenario considered, the seventeen-mile Passaic River sediment remediation scenario produces the lowest projected future contaminant concentrations throughout the model domain. This scenario considers the impact of complete cleansing of the full seventeen miles of the Passaic River as well as the anticipated improvements in PCB loading from the Upper Hudson River. Specifically, the sediment concentrations in the Passaic River were set to zero at the end of the sixth year of the simulation to approximate the impact of remediation of sediments

throughout the Passaic River. In addition, reductions in the Upper Hudson PCB load were made based on EPA estimates as indicated above. Figure 13-8 shows the time history of the anticipated PCB load over the Federal Dam at Troy, NY under the future with current loading and Upper Hudson River remediation cases. Consistent with EPA's specification, the loads on Figure 13-8 are presented as "tri + " PCB although di-CB was also modeled.

Worm 2,3,7,8-TCDD concentrations were calculated for the 17-mile remediation run in the same fashion as the "future with current loads" scenario. 2,3,7,8-TCDD results for worms using field-derived and Schrock et al. 1997 BSAFs are shown in Figure 13-9, 13-10, 13-11, and 13-12. With complete remediation of all of the sediments in the Passaic River, using field-derived BSAFs, the only locations expected to fail to attain HARS criteria for TCDD are the sediments near the dams at head-of-tide on the Passaic and Hackensack Rivers and Jamaica Bay. Approximately one third of the segments expected to fail under the "future with current loads" conditions are expected to remain under the full 17-mile remediation conditions. Under the 17-mile remediation conditions, the lower 7 miles of the Passaic River and Newark Bay are expected to attain HARS TCDD disposal criteria. If the Schrock et al. BSAFs are used, all sediments system-wide are expected to attain the HARS TCDD criterion prior to the end of the 37 year projection period.

The sediments in the Passaic River immediately below Dundee Dam are expected to re-contaminate with 2,3,7,8-TCDD by the end of the 37 year simulation period. Based on above head-of-tide data collected by CARP, the log mean Passaic River head-of-tide 2,3,7,8-TCDD particulate concentration, on an organic carbon normalized basis, is approximately 10 times greater than any of the other headwater log mean concentrations measured by CARP. This suggests that there is possibly a source of 2,3,7,8-TCDD on the Passaic River above Little Falls (i.e., where CARP sampled) that may need some remedial action. It is advisable to collect additional head-of-tide data to better characterize this load given the implications of recontamination. Sampling just above Dundee Dam, rather than at Little Falls, would give a better representation of contaminants entering the Harbor.

With the improvements in PCB loading and Passaic River remediation action considered in this run, projected worm PCB concentrations, based on field-derived BSAFs, are expected to be lower than HARS PCB values for the full reach of the Hudson from the Federal Dam to the Battery (Figures 13-9 and 13-13). Using DMT BSAFs (and the testing program's doubling practice), the Hudson River, as well as the majority of Raritan Bay and the majority of the Newark Bay complex, are also expected to meet the HARS criterion for PCBs (Figures 13-10 and 13-14). Under the full Passaic River remediation conditions, almost all waterbodies throughout the Harbor have a number of segments that would not attain the HARS criterion for PCBs using the field-derived BSAFs. Of these segments, most would attain

HARS suitable levels of PCBs based upon the DMT BSAFs. The exceptions are in the East River, Jamaica Bay, and the Lower Bay near the mouth of Rockaway Inlet.

13.2.2 7-Mile Remediation

For the 7-mile Passaic River and Upper Hudson remediation conditions, in addition to loading reductions for the Upper Hudson, only the sediments in the lower seven miles of the Passaic River are remediated. Specifically, as in the 17-mile scenario, the sediment concentrations in the 7-mile remediation section of the model were set to zero for all contaminants at the end of the sixth year of the run to approximate the impact of a full remediation action. In addition this run also had the reductions in the Upper Hudson PCB load. Results are shown in Figures 13-15 thru 13-20.

Worm 2,3,7,8-TCDD concentrations were calculated using both field-derived and DMT BSAFs. Locations expected to attain the HARS TCDD criterion and those that do not, look similar to those calculated for the "future with current loads" run. Worm 2,3,7,8-TCDD concentrations calculated using field-derived BSAFs are, in most of the area of remedial action, reduced enough to attain the HARS suitable value of 1 ppt in worm tissue. A number of locations that were part of the Passaic River remedy are expected to become re-contaminated enough to ultimately fail HARS suitability (Figures 13-15 and 13-17). As in the 17-mile Passaic River remediation run, the head-of- tide load for the Passaic River likely plays a role in the recontamination and should be more rigorously measured than was done for CARP. It is noted though that Newark Bay would be HARS suitable under a 7-mile cleanup. The CARP model calculations based on DMT BSAFs suggest that HARS suitable levels of 2,3,7,8-TCDD would be expected throughout the domain (Figures 13-16 and 13-18).

Worm PCB concentrations were also calculated for the 7 mile remediation case. In this case, the Hudson River from the Federal Dam to the Battery would be expected to attain HARS suitable PCB levels regardless of whether or not field-derived or DMT BSAF values (with doubling) are used. When field-derived BSAF values are used, however, the number of segments throughout the rest of the domain outside the Hudson River that would be expected to attain HARS suitable PCB levels is reduced with the expectation that model segments would have elevated worm concentrations (Figures 13-15 and 13-19). Attainment of HARS suitability is better when the DMT BSAFs are used. As in the 17-mile remediation scenario, the East River, Jamaica Bay, and the Upper Bay near the mouth of Rockaway Inlet are expected to exceed HARS PCB worm values using DMT BSAFs (Figures 13-16 and 13-20).

Clearly, from the discussions above, the level of remediation required to attain, and the timining of attaining, HARS suitable levels in surface sediments are dependent on the selected BSAFs for both TCDD and PCBs. If DMT BSAFs are used as recommended by the CARP MEG and Management

Committee, most sediments will attain HARS suitable levels without any action within thirty-seven years. In order to attain HARS suitable levels throughout the domain using field-derived BSAFs, a somewhat greater level of remediation than any of the scenarios run would be needed or a longer time horizon would be required. Based on the scenarios evaluated, it appears that outside of the Hackensack and Passaic Rivers, Arthur Kill, and Newark and Jamiaca Bays, PCB contamination generally controls the attainment of HARS suitability. It is noted that our consideration of HARS suitability for PCBs is based upon using twice the sum of four PCB homolog concentrations to approximate total PCB concentrations and, when DMT BSAFs are used, a second doubling as adopted by the dredged material testing program. A further limitation of our analysis is that sediments expected to achieve HARS suitable values for both TCDD and total PCB might still fail to meet HARS suitability for contaminants not considered in the projection scenarios. The reader is reminded that the results of the projection scenarios have application beyond determination of HARS suitability. Projection results contained in Appendix 14 are appropriate for further application uses.

Given the implications of understanding the quality of dredged material in the future, greater effort within the region should focus on both additional field measurements and dredged material test condition measurements of BSAFs. Additional measurements of BSAFs are needed not only for worms (as presented here), but also for clams, the other dredged material testing organism. Although some clams were sampled in CARP, samples were collected outside of areas likely to be dredged and the samples did not include the dredged material testing species.

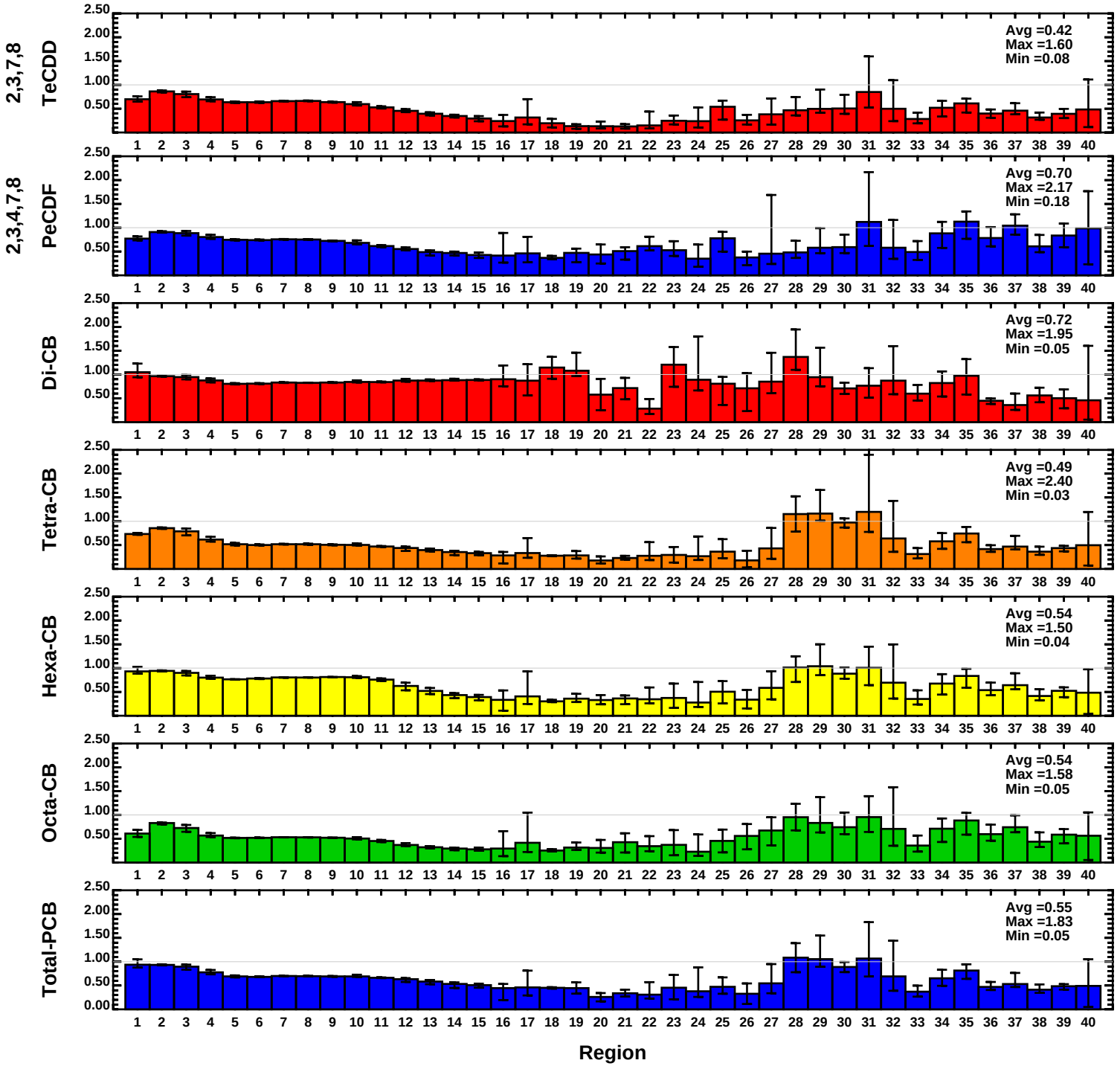

1 Hudson River (150.8 to 143.9)
2 Hudson River (143.9 to 133.8)
3 Hudson River (133.8 to 123.6)
4 Hudson River (123.6 to 112.7)
5 Hudson River (112.7 to 102.8)
6 Hudson River (102.8 to 92.5)
7 Hudson River (92.5 to 83.8)
8 Hudson River (83.8 to 74.8)
9 Hudson River (74.8 to 64.8)
10 Hudson River (64.8 to 55.2)
11 Hudson River (55.2 to 46.2)
12 Hudson River (46.2 to 34.8)
13 Hudson River (34.8 to 24.6)
14 Hudson River (24.6 to 13.9)
15 Hudson River (13.9 to 0)
16 Upper Bay (0 to -6.7)
17 Lower Bay (-6.7 to -17.2)
18 Kill Van Kull
19 Newark Bay
20 Hackensack River
21 Passaic River lower 7 Miles
22 Passaic River upper 10 Miles
23 Arthur Kill
24 Raritan Bay
25 Raritan River
26 Harlem River and Lower East Rivers (0 to 7.6)
27 Upper East River and Western LIS (7.6 to 21.5)
28 LIS (21.5 to 43.8)
29 LIS (43.8 to 78.6)
30 LIS (78.6 to 104.2)
31 LIS (104.2 to 135.1)
32 Jamaica Bay
33 Bight Apex (Sandy Hook /Rockaway) (-17.2 to -30.8)
34 Bight Apex (NJ)
35 Bight Apex (NJ)
36 Bight Apex (NY / NJ) (-30.8 to -53.2)
37 Bight Apex (NY / NJ) (-53.2 to -92.8)
38 Bight Apex (NY)
39 Bight Apex (NY)
40 Open Ocean

Future with Current Loads Projection, Year 37
Ratio of Final to Initial Sediment Concentration

Figure 13-1

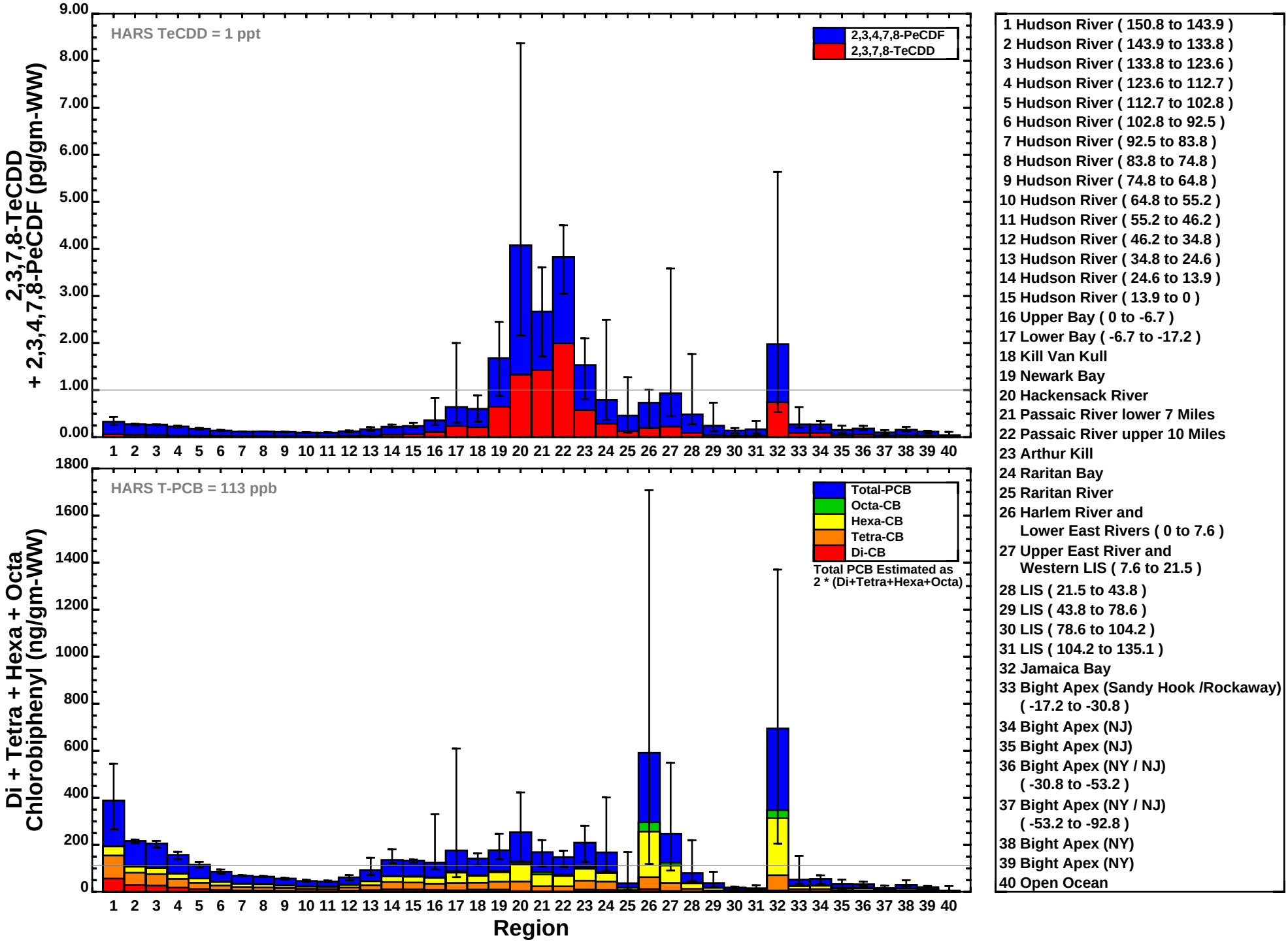

Future with Current Loads Projection, Year 37
Polychaete Worm Concentration Calculated Using CARP Data BSAFs

Figure 13-2

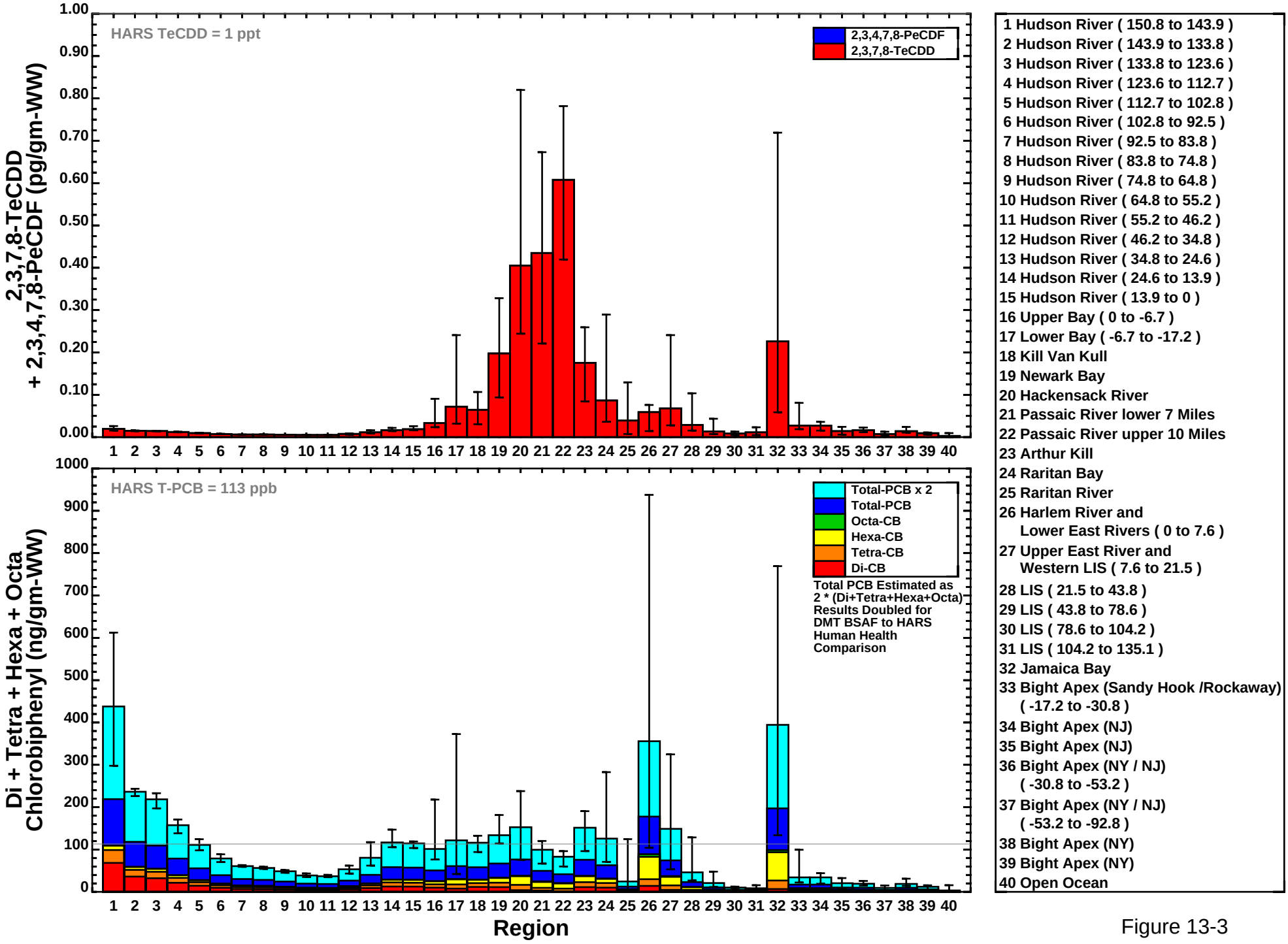

Figure 13-3

Future with Current Loads Projection, Year 37
Neries Virens, Worm Concentration Calculated Using Schrock / Reiss , 28 Day Dredged Material Test Data, BSAFs

Results for Year 37
Future with Current Loads

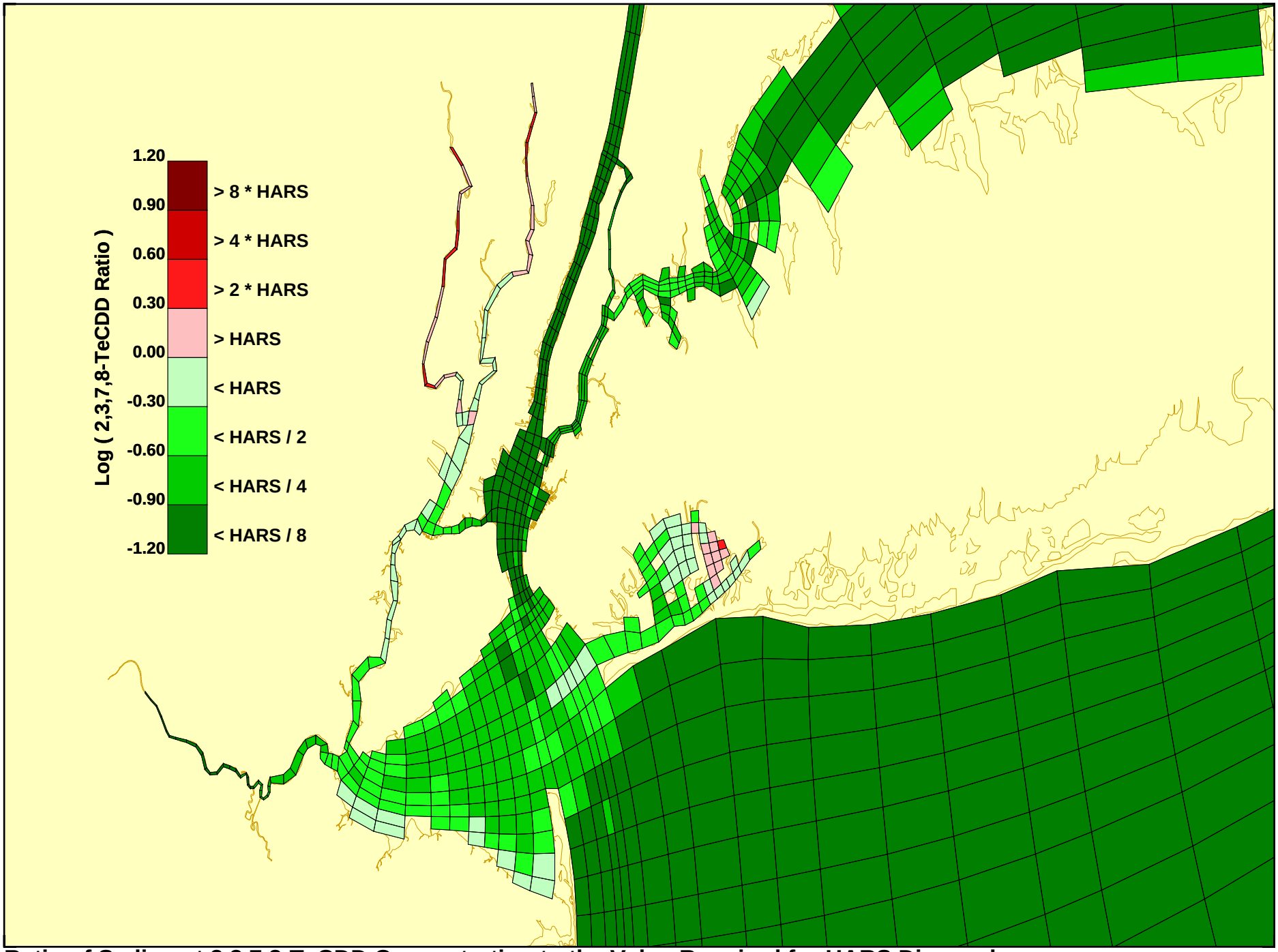

Ratio of Sediment 2,3,7,8-TeCDD Concentration to the Value Required for HARS Disposal Based on a BSAF of 0.17 (gm-DW / gm-WW) From CARP Data and a Worm Target Concentration of 1 ppt

Figure 13-4

Results for Year 37
Future with Current Loads

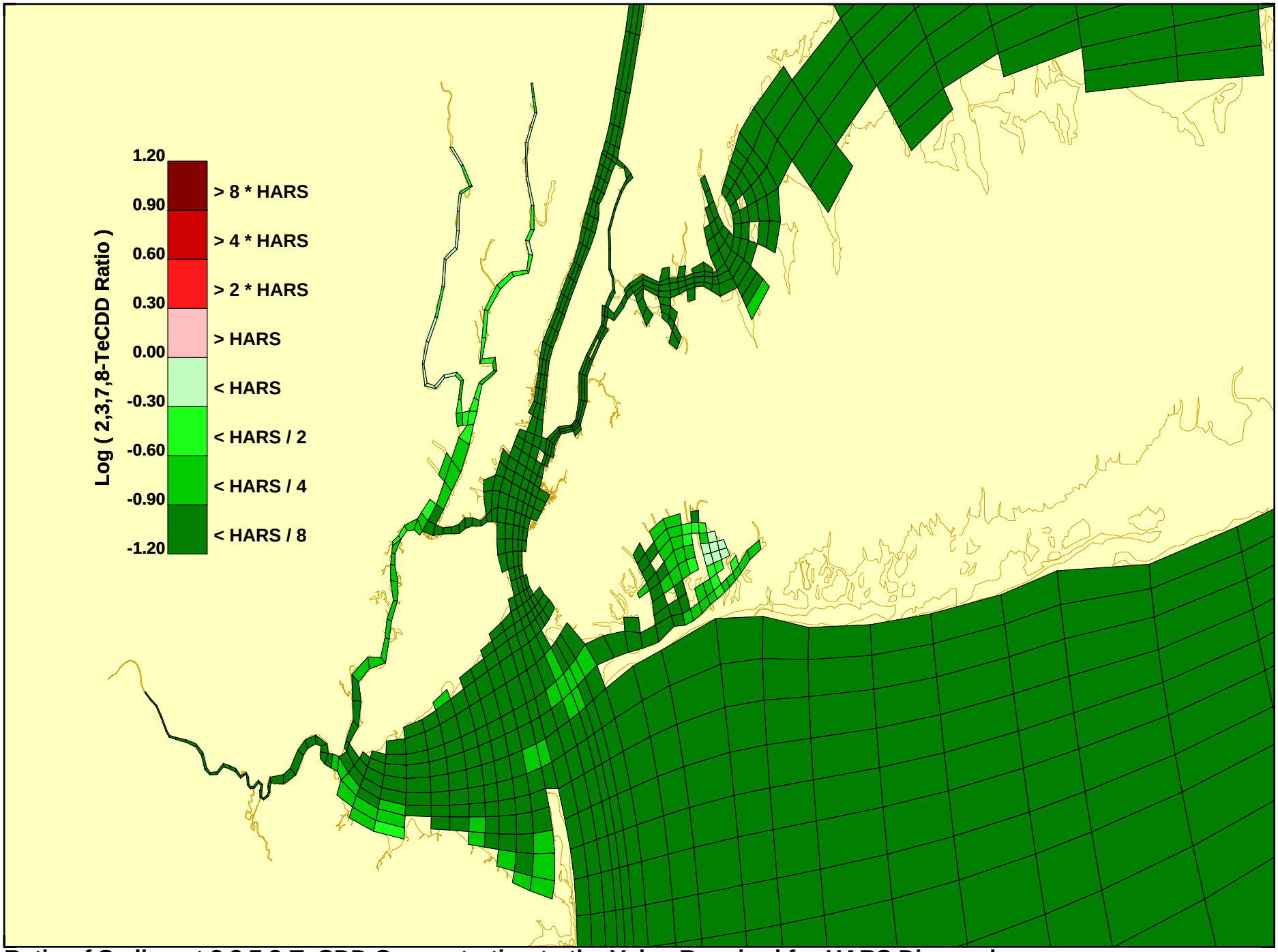

Ratio of Sediment 2,3,7,8-TeCDD Concentration to the Value Required for HARS Disposal
Based on a BSAF of 0.363 (gm-DW/gm-DW) From Schrock Data / 7 (gm-WW/gm-DW) = 0.052 (gm-DW/gm-WW) and a Worm Target Concentration of 1 ppt

Figure 13-5

Results for Year 37
Future with Current Loads

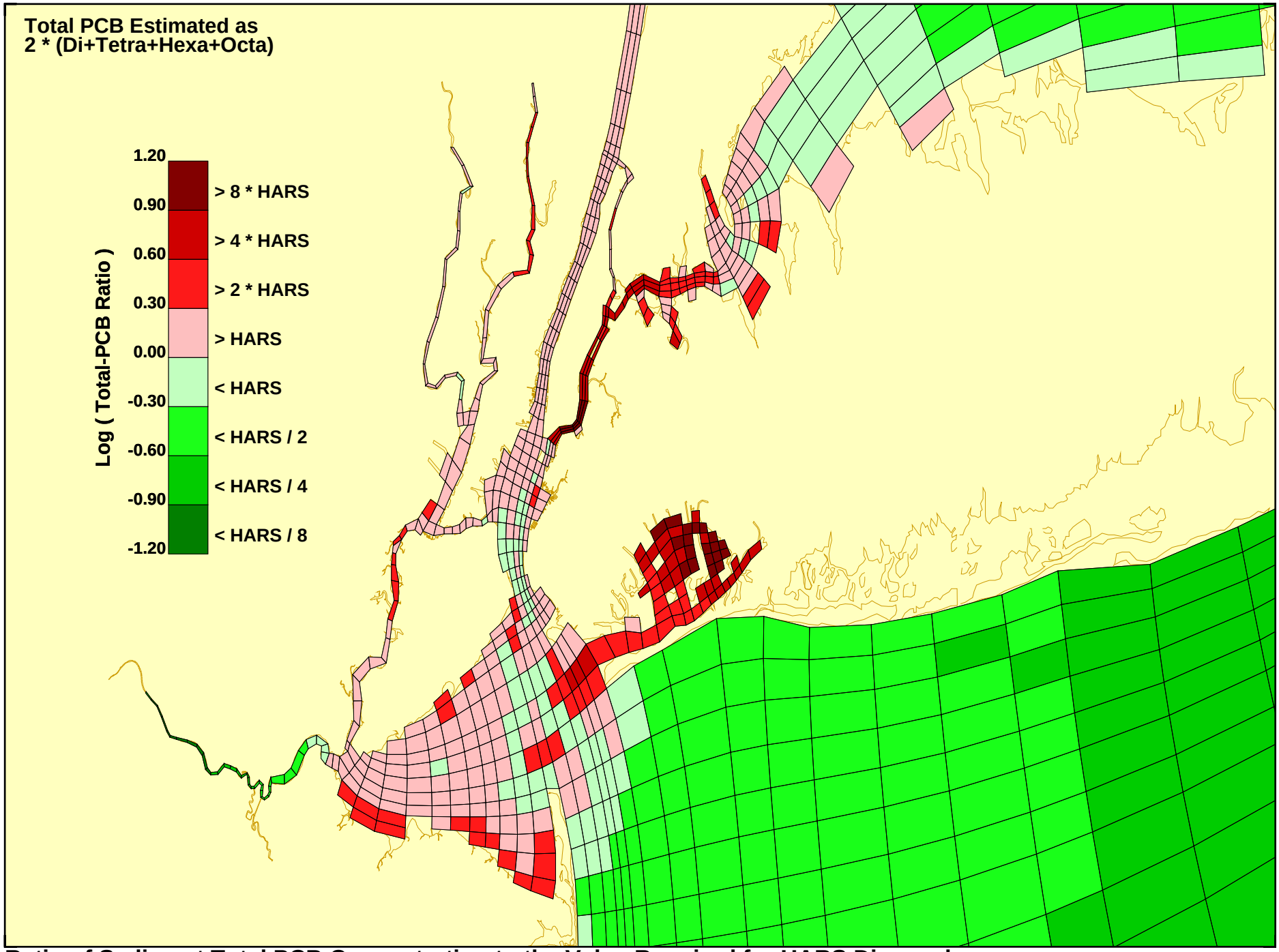

Ratio of Sediment Total PCB Concentration to the Value Required for HARS Disposal
Based on Di, Tetra, Hexa, and Octa BSAFs = 0.20, 0.97, 1.81, and 1.41 (gm-DW/gm-WW) from CARP Data and a Worm Target Concentration of 113 ppb (Interim HARS Non-Cancer)

Figure 13-6

Results for Year 37
Future with Current Loads

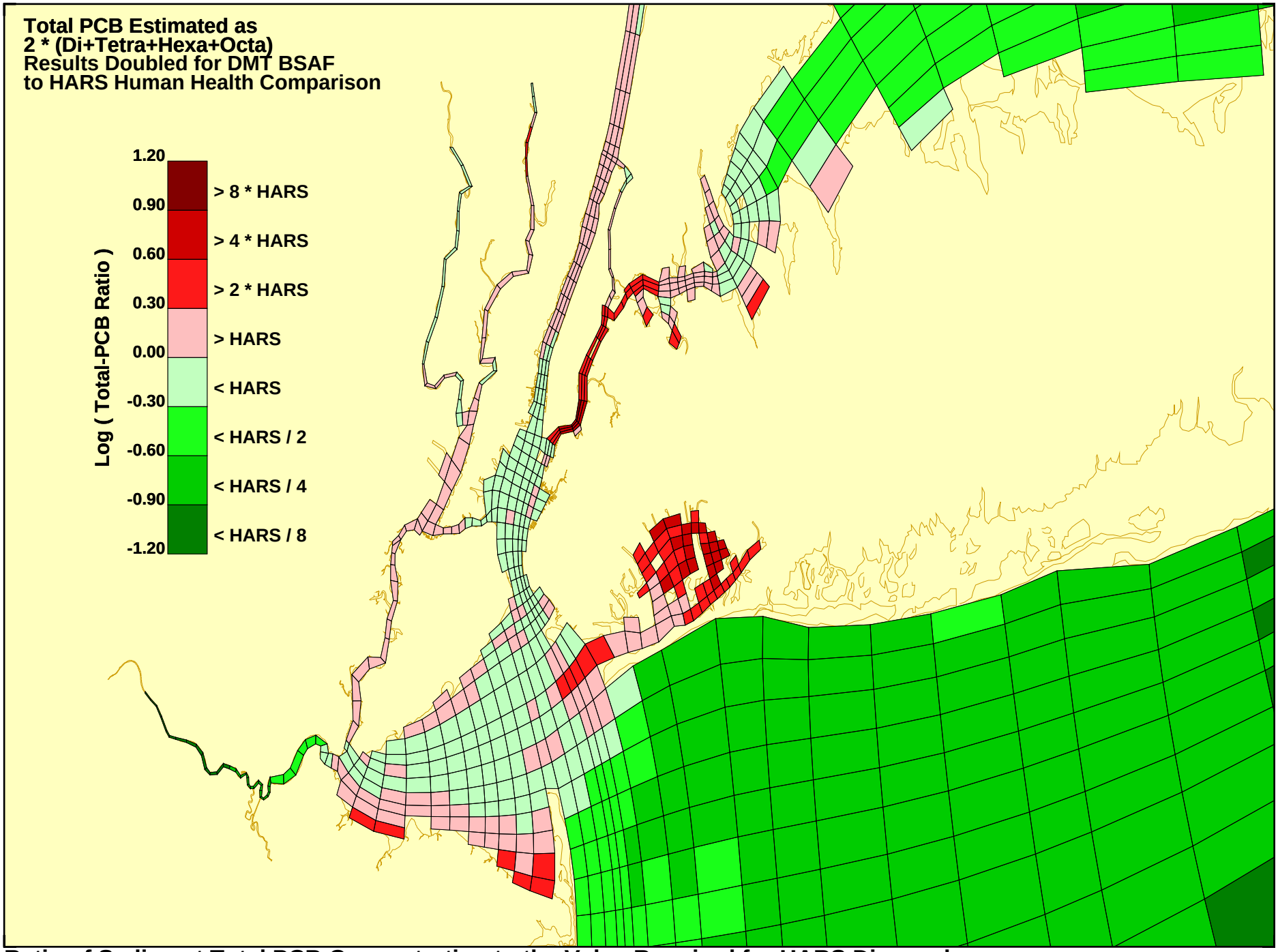

Ratio of Sediment Total PCB Concentration to the Value Required for HARS Disposal
Based on Di, Tetra, Hexa, and Octa BSAFs = 0.24, 0.30, 0.50, and 0.22 (gm-DW/gm-WW) from Reiss Data and a Worm Target Concentration of 113 ppb (Interim HARS Non-Cancer)

Figure 13-7

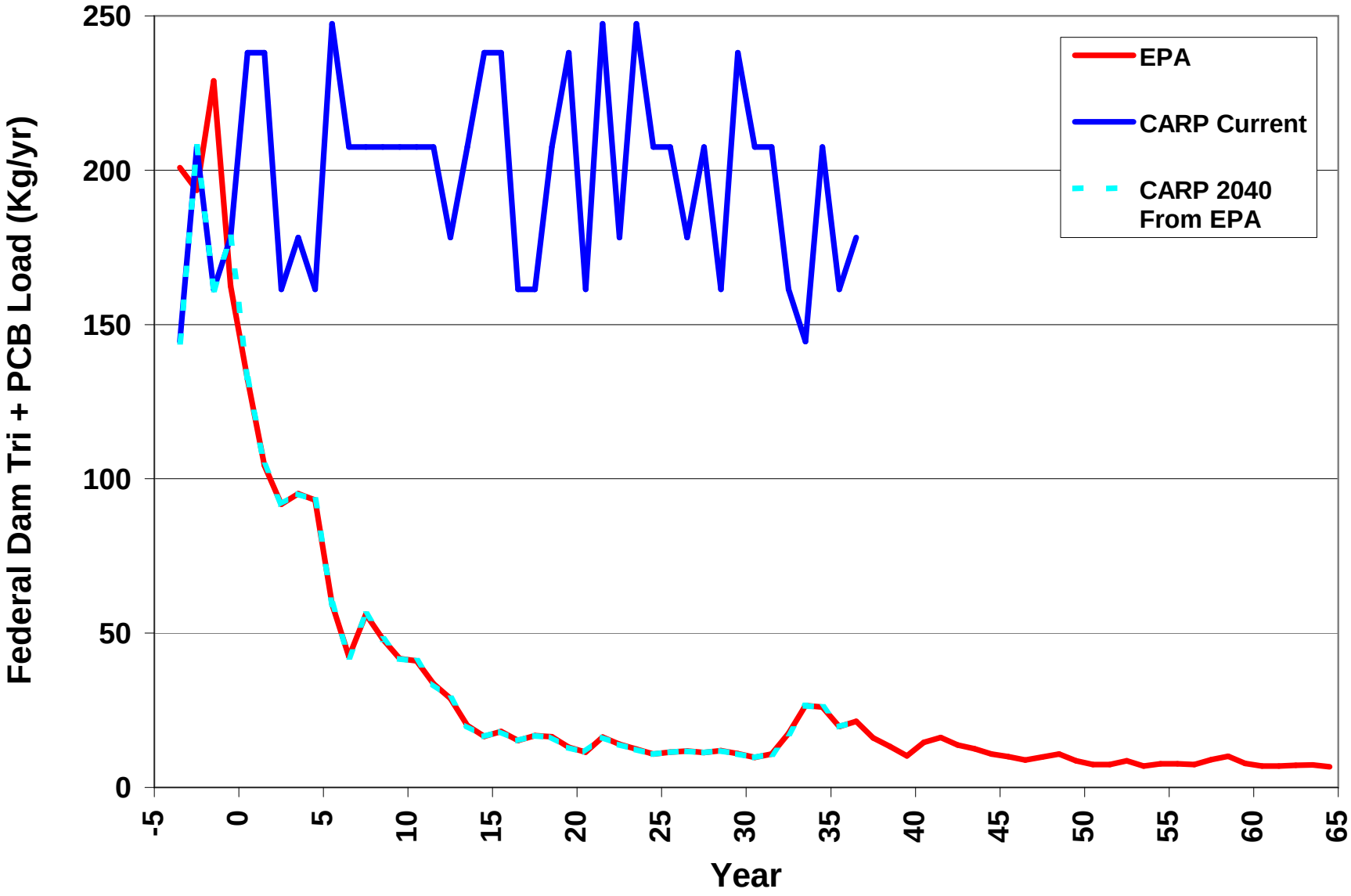
Federal Dam Tri + PCB Load (Kg/yr)
250
200
150
100
50
0
-5
0
5
10
15
20
25
30
35
40
45
50
55
60
65
Year
EPA
CARP Current
CARP 2040
From EPA

Figure 13-8

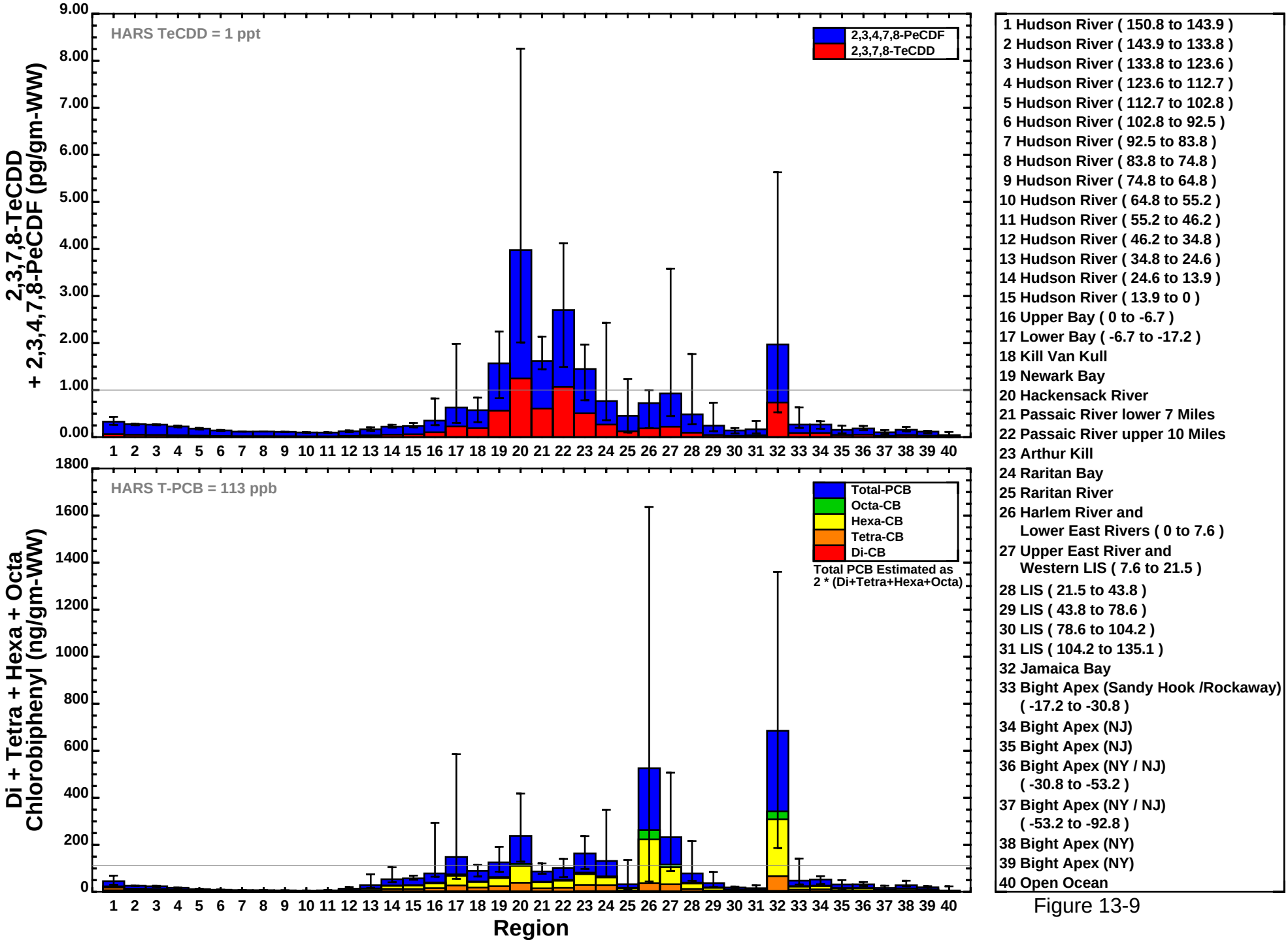

Figure 13-9

Year 7 Dredging in the Full 17 Miles of the Passaic River + Upper Hudson PCB Attenuation Projection, Year 37 Polychaete Worm Concentration Calculated Using CARP Data BSAFs

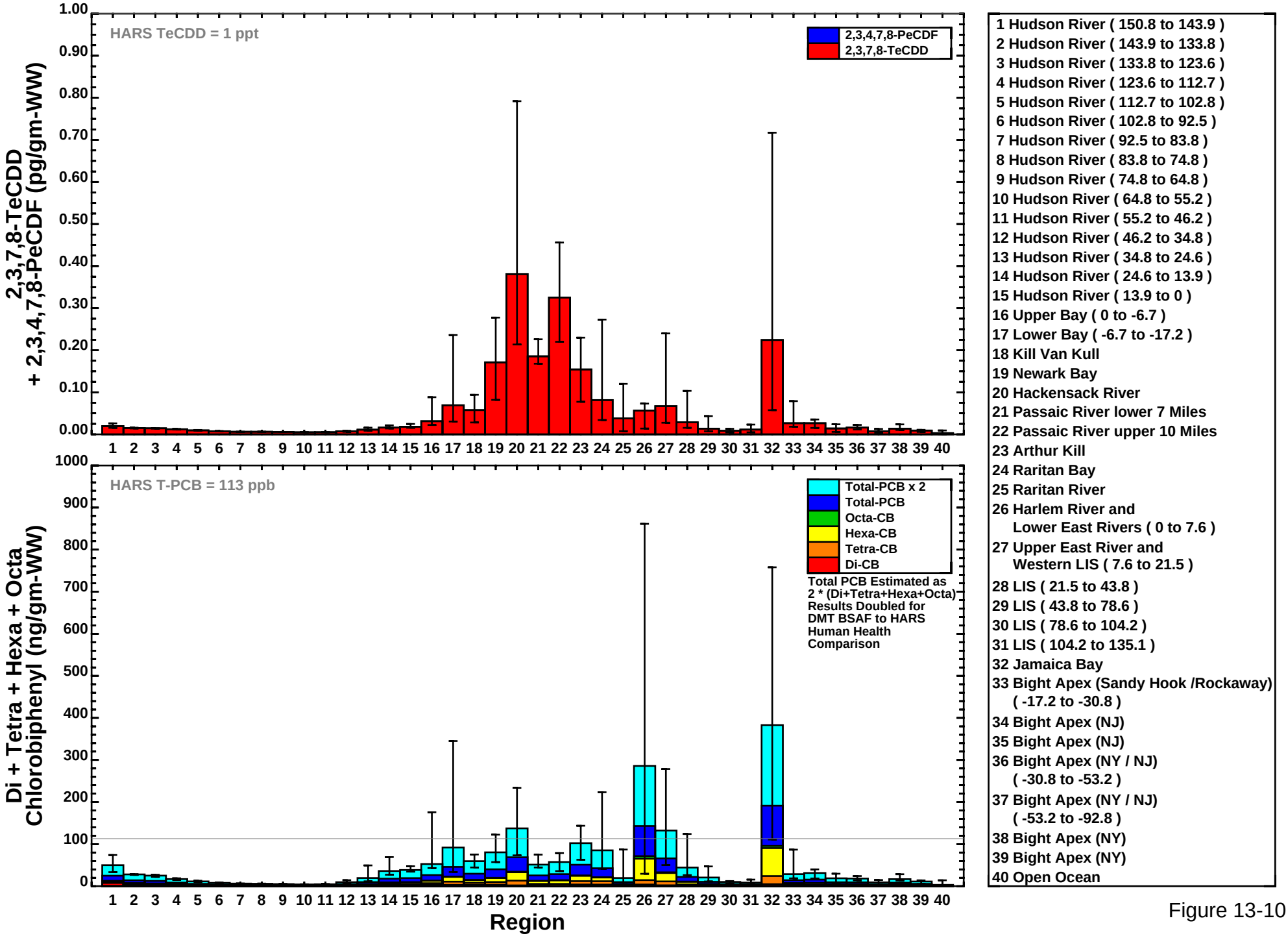

Figure 13-10

Year 7 Dredging in the Full 17 Miles of the Passaic River + Upper Hudson PCB Attenuation Projection, Year 37
Neries Virens, Worm Concentration Calculated Using Schrock / Reiss , 28 Day Dredged Material Test Data, BSAFs

Results for Year 37
Dredging in the Full 17 Miles of the Passaic, End of Year 6

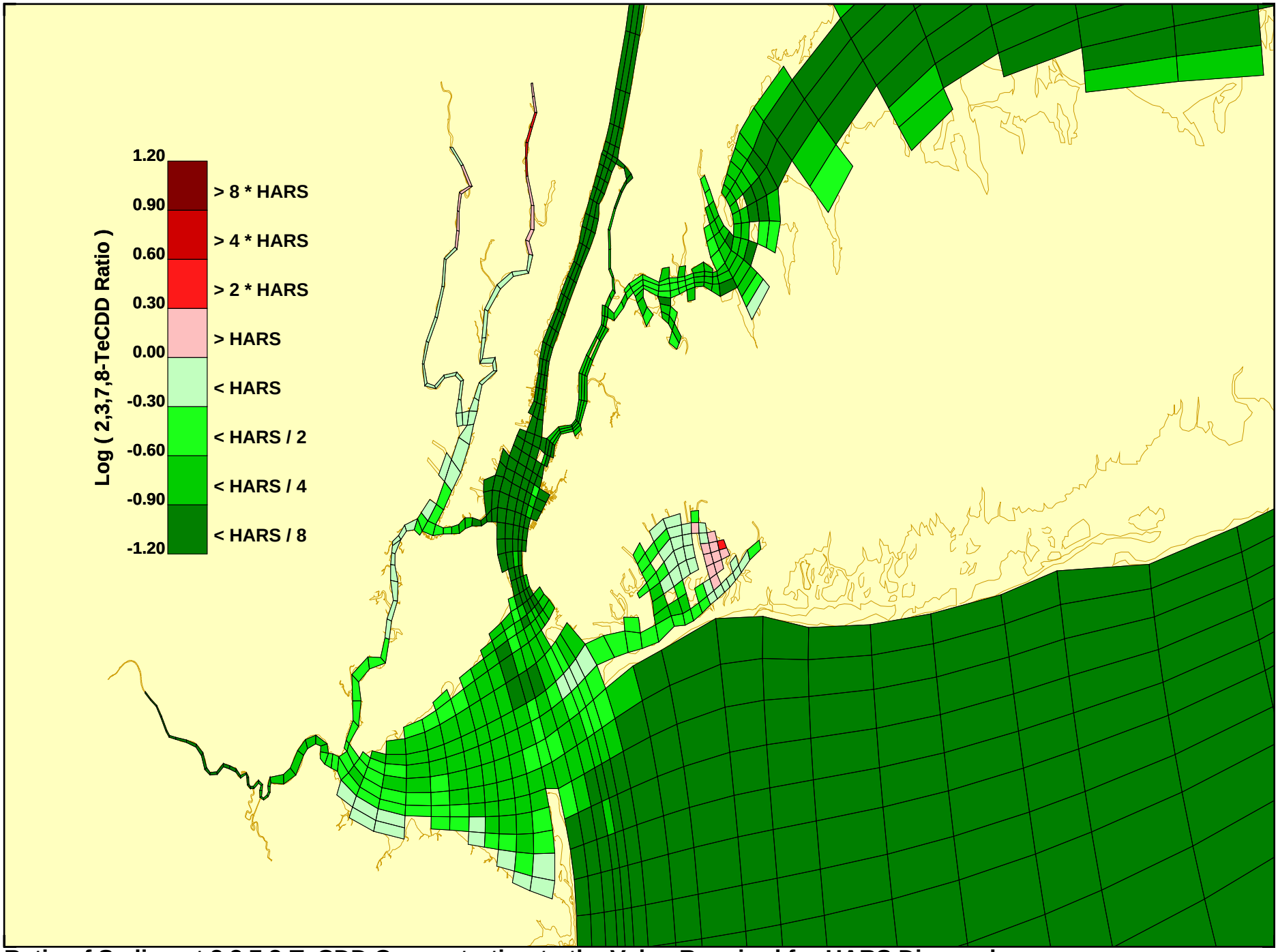

Ratio of Sediment 2,3,7,8-TeCDD Concentration to the Value Required for HARS Disposal Based on a BSAF of 0.17 (gm-DW / gm-WW) From CARP Data and a Worm Target Concentration of 1 ppt

Figure 13-11

Results for Year 37
Dredging in the Full 17 Miles of the Passaic, End of Year 6

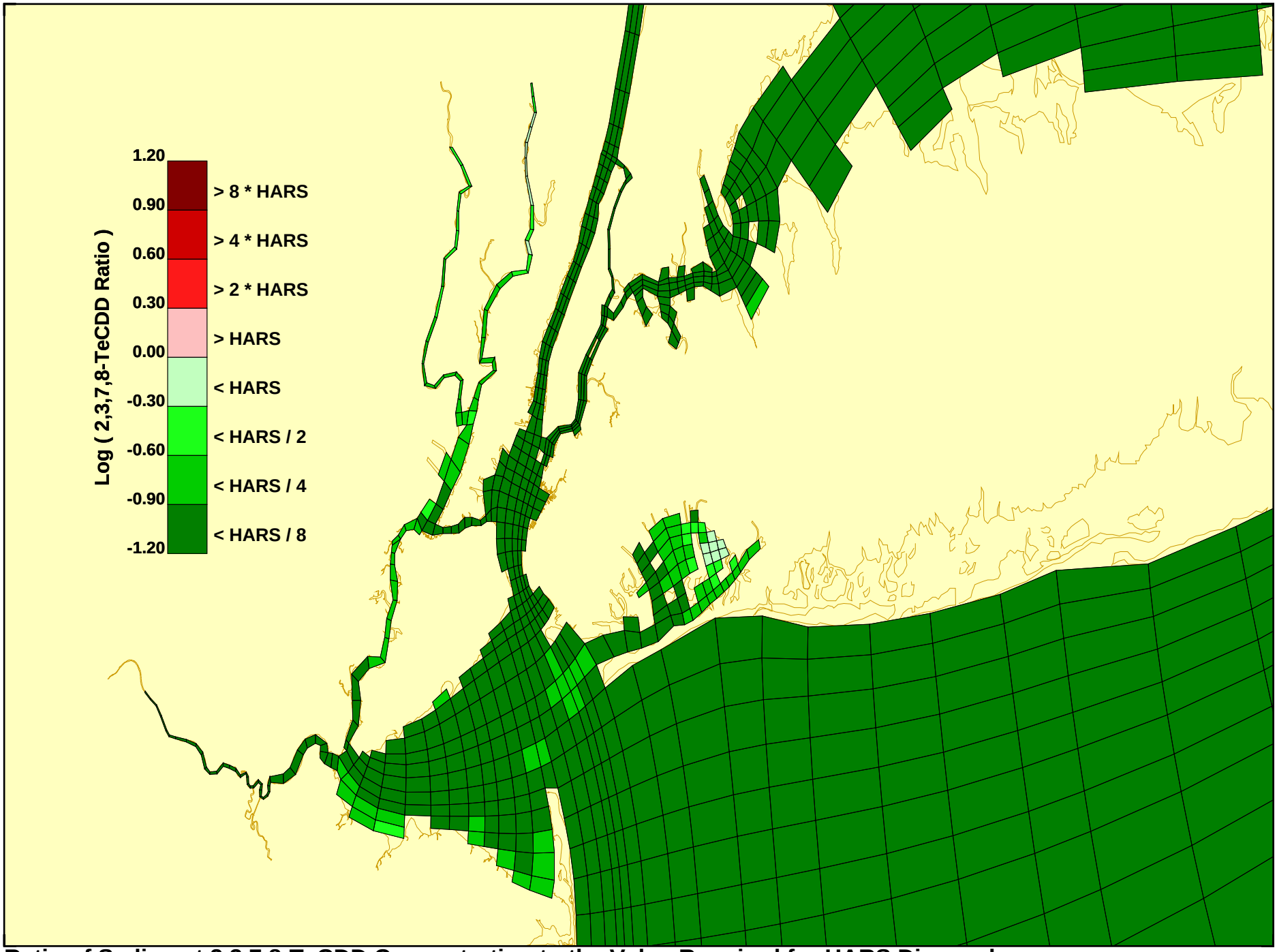

Ratio of Sediment 2,3,7,8-TeCDD Concentration to the Value Required for HARS Disposal
Based on a BSAF of 0.363 (gm-DW/gm-DW) From Schrock Data / 7 (gm-WW/gm-DW) = 0.052 (gm-DW/gm-WW) and a Worm Target Concentration of 1 ppt

Figure 13-12

Results for Year 37
Dredging in the Full 17 Miles of the Passaic, End of Year 6

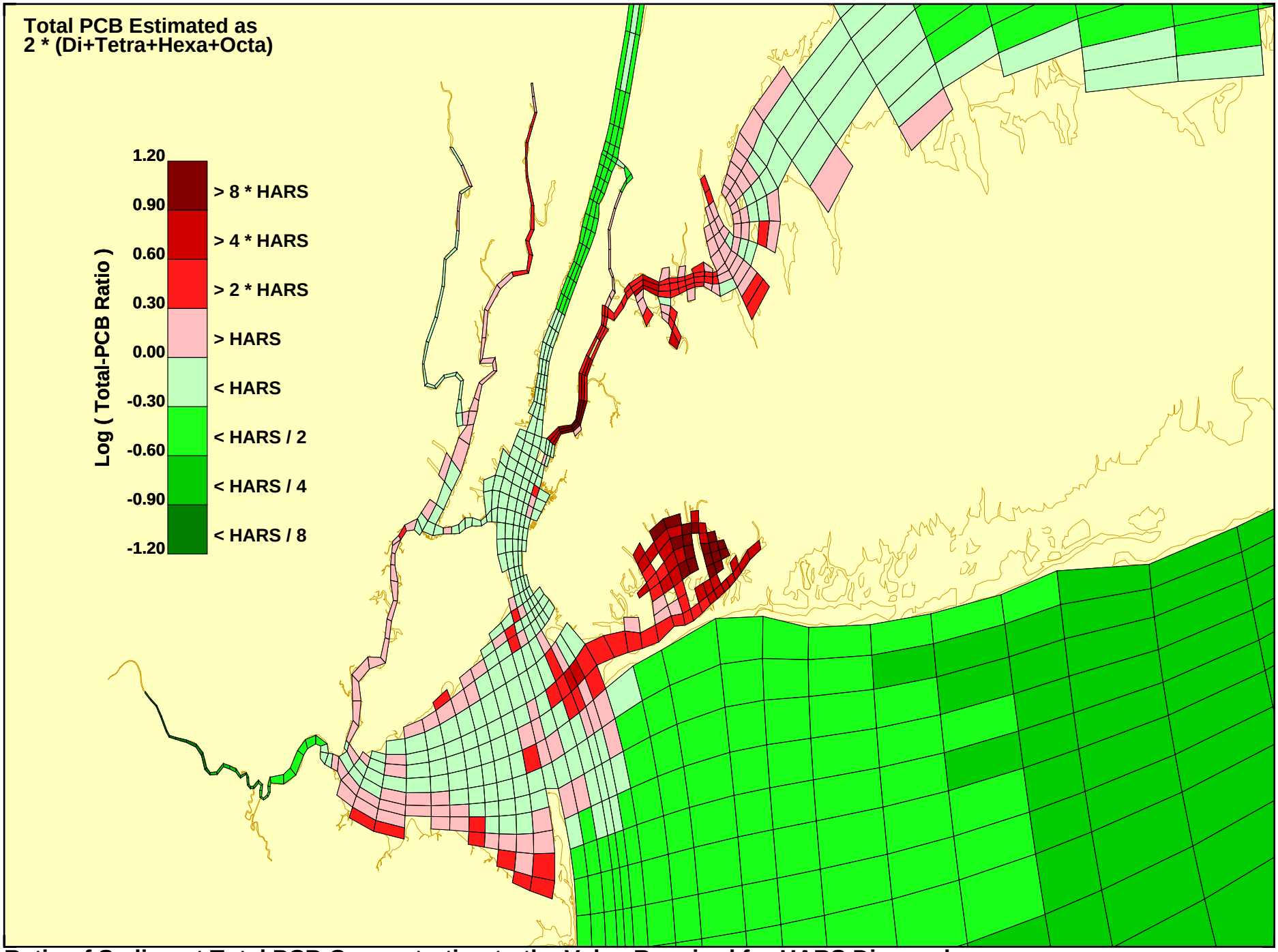

Ratio of Sediment Total PCB Concentration to the Value Required for HARS Disposal
Based on Di, Tetra, Hexa, and Octa BSAFs = 0.20, 0.97, 1.81, and 1.41 (gm-DW/gm-WW) from CARP Data and a Worm Target Concentration of 113 ppb (Interim HARS Non-Cancer)

Figure 13-13

Results for Year 37
Dredging in the Full 17 Miles of the Passaic, End of Year 6

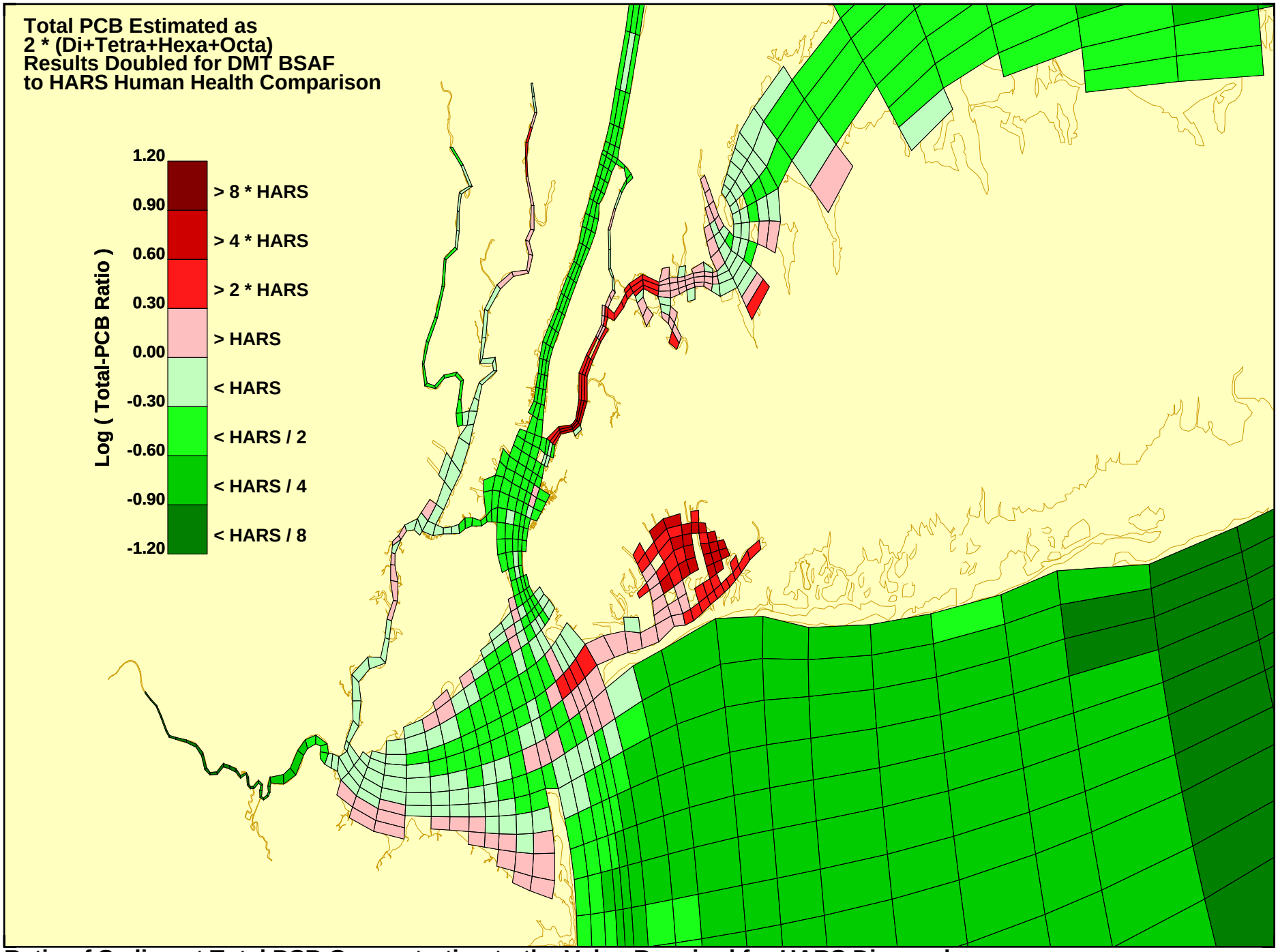

Ratio of Sediment Total PCB Concentration to the Value Required for HARS Disposal
Based on Di, Tetra, Hexa, and Octa BSAFs = 0.24, 0.30, 0.50, and 0.22 (gm-DW/gm-WW) from Reiss Data and a Worm Target Concentration of 113 ppb (Interim HARS Non-Cancer)

Figure 13-14

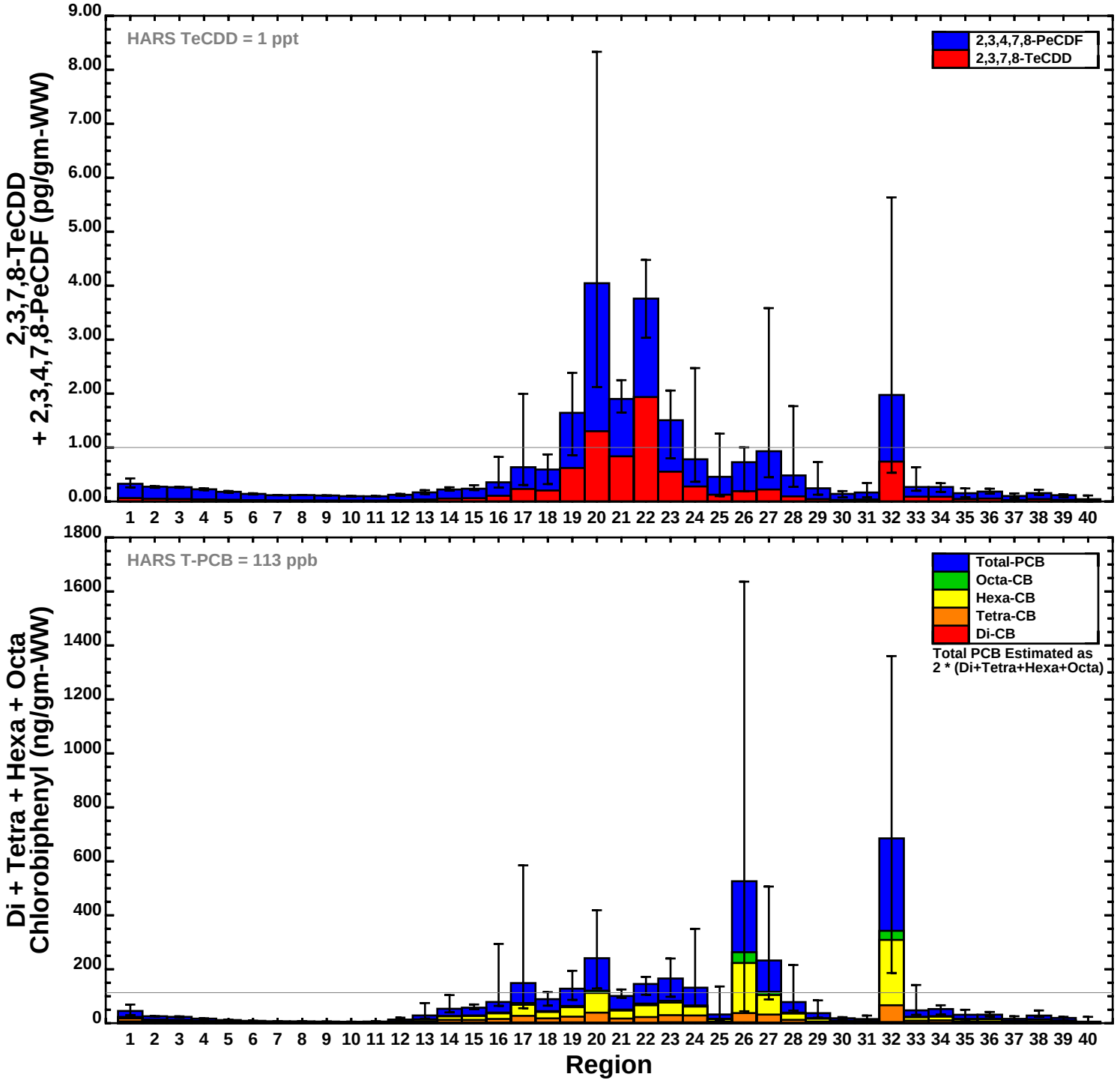

1 Hudson River (150.8 to 143.9)
2 Hudson River (143.9 to 133.8)
3 Hudson River (133.8 to 123.6)
4 Hudson River (123.6 to 112.7)
5 Hudson River (112.7 to 102.8)
6 Hudson River (102.8 to 92.5)
7 Hudson River (92.5 to 83.8)
8 Hudson River (83.8 to 74.8)
9 Hudson River (74.8 to 64.8)
10 Hudson River (64.8 to 55.2)
11 Hudson River (55.2 to 46.2)
12 Hudson River (46.2 to 34.8)
13 Hudson River (34.8 to 24.6)
14 Hudson River (24.6 to 13.9)
15 Hudson River (13.9 to 0)
16 Upper Bay (0 to -6.7)
17 Lower Bay (-6.7 to -17.2)
18 Kill Van Kull
19 Newark Bay
20 Hackensack River
21 Passaic River lower 7 Miles
22 Passaic River upper 10 Miles
23 Arthur Kill
24 Raritan Bay
25 Raritan River
26 Harlem River and Lower East Rivers (0 to 7.6)
27 Upper East River and Western LIS (7.6 to 21.5)
28 LIS (21.5 to 43.8)
29 LIS (43.8 to 78.6)
30 LIS (78.6 to 104.2)
31 LIS (104.2 to 135.1)
32 Jamaica Bay
33 Bight Apex (Sandy Hook /Rockaway) (-17.2 to -30.8)
34 Bight Apex (NJ)
35 Bight Apex (NJ)
36 Bight Apex (NY / NJ) (-30.8 to -53.2)
37 Bight Apex (NY / NJ) (-53.2 to -92.8)
38 Bight Apex (NY)
39 Bight Apex (NY)
40 Open Ocean

Figure 13-15

Year 7 Dredging in the Lower 7 Miles of the Passaic River + Upper Hudson PCB Attenuation Projection, Year 37 Polychaete Worm Concentration Calculated Using CARP Data BSAFs

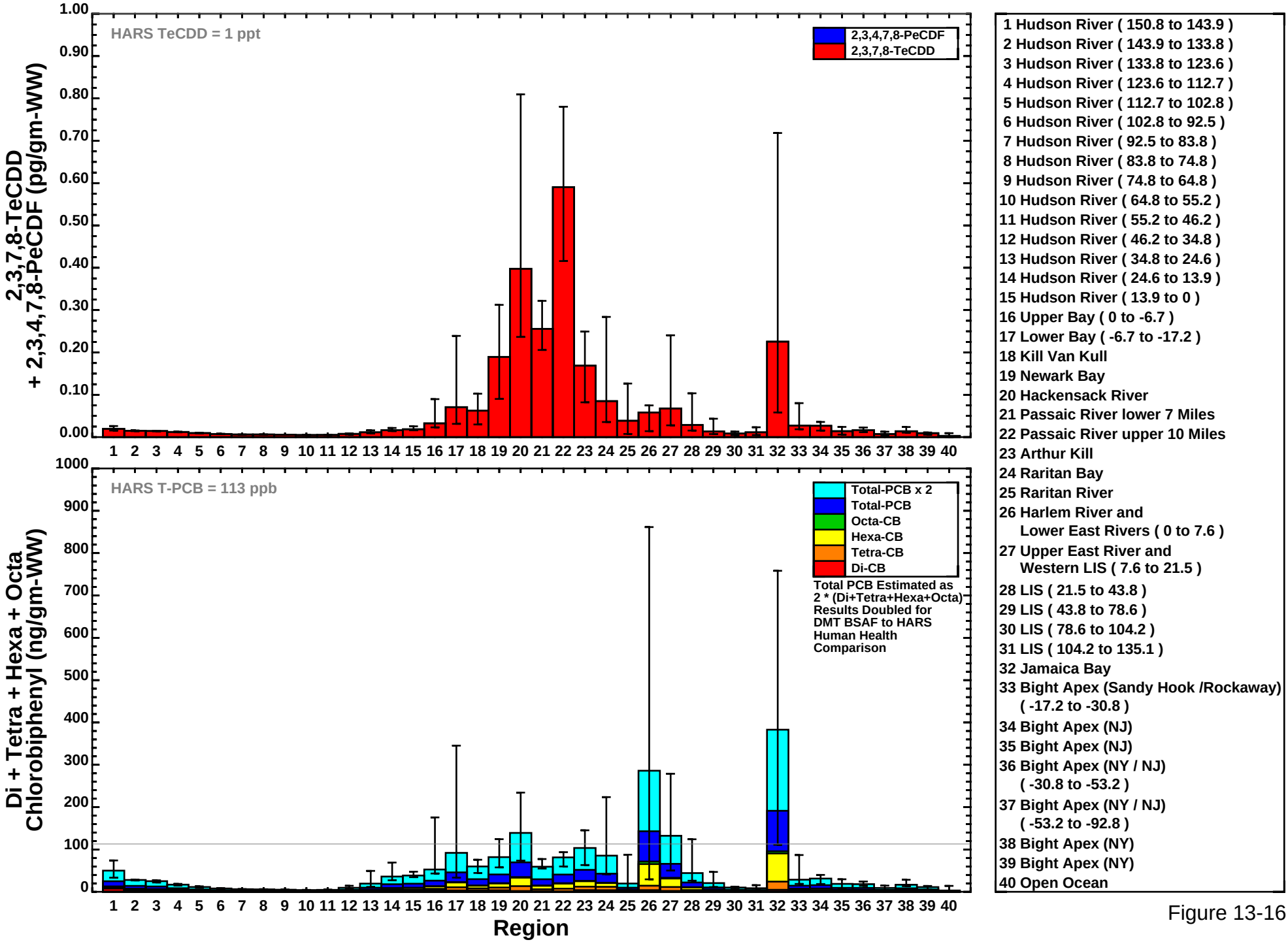

Figure 13-16

Year 7 Dredging in the Lower 7 Miles of the Passaic River + Upper Hudson PCB Attenuation Projection, Year 37 Neries Virens, Worm Concentration Calculated Using Schrock / Reiss , 28 Day Dredged Material Test Data, BSAFs

Results for Year 37
Dredging in the Lower 7 Miles of the Passaic, End of Year 6

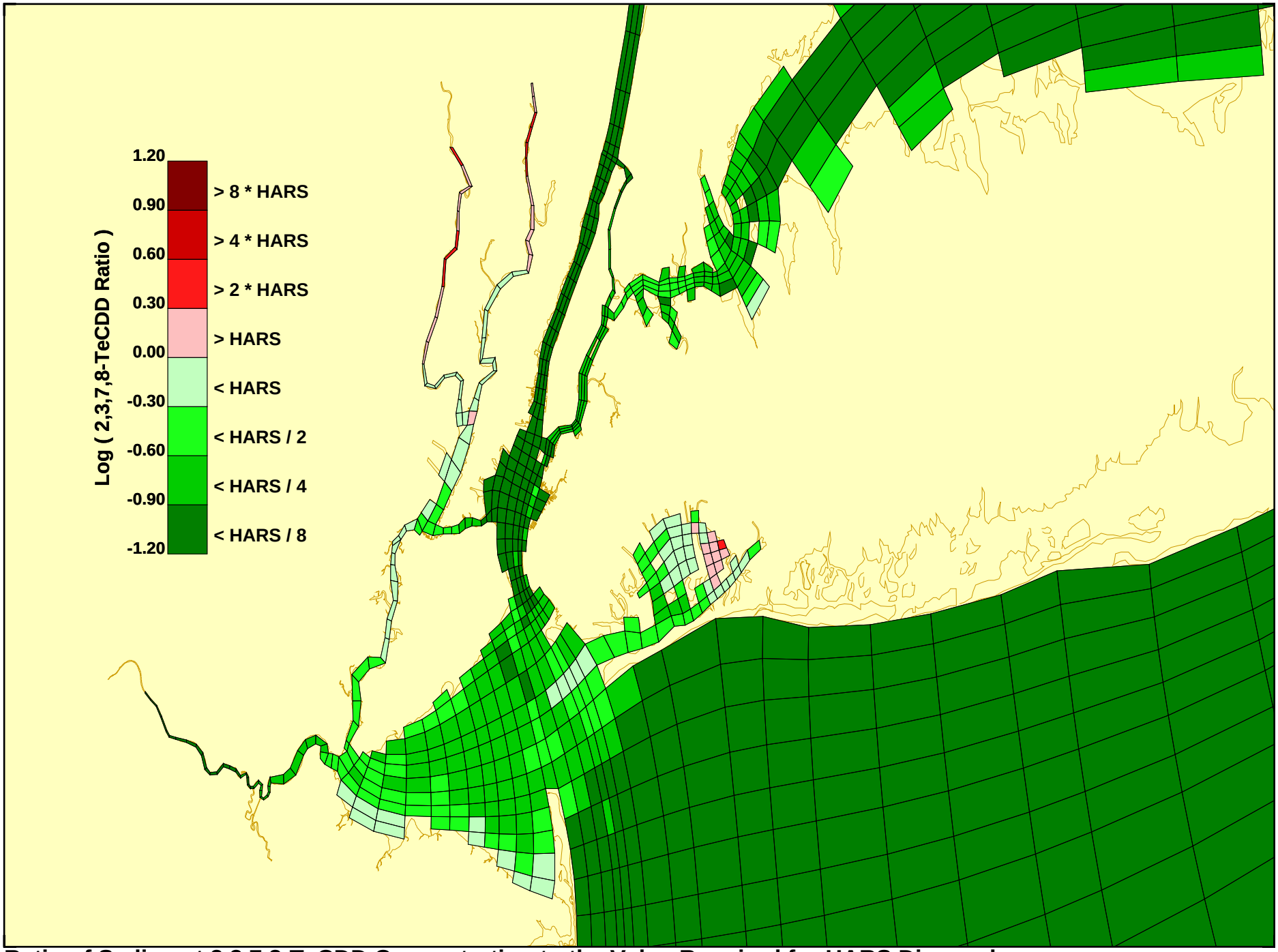

Ratio of Sediment 2,3,7,8-TeCDD Concentration to the Value Required for HARS Disposal Based on a BSAF of 0.17 (gm-DW / gm-WW) From CARP Data and a Worm Target Concentration of 1 ppt

Figure 13-17

Results for Year 37
Dredging in the Lower 7 Miles of the Passaic, End of Year 6

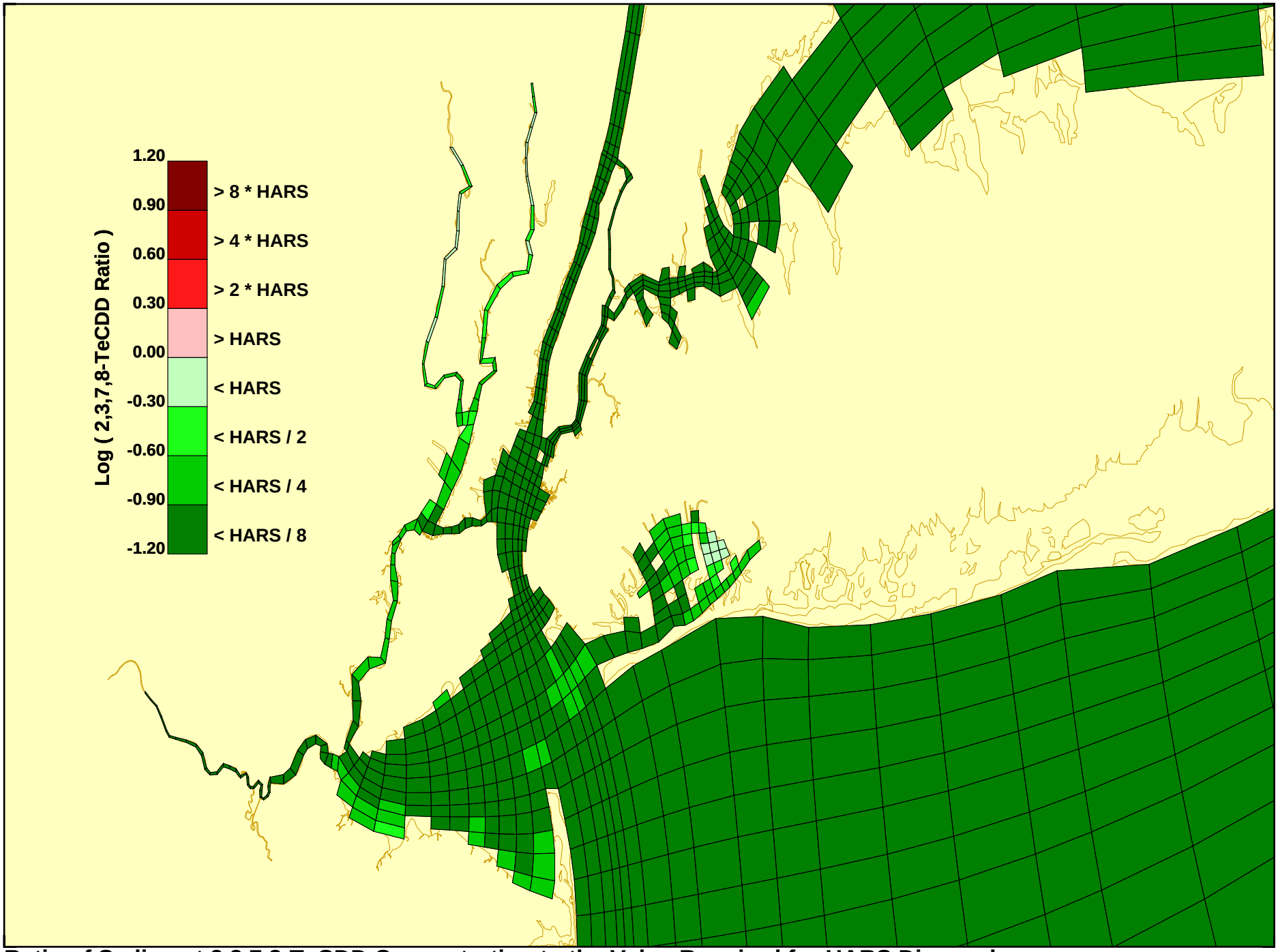

Ratio of Sediment 2,3,7,8-TeCDD Concentration to the Value Required for HARS Disposal
Based on a BSAF of 0.363 (gm-DW/gm-DW) From Schrock Data / 7 (gm-WW/gm-DW) = 0.052 (gm-DW/gm-WW) and a Worm Target Concentration of 1 ppt

Figure 13-18

Results for Year 37
Dredging in the Lower 7 Miles of the Passaic, End of Year 6

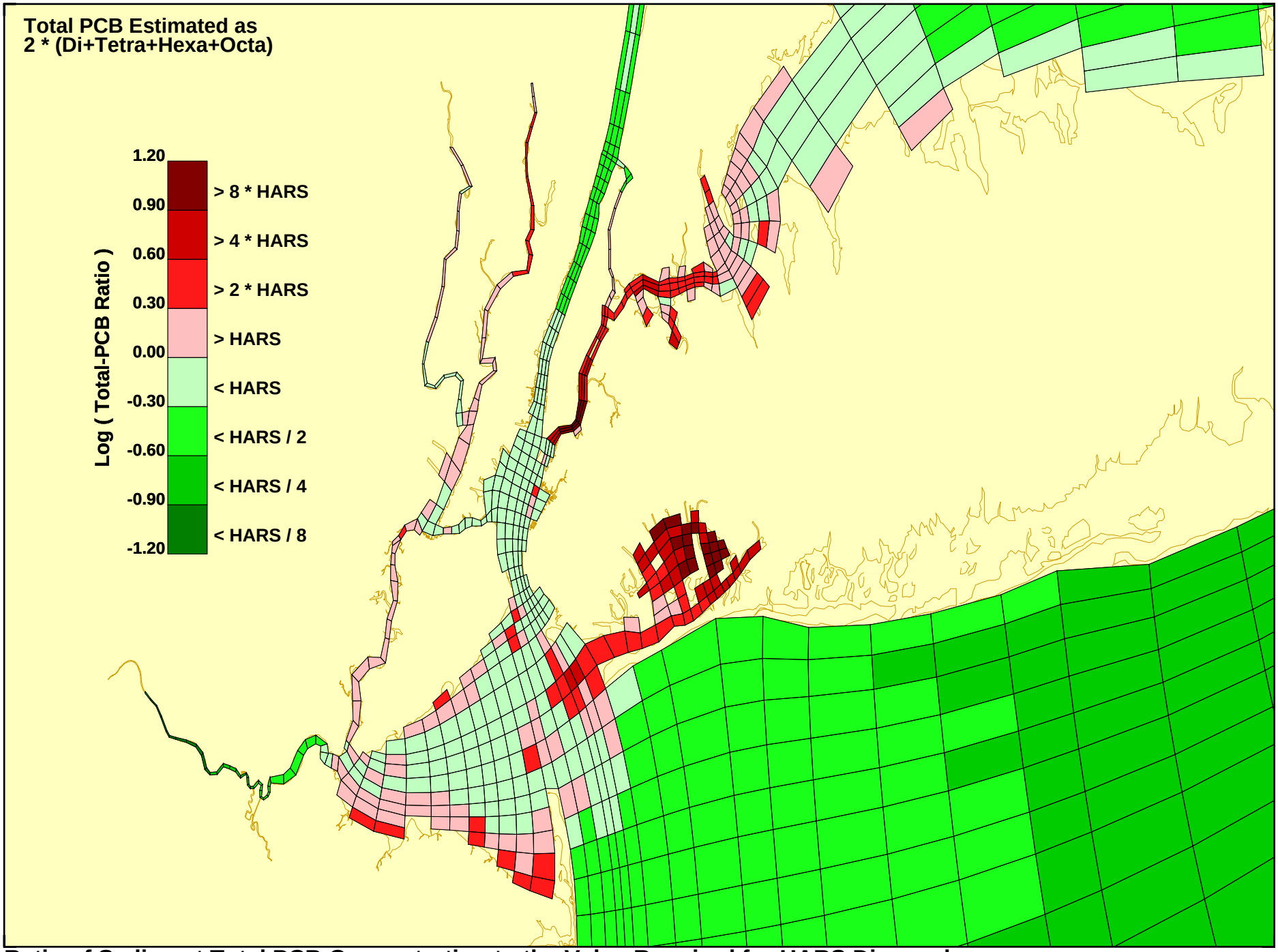

Ratio of Sediment Total PCB Concentration to the Value Required for HARS Disposal
Based on Di, Tetra, Hexa, and Octa BSAFs = 0.20, 0.97, 1.81, and 1.41 (gm-DW/gm-WW) from CARP Data and a Worm Target Concentration of 113 ppb (Interim HARS Non-Cancer)

Figure 13-19

Results for Year 37
Dredging in the Lower 7 Miles of the Passaic, End of Year 6

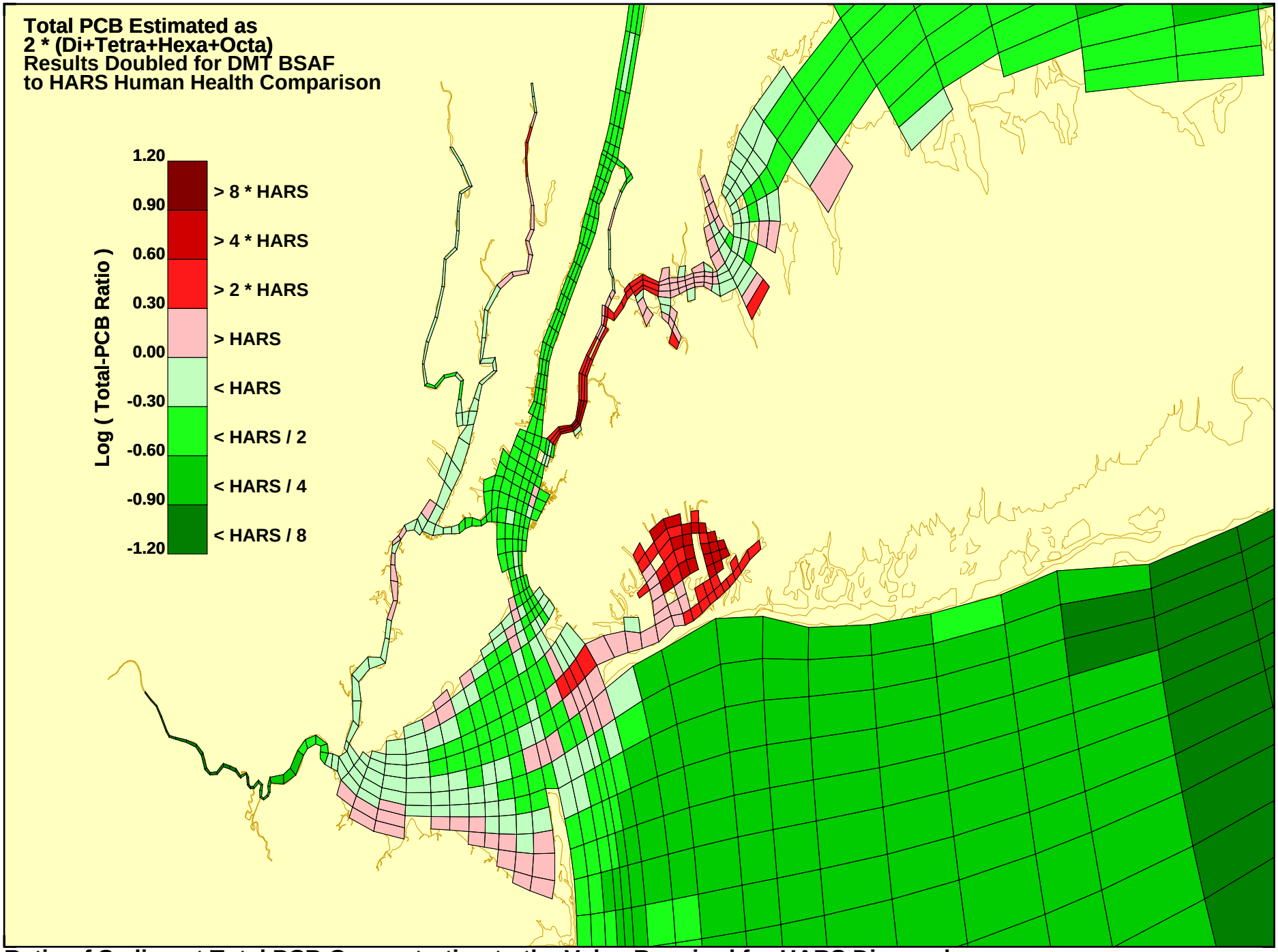

Ratio of Sediment Total PCB Concentration to the Value Required for HARS Disposal
Based on Di, Tetra, Hexa, and Octa BSAFs = 0.24, 0.30, 0.50, and 0.22 (gm-DW/gm-WW) from Reiss Data and a Worm Target Concentration of 113 ppb (Interim HARS Non-Cancer)

Figure 13-20

SECTION 14.0

REFERENCES

Adams, D. & Benyi, S. 2003. Final Report. Sediment Quality of the NY/NJ Harbor System: A 5-Year Revisit 1993/4 -1998. Investigation under the Regional Environmental Monitoring and Assessment Program (REMAP). *EPA/902-R-03-002.* USEPA-Region2, Division of Environmental Science and Assessment. Edison, New Jersey.

Aller, R.C. 1988. Benthic fauna and bio-geochemical processes in marine sediments: The role of burrow structures. Nitrogen cycling in coastal marine environments. New York, NY, Wiley, Chichester. 301-340.

Ayers, R.U., Ayres, L.W., Tarr, J.A., and Widgery, R.C. 1985. An historical reconstruction of major pollutant levels in the Hudson-Raritan Basin:1880-1980 Volume 1 Summary. March 1985 (Revised May, 1988). Prepared by Variflex Corporation for Martin-Marietta Environmental Systems (MMES) Grant #NA 83AA-D-00059 Ocean Assessments Division National Oceanographic and Atmospheric Administration. 99 pp.

Back, R., P. Gorski, L. Cleckner, and J. Hurley, 2003. Mercury content and speciation in the plankton and benthos of Lake Superior. *The Science of the Total Environment*, 304: 349-354.

Balcom, P.H., C.R. Hammerschmidt, W.F. Fitzgerald, C.H. Lamborg, J.S. O'Connor, submitted. Seasonal Distributions and Cycling of Mercury and Methylmercury in the waters of New York/New Jersey Harbor Estuary. *Mar. Chem.*

Balcom, P.H., W.F. Fitzgerald, G.M. Vandal, C.H. Lamborg, K.R. Rolfhus, C.S. Langer, C.R. Hammerschmidt, 2004. Mercury Sources and Cycling in the Connecticut River and Long Island Sound. *Mar. Chem.*, 90: 53-74.

Balzer, W., 1996. Particle mixing processes of Chernobyl fallout in deep Norwegian Sea sediments: Evidence for seasonal effects. *Geochim. Cosmochim. Acta* 60: 3425-3433.

Bamford, H.A., Offenberg, J.H., Larsen, R.K., Ko, F-C, and Baker, J.E., 1999. Diffusive exchange of polycyclic aromatic hydrocarbons across the air-water interface of the Patapsco River, an urbanized subestuary of the Chesapeake Bay. *Environ. Sci. Technol.* 33:2139-2144.

Bamford, H.A., Poster, D.L., Huie, R.E., and Baker, J.E., 2002. Using extra thermodynamic relationships to model the temperature dependence of Henry's Law constants of 209 PCB Congeners. *Environ. Sci. Technol.* 36:4395-4402.

Barber, M.C., Suarez, L.A., and Lassiter, R.R. 1991. Modelling bioaccumulation of organic pollutants in fish with an application to PCBs in Lake Ontario salmonids. *Can. J. Fish. Aquat. Sci.*, 48: 318-337.

Bath, D.W. and J.M. O'Connor, 1982. The biology of the white perch, *Morone americana*, in the Hudson River Estuary. *Fisheries Bulletin*, 80: 599-610.

Battelle Memorial Institute. 1996a. Evaluation of Dredged Material Proposed for Ocean Disposal from the Eastchester Project Area, New York. Technical report prepared for the U.S. Army Corps of Engineers New York District under service agreement with the U.S. Department of Energy under contract DE-AC06-76RLO 1830. Report PNNL-11232.

Battelle Memorial Institute. 1996b. Evaluation of Dredged Material Proposed for Ocean Disposal from Hudson River, New York. Technical report prepared for the U.S. Army Corps of Engineers New York District under service agreement with the U.S. Department of Energy under contract DE-AC06-76RLO 1830. Report PNNL-11342.

Battelle Memorial Institute. 1996c. Evaluation of Dredged Material Proposed for Ocean Disposal from Westchester Creek Project Area, New York. Technical report prepared for the U.S. Army Corps of Engineers New York District under service agreement with the U.S. Department of Energy under contract DE-AC06-76RLO 1830. Report PNNL-11404.

Battelle Memorial Institute. 1996d. Evaluation of Dredged Material Proposed for Ocean Disposal from Bronx River Project Area, New York. Technical report prepared for the U.S. Army Corps of Engineers New York District under service agreement with the U.S. Department of Energy under contract DE-AC06-76RLO 1830. Report PNNL-11443.

Battelle Memorial Institute. 1996e. Evaluation of Dredged Material Proposed for Ocean Disposal from Federal Projects in New York and New Jersey and the Military Ocean Terminal (MOTBY) Technical report prepared for the U.S. Army Corps of Engineers New York District under service agreement with the U.S. Department of Energy under contract DE-AC06-76RLO 1830. Report PNNL-11280.

Benoit, J., Gilmour, C., Mason, R. and Heyes, A., 1999. Sulfide Controls on Mercury Speciation and Bioavailability to Methylating Bacteria in Sediment Pore Waters. Environmental Science and Technology, 33: 951-957.

Blasland, Bouck and Lee, Inc. 1997. *Summary of Lower Fox River IPX Model Review by Blasland, Bouck, and Lee, Inc.* Syracuse, New York.

Bopp, R.F., S.N. Chillrud, A.E. Kroenke, D.A. Chaky, E.L. Shuster, F.D. Estabrooks, and J. Swart. Mercury Deposition in Sediments of the NY/NJ Harbor Area. Manuscript in preparation.

Bopp, R. F., S.N. Chillrud, E.L. Shuster, and H.J. Simpson, 2006. Contaminant Chronologies from Hudson River Sedimentary Records. In, *The Hudson River Estuary*, J. Levinton and J. Waldman eds., 26: 383-397, Cambridge University Press.

Bopp, R.F., et al. 1991. A Major Incident of Dioxin Contamination: Sediments of New Jersey Estuaries. *Environ. Sci. Technol.* 25(5): 951-956.

Bopp, R.F., et al. 1982. Chlorinated Hydrocarbons and Radionuclide Chronologies in Sediments of the Hudson River and Estuary, New York. *Environ. Sci. Technol.* 16(10): 666-675.

Borchardt, T., 1983. Influence of Food Quantity on the Kinetics of Cadmium Uptake and Loss via Food and Seawater in Mytilus edulis," *Marine Biology*, 76: 67-76.

Borchardt, T., 1985. Relationships Between Carbon and Cadmium Uptake in Mytilus edulis. *Marine Biology*, 85: 233-244.

Boudreau, B.P., 1994. Is burial velocity a master parameter for bioturbation?: *Geochim. Cosmochim. Acta.* 58: 1243-1249.

Brievik, K., Sweetman, A., Pacyna, J.M., and Jones, K.C. 2002a. Towards a global historical emission inventory for selected PCB congeners - a mass balance approach 1. Global production and consumption. *The Science of the Total Environment*, 290: 181-198.

Brievik, K., Sweetman, A., Pacyna, J.M., and Jones, K.C. 2002b. Towards a global historical emission inventory for selected PCB congeners - a mass balance approach 2. Emissions. *The Science of the Total Environment*, 290: 199-224.

Broman, D., C. Naf, C. Rolff and Y. Zebuhr. 1991. Occurrence and dynamics of polychlorinated dibenzo-p-dioxins and dibenzofurans and polycyclic aromatic hydrocarbons in the mixed surface layer of remote coastal and offshore waters of the Baltic. *Environ. Sci. Technol.,* 25: 1850-1864.

Burkhard, L.P. and D.W. Kuehl. 1986. N-octanol/water partition coefficients by reverse phase liquid chromatography/mass spectrometry for eight tetrachlorinated planar molecules. *Chemosphere*, 15: 163-167.

Burkhard, L. P. 1998. Comparison of two models for predicting bioaccumulation of hydrophobic organic chemicals in a Great Lakes food web. *Environ. Toxicol. Chem.* 17(3): 383-393.

Burkhard, L.P. 2000. Estimating dissolved organic carbon partition coefficients for nonionic organic chemicals. Environ. Sci. Technol. 34(22):4663-4668.

Caplow, T., Schlosser, P., Ho, D.T., and Enriquez, R.C. 2004. Effect of Tides on Solute Flushing from a Strait: Imaging Flow and Transport in the East River with SF_6. *Environ. Sci. Technol.* 38: 4562-4571.

Caplow, T., Schlosser, P., Ho, D.T., and Santella, N. 2003. Transport Dynamics in a Sheltered Estuary and Connecting Tidal Straits: SF_6 Tracer Study in New York Harbor. *Environ. Sci. Technol.* 37:5116-5126.

Chaky, D.A. 2003. *Polychlorinated Biphenyls, Polychlorinated Dibenzo-P-Dioxins and Furans in the New York Metropolitan Area: Interpreting Atmospheric Deposition and Sediment Chronologies.* Doctoral thesis. Rensselaer Polytechnic Institute, Troy, New York. 431 pp.

Chillrud, S.N. 1996. *Transport and Fate of Particle Associated Contaminants in the Hudson River Basin.* Doctoral thesis. Columbia University, New York, New York. 277 pp.

Ciffroy, P., Garnier, J., and Benyahya, L. 2003. Kinetic partitioning of Co, Mn, Cs, Fe, Ag, Zn and Cd in waters (Loire) mixed with brakish waters (Loire estuary): experimental and modelling approaches. *Marine Pollution Bulletin* 46: 626-641.

Clark, J.F., Schlosser, P., Stute, M., and Simpson, H.J. 1996. SF_6-^{3}HE tracer release experiment: A new method for determining longitudinal dispersion coefficients in large rivers. *Environ. Sci. Technol.* 30:1527-1532.

Compeau, G. and Bartha, R., 1984. Methylation and Demethylation of Mercury Under Controlled Redox, pH, and Salinity Conditions. *Applied and Environmental Microbiology*, 48(6): 1203-1207.

Connell, D.B. and J.G. Sanders, 1999. Variation in Cadmium Uptake by Phytoplankton and Transfer to the Copepod Eurytemora affinis. *Marine Biology*, 133: 259-265.

Connolly, J.P. and R. Tonelli, 1985. Modeling Kepone in the striped bass food chain of the James River Estuary. *Estuarine, Coastal and Shelf Sciences*, 20: 349-366.

Connolly, J.P. 1991. Users Guide for WASTOX2, Version 2.51. Manhattan College, Riverdale, NY.

Connolly, J.P. & Thomann, R.V. 1985. WASTOX, A Framework for Modeling the Fate of Toxic Chemicals in Aquatic Environments: Part 2 Food Chain. Manhattan College, Riverdale, NY.

Dankwerts, P.V. 1951. Significance of liquid-film coefficients in gas absorption. *Ind. Eng. Chem.* 43:1460-67.

DiToro, D.M., J.J. Fitzpatrick, and R.V. Thomann. 1981. (Rev. 1983) Water Quality Analysis Simulation Program (WASP) and Model Verification Program (MVP) Documentation. Report prepared for USEPA Duluth, MN. Contract No. 68-01-3872. Hydroscience, Inc.

DiToro, D.M. & Paquin, P.R. 1984. Time variable model of the fate of DDE and lindane in a quarry. *Environ. Toxicol. Chem.* 3: 335-353.

Elliott, A.H. 1990. Transfer of solutes into and out of streambeds. PhD Thesis. California Institute of Technology, Pasadena, CA.

Eitzer, B.D. and Hites, R.A. 1989. Atmospheric Transport and Deposition of Polychlorinated Dibenzo-p-dioxins and Dibenzofurans. *Environ. Sci. Technol.*, 23: 1396-1401.

EMEP/MSC-E. 1998. Long-Range Transport of Selected POPs, PART II: Physical-Chemical Properties of Dioxins and Furans and Factors Influencing the Transport and Accumulation of Persistent Organic Pollutants. August 1998 report

Farley, K.J., R.V. Thomann, T.F. Cooney III, D.R. Damiani, and J.R. Wands. 1999. An Integrated Model of Organic Chemical Fate and Bioaccumulation in the Hudson River Estuary. Final Report prepared for the Hudson River Foundation. Manhattan College, Riverdale, NY.

Farley, K.J., Wands, J.R., Damiani, D.R. and Cooney T.F., 2006. Transport, Fate and Bioaccumulation of PCBs in the Lower Hudson River, in The Hudson River Ecosystem, J. Levington, (Ed).

Florida Department of Environmental Protection, 2003.

Gagne, A.Y. 2006. Atmospheric Mercury Deposition in Lakes of the Adirondacks, New York. M.S. Thesis, Rensselaer Polytechnic Institute, pp 184.

Gardinier, M.N. and T.B. Hoff, 1982. Diet of striped bass in Hudson River Estuary. *New York Fish Game Journal*, 29: 152-165.

George, S. G. and T. L. Coombs 1977. The Effects of Chelating Agents on the Uptake and Accumulation of Cadmium by Mytilus edulis. *Marine Biology* 39: 261-268.

Gerino, M., R.C. Aller, et al. 1998. "Comparison of different tracers and methods used to quantify bioturbation during a spring bloom: 234-thorium, luminophores and chlorophyll a." *Estuarine Coastal and Shelf Sci.*, 46: 531-547.

Gioia, R. In preparation. The New Jersey Atmospheric Deposition Network: Atmospheric Concentrations and Deposition of Organo-Chlorine Pesticides to the Hudson River Estuary. Final report to the Hudson River Foundation.

Gobas, F.A.P.C., Zhang, X., and Wells, R., 1993. Gastrointestinal magnification: The mechanism of biomagnification and food chain accumulation of organic chemicals. *Environ. Sci. Technol.*, 17(13): 2855-2863.

Gobas, F.A.P.C., Muir, O.C.G., and Mackay, D. 1988. Dynamics of dietary bioaccumulation and fecal elimination of hydrophobic organic chemicals in fish. *Chemosphere,* 17: 943-962.

Griscom, S. B., N. S. Fisher, et al. 2002. Kinetic modeling of Ag, Cd and Co bioaccumulation in the clam Macoma balthica: quantifying dietary and dissolved sources. Marine Ecology Progress Series 240: 127-141.

Griscom, S. B. and N. S. Fisher 2002. Uptake of Dissolved Ag, Cd, and Co by the Clam, Macoma balthica: Relative Importance of Overlying Water, Oxic Pore Water, and Burrow Water. *Environmental Science and Technology* 36: 2471-2478.

Hairr, L. 1974. An investigation of factors influencing radiocesium cycling in estuarine sediments of the Hudson River. Ph.D. Thesis, New York University, New York, 183pp.

Haitzer, M., Aiken, G. and Ryan, J. 2003. Binding of Mercury(II) to Aquatic Humic Substances: Influence of pH and Source of Humic Substances. *Environmental Science and Technology*, 37: 2436-2441.

Hammerschmidt, C.R., W.F. Fitzgerald, submitted. Sediment-water Exchange of Methylmercury Determined from Shipboard Benthic Flux Chambers. *Mar. Chem.*

Hammerschmidt, C.R., W.F. Fitzgerald, 2006a. Bioaccumulation and Trophic Transfer of Methylmercury in Long Island Sound. *Arch. Environ. Contam. Toxicol.*, 51: 416-424.

Hammerschmidt, C.R., W.F. Fitzgerald, P.H. Balcom, P.T. Visscher, submitted. Organic Matter and Sulfide Inhibit Methylmercury Production in Coastal Marine Sediments, *Mar. Chem.*

Hammerschmidt, C. and Fitzgerald, W., 2004. Geochemical Controls on the Production and Distribution of Methylmercury in Near-Shore Marine Sediments. Environmental Science and Technology, 38: 1487-1495.

Hawker, D.W., and Connell, D.W. 1988. Octanol-water partition coefficients of polychlorinated biphenyl congeners. *Environ Sci. Technol.* 22:382-387.

Hetling. L., et al. 1978. *Summary of Hudson River PCB Study Results.* NYSDEC Technical Paper #51, April 1978. 88 pp.

Heyes, A., R.P. Mason, E.-H. Kim, E. Sunderland, 2006. Mercury Methylation in Estuaries: Insights from Using Measuring Rates using Stable Mercury Isotopes, *Mar. Chem.*, 102: 134-147.

Heyes, A., Miller, C. and Mason, R., 2004. Mercury and methylmercury in Hudson River sediment: impact of tidal resuspension on partitioning and methylation. *Marine Chemistry*, 90: 75-89.

Hilal, S.H., et al. 1994. Estimation of Chemical Reactivity and Parameters and Physical Properties of Organic Molecules Using SPARC, p. 291-353. In: *Quantitative Treatments of Solute/Solvent Interactions: Theoretical and Computational Chemistry* Vol. 1, Politzer, P. and Murray, J. S, Editors. Elsevier, Amsterdam.

Ho, D.T., Schlosser, P., and Caplow, T. 2002. Determination of Longitudinal Dispersion Coefficient and Net Advection in the Tidal Hudson River with a Large-Scale, High Resolution SF_6 Tracer Release Experiment. *Environ. Sci. Technol.* 36: 3234-3241.

HydroQual, 2007a. A model for the evaluation and management of contaminants of concern in water, sediment, and biota in the NY/NJ harbor estuary. Hydrodynamic sub-model. Report prepared for the Hudson River Foundation on behalf of the Contaminant Assessment and Reduction Project (CARP). 552 pp.

HydroQual, 2007b. A model for the evaluation and management of contaminants of concern in water, sediment, and biota in the NY/NJ harbor estuary. Sediment Transport/Organic Carbon Production Sub-model. Report prepared for the Hudson River Foundation on behalf of the Contaminant Assessment and Reduction Project (CARP).

Jackson, D.R., M.H. Roulier, H.M. Grotton, S.W. Rust, J.S. Warner, M.F. Arthur and F.L. DeRoos. 1985. Leaching potential of 2,3,7,8-TCDD in contaminated soils. In: Land Disposal of Hazardous Waste, Proceedings of the eleventh annual research symposium. EPA/600/9-85/013. pp. 153-168.

Janssen, H.H. and Scholz, N., 1979. Uptake and cellular distribution of cadmium in *Mytilus edulis*. *Marine Biology*, 55: 133-141.

Jinks, S.M. and Wrenn, M.E. 1976. Radiocesium Transport in the Hudson River Estuary. In: *Environmental toxicity of aquatic radionuclides: models and mechanisms. Proceedings of the 8th Rochester International Conference on Environmental Toxicity 1975*. Miller, M.W. and Stannard, J.N, eds. Ann Arbor Science, Ann Arbor Michigan. pp. 207- 227.

Kainz, M., M. Lucotte and C. Parrish, 2002. Methyl Mercury in Zooplankton – The Role of Size, Habitat and Food Quality. *Canadian Journal of Fisheries and Aquatiac Sciences*, 59: 1606-1615.

Kelly, B.C., F.A.P.C. Gobas and M.S. McLachlan. 2004. Intestinal Absorption and Biomagnification of Organic Contaminants in Fish, Wildlife and Humans. *Environ. Toxicol. Chem.*, 23: 2324-2336.

Kerin, E.J., C.C. Gilmour, E. Roden, M.T. Suzuki, J.D. Coates, R.P. Mason, 2006. Mercury Methylation by Dissimilatory Iron-reducing Bacteria, *Appl. Environ. Microbiol.*, 72: 7919-7921.

King, J., Kostka, J., Frischer, M. and Saunders, F., 2000. Sulfate-Reducing Bacteria Methylate Mercury at Variable Rates in Pure Culture and in Marine Sediments. *Applied and Environmental Microbiology*, 66(6): 2430-2437.

King, J., Kostka, J., Frischer, M., Saunders, F. and Jahnke, R., 2001. A Quantitative Relationship that Demonstrated Mercury Methylation Rates in Marine Sediments are Based on the Community Composition and Activity of Sulfate-Reducing Bacteria. *Environmental Science and Technology*, 35: 2491-2496.

King, J., Saunders, F., Lee, R. and Jahnke, R., 1999. Coupling Mercury Methylation Rates to Sulfate Reduction Rates in Marine Sediments. Environmental Toxicology and Chemistry, 18(7): 1362-1369.

Kroenke, A.E., 2003. Atmospheric Mercury Deposition to Sediments of New Jersey and Southern New York State: Interpretations from Dated Sediment Cores. Ph.D. Thesis, Rensselaer Polytechnic Institute, pp 283.

Lambertsson, L., M. Nilsson, 2006. Organic material: The primary Control on Mercury Methylation and Ambient Methyl Mercury Concentrations in Estuarine Sediments, *Environ. Sci. Technol.*, 40: 1822-1829.

Leo, A. and D. Weininger. 1989. CLOGP version 3.54 for VAX-11. Medicinal Chemistry Project, Pomona College, Claremont, CA.

Li, N. Wania, F., Lei, Y., and Daly, G. 2003. A comprehensive and critical compilation, evaluation, and selectyion of physical-chemical property data for selected polychlorinated biphenyls. *J. Phys. Chem. Ref. Data*, 32(4): 1545-1590.

Limno-Tech, Inc. 1998. *Fox River and Green Bay PCB Fate and Transport Model Evaluation: Technical Memorandum 4a - Alternative Sediment Bed Handling in IPX Lower Fox River Model.* AnnArbor, MI.

Linsalata, P. 1984. Sources, distribution, and mobility of plutonium and radiocesium in soils, sediments and water of the Hudson River estuary and watershed. Ph.D. thesis, New York University, New York, NY. 401pp.

Linsalata, P., Simpson, H.J., Olsen, C.R., Cohen, N., and Trier, R.M. 1985. Plutonium and radiocesium in the water column of the Hudson River estuary. *Environ Geol Water Sci.* 7(4):193-204.

Litten, S. 2003. Contaminant Assessment and Reduction Project (CARP) Water. Draft Final Report. Prepared by NYSDEC Division of Water Bureau of Water Assessment and Management.

Litten, S. 2005. PCDD/Fs and PCBs in Stormwater. Final Stormwater Toxics Report. New York State Department of Environmental Conservation. 14 pp.

Lodge, K.B. and P.M. Cook. 1989. Partitioning studies of dioxin between sediment and water: The measurement of K_{oc} for Lake Ontario sediment. *Chemosphere*, 19: 439-444.

Lohmann, R., Macfarlane, J.K., and Gschwend, P.M. 2005. Importance of black carbon to sorption of native PAHs, PCBs, and PCDDs in Boston and New York Harbor Sediments. *Environ. Sci. Technol.,* 39: 141-148.

Mason, R., J. Laport and S. Andres, 2000. Factors Controlling the Bioaccumulation of Mercury, Methylmercury, Arsenic, Selenium, and Cadmium by Freshwater Invertabrates and Fish. *Arch. Environ. Contam. Toxicol.*, 38: 283-297.

Mason, R., J. Reinfelder and F. Morel, 1996. Uptake, Toxicity and Trophic Transfer of Mercury in a Coastal Diatom. *Environmental Science and Technology*, 30: 1835-1845.

Marple, L., B. Berridge and L. Throop. 1986b. Measurement of the water-octanol partition coefficient of 2,3,7,8-tetrachlorobenzo-p-dioxin. *Environ. Sci. Technol.*, 20: 397-399.

Marvin-DiPasquale, M. et al., 2000. Methyl-Mercury Degradation Pathways: A Comparison among Three Mercury-Impacted Ecosystems. *Environmental Science and Technology*, 34(23): 4908-4916.

Matisoff, G., 1982. Mathematical Models of Bioturbation. Animal-Sediment Relations. The Biogenic Alteration of Sediments. New York, Plenum Press. 289-330.

Martell, A., Smith, R., and Motekaitis, R. 2004. NIST Critically Selected Stability Constants of Metal Complexes Database, Version 8, U.S. Department of Commerce, Gaithersburg, MD.

Meador, J.P., Adams, N.G., Casillas, E., and Bolton, J.L. 1997. Comparative bioaccumulation of chlorinated hydrocarbons from sediment by two infaunal invertebrates. *Arch. Environ. Contam. Toxicol.*, 33: 388-400.

Mersch, J., Morhain, E., and Mouvet, C. 1993. Laboratory accumulation of copper and cadmium in freshwater mussel *Dreissina polymorpha* and the aquatic moss *Rhynchostegium riparioides*. *Chemosphere*, 27(8): 1475-1485.

Miller, C.L., R.P. Mason, C.C. Gilmour, and A. Heyes. 2007. Influence of Dissolved Organic Matter on the Complexation of Mercury under Sulfidic Conditions. *Environmental Toxicology and Chemistry*. 26(4): 624-633.

Miller, M.M., S.P. Waslk, G.L. Huang, W.Y. Shiu and D. Mackay. 1985. Relationships between octanol-water partition coefficient and aqueous solubility. *Environ. Sci. Technol.*, 19: 522-529.

Mulholland, P.J. and Olsen, C.R. 1992. Marine Origin of Savannah River Estuary Sediments: Evidence from Radioactive and Stable Isotope Tracers. *Estuarine, Coastal, and Shelf Science.* 34:95-107.

McKim, J., Schmieder, P., and Veith, G. 1985. Absorption dynamics of organic chemical transport across trout gills as related to octanol-water partition coefficient. *Toxicol. Appl. Pharmacol.*, 77: 1-10.

O'Connor, D.J. and Dobbins, W.E. 1958. Mechanisms of reaeration in natural streams. *Transactions ASCE*. 641:123.

O'Connor, J.M., 1984. PCBs: Dietary dose and burdens in striped bass from the Hudson River. *Northeastern Environmental Science*, 3(3/4): 152-158.

O'Driscoll, N. and Evans, R. 2000. Analysis of Methyl Mercury Binding to Freshwater Humic and Fulvic Acids by Gel Permeation Chromatography/Hydride Generation ICP-MS. *Environmental Science and Technology*, 34: 4039-4043.

Olsen, C.R., Larsen, I.L., Brewster, R.H., Cutshall, N.H., Bopp, R.F., and Simpson, H.J. 1984. A Geochemical Assessment of Sedimentation and contaminant Distributions in the Hudson-Raritan Estuary. NOAA Technical Report NOS OMS 2. 101 pp.

Olsen, C.R. 1979. Radionuclides, sedimentation, and the accumulation of pollutants in the Hudson estuary. Ph.D. thesis, Columbia University, New York, N.Y. 343 pp.

Oremland, R., Culbertson, C. and Winfrey, M., 1991. Methylmercury Decomposition in Sediments and Bacterial Cultures: Involvement of Methanogens and Sulfate Reducers in Oxidative Demethylation. *Applied and Environmental Microbiology*, 57(1): 130-137.

Oremland, R., Miller, L., Dowdle, P., Connell, T. and Barkay, T., 1995. Methylmercury Oxidative Degradation Potentials in Contaminated and Pristine Sediments of the Carson River, Nevada. *Applied and Environmental Microbiology*, 61(7): 2745-2753.

Pak, K. and Bartha, R., 1998. Mercury Methylation by Interspecies Hydrogen and Acetate Transfer between Sulfidogens and Methanogens. *Applied and Environmental Microbiology*, 64(6): 1987-1990.

Park, R.A., 1998. AQUATOX for Windows: A Modular Toxic Effects Model for Aquatic Ecosystems, Eco Modeling, Montgomery Village, MD.

Poissant, L., Amyot, M., Pilote, M. and Lean, D. 2000. Mercury Water-Air Exchance over the Upper St. Lawrence River and Lake Ontario. *Environmental Science and Technology*, 34: 3069-3078.

Poje, G.V., S.A. Riordan and J.M. O'Connor, 1988. Food habits of the amphipod *Gammarus tigrinus* in the Hudson River and the effects of diet upon its growth and reproduction, p. 255-270. In C.L. Smith (Ed.), Fisheries Research in the Hudson River, State University of New York Press, Albany, NY.

Post, J., R. Vandenbos and D. McQueen, 1996. Uptake rates of food-chain and waterborne mercury by fish: field measurements, a mechanistic model, and an assessment of uncertainties. *Canadian Journal of Fisheries and Aquatic Science*, 53: 395-407.

Reinfelder, J.R., L.A. Totten, and S.J. Eisenreich, 2004. The New Jersey Atmospheric Deposition Network (NJADN). Final Report to the New Jersey Department of Environmental Protection.

Rice, C.A., Plesha, P.D., Casillas, E., Misitano, D.A., and Meador, J.P. 1995. Growth and survival of three marine invertebrate species in sediments from the Hudson-Raritan estuary, New York. *Environ. Toxicol. Chem.*, 14(11): 1931-1940.

Roditi, H. A., N. S. Fisher, et al. 2000. Field Testing a Metal Bioaccumulation Model for Zebra Mussels. *Environmental Science and Technology* 34(13): 2817-2825.

Rolfhus, K.R. and Fitzgerald, W.F. 2001. The Evasion and Spatial/Temporal Distribution of Mercury Species in Long Island Sound, CT-NY. *Geochim. Cosmochim, Acta.* , 65(3): 407-418.

Schluter, M., Sauter, E., et al. 2000. Seasonal variations of bioirrigation in coastal sediments: Modeling of field data. *Geochim. Cosmochim. Acta* 64: 821-834.

Schmolke, S. et al. 1998. Estimates of the Air-Sea Exchange of Mercury Derived from Summer and Winter measurements. MAST Project BASYS., Poster; Second Annual Science Conference 23.-25.09.1998, University Stockholm, Sweden, EU.

Schrock, M.E., Barrows, E.S., and Rosman, L.B. , 1997. Biota-to-Sediment Accumulation Factors for TCDD and TCDF in Worms from 28-Day Bioaccumulation Tests. *Chemosphere*, 34(5-7): 1333-1339.

Schwarzenbach, R.P., Gschwend, P.M., and Imboden, D.M. 1993. *Environmental Organic Chemistry*. John Wiley & Sons, Inc. New York, New York.

Selck, H., V.E. Forbes, and T.L. Forbes, 1998. Toxicity and Toxicokinetics of Cadmium in Capitella Sp. I: Relative Importance of Water and Sediment as Routes of Cadmium Uptake. *Marine Ecology Progress Series*, 164: 167-178.

Sellers, P., Kelly, C., Rudd, J. and MacHutchon, A., 1996. Photodegradation of Methylmercury in Lakes. *Nature*, 380: 694-697.

Setzler, E.M., W.R. Boynton, K.V. Wood, H.H. Zion, L. Lubbers, N.K. Mountford, P. Fere, L. Tucker and J.A. Mihursky. 1980. Synopsis of biological data on striped bass, *Morone saxatilis* (Waldbaum). NMFS Cir. 433, FAO Synopsis No. 121, U.S. Department of Commerce, Rockville, MD.

Shlu, W.Y., W. Doucette, F.A.P.C. Gobas, A. Andren, and D. Mackay. 1988. Physical-Chemical Properties of Chlorinated Dibenzo-p-dioxins. *Environ. Sci. Technol.*, 22: 651-658.

Sijm, D.T.H.M., H. Wever, P.J. de Vries and A. Opperhuizen. 1989. Octan-1-ol/water Coefficients of Polychlorinated Dibenzo-p-dixoins and Dibenzofurans: Experimental Values Determined with a Stirring Method. *Chemosphere*, 19: 263-266.

Skoglund, R.S. and D.L. Swackhamer. 1999. Evidence for the use of organic carbon as the sorbing matrix in the modeling of PCB accumulation in phytoplankton. *Environ. Sci. Technol.*, 33: 1516-1519.

Smith, D., Bell, R., Valliant, J. and Kramer, J. 2003. Determination of Strong Ligand Sites in Natural Waters by Competitive Ligand Titration with Silver. *Environmental Science and Technology*, Submitted.

Smith, D., Bell, R., Valliant, J. and Kramer, J., 2004. Determination of Strong Ligand Sites in Sewage Effluent-Impacted Waters by Competitive Ligand Titration with Silver. *Environmental Science and Technology*, 38(7): 2120-2125.

Sobek, A., Gustafsson, O., Hajdu, S., and Larsson, U. 2004. Particle-Water partitioning of PCBs in the photic zone: a 25-month study in the open Baltic Sea. *Environ. Sci. Technol.* 38:1375-1382.

Sunderland, E.M., F.A.P.C. Gobas, B.A. Branfireun, A. Heyes, 2006. Environmental Controls on the Speciation and Distribution of Mercury in Coastal Sediments. *Mar. Chem.*, 102: 111-123.

TAMS Consultants, Inc. 2005. The Hudson River PCB Reassessment Database. Phase 2 High Resolution cores. Electronic files provided upon request from Mr. Edward Garvey. TetraTech, 1999.

Thomann, R.V., and Connolly, J.P. 1984. Model of PCB in the Lake Michigan trout food chain. *Environ. Sci. Technol.*, 18(2): 65-71..

Thomann, R.V., Mueller, J.A., Winfield, R.P., and Huang, C. 1989. Mathematical Model of the Long-Term Behavior of PCBs in the Hudson River Estuary. Report prepared for the Hudson River Foundation. Grant Nos. 007/87A/30 and 011/88A/030. 8 chapters and appendices.

Thomann, R.V., Mueller, J.A., Winfield, R.P., and Huang, C. 1991. Model of fate and accumulation of PCB homologues in Hudson Estuary. *Journal of Environmental Engineering*, 117(2): 1651-178.

Thomann, R.V., J.P. Connolly and T.F. Parkerton. 1992a. An equilibrium model of organic chemical accumulation in aquatic food webs with sediment interaction. *Environmental Toxicology and Chemistry*, 11: 615-629.

Thomann, R.V., J.P. Connolly and T.F. Parkerton. 1992b. Modeling accumulation or organic chemicals in aquatic food webs, p. 153-186. In F.A.P.C. Gobas and J.A. McCorquodale (Eds.), Chemical Dynamics in Fresh Water Ecosystems, Lewis Publishers, Chelsea, MI.

Tipping, E. 1994. WHAM- A Chemical Equilibrium Model and Computer Code for Waters, Sediments and Soils Incorporating a Discrete Site/Electrostatic Model of Ion Binding by Humic Substances. *Comp. Geosci.*, 20: 973-1023.

Tipping, E. 1998. Humic Ion-Binding Model VI: An Improved Description of the Interactions of Protons and Metal Ions with Humic Substances. *Aquat. Geochem.*, 4: 3-48.

Totten, L.A., et al. In press. The New Jersey Atmospheric Deposition Network: Atmospheric Concentrations and Deposition of PCBs to the Hudson River Estuary.

Tseng, C.M., Balcom, P.H., Lamborg, C.H., and Fitzgerald, W.F. 2003. Dissolved Elemental Mercury Investigations in Long Island Sound using On-line Au Amalgamation-flow Injection Analysis, *Environ. Sci. Technol.*, 37: 1183-1188.

Turner, A. and Millward, G.E. 1994. Partitioning of Trace Metals in a Macrotidal Estuary. Implications for Contaminant Transport Models. *Estuarine, Coastal and Shelf Science.* 39:45-58.

U.S. EPA. 1993. Interim report on data and methods for assessment of 2,3,7,8-tetrachlorodibenzo-p-dioxin risks to aquatic life and associated wildlife. EPA/600/R-93/055. Office of Research and development, Duluth, MN.

U.S. EPA. 2005. *Contaminated Sediment Remediation Guidance for Hazardous Waste Sites.* EPA-540-R-05-012. OSWER 9355.0-85. Available to download at http://www.epa.gov/superfund/resources/sediment/guidance.htm, 236p.

van der Linde, A., Jhendriks, A.J., and Sijm, D.T.H.M. 2001. Estimating biotransformation rate constants of organic chemicals from modeled and measured elimination rates. *Chemosphere*, 44: 423-435.

Waldman, J.R. 1988. 1986 Hudson River striped bass tag recovery program. Hudson River Foundation, New York, NY.

Waldman, J.R., D.J. Dunning, Q.E. Ross, and M.T. Mattson. 1990. Range dynamics of Hudson River striped bass along the Atlantic coast. *Transactions of the American Fisheries Society*, 119: 910-919.

Walters, R.W., S.A. Ostaeski and A. Guiseppi-Elie. 1989. Sorption of 2,3,7,8-tetrachlorodizenzo-p-dioxin from water by surface soils. *Environ. Sci. Technol.*, 23: 480-484.

Wang, W. and N. Fisher, 1998a. Accumulation of Trace Elements in a Marine Copepod. *Limnol. Oceanogr.*, 43(2): 273-283.

Wang, W. and N. Fisher, 1998b. Excretion of Trace Elements by Marien Copepods and their Bioavailability to Diatoms. *Journal of Marine Research*, 56: 713-729.

Wang, W. and N. Fisher, 1999. Delineating Metal Accumulation Pathways for Marine Invertabrates. *The Science of the Total Environment*, 237/238: 459-472.

Watras, C. et al., 1998. Bioaccumulation of mercury in pelagic freshwater food webs. *The Science of the Total Environment*, 219: 183-208.

Williams, D.R. and J.P. Giesy, Jr., 1978. Relative Importance of Food and Water Sources to Cadmium Uptake by Gambusia affinis (Poeciliidae). Environmental Research, 16: 326-332.

Wrenn, M.E., et al. 1972. Natural Activity in Hudson River Estuary Samples and their Influence on the Detection Limits for Gamma Emitting Radionuclides Using NaI Gamma Spectrometry. In: *The Natural Radiation Environment II. Proceedings of the Second International Symposium on the Natural Radiation Environment August 7-11, 1972.* Adams, J.A.S. et al., eds. Rice University, Houston, Texas. Conf-720805-P2. pp. 897-916.

Young, R.A. 1988. A Report on striped bass in New York marine waters. New York State Marine Fisheries, Stony Brook, NY.

HydroQual Response: No measurements of metal concentrations in phytoplankton were made in the CARP monitoring program. Differences in metal partitioning for top and bottom water samples did not appear to be significantly different (We will recommend that this be more rigorously explored as part of potential future CARP model application efforts). Therefore, we have no basis for expecting or for assigning different partitioning values for POC and phytoplankton. Also, the fact that observed particle-specific concentrations of Hg and MMHg are in good agreement with those in underlying sediments at locations throughout the Harbor is consistent with our model results and indicates the importance of tidally-induced resuspension and settling in controlling the exchange of contaminants between the sediment and the overlying water.

37) Section 9.2.3, fifth paragraph. The gill transfer efficiency (b) was set at 0.6 for cadmium, mercury, and methylmercury. How was this value derived (literature reference?)? While uptake of Cd via gills is known to be important, it appears that aqueous exposures are insignificant for Hg/MMHg accumulation in fish (Hall et al., 1997), for which dietary uptake is the principal exposure pathway. While 0.6 may indeed be the gill transfer efficiency for Hg species, this pathway of uptake is not relevant.

HydroQual Response: Model results also show that dietary exposure is the primary exposure pathway for Hg/MMHg accumulation in fish. Our understanding is that the selection of gill transfer efficiency is not sensitive in the mercury bioaccumulation model calculation. This pathway is still active in the CARP model calculations, though of lesser importance.

38) Section 10.3, first paragraph. Again, free Hg^{2+} and CH_3Hg^+ should not be used to estimate BAFs; total dissolved concentrations of Hg(II) and MMHg should be used instead. Additionally, and as part of defining terms in the BAF calculation (Comment 29), the conventional unit for BAF is L kg^{-1} wet weight. This unit was used for many, if not all, contaminants in this section except Hg and MMHg (Figure 10-6), although L kg^{-1} was used in the tabulation of the same data in Appendix 11. In appendix 11, log BAFs (L/kg) for total Hg (nearly all of which is MMHg except in zooplankton) range from about 17 to 18 for the various biological species. These values are more than 10^{10} greater than BAFs determined for other coastal marine biota (Hammerschmidt and Fitzgerald, 2006a; Fitzgerald et al., 2007), which are calculated from total dissolved concentrations of Hg species (i.e., the conventional method). As noted several times above, we suggest that the authors use the conventional (i.e., U.S. EPA) method to calculate BAFs for biota in their model. This will aid in interpreting and comparing modeled results with empirical studies. Moreover, it is not free Hg^{2+} and CH_3Hg^+ that are accumulated by biota.

HydroQual Response:
Calculating BAF and BSAF on total dissolved concentrations would likely give values closer to other published values. CARP model calculations of free Hg^{+2} concentrations are very low.

39) Section 10.3, second paragraph. "These results [Fig. 10-5] which show lower BAFs for higher trophic organisms suggest that cadmium uptake through dietary exposure is not an important pathway." It is unclear how this conclusion can be drawn from the data. While the fish certainly have lower levels of cadmium than zooplankton, relative to Cd in water, this may be attributed to fish being more adept at removing (depurating) Cd from their bodies than zooplankton.

HydroQual Response: This could be considered an alternative explanation. In any event, the final conclusion from a management perspective is that Cd is not biomagnified. Cd bioaccumulation can be modeled either way successfully.

40) Section 10.3, second paragraph. "This is consistent with reports of strong binding of cadmium in organisms (e.g., by metallothioneins) which in effect may limit dietary exposure." It is unclear how an internal chelation of cadmium affects the amount that is passed from one trophic level to the next, except if metallothioneins were to aid in the depuration of Cd.

HydroQual Response: The basis idea is that strong binding of Cd to metallothioneins would limit the chemical potential of Cd in the gut and hence limit transfer across the gut wall and into the organism. We will try to provide a specific reference. Note that these issues are important and were appropriately explored using the bioaccumulation model. However, since we do not completely understand all the aspects of bioaccumulation, we used the bioaccumulation model to critically examine the data, but we recommend this use of field-derived BAFs and BSAFs for CARP management applications.

41) Section 10.7. Suggested revision of the title; replace "sediment species" with "benthic species". Sediment is not an adjective.

HydroQual Response: We appreciate your suggestion.

42) Section 10.7, second paragraph. BAFs should not be calculated for specific tissues or organs (e.g., hepatopancreas), they should be used only for whole organisms (Gray, 2002). Additionally, references for enhanced metal accumulation in the hepatopancreas should be included, if this statement were retained.

HydroQual Response: We will consider the Gray, 2002 reference in future applications. The BAFs for the hepatopancreas provide an initial descriptor for the "steady state" (or pseudo-steady state) accumulation in a specific organ. We believe estimates of Cd concentrations in the hepatopancreas are important for ecological or human health assessments.

43) Section 10.8, equation 10-8. Here, BAF is defined as having units of L/kg. These units should be used throughout the report.

HydroQual Response: They are.

44) Section 11.3, third paragraph. The model-predicted fraction of total Hg as MMHg is about 50% for zooplankton, but empirical determinations indicate the fraction is 10-20%. Both values are within the range commonly found in freshwater and marine zooplankton. We do not recommend "re-evaluating" the empirical results because they do not fit the model, but rather, re-evaluate the model. A principal weakness of the model is its ability to accurately predict MMHg concentrations in most of the media considered in this analysis, especially sediments (Comment 25) and dissolved, total, and particulate concentrations in the water column (Comment 34).

HydroQual Response: We disagree.

References

Balcom, P. H., Hammerschmidt, C. R., Fitzgerald, W. F., Lamborg, C. H., O'Connor, J. S., submitted. Seasonal distributions and cycling of mercury and methylmercury in the waters of New York/New Jersey Harbor estuary. *Mar. Chem.*

Balcom, P. H., Fitzgerald, W. F., Vandal, G. M., Lamborg, C. H., Rolfhus, K. R., Langer, C. S., Hammerschmidt, C. R., 2004. Mercury sources and cycling in the Connecticut River and Long Island Sound. *Mar. Chem.* 90, 53-74.

Benoit, J. M., Gilmour, C. C., Mason, R. P., Riedel, G. S., Riedel, G. F., 1998. Behavior of mercury in the Patuxent River estuary. *Biogeochemistry* 40, 249-265.

Benoit, J. M., Gilmour, C. C., Mason, R. P., Heyes, A., 1999. Sulfide controls on mercury speciation and bioavailability to methylating bacteria in sediment pore waters. *Environ. Sci. Technol.* 33, 951-957.

Benoit, J. M., Gilmour, C. C., Mason, R. P., 2001a. The influence of sulfide on solid-phase mercury bioavailability for methylation by pure cultures of *Desulfobulbus propionicus* (1pr3). *Environ. Sci. Technol.* 35, 127-132.

Benoit, J. M., Gilmour, C. C., Mason, R. P., 2001b. Aspects of bioavailability of mercury for methylation in pure cultures of *Desulfobulbus propionicus* (1pr3). *Appl. Environ. Microbiol.* 67, 51-58.

Benoit, J. M., Mason, R. P., Gilmour, C. C., Aiken, G. R., 2001c. Constants for mercury binding by dissolved organic matter isolates from the Florida Everglades. *Geochim. Cosmochim. Acta* 65, 4445-4451.

Dauer, D. M., Rodi, A. J., Jr., Ranasinghe, J. A., 1992. Effects of low dissolved oxygen events on the macrobenthos of the lower Chesapeake Bay. *Estuaries* 15, 384-391.

Diaz, R. J., Rosenberg, R., 1995. Marine benthic hypoxia: a review of its ecological effects and the behavioural responses of benthic macrofauna. *Oceanogr. Mar. Biol. Ann. Rev.* 33, 245-303.

Fitzgerald, W. F., Lamborg, C. H., Hammerschmidt, C. R., 2007. Marine biogeochemical cycling of mercury. *Chem. Rev.* doi: 10.1021/cr050353m.

Fleming, E. J., Mack, E. E., Green, P. G., Nelson, D. C., 2006. Mercury methylation from unexpected sources: Molybdate-inhibited freshwater sediments and an iron-reducing bacterium. *Appl. Environ. Microbiol.* 72, 457-464.

Gagnon, C., Pelletier, E., Mucci, A., Fitzgerald, W. F., 1996. Diagenetic behavior of methylmercury in organic-rich coastal sediments. *Limnol. Oceanogr.* 41, 428-434.

Gray, J. S., 2002. Biomagnification in marine systems: The perspective of an ecologist. *Mar. Poll. Bull.* 45, 46-52.

Hall, B. D., Bodaly, R. A., Fudge, R. J. P., Rudd, J. W. M., Rosenberg, D. M., 1997. food as the dominant pathway of methylmercury uptake by fish. *Water Air Soil Pollut.* 100, 13-24.

Hammerschmidt, C. R., Fitzgerald, W. F., submitted. Sediment-water exchange of methylmercury determined from shipboard benthic flux chambers. *Mar. Chem.*

Hammerschmidt, C. R., Fitzgerald, W. F., 2004. Geochemical controls on the production and distribution of methylmercury in near-shore marine sediments. *Environ. Sci. Technol.* 38, 1487-1495.

Hammerschmidt, C. R., Fitzgerald, W. F., 2006a. Bioaccumulation and trophic transfer of methylmercury in Long Island Sound. *Arch. Environ. Contam. Toxicol.* 51, 416-424.

Hammerschmidt, C. R., Fitzgerald, W. F., 2006b. Methylmercury cycling in sediments on the continental shelf of southern New England. *Geochim. Cosmochim. Acta* 70, 918-930.

Hammerschmidt, C. R., Fitzgerald, W. F., Lamborg, C. H., Balcom, P. H., Visscher, P. T., 2004. Biogeochemistry of methylmercury in sediments of Long Island Sound. *Mar. Chem.* 90, 31-52.

Hammerschmidt, C. R., Fitzgerald, W. F., Balcom, P. H., Visscher, P. T., submitted. Organic matter and sulfide inhibit methylmercury production in coastal marine sediments. *Mar. Chem.*

Han, S., Gill, G. A., 2005. Determination of mercury complexation in coastal and estuarine waters using competitive ligand exchange method. *Environ. Sci. Technol.* 39, 6607-6615.

Hayduk, W., Laudie, H., 1974. Prediction of diffusion coefficients for non-electrolytes in dilute aqueous solutions. *Am. Inst. Chem. Eng. J.* 20, 611-615.

Heyes, A., Mason, R. P., Kim, E.-H., Sunderland, E., 2006. Mercury methylation in estuaries: Insights from using measuring rates using stable mercury isotopes. *Mar. Chem.* 102, 134-147.

Kerin, E. J., Gilmour, C. C., Roden, E., Suzuki, M. T., Coates, J. D., Mason, R. P., 2006. Mercury methylation by dissimilatory iron-reducing bacteria. *Appl. Environ. Microbiol.* 72, 7919-7921.

Kola, H., Wilkinson, K. J., 2005. Cadmium uptake by a green alga can be predicted by equilibrium modeling. *Environ. Sci. Technol.* 39, 3040-3047.

Lambertsson, L., Nilsson, M., 2006. Organic material: The primary control on mercury methylation and ambient methyl mercury concentrations in estuarine sediments. *Environ. Sci. Technol.* 40, 1822-1829.

Lamborg, C. H., Fitzgerald, W. F., Skoog, A., Visscher, P. T., 2004. The abundance and source of mercury-binding organic ligands in Long Island Sound. *Mar. Chem.* 90, 151-163.

Lindberg, S. E., Harriss, R. C., 1974. Mercury-organic matter associations in estuarine sediments and interstitial water. *Environ. Sci. Technol.* 5, 459-462.

Marvin-DiPasquale, M., Agee, J., McGowan, C., Oremland, R. S., Thomas, M., Krabbenhoft, D., Gilmour, C. C., 2000. Methyl-mercury degradation pathways: A comparison among three mercury-impacted ecosystems. *Environ. Sci. Technol.* 34, 4908-4916.

Mason, R. P., Reinfelder, J. R., Morel, F. M. M., 1996. Uptake, toxicity, and trophic transfer of mercury in a coastal diatom. *Environ. Sci. Technol.* 30, 1835-1845.

MDN (Mercury Deposition Network), 2006. National Atmospheric Deposition Program, URL http://nadp.sws.uiuc.edu.

Mikac, N., Niessen, S., Ouddane, B., Wartel, M., 1999. Speciation of mercury in sediments of the Seine Estuary (France). *Appl. Organometal. Chem.* 13, 715-725.

Montagna, P. A., Ritter, C., 2006. Direct and indirect effects of hypoxia on benthos in Corpus Christi Bay, Texas, U.S.A. *J. Exper. Mar. Biol. Ecol.* 330, 119-131.

Robinson, J. B., Tuovinen, O. H., 1984. Mechanisms of microbial resistance and detoxification of mercury and organomercury compounds: Physiological, biochemical, and genetic analyses. *Microbiol. Rev.* 48, 95-124.

Schlüter, M., Sauter, E., Hansen, H.-P., Suess, E., 2000. Seasonal variations of bioirrigation in coastal sediments: Modelling of field data. *Geochim. Cosmochim. Acta* 64, 821-834.

Spry, D. J., Wiener, J. G., 1991. Metal bioavailability and toxicity to fish in low-alkalinity lakes: A critical review. *Environ. Pollut.* 71, 243-304.

Sunda, W. g., Engel, d. W., Thuotte, R. M., 1978. Effects of chemical speciation on the toxicity of cadmium to grass shrimp *Palaemonetes pugio*: Important of free cadmium ion. *Environ. Sci. Technol.* 12, 409-413.

Sunderland, E. M., Gobas, F. A. P. C., Branfireun, B. A., Heyes, A., 2006. Environmental controls on the speciation and distribution of mercury in coastal sediments. *Mar. Chem.* 102, 111-123.

U.S. Environmental Protection Agency. 2000. Methodology for deriving ambient water quality criteria for the protection of human health (2000). Office of Water, Washington, D.C. EPA-822-B-00-004.

Additional HydroQual References Cited

Benoit JM, Gilmour CC, Mason RP, Heyes A. 1999. Sulfide Controls on Mercury Speciation and Bioavailability to Methylating Bacteria in Sediment Pore *Waters. Environ. Sci. Technol.* 33:951-957

DiToro, Dominic M. *Sediment Flux Modeling.* New York: Wiley, 2001.

Haitzer M, Aiken GR, Ryan JN. 2003. Binding of Mercury(II) to Aquatic Humic Substances: Influence of pH and Source of Humic Substances. *Environ. Sci. Technol.* 37:2436-2441

Miller, C.L., Mason, R.P., Gilmour, C.C., and Heyes, A. 2007. Influence of dissolved organic matter on the complexation of mercury under sulfidic conditions. *Environmental Toxicology and Chemistry* 26(4):624-633).

Rolfhus, K.R.and Fitzgerald, W.F. 2001. The evasion and spatial/temporal distribution of mercury species in Long Island Sound, CT-NY. *Geochim. Cosmochim, Acta.* 65(3):407-418.

Sellers, P., Kelly, C., Rudd, J., and MacHutchon, A. 1996. Photodegradation of methylmercury in lakes. *Nature.* 380:694-697.

Skyllberg U, Xia K, Bloom PR, Nater EA, Bleam WF. 2000. Binding of Mercury(II) to Reduced Sulfur in Soil Organic Matter along Upland-Peat Soil Transects. *J. Environ. Quality* 29:855-865

HydroQual Response: No measurements of metal concentrations in phytoplankton were made in the CARP monitoring program. Differences in metal partitioning for top and bottom water samples did not appear to be significantly different (We will recommend that this be more rigorously explored as part of potential future CARP model application efforts). Therefore, we have no basis for expecting or for assigning different partitioning values for POC and phytoplankton. Also, the fact that observed particle-specific concentrations of Hg and MMHg are in good agreement with those in underlying sediments at locations throughout the Harbor is consistent with our model results and indicates the importance of tidally-induced resuspension and settling in controlling the exchange of contaminants between the sediment and the overlying water.

37) Section 9.2.3, fifth paragraph. The gill transfer efficiency (b) was set at 0.6 for cadmium, mercury, and methylmercury. How was this value derived (literature reference?)? While uptake of Cd via gills is known to be important, it appears that aqueous exposures are insignificant for Hg/MMHg accumulation in fish (Hall et al., 1997), for which dietary uptake is the principal exposure pathway. While 0.6 may indeed be the gill transfer efficiency for Hg species, this pathway of uptake is not relevant.

HydroQual Response: Model results also show that dietary exposure is the primary exposure pathway for Hg/MMHg accumulation in fish. Our understanding is that the selection of gill transfer efficiency is not sensitive in the mercury bioaccumulation model calculation. This pathway is still active in the CARP model calculations, though of lesser importance.

38) Section 10.3, first paragraph. Again, free Hg^{2+} and CH_3Hg^+ should not be used to estimate BAFs; total dissolved concentrations of Hg(II) and MMHg should be used instead. Additionally, and as part of defining terms in the BAF calculation (Comment 29), the conventional unit for BAF is L kg^{-1} wet weight. This unit was used for many, if not all, contaminants in this section except Hg and MMHg (Figure 10-6), although L kg^{-1} was used in the tabulation of the same data in Appendix 11. In appendix 11, log BAFs (L/kg) for total Hg (nearly all of which is MMHg except in zooplankton) range from about 17 to 18 for the various biological species. These values are more than 10^{10} greater than BAFs determined for other coastal marine biota (Hammerschmidt and Fitzgerald, 2006a; Fitzgerald et al., 2007), which are calculated from total dissolved concentrations of Hg species (i.e., the conventional method). As noted several times above, we suggest that the authors use the conventional (i.e., U.S. EPA) method to calculate BAFs for biota in their model. This will aid in interpreting and comparing modeled results with empirical studies. Moreover, it is not free Hg^{2+} and CH_3Hg^+ that are accumulated by biota.

HydroQual Response:
Calculating BAF and BSAF on total dissolved concentrations would likely give values closer to other published values. CARP model calculations of free Hg^{+2} concentrations are very low.

39) Section 10.3, second paragraph. "These results [Fig. 10-5] which show lower BAFs for higher trophic organisms suggest that cadmium uptake through dietary exposure is not an important pathway." It is unclear how this conclusion can be drawn from the data. While the fish certainly have lower levels of cadmium than zooplankton, relative to Cd in water, this may be attributed to fish being more adept at removing (depurating) Cd from their bodies than zooplankton.

HydroQual Response: This could be considered an alternative explanation. In any event, the final conclusion from a management perspective is that Cd is not biomagnified. Cd bioaccumulation can be modeled either way successfully.

40) Section 10.3, second paragraph. "This is consistent with reports of strong binding of cadmium in organisms (e.g., by metallothioneins) which in effect may limit dietary exposure." It is unclear how an internal chelation of cadmium affects the amount that is passed from one trophic level to the next, except if metallothioneins were to aid in the depuration of Cd.

HydroQual Response: The basis idea is that strong binding of Cd to metallothioneins would limit the chemical potential of Cd in the gut and hence limit transfer across the gut wall and into the organism. We will try to provide a specific reference. Note that these issues are important and were appropriately explored using the bioaccumulation model. However, since we do not completely understand all the aspects of bioaccumulation, we used the bioaccumulation model to critically examine the data, but we recommend this use of field-derived BAFs and BSAFs for CARP management applications.

41) Section 10.7. Suggested revision of the title; replace "sediment species" with "benthic species". Sediment is not an adjective.

HydroQual Response: We appreciate your suggestion.

42) Section 10.7, second paragraph. BAFs should not be calculated for specific tissues or organs (e.g., hepatopancreas), they should be used only for whole organisms (Gray, 2002). Additionally, references for enhanced metal accumulation in the hepatopancreas should be included, if this statement were retained.

HydroQual Response: We will consider the Gray, 2002 reference in future applications. The BAFs for the hepatopancreas provide an initial descriptor for the "steady state" (or pseudo-steady state) accumulation in a specific organ. We believe estimates of Cd concentrations in the hepatopancreas are important for ecological or human health assessments.

43) Section 10.8, equation 10-8. Here, BAF is defined as having units of L/kg. These units should be used throughout the report.

HydroQual Response: They are.

44) Section 11.3, third paragraph. The model-predicted fraction of total Hg as MMHg is about 50% for zooplankton, but empirical determinations indicate the fraction is 10-20%. Both values are within the range commonly found in freshwater and marine zooplankton. We do not recommend "re-evaluating" the empirical results because they do not fit the model, but rather, re-evaluate the model. A principal weakness of the model is its ability to accurately predict MMHg concentrations in most of the media considered in this analysis, especially sediments (Comment 25) and dissolved, total, and particulate concentrations in the water column (Comment 34).

HydroQual Response: We disagree.

References

Balcom, P. H., Hammerschmidt, C. R., Fitzgerald, W. F., Lamborg, C. H., O'Connor, J. S., submitted. Seasonal distributions and cycling of mercury and methylmercury in the waters of New York/New Jersey Harbor estuary. *Mar. Chem.*

Balcom, P. H., Fitzgerald, W. F., Vandal, G. M., Lamborg, C. H., Rolfhus, K. R., Langer, C. S., Hammerschmidt, C. R., 2004. Mercury sources and cycling in the Connecticut River and Long Island Sound. *Mar. Chem.* 90, 53-74.

Benoit, J. M., Gilmour, C. C., Mason, R. P., Riedel, G. S., Riedel, G. F., 1998. Behavior of mercury in the Patuxent River estuary. *Biogeochemistry* 40, 249-265.

Benoit, J. M., Gilmour, C. C., Mason, R. P., Heyes, A., 1999. Sulfide controls on mercury speciation and bioavailability to methylating bacteria in sediment pore waters. *Environ. Sci. Technol.* 33, 951-957.

Benoit, J. M., Gilmour, C. C., Mason, R. P., 2001a. The influence of sulfide on solid-phase mercury bioavailability for methylation by pure cultures of *Desulfobulbus propionicus* (1pr3). *Environ. Sci. Technol.* 35, 127-132.

Benoit, J. M., Gilmour, C. C., Mason, R. P., 2001b. Aspects of bioavailability of mercury for methylation in pure cultures of *Desulfobulbus propionicus* (1pr3). *Appl. Environ. Microbiol.* 67, 51-58.

Benoit, J. M., Mason, R. P., Gilmour, C. C., Aiken, G. R., 2001c. Constants for mercury binding by dissolved organic matter isolates from the Florida Everglades. *Geochim. Cosmochim. Acta* 65, 4445-4451.

Dauer, D. M., Rodi, A. J., Jr., Ranasinghe, J. A., 1992. Effects of low dissolved oxygen events on the macrobenthos of the lower Chesapeake Bay. *Estuaries* 15, 384-391.

Diaz, R. J., Rosenberg, R., 1995. Marine benthic hypoxia: a review of its ecological effects and the behavioural responses of benthic macrofauna. *Oceanogr. Mar. Biol. Ann. Rev.* 33, 245-303.

Fitzgerald, W. F., Lamborg, C. H., Hammerschmidt, C. R., 2007. Marine biogeochemical cycling of mercury. *Chem. Rev.* doi: 10.1021/cr050353m.

Fleming, E. J., Mack, E. E., Green, P. G., Nelson, D. C., 2006. Mercury methylation from unexpected sources: Molybdate-inhibited freshwater sediments and an iron-reducing bacterium. *Appl. Environ. Microbiol.* 72, 457-464.

Gagnon, C., Pelletier, E., Mucci, A., Fitzgerald, W. F., 1996. Diagenetic behavior of methylmercury in organic-rich coastal sediments. *Limnol. Oceanogr.* 41, 428-434.

Gray, J. S., 2002. Biomagnification in marine systems: The perspective of an ecologist. *Mar. Poll. Bull.* 45, 46-52.

Hall, B. D., Bodaly, R. A., Fudge, R. J. P., Rudd, J. W. M., Rosenberg, D. M., 1997. food as the dominant pathway of methylmercury uptake by fish. *Water Air Soil Pollut.* 100, 13-24.

Hammerschmidt, C. R., Fitzgerald, W. F., submitted. Sediment-water exchange of methylmercury determined from shipboard benthic flux chambers. *Mar. Chem.*

Hammerschmidt, C. R., Fitzgerald, W. F., 2004. Geochemical controls on the production and distribution of methylmercury in near-shore marine sediments. *Environ. Sci. Technol.* 38, 1487-1495.

Hammerschmidt, C. R., Fitzgerald, W. F., 2006a. Bioaccumulation and trophic transfer of methylmercury in Long Island Sound. *Arch. Environ. Contam. Toxicol.* 51, 416-424.

Hammerschmidt, C. R., Fitzgerald, W. F., 2006b. Methylmercury cycling in sediments on the continental shelf of southern New England. *Geochim. Cosmochim. Acta* 70, 918-930.

Hammerschmidt, C. R., Fitzgerald, W. F., Lamborg, C. H., Balcom, P. H., Visscher, P. T., 2004. Biogeochemistry of methylmercury in sediments of Long Island Sound. *Mar. Chem.* 90, 31-52.

Hammerschmidt, C. R., Fitzgerald, W. F., Balcom, P. H., Visscher, P. T., submitted. Organic matter and sulfide inhibit methylmercury production in coastal marine sediments. *Mar. Chem.*

Han, S., Gill, G. A., 2005. Determination of mercury complexation in coastal and estuarine waters using competitive ligand exchange method. *Environ. Sci. Technol.* 39, 6607-6615.

Hayduk, W., Laudie, H., 1974. Prediction of diffusion coefficients for non-electrolytes in dilute aqueous solutions. *Am. Inst. Chem. Eng. J.* 20, 611-615.

Heyes, A., Mason, R. P., Kim, E.-H., Sunderland, E., 2006. Mercury methylation in estuaries: Insights from using measuring rates using stable mercury isotopes. *Mar. Chem.* 102, 134-147.

Kerin, E. J., Gilmour, C. C., Roden, E., Suzuki, M. T., Coates, J. D., Mason, R. P., 2006. Mercury methylation by dissimilatory iron-reducing bacteria. *Appl. Environ. Microbiol.* 72, 7919-7921.

Kola, H., Wilkinson, K. J., 2005. Cadmium uptake by a green alga can be predicted by equilibrium modeling. *Environ. Sci. Technol.* 39, 3040-3047.

Lambertsson, L., Nilsson, M., 2006. Organic material: The primary control on mercury methylation and ambient methyl mercury concentrations in estuarine sediments. *Environ. Sci. Technol.* 40, 1822-1829.

Lamborg, C. H., Fitzgerald, W. F., Skoog, A., Visscher, P. T., 2004. The abundance and source of mercury-binding organic ligands in Long Island Sound. *Mar. Chem.* 90, 151-163.

Lindberg, S. E., Harriss, R. C., 1974. Mercury-organic matter associations in estuarine sediments and interstitial water. *Environ. Sci. Technol.* 5, 459-462.

Marvin-DiPasquale, M., Agee, J., McGowan, C., Oremland, R. S., Thomas, M., Krabbenhoft, D., Gilmour, C. C., 2000. Methyl-mercury degradation pathways: A comparison among three mercury-impacted ecosystems. *Environ. Sci. Technol.* 34, 4908-4916.

Mason, R. P., Reinfelder, J. R., Morel, F. M. M., 1996. Uptake, toxicity, and trophic transfer of mercury in a coastal diatom. *Environ. Sci. Technol.* 30, 1835-1845.

MDN (Mercury Deposition Network), 2006. National Atmospheric Deposition Program, URL http://nadp.sws.uiuc.edu.

Mikac, N., Niessen, S., Ouddane, B., Wartel, M., 1999. Speciation of mercury in sediments of the Seine Estuary (France). *Appl. Organometal. Chem.* 13, 715-725.

Montagna, P. A., Ritter, C., 2006. Direct and indirect effects of hypoxia on benthos in Corpus Christi Bay, Texas, U.S.A. *J. Exper. Mar. Biol. Ecol.* 330, 119-131.

Robinson, J. B., Tuovinen, O. H., 1984. Mechanisms of microbial resistance and detoxification of mercury and organomercury compounds: Physiological, biochemical, and genetic analyses. *Microbiol. Rev.* 48, 95-124.

Schlüter, M., Sauter, E., Hansen, H.-P., Suess, E., 2000. Seasonal variations of bioirrigation in coastal sediments: Modelling of field data. *Geochim. Cosmochim. Acta* 64, 821-834.

Spry, D. J., Wiener, J. G., 1991. Metal bioavailability and toxicity to fish in low-alkalinity lakes: A critical review. *Environ. Pollut.* 71, 243-304.

Sunda, W. g., Engel, d. W., Thuotte, R. M., 1978. Effects of chemical speciation on the toxicity of cadmium to grass shrimp *Palaemonetes pugio*: Important of free cadmium ion. *Environ. Sci. Technol.* 12, 409-413.

Sunderland, E. M., Gobas, F. A. P. C., Branfireun, B. A., Heyes, A., 2006. Environmental controls on the speciation and distribution of mercury in coastal sediments. *Mar. Chem.* 102, 111-123.

U.S. Environmental Protection Agency. 2000. Methodology for deriving ambient water quality criteria for the protection of human health (2000). Office of Water, Washington, D.C. EPA-822-B-00-004.

Additional HydroQual References Cited

Benoit JM, Gilmour CC, Mason RP, Heyes A. 1999. Sulfide Controls on Mercury Speciation and Bioavailability to Methylating Bacteria in Sediment Pore *Waters. Environ. Sci. Technol.* 33:951-957

DiToro, Dominic M. *Sediment Flux Modeling.* New York: Wiley, 2001.

Haitzer M, Aiken GR, Ryan JN. 2003. Binding of Mercury(II) to Aquatic Humic Substances: Influence of pH and Source of Humic Substances. *Environ. Sci. Technol.* 37:2436-2441

Miller, C.L., Mason, R.P., Gilmour, C.C., and Heyes, A. 2007. Influence of dissolved organic matter on the complexation of mercury under sulfidic conditions. *Environmental Toxicology and Chemistry* 26(4):624-633).

Rolfhus, K.R.and Fitzgerald, W.F. 2001. The evasion and spatial/temporal distribution of mercury species in Long Island Sound, CT-NY. *Geochim. Cosmochim, Acta.* 65(3):407-418.

Sellers, P., Kelly, C., Rudd, J., and MacHutchon, A. 1996. Photodegradation of methylmercury in lakes. *Nature.* 380:694-697.

Skyllberg U, Xia K, Bloom PR, Nater EA, Bleam WF. 2000. Binding of Mercury(II) to Reduced Sulfur in Soil Organic Matter along Upland-Peat Soil Transects. *J. Environ. Quality* 29:855-865

HydroQual Response: No measurements of metal concentrations in phytoplankton were made in the CARP monitoring program. Differences in metal partitioning for top and bottom water samples did not appear to be significantly different (We will recommend that this be more rigorously explored as part of potential future CARP model application efforts). Therefore, we have no basis for expecting or for assigning different partitioning values for POC and phytoplankton. Also, the fact that observed particle-specific concentrations of Hg and MMHg are in good agreement with those in underlying sediments at locations throughout the Harbor is consistent with our model results and indicates the importance of tidally-induced resuspension and settling in controlling the exchange of contaminants between the sediment and the overlying water.

37) Section 9.2.3, fifth paragraph. The gill transfer efficiency (b) was set at 0.6 for cadmium, mercury, and methylmercury. How was this value derived (literature reference?)? While uptake of Cd via gills is known to be important, it appears that aqueous exposures are insignificant for Hg/MMHg accumulation in fish (Hall et al., 1997), for which dietary uptake is the principal exposure pathway. While 0.6 may indeed be the gill transfer efficiency for Hg species, this pathway of uptake is not relevant.

HydroQual Response: Model results also show that dietary exposure is the primary exposure pathway for Hg/MMHg accumulation in fish. Our understanding is that the selection of gill transfer efficiency is not sensitive in the mercury bioaccumulation model calculation. This pathway is still active in the CARP model calculations, though of lesser importance.

38) Section 10.3, first paragraph. Again, free Hg^{2+} and CH_3Hg^+ should not be used to estimate BAFs; total dissolved concentrations of Hg(II) and MMHg should be used instead. Additionally, and as part of defining terms in the BAF calculation (Comment 29), the conventional unit for BAF is L kg^{-1} wet weight. This unit was used for many, if not all, contaminants in this section except Hg and MMHg (Figure 10-6), although L kg^{-1} was used in the tabulation of the same data in Appendix 11. In appendix 11, log BAFs (L/kg) for total Hg (nearly all of which is MMHg except in zooplankton) range from about 17 to 18 for the various biological species. These values are more than 10^{10} greater than BAFs determined for other coastal marine biota (Hammerschmidt and Fitzgerald, 2006a; Fitzgerald et al., 2007), which are calculated from total dissolved concentrations of Hg species (i.e., the conventional method). As noted several times above, we suggest that the authors use the conventional (i.e., U.S. EPA) method to calculate BAFs for biota in their model. This will aid in interpreting and comparing modeled results with empirical studies. Moreover, it is not free Hg^{2+} and CH_3Hg^+ that are accumulated by biota.

HydroQual Response:
Calculating BAF and BSAF on total dissolved concentrations would likely give values closer to other published values. CARP model calculations of free Hg^{+2} concentrations are very low.

39) Section 10.3, second paragraph. "These results [Fig. 10-5] which show lower BAFs for higher trophic organisms suggest that cadmium uptake through dietary exposure is not an important pathway." It is unclear how this conclusion can be drawn from the data. While the fish certainly have lower levels of cadmium than zooplankton, relative to Cd in water, this may be attributed to fish being more adept at removing (depurating) Cd from their bodies than zooplankton.

HydroQual Response: This could be considered an alternative explanation. In any event, the final conclusion from a management perspective is that Cd is not biomagnified. Cd bioaccumulation can be modeled either way successfully.

40) Section 10.3, second paragraph. "This is consistent with reports of strong binding of cadmium in organisms (e.g., by metallothioneins) which in effect may limit dietary exposure." It is unclear how an internal chelation of cadmium affects the amount that is passed from one trophic level to the next, except if metallothioneins were to aid in the depuration of Cd.

HydroQual Response: The basis idea is that strong binding of Cd to metallothioneins would limit the chemical potential of Cd in the gut and hence limit transfer across the gut wall and into the organism. We will try to provide a specific reference. Note that these issues are important and were appropriately explored using the bioaccumulation model. However, since we do not completely understand all the aspects of bioaccumulation, we used the bioaccumulation model to critically examine the data, but we recommend this use of field-derived BAFs and BSAFs for CARP management applications.

41) Section 10.7. Suggested revision of the title; replace "sediment species" with "benthic species". Sediment is not an adjective.

HydroQual Response: We appreciate your suggestion.

42) Section 10.7, second paragraph. BAFs should not be calculated for specific tissues or organs (e.g., hepatopancreas), they should be used only for whole organisms (Gray, 2002). Additionally, references for enhanced metal accumulation in the hepatopancreas should be included, if this statement were retained.

HydroQual Response: We will consider the Gray, 2002 reference in future applications. The BAFs for the hepatopancreas provide an initial descriptor for the "steady state" (or pseudo-steady state) accumulation in a specific organ. We believe estimates of Cd concentrations in the hepatopancreas are important for ecological or human health assessments.

43) Section 10.8, equation 10-8. Here, BAF is defined as having units of L/kg. These units should be used throughout the report.

HydroQual Response: They are.

44) Section 11.3, third paragraph. The model-predicted fraction of total Hg as MMHg is about 50% for zooplankton, but empirical determinations indicate the fraction is 10-20%. Both values are within the range commonly found in freshwater and marine zooplankton. We do not recommend "re-evaluating" the empirical results because they do not fit the model, but rather, re-evaluate the model. A principal weakness of the model is its ability to accurately predict MMHg concentrations in most of the media considered in this analysis, especially sediments (Comment 25) and dissolved, total, and particulate concentrations in the water column (Comment 34).

HydroQual Response: We disagree.

References

Balcom, P. H., Hammerschmidt, C. R., Fitzgerald, W. F., Lamborg, C. H., O'Connor, J. S., submitted. Seasonal distributions and cycling of mercury and methylmercury in the waters of New York/New Jersey Harbor estuary. *Mar. Chem.*

Balcom, P. H., Fitzgerald, W. F., Vandal, G. M., Lamborg, C. H., Rolfhus, K. R., Langer, C. S., Hammerschmidt, C. R., 2004. Mercury sources and cycling in the Connecticut River and Long Island Sound. *Mar. Chem.* 90, 53-74.

Benoit, J. M., Gilmour, C. C., Mason, R. P., Riedel, G. S., Riedel, G. F., 1998. Behavior of mercury in the Patuxent River estuary. *Biogeochemistry* 40, 249-265.

Benoit, J. M., Gilmour, C. C., Mason, R. P., Heyes, A., 1999. Sulfide controls on mercury speciation and bioavailability to methylating bacteria in sediment pore waters. *Environ. Sci. Technol.* 33, 951-957.

Benoit, J. M., Gilmour, C. C., Mason, R. P., 2001a. The influence of sulfide on solid-phase mercury bioavailability for methylation by pure cultures of *Desulfobulbus propionicus* (1pr3). *Environ. Sci. Technol.* 35, 127-132.

Benoit, J. M., Gilmour, C. C., Mason, R. P., 2001b. Aspects of bioavailability of mercury for methylation in pure cultures of *Desulfobulbus propionicus* (1pr3). *Appl. Environ. Microbiol.* 67, 51-58.

Benoit, J. M., Mason, R. P., Gilmour, C. C., Aiken, G. R., 2001c. Constants for mercury binding by dissolved organic matter isolates from the Florida Everglades. *Geochim. Cosmochim. Acta* 65, 4445-4451.

Dauer, D. M., Rodi, A. J., Jr., Ranasinghe, J. A., 1992. Effects of low dissolved oxygen events on the macrobenthos of the lower Chesapeake Bay. *Estuaries* 15, 384-391.

Diaz, R. J., Rosenberg, R., 1995. Marine benthic hypoxia: a review of its ecological effects and the behavioural responses of benthic macrofauna. *Oceanogr. Mar. Biol. Ann. Rev.* 33, 245-303.

Fitzgerald, W. F., Lamborg, C. H., Hammerschmidt, C. R., 2007. Marine biogeochemical cycling of mercury. *Chem. Rev.* doi: 10.1021/cr050353m.

Fleming, E. J., Mack, E. E., Green, P. G., Nelson, D. C., 2006. Mercury methylation from unexpected sources: Molybdate-inhibited freshwater sediments and an iron-reducing bacterium. *Appl. Environ. Microbiol.* 72, 457-464.

Gagnon, C., Pelletier, E., Mucci, A., Fitzgerald, W. F., 1996. Diagenetic behavior of methylmercury in organic-rich coastal sediments. *Limnol. Oceanogr.* 41, 428-434.

Gray, J. S., 2002. Biomagnification in marine systems: The perspective of an ecologist. *Mar. Poll. Bull.* 45, 46-52.

Hall, B. D., Bodaly, R. A., Fudge, R. J. P., Rudd, J. W. M., Rosenberg, D. M., 1997. food as the dominant pathway of methylmercury uptake by fish. *Water Air Soil Pollut.* 100, 13-24.

Hammerschmidt, C. R., Fitzgerald, W. F., submitted. Sediment-water exchange of methylmercury determined from shipboard benthic flux chambers. *Mar. Chem.*

Hammerschmidt, C. R., Fitzgerald, W. F., 2004. Geochemical controls on the production and distribution of methylmercury in near-shore marine sediments. *Environ. Sci. Technol.* 38, 1487-1495.

Hammerschmidt, C. R., Fitzgerald, W. F., 2006a. Bioaccumulation and trophic transfer of methylmercury in Long Island Sound. *Arch. Environ. Contam. Toxicol.* 51, 416-424.

Hammerschmidt, C. R., Fitzgerald, W. F., 2006b. Methylmercury cycling in sediments on the continental shelf of southern New England. *Geochim. Cosmochim. Acta* 70, 918-930.

Hammerschmidt, C. R., Fitzgerald, W. F., Lamborg, C. H., Balcom, P. H., Visscher, P. T., 2004. Biogeochemistry of methylmercury in sediments of Long Island Sound. *Mar. Chem.* 90, 31-52.

Hammerschmidt, C. R., Fitzgerald, W. F., Balcom, P. H., Visscher, P. T., submitted. Organic matter and sulfide inhibit methylmercury production in coastal marine sediments. *Mar. Chem.*

Han, S., Gill, G. A., 2005. Determination of mercury complexation in coastal and estuarine waters using competitive ligand exchange method. *Environ. Sci. Technol.* 39, 6607-6615.

Hayduk, W., Laudie, H., 1974. Prediction of diffusion coefficients for non-electrolytes in dilute aqueous solutions. *Am. Inst. Chem. Eng. J.* 20, 611-615.

Heyes, A., Mason, R. P., Kim, E.-H., Sunderland, E., 2006. Mercury methylation in estuaries: Insights from using measuring rates using stable mercury isotopes. *Mar. Chem.* 102, 134-147.

Kerin, E. J., Gilmour, C. C., Roden, E., Suzuki, M. T., Coates, J. D., Mason, R. P., 2006. Mercury methylation by dissimilatory iron-reducing bacteria. *Appl. Environ. Microbiol.* 72, 7919-7921.

Kola, H., Wilkinson, K. J., 2005. Cadmium uptake by a green alga can be predicted by equilibrium modeling. *Environ. Sci. Technol.* 39, 3040-3047.

Lambertsson, L., Nilsson, M., 2006. Organic material: The primary control on mercury methylation and ambient methyl mercury concentrations in estuarine sediments. *Environ. Sci. Technol.* 40, 1822-1829.

Lamborg, C. H., Fitzgerald, W. F., Skoog, A., Visscher, P. T., 2004. The abundance and source of mercury-binding organic ligands in Long Island Sound. *Mar. Chem.* 90, 151-163.

Lindberg, S. E., Harriss, R. C., 1974. Mercury-organic matter associations in estuarine sediments and interstitial water. *Environ. Sci. Technol.* 5, 459-462.

Marvin-DiPasquale, M., Agee, J., McGowan, C., Oremland, R. S., Thomas, M., Krabbenhoft, D., Gilmour, C. C., 2000. Methyl-mercury degradation pathways: A comparison among three mercury-impacted ecosystems. *Environ. Sci. Technol.* 34, 4908-4916.

Mason, R. P., Reinfelder, J. R., Morel, F. M. M., 1996. Uptake, toxicity, and trophic transfer of mercury in a coastal diatom. *Environ. Sci. Technol.* 30, 1835-1845.

MDN (Mercury Deposition Network), 2006. National Atmospheric Deposition Program, URL http://nadp.sws.uiuc.edu.

Mikac, N., Niessen, S., Ouddane, B., Wartel, M., 1999. Speciation of mercury in sediments of the Seine Estuary (France). *Appl. Organometal. Chem.* 13, 715-725.

Montagna, P. A., Ritter, C., 2006. Direct and indirect effects of hypoxia on benthos in Corpus Christi Bay, Texas, U.S.A. *J. Exper. Mar. Biol. Ecol.* 330, 119-131.

Robinson, J. B., Tuovinen, O. H., 1984. Mechanisms of microbial resistance and detoxification of mercury and organomercury compounds: Physiological, biochemical, and genetic analyses. *Microbiol. Rev.* 48, 95-124.

Schlüter, M., Sauter, E., Hansen, H.-P., Suess, E., 2000. Seasonal variations of bioirrigation in coastal sediments: Modelling of field data. *Geochim. Cosmochim. Acta* 64, 821-834.

Spry, D. J., Wiener, J. G., 1991. Metal bioavailability and toxicity to fish in low-alkalinity lakes: A critical review. *Environ. Pollut.* 71, 243-304.

Sunda, W. g., Engel, d. W., Thuotte, R. M., 1978. Effects of chemical speciation on the toxicity of cadmium to grass shrimp *Palaemonetes pugio*: Important of free cadmium ion. *Environ. Sci. Technol.* 12, 409-413.

Sunderland, E. M., Gobas, F. A. P. C., Branfireun, B. A., Heyes, A., 2006. Environmental controls on the speciation and distribution of mercury in coastal sediments. *Mar. Chem.* 102, 111-123.

U.S. Environmental Protection Agency. 2000. Methodology for deriving ambient water quality criteria for the protection of human health (2000). Office of Water, Washington, D.C. EPA-822-B-00-004.

Additional HydroQual References Cited

Benoit JM, Gilmour CC, Mason RP, Heyes A. 1999. Sulfide Controls on Mercury Speciation and Bioavailability to Methylating Bacteria in Sediment Pore *Waters. Environ. Sci. Technol.* 33:951-957

DiToro, Dominic M. *Sediment Flux Modeling.* New York: Wiley, 2001.

Haitzer M, Aiken GR, Ryan JN. 2003. Binding of Mercury(II) to Aquatic Humic Substances: Influence of pH and Source of Humic Substances. *Environ. Sci. Technol.* 37:2436-2441

Miller, C.L., Mason, R.P., Gilmour, C.C., and Heyes, A. 2007. Influence of dissolved organic matter on the complexation of mercury under sulfidic conditions. *Environmental Toxicology and Chemistry* 26(4):624-633).

Rolfhus, K.R.and Fitzgerald, W.F. 2001. The evasion and spatial/temporal distribution of mercury species in Long Island Sound, CT-NY. *Geochim. Cosmochim, Acta.* 65(3):407-418.

Sellers, P., Kelly, C., Rudd, J., and MacHutchon, A. 1996. Photodegradation of methylmercury in lakes. *Nature.* 380:694-697.

Skyllberg U, Xia K, Bloom PR, Nater EA, Bleam WF. 2000. Binding of Mercury(II) to Reduced Sulfur in Soil Organic Matter along Upland-Peat Soil Transects. *J. Environ. Quality* 29:855-865

APPENDICES 1- 14

INCLUDED IN SEPARATE FILE (CFTP_Appendies.pdf)

APPENDIX 15

MODEL EVALUATION GROUP (MEG)

FINAL CONTAMINANT FATE TRANSPORT AND BIOACCUMULATION REVIEW COMMENTS AND HYDROQUAL RESPONSE

Appendix 15
Model Evaluation Group (MEG) Final Contaminant Fate Transport and Bioaccumulation

Review Comments and HydroQual Response

This report appendix includes final review comments provided by the Model Evaluation Group (MEG). It also includes HydroQual's response to comments. The appendix has been organized into four subsections. Appendix 15.1 contains summary review comments prepared by Joel Baker, the MEG chairperson. These comments summarize responses prepared by other MEG members on specific aspects of the CARP model. In addition to summarizing the MEG's findings related to contaminants, MEG comments on hydrodynamics and sediment transport, which appear fully in the CARP modeling reports for those models, are also summarized here. Appendix 15.2 contains the MEG comments and HydroQual responses for HOC fate and transport modeling. Appendix 15.3 contains the MEG comments and HydroQual responses for HOC bioaccumulation. Appendix 15.4 contains the MEG comments and HydroQual responses for metals modeling.

APPENDIX 15.1
SUMMARY MEG COMMENTS

New York & New Jersey Harbor

Contaminant Assessment and Reduction Project (CARP)

Model Evaluation Group Final Peer-Review Report

Joel Baker
Chair, CARP Model Evaluation Group
Chesapeake Biological Laboratory
University of Maryland

1. Overall scope of review.

The overall objective of the Contaminant Assessment and Reduction Project (CARP) is to quantify loadings and movement of chemical contaminants in the New York & New Jersey Harbor with sufficient accuracy to explain current and to predict future concentrations of chemicals in Harbor sediments and organisms. Integral to this effort is the development of a coupled water quality model. Due to the complexity of contaminant transport in the estuary and the range of chemical classes of interest (PCBs, PAHs, pesticides, mercury, and metals), no existing model was suitable to meet the needs of the CARP program. Specifically, it was recognized at the beginning of CARP that a linked model that combines hydrodynamics, sediment transport, organic carbon dynamics, oxygen and sulfur cycling, and contaminant partitioning and bioaccumulation would be needed. These design specifications were detailed in a request for proposals, and subsequent proposals were evaluated by an external peer review group.

Developing models of this nature requires a large number of decisions and interpretations, each of which impacts the final model performance and capability. Given the complexity, it is very difficult to review the structure of the final model without first participating in reviews throughout the course of the model development. For this reason, CARP established a Model Evaluation Group (MEG). The purpose of the MEG was to provide technical review and guidance to the model development group throughout the process to insure that each component of the overall model was thoroughly evaluated and its performance understood before the linked model was assembled. The MEG met regularly with CARP participants throughout the study, including those responsible for the CARP field programs and

the model development group. When necessary, targeted meetings or conference calls were arranged to address specific issues that arose during the field program and the model development. The Hudson River Foundation aided the MEG by providing meeting space and logistics. The MEG reviewed each component of the field program (ambient monitoring, loadings calculations) and model as they were completed.

Throughout the CARP program, the MEG continually evaluated the model against the following core questions:

1. Does each component of the CARP model reflect the best available science?
2. Are all available field data appropriately used in model development and calibration?
3. Does the model structure and complexity, especially spatial and temporal resolution, match the intended uses and the available data from the study area?
4. How accurate are the model results, and what tools are available to evaluate and communicate model uncertainty?

2. MEG Members

Joel Baker, University of Maryland	organic contaminant cycling
Frank Bohlen, University of Connecticut	sediment transport, dredging
Richard Bopp, RPI	organic contaminant cycling
Joe DePinto, LimnoTech, Inc.	water quality modeling
Joe DiLorenzo, Najarian and Associates	hydrodynamics
William Fitzgerald, University of Connecticut	mercury and metals cycling
W. Rockwell Geyer	
Woods Hole Oceanographic Institution	sediment transport/hydrodynamics
Lawrence Sanford*, University of Maryland	sediment transport
Jay Taft, Harvard University	organic carbon/water quality modeling

*resigned

3. Overall Evaluation of the CARP Model

The design of the CARP model was driven by the original objective to predict contaminant concentrations in water, sediments, and biota throughout the Harbor over time scales of years to decades. These spatial and temporal scales, coupled with the available field observations for calibration, dictated to some extent the model resolution. The model is designed to, and best used for, exploring

spatial trends across the entire Harbor, rather than detailed analysis within specific tributaries, berthings, or embayments. For example, the model grid is fairly coarse in many tributaries-this is likely suitable for predicting transport of chemicals on the scale of the entire Harbor, but insufficient to predict detailed behavior within these tributaries. Based on our review, the MEG makes the following conclusions:

1. The CARP model provides an important framework to organize and interpret field data and to identify gaps in data and knowledge.
2. The CARP model is technically sound and represents the best and latest science available at the time of model development.
3. The CARP model development utilizes available data to the greatest extent possible in terms of it complexity (i.e., the spatial and temporal resolution and the process kinetics).
4. The CARP model is suitable for use in predicting general spatial and temporal relationships between external contaminant loadings and concentrations in water and sediment throughout the NY/NJ Harbor. Specific limitations are discussed below. Predictions of concentrations in biota are less certain due to, among other things, relatively few calibration data.
5. Of the chemical classes modeled, mercury is the most difficult due to its complex geochemistry in the estuary, especially the processes controlling conversion of inorganic mercury to methylmercury.
6. The relationships between current loadings and ambient chemical concentrations are fairly well characterized, but it is more difficult to predict the long-term rate of change in concentrations.
7. The response time of the system is long due to storage in sediments, and the projections are sensitive to the sediment initial conditions and especially to the model parameterization of net sedimentation rates in various parts of the system.
8. Uncertainties increase with time in the projections. This is a characteristic of all models.
9. The model is based on six years of observations. Extreme events for all parts of the system are not included in the projections.
10. The influence of the Hudson River on Newark Bay is uncertain. The CARP model shows a relatively high amount of sediment entering Newark Bay from the Hudson River, which might have important management implications. This behavior needs to be verified by further field studies.
11. The CARP Program has advanced the understanding of contaminant behavior in the Harbor. This increase in understanding should continue to evolve by further field investigations and model refinement.
12. The model should be continually maintained and improved. Findings from the CARP model should drive these studies, i.e., investigate transport of sediments into Newark Bay.
13. A particular research need identified by the CARP model development exercise is to improve the empirical relationships and mechanistic understanding of contaminant levels in biota,

sediment, and water. A related need with respect to the bioaccumulation model is the quantitative formulation of food web bioenergetics and trophic transfer processes.

4. Results of Individual Model Component Reviews

Hydrodynamics.

Overall, the report demonstrates that the model is a useful tool for simulating the hydrodynamics of the system during the CARP years. The model passes accurate water depths to other sub-models. Generally, the model passes representative water temperatures for computation of temperature-dependent rate constants and kinetics. The model passes representative bottom velocities for the computation of bottom stress, except in upper Newark Bay. The model appears to provide an adequate simulation of constituent (salt) transport, except during the summer of 2002.

Specific recommendations for the hydrodynamic model include:

1. Investigate why the model appears to: (1) underestimate bottom velocity in Upper Newark Bay; (2) underestimate salinity in summer 2002; and (3) reduce semi-diurnal tidal variations in salinity.
2. Characterize the system's salient hydrodynamic features and transport processes and discuss how well the model reproduces such features.
3. Provide values for all adjustable model coefficients and revise and expand error analysis methods and discussion.
4. In the linkage section of the report, describe how diffusivities are computed and aggregated for passage to sub-models

In the future, additional salinity comparisons for the CARP years may be performed using available NOAA data at Sandy Hook and WHOI data at various Hudson Estuary locations. The latter would provide an excellent test of the model's ability to reproduce documented patterns of fortnightly variability in salinity stratification/de-stratification and provide greater model confidence.

Sediment Transport.

Strengths: The CARP model is a state-of-the-art model, with prognostic equations for sediment and carbon distributions. The carbon model is well calibrated and shows significant predictive skill. Predicted suspended sediment distributions often in agreement with observations (except near turbidity-maximum region).

Weaknesses: In the lower Hudson River section of the model, sediment trapping distributions are inconsistent with observations of temporally-variable sediment storage, especially along the river flanks (e.g., dredging data, Woodruff et al., 2001). The fine scale temporal and spatial sediment transport processes in this are not captured by the model, but the implications of this on the broader, system-wide scale are not known. Significant adjustment of parameters were required to achieve reasonable fit to field data. In the draft CARP model documentation, justification of the values chosen for various parameters and the detailed description of the model set-up generally were not consistent with peer-reviewed publication-quality.

Hydrophobic Organic Contaminant (HOC) Fate and Transport.

Overall, the CARP modeling group has done an excellent job of developing this model. They had to model a very complex system and include a large suite of chemicals, with somewhat marginal data considering the size and complexity of the system and the questions. This made the task quite difficult, and the MEG is overall impressed with their compilation and synthesis of data from all possible sources, including the literature and previous theory, to pull together a well-integrated whole system model. Having said that, the summation of the utility of this model is that it has value in predicting the direction and rate of surface sediment response in various zones of the model (i.e., Newark Bay, lower Hudson River, etc.) to a change in loading from a given source category or from a given source area. It is not clear how much of the uncertainty that will be encountered in trying to predict the absolute value of a chemical's response to a specific load change or the time it will take to achieve that value.

Bioaccumulation Modeling.

Strengths:

1. Linked carbon flow and contaminant models allow investigation of potential impacts of changing nutrient loads and food web structure on HOC accumulation.
2. Ratio approach is straightforward and consistent with regulatory programs; bioaccumulation modeling allows mechanisms underlying trends in ratio-derived values to be explored.
3. Structure allows further integration/expansion with fisheries models (IBMs, bioenergetics).

Weaknesses:

1. Uniform food web structure and ratios (BAF/BSAF) in space and time.
2. Relatively sparse Harbor-specific data describing BAF and BSAF for key species
3. Predicts 'average' concentrations in biota, but risk assessors may be more interested in extremes (especially for human health assessments).

Mercury and Metals Modeling.

At the beginning of the CARP program, it was recognized that modeling mercury accumulation in NY & NJ Harbor organisms would be one of the most challenging aspects of model development. Unlike most target organic pollutants, mercury must undergo a key biogeochemical process in the environment (methylation) to be transformed to the species that bioaccumulates in organisms. Modeling the relationship between external loadings (of both inorganic and methyl mercury) and resulting mercury concentrations in biota requires explicit calculation of methylation and demethylation rates within the estuary. These rates depend upon several factors, including sulfate reduction rates (sulfate-reducing microorganisms are thought to be responsible for mercury methylation) and inorganic mercury bioavailability (controlled in turn by speciation with organic matter, sulfides, and other phases). The overall rate of in situ mercury methylation depends in the 'controlling' (e.g. slowest) process, which is likely either microbial activity (which scales to the sulfate reduction rate) or inorganic mercury bioavailability (which depends on geochemical speciation in the sediments). In addition, the concentration of methyl mercury in the estuary is a balance between production via methylation and loss by demethylation reactions. It is likely that the relative importance of these competing processes differs spatially across the NY&NJ Harbor.

The initial CARP modeling strategy sought to take advantage of the existing calibrated sulfur and redox chemistry modules of the System-Wide Eutrophication Model (SWEM) as a chassis for developing the CARP mercury cycling model. The approach was to calculate the mercury methylation rates from modeled sulfate reduction rates. Independent research conducted concurrently with the CARP model development shows that in certain areas of the NY & NJ Harbor model domain that mercury bioavailability may be the controlling process rather than sulfate reduction rates. Overall, our knowledge of mercury dynamics in estuaries was relatively incomplete at the beginning of the CARP program and has rapidly evolved in recent years. Modeling always lags a bit behind the most recent research finding-this is not a criticism but rather reflects the dynamic between model development and fundamental research. The CARP mercury model is an appropriate framework, and as additional research results become available, they should be incorporated into subsequent versions of the CARP model.

APPENDIX 15.2
HOC FATE AND TRANSPORT

Review and Comments on CARP HOC Fate and Transport Modeling Component

Joseph V. DePinto
August 30, 2006

General Approach

The CARP modeling framework includes a linked series of fine-scale models (hydrodynamic, sediment transport, organic carbon sorbent, contaminant fate and transport, and bioaccumulation) to allow the prediction of water column, sediment and biota concentrations of a suite of contaminants in the NY-NJ Harbor system as a function of various potential source control measures that might be implemented. The MEG has been conducting an ongoing peer review of this model development effort that includes model construction and configuration, model calibration, model evaluation including diagnostic analysis, and ultimately model evaluation. This document presents a review of the HOC fate and transport part of the overall CARP model. The primary question is our assessment of the strengths and weaknesses of the model and our recommendation as to what it can be used for with confidence and what uses of the model may be problematic or entail excess uncertainty.

In assessing the above primary question, I have reviewed three aspects of the overall model development process: 1) model framework; 2) model calibration; and 3) model diagnostic and evaluation results. Comments on each of these three aspects are presented below followed by a general overview statement on this part of the overall CARP model.

Model Framework

Spatial resolution - fine enough to assess relative contamination in different areas of the system including navigation channels, but not fine enough to determine response of specific port/slip areas to load changes

Processes and process formulations –

- three phase, site-specific partitioning on homolog basis is well developed and reasonable. Use a value of $A_{DOC} = 0.08$; seems reasonable. Also, use three-phase partitioning in bed with a higher value of A_{DOC}.
- chemical transformations not used for PCBs or dioxins/furans – seems OK;
- Volatilization uses a single, temperature corrected mass transfer rate of 1 m/d based on SF_6 experiments. Model does not include wind effects on this rate, claiming dominance of tidal velocities. **I am not sure this is valid throughout the system; provide evidence of lack of sensitivity to wind**.
- sediment bed processes – porewater diffusion uses values from SWEM (2-3 X molecular diffusion) seems OK unless bioturbation is causing this rate to be higher – bed mixing process is based on bioturbation with benthic biomass proportional to deposition of labile organic carbon. This process is crucial to establishing the upper mixed layer depth, which strongly impacts system response time. **Are there dated cores that can provide data-based estimate of mixing depth?**

Model Calibration

- Model input data development for the current conditions calibration was a major part of the study. Tributary load estimates were very important. The approach to develop tributary loads was reasonable, given the level of data available.
- Configuration of sediment bed for F&T model and establishment of initial conditions is crucial for a short-term calibration. This is a source of uncertainty.
- **Current calibration using 1998-2002 really only looks at water column relative to current external loads; cannot really calibrate the sediment and sediment-water exchange processes that govern long-term trends. See later where they estimate ~30 years for system to come to steady-state with current loads; this is because the sediment response is much slower than the water column. So, a four year start up for calibration does not really eliminate errors in setting sediment initial conditions.**
- Calibration is evaluated with three types of plots: plots of model versus data for pairs that match in space and time; cumulative probability plots (these allow one to look for bias at either high or low values of state variables in the system); and traditional time series plots at various locations in the system. My qualitative evaluation of the current conditions calibration for PCBs and dioxins is as follows (see Figures 4.7 and 4.8 for summary; detailed results in Appendices 4B-PCBs and 4C-dioxins/furans):
  - For mono- and di-PCBs model is biased high throughout the concentration range;
  - For tri- and tetra-PCBs model is biased high at low concentrations, which occur largely in the bight – perhaps model is not volatilizing these lower chlorinated compounds fast enough and it shows up as the model accumulating more in the bight than is being measured;
  - For the higher PCB homologs, the calibration is pretty good, within a factor of 10 in water column;
  - For the dioxins/furans, the model calibration is fairly good – within a factor of 10 throughout. But it tends to be biased a little high for water column concentration (due to dissolved phase) of most congeners.

Model Diagnostic and Evaluation

- HQI claimed that model uncertainty analysis was beyond the scope of the project and stated that EPA said it was difficult to do a quantitative uncertainty analysis for contaminant fate and transport models; and, therefore, they did not perform it.
- HQI did a long-term (96 years) run to steady-state with the current loads and zero sediment initial conditions. Found that 32 years is sufficient to reach sediment steady-state for this scenario. In addition to the time to steady-state, the endpoint sediment concentrations indicate where the sediments will end up when the current higher sediment concentrations come into steady-state with the current loads. This is a very useful diagnostic (see figure 5-1 for example and figure on penta-PCB from appendix 10). This and other plots show that the sediments in many areas are declining under the current load conditions (i.e., the sediments are still reflecting historic loads). **I would have liked to have seen a time plot of surface sediment concentrations for a few model cells beginning with initial interpolated conditions and running to steady-state.**

- I would have been very interested in seeing rusults of model runs for site-specific K_{oc}'s very K_{ow}-based K_{oc}'s. Does it make a different in the steady-state surface sediment concentrations?
- **We were told that wind effects were not important for air-water gas phase exchange, because tidal effects were dominant. I am not sure I believe this for New York harbor area and in the Bight. I would like to see a plot of computed mass transfer for this area for a velocity-driven formulation in comparison with a wind-driven formulation for the typical range of velocities and wind.**
- **Section 6 contained results of a 1965 – 2002 hindcast confirmation of the model.**
    - Hydrodynamics, sediment transport, and organic carbon were simulated using surrogate years from 1988-89, 1994-95, and 1998-2002 based on comparison with Hudson River flow for a given year. **It is not clear to me that there was any consideration of a change in nutrient loads that might have affected organic carbon production during a given period in the simulation. A significantly higher carbon production in early years might have meant a larger sedimentation rate and hence contaminant burial rate during this period. Is this possible?**
    - Cs hindcast looks quite good. They have done a good job of capturing the time and space (especially in the HR, upper, and lower bay) gradients in sediments. **This result speaks well of the models ability to capture the sediment response time. This is a very important model evaluation result.**
    - The PCB hindcast was conducted by re-constructing the historical PCB loading in the system in a manner similar to what was done for the Delaware River problem. Appendix 7A (time series) and 7B (spatial transects) display the results. The PCB hindcast is not nearly as good as the Cs hindcast, probably because of larger uncertainty in reproducing historical time series of loads. There are some fairly bad time series for some cells in the upper HR (see plots for cells 10,44 and 14,83). Also, the dry weight normalized sediment concentrations seem to compare better to data than the organic carbon normalized values; this is probably due to changes in f_{oc} over time that are not captured by the model.
- **Section 12: Loading Component Analysis**
    - This section looked at the contribution of various loading categories (atmospheric, ocean boundary, CSO's, STP's, tributaries, head of tide, and in-place sediment) to the sediment and water column concentrations over time. In general, the results indicate that it is almost all about in-place sediment levels (and the HR load for PCBs) and the rate at which they decline. Some examples (see Figures 12.2 and 12.3) demonstrate this result. This finding places a premium on getting the sediment – water exchange and sediment burial rates correct, and I think for the most part this model does that well in those areas that are important for management questions.

Summary

Overall, HQI has done an excellent job of developing this model. They had to model a very complex system and include a large suite of chemicals, with somewhat marginal data considering the size and complexity of the system and the questions. This made the task quite difficult, and I was overall impressed with their compilation and synthesis of data from all possible sources, including the literature and previous theory, to pull together a well-integrated whole system model. **Having said that, my summation of the utility of this model is that it has value in predicting the direction and rate of surface sediment response in various zones of the model (i.e., Newark Bay, lower Hudson River, etc.) to a change in loading from a given source category or from a given source area. It is not clear of the uncertainty that will be encountered in trying to predict the absolute value of a chemical's response to a specific load change or the time it will take to achieve that value.**

HydroQual Inc. Response to: Review and Comments on CARP HOC Fate and Transport Modeling Component

HydroQual's effort on the CARP contaminant fate and transport models for HOCs included development, calibration, hindcast verification, sensitivity evaluations, and management application of new models. Emphasis was placed on PCB homolog and dioxin/furan congener calibrations with individual PAHs and organochlorine pesticides being modeled as a further opportunity to test the protocols and methods develped for the calibration of PCB homologs and dioxin/furan congeners. Results of HOC contaminant fate and transport modeling were used to drive pelagic and benthic bioaccumulation model calculations. HydroQual is appreciative of the MEG's involvement in the development of the HOC fate and transport models and the review provided above.

It was not intended that HydroQual would formally respond to or act upon the final MEG review comments. Accordingly, no scope or budget had been alotted for this purpose in HydroQual's contract agreement with the Hudson River Foundation. Rather the intention of the final MEG review was to provide guidance for future users of the CARP model. It is noted that HydroQual had been working cooperatively with the MEG throughout the CARP model development process and that many interim MEG recommendations and suggestions were incorporated into the CARP model along the way. In that sense, there has already been a significant effort by HydroQual to respond to MEG comments and feedback.

While the purposes of HydroQual's response is not to refute or rebut the MEG's final review, the HydroQual response is intended to provide HydroQual with the opportunity to clarify for potential future users of the model (e.g., EPA and State TMDL programs, Superfund, restoration, etc.) any misunderstandings that may be inherent in the MEG review. Overall, HydroQual has found the final MEG review of the HOC contaminant fate and transport model to be technically accurate with few exceptions. These few exceptions and other points of clarification are noted below. Specifically, our response focuses on review comments related to (1) phase partitioning, (2) volatilization and the mass transfer rate across the air-water interface, (3) sediment bed mixing depth and system response time, and (4) assumptions for hindcasting conditions.

As correctly stated in the review, three-phase, site-specific partitioning was used in both the water column and the sediment bed. The A_{DOC} value (i.e., a factor or multiplier applied to the octanol-water partitioning coefficient to specify the partitioning coefficient for contaminants between freely-dissolved and DOC-complexed dissolved phases) was set to 0.08 in both the water column and sediment bed. A higher value for A_{DOC}, however, was not used in the sediment bed as indicated in the review. Although higher values for A_{DOC} in the sediment bed have been used in other studies for other systems, we did not have any justification for doing so in this model. The framework for the CARP model is capable of calculating partitioning with distinct values of A_{DOC} for water column labile, water column refractory, and sediment bed DOC pools. If future data collection efforts provide more detailed information on dissolved phase partitioning, distinct values of A_{DOC} could be implemented with the CARP HOC fate and transport model.

The review incorrectly indicates that volatilization was specified using a single, temperature-corrected mass transfer rate of 1 m/d based on SF_6 experiments. In the final calibrations for all contaminants, volatilization rates were calculated as a function of velocity, diffusivity, and depth acording to equations 2-11 through 2-14 rather than the 1 m/d which was used initially. In addition, the volatilization calculations for PCBs include the effects of temperature on volatilization. HydroQual agrees with the

MEG that at certain locations and for certain conditions, the effects of wind on exchange may dominate transfer, particularly in areas with relatively lower tidal velocities such as the Bight. Tidal velocities in the Harbor proper, the focus of the project, are sufficiently high enough to control volatilization. Further, due to a lack of available wind velocity data over the expanse of the CARP domain at high spatial and temporal resolution, it is unlikely that wind velocities could have been used to drive the volatilization calculations with any more rigor than was achieved by using tidal velocities.

A test was run, specifically for purposes of responding to these comments, to check the sensitivity of the CARP model to the volatilization rate for the di- through hexa- CB homologs. The volatilization mass transfer rates used in the calibration were increased by a factor of ten throughout the model simulation period (i.e., four years of spin-up and four years of calibration). This sensitivity could be cast as examing the effects of a hypothetical wind condition which changed mass transfer by an order of magnitude. Model results from the calibration and sensitivity were compared. The most sensitive homolog run, di-CB, showed modest (i.e., at most 50%) reductions in water column concentrations. The reductions for di-CB suggested in this sensitivity analysis would tend to improve the comparability between ambient data and model outputs for the water column. Future work using the CARP model should revisit the volatilization calculation to determine if the accuracy of the CARP model could be improved for contaminants with relatively low Henry's constants and octanol-water partition coefficients.

In addition to the test run for the di- through hexa- CB homologs described above, two additional calculations for di-CB, the most sensitive homolog to volatilization, were also done specifically for purposes of responding to MEG comments and concerns related to the potential effects of wind on exchange between the atmosphere and water column. Wind driven mass transfer rates were calculated using independent formulations developed by O'Connor and MacKay. The values calculated with the O'Connor and MacKay equations were compared to the mass transfer rates calculated by the CARP model using tidal velocities. For purposes of these comparisons, average tidal velocities were used. For the comparisons, the average wind velocity at JFK airport from 1996 through 2004, 11.3 mph, was used as the wind velocity. Under these conditions, the mass transfer rates calculated were 0.21 and 0.38 m/d for the O'Connor and MacKay equations, respectively. The domain-wide average mass transfer rate calculated with the CARP model volatilization formulation for di-CB, based on average tidal velocities, was 0.15 m/d with a range from 0.02 to 0.32 m/d. Regional average CARP model calculations for mass transfer in the Bight, Long Island Sound, and the remainder of the CARP model domain (i.e., the Harbor and Hudson River) were 0.10, 0.15, and 0.20 m/d. In the core area of the NY/NJ Harbor proper, the mass transfer rates calculated for CARP modeling are within 50% of estimates based on MacKay's formulation and are approximately equal to estimates based on O'Connor's formulation. For the majority of grid cells in the CARP model domain outside the core area (i.e., the Bight and Sound), under average tidal velocity and average wind conditions, estimated rates of mass transfer would be within a factor of 2 to 3 of each other depending on the formulation (i.e., O'Connor, MacKay, or CARP model approach) used. Future users of the CARP model may wish to more rigorously consider these and other formulations, or combinations of formulations, that best represent volatilization.

Dated sediment cores were not collected specifically as part of CARP. Dated sediment cores available from other researchers were considered as part of model verification. HydroQual did not seek out dated sediment cores from other researchers specifically for purposes of estimating the sediment mixing depth in the contaminant fate model current conditions calibrations for several reasons: (1) Dated sediment cores are often biased toward representing a few high depositional areas of the Harbor rather than broad regions (2) Dated sediment cores tend to track long-term rather than seasonal scale trends

and (3) Measured flux data for SOD, ammonia, nitrate plus nitrite, phopshate, and silica and the previously calibrated/validated CARP organic carbon production model were readily available for estimating the sediment mixing depth over space and time. Measured and calculated nutrient fluxes vary greatly both in space and time, more so than could be represented with the available dated sediment cores. The CARP organic carbon production model calculates in space and time the depth of aereobic and anaerobic zones within the top 10 cm of the sediment bed. The mixing depth in the contaminant model based on the nutrient flux calibrations was further tested for contaminants against available dated sediment cores as part of the long-term hindcast analysis.

The CARP model hindcast runs used current condition organic carbon and nutrient loadings for the duration of the model run. Accurate estimates of historical (i.e., potentially higher or lower) loadings were not available to properly estimate the impact of changing (beyond seasonal and recent interannual) carbon loadings and production levels on the system. Had the chronology of previous carbon and nutrient loadings been available, it would have entailed a much greater level of effort than anticipated for in the project scope to produce forcing functions for thirty-seven individual years for all sources. It was intended in the project scope that the sequence of carbon results used for the hindcast would also be used for future projections. Considering historical carbon loadings and anticipated future changes to carbon loadings would have necessitated running two rather than one thirty-seven year sequence of sediment transport/organic carbon production. Although not addressed under the current project, the point raised by the MEG is certainly relevant and poses an excellent research question worthy of future study.

HydroQual acknowledges the many excellent suggestions that the MEG has made regarding future endeavors related to enhancing the CARP HOC fate and transport model . Hopefully, these may be incorporated in future modeling work or other upcoming efforts within the region. Once again, HydroQual gratefully acknowledges and thanks the MEG members for all of their assistance with the CARP modeling effort. In particular, HydroQual thanks Joe DePinto who was the lead author of the MEG final review comments for the CARP HOC fate and transport models.

APPENDIX 15.3
HOC BIOACCUMULATION

Review of Sections 8 - 11 of CARP Report: Food Chain/Bioaccumulation J.E. Baker

Overall, the CARP Food Chain/Bioaccumulation model is based upon a well-established framework that has been successfully used to model PCB accumulation in the Hudson River and elsewhere. The formulations describing accumulation from water, diet, and sediment are consistent with the literature and represent the state-of-the-science for this type of aggregated modeling. The model is constructed to predict the average concentration of each target contaminant based on the properties of the contaminant (PCB homolog, etc.) in the 'average' biota (*e.g.*, an individual fish or worm that exhibits average behavior) throughout the study area. The model parameters are derived from literature values (physical properties of chemicals, bioenergetic rates) and field measurements (concentrations of target contaminants in biota and sediment). While little new conceptual ground was broken during the development of the CARP Food Chain/Bioaccumulation model, Hydroqual did an excellent job of applying their existing model, with minor modifications, to the task at hand.

Strengths of the model: The CARP model is the first comprehensive contaminant model that links hydrodynamics, sediment transport, organic carbon and dissolved oxygen dynamics, and contaminant partitioning and bioaccumulation in one integrated model. This linked approach allows for interesting integrated management questions to be addressed, such as 'how will altering nutrient conditions indirectly affect PCB or mercury bioaccumulation as moderated by changes to the carbon and sulfur cycles in the Harbor?'. The model rests on a sound fundamental footing, and although calibration issues remain (as described below), I have confidence in the overall ability of the model to predict concentrations of target contaminants in the NY/NJ Harbor food web. Weaknesses of the model: The model calibration is best for PCB homologs, PAHs, and most pesticides (I did not review the cadmium and mercury sections; this is left for other MEG members to complete as part of the metals/mercury review). The model's ability to reproduce observed levels of dioxins and furans in the food web is much poorer. Whether this reflects problems with the field calibration data, errors in parameter estimation, or some missing process in the model will require further investigation. Since the model behaves well for the other organic contaminants, it is difficult to see how problems with the dioxin/furan calibration stem from errors in the model structure.

An inherent characteristic of the model is that it predicts time- and space-averaged concentrations of contaminants in the food web. Numerous studies in the NY/NJ Harbor and elsewhere demonstrate that contaminant levels vary considerably within a species at a site, likely due to differences in energetics, mobility, migration patterns, etc. While the model in most cases captures the average behavior, risk assessors may be more interested in the distribution of contaminant concentrations within a species. A complementary but more probabilistic model would be required.

Specific discussion points.

Section 8

1. What are the consequences of using modeled dissolved phase and sediment concentrations to calculate BAFs and BSAFs? While this is addressed later (Section 11), it would be helpful to have a direct comparison of modeled and field measured concentrations for each bioaccumulation zone.

Section 9

2. Why was the top 10 cm of sediment chosen? What are the consequences? What is the oxygen penetration depth in each zone, and how does this affect the vertical distribution of biota?
3. Lipid content of 5% for phytoplankton seems very high. What is the reference for this?
4. Minor typo of pg 26: type aerial = areal
5. Migration of striped bass-how important is this in moderating the PCB levels? What would a 'worse case' scenario look like with adult striped bass remaining in contaminated zones?
6. How important is making the gill uptake rate inversely proportional to the dissolved oxygen concentration? Is this a necessary complication? It is nice to do here since DO is modeled, but is this necessarily a requirement for other models?
7. Chemical assimilation efficiency is not a function of Kow in the model. Comment on the implications on homolog profiles. Also, the chemical assimilation rates seem to be low relative to the literature.

Section 10.

8 BAF for zooplankton = 6xKow with no further increase at higher trophic levels BAF in fish are lower than zooplankton for lower homologs–dietary exposure is less or that metabolism is occurring–what about kinetics? Not wild about metabolic explanations–need more literature review to support.
9. Dioxin/furan BAFs are way too low–look at chapter 11 for explanation–this is a big deal, may be a problem with the fish data OR indicate the model is over-predicting dissolved dioxin/furan concentrations.
10. Pg 36. Not clear you can argue that PAHs reach equilibrium with surrounding water while PCBs of comparable size/hydrophobicity do not. Will defer the cadmium BAF review to others on the MEG.
11. Pg 38. How much of this discussion could be influenced by bias in the sediment concentrations–either being off spatially or by assuming 10 cm depth?
12. Pg 40. I agree that the 28 day bioaccumulation test (dredge material bioaccumulation protocols) under-predict BSAF due to slow accumulation rates. We recently found similar results in Baltimore Harbor.
13. Pg 42. Why do metals BSAFs from field sediment measurements agree with those from model but PCBs do not? Cannot argue that the field grab samples do not represent the biota zones for PCBs but do for metals.
14. What are the consequences of using the same BSAF and BAF across the study domain as compared with zone specific numbers?

Section 11.

15. Since field collected biota were used to determine the parameters (BAF and BSAF), it is a bit circular to compare the model results to the field data–not a criticism, just a recognition of the limited biota data.
16. Pg 72 dioxin/furan in white perch and striped bass are overpredicted by 10 to 1000, even though the BSAF/BAF are unusually low. Does this suggest even a larger problem?
17. Check van der Linde et al (2001) reference. CARP is using the upper end of estimated metabolism rate constants for dioxin/furans.
18. Reference for 6% of sediment organic carbon = black carbon?
19. Sensitivity analysis for dioxin/furan metabilism is not very convincing. Reduces overall modeled/measured concentration ration, but homolog differences remain.

HydroQual Inc. Response to: Review of Sections 8 - 11 of CARP Report: Food Chain/Bioaccumulation

The approach taken with the CARP models to account for the bioaccumulation of contaminants included (1) calculation of site-specific observed BAFs and BSAFs based on contaminant measurements in organisms collected specifically for CARP and exposure concentrations calculated by the CARP contaminant fate and transport models and (2) use of steady-state and time variable bioaccumulation modeling to help explain and better understand the observed BAFs and BSAFs. Based on the MEG review comments, it does not appear that this approach was fully understood. Many of the MEG comments appear to stem from an expectation that the models were used to develop BAFs and BSAFs and model results for BAFs and BSAFs were compared to measurements. Since some of the fundamentals of the modeling approach were misunderstood by the MEG, additional text was subsequently added to report sections 8 through 11 to better clarify this point and the overall bioaccumulation approach. The BAFs and BSAFs used in this study were all field-derived from measured biological data. Bioaccumulation model runs were performed for sensitivity purposes and to help better understand or explain the field-derived BAFs and BSAFs.

While the purposes of HydroQual's response is not to refute or rebut the MEG's final review, the HydroQual response is intended to provide HydroQual with the opportunity to clarify for potential future users of the model (e.g., EPA and State TMDL programs, Superfund, restoration, etc.) any misunderstandings that may be inherent in the MEG review. In the section below, HydroQual will address those MEG comments which are still relevant separate and apart from the basic misunderstanding of the approach. Any remarks made by the MEG (e.g., #13, #15, #16) regarding the calibration of the bioaccumulation model were withdrawn once the approach was clarified.

(#2, #1, #11) Regarding the use of exposure concentrations from sediments averaged over the top ten cm, we found that contaminant concentrations within the top one cm were within 20% of contaminant concentrations in the nine to ten cm sediment depth layer. Oxygen penetration depth varies over space and time and can be over the full ten cm. In this regard, the top 10 cm potentially represents a biologically active zone and is an appropriate averaging interval for exposure concentrations. We do not believe that using calculated exposure concentrations averaged over this depth, when ambient data collocated with biological data were absent, introduces any bias into the observed BAFs and BSAFs. Direct comparisons of model calculated concentrations and measured data are presented in the model calibration sections (i.e., sections 4, 5, and 7) of this report and were not repeated in the bioaccumulation report chapters.

(#3) The lipid content of 5% assigned for phytoplankton may be more accurately described as a sorbing matrix fraction. The 5%, reported on a wet weight basis, includes the effects of contaminant binding to both lipid and non-lipid organic matter in phytoplankton. 5% on a wet weight basis is consistent with the dry weight organic carbon and lipid fractions reported for phytoplankton in Skoglund and Swackhamer (1999).

(#5) The question was raised as to how important the migration pattern developed for stiped bass is in moderating projected PCB levels within bass and a worst case scenario description was requested. Since all projections were done using field-derived BAFs, this issue could be addressed simply by looking at the highest field-derived BAF for striped bass. Further, this issue was previously addressed during the conduct of research funded by the Hudson River Foundation (Farley et al., 1999).

(#6) We believe that modeling the gill uptake rate as inversely proportional to the dissolved oxygen concentration is technically correct and not an unnecessary complication.

(#7) We do not agree with the assessment that CARP model chemical assimilation rates seem low relative to the literature. Chemical assimilation rates were calculated using equation 11-4 which is based on the work of Kelly and Gobas and includes a K_{OW} effect.

(#8, #1, #9, #11, #17, #19) The reader/model user is reminded to disregard concerns expressed that there is a flaw in the bioaccumulation model because BAFs for dioxin are higher in zooplankton than in fish. The BAFs were observed (i.e., Contaminant concentrations in organisms were measured. Coincident sediment exposure concentrations were also measured for worms. Exposure concentrations for other organisms came from the calibrated contaminant fate and transport model). The bioaccumulation model was used to explore and possibly explain the observed BAF behavior. The bioaccumulation modeling analysis suggests that metabolism of dioxins by fish provides a possible explanation for the observed BAF behavior. We provided a literature reference which indicates that dioxins are metabolized by fish. In using this reference, the metabolism rate constants for dioxin/furans selected for use in the model are on the low end of the reported range for bass and more at the upper end of the reported range for perch. We do not imply that the demonstration with the bioaccumulation model that metabolism of dioxins is possibly occurring in fish is exhaustive or definitive. It merely indicates the need for further investigation to explain observed BAFs.

The suggestion that lower BAFs for fish were calculated because the contaminant fate and transport model over-predicts dissolved dioxin/furan concentrations is not true (i.e., the lower BAFs in fish were observed rather than modeled, there were limited and questionable dissolved data with which to make that judgement, and the model does a very good job of reproducing BAFs observed for zooplankton which suggests that calculated dissolved dioxin concentrations are reasonable.). It is true that BAFs in fish could have been underestimated because the freely dissolved fraction of dissolved contaminant was overestimated. This argument, however, would not be consistent with the measured zooplankton BAFs. Metabolism of dioxin/furans occurring in fish appears to be a way to explain both the fish and zooplankton BAFs.

(#10) As a point of clarification, there are three mechanisms by which HOCs in organisms can reach equilibrium with surrounding waters: back diffusion loss, growth dilution, and metabolism. Certain PAHs (those with octanol-water partition coefficients less than 4), in particular, would likely have back diffusion loss mechanisms that are faster than metabolism. In comparing PAHs and PCBs, it is therefore possible that PAHs in organisms could reach equilibrium with the surrounding water faster than PCBs with octanol-water partition coefficients of 4.5 and greater.

(#14) Although we observed spatial differences in BAFs and BSAFs, we used spatially constant BAFs and BSAFs for projection work. The rationale for this decision is that using a geometric mean was more defensible. Although we expended significant effort trying to explain the causality of the observed spatial variability, we don't at this time have conclusive explanations for the observed variability. Further, the relative sparseness of the BAF and BSAF data was another consideration.

(#18) The definition of black carbon as 6% sediment organic carbon is derived from personal communications with and knowledge of publications by Phil Gschwend. We did sensitivity calculations using 0% black carbon and 6% black carbon. 6% black carbon represents the high end based on sediments collected in New York and Boston Harbors (Lohmann et al., 2005).

HydroQual acknowledges the many excellent suggestions that the MEG has made regarding future endeavors related to enhancing the CARP HOC bioaccumulation model . Hopefully, these may be incorporated in future modeling work or other upcoming efforts within the region. Once again, HydroQual gratefully acknowledges and thanks the MEG members for all of their assistance with the CARP modeling effort. In particular, HydroQual thanks Joel Baker who was the lead author of the MEG final review comments for CARP HOC bioaccumulation.

APPENDIX 15.4
METALS FATE AND TRANSPORT

Planning Document for CARP MEG Metals Modeling Review Early April 2007 Conference Call: HydroQual, Inc. Initial Responses

The following is HydroQual's response to comments on CARP metals modeling prepared by Chad Hammerschmidt and William Fitzgerald on behalf of the CARP MEG. The purpose of this set of comments was initially to allow the MEG to prioritize those comments that required further discussion during a conference call planned for April 2 or 3, 2007.

The format of HydroQual's response is on a comment by comment basis with HydroQual's brief initial responses embedded in the comments prepared by the MEG's reviewers.

Comments on the Sub-modeling for Cadmium, Mercury, and Methylmercury in the "HydoQual Model for the Evaluation and Management of Contaminants of Concern in Water, Sediment, and Biota in the NY/NJ Harbor Estuary"

Chad R. Hammerschmidt[†] *and William F. Fitzgerald*[‡]

[†]Department of Marine Chemistry and Geochemistry, Woods Hole Oceanographic Institution
[‡]Department of Marine Sciences, University of Connecticut

1) Section 2.1.1.3.1. A relationship is presented between molecular diffusivity and molecular weight, according to Schwarzenbach et al. (1993). We recall the association to be different from what is described as we have applied the relationship in our own work (Hammerschmidt et al., 2004). That is, and according to Schwarzenbach et al. (1993), who draw from the work of Hayduk and Laudie (1974), $D_w = (2.3 \times 10^{-4})/V^{0.71}$, where V is the molar volume of the molecule ($cm^3\ mol^{-1}$), which is estimated from the molecular weight and density. This approach may provide a more accurate estimate of D_w than the approximation presented here.

HydroQual Response: D_w is given as a function of both V and MW in Figure 9.7 in Schwarzenbach et al. (1993). The relationships presented in Schwarzenbach imply that there is a direct correlation between V and MW. However, we acknowledge, as discussed in Schwarzenbach et al. (1993), that some compounds, such as radon, deviate from the V-MW correlation. Further consideration could be given to comparable effects for mercury and how differences in the molecular diffusivity may affect the CARP model estimate of the gas exchange rate coefficient.

1A) Section 2.1.2.1. The partitioning of Hg to organic matter can be about 10x greater in the water column relative to the sediments. This observation is not reflected in the model, which assumes that the partitioning between the "freely dissolved contaminant" (C_D) and the POC-complexed contaminant (C_{POC}) does not change between the water column and the sediment.

HydroQual Response: Can the reviewers provide a reference? Also, how are the reviewers describing partition coefficients (as apparent coefficients or as intrinsic coefficients)? Partitioning is perhaps the wrong way to describe the way POC binds mercury in the CARP model. The binding of Hg to POC is simulated by a multi-site specific binding model, and the strength of the interactions of those sites with Hg is assumed to be constant for POC in both the water column and sediment. Since the word

"partitioning" often refers to the apparent binding of substances, without consideration of detailed speciation and other competing reactions, the partitioning may indeed be quite different when comparing the water column and sediments, even if the underlying binding strengths are the same.

It is not clear if the comment made by the reviewer refers to apparent binding (partitioning) or if there is evidence to suggest that the nature of POC in sediments and suspended matter is different, with 10x greater binding strengths for suspended particulate matter.

2) Section 2.1.2.2.1. It is stated that bioturbation varies as a function of temperature and biomass of macrobenthos inhabiting sediment. Further, "benthic biomass was not modeled directly in the CARP contaminant fate and transport sub-model, but rather it was assumed that the benthic biomass present is proportional to the concentration of labile organic carbon in the sediment," which also was estimated with the model. In this approach, organic carbon loadings to the benthos are the principal factor driving benthic biomass and associated particle mixing, and thus, greater organic carbon burial leads to greater particle mixing. However, organic carbon burial may have the opposite effect on bioturbation. Among many factors, dissolved oxygen is an important control on the abundance and/or activity of macrofauna (Dauer et al., 1992; Diaz and Rosenberg, 1995; Schlüter et al., 2000; Montagna and Ritter, 2006). Accordingly, greater organic carbon burial and subsequent metabolism/remineralization of this material may result in reduced benthic oxygen levels that inhibit the colonization and activity of macrofauna in sediments. Indeed, we have found that the bioirrigation of pore fluids (i.e., bioturbation) in sediments of NY/NJ Harbor is related positively to oxygen levels at the sediment-water interface, which is correlated with infauna abundance (Hammerschmidt and Fitzgerald, submitted; see Figures 1 and 2 below). Bioturbation of sediments was independent of temperature and sediment organic content in this study.

HydroQual Response: Di Toro 2001, *Sediment Flux Modeling* descibes the calibration of sediment processes. The sediment nutrient flux model calculates three terms used in the determination of the transport of contaminants within the sediment and between the sediment and overlying water column. These terms in many locations are negligible in comparison to the deposition and resuspension terms calculated in the sediment transport model. Particle mixing rates between sediment layers are a function of labile organic carbon, temperature, and time-varying benthic stress. The benthic stress is calculated as a function of the time history of dissolved oxygen in the overlying water column. Specifically, a recovery time after a low dissolved oxygen event is required for the mixing effects of the organisms to become active again in the model calculations. Dissolved phase mixing between the sediment and the water column is calculated as a function of the SOD and the overlying water column dissolved oxygen. Both of these terms, SOD and overlying water column dissolved oxygen, are controlled directly and indirectly by dissolved oxygen and temperature effects included in the sediment diagenesis and water column eutrophication kinetics that are part of the CARP organic carbon production sub-model.

3) Section 2.1.2.2.2. The title of this subsection infers molecular diffusion only. However, "diffusion" in the model also includes biodiffusion/advection. "Sediment-Water Exchange" may be a more appropriate title for this subsection.

   D_d, the pore water diffusion coefficient, is assumed by the model to be "approximately two to three times higher than molecular diffusion." Firstly, which is it—two, three, or 2.5? Secondly, how might D_d vary seasonally in the Harbor? It was noted previously (Section 2.1.2.2.1) that bioturbation, as it relates to particle mixing, varies as a function of temperature and macrofauna abundance in sediments. It is expected that the some of the activities of infauna that redistribute

sediment particles also should influence sediment-water exchange of dissolved constituents.

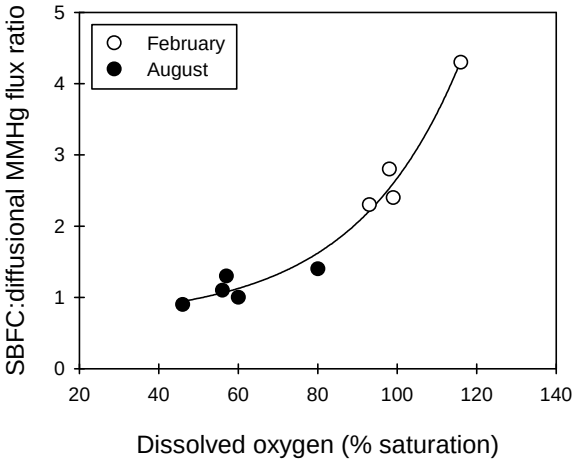

Figure 1. Ratio of methylmercury (MMHg) fluxes measured with shipboard benthic flux chambers:diffusional estimates based on pore-water gradients (SBFC:diffusional) versus the relative concentration of dissolved oxygen in water overlying sediments at each of the sampling locations in NY/NJ Harbor in August 2003 and February 2004 (Hammerschmidt and Fitzgerald, submitted).

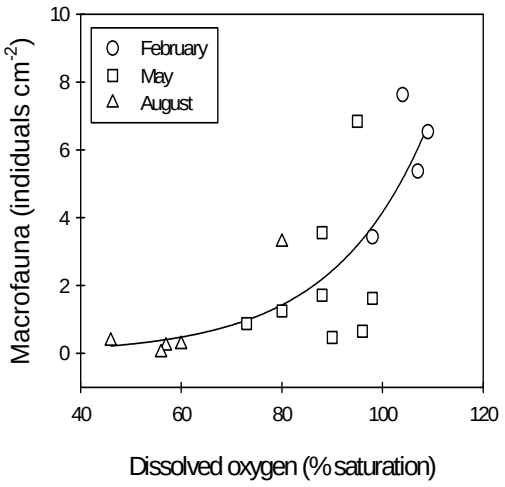

Figure 2. Variation of macrofauna (> 300 μm) abundance with relative concentration of dissolved oxygen in water overlying sediments at multiple locations in NY/NJ Harbor in February, May, and August 2003 (Hammerschmidt and Fitzgerald, submitted).

Moreover, and as noted in Comment 2, dissolved oxygen appears to be an important factor influencing infauna abundance and associated sediment-water exchange of monomethylmercury (MMHg; Figs. 1 and 2). Sediment-water fluxes of MMHg are largely diffusional when dissolved oxygen is less than 80% of the saturation concentration, and enhanced relative to diffusion (i.e., bioirrigation) when oxygen levels are greater.

HydroQual Response: Diffusion is used to denote all processes that affect the exchange of dissolved chemical between the overlying water and pore water. Calibration of the diffusive exchange rate coefficient is based on Di Toro (2001). The direct or indirect effects of dissolved oxygen and temperature on diffusive exchange rates are discussed above in HydroQual's response to comment 2 above. For many parts of the Harbor, particle exchange (by tidal resuspension and settling) will dominate over diffusive exchange.

4) Section 2.2.1.1. It is stated that "free ions, Cd^{2+} and Hg^{2+}, from speciation calculations were used as the bioavailable form of the metals for bioaccumulation model calculations." While this may be appropriate for cadmium, which is acquired by unicellular (e.g., Kola and Wilkinson, 2005) and multicellular organisms (e.g., Sunda et al., 1978; Spry and Wiener, 1991) by active transport through membranes, it most probably is not applicable to Hg^{2+} and CH_3Hg^+. Phytoplankton accumulate both Hg^{2+} and CH_3Hg^+ by passive uptake of uncharged, lipophilic chloride complexes (Mason et al., 1996), and methylating bacteria in sediments are thought to take up Hg^{2+} by passive diffusion of neutrally charged sulfide complexes (Benoit et al., 2001a; 2001b).

HydroQual Response: The uptake of neutral HgCl complexes (Mason et al., 1996) is an interesting point. Certainly $HgCl_2$ uptake is possible, but such non-ionic species in non-sulfidic surface waters are not prevalent. Binding of Hg and Cd to algal surfaces is also a likely (i.e., we do not have any references to point to at the moment) mechanism of accumulation for algae. Hg in zooplankton is important but was not transferred efficiently to fish. MeHg uptake by algae was modeled in the same way (meHg + POC(algae) = meHg-Algae). LogKow values for all lipiphilic Hg and meHg species are less than 1 (Miller et al., 2007). The influence of dissolved organic matter on the complexation of mercury under sulfidic conditions is discussed.

Also, Mason et al., 1996 acknowledge binding of Hg and meHg to algal cells but they are looking specifically at the transfer of dissolved species into the cell. They were trying to identify reasons why meHg is biomagnified and Hg is not. They were hypothesizing that Hg is strongly bound to cell membranes while some meHg is transported into the cell. This would be reflected in a higher assimilation coefficient. Their calculations did not include the presence of DOC,. assuming that in their laboratory study it would not be appreciable. Only Cl, which has a relatively much smaller binding affinity for Hg and meHg than DOC, changed.

5) Table 2-2. A log K_f of 28.7 is used for the complexation of Hg^{2+} with the relatively abundant, yet lower-affinity, binding sites in DOC. This value is at the high end of measured stability constants for these complexes, and should be revised to reflect the more common range of values. Lamborg et al. (2004) found that log *K*' for Hg-L complexes ranged from 22 to 25 among a wide range of surface waters, including the East River, Mid-Atlantic Bight, and Long Island Sound. This range is comparable to that determined for Hg-L complexes in other studies (Benoit et al., 2001c; Han and Gill, 2005).

HydroQual Response: The CARP model log K_f is consistent with the values reported in Hann and Gill (2006) and Lamborg et al (2004). Haitzer, Skyllberg, and Benoit also support higher values.

6) Section 2.2.1.2.1. The rate constant in the photolysis equation (i.e., eq. 2-11) can be simplified; it currently has units of time in both the numerator and denominator.

HydroQual Response: Sellars et al. (1996) presented meHg degradation rates in ng L^{-1} d^{-1} and coincident light intensity measurements (photosynthetically active radiation or PAR) which have units of Einstein m^{-2} d^{-1}. We derived the K term to make use of light intensity values in SWEM: Degradation rate (ng L^{-1} d^{-1}) = K * PAR * C_{meHg} (ng L^{-1}) so K has units of PAR^{-1} d^{-1}.

7) Section 2.2.1.3.1. Use of the "2-film" model for gas exchange of elemental Hg is fine. However, it is unclear how the levels of Hg^0 in the atmosphere and surface waters were estimated for the flux calculation. The concentration of Hg^0 in the atmosphere can be assumed to be relatively constant (~3 ng m^{-3} in southern New England). This amount is within a factor of 10 or less of Hg^0 levels in surface waters. The cycling of Hg^0 is surface waters is dynamic and governs the flux gradient. Hg^0 is controlled by photochemical and biological reactions that reduce and oxidize inorganic Hg species. Given that Hg^0 appears to be a model estimate, are these reactions and substrates considered in the model?

HydroQual Response: These substrates are not considered in the model. Hg^0 is calculated as 10% of the computed dissolved mercury consistent with the general observations in Rolfhus and Fitzgerald (2001).

8) Section 2.2.2.1. The significance of AVS in controlling Hg partitioning in sediments is overstated. In the upper 10 cm of most coastal marine sediments, Hg^{2+} and CH_3Hg^+ are associated largely with the organic material in sediment solid phases. This is evidenced by (1) strong relationships between the distribution coefficient (K_D) of Hg^{2+} and CH_3Hg^+ with sediment organic content (e.g., Hammerschmidt et al., 2004; Hammerschmidt and Fitzgerald, 2006b), (2) selective leaching experiments (e.g, Hammerschmidt et al., 2004; Gagnon et al., 1996), and (3) solid-phase total Hg often is correlated with the level of organic material among surface deposits within a given coastal marine system (e.g., Lindberg and Harriss, 1974; Benoit et al., 1998; Mikac et al., 1999; Heyes et al., 2006; Sunderland et al., 2006; Hammerschmidt and Fitzgerald, 2004,2006b; Lambertsson and Nilsson, 2006).

HydroQual Response: We agree with the reviewer that methylmercury would largely be associated with organic matter in bed sediments. The section of the report that the reviewer is citing states "Binding of mercury and cadmium with AVS is strong". The statement refers to divalent mercury, not methylmercury. The effects of Hg binding to organic matter are included in the model formulation. In NY-NJ Harbor, the aerobic sediment layer is often on the order of 1 millimeter. AVS is therefore expected to play a more significant role in controlling Hg "partitioning" in sediment throughout NY-NJ Harbor.

9) Section 2.2.2.2.1. The second sentence of this subsection states that mercury methylation "is also influenced by pore water sulfide concentration (Benoit et al., 1999)." This statement should be revised to reflect that Hg availability to methylating bacteria is the other key control on MMHg production: Mercury methylation is also influenced by Hg bioavailability, which is mediated by sulfide and organic matter (Benoit et al., 1999; Hammerschmidt and Fitzgerald, 2004, 2006).

Second paragraph, second sentence, section 2.2.2.2.1. It has been *hypothesized* that neutrally charged Hg-S complexes are the primary forms of Hg^{2+} that are available to methylating bacteria in sediment pore fluids (Benoit et al., 1999). Accordingly, this sentence should be modified; insert "thought to be" between "are" and "available"

HydroQual Response: We'll consider the suggested wording changes. We emphatically agree that bioavailability is another control on methylation kinetics and have a detailed discussion about this in section 4.4.4. In 2.2.2.2.1 we do say that methylation is "influenced by pore water sulfide concentrations" although this statement could be clarified to add more of the information on bioavailability we present later on in section 4.4.4.

10) Section 2.2.2.2.1., mercury methylation rate equation. The constant "k" in this equation has units of m^2 mg O_2, and the sulfate reduction rate has units of mg O_2 m^{-2} d^{-1}. The mass units of O_2 do not cancel in this expression, and either the equation or typographical error should be corrected. Secondly, the constant "k" has a value of 44140 m^2 mg O_2. How was the value derived, and what is its meaning?

    The rate expression includes a term for microbial sulfate reduction rate (SRR), which is hypothesized to have a primary control on mercury methylation rates (MMR). Empirical results for sediments in Long Island Sound (Hammerschmidt and Fitzgerald, 2004), the continental shelf of southern New England (Hammerschmidt and Fitzgerald, 2006b), and NY/NJ Harbor (Hammerschmidt et al., submitted) suggest that there is excess methylating potential in coastal marine deposits and that availability of Hg largely limits Hg methylation. Moreover, and not considered in this model, microbes other than sulfate-reducing bacteria (e.g., iron-reducing bacteria) can also methylate Hg (Fleming et al., 2006; Kerin et al., 2006). These results suggest that SRR may not be a primary factor influencing MMHg production in surface sediments of coastal systems. How do results of the model change if methylating potential (i.e., SRR) is assumed to be in excess?

HydroQual Response: It was assumed that that SRR is the major process in marine sediments. K was determined by calibration. We believe there is an error in the units of K (m^2 mg O_2^{-1}) that we will correct.

11) Section 2.2.2.2.2. It is stated that MMHg demethylation "is largely a microbial process in sediment and is strongly tied to redox (Compeau and Bartha, 1984) and sulfate reduction rates (Oremland et al., 1991) with greater rates of demethylation generally occurring under anoxic conditions." While demethylation is linked to redox poise and microbial processes, the connection to SRR is weak. That is, in comparison to anaerobic bacteria (e.g., sulfate-reducers, methanogens) under anoxic conditions, aerobic bacteria (i.e., oxic/hypoxic conditions) were the most significant demethylators of MMHg in the estuarine sediments examined by Oremland et al. (1991), where demethylation appeared to proceed by the organomercurial-lyase pathway and yield CH_4. This pathway/process is mediated by a suite of enzymes that are produced by bacteria when exposed to high levels of Hg (Robinson and Tuovinen, 1984). It is presumed that MMHg demethylation by this pathway is a detoxification mechanism. The organomercurial-lyase pathway is different from demethylation via a generalized oxidative pathway, where it appears that the methyl group of MMHg is metabolized and oxidized similar to other C_1-compounds (e.g., CH_3Br). This oxidative pathway is most pronounced in sediments that have low to moderate Hg contamination (< 0.5 μg g^{-1} dry weight; Marvin-DiPasquale et al., 2000). Accordingly, MMHg demethylation in sediments of NY/NJ Harbor (where Hg contamination is severe, ~1 μg g^{-1} dry weight; Hammerschmidt et al., submitted) is mediated largely by aerobic bacteria that use the organomercurial-lyase pathway.

HydroQual Response: Data and the state-of-the-science did not support further development. We will be more specific in future discussions of demethylation.

12) Section 2.2.2.2.2., methylmercury demethylation rate expression. Firstly, the constant "k" in this equation has units of m^2 mg O_2, and the carbon decay rate has units of mg O_2 m^{-2} d^{-1}. Accordingly, mass units of O_2 do not cancel in this expression, and either the equation or typographical error should be corrected.

Secondly, the model expression for MMHg demethylation is not environmentally realistic. It should be assumed that only a fraction of total sediment MMHg is available for demethylation, as is the case with Hg(II) methylation (section 2.2.2.2.1). Indeed, it would more reasonable to simulate this bioavailable fraction of MMHg as a dissolved, neutrally charged complex (e.g., CH_3HgSH^0), not the entire sedimentary reservoir. Modeling MMHg bioavailability in this manner may allow prediction of more meaningful rate constants that can be compared with methylation rates. Rate constants for methylation and demethylation may be of the same order of magnitude, if not comparable.

Thirdly, the modeled Demethylation Rate is a function of the Carbon Decay Rate, which is set equal to the sulfate-reduction rate, an anaerobic process. As noted in Comment 11, MMHg demethylation appears to mediated largely by aerobic bacteria (Oremland et al., 1991), and this is supported by the results of Compeau and Bartha (1984; cited above), who found that MMHg demethylation was favored under positive redox conditions (+ 110 mV). Thus, the carbon decay rate (i.e., sulfate-reduction rate) is not likely the most appropriate measure of demethylating bacterial activity. Sediment oxygen demand may be a more useful and environmentally realistic alternative, especially if chemical oxygen demand of the sediments can be removed from this term.

HydroQual Response: An "active" MMHg is an interesting idea. Again, data and the state-of-the-science did not support further development.

13) Section 2.2.2.3. What is the assumed speciation and associated molecular diffusion coefficients for Hg(II), Cd(II), and MMHg?

HydroQual Response: Speciation was given in tables 2-1 and 2-2.

14) Section 3.3.1. It is stated that "the mercury methylation kinetics are so fast that any external inputs into the systems of methyl mercury are likely masked by the in-situ net methylation/demethylation processes…." This statement is not correct. While the kinetics of in situ production appear to be very fast, external loadings are the primary source of MMHg to NY/NJ Harbor. The efflux of MMHg from the benthos in the Harbor (8 ± 4 mol y^{-1}) is less than that from rivers (21 ± 4 mol y^{-1}; Balcom et al., submitted). The assumption that MMHg (25 mol y^{-1}) is a trivial fraction of external Hg loadings (~2500 mol y^{-1}) to the Harbor is correct (Balcom et al., submitted).

HydroQual Response: If the "kinetics of in situ production appear to be very fast" how can external loadings be the primary source of MMHg to NY/NJ Harbor? This statement in the review seems to contradict itself so we are not sure that we are interpreting the comment correctly. Also, what were the specific conditions (i.e., location, season, etc.) of measurements used to estimate MMHg efflux from sediment and riverine inputs?

15) Appendix 1A. Given the typical precision of trace-level analyses of Hg, Cd, and MMHg in natural waters, median concentrations should be reported with only two non-zero numbers (e.g., 1.7 ng/L Hg, 17 μg/g Cd, and 0.034 ng/L MMHg).

HydroQual Response: The CARP principal investigators provided the ambient measurements of metals with more than two non-zero numbers. Further, we were more concerned about the significant figures associated with the analytical precision. Consider the following hypothetical example: Dissolved oxygen can be measured accurately to the hundredth of a mg/L level. Accordingly, reports of dissolved oxygen as 0.071 and 11.612 would both be valid measurements. The thousandth place digits are the doubtful digits and all other digits are considered certain digits. The certain digits and one doubtful digit are both considered significant figures. Notice in one case there are two significant figures and in the other case there are five. Was the comment intended to suggest that a better reporting would have been 0.071 and 12, maintaining the same number of non-zero digits and ignoring measurement precision? Wouldn't maintaining the same number of non-zero numbers be a concern for any subsequent manipulations of these measurements?

16) Section 3.3.1.2.1., Tributary Contaminant Loads. It is stated that "New York [tributary Hg concentrations] were also applied to the Connecticut tributaries." There are data for the CT tributaries. Balcom et al. (2004) have reported dissolved and particulate total Hg and MMHg concentrations in many of the major rivers that discharge to Long Island Sound, including the Connecticut, Quinnipiac, Thames, and Housatonic Rivers.

HydroQual Response: Balcom et al. 2004 results were not yet available during the phase of the project when loading estimates were developed. Schedule and budget would not have allowed for us to rework loading estimates after 2004. Further, we had no knowledge that Balcom et al. were collecting data in the Connecticut tributaries. It is regrettable that there wasn't any communication of the effort to CARP or the Hudson River Foundation or any collaboration with the CARP principal investigators who collected similar data in New York and New Jersey waters. We would have liked to have been able to work with these data. How do Balcom et al. concentrations compare to concentrations used for CARP? During what period were Balcom et al. sampling (CARP data were collected between 1998 and 2002)? Did Balcom et al. sample above head-of-tide? We would not expect that differences, if any, in CARP estimates versus estimates for the CT tributaries at head-of-tide from Balcom et al. data would have a significant effect on ambient concentrations in the New York/New Jersey Harbor. Nonetheless, we will recommend that these data be considered as part of future CARP model application efforts.

17) Section 3.3.1.2.1., second protocol for developing daily contaminant loads. Figure 3-6 shows a disconnected log-log relationship between POC and suspended sediment. It is stated in the text that "much of the data came from the Mohawk River, particularly for suspended sediment values greater than 200 mg/L." Exactly how much of the data is from the Mohawk River, and is this system representative? Is it reasonable to expect that the mass fraction of suspended material as POC will vary disproportionately when suspended sediment exceeds about 50 mg/L? Does the disconnect between POC and suspended sediment exist when results from the Mohawk are excluded?

HydroQual Response: The Mohawk provides a dominant source of sediment and organic carbon to the Hudson River Estuary. Also, wastewater treatment plants and in situ production are likely to be the dominant sources of organic carbon to the Harbor. Although the relationship between suspended matter and organic carbon may be somewhat different for the Connecticut tributaries, we would not expect these differences to have a large effect on model results for main portions of NY-NJ Harbor. Site specific NPL POC loading functions were developed where the available data supported them. The Hudson, Mohawk, Passaic, Raritan, Elizabeth, Rahway, Saddle, Wallkill, Roundout, Connecticut, Toms and Great Egg Rivers all had sufficient data to support the development of site specific NPL functions. The inputs from these rivers cover between 1/3 and 1/2 of the rivers considered in the model and

about 80% of the total head of tide volume entering the model domain. The breakdown of the data used to develop the relationship in figure 3-6 is as follows: Mohawk River at Cohoes, NY - 55%, Raritan River - 8%, Passaic River - 8%, Hudson River - 7%, Connecticut River - 6%, Wallkill River - 3%, Rahway River at Rahway, NJ - 3%, Saddle River - 2%, Toms River - 2%, Great Egg - 2%, Elizabeth River at Elizabeth, NJ - 2%, Quinnebaug River - 2%, Housatonic River - 1%. Few of the rivers aside from the Mohawk had measured SS values above 50 mg/L. All of the rivers with SS measurements above 50 mg/L had site specific NPL functions. If the Mohawk River is excluded from the analysis, the low solids relationship remains approximately the same while the high flow relationship remains within a factor of two for the remaining range of observed values. Specifically, the Connecticut River had a site specific NPL using 57 samples from the period of 1978 through 1995.

18) Section 3.3.1.2.2., Unmeasured STPs. "For purposes of assigning effluent contaminant concentrations to unmeasured [sewage treatment] plants, the STP effluent data for each state [i.e., NY and NJ] were screened to eliminate facilities with elevated effluent concentrations potentially attributable to industrial dischargers in their headworks." We question whether the exclusion of these facilities is necessary or warranted. Firstly, the "unmeasured plants" are not the major STPs and, therefore, their volume flux is presumed to be a minor component of total effluent discharge. Secondly, the small "unmeasured plants" also may have elevated contaminant concentrations, so removal of high contaminant values from the median estimate may underestimate the contribution from these sources.

HydroQual Response: The method used to estimate loads from unmeasured sewage treatment plants is reasonable. Any error that may be introduced in our estimates is not considered significant because the unmeasured plants do not have high flow rates. Better estimates would require a large supplemental sampling survey.

19) Section 3.3.1.2.5, second paragraph. An atmospheric Hg deposition flux of 0.0067 mg m^{-2} y^{-1} is used in the model, based on data from the NJ Atmospheric Deposition Network. We have estimated the atmospheric deposition of total Hg to NY/NJ Harbor with data from the Mercury Deposition Network (MDN). The combined mean annual wet depositional Hg flux for MDN sites in Ulster County, New York (NY68; March 2004-March 2005, 0.0118 mg m^{-2} y^{-1}) and Pike County, Pennsylvania (PA72; September 2000-September 2005, 0.0096 mg m^{-2} y^{-1}) is 0.0107 mg m^{-2} y^{-1} (MDN, 2006), which is comparable to the average flux measured in coastal Connecticut (0.008 mg m^{-2} y^{-1}; Balcom et al., 2004). While the atmospheric Hg flux used in the current model (0.0067 mg Hg m^{-2} y^{-1}) is within a factor of two of the other estimates, it appears to be low based on the results of other studies.

The reference to Tseng and coworkers (2003) in this section is neither relevant nor correct. The Tseng et al. (2003) study is largely a "methods paper," and the only reference made to atmospheric Hg in this article is the concentration of Hg^0 (~3 ng m^{-3}), which is borrowed from the Ph.D. thesis of Kris Rolfhus. This article makes no reference to atmospheric Hg deposition.

HydroQual Response: The CARP model Hg atmospheric deposition flux estimate is from the work of Yuan Gao sponsored by the Hudson River Foundation and New Jersey Sea Grant. Gao's measurements were collected at NJADN monitoring stations in the core of the New York/New Jersey Harbor estuary and include Sandy Hook, New Brunswick, and Jersey City. The reviewer is citing estimates from monitoring stations that are located further away from the core area of the Harbor. (Note that the different estimates are within a factor of two!) While the Hg deposition flux relative to

the overall loading of Hg is very important over the open waters the New York Bight, it is less so in Long Island Sound open waters and of only minimal importance over waters in the core area of the Harbor. The CARP Hg atmospheric deposition flux is applied only to the open water surface. Hg atmospheric deposition flux over land is reflected in measured runoff and headwater concentrations both of which represent significant loading sources. Tseng et al. should not have been referenced in this section.

20) Section 3.3.1.2.6. Are not landfill contaminant loadings included in either the CSO, runoff, or river flux estimates?

HydroQual Response: Landfill leachates were monitored as part of CARP. Several landfills within the study domain discharge either directly to the estuary or to treatment plants. Those discharging to treatment plants are included in the CARP model as part of the treatment plant discharge. Those landfills within the model domain discharging directly to the estuary for which both discharge volume rates and concentration estimates were available were included in the model as direct inputs. The input structure of the CARP contaminant model source code has only a limited number of input files for handling the various point and non-point source loading types so mechanistically the discrete landfill inputs were included in an input file that had various other discrete loadings in it. Unfortunately, those landfills for which we had only leachate concentration estimates but no estimate of leachate volume could not be included in the model. We did not make the assumption that landfill leachate was generically represented in overland runoff as suggested by the reviewer. Landfills located above the heads-of-tide of the varios rivers are considered to be included as part of the tributary loads at head-of-tide. Overall, this is really a minor point given the small magnitude of the landfill loadings relative to other loadings.

21) Section 4.4.4., second paragraph. It is stated that "only non-ionic forms of mercury are available for methylation." The word "certain" (or similar) should be inserted between "only" and "non-ionic"

HydroQual Response: We agree. All non-ionic forms of Hg were considered bioavailable for methylation but sulfide species were by far the most abundant non-ionic species of Hg such that the concentrations of all other non-ionic species were irrelevant.

22) Section 4.4.4., second paragraph. It is stated that the conceptual model presented in Figure 4-10 "is supported by studies that have documented relationships between measured methylation rate and measured sulfate reduction." It is important to understand that the relationship in Figure 4-10 is not driven entirely by sulfate-reduction rate. Hg availability/speciation is the other critical factor. Reduced Hg bioavailability inhibits MMHg production when sulfate exceeds about 1 mM in the conceptual model. All sediments in the CARP model domain have greater than 1 mM sulfate, and accordingly, one would expect that Hg bioavailability (not activity of sulfate-reducing bacteria) would be the limiting/primary factor governing MMHg production in this system.

This is supported by the results shown in Figure 4-11. Mercury methylation rates (MMR) are largely independent of sulfate reduction rates (SRR) when SRR is greater than about 0.07 mg d^{-1}, which includes all sediments in the studies of Hammerschmidt & Fitzgerald (2004), Heyes et al. (2004), and by extension, presumably all other deposits within the CARP model domain. This suggests that SRR is not the limiting factor, and implies that Hg availability is the primary control. Accordingly,

and as suggested, SRR might be considered to be in excess, and MMR modeled versus bioavailable Hg.

HydroQual Response: We agree. The paragraph in question specifically states that methylation is a function of sulfate reduction and bioavailability. We are concerned there is a fundamental misunderstanding on the part of the reviewer as to how the CARP methylation model was formulated. We do clearly discuss the importance of bioavailability of mercury, in addition to SRR, in the control of methylation rates. We also have indicated bioavailability controls on Figure 4-11 and shown predictions of the bioavailabile fraction in Figure 4-12. We think the CARP model already has the behavior the review specifies as appropriate in comment 22.

23) Section 4.4.4., third paragraph. We infer that the model assumes partitioning of Hg species between solid and dissolved is very rapid and not the rate limiting step for methylation. Is that correct? Is the concentration of organic carbon a factor influencing steady-state pore fluid concentrations of Hg(II) and MMHg, as suggested by Hammerschmidt and Fitzgerald (2004, 2006b)?

HydroQual Response: Yes. Effects of AVS and organic carbon are both considered in determining Hg "partitioning."

24) Figure 4-13. The model predicts that mercury methylation rates are elevated significantly in sedimentary environs within a few miles of Battery Park, although there are no data to support this result. Hammerschmidt et al. (submitted) have measured the key geochemical parameters which can be used to constrain these model predictions.

HydroQual Response: Available estimates of Hg methylation were used in model calibration. The predicted methylation rates near Battery Park were a feature of the CARP model predictions that generated much discussion during CARP MEG meetings and we all agreed that measurements in this vicinity would be a very useful check on the CARP model. We are curious to know if your more recent estimates of methylation are consistent or not consistent with CARP model predictions and appreciate your willingness to share the unpublished results with us at this time for preliminary discussion purposes in the early April call. We will recommend that as part of any future (i.e., after the paper is actually published) CARP model application projects that a post-audit of the metals model calibration be included to make comparisons between these and potentially other soon to be available data.

25) Figure 4-14. MMHg concentrations predicted by the model for sediments in NY/NJ Harbor are too high. Hammerschmidt et al. (submitted) measured solid-phase MMHg at 10 primary locations in the Harbor in August 2002 and February and May 2003. Measured MMHg levels in Harbor deposits generally range from 2 to 8 ng/g dry weight, and average about 5 ng/g. Accordingly, the model overestimates either net MMHg production or its sequestration by the solid phase. This could result from either overestimation of the MMR, underestimation of demethylation, or possibly, that a greater fraction of the MMHg produced in sediments is mobilized to overlying water.

HydroQual Response: A copy of Hammerschmidt et al. (submitted) wast just provided to us this week. We'll need to review it before providing a preliminary response. We will recommend that a comparison between these not yet publicly available measurements and CARP model results should be discussed as part of a potential CARP metals model calibration post-audit that should be included in any future (i.e., after publication) CARP model application projects.

26) Section 4.4.4, last paragraph. It is noted here that "the agreement between model calculations and the limited available methylmercury data is not as good as for other contaminants," and that there are a couple of reasons for the discrepancies, one of which is questionable quality of the MMHg data.

We suggest that the authors consider revising the model rather than pointing a finger at questionable or "uncertain" data. It is unwise to state or infer that empirical data might be flawed because it doesn't fit a model. We suspect that the MMHg data is just fine. Firstly, the CARP dissolved MMHg results from 1999-2000 are in very good agreement with those reported by Balcom et al. (submitted), who used a method other than aqueous distillation to determine MMHg. Secondly, a recovery factor of 90% is acceptable for the MMHg distillation technique, and the results were corrected appropriately for this minor deficit. Even if they were not corrected, the less-than-perfect recovery would result in a bias/uncertainty of about 10%. The modeled results, however, differ from measured values more significantly. Indeed, less than 50% of model predictions for total, particulate, and dissolved MMHg were within a factor of five (i.e., 500%) of the measured concentrations (Appendix 4D). In most cases, the model overestimates MMHg in the water column, as is the case in sediments (Comment 25), and most probably MMR in sediments. The model should be modified to reflect reality.

HydroQual Response: We did not intend to "point a finger" at the data because it didn't fit the model as the reviewer suggests. Uncertainty in the CARP methylmercury data is a claim that can be made independent of the CARP model. There were relatively few water column methylmercury measurements as compared to the other contaminants with which to represent ambient conditions throughout such an expansive spatial domain over a four year period. Also, there were no measurements of methylmercury in the sediment bed collected specifically as part of the CARP sediment bed sampling program. We had only a few literature measurements to rely on for the sediment bed which were not necessarily collected during our calibration period. In addition, we had some concerns regarding the limited CARP water-column data that we had based on what was reported to us by the CARP principal investigators who collected the data. We were very careful and responsible in wording the text in section 4.4.4 which is repeated here to emphasize our use of words like "some", "may not be", etc. The wording used is very similar, if not exact, with that used in documents prepared by the CARP data collectors.

Section 4.4.4 text excerpt:

"Some of the reasons for discrepancies include:

- The laboratory analysis method for methylmercury involved a distillation which does not have a full recovery. All of the net methylmercury measurements were corrected using an historic mean methylmercury distillation recovery of 90.6%. This historic mean efficiency factor may not be exactly correct for each measurement to which it was applied. In this sense, the methylmercury measurements have some uncertainty.
- The methylmercury data are the weakest of the CARP metal measurements. These measurements were most often non-detect, showed the worst reproducibility, and most frequently had blank contamination."

It is noted that the second bullet point above was taken verbatim from the NYSDEC CARP data report prepared by Simon Litten.

We would be very interested to know how many locations in the core area of the NY-NJ Harbor and the Newark Bay complex and repetitions are represented in the the not yet publicly available Balcom et al. data and we will examine the manuscript we received from the reviewers this week. Again, we will recommend that a comparison between these not yet available measurement and CARP model results should be discussed as part of a potential CARP metals model calibration post-audit that should be included in any future (i.e., after the data are published) CARP model application projects.

27) Section 8.1. The model calculates bioaccumulation factors (BAF) for Hg and Cd based on free ion concentrations in water; this is not an appropriate approach. The widely accepted method for calculating the BAF is the ratio of the contaminant concentration in an organism to the <u>total</u> concentration dissolved in water (U.S. EPA, 2000), not just the free ion, in the case of metals. In the current model, BAF for Cd and Hg are calculated from model estimates of both dissolved metal concentration and speciation, with the speciation estimates adding another source of uncertainty that is neither necessary nor appropriate, especially in the case of Hg. <u>As noted in comment 4, neither Hg (II) nor MMHg is accumulated as free ion species, but rather as neutrally charged inorganic complexes.</u>

<u>HydroQual Response</u>: We will look more closely at this issue of biological uptake being controlled by neutrally charged HgCl and MMHg complexes in future CARP model applications.

28) Section 8.1. Tissue concentrations used in the calculation of BAFs are usually (at least, they should be; Gray, 2002) for whole organisms; that is, not just the concentration in axial muscle. For example, while this is not a problem for small organisms that are readily homogenized (e.g., zooplankton, polychaete worms, small fish), it is challenging for large fish species, such as striped bass. Are BAFs for striped bass (and other fish species) derived from whole fish homogenates?

<u>HydroQual Response</u>:
Fish concentrations were measured as at least one of whole fish homogenized, whole fish minus head and viscera, or standard fillet. Liver samples were eliminated. When more than one of whole fish homogenized, whole fish minus head and viscera, or standard fillet were measured for a given species, it did not show a noticeable discontinuity between the different medium.

29) Equations 8-1 and 8-2. Each of the variables, and their respective units, should be identified and described in the text. By convention, units for BAF are L/kg.

<u>HydroQual Response</u>: We agree with the BAF units which are described in the report text without denoting symbols.

30) Section 8.2. Biota-Sediment Accumulation Factors (BSAFs) were derived for benthic species. The identity of these "benthic species" should be provided here. As corresponding/co-located sediment was not collected with each sample of benthic fauna, sediment concentrations were *estimated* from the CARP contaminant fate model. Accordingly, there is a good deal of uncertainty associated with the BSAFs for sediments in NY/NJ Harbor.

<u>HydroQual Response</u>: Looking at the model-data comparisons for sediment Hg included in the report provides a good sense of the uncertainty in BSAFs. For 79 total Hg measurements, the model predicts 78 within a factor of ten, 76 within a factor of five, 66 within a factor of three, and 52 within a factor

of two – so these BSAF calculations do not show large variations. Cadmium had similar statistics. The CARP sediment sampling program did not include methylmercury; however looking at the few meHg sediment measurements we had from other programs (shown on the transect plots even though not from the same period in most cases), approximately 25 of 30 or so measurements are within a factor of ten of the model results. Sediment concentrations were used because of the lack of sediment data collocated with biological data. The only other choice would have been not to do any calculations which would have violated our contractual agreement with the Hudson River Foundation. The clams and crabs for which body burdens of contaminants were measured included a random number of species based solely on the happenstance of the location and timing of sample collection. We can provide a listing of the species found.

31) Section 8.3, second paragraph. C_{dis} is defined as "the freely dissolved contaminant concentration (μg contaminant/L) and typically does not include complexed forms of the contaminant." This concentration is applied to a rate constant for diffusive uptake in model equation 8-3. We are concerned with the metals Cd and Hg. Uptake of Cd is known to occur by active/facilitated transport of either the free ion (Cd^{2+}) or complexes of Cd with an organic ligand—neither of these processes are diffusional, but they might be modeled as such. Moreover, uptake of Hg by phytoplankton, for example, is by passive diffusion of the $HgCl_2$ complex, not the free ion. While all of these species are dissolved, the meaning of freely dissolved (which also shouldn't be hyphenated) is unclear. That is, exactly what species of Cd and Hg are being considered for "diffusional" uptake, and how are the diffusive rate constants determined or known? In addition, these rate constants are on a mass basis (i.e., L/g organism/d). Is not surface area of the organism an important factor when considering diffusional uptake?

HydroQual Response: We will re-examine the use of Hg^{2+} in future bioaccumulation calculations. Uptake rates (from water exposure) are described in L/g organism/day and are expressed as a function of water rates passing over the gills per day (and are computed from the required respiratory requirements of the organism). For phytoplankton (where surface area would be an appropriate metric for diffusional uptake), we are assuming that kinetics are relatively fast and that equilibrium partitioning applies. See bottom of 2nd paragraph in Section 8.4.

32) Section 8.4, first paragraph. Why was *Gammarus* selected as the model zooplankton species. We do not consider this amphipod to be representative of most coastal zooplankton given its large size, affinity for the benthos, and varied diet of phytoplankton, detritus, and other zooplankton. Copepods (e.g., *Acartia*) would have been better model organisms.

HydroQual Response: Gammarus was used as the model zooplankton species based on previous work by Thomann et al (1989, 1991) for the Hudson River Estuary. For our bioaccumulation model calculations, description of the Hudson River striped bass food chain and the corresponding bioenergetic parameters were taken from Thomann et al. (1989, 1991).

33) Section 8.4, first paragraph. It is stated that the "small fish compartment, which feeds on zooplankton, is meant to reflect a mixed diet of fish of about 10 g in weight and includes age 0-1 tomcod and herring." This is confusing: Does the small fish compartment feed on zooplankton, a mixed diet, or a mixed diet of fish? Herring is an excellent choice for a zooplanktivorous fish, but the tomcod is omnivorous, often feeding on amphipods, worms, squid, fish fry, and mollusks. White perch *Morone americana* do NOT feed exclusively on zooplankton; they also feed on small fish and benthic critters.

HydroQual Response: The Hudson River striped bass food chain provides an idealized description of feeding structure and is based on pervious work by Thomann et al. (1989, 1991). (Note that words like "assumed" are use throughout the description of the model food chain.) The idealized food chain is used as a reasonable description of reality. Inclusion of more species and more food web interactions within the model would result in a much more complex model with too many degrees of freedom. The "mixed diet" in the description refers to a mixed diet of fish for the next trophic level.

It is important to note that management application of the CARP model will be performed using field-derived BAFs. Model calculations are presented to examine mechanisms controlling bioaccumulation and trophic transfer, and to provide additional evaluation of the field-derived BAFs.

34) Section 8.4, second paragraph. Again, free mercury and MMHg (i.e., Hg^{2+} and CH_3Hg^{+}) are not the species accumulated at the base of the food web.

    Furthermore, the CARP bioaccumulation model is applied to the Lower Hudson by taking concentrations in water "directly from the CARP contaminant fate model." This is of concern especially for MMHg, because the model provides poor estimates of total, dissolved, and particulate MMHg in the water column of the Harbor (Figure 4-9).

HydroQual Response: We will check how model calculations are affected before proceeding with future application work.

35) Section 9.0. The topic sentence of this section states that the BAFs and BSAFs are "field-derived." This is only partly true. While the BAFs and BSAFs are based in part on measured contaminant concentrations in biota, levels in the water column and sediments are based on uncertain model predictions.

HydroQual Response: Correct. As explained in the report text, BAFs and BSAFs are hybrid calculations based on measured concentrations in the biota and model water and sediment concentrations. Since co-located biota and exposure concentrations are not available, the use of results from a calibrated model provides our best estimate of BAFs and BSAFs for mercury. We will recommend that as part of any potential future application effort of the CARP model, an assessment of the uncertainties in BAFs and BSAFs associated with the accuracy of the model calculations be prepared and/or that consideration be given to collecting coincident measurements for selected contaminants.

36) Section 9.2.1. "Metal concentrations in phytoplankton were assumed to be equal to POC-bound concentrations…." While this approach may be practical for some aquatic systems, it is questionable whether it should be used in river-dominated estuaries such as NY/NJ Harbor. A considerable amount of suspended solid in the water column of the Harbor is resuspended sediment and/or particulate material delivered from the watershed by rivers. These particles also contain organic carbon, and therefore a burden of organic contaminants as well as Hg and MMHg (and to a lesser extent Cd). Balcom et al., (submitted) have found particle-specific concentrations of total Hg and MMHg (ng g^{-1} suspend solids) are in good agreement with those in underlying sediments at locations throughout the Harbor. Thus, contaminant levels in suspended POC appear to be influenced significantly by resuspension and may not be representative of bioconcentration by phytoplankton.

HydroQual Response: No measurements of metal concentrations in phytoplankton were made in the CARP monitoring program. Differences in metal partitioning for top and bottom water samples did not appear to be significantly different (We will recommend that this be more rigorously explored as part of potential future CARP model application efforts). Therefore, we have no basis for expecting or for assigning different partitioning values for POC and phytoplankton. Also, the fact that observed particle-specific concentrations of Hg and MMHg are in good agreement with those in underlying sediments at locations throughout the Harbor is consistent with our model results and indicates the importance of tidally-induced resuspension and settling in controlling the exchange of contaminants between the sediment and the overlying water.

37) Section 9.2.3, fifth paragraph. The gill transfer efficiency (b) was set at 0.6 for cadmium, mercury, and methylmercury. How was this value derived (literature reference?)? While uptake of Cd via gills is known to be important, it appears that aqueous exposures are insignificant for Hg/MMHg accumulation in fish (Hall et al., 1997), for which dietary uptake is the principal exposure pathway. While 0.6 may indeed be the gill transfer efficiency for Hg species, this pathway of uptake is not relevant.

HydroQual Response: Model results also show that dietary exposure is the primary exposure pathway for Hg/MMHg accumulation in fish. Our understanding is that the selection of gill transfer efficiency is not sensitive in the mercury bioaccumulation model calculation. This pathway is still active in the CARP model calculations, though of lesser importance.

38) Section 10.3, first paragraph. Again, free Hg^{2+} and CH_3Hg^+ should not be used to estimate BAFs; total dissolved concentrations of Hg(II) and MMHg should be used instead. Additionally, and as part of defining terms in the BAF calculation (Comment 29), the conventional unit for BAF is L kg^{-1} wet weight. This unit was used for many, if not all, contaminants in this section except Hg and MMHg (Figure 10-6), although L kg^{-1} was used in the tabulation of the same data in Appendix 11. In appendix 11, log BAFs (L/kg) for total Hg (nearly all of which is MMHg except in zooplankton) range from about 17 to 18 for the various biological species. These values are more than 10^{10} greater than BAFs determined for other coastal marine biota (Hammerschmidt and Fitzgerald, 2006a; Fitzgerald et al., 2007), which are calculated from total dissolved concentrations of Hg species (i.e., the conventional method). As noted several times above, we suggest that the authors use the conventional (i.e., U.S. EPA) method to calculate BAFs for biota in their model. This will aid in interpreting and comparing modeled results with empirical studies. Moreover, it is not free Hg^{2+} and CH_3Hg^+ that are accumulated by biota.

HydroQual Response:
Calculating BAF and BSAF on total dissolved concentrations would likely give values closer to other published values. CARP model calculations of free Hg^{+2} concentrations are very low.

39) Section 10.3, second paragraph. "These results [Fig. 10-5] which show lower BAFs for higher trophic organisms suggest that cadmium uptake through dietary exposure is not an important pathway." It is unclear how this conclusion can be drawn from the data. While the fish certainly have lower levels of cadmium than zooplankton, relative to Cd in water, this may be attributed to fish being more adept at removing (depurating) Cd from their bodies than zooplankton.

HydroQual Response: This could be considered an alternative explanation. In any event, the final conclusion from a management perspective is that Cd is not biomagnified. Cd bioaccumulation can be modeled either way successfully.

40) Section 10.3, second paragraph. "This is consistent with reports of strong binding of cadmium in organisms (e.g., by metallothioneins) which in effect may limit dietary exposure." It is unclear how an internal chelation of cadmium affects the amount that is passed from one trophic level to the next, except if metallothioneins were to aid in the depuration of Cd.

HydroQual Response: The basis idea is that strong binding of Cd to metallothioneins would limit the chemical potential of Cd in the gut and hence limit transfer across the gut wall and into the organism. We will try to provide a specific reference. Note that these issues are important and were appropriately explored using the bioaccumulation model. However, since we do not completely understand all the aspects of bioaccumulation, we used the bioaccumulation model to critically examine the data, but we recommend this use of field-derived BAFs and BSAFs for CARP management applications.

41) Section 10.7. Suggested revision of the title; replace "sediment species" with "benthic species". Sediment is not an adjective.

HydroQual Response: We appreciate your suggestion.

42) Section 10.7, second paragraph. BAFs should not be calculated for specific tissues or organs (e.g., hepatopancreas), they should be used only for whole organisms (Gray, 2002). Additionally, references for enhanced metal accumulation in the hepatopancreas should be included, if this statement were retained.

HydroQual Response: We will consider the Gray, 2002 reference in future applications. The BAFs for the hepatopancreas provide an initial descriptor for the "steady state" (or pseudo-steady state) accumulation in a specific organ. We believe estimates of Cd concentrations in the hepatopancreas are important for ecological or human health assessments.

43) Section 10.8, equation 10-8. Here, BAF is defined as having units of L/kg. These units should be used throughout the report.

HydroQual Response: They are.

44) Section 11.3, third paragraph. The model-predicted fraction of total Hg as MMHg is about 50% for zooplankton, but empirical determinations indicate the fraction is 10-20%. Both values are within the range commonly found in freshwater and marine zooplankton. We do not recommend "re-evaluating" the empirical results because they do not fit the model, but rather, re-evaluate the model. A principal weakness of the model is its ability to accurately predict MMHg concentrations in most of the media considered in this analysis, especially sediments (Comment 25) and dissolved, total, and particulate concentrations in the water column (Comment 34).

HydroQual Response: We disagree.

References

Balcom, P. H., Hammerschmidt, C. R., Fitzgerald, W. F., Lamborg, C. H., O'Connor, J. S., submitted. Seasonal distributions and cycling of mercury and methylmercury in the waters of New York/New Jersey Harbor estuary. *Mar. Chem.*

Balcom, P. H., Fitzgerald, W. F., Vandal, G. M., Lamborg, C. H., Rolfhus, K. R., Langer, C. S., Hammerschmidt, C. R., 2004. Mercury sources and cycling in the Connecticut River and Long Island Sound. *Mar. Chem.* 90, 53-74.

Benoit, J. M., Gilmour, C. C., Mason, R. P., Riedel, G. S., Riedel, G. F., 1998. Behavior of mercury in the Patuxent River estuary. *Biogeochemistry* 40, 249-265.

Benoit, J. M., Gilmour, C. C., Mason, R. P., Heyes, A., 1999. Sulfide controls on mercury speciation and bioavailability to methylating bacteria in sediment pore waters. *Environ. Sci. Technol.* 33, 951-957.

Benoit, J. M., Gilmour, C. C., Mason, R. P., 2001a. The influence of sulfide on solid-phase mercury bioavailability for methylation by pure cultures of *Desulfobulbus propionicus* (1pr3). *Environ. Sci. Technol.* 35, 127-132.

Benoit, J. M., Gilmour, C. C., Mason, R. P., 2001b. Aspects of bioavailability of mercury for methylation in pure cultures of *Desulfobulbus propionicus* (1pr3). *Appl. Environ. Microbiol.* 67, 51-58.

Benoit, J. M., Mason, R. P., Gilmour, C. C., Aiken, G. R., 2001c. Constants for mercury binding by dissolved organic matter isolates from the Florida Everglades. *Geochim. Cosmochim. Acta* 65, 4445-4451.

Dauer, D. M., Rodi, A. J., Jr., Ranasinghe, J. A., 1992. Effects of low dissolved oxygen events on the macrobenthos of the lower Chesapeake Bay. *Estuaries* 15, 384-391.

Diaz, R. J., Rosenberg, R., 1995. Marine benthic hypoxia: a review of its ecological effects and the behavioural responses of benthic macrofauna. *Oceanogr. Mar. Biol. Ann. Rev.* 33, 245-303.

Fitzgerald, W. F., Lamborg, C. H., Hammerschmidt, C. R., 2007. Marine biogeochemical cycling of mercury. *Chem. Rev.* doi: 10.1021/cr050353m.

Fleming, E. J., Mack, E. E., Green, P. G., Nelson, D. C., 2006. Mercury methylation from unexpected sources: Molybdate-inhibited freshwater sediments and an iron-reducing bacterium. *Appl. Environ. Microbiol.* 72, 457-464.

Gagnon, C., Pelletier, E., Mucci, A., Fitzgerald, W. F., 1996. Diagenetic behavior of methylmercury in organic-rich coastal sediments. *Limnol. Oceanogr.* 41, 428-434.

Gray, J. S., 2002. Biomagnification in marine systems: The perspective of an ecologist. *Mar. Poll. Bull.* 45, 46-52.

Hall, B. D., Bodaly, R. A., Fudge, R. J. P., Rudd, J. W. M., Rosenberg, D. M., 1997. food as the dominant pathway of methylmercury uptake by fish. *Water Air Soil Pollut.* 100, 13-24.

Hammerschmidt, C. R., Fitzgerald, W. F., submitted. Sediment-water exchange of methylmercury determined from shipboard benthic flux chambers. *Mar. Chem.*

Hammerschmidt, C. R., Fitzgerald, W. F., 2004. Geochemical controls on the production and distribution of methylmercury in near-shore marine sediments. *Environ. Sci. Technol.* 38, 1487-1495.

Hammerschmidt, C. R., Fitzgerald, W. F., 2006a. Bioaccumulation and trophic transfer of methylmercury in Long Island Sound. *Arch. Environ. Contam. Toxicol.* 51, 416-424.

Hammerschmidt, C. R., Fitzgerald, W. F., 2006b. Methylmercury cycling in sediments on the continental shelf of southern New England. *Geochim. Cosmochim. Acta* 70, 918-930.

Hammerschmidt, C. R., Fitzgerald, W. F., Lamborg, C. H., Balcom, P. H., Visscher, P. T., 2004. Biogeochemistry of methylmercury in sediments of Long Island Sound. *Mar. Chem.* 90, 31-52.

Hammerschmidt, C. R., Fitzgerald, W. F., Balcom, P. H., Visscher, P. T., submitted. Organic matter and sulfide inhibit methylmercury production in coastal marine sediments. *Mar. Chem.*

Han, S., Gill, G. A., 2005. Determination of mercury complexation in coastal and estuarine waters using competitive ligand exchange method. *Environ. Sci. Technol.* 39, 6607-6615.

Hayduk, W., Laudie, H., 1974. Prediction of diffusion coefficients for non-electrolytes in dilute aqueous solutions. *Am. Inst. Chem. Eng. J.* 20, 611-615.

Heyes, A., Mason, R. P., Kim, E.-H., Sunderland, E., 2006. Mercury methylation in estuaries: Insights from using measuring rates using stable mercury isotopes. *Mar. Chem.* 102, 134-147.

Kerin, E. J., Gilmour, C. C., Roden, E., Suzuki, M. T., Coates, J. D., Mason, R. P., 2006. Mercury methylation by dissimilatory iron-reducing bacteria. *Appl. Environ. Microbiol.* 72, 7919-7921.

Kola, H., Wilkinson, K. J., 2005. Cadmium uptake by a green alga can be predicted by equilibrium modeling. *Environ. Sci. Technol.* 39, 3040-3047.

Lambertsson, L., Nilsson, M., 2006. Organic material: The primary control on mercury methylation and ambient methyl mercury concentrations in estuarine sediments. *Environ. Sci. Technol.* 40, 1822-1829.

Lamborg, C. H., Fitzgerald, W. F., Skoog, A., Visscher, P. T., 2004. The abundance and source of mercury-binding organic ligands in Long Island Sound. *Mar. Chem.* 90, 151-163.

Lindberg, S. E., Harriss, R. C., 1974. Mercury-organic matter associations in estuarine sediments and interstitial water. *Environ. Sci. Technol.* 5, 459-462.

Marvin-DiPasquale, M., Agee, J., McGowan, C., Oremland, R. S., Thomas, M., Krabbenhoft, D., Gilmour, C. C., 2000. Methyl-mercury degradation pathways: A comparison among three mercury-impacted ecosystems. *Environ. Sci. Technol.* 34, 4908-4916.

Mason, R. P., Reinfelder, J. R., Morel, F. M. M., 1996. Uptake, toxicity, and trophic transfer of mercury in a coastal diatom. *Environ. Sci. Technol.* 30, 1835-1845.

MDN (Mercury Deposition Network), 2006. National Atmospheric Deposition Program, URL http://nadp.sws.uiuc.edu.

Mikac, N., Niessen, S., Ouddane, B., Wartel, M., 1999. Speciation of mercury in sediments of the Seine Estuary (France). *Appl. Organometal. Chem.* 13, 715-725.

Montagna, P. A., Ritter, C., 2006. Direct and indirect effects of hypoxia on benthos in Corpus Christi Bay, Texas, U.S.A. *J. Exper. Mar. Biol. Ecol.* 330, 119-131.

Robinson, J. B., Tuovinen, O. H., 1984. Mechanisms of microbial resistance and detoxification of mercury and organomercury compounds: Physiological, biochemical, and genetic analyses. *Microbiol. Rev.* 48, 95-124.

Schlüter, M., Sauter, E., Hansen, H.-P., Suess, E., 2000. Seasonal variations of bioirrigation in coastal sediments: Modelling of field data. *Geochim. Cosmochim. Acta* 64, 821-834.

Spry, D. J., Wiener, J. G., 1991. Metal bioavailability and toxicity to fish in low-alkalinity lakes: A critical review. *Environ. Pollut.* 71, 243-304.

Sunda, W. g., Engel, d. W., Thuotte, R. M., 1978. Effects of chemical speciation on the toxicity of cadmium to grass shrimp *Palaemonetes pugio*: Important of free cadmium ion. *Environ. Sci. Technol.* 12, 409-413.

Sunderland, E. M., Gobas, F. A. P. C., Branfireun, B. A., Heyes, A., 2006. Environmental controls on the speciation and distribution of mercury in coastal sediments. *Mar. Chem.* 102, 111-123.

U.S. Environmental Protection Agency. 2000. Methodology for deriving ambient water quality criteria for the protection of human health (2000). Office of Water, Washington, D.C. EPA-822-B-00-004.

Additional HydroQual References Cited

Benoit JM, Gilmour CC, Mason RP, Heyes A. 1999. Sulfide Controls on Mercury Speciation and Bioavailability to Methylating Bacteria in Sediment Pore *Waters. Environ. Sci. Technol.* 33:951-957

DiToro, Dominic M. *Sediment Flux Modeling.* New York: Wiley, 2001.

Haitzer M, Aiken GR, Ryan JN. 2003. Binding of Mercury(II) to Aquatic Humic Substances: Influence of pH and Source of Humic Substances. *Environ. Sci. Technol.* 37:2436-2441

Miller, C.L., Mason, R.P., Gilmour, C.C., and Heyes, A. 2007. Influence of dissolved organic matter on the complexation of mercury under sulfidic conditions. *Environmental Toxicology and Chemistry* 26(4):624-633).

Rolfhus, K.R.and Fitzgerald, W.F. 2001. The evasion and spatial/temporal distribution of mercury species in Long Island Sound, CT-NY. *Geochim. Cosmochim, Acta.* 65(3):407-418.

Sellers, P., Kelly, C., Rudd, J., and MacHutchon, A. 1996. Photodegradation of methylmercury in lakes. *Nature.* 380:694-697.

Skyllberg U, Xia K, Bloom PR, Nater EA, Bleam WF. 2000. Binding of Mercury(II) to Reduced Sulfur in Soil Organic Matter along Upland-Peat Soil Transects. *J. Environ. Quality* 29:855-865